

AD\_\_\_\_\_

Award Number: W81XWH-07-2-0034

TITLE: Mass spectrometry to identify new biomarkers of nerve agent exposure

PRINCIPAL INVESTIGATOR: Oksana Lockridge Ph.D.

CONTRACTING ORGANIZATION: University of Nebraska Medical Center  
Omaha, NE 55198-7835

REPORT DATE: April 20F€

TYPE OF REPORT: ~~Other~~

PREPARED FOR: U.S. Army Medical Research and Materiel Command  
Fort Detrick, Maryland 21702-5012

DISTRIBUTION STATEMENT: Approved for Public Release;  
Distribution Unlimited

The views, opinions and/or findings contained in this report are those of the author(s) and should not be construed as an official Department of the Army position, policy or decision unless so designated by other documentation.

<b>REPORT DOCUMENTATION PAGE</b>			<i>Form Approved</i> <b>OMB No. 074-0188</b>	
Public reporting burden for this collection of information is estimated to average 1 hour per response, including the time for reviewing instructions, searching existing data sources, gathering and maintaining the data needed, and completing and reviewing this collection of information. Send comments regarding this burden estimate or any other aspect of this collection of information, including suggestions for reducing this burden to Washington Headquarters Services, Directorate for Information Operations and Reports, 1215 Jefferson Davis Highway, Suite 1204, Arlington, VA 22202-4302, and to the Office of Management and Budget, Paperwork Reduction Project (0704-0188), Washington, DC 20503				
<b>1. F Ydcfh8 UH</b> April 1, 2010		<b>2. F YdcfhHndY</b> A Final		<b>' "F YdcfhDYfjcX'7 cj YfYX fl"Y'XUHgk</b> 1 APR 2007 - 31 MAR 2010
<b>4. Title and Subtitle</b> Mass spectrometry to identify new biomarkers of nerve agent exposure			<b>5. Award Number</b> W81XWH-07-2-0034	
<b>6. Author(s)</b> Oksana Lockridge, Ph.D. ÎÃ~→~'←ã↔äM  ^↑'Èæä			<b>8. Performing Organization Report Number (Leave Blank)</b>	
<b>7. Performing Organization Name (Include Name, City, State, Zip Code and Email for Principal Investigator)</b> University of Nebraska Medical Center, Omaha, NE 68198-5950 Ã				
<b>9. Sponsoring/Monitoring Agency Name and Address</b> U.S. Army Medical Research and Materiel Command Fort Detrick, Maryland 21702-5012			<b>10. Sponsoring/Monitoring Agency Report Number (Leave Blank)</b>	
<b>11. Supplementary Notes (i.e., report contains color photos, report contains appendix in non-print form, etc.)</b>				
<b>12a. Distribution/Availability Statement (check one)</b> <input checked="" type="checkbox"/> Approved for public release; distribution unlimited Distribution limited to U.S. Government agencies only - report contains proprietary information				<b>12b. Distribution Code</b> (Leave Blank)
<b>13. Abstract (Maximum 200 Words) (abstract should contain no proprietary or confidential information)</b> The accepted target for organophosphorus agent (OP) binding to enzymes is the active site serine in the consensus sequence GlyXSerXGly of acetylcholinesterase. By using mass spectrometry to fragment OP-labeled peptides, we have found that OP can make covalent bonds not only with serine, but also with tyrosine and lysine in proteins that have no active site serine. The OP-tyrosine bond is stable, and does not undergo the decay seen with OP-serine. Human blood treated with nerve agents in vitro has adducts on tyrosine 411 of albumin. To test whether adducts on tyrosine are formed when people are exposed to OP, we analyzed blood from humans poisoned by pesticides, a surrogate for nerve agents. Humans exposed to dichlorvos had OP-labeled tyrosine 411 in plasma albumin. We conclude that albumin is a new biomarker of OP exposure. Mice treated with chlorpyrifos at doses too low to inhibit acetylcholinesterase had OP-labeled tubulin in brain. It is expected that the new OP binding motif will aid in the search for a mechanism of low dose OP toxicity.				
<b>14. Subject Terms (keywords previously assigned to proposal abstract or terms which apply to this award)</b> mass spectrometry, organophosphorus nerve agent binding motif, detection, biomarker			<b>15. Number of Pages (count all pages including appendices) 257</b>	
			<b>16. Price Code</b>	
<b>17. Security Classification of Report</b> Unclassified	<b>18. Security Classification of this Page</b> Unclassified	<b>19. Security Classification of Abstract</b> Unclassified	<b>20. Limitation of Abstract</b>	

## Table of Contents

Abbreviations .....	4
Introduction .....	4-5
Brief Synopsis of Research Results for the Period of this Award.....	5-6
New Directions for Future Research Based on the Results in this Report .....	6
Approved Statement of Work.....	7
Body .....	7-24
Task 1.....	7-10
Task 2.....	11-16
Task 3.....	17-19
Task 4.....	19-20
Task 5.....	20-22
Task 6.....	22-23
Task 7.....	23-24
Key Research Accomplishments .....	24
Reportable Outcomes.....	24-26
Conclusions .....	26-27
Personnel .....	27
References Cited.....	27-29
Appendix: .....	30-258

26 publications are attached as pdf files

## ABBREVIATIONS

amu	atomic mass units
BChE	butyrylcholinesterase
CPO	chlorpyrifos oxon
DFP	diisopropylfluorophosphate
FP-biotin	biotin-tagged organophosphorus agent; 10-fluoroethoxyphosphinyl-N-biotinamidopentyldecanamide
HPLC	high performance liquid chromatography
MALDI-TOF	matrix assisted laser desorption ion – time of flight mass spectrometer; used for acquisition of MS spectra
MALDI-TOF-TOF	matrix assisted laser desorption ion – time of flight mass spectrometer – time of flight mass spectrometer; used for acquisition of MSMS spectra
MS	mass spectrum
MSMS	tandem mass spectrometry in which the mass of a molecule is determined in the first MS and the masses of the fragment ions are determined in the second MS
m/z	mass to charge ratio
NCBI	National Center for Biotechnology Information, US library of medicine
OP	organophosphorus toxicant
QTRAP	Hybrid Triple Quadrupole/Linear Ion trap mass spectrometer from Applied Biosystems
sarin	O-isopropylmethylphosphonofluoridate
soman	O-pinacolylmethylphosphonofluoridate

## INTRODUCTION

There is overwhelming evidence that the acute toxicity of organophosphorus nerve agents and pesticides (OP) is due to inhibition of acetylcholinesterase. The OP binds covalently to the active site serine to make an irreversible adduct. The active site serine of acetylcholinesterase is located in a conserved sequence GlyXSerXGly common to all serine esterases and serine proteases (Taylor and Radic, 1994). The OP-modified acetylcholinesterase is incapable of performing its physiological function of hydrolyzing the neurotransmitter acetylcholine. Excess acetylcholine overstimulates receptors, initiating a cascade of reactions that results in uncontrolled seizures and respiratory arrest (McDonough and Shih, 1997).

What is not understood is why some people suffer chronic illness from a dose of OP too low to inhibit acetylcholinesterase (Ray and Richards, 2001; Salvi et al., 2003; Kamel and Hoppin, 2004; Beseler et al., 2008; Golomb, 2008). The implication is that OP-reactive proteins exist that are more sensitive than acetylcholinesterase to OP. When we began this work we assumed that these highly reactive proteins would have serine at the active site. But when we searched for these proteins using a biotinylated OP we consistently found proteins that had no active site serine. At first we suspected that the avidin beads had nonspecifically bound these proteins and that we were looking at artifacts. To convince ourselves that a protein like tubulin actually binds OP covalently, we studied OP binding to pure tubulin. We used mass

spectrometry to identify the OP binding site (Grigoryan et al., 2008). The labeled amino acid was tyrosine. We studied other pure proteins, and finally synthetic peptides (Grigoryan et al., 2009a; Li et al., 2009a). A consistent pattern emerged of OP binding to tyrosine (Schopfer et al., 2010b). More recently we have also identified covalent binding of OP to lysine in proteins that have no active site serine (Grigoryan et al., 2009b; Lockridge and Schopfer, 2010).

Evidence that OP binding to tyrosine occurs *in vivo* comes from our study of mice and humans. Mice treated with chlorpyrifos at doses that did not inhibit acetylcholinesterase had diethoxyphosphorylated tubulin in brain (Jiang et al., 2010). Humans poisoned by dichlorvos had dimethoxyphosphorylated albumin in plasma (Li et al., 2010b). Human studies used OP pesticides as surrogates for nerve agents because humans exposed to nerve agents are not available. Our results suggest new directions to search for a mechanism of low dose OP toxicity. Proteins involved in axonal transport, especially proteins whose function depends on reversible phosphorylation, are prime candidates for a role in OP-induced low dose toxicity.

## BRIEF SYNOPSIS OF RESEARCH RESULTS

Oganophosphorus toxicants (OP) include chemical nerve agents and pesticides. We have identified a new motif for OP binding to proteins. OP agents make a covalent bond not only with serine but also with tyrosine and lysine. The reaction of OP with tyrosine occurs at physiological conditions. Mice treated with low doses of chlorpyrifos that do not inhibit acetylcholinesterase, have OP-modified tubulin in their brains (Jiang et al., 2010). Humans poisoned with dichlorvos have OP-modified albumin in plasma (Li et al., 2010b).

Butyrylcholinesterase in plasma is a biomarker of exposure to OP nerve agents, OP pesticides and carbamate exposures. We developed mass spectrometry methods to detect soman and sarin adducts on butyrylcholinesterase in human plasma that had been treated with these nerve agents *in vitro* (Li et al., 2008c). In addition we used mass spectrometry to identify butyrylcholinesterase adducts after treatment of purified butyrylcholinesterase with nerve agent analogs of tabun, soman, sarin, and cyclosarin (Gilley et al., 2009). This *in vitro* work laid the groundwork for studies on plasma from live humans exposed to various agents. Plasma from humans poisoned by nerve agents was not available to us because nerve agent exposures are uncommon. However, we were able to obtain plasma from humans poisoned by OP and carbamate pesticides. These agents are surrogates for nerve agents because their mechanism of toxicity is the same as for nerve agents. Furthermore, exposure to the surrogates can be tracked in the same way as exposure to nerve agents, namely by binding to plasma butyrylcholinesterase. Our mass spectrometry analysis showed that plasma samples from humans poisoned by dichlorvos, chlorpyrifos, carbofuran, or aldicarb had adducts on butyrylcholinesterase (Li et al., 2009b; Li et al., 2010a).

Nanoimaging of microtubules was introduced as a method to visualize the effect of OP exposure (Grigoryan and Lockridge, 2009b). Mice treated with OP have thin microtubules that are depleted of the normal amount of associated proteins (Jiang et al., 2010). This result is relevant to understanding noncholinesterase mechanisms of OP toxicity.

Mass spectrometry was used to demonstrate that the esterase activity of albumin is not a real esterase activity because there is no turnover. Many lysines become acetylated but the acetylation is stable (Lockridge et al., 2008; Liyasova et al., 2010). Tyrosine 411 of albumin is acetylated by p-nitrophenyl acetate, but not by aspirin. These studies are relevant to the study of

nerve agent exposure because nerve agents make stable adducts with albumin on Tyrosine 411. Aspirin use will not interfere with OP binding to Tyrosine 411 of albumin.

Butyrylcholinesterase purified from human plasma is not simply a tetramer of 4 identical subunits. Using mass spectrometry we found that the purified butyrylcholinesterase includes polyproline peptides with the sequence PSPPLPPPPPPPPPPPPPPPPPLP . The function of the polyproline peptides is to organize the 4 subunits into a 340 kDa tetramer, by interacting with the C-terminal tetramerization domain (Li et al., 2008b). This finding is relevant to protection from nerve agent toxicity because butyrylcholinesterase is being developed as a bioscavenger for protection. The tetrameric form of butyrylcholinesterase has a much longer residence time in the circulation (weeks) than the monomeric form (minutes). The information that tetramers are produced by coexpression with a polyproline rich peptide makes it possible to make butyrylcholinesterase tetramers by recombinant DNA methods. The Department of Defense will save a lot of money by using tetrameric butyrylcholinesterase because a single dose will last a long time in the body.

#### NEW DIRECTIONS FOR FUTURE RESEARCH BASED ON THE RESULTS IN THIS REPORT

- Antibodies for detection of OP exposure could be developed that recognize OP-tyrosine adducts on proteins in plasma. The rationale for this approach are the findings that 1) people poisoned with dichlorvos have OP-albumin adducts in their plasma, where the OP is covalently bound to Tyrosine 411. This demonstrates that it makes sense to make an antibody for detection of OP-tyrosine. 2) OP-tyrosine adducts are stable compared to OP-serine adducts, making it likely that OP-tyrosine adducts could be detected weeks after exposure.
- The finding that OP agents bind covalently to tyrosine and lysine on proteins suggests new directions to search for a mechanism to explain neurotoxicity from low dose exposure to OP. The most likely candidates are a) low abundance signaling proteins, possibly kinases, whose function is disrupted by binding OP, and b) proteins involved in axonal transport whose function depends on reversible phosphorylation and dephosphorylation.
- The mass spectrometry methods developed in this work can be applied to study toxicity from exposures that have no laboratory verification method to date. For example, the unfiltered bleed air in jet aircraft causes severe toxicity in some air crew and passengers (Ross, 2008). The likely toxicant is tricesyl phosphate, an additive in jet oil (Ross, 2008). Tricesyl phosphate is converted to a potent cyclic phosphate in the liver (Casida et al., 1961). Mass spectrometry is expected to detect butyrylcholinesterase adducts in plasma.
- Tetrameric butyrylcholinesterase can be produced by coexpression of butyrylcholinesterase with a polyproline rich peptide. The advantage of tetrameric butyrylcholinesterase is that it is stable in the circulation. In contrast, monomeric butyrylcholinesterase is cleared within minutes. A single dose will last for days or weeks and therefore a single dose will protect from nerve agent toxicity for a long time.

## APPROVED STATEMENT OF WORK

- Task 1. Determine the characteristic fragmentation pattern of soman covalently bound to a serine hydrolase (trypsin).
- Task 2. Determine the characteristic fragmentation pattern of soman covalently bound to a tyrosine esterase (albumin)
- Task 3. Identify the proteins in human plasma that bind the nerve agent simulant, FP-biotin.
- Task 4. Set up a Multiple Reaction Monitoring method to identify soman-labeled proteins, using purified proteins.
- Task 5. Use Multiple Reaction Monitoring to identify soman-labeled proteins in human plasma.
- Task 6. Use a second method, for example enzyme activity assays or immunoprecipitation, to confirm the identity of soman-labeled proteins from plasma.
- Task 7. Determine the limit of detection of soman-labeled proteins in human plasma.

## Task 1. Determine the characteristic fragmentation pattern of soman covalently bound to a serine hydrolase (trypsin).

### SUMMARY

The goal was to search for characteristic fragment ions that would indicate covalent binding of soman to serine in proteins. Two highly purified proteins, bovine trypsin and human butyrylcholinesterase, were labeled with soman and their tryptic peptides analyzed by mass spectrometry. Aged soman adducts on serine that had lost the pinacolyl group were found for both proteins (Figures 1.1 and 1.2). MSMS spectra of the butyrylcholinesterase adduct showed dehydroalanine ions, where the active site serine had been converted to dehydroalanine by loss of the entire soman molecule as well as loss of a molecule of water (Figure 1.1). In contrast, MSMS spectra of the soman-trypsin adduct contained no dehydroalanine ions (Figure 1.2). It is concluded that the search for soman-labeled serine peptides with Mascot software should use the variable modifications named “dehydrated (S)” and “methylphosphonate (S)”.

We used this information to identify soman-labeled butyrylcholinesterase in human plasma in the attached paper by (Li et al., 2008c). We also used this information to study the reaction of soman analogs with purified human butyrylcholinesterase in the attached paper by (Gilley et al., 2009). This information was also useful for comparison of reaction products of butyrylcholinesterase with other nerve agents in the attached papers by (Carletti et al., 2008) and (Masson and Lockridge, 2010).

### **Attached are pdf files for published papers related to this task.**

Li H, Tong L, Schopfer LM, Masson P, Lockridge O. Fast affinity purification coupled with mass spectrometry for identifying organophosphate labeled plasma butyrylcholinesterase. Chem

Biol Interact. 2008 Sep 25;175(1-3):68-72. PMID: 18586231

Carletti E, Li H, Li B, Ekström F, Nicolet Y, Loiodice M, Gillon E, Froment MT, Lockridge O, Schopfer LM, Masson P, Nachon F. Aging of Cholinesterases Phosphylated by Tabun Proceeds through O-Dealkylation. J Am Chem Soc. 2008 Nov 26; 130 (47): 16011-20. PMID: 18975951

Gilley C, MacDonald M, Nachon F, Schopfer LM, Zhang J, Cashman JR, Lockridge O. Nerve agent analogues that produce authentic soman, sarin, tabun, and cyclohexyl methylphosphonate-modified human butyrylcholinesterase. Chem Res Toxicol. 2009 Oct; 22(10):1680-8. PMID: 19715348

Masson P, Lockridge O. Butyrylcholinesterase for protection from organophosphorus poisons; catalytic complexities and hysteretic behavior. Arch Biochem Biophys. 2010. Feb15; 494(2): 107-20. PMID: 20004171

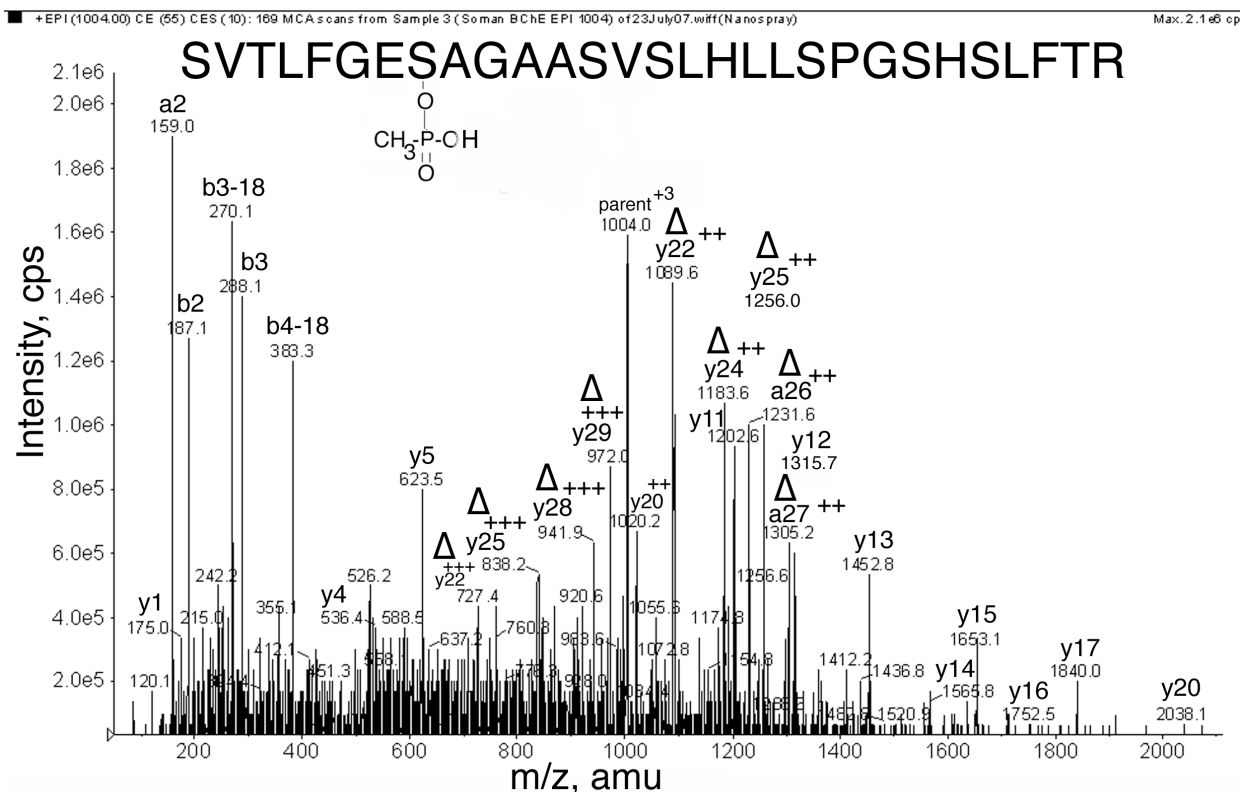


Figure 1.1. MSMS spectrum of aged soman-labeled human butyrylcholinesterase tryptic peptide. The parent ion at 1004.0 m/z is triply charged. Dehydroalanine forms of the peptide are indicated by the symbol Δ. The MSMS spectrum was acquired on the QTRAP 4000 mass spectrometer. The accession number for human butyrylcholinesterase in the National Center for Biotechnology Information database is gi: 116353. Experimental details are in the Annual report for W81XWH-07-2-0034 year 2009 by Lockridge.

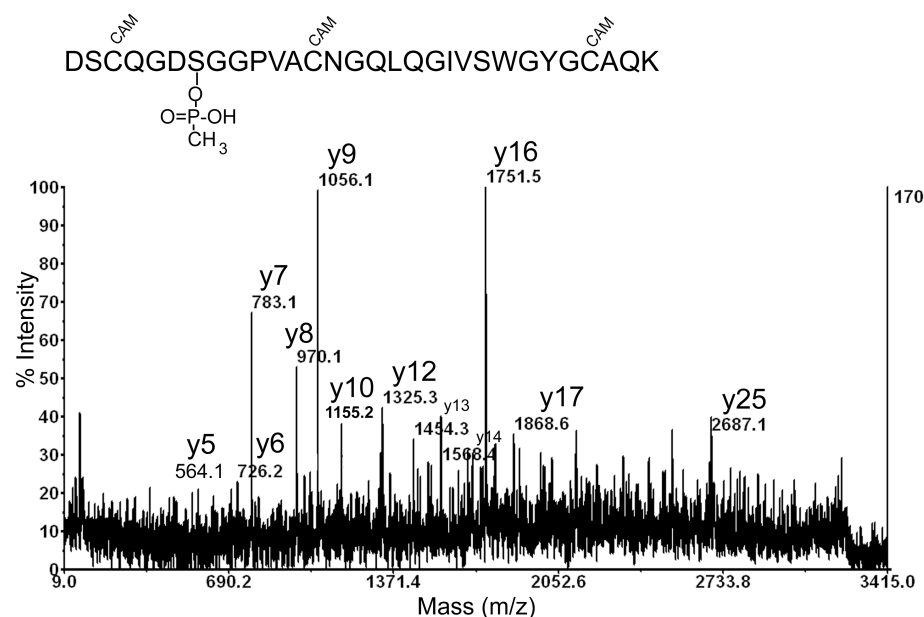


Figure 1.2. Tryptic peptide of bovine trypsin covalently modified on serine with aged soman. The MSMS spectrum of the singly charged parent ion of mass 3234 was obtained on the MALDI-TOF-TOF mass spectrometer. CAM indicates carbamidomethylated cysteine. The y-ion series from y5 to y25 is consistent with the sequence for the 30 amino acid residue peptide. The y25 ion is of particular note because the 2687.1 mass includes the methylphosphonate from aged soman. The methylphosphonate has remained bound to serine during the fragmentation procedure. No masses were found for a dehydroalanine form of this peptide. The accession number for the sequence is gi:830 in the NCBI database. Experimental details are in the Annual report for W81XWH-07-2-0034 year 2009 by Lockridge.

**Summary of information derived from our study, that is useful for identifying soman exposure.** Identification of soman exposure by mass spectrometry requires one to know exactly what ion masses are expected. Theoretical calculations are helpful but may not foresee exceptions to a theoretical model. Human butyrylcholinesterase is a good example of this point. Human butyrylcholinesterase is an excellent biomarker of exposure because it rapidly forms an adduct with soman that can be detected by mass spectrometry. Furthermore, a blood sample can be analyzed for soman exposure because butyrylcholinesterase is present in human plasma. The theoretical mass of the soman-labeled tryptic peptide of butyrylcholinesterase is 3090 daltons if serine 198 is modified by O-pinacolylmethylphosphonate. However, such a mass is not found. What is found is a mass of 3006 daltons for the O-methylphosphonate adduct on serine 198. (A singly charged mass of 3006 is equivalent to the triply charged mass of 1004 m/z in Figure 1.1). The difference between the theoretical and actual masses is explained by loss of the pinacolyl group of soman.

A second deviation from a theoretical model is in the MSMS spectrum. The collision energy in the mass spectrometer fragments the soman-labeled tryptic peptide of butyrylcholinesterase into a set of y-ions that have lost the methylphosphonate as well as a molecule of water, converting the active site serine 198 to dehydroalanine. The dehydroalanine

ions are highly characteristic of OP-labeling on the active site serine of butyrylcholinesterase (Fidder et al., 2002).

Both soman-labeled bovine trypsin and soman-labeled butyrylcholinesterase have O-methylphosphonate rather than O-pinacolylmethylphosphonate adducts on their active site serine. However, MSMS spectra of soman-labeled bovine trypsin showed no dehydroalanine ions. Consistent with our finding is the report that DFP-treated chymotrypsin yielded no dehydroalanine ions in the MSMS spectrum (Tsuge and Seto, 2002).

MSMS data are often searched for peptide modifications with the Mascot search engine. The Mascot software can only identify a modification if the expected possible modifications are listed as variable options during the search. To make it possible to search for soman modifications we have added soman as a variable modification option. The Mascot modification file is an open source software called Unimod. We introduced soman modification on serine, threonine, and tyrosine according to the instructions on the web site <http://www.unimod.org>. Access to soman modification is freely available to all Mascot users in the variable modifications menu under the name “O-pinacolylmethylphosphonate” for unaged soman bound to oxygen and “methylphosphonate” for aged soman. Dehydrated serine (equivalent to dehydroalanine) can be found in the variable modifications menu under the name “dehydrated (S)”.

### Key Accomplishments

- Our mass spectrometry work confirmed that soman covalently modifies human butyrylcholinesterase and bovine trypsin on the active site serine, and that the pinacolyl group of soman is rapidly lost to yield a methylphosphonate adduct with an added mass of +78.
- Fragmentation of the soman-labeled active site peptide of butyrylcholinesterase showed that the labeled serine easily releases methylphosphonate and a molecule of water, converting the active site serine to dehydroalanine. The conversion to dehydroalanine was prominent for soman-modified butyrylcholinesterase, but was not seen for soman-labeled trypsin. The presence of dehydroalanine in the MSMS spectrum is characteristic for adducts on the active site serine of butyrylcholinesterase.
- The Mascot search engine is used by investigators all over the world. To make it possible for other investigators to identify soman-labeled proteins we have added O-pinacolylmethylphosphonate and methylphosphonate to the variable modifications database in Mascot.

## Task 2. Determine the characteristic fragmentation pattern of soman covalently bound to a tyrosine esterase (albumin).

### SUMMARY

The goal was to determine the characteristic fragmentation pattern of soman covalently bound to tyrosine. Three pure proteins, human albumin, human transferrin, and bovine tubulin, were treated with soman, digested with trypsin and analyzed by mass spectrometry (Li et al., 2007; Grigoryan et al., 2008; Li et al., 2008a; Grigoryan et al., 2009c; Li et al., 2009a; Lockridge and Schopfer, 2010). It was found that soman made a covalent bond with tyrosine in each of these proteins (Figures 2.1, 2.2, 2.3, 2.4). The soman adduct on tyrosine did not undergo dealkylation so that the pinacolyl group remained bound in the parent ion. However, during MSMS fragmentation the pinacolyl group was readily released to yield ions that had lost 84 mass units. Soman adducts on tyrosine are stable, having a half-life of 20 days at pH 7.4 (Figure 2.5). This stability suggests that soman exposure could be monitored by analyzing soman-tyrosine adducts in blood samples taken weeks after the exposure incident.

### Attached are pdf files for published papers related to this task.

Li B., Schopfer LM, Hinrichs SH, Masson P, Lockridge O. Matrix-assisted laser desorption/ionization time-of-flight mass spectrometry assay for organophosphorus toxicants bound to human albumin at Tyr411. *Anal Biochem.* 2007 Feb 15; 361(2): 263-272. PMID: 17188226

Li H, Schopfer LM, Nachon F, Froment MT, Masson P, Lockridge O. Aging pathways for organophosphate-inhibited human butyrylcholinesterase, including novel pathways for isomalathion, resolved by mass spectrometry. *Toxicol Sci.* 2007 Nov; 100(1):136-145. PMID: 17698511

Li B, Nachon F, Froment MT, Verdier L, Debouzy JC, Brasme B, Gillon E, Schopfer LM, Lockridge O, Masson P. Binding and hydrolysis of soman by human serum albumin. *Chem Res Toxicol.* 2008 Feb;21(2):421-31. PMID: 18163544

Grigoryan H, Schopfer LM, Thompson CM, Terry AV, Masson P, Lockridge O. Mass spectrometry identifies covalent binding of soman, sarin, chlorpyrifos oxon, diisopropyl fluorophosphate, and FP-biotin to tyrosines on tubulin: a potential mechanism of long term toxicity by organophosphorus agents. *Chem Biol Interact.* 2008 Sep 25;175(1-3):180-6. PMID: 18502412

Lockridge O, Xue W, Gaydess A, Grigoryan H, Ding SJ, Schopfer LM, Hinrichs SH, Masson P. Pseudo-esterase activity of human albumin: slow turnover on tyrosine 411 and stable acetylation of 82 residues including 59 lysines. *J Biol Chem.* 2008 Aug 15;283(33):22582-90. PMID: 18577514

Li H, Schopfer LM, Masson P, Lockridge O (2008) Lamellipodin proline rich peptides associated with native plasma butyrylcholinesterase tetramers. *Biochem J.* 2008 Apr 15; 411(2): 425-432. PMID: 18076380

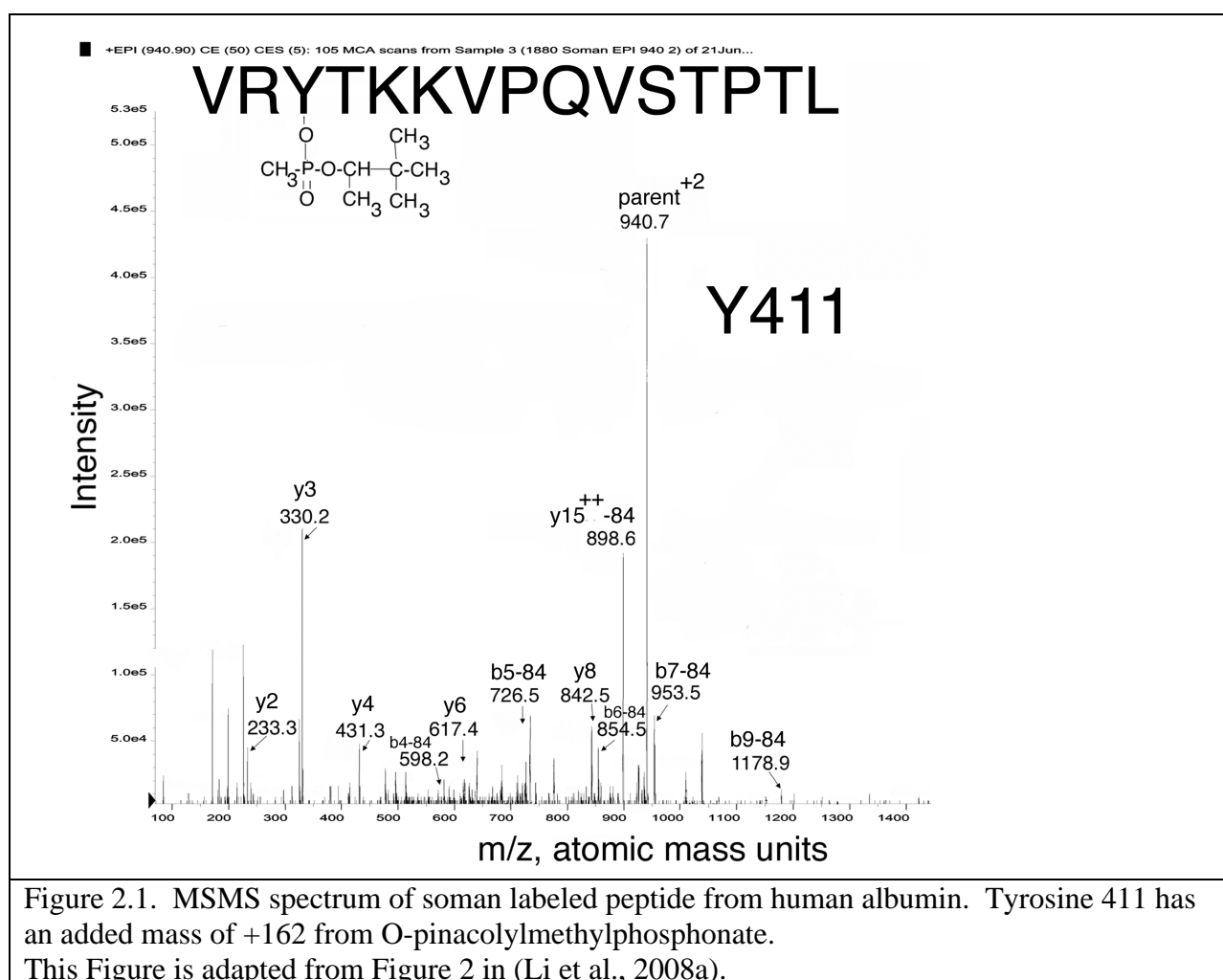
Grigoryan H, Schopfer LM, Peeples ES, Duysen EG, Grigoryan M, Thompson CM, Lockridge O. Mass spectrometry identifies multiple organophosphorylated sites on tubulin. *Toxicol Appl Pharmacol.* 2009 Oct 15;240(2):149-158. PMID: 19632257

Grigoryan H, Li B, Xue W, Grigoryan M, Schopfer LM, Lockridge O. Mass spectral characterization of organophosphate-labeled lysine in peptides. *Anal Biochem.* 2009 Nov 1; 304(1):92-100. PMID: 19596251

Li B, Schopfer LM, Grigoryan H, Thompson CM, Hinrichs SH, Masson P, Lockridge O. Tyrosines of human and mouse transferrin covalently labeled by organophosphorus agents: a new motif for binding to proteins that have no active site serine. *Toxicol Sci.* 2009 Jan;107(1):144-55. PMID: 18930948.

Liyasova MS, Schopfer LM, Lockridge O. Reaction of human albumin with aspirin in vitro: mass spectrometric identification of acetylated lysines 199, 402, 519, and 545. *Biochem Pharmacol* 2010;79(5):784-91. PMID:19836360

Lockridge O, Schopfer LM. Review of tyrosine and lysine as new motifs for organophosphate binding to proteins that have no active site serine. *Chem Biol Interact.* 2010 Sep 6;187(1-3):344-348. PMID: 20211158



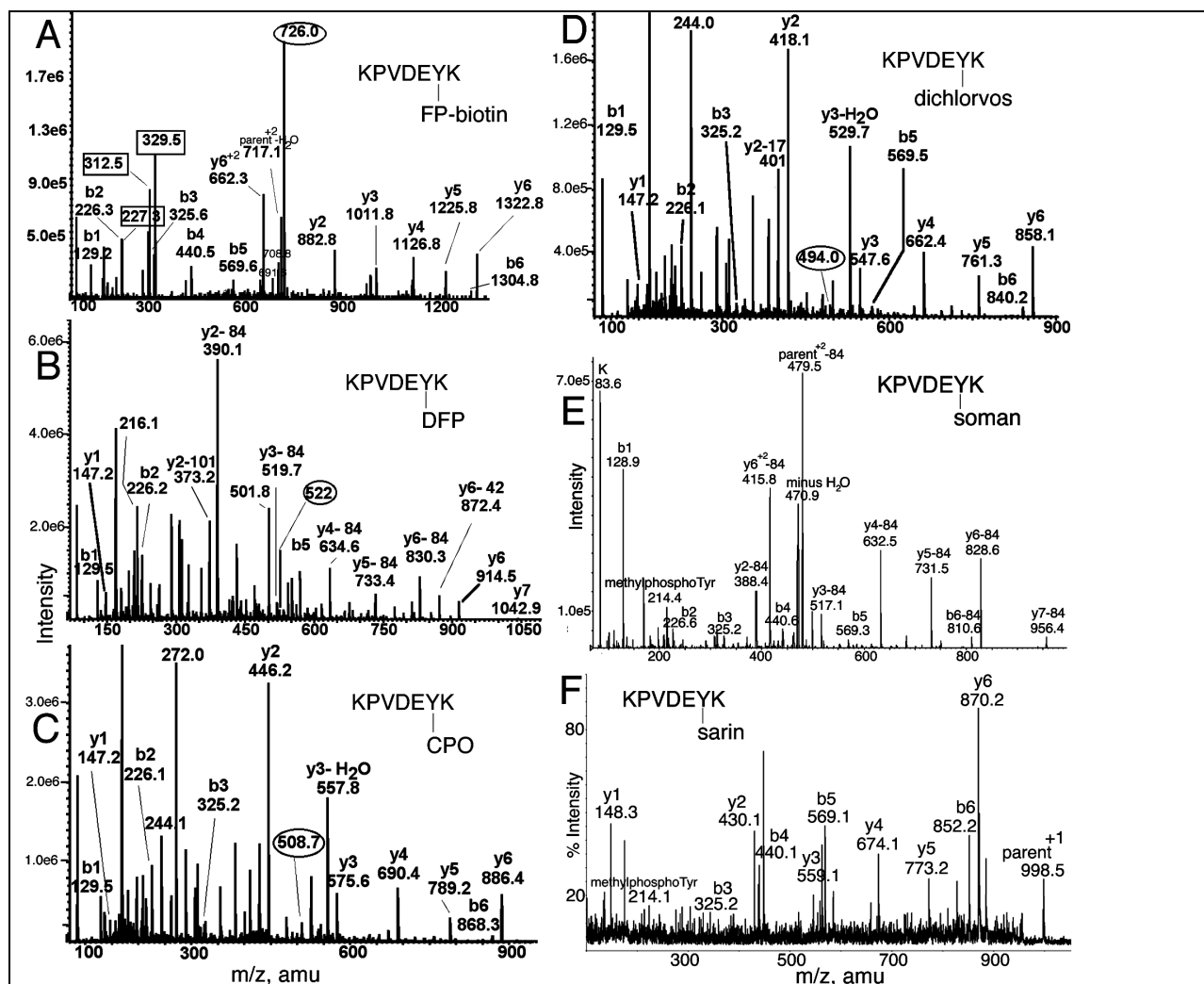


Figure 2.2. MSMS spectra of OP labeled Tyr 238 in peptide KPVDEYK of human transferrin. The b and y ion masses in all panels are consistent with OP covalently bound to Tyr 238. A) The doubly charged parent ion of the FP-biotin labeled peptide is at 726 m/z. Masses enclosed in boxes at 227.3, 312.5, and 329.5 are fragments of FP-biotin. The immonium ion of FP-biotinylated tyrosine is at 708.8 amu. B) The doubly charged parent ion of the DFP-labeled peptide is at 522 m/z. Loss of one or both isopropyl groups during collision induced dissociation yields y-ions minus 42 or minus 84 amu, confirming the presence of diisopropylphosphate on the parent ion. C) The doubly charged parent ion of the chlorpyrifos oxon labeled peptide is at 508.7 m/z. The mass difference between y1 (147.2) and y2 (446.2) shows the diethoxyphosphate on tyrosine in fragment y2. D) The doubly charged parent ion of the dichlorvos labeled peptide is at 494 m/z. E) The parent ion of the **soman labeled peptide** has a mass to charge ratio of 520.7, but this mass does not appear in the scan. The prominent peak at 479.5 is the doubly charged parent ion that has lost the pinacolyl group from soman. The y2-y7 ions have all lost 84 amu due to release of pinacolyl from soman. The peak at 214.4 is the methylphosphotyrosine immonium ion. F) The parent ion of the sarin labeled peptide is the singly charged ion at 998.5 amu. The masses of the y-ion series, and the 214.1 mass for methylphosphotyrosine immonium support labeling on tyrosine.

This is Figure 4 from (Li et al., 2009a).

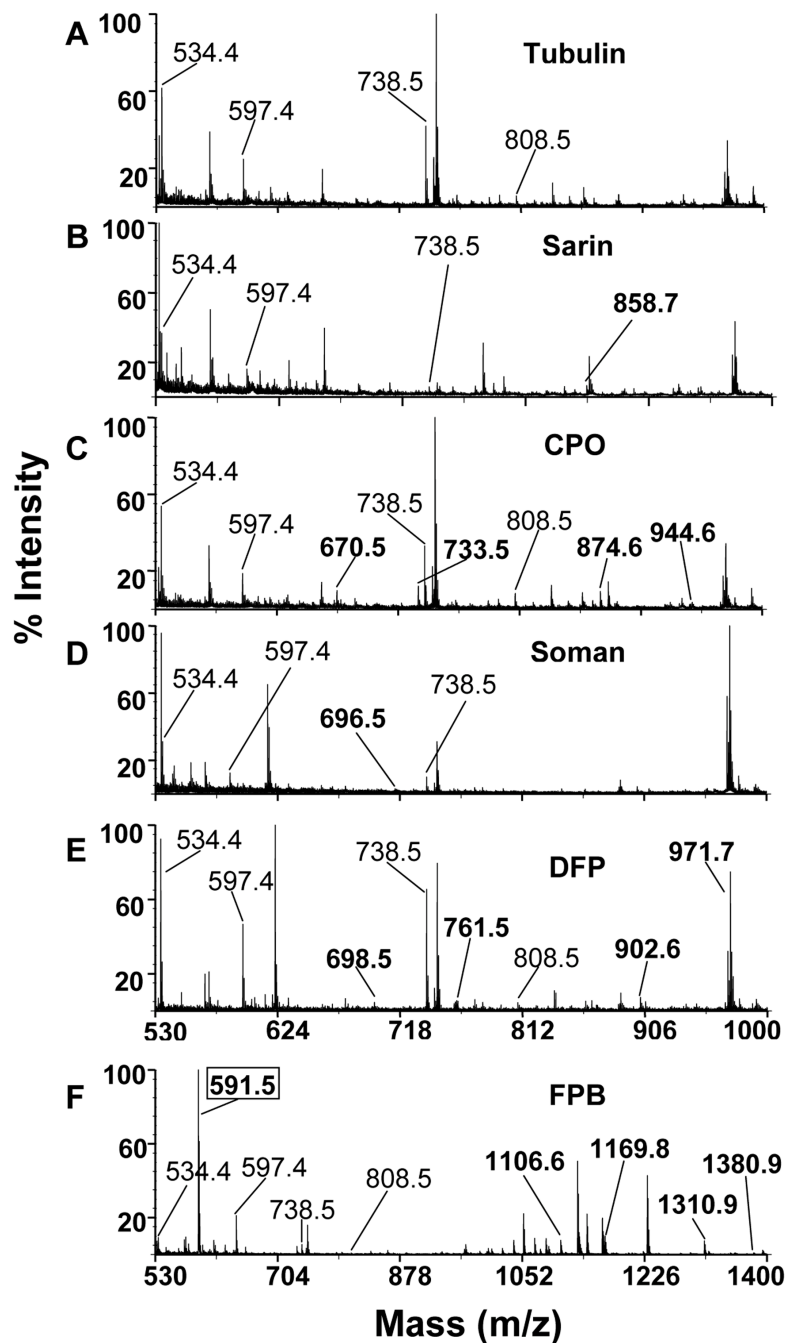
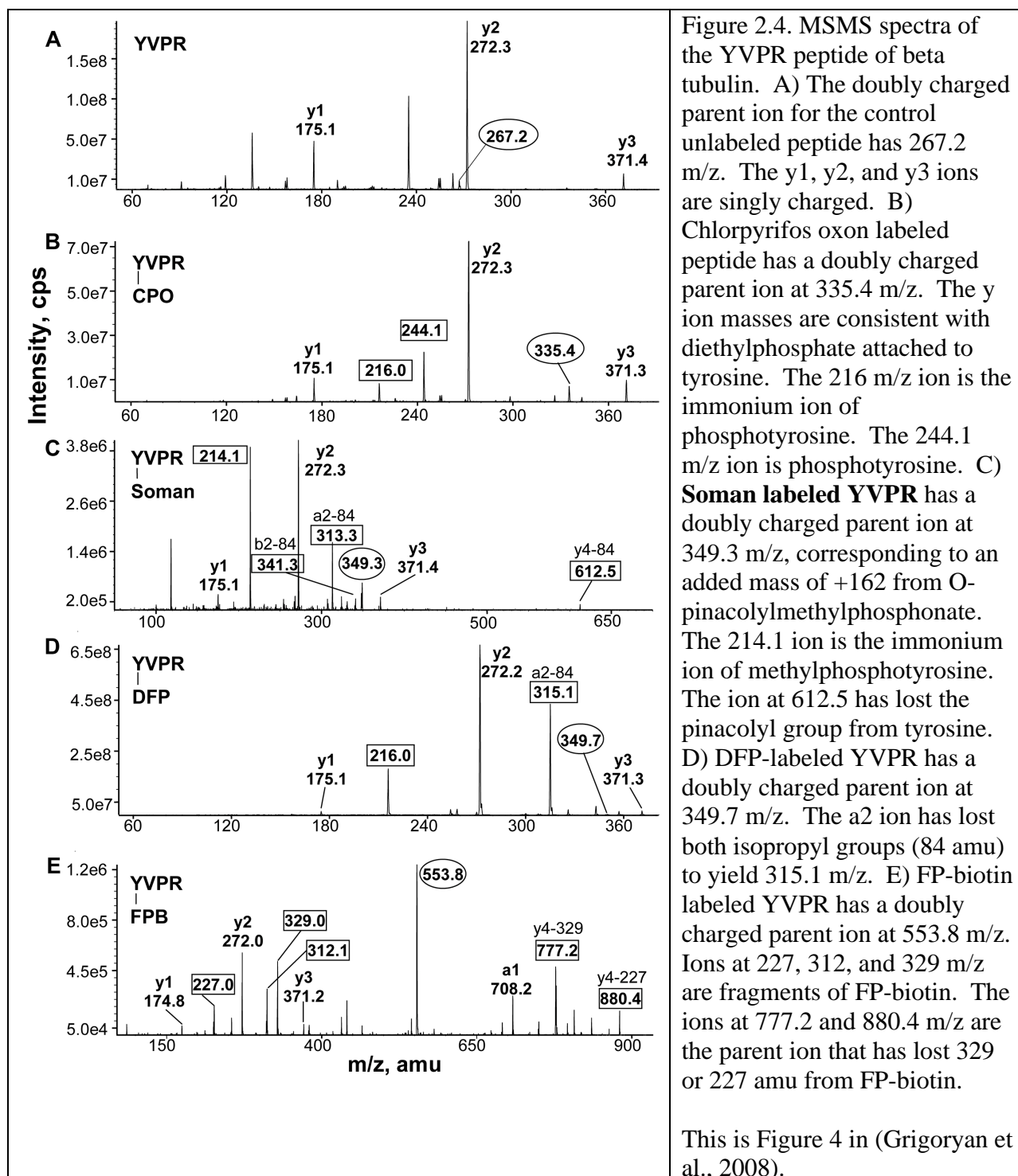


Figure 2.3. MALDI-TOF mass spectra of tryptic peptides of bovine tubulin before and after labeling with OP. Peptides from A) control bovine tubulin, B) sarin treated tubulin, C) chlorpyrifos oxon (CPO) treated tubulin, D) **soman treated tubulin**, F) FP-biotin (FPB) treated tubulin. OP-labeled peptides are in bold. The sarin labeled peptide has a mass of 858.7 amu. The soman labeled peptide has a mass of 696.5 amu. Four peptides indicated in bold letters are labeled with CPO, DFP, and FP-biotin.

This is Figure 2 in (Grigoryan et al., 2008).



This is Figure 4 in (Grigoryan et al., 2008).

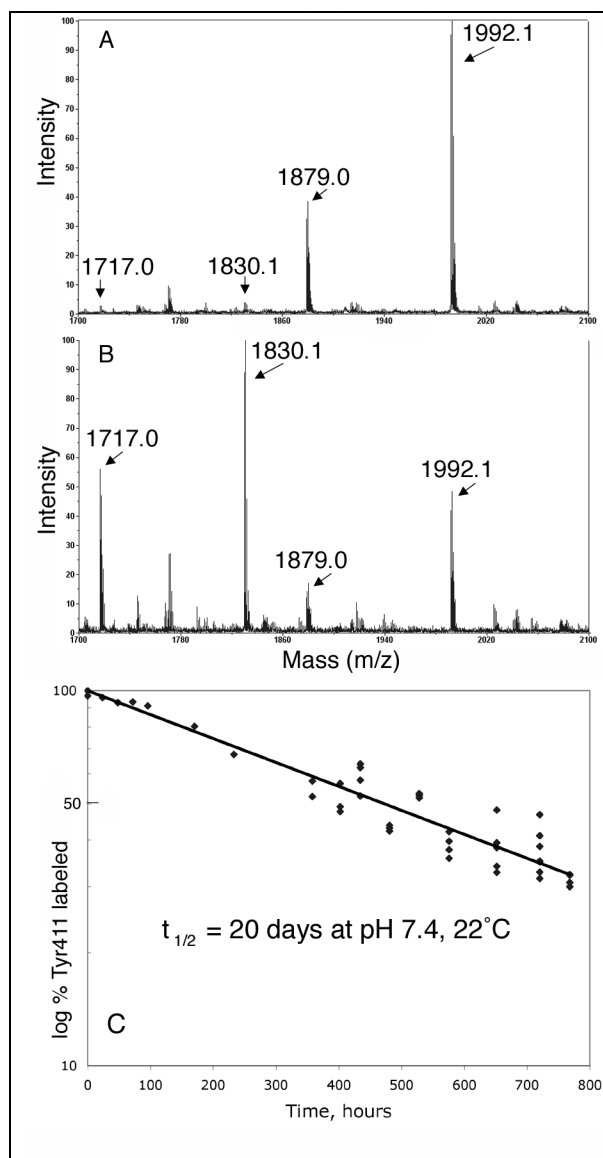


Figure 2.5. Stability of the **soman-albumin** adduct calculated from mass spectrometer data. Panels A and B are MALDI-TOF spectra of pepsin-digested, soman-labeled human albumin after 24 and 768 hours incubation at pH 7.4 and 22°C. The masses at 1717 and 1830 are unlabeled peptides VRYTKKVPQVSTPTL and LVRYTKKVPQVSTPTL. The masses at 1879 and 1992 are the same peptides with an added mass of +162 from O-pinacolylmethylphosphonate. Percent labeled Tyr411 was calculated by comparing the areas for the peaks of mass 1879 and 1992 with the areas for 1717 and 1830. Panel C is a plot of % Tyr411 labeled by soman, as a function of time of incubation of the soman albumin adduct. The soman-albumin adduct decays with a half-life of 20 days.

This is Figure 7 in (Li et al., 2008a).

### Key accomplishments

- Soman (as well as sarin, DFP, chlorpyrifos oxon, dichlorvos, and FP-biotin) binds covalently to tyrosine in albumin, transferrin, and tubulin. Covalent binding to tyrosine identifies a new binding motif for OP in proteins that have no active site serine.
- Adducts of soman on tyrosine do not age. That is, they do not lose the pinacolyl group of soman. This is significant because it means exposure to soman can be distinguished from exposure to sarin, cyclosarin, and VX.
- Soman adducts on tyrosine are stable, decaying with a half-life of 20 days at pH 7.4. This stability suggests that soman exposure could be monitored by analyzing soman-tyrosine adducts in blood samples taken weeks after the exposure incident.

## Task 3. Identify the proteins in human plasma that bind the nerve agent simulant, FP-biotin.

### SUMMARY

Many proteins in human plasma are modified by FP-biotin, a biotinylated OP, by treatment of plasma with 0.1 mM FP-biotin (Li et al., 2009a). The modified proteins are visualized by fluorescence after the proteins have been separated on a nondenaturing gel and hybridized to avidin conjugated to Alexa Fluor 680. We tested several strategies to identify the modified proteins (Ding et al., 2008). 1) Purification of FP-biotinylated proteins by binding to tetrameric or monomeric avidin beads, followed by mass spectrometry of bound proteins. 2) Purification of tryptic peptides bound to tetrameric or monomeric avidin beads, followed by mass spectrometry of bound peptides. 3) Depletion of the most abundant proteins in plasma on antibody depletion columns, followed by binding to monomeric avidin beads and mass spectrometry of bound proteins and peptides. 4) Extraction of proteins from gel bands followed by mass spectrometry. 5) Purification of butyrylcholinesterase from plasma, followed by mass spectrometry to identify the labeled peptide. The proteins in human plasma modified by reaction with FP-biotin are listed in **Table 3.1**. In addition we found FP-biotinylated peptides containing 2 to 4 amino acids that could not be assigned to a specific protein because the sequences were too short (Schopfer et al., 2010a).

What we learned from this task was the difficulty of identifying nonabundant OP-labeled proteins in plasma. The abundant proteins in plasma overwhelmed the analysis. Even though we depleted plasma of the 12 most abundant proteins, the residual albumin interfered with recovery of nonabundant FP-biotinylated proteins. We had to purify butyrylcholinesterase using protocols specifically designed for purification of butyrylcholinesterase from small volumes of plasma before we could detect OP-modified butyrylcholinesterase by mass spectrometry (Li et al., 2008c). This lesson has significance for projects that aim to identify the mechanism of low dose OP neurotoxicity. It will be necessary to specifically purify a particular protein before it will be possible to identify it as OP-modified.

### Attached are pdf files for published papers related to this task.

Ding SJ, Carr J, Carlson JE, Tong L, Xue W, Li Y, Schopfer LM, Li B, Nachon F, Asojo O, Thompson CM, Hinrichs SH, Masson P, Lockridge O. Five tyrosines and two serines in human albumin are labeled by the organophosphorus agent FP-biotin. *Chem Res Toxicol*. 2008 Sep;21(9):1787-94. PMID: 18707141

Masson P, Nachon F, Broomfield CA, Lenz DE, Verdier L, Schopfer LM, Lockridge O. A collaborative endeavor to design cholinesterase-based catalytic scavengers against toxic organophosphorus esters. *Chem Biol Interact*. 2008 Sep 25; 175(1-3): 273-280. PMID: 18508040

Grigoryan H, Li B, Anderson EK, Xue W, Nachon F, Lockridge O, Schopfer LM. Covalent binding of the organophosphorus agent FP-biotin to tyrosine in eight proteins that have no active site serine. *Chem Biol Interact*. 2009 Aug 14; 180(3):492-8. PMID: 19539807

Schopfer LM, Grigoryan H, Li B, Nachon F, Masson P, Lockridge O. Mass spectral characterization of organophosphate-labeled tyrosine-containing peptides: characteristic mass

fragments and a new binding motif for organophosphates. J Chromatogr B 2010 July 24; 878: 1297-1311. PMID:19762289

Masson P, Nachon F, Lockridge O. Structural approach to the aging of phosphorylated cholinesterases. Chem Biol Interact. 2010 Sep 6;187(1-3):157-162. PMID: 20338153

**Table 3.1. Proteins in human plasma modified by covalent binding of FP-biotin**

Protein	Accession #	modified peptide	reference
albumin	gi:3212456	Y <sub>138</sub> LYEIAR	(Ding et al., 2008)
albumin	gi:3212456	HPY <sub>148</sub> FYAPPELLFFAK	(Ding et al., 2008)
albumin	gi:3212456	AEFAEVS <sub>232</sub> K	(Ding et al., 2008)
albumin	gi:3212456	S <sub>287</sub> HCIAEVENDEMPADLPSLA ADFVESK	(Ding et al., 2008)
albumin	gi:3212456	QNCELFEQLGEY <sub>401</sub> K	(Ding et al., 2008)
albumin	gi:3212456	Y <sub>411</sub> TK	(Ding et al., 2008)
albumin	gi:3212456	MPCAEDY <sub>452</sub> LSVVLNQLCVLHE K	(Ding et al., 2008)
butyrylcholinesterase	gi:34810862	SVTLFGES <sub>198</sub> AGAASVSLHLLSP GSHSLFTR	not published
transferrin	gi:15021381	KPVDEY <sub>238</sub> K	(Li et al., 2009a)
transferrin	gi:15021381	KPVEEY <sub>574</sub> ANCHLAR	(Li et al., 2009a)
alpha-2-glycoprotein 1 zinc	gi:52790422	WEAEPVY <sub>174</sub> VQR	(Grigoryan et al., 2009a)
alpha-2-glycoprotein 1 zinc	gi:52790422	AY <sub>181</sub> LEECPATLR	(Grigoryan et al., 2009a)
alpha-2-glycoprotein 1 zinc	gi:52790422	YY <sub>138</sub> YDGKDYIEFNK	(Grigoryan et al., 2009a)
alpha-2-macroglobulin	gi:25303946	not known	(Li et al., 2009a)
alpha-1-antitrypsin	gi:54695780	not known	(Li et al., 2009a)
complement C3	gi:40786791	not known	(Li et al., 2009a)
Ig G1 H Nie	gi:229601	not known	not published
Immunoglobulin k VLJ region	gi:21669317	not known	not published
Ig mu chain C region	gi:127514	not known	not published
unknown	unknown	AY*PR	(Schopfer et al., 2010a)
unknown	unknown	Y*PR	(Schopfer et al., 2010a)
unknown	unknown	Y*L/IK	(Schopfer et al., 2010a)
unknown	unknown	Y*K	(Schopfer et al., 2010a)

The modified amino acid is indicated by the lower case number; for example in peptide Y<sub>138</sub>LYEIAR the modified amino acid is tyrosine 138. The evidence for FP-biotin binding to human albumin, butyrylcholinesterase, transferrin, alpha-2-glycoprotein 1 zinc, and to the 4 short peptides (listed at the bottom of the table) is very strong because the modified peptides and the binding site were identified by mass spectrometry. The evidence for FP-biotin binding to human alpha-2-macroglobulin, alpha-1-antitrypsin, and complement C3 is also strong because binding was confirmed using pure proteins, though the modified amino acids have not been identified. The evidence for FP-biotin binding to immunoglobins is weak because the modified peptides have not been found and the experiments have not been repeated with highly purified immunoglobulins. The 4 short peptides listed at the bottom of the table could originate from several proteins in human plasma.

**Key accomplishments**

- Several proteins in human plasma make a covalent bond with FP-biotin. The best biomarkers for OP exposure are butyrylcholinesterase and albumin.

## Task 4. Set up a Multiple Reaction Monitoring method to identify soman-labeled proteins, using purified proteins.

**SUMMARY**

Multiple reaction monitoring methods were developed to detect the soman-modified active site peptide of human butyrylcholinesterase and soman-modified human albumin. The methods were developed using pure human butyrylcholinesterase and pure human albumin modified with soman. Tables 4.1 and 4.2 list the amino acid sequences of the peptides that are labeled by soman, the masses and charge of the parent ions and the masses and charge of the product ions. The information in Tables 4.1 and 4.2 was derived experimentally and shows the set of values that need to be used in the multiple reaction monitoring method for detection of soman exposure. The results in Tables 4.1 and 4.2 completed Task 4.

Having completed Task 4, we set out to test actual samples from humans poisoned by pesticides. Cases of pesticide exposure rather than soman exposure were tested because only pesticide exposure cases were available to us. Very few humans are poisoned by nerve agents, and their blood is sent to military laboratories or to the Centers for Disease Control and is unavailable to a university laboratory for testing.

Our first test cases were plasma samples from two patients poisoned by carbofuran. Multiple reaction monitoring in the QTRAP mass spectrometer was selected as the method for identification because this method has the highest sensitivity, and therefore the highest likelihood of success. Its high sensitivity comes from the fact that it ignores all masses except those listed by the investigator as the masses of interest. The investigator has to know exactly what he is looking for before this method can be used. We did preliminary work with purified butyrylcholinesterase labeled on serine 198 with various agents, in preparation for analyzing the patient samples. From the work in Task 3 we knew that we had to purify the butyrylcholinesterase from patient plasma to have a chance of seeing the labeled peptide in the mass spectrometer. We purified the patients' butyrylcholinesterase by chromatography on procainamide-Sepharose, digested the butyrylcholinesterase with trypsin, and enriched for the labeled peptide by offline HPLC. The partially purified labeled peptide was analyzed by liquid chromatography/tandem mass spectrometry in the multiple reaction mode. Carbofuran was found covalently bound to serine 198 of human butyrylcholinesterase in both poisoning cases (Li et al., 2009b). Our study is the first to report success using multiple reaction monitoring to identify an adduct on butyrylcholinesterase in samples from poisoned humans. The methods developed in our carbofuran study are applicable to analysis of soman exposure in humans.

**A PDF file of the published paper is attached.**

Li H, Ricordel I, Tong L, Schopfer LM, Baud F, Mégarbane B, Maury E, Masson P, Lockridge O. Carbofuran poisoning detected by mass spectrometry of butyrylcholinesterase adduct in human serum. *J Appl Toxicol.* 2009 Mar;29(2):149-55. PMID: 18937214

Table 4.1. Multiple Reaction Monitoring transitions for detection of soman exposure, using human butyrylcholinesterase as the biomarker of exposure.

butyrylcholinesterase peptide SVTLFGESAGAASVSLHLLSPGSHSLFTR	parent ion,m/z charge+4	product ion,m/z charge+1	product ion,m/z charge+1
no label	733.3	1001.5 (y9)	1088.5 (y10)
aged soman labeled; added mass +78	752.8	1001.5 (y9)	1088.5 (y10)

Table 4.2. Multiple Reaction Monitoring transitions for detection of soman exposure, using human albumin as the biomarker of exposure.

albumin peptide VRYTKKVPQVSTPTL	parent ion, m/z charge +3	product ion, m/z charge +2	product ion, m/z charge +2
no label	573.3	694.4 (b12)	742.9 (b13)
soman labeled; added mass +162	627.3	775.4 (b12)	823.9 (b13)
albumin peptide LVRYTKKVPQVSTPTL			
no label	611.1	700.4 (b12)	750.9 (b13)
soman labeled; added mass +162	665.1	781.4 (b12)	831.9 (b13)

### Key Accomplishments

- A multiple reaction monitoring method for detection of soman exposure was developed using pure human proteins modified by soman.
- The multiple reaction monitoring method was applied to clinical cases of pesticide exposure, because cases of soman exposure were not available to us. Plasma from two live patients was successfully identified as having carbofuran adducts on plasma butyrylcholinesterase.

## Task 5. Use Multiple Reaction Monitoring to identify soman-labeled proteins in human plasma.

### SUMMARY

Finding a labeled peptide in human plasma is challenging because human plasma contains at least 3000 proteins. We had to develop methods to purify butyrylcholinesterase from 1 ml of plasma before we could detect the soman labeled peptide in the mass spectrometer. We achieved purification by affinity chromatography on 0.2 ml of procainamide-Sepharose beads, followed by gel electrophoresis (Li et al., 2008c). An example of the Coomassie stained gel from which the butyrylcholinesterase band was extracted for mass spectrometry analysis is shown in Figure 5.1. Mass spectrometry successfully identified the soman labeled butyrylcholinesterase peptide. Soman labeled butyrylcholinesterase could be detected when the soman concentration was low, inhibiting as little as 2% of the butyrylcholinesterase in plasma. In contrast, soman labeled albumin could not be detected when the soman concentration was low. The soman concentration had to be raised to 0.2 mM (a lethal concentration) before 1% of the albumin in plasma was labeled, and before we could detect soman labeled albumin in the mass spectrometer. It was surprising that soman labeled albumin could not be detected in human plasma when

soman concentrations were sublethal, because we were able to detect dichlorvos labeled albumin in human plasma from live patients poisoned by dichlorvos (Li et al., 2010b).

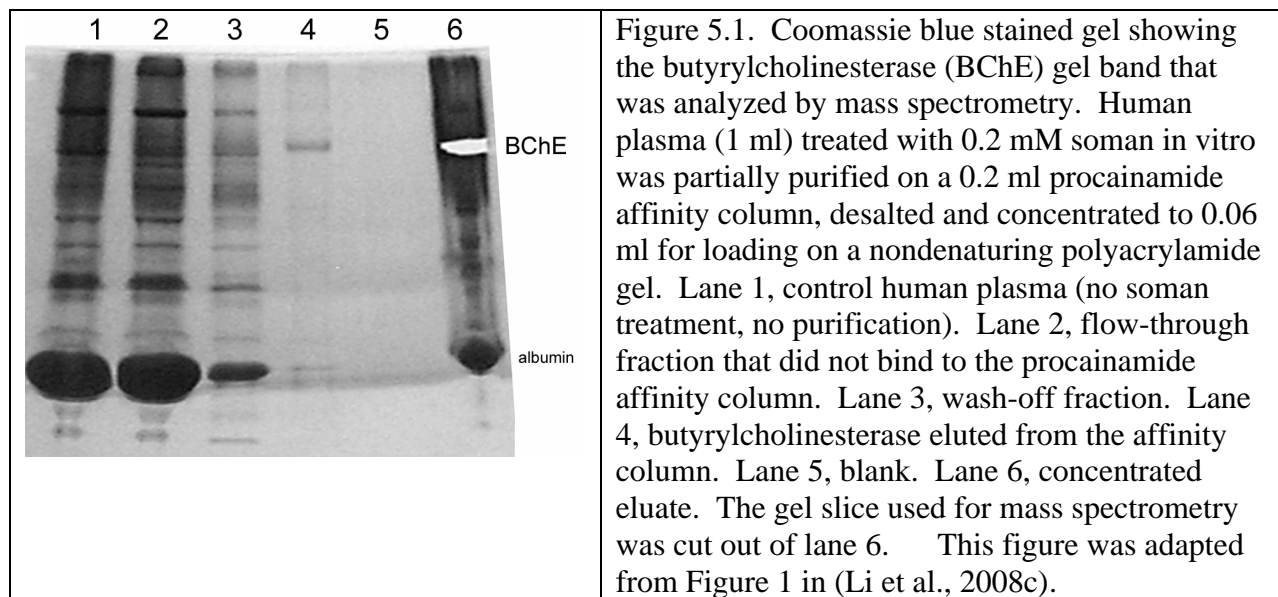
The methods we developed to purify butyrylcholinesterase from 1 ml plasma and to analyze the peptides by mass spectrometry were applied to analysis of patient plasma. We also analyzed patient plasma for the presence of OP adducts on albumin, and found dichlorvos labeled albumin. Multiple reaction monitoring was used to identify OP-modified butyrylcholinesterase in the plasma of patients poisoned by dichlorvos and by chlorpyrifos (Li et al., 2010a). Mass spectrometry was also successful in identifying OP-modified albumin in patients poisoned by dichlorvos (Li et al., 2010b). Our study is the first to have identified OP-modified albumin in patient plasma. The methods developed for analyzing plasma from OP poisoned patients are applicable to analyzing exposure to soman.

### Attached are pdf files for published papers related to this task.

Li H, Tong L, Schopfer LM, Masson P, Lockridge O. Fast affinity purification coupled with mass spectrometry for identifying organophosphate labeled plasma butyrylcholinesterase. *Chem Biol Interact.* 2008 Sep 25;175(1-3):68-72. PMID: 18586231

Li B, Ricordel I, Schopfer LM, Baud F, Mégarbane B, Masson P, Lockridge O. Dichlorvos, Chlorpyrifos Oxon, and Aldicarb adducts of butyrylcholinesterase, detected by mass spectrometry in human plasma following deliberate overdose. *J Appl Toxicol.* 2010 Aug;30(6):559-565. PMID: 2080944

Li B, Ricordel I, Schopfer LM, Baud F, Mégarbane B, Nachon F, Masson P, Lockridge O. Detection of adduct on tyrosine 411 of albumin in humans poisoned by dichlorvos. *Toxicol Sci.* 2010 Jul;116(1)23-31. PMID:20395308



### Key accomplishments

- Soman labeled butyrylcholinesterase was detected by mass spectrometry in human plasma treated in vitro with soman. It was necessary to enrich the plasma for butyrylcholinesterase before the labeled peptide could be detected in the mass

spectrometer. Enrichment was achieved by partially purifying butyrylcholinesterase from 1 ml of human plasma.

- The methods developed for analysis of soman exposure were applied to analysis of plasma samples from patients poisoned by OP pesticides. Mass spectrometry identified dichlorvos modified butyrylcholinesterase and chlorpyrifos oxon modified butyrylcholinesterase in clinical samples from patients poisoned by OP pesticides.
- Mass spectrometry identified dichlorvos modified albumin in patients poisoned by dichlorvos.

**Task 6.** Use a second method, for example enzyme activity assays or immunoprecipitation, to confirm the identity of soman-labeled proteins from plasma.

#### SUMMARY

In addition to mass spectrometry, we used enzyme activity assays, migration on polyacrylamide gels, and nanoimaging to confirm the identity of soman-labeled proteins from plasma. Activity assays showed that OP labeling of transferrin did not inhibit transferrin activity (Li et al., 2009a). On the other hand, activity assays showed that OP labeling of butyrylcholinesterase inhibited butyrylcholinesterase activity (Li et al., 2008c) but did not affect migration on polyacrylamide gels (Li et al., 2008c), a result consistent with the scientific literature. Nanoimaging by atomic force microscopy was introduced for visualizing the effect of OP modification of tubulin (Grigoryan and Lockridge, 2009a). Chlorpyrifos oxon was used as a surrogate for soman in the nanoimaging experiments because we do not have soman in our University. Pure bovine tubulin treated with various concentrations of chlorpyrifos oxon polymerized to abnormal microtubule structures. Low concentrations of chlorpyrifos oxon resulted in abnormally short microtubules as shown in Figure 6.1B. High concentrations caused aggregation and depletion of associated proteins (Figure 6.1C and 6.1D). Nanoimages were also acquired for microtubules prepared from tubulin purified from mouse brain. Mice treated with low doses of chlorpyrifos oxon had thin microtubules and few associated proteins, whereas control untreated mice had thick microtubules decorated with many proteins (Jiang et al., 2010). Nanoimaging is a new method for demonstrating the effect of OP exposure on the brain. Another significant finding from the study of mice treated with low doses of chlorpyrifos oxon was that the mice had chlorpyrifos modified tubulin in their brains. Acetylcholinesterase was not inhibited by the low doses, yet tubulin was covalently modified.

**Attached are pdf files for published papers related to this task.**

Li B, Schopfer LM, Grigoryan H, Thompson CM, Hinrichs SH, Masson P, Lockridge O. Tyrosines of human and mouse transferrin covalently labeled by organophosphorus agents: a new motif for binding to proteins that have no active site serine. *Toxicol Sci.* 2009 Jan;107(1):144-55. PMID: 18930948.

Grigoryan H, Lockridge O. Nanoimages show disruption of tubulin polymerization by chlorpyrifos oxon: Implications for neurotoxicity. *Toxicol Appl Pharmacol.* 2009 Oct 15; 240(2): 143-148. PMID: 19631231

Tacal O, Lockridge O. Methamidophos, dichlorvos, O-methoate and diazinon pesticides used in Turkey make a covalent bond with butyrylcholinesterase detected by mass spectrometry. *J Appl Toxicol.* 2010 Jul;30(5) 469-475. PMID: 20229498

Jiang W, Duysen EG, Hansen H, Shlyakhtenko L, Schopfer LM, Lockridge O. Mice treated with chlorpyrifos or chlorpyrifos oxon have organophosphorylated tubulin in the brain and disrupted microtubule structures, suggesting a role for tubulin in neurotoxicity associated with exposure to organophosphorus agents. *Toxicol Sci.* 2010 May;115(1):183-93. PMID: 20142434

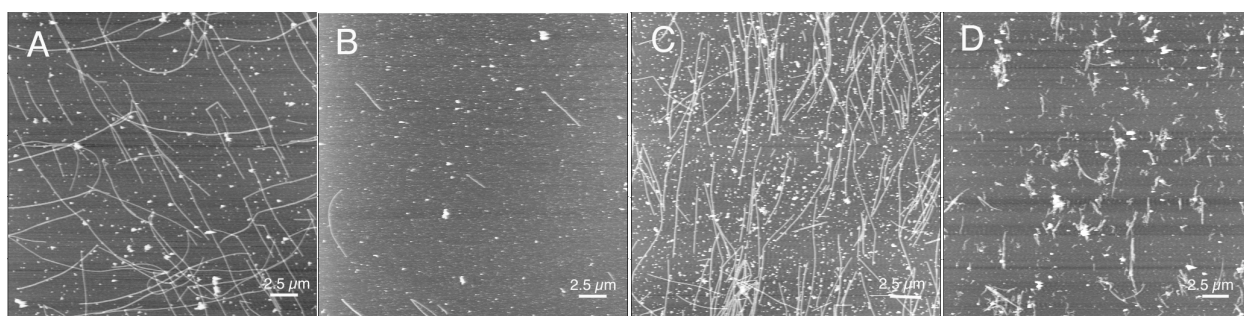


Figure 6.1. Effect of chlorpyrifos oxon (CPO) on tubulin polymerization visualized by atomic force microscopy. (A) Control, 5 mg/ml (91  $\mu$ M) bovine brain tubulin polymerized with 1 mM GTP in pH 7.0 buffer (B) Pre treated with 5  $\mu$ M CPO. (C) Pretreated with 25  $\mu$ M CPO. (D) Pretreated with 100  $\mu$ M CPO. The bar is 2.5  $\mu$ m. Adapted from Fig 1 in (Grigoryan and Lockridge, 2009a).

#### Key accomplishments

- Nanoimaging was introduced as a method to monitor the effect of OP toxicants on the function of tubulin and microtubules. Nanoimaging revealed stunning effects of the nerve agent surrogate, chlorpyrifos oxon, on tubulin polymerization.
- Doses of the nerve agent surrogate, chlorpyrifos oxon, that did not inhibit acetylcholinesterase, reacted with tubulin in the brains of mice to yield OP modified tubulin detectable by mass spectrometry.

## Task 7. Determine the limit of detection of soman-labeled proteins in human plasma.

### SUMMARY

The goal was to establish a method to detect exposure to low levels of soman. Human plasma was treated ex vivo with 0.01 to 0.18  $\mu$ M soman. The butyrylcholinesterase in 1 ml plasma was purified by affinity chromatography on procainamide gel followed by nondenaturing gel electrophoresis. The gel band containing butyrylcholinesterase (see Figure 5.1) was reduced,

carbamidomethylated, and digested with trypsin. The tryptic peptides were analyzed by multiple reaction monitoring in a QTRAP 2000 mass spectrometer. Parent/daughter ion pairs 752.8/1001.5 and 752.8/1088.5 and 752.8/1201.6 atomic mass units gave MSMS spectra that proved the peptide masses were those of butyrylcholinesterase modified by aged soman. A representative MSMS figure of soman labeled butyrylcholinesterase peptide is in Figure 1.1. The limit of detection was for plasma treated with 0.01  $\mu$ M soman, a concentration which inhibited the butyrylcholinesterase 2%. We were unable to detect soman labeled albumin in these plasma samples.

These results have not been published because we have no plasma from humans exposed to soman. In lieu of humans exposed to soman, we have studied humans exposed to the carbamate pesticides, carbofuran and Aldicarb, and the OP pesticides, dichlorvos and chlorpyrifos oxon (Li et al., 2009b; Li et al., 2010a; Li et al., 2010b). We found OP and carbamate adducts in the patients' plasma butyrylcholinesterase and OP adducts on the patients' plasma albumin.

## KEY RESEARCH ACCOMPLISHMENTS

- A new motif for OP binding to proteins that have no active site serine was established. Mass spectrometry conclusively identified tyrosine and lysine as covalent binding sites for soman, sarin, dichlorvos, chlorpyrifos oxon, diisopropylfluorophosphate, and FP-biotin.
- OP-tyrosine adducts are stable. For example, soman bound to tyrosine 411 in human albumin does not lose the pinacolyl group.
- The finding that the OP-tyrosine adduct is stable suggests that antibodies could be made against OP-tyrosine to use for detection of OP exposure.
- Humans poisoned by dichlorvos have OP-modified albumin in blood, detectable by mass spectrometry.
- The finding that tyrosine 411 of albumin is modified by OP in poisoned humans, suggests that tyrosine in other proteins may also be modified. This suggests new directions to search for a mechanism to explain low dose neurotoxicity.
- Tubulin protein in the brains of mice was modified by OP after the mice had been treated with chlorpyrifos at doses that did not inhibit acetylcholinesterase. This suggests a mechanism for low dose OP neurotoxicity independent of acetylcholinesterase inhibition.
- A mass spectrometry method called multiple reaction monitoring was developed that successfully identifies OP-modified butyrylcholinesterase in plasma from humans poisoned by OP.

## REPORTABLE OUTCOMES

*Published papers (pdf copies attached)*

1. Carletti E, Li H, Li B, Ekström F, Nicolet Y, Loiodice M, Gillon E, Froment MT, Lockridge O, Schopfer LM, Masson P, Nachon F. Aging of Cholinesterases Phosphorylated by Tabun Proceeds through O-Dealkylation. J Am Chem Soc. 2008 Nov 26; 130 (47): 16011-20. PMID: 18975951
2. Ding SJ, Carr J, Carlson JE, Tong L, Xue W, Li Y, Schopfer LM, Li B, Nachon F, Asojo O, Thompson CM, Hinrichs SH, Masson P, Lockridge O. Five tyrosines and two serines in human albumin are labeled by the organophosphorus agent FP-biotin. Chem Res Toxicol. 2008 Sep;21(9):1787-94. PMID: 18707141

3. Gilley C, MacDonald M, Nachon F, Schopfer LM, Zhang J, Cashman JR, Lockridge O. Nerve agent analogues that produce authentic soman, sarin, tabun, and cyclohexyl methylphosphonate-modified human butyrylcholinesterase. *Chem Res Toxicol*. 2009 Oct; 22(10):1680-8. PMID: 19715348
4. Grigoryan H, Li B, Anderson EK, Xue W, Nachon F, Lockridge O, Schopfer LM. Covalent binding of the organophosphorus agent FP-biotin to tyrosine in eight proteins that have no active site serine. *Chem Biol Interact*. 2009 Aug 14; 180(3):492-8. PMID: 19539807
5. Grigoryan H, Li B, Xue W, Grigoryan M, Schopfer LM, Lockridge O. Mass spectral characterization of organophosphate-labeled lysine in peptides. *Anal Biochem*. 2009 Nov 1; 304(1):92-100. PMID: 19596251
6. Grigoryan H, Lockridge O. Nanoimages show disruption of tubulin polymerization by chlorpyrifos oxon: Implications for neurotoxicity. *Toxicol Appl Pharmacol*. 2009 Oct 15; 240(2): 143-148. PMID: 19631231
7. Grigoryan H, Schopfer LM, Peeples ES, Duysen EG, Grigoryan M, Thompson CM, Lockridge O. Mass spectrometry identifies multiple organophosphorylated sites on tubulin. *Toxicol Appl Pharmacol*. 2009 Oct 15;240(2):149-158. PMID: 19632257
8. Grigoryan H, Schopfer LM, Thompson CM, Terry AV, Masson P, Lockridge O. Mass spectrometry identifies covalent binding of soman, sarin, chlorpyrifos oxon, diisopropyl fluorophosphate, and FP-biotin to tyrosines on tubulin: a potential mechanism of long term toxicity by organophosphorus agents. *Chem Biol Interact*. 2008 Sep 25;175(1-3):180-6. PMID: 18502412
9. Jiang W, Duysen EG, Hansen H, Shlyakhtenko L, Schopfer LM, Lockridge O. Mice treated with chlorpyrifos or chlorpyrifos oxon have organophosphorylated tubulin in the brain and disrupted microtubule structures, suggesting a role for tubulin in neurotoxicity associated with exposure to organophosphorus agents. *Toxicol Sci* 2010 May;115(1):183-93. PMID: 20142434
10. Li B, Nachon F, Froment MT, Verdier L, Debouzy JC, Brasme B, Gillon E, Schopfer LM, Lockridge O, Masson P. Binding and hydrolysis of soman by human serum albumin. *Chem Res Toxicol*. 2008 Feb;21(2):421-31. PMID: 18163544
11. Li B, Ricordel I, Schopfer LM, Baud F, Mégarbane B, Masson P, Lockridge O. Dichlorvos, Chlorpyrifos Oxon, and Aldicarb adducts of butyrylcholinesterase, detected by mass spectrometry in human plasma following deliberate overdose. *J Appl Toxicol*. 2010 Aug;30(6):559-565. PMID: 20809544
12. Li B, Ricordel I, Schopfer LM, Baud F, Mégarbane B, Nachon F, Masson P, Lockridge O. Detection of adduct on tyrosine 411 of albumin in humans poisoned by dichlorvos. *Toxicol Sci*. 2010 Jul;116(1):23-31. PMID:20395308
13. Li B, Schopfer LM, Grigoryan H, Thompson CM, Hinrichs SH, Masson P, Lockridge O. Tyrosines of human and mouse transferrin covalently labeled by organophosphorus agents: a new motif for binding to proteins that have no active site serine. *Toxicol Sci*. 2009 Jan;107(1):144-55. PMID: 18930948.
14. Li B., Schopfer LM, Hinrichs SH, Masson P, Lockridge O. Matrix-assisted laser desorption/ionization time-of-flight mass spectrometry assay for organophosphorus toxicants bound to human albumin at Tyr411. *Anal Biochem*. 2007 Feb 15; 361(2): 263-272. PMID: 17188226
15. Li H, Ricordel I, Tong L, Schopfer LM, Baud F, Mégarbane B, Maury E, Masson P, Lockridge O. Carbofuran poisoning detected by mass spectrometry of butyrylcholinesterase

- adduct in human serum. *J Appl Toxicol*. 2009 Mar;29(2):149-55. PMID: 18937214
16. Li H, Schopfer LM, Nachon F, Froment MT, Masson P, Lockridge O. Aging pathways for organophosphate-inhibited human butyrylcholinesterase, including novel pathways for isomalathion, resolved by mass spectrometry. *Toxicol Sci*. 2007 Nov; 100(1):136-145. PMID: 17698511
  17. Li H, Schopfer LM, Masson P, Lockridge O (2008) Lamellipodin proline rich peptides associated with native plasma butyrylcholinesterase tetramers. *Biochem J*. 2008 Apr 15; 411(2): 425-432. PMID: 18076380
  18. Li H, Tong L, Schopfer LM, Masson P, Lockridge O. Fast affinity purification coupled with mass spectrometry for identifying organophosphate labeled plasma butyrylcholinesterase. *Chem Biol Interact*. 2008 Sep 25;175(1-3):68-72. PMID: 18586231
  19. Liyasova MS, Schopfer LM, Lockridge O. Reaction of human albumin with aspirin in vitro: mass spectrometric identification of acetylated lysines 199, 402, 519, and 545. *Biochem Pharmacol* 2010 Mar 1;79(5):784-91. PMID: 19836360
  20. Lockridge O, Schopfer LM. Review of tyrosine and lysine as new motifs for organophosphate binding to proteins that have no active site serine. *Chem Biol Interact*. 2010 Sep 6;187(1-3):344-348. PMID: 20211158
  21. Lockridge O, Xue W, Gaydoss A, Grigoryan H, Ding SJ, Schopfer LM, Hinrichs SH, Masson P. Pseudo-esterase activity of human albumin: slow turnover on tyrosine 411 and stable acetylation of 82 residues including 59 lysines. *J Biol Chem*. 2008 Aug 15;283(33):22582-90. PMID: 18577514
  22. Masson P, Lockridge O. Butyrylcholinesterase for protection from organophosphorus poisons; catalytic complexities and hysteretic behavior. *Arch Biochem Biophys*. 2010. Feb15;494(2):107-20. PMID: 20004171
  23. Masson P, Nachon F, Broomfield CA, Lenz DE, Verdier L, Schopfer LM, Lockridge O. A collaborative endeavor to design cholinesterase-based catalytic scavengers against toxic organophosphorus esters. *Chem Biol Interact*. 2008 Sep 25; 175(1-3): 273-280. PMID: 18508040
  24. Masson P, Nachon F, Lockridge O. Structural approach to the aging of phosphorylated cholinesterases. *Chem Biol Interact*. 2010 Sep 6;187(1-3):157-162. PMID: 20338153
  25. Schopfer LM, Grigoryan H, Li B, Nachon F, Masson P, Lockridge O. Mass spectral characterization of organophosphate-labeled tyrosine-containing peptides: characteristic mass fragments and a new binding motif for organophosphates. *J Chromatogr B* 2010 July 24; 878: 1297-1311. PMID:19762289
  26. Tacal O, Lockridge O. Methamidophos, dichlorvos, O-methoate and diazinon pesticides used in Turkey make a covalent bond with butyrylcholinesterase detected by mass spectrometry. *J Appl Toxicol*. 2010 Jul;30(5):469-475. PMID: 20229498

## CONCLUSIONS

Our mass spectrometry results contradict the dogma that serine esterases and serine proteases are the only class of proteins modified by exposure to OP. We have identified 12 proteins that are labeled by OP. The significance of this finding is in diagnosis of OP exposure. It now becomes possible to look for several proteins in human tissues, in addition to butyrylcholinesterase and acetylcholinesterase, for evidence of OP exposure. In vivo exposure of humans to the pesticides carbofuran, aldicarb, dichlorvos, and chlorpyrifos was identified using the multiple reaction

monitoring function of the QTRAP mass spectrometer. The limit of detection after exposure to soman was determined to be a dose that inhibited plasma butyrylcholinesterase 2%. Mass spectrometry detected OP-modified tubulin in the brains of mice treated with a low dose of chlorpyrifos that did not inhibit acetylcholinesterase. This finding suggests new directions to search for a mechanism to explain neurotoxicity from low dose OP exposure.

#### PERSONNEL

Shi-Jian Ding, Ph.D.

Ellen G. Duysen, BS

Hasmik Grigoryan, Ph.D.

Wei Jiang

Mariya Liyasova

Oksana Lockridge, Ph.D.

Bin Li, Ph.D.

He Li, Ph.D.

Lawrence M. Schopfer, Ph.D.

Weihua Xue, BS

#### REFERENCES CITED

- Beseler CL, Stallones L, Hoppin JA, Alavanja MC, Blair A, Keefe T and Kamel F (2008) Depression and pesticide exposures among private pesticide applicators enrolled in the Agricultural Health Study. *Environ Health Perspect* **116**:1713-1719.
- Carletti E, Li H, Li B, Ekstrom F, Nicolet Y, Loiodice M, Gillon E, Froment MT, Lockridge O, Schopfer LM, Masson P and Nachon F (2008) Aging of Cholinesterases Phosphylated by Tabun Proceeds through O-Dealkylation. *J Am Chem Soc*.
- Casida JE, Eto M and Baron RL (1961) Biological activity of a trio-cresyl phosphate metabolite. *Nature* **191**:1396-1397.
- Ding SJ, Carr J, Carlson JE, Tong L, Xue W, Li Y, Schopfer LM, Li B, Nachon F, Asojo O, Thompson CM, Hinrichs SH, Masson P and Lockridge O (2008) Five tyrosines and two serines in human albumin are labeled by the organophosphorus agent FP-biotin. *Chem Res Toxicol* **21**:1787-1794. PMID:2646670.
- Fidder A, Hulst AG, Noort D, de Ruiter R, van der Schans MJ, Benschop HP and Langenberg JP (2002) Retrospective detection of exposure to organophosphorus anti-cholinesterases: mass spectrometric analysis of phosphylated human butyrylcholinesterase. *Chem Res Toxicol* **15**:582-590.
- Gilley C, MacDonald M, Nachon F, Schopfer LM, Zhang J, Cashman JR and Lockridge O (2009) Nerve agent analogues that produce authentic soman, sarin, tabun, and cyclohexyl methylphosphonate-modified human butyrylcholinesterase. *Chem Res Toxicol* **22**:1680-1688.
- Golomb BA (2008) Acetylcholinesterase inhibitors and Gulf War illnesses. *Proc Natl Acad Sci U S A* **105**:4295-4300.
- Grigoryan H, Li B, Anderson EK, Xue W, Nachon F, Lockridge O and Schopfer LM (2009a) Covalent binding of the organophosphorus agent FP-biotin to tyrosine in eight proteins that have no active site serine. *Chem Biol Interact* **180**:492-498 PMID:2700782.
- Grigoryan H, Li B, Xue W, Grigoryan M, Schopfer LM and Lockridge O (2009b) Mass spectral characterization of organophosphate-labeled lysine in peptides. *Anal Biochem* **394**:92-100.
- Grigoryan H and Lockridge O (2009a) Nanoimages show disruption of tubulin polymerization by chlorpyrifos oxon: implications for neurotoxicity. *Toxicol Appl Pharmacol* **240**:143-148.

- Grigoryan H and Lockridge O (2009b) Nanoimages show disruption of tubulin polymerization by chlorpyrifos oxon: Implications for neurotoxicity. *Toxicol Appl Pharmacol* **240**:143-148 NIHMS:134468.
- Grigoryan H, Schopfer LM, Peeples ES, Duysen EG, Grigoryan M, Thompson CM and Lockridge O (2009c) Mass spectrometry identifies multiple organophosphorylated sites on tubulin. *Toxicol Appl Pharmacol* **240**:149-158 NIHMS:135197.
- Grigoryan H, Schopfer LM, Thompson CM, Terry AV, Masson P and Lockridge O (2008) Mass spectrometry identifies covalent binding of soman, sarin, chlorpyrifos oxon, diisopropyl fluorophosphate, and FP-biotin to tyrosines on tubulin: a potential mechanism of long term toxicity by organophosphorus agents. *Chem Biol Interact* **175**:180-186 PMID:2577157.
- Jiang W, Duysen EG, Hansen H, Shlyakhtenko L, Schopfer LM and Lockridge O (2010) Mice treated with chlorpyrifos or chlorpyrifos oxon have organophosphorylated tubulin in brain and disrupted microtubule structures, suggesting a role for tubulin in neurotoxicity associated with exposure to organophosphorus agents. *Tox Sci* **115**:183-193.
- Kamel F and Hoppin JA (2004) Association of pesticide exposure with neurologic dysfunction and disease. *Environ Health Perspect* **112**:950-958.
- Li B, Nachon F, Froment MT, Verdier L, Debouzy JC, Brasme B, Gillon E, Schopfer LM, Lockridge O and Masson P (2008a) Binding and hydrolysis of soman by human serum albumin. *Chem. Res. Toxicol.* **21**:421-431.
- Li B, Ricordel I, Schopfer LM, Baud F, Megarbane B, Masson P and Lockridge O (2010a) Dichlorvos, chlorpyrifos oxon, and aldicarb adducts of butyrylcholinesterase detected by mass spectrometry in human plasma following deliberate overdose. *J Appl Toxicol* **30**:559-565.
- Li B, Ricordel I, Schopfer LM, Baud F, Megarbane B, Nachon F, Masson P and Lockridge O (2010b) Detection of adducts on tyrosine 411 of albumin in humans poisoned by dichlorvos. *Toxicol Sci* **116**:23-31.
- Li B, Schopfer LM, Grigoryan H, Thompson CM, Hinrichs SH, Masson P and Lockridge O (2009a) Tyrosines of human and mouse transferrin covalently labeled by organophosphorus agents: a new motif for binding to proteins that have no active site serine. *Toxicol Sci* **107**:144-155 PMID:2638647.
- Li B, Schopfer LM, Hinrichs SH, Masson P and Lockridge O (2007) Matrix-assisted laser desorption/ionization time-of-flight mass spectrometry assay for organophosphorus toxicants bound to human albumin at Tyr411. *Anal. Biochem.* **361**:263-272 PMID:1828685.
- Li H, Ricordel I, Tong L, Schopfer LM, Baud F, Megarbane B, Maury E, Masson P and Lockridge O (2009b) Carbofuran poisoning detected by mass spectrometry of butyrylcholinesterase adduct in human serum. *J Appl Toxicol* **29**:149-155.
- Li H, Schopfer LM, Masson P and Lockridge O (2008b) Lamellipodin proline rich peptides associated with native plasma butyrylcholinesterase tetramers. *Biochem J* **411**:425-432.
- Li H, Tong L, Schopfer LM, Masson P and Lockridge O (2008c) Fast affinity purification coupled with mass spectrometry for identifying organophosphate labeled plasma butyrylcholinesterase. *Chem Biol Interact* **175**:68-72.
- Liyasova MS, Schopfer LM and Lockridge O (2010) Reaction of human albumin with aspirin in vitro: mass spectrometric identification of acetylated lysines 199, 402, 519, and 545. *Biochem Pharmacol* **79**:784-791.

- Lockridge O and Schopfer LM (2010) Review of tyrosine and lysine as new motifs for organophosphate binding to proteins that have no active site serine. *Chem Biol Interact* **187**:344-348.
- Lockridge O, Xue W, Gaydess A, Grigoryan H, Ding SJ, Schopfer LM, Hinrichs SH and Masson P (2008) Pseudo-esterase activity of human albumin: slow turnover on tyrosine 411 and stable acetylation of 82 residues including 59 lysines. *J Biol Chem* **283**:22582-22590.
- Masson P and Lockridge O (2010) Butyrylcholinesterase for protection from organophosphorus poisons: catalytic complexities and hysteretic behavior. *Arch Biochem Biophys* **494**:107-120.
- McDonough JH, Jr. and Shih TM (1997) Neuropharmacological mechanisms of nerve agent-induced seizure and neuropathology. *Neurosci Biobehav Rev* **21**:559-579.
- Ray DE and Richards PG (2001) The potential for toxic effects of chronic, low-dose exposure to organophosphates. *Toxicol Lett* **120**:343-351.
- Ross SM (2008) Cognitive function following exposure to contaminated air on commercial aircraft: a case series of 27 pilots seen for clinical purposes. *J Nutr Environ Med* **17**:111-126.
- Salvi RM, Lara DR, Ghisolfi ES, Portela LV, Dias RD and Souza DO (2003) Neuropsychiatric evaluation in subjects chronically exposed to organophosphate pesticides. *Toxicol Sci* **72**:267-271.
- Schopfer LM, Grigoryan H, Li B, Nachon F, Masson P and Lockridge O (2010a) Mass spectral characterization of organophosphate-labeled, tyrosine-containing peptides: characteristic mass fragments and a new binding motif for organophosphates. *J Chromatogr B Analyt Technol Biomed Life Sci* **878**:1297-1311.
- Schopfer LM, Grigoryan H, Li B, Nachon F, Masson P and Lockridge O (2010b) Mass spectral characterization of organophosphate-labeled, tyrosine-containing peptides: Characteristic mass fragments and a new binding motif for organophosphates. *J Chromatogr B Analyt Technol Biomed Life Sci*.
- Taylor P and Radic Z (1994) The cholinesterases: from genes to proteins. *Annu Rev Pharmacol Toxicol* **34**:281-320.
- Tsuge K and Seto Y (2002) Analysis of organophosphorus compound adducts of serine proteases by liquid chromatography-tandem mass spectrometry. *J Chromatogr B Analyt Technol Biomed Life Sci* **776**:79-88.

## Aging of Cholinesterases Phosphylated by Tabun Proceeds through O-Dealkylation

Eugénie Carletti,<sup>†</sup> He Li,<sup>‡</sup> Bin Li,<sup>‡</sup> Fredrik Ekström,<sup>§</sup> Yvain Nicolet,<sup>#</sup>  
Mélanie Loidice,<sup>†</sup> Emilie Gillon,<sup>†</sup> Marie T. Froment,<sup>†</sup> Oksana Lockridge,<sup>‡</sup>  
Lawrence M. Schopfer,<sup>‡</sup> Patrick Masson,<sup>†</sup> and Florian Nachon<sup>\*†</sup>

*Département de Toxicologie, Centre de Recherches du Service de Santé des Armées (CRSSA),  
24 avenue des Maquis du Grésivaudan, 38700 La Tronche, France, Eppley Institute and  
Department of Biochemistry and Molecular Biology, University of Nebraska Medical Center,  
Omaha, Nebraska 68198-6805, FOI CBRN Defence and Security, S-901 82 Umeå, Sweden, and  
Laboratoire de Cristallogénèse et Cristallographie des Protéines, Institut de Biologie Structurale  
(CEA-CNRS-UJF), 41 rue Jules Horowitz, 38027 Grenoble, France*

Received June 27, 2008; E-mail: fnachon@crssa.net

**Abstract:** Human butyrylcholinesterase (hBChE) hydrolyzes or scavenges a wide range of toxic esters, including heroin, cocaine, carbamate pesticides, organophosphorus pesticides, and nerve agents. Organophosphates (OPs) exert their acute toxicity through inhibition of acetylcholinesterase (AChE) by phosphorylation of the catalytic serine. Phosphylated cholinesterase (ChE) can undergo a spontaneous, time-dependent process called “aging”, during which the OP–ChE conjugate is dealkylated. This leads to irreversible inhibition of the enzyme. The inhibition of ChEs by tabun and the subsequent aging reaction are of particular interest, because tabun–ChE conjugates display an extraordinary resistance toward most current oxime reactivators. We investigated the structural basis of oxime resistance for phosphoramidated ChE conjugates by determining the crystal structures of the non-aged and aged forms of hBChE inhibited by tabun, and by updating the refinement of non-aged and aged tabun-inhibited mouse AChE (mAChE). Structures for non-aged and aged tabun–hBChE were refined to 2.3 and 2.1 Å, respectively. The refined structures of aged ChE conjugates clearly show that the aging reaction proceeds through O-dealkylation of the P(R) enantiomer of tabun. After dealkylation, the negatively charged oxygen forms a strong salt bridge with protonated His438Nε2 that prevents reactivation. Mass spectrometric analysis of the aged tabun-inhibited hBChE showed that both the dimethylamine and ethoxy side chains were missing from the phosphorus. Loss of the ethoxy is consistent with the crystallography results. Loss of the dimethylamine is consistent with acid-catalyzed deamidation during the preparation of the aged adduct for mass spectrometry. The reported 3D data will help in the design of new oximes capable of reactivating tabun–ChE conjugates.

### Introduction

Acetylcholinesterase (AChE; EC 3.1.1.7) and butyrylcholinesterase (BChE; EC 3.1.1.8) are closely related serine hydrolases with different substrate specificities and inhibitor sensitivities. AChE terminates the action of the neurotransmitter acetylcholine at postsynaptic membranes and neuromuscular junctions. Although BChE is present in numerous vertebrate tissues, its physiological role remains unclear.<sup>1,2</sup>

Human butyrylcholinesterase (hBChE) is toxicologically relevant because it hydrolyzes or scavenges a wide range of toxic esters, including heroin, cocaine, carbamate pesticides, organophosphorus pesticides, and nerve agents.<sup>3</sup> Organophosphates (OPs) exert their acute toxicity through inhibition of AChE by phosphorylation of the catalytic serine. Subsequent

accumulation of acetylcholine at neuronal synapses and neuromuscular junctions results in paralysis, seizures, and other symptoms of cholinergic syndrome.<sup>4,5</sup>

Phosphylated ChEs can be reactivated by nucleophilic agents such as oximes. The most effective oximes used for emergency treatment of nerve agent poisoning are the monopyridinium oximes (2-PAM and HI-6) and bispyridinium oximes (TMB-4, MMB-4, obidoxime, and HLö-7).<sup>6</sup> Kinetic analysis of the interactions between different AChE–OP conjugates and different oximes shows that the most effective oximes are HLö-7 for phosphonylated AChE and obidoxime for phosphorylated AChE.<sup>6</sup> Unfortunately, a universal antidote, efficient against all known nerve agents and capable of crossing the blood–brain barrier, is not yet available.

Subsequent to formation of the OP–ChE adduct, the phosphylated ChEs can undergo a spontaneous, time-dependent

<sup>†</sup> Département de Toxicologie, CRSSA.

<sup>‡</sup> University of Nebraska Medical Center.

<sup>§</sup> FOI CBRN Defence and Security.

<sup>#</sup> Institut de Biologie Structurale.

(1) Chatonnet, A.; Lockridge, O. *Biochem. J.* **1989**, *260*, 625–634.

(2) Mack, A.; Robitzki, A. *Prog. Neurobiol.* **2000**, *60*, 607–628.

(3) Lockridge, O.; Masson, P. *Neurotoxicology* **2000**, *21*, 113–126.

(4) Eddleston, M.; Mohamed, F.; Davies, J. O.; Eyer, P.; Worek, F.; Sheriff, M. H.; Buckley, N. A. *Qim* **2006**, *99*, 513–522.

(5) Konradsen, F.; Dawson, A. H.; Eddleston, M.; Gunnell, D. *Lancet* **2007**, *369*, 169–170.

(6) Worek, F.; Thiermann, H.; Szinicz, L.; Eyer, P. *Biochem. Pharmacol.* **2004**, *68*, 2237–2248.

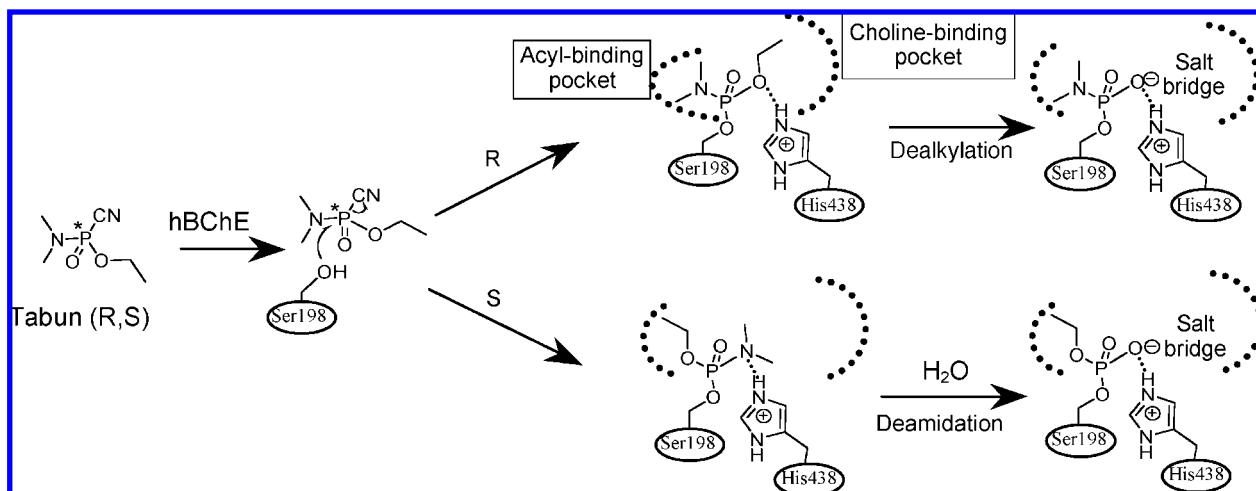


**Figure 1.** Mechanism proposed for aging of hBChE phosphorylated by tabun.

process called “aging”, during which the OP–ChE conjugate is dealkylated. This leads to irreversibly inhibited enzyme.<sup>7–10</sup> The rate of aging depends on the nature of the OP. The  $t_{1/2}$  is a few minutes for ChE inhibited by soman<sup>11</sup> and several hours for ChE inhibited by tabun.<sup>12</sup>

Early studies showed that tabun-inhibited ChEs from different animals display different rates of aging.<sup>13</sup> The rate constant for aging of tabun-inhibited human AChE (hAChE) *in vitro* was found to be  $8.7 \times 10^{-4} \text{ min}^{-1}$  (i.e.,  $t_{1/2} = 13.3 \text{ h}$ ) at 37° and pH 7.4.<sup>12</sup>

Inhibition of ChEs by tabun and the subsequent aging reaction are of particular interest, because tabun–ChE conjugates display an extraordinary resistance toward most oxime reactivators. As tabun is racemic, the two enantiomers, P(R) and P(S), can react with the enzyme and form adducts with different stereochemistry. These adducts could respectively age through “dealkylation” or “deamidation” (Figure 1).

Mass spectrometry (MS) studies on the aging of hAChE inhibited by tabun suggested that the mechanism involved a P–N bond cleavage and elimination of the dimethylamine group.<sup>14,15</sup> Intriguingly, the 2.5 Å crystal structure of non-aged *Mus musculus* AChE (mAChE) inhibited by tabun suggested that the ethoxy moiety is placed close to the catalytic His447, with the dimethylamine group distant from catalytic residues able to facilitate the aging reaction.<sup>16</sup> In the structure, the His447 and Phe338 side chains have undergone a structural change

relative to the conformation found in the apoenzyme structure. The authors proposed that this displacement might interfere with the accessibility of oximes, thereby contributing to the high resistance of tabun conjugates to reactivators.

Kinetic analysis of the oxime-induced reactivation and aging of hAChE inhibited by various tabun-related *N*-monoalkyl phosphoramidates showed that the rate constants for both were dependent on the length of the *N*-alkyl chain.<sup>17</sup>

In order to better understand the structural basis of both the oxime resistance of the conjugates and the aging mechanism of tabun-inhibited ChEs, we analyzed peptides from tabun–hBChE by MS, determined the crystal structures of non-aged and aged forms of hBChE inhibited by tabun, and updated the previous crystal structure model of tabun–mAChE. The X-ray structures will help in the design of new oximes capable of reactivating tabun–ChEs conjugates.

## Materials and Methods

**Caution:** As tabun is highly toxic and is classified as a schedule 1 chemical as defined in the Chemical Weapons Convention, all work with tabun is regulated by the convention. The handling of tabun is dangerous and requires suitable personal protection, training, and facilities.

**Titration of Tabun by Ionometry and NMR.** Racemic tabun in solution in 2-propanol was from CEB (Vert-le-Petit, France). <sup>31</sup>P, <sup>1</sup>H, and <sup>13</sup>C NMR spectra for tabun in 2-propanol were recorded to determine its purity and integrity. After complete hydrolysis at pH 13.6, tabun was titrated by ionometry using a thermostatted ionometer (Radiometer IONcheck 45) equipped with an ion-selective electrode for cyanide (Radiometer Analytical ISE25CN-9), as described by the electrode provider.

**Production of Recombinant hBChE.** The recombinant hBChE was a truncated monomer containing residues 1–529.<sup>18</sup> The 45-amino acid tetramerization domain at the carboxy terminus was deleted. The carbohydrate content was reduced by site-directed mutagenesis from nine to six glycans.<sup>18</sup> The recombinant hBChE gene was expressed in Chinese hamster ovary (CHO) cells. The enzyme, secreted into serum-free culture medium, was purified by affinity and ion-exchange chromatographies and crystallized as

- (7) Benschop, H. P.; Keijer, J. H. *Biochim. Biophys. Acta* **1966**, *128*, 586–588.
- (8) Viragh, C.; Kovach, I. M.; Pannell, L. *Biochemistry* **1999**, *38*, 9557–9561.
- (9) Millard, C. B.; Kryger, G.; Ordentlich, A.; Greenblatt, H. M.; Harel, M.; Raves, M. L.; Segall, Y.; Barak, D.; Shafferman, A.; Silman, I.; Sussman, J. L. *Biochemistry* **1999**, *38*, 7032–7039.
- (10) Nachon, F.; Asojo, O. A.; Borgstahl, G. E.; Masson, P.; Lockridge, O. *Biochemistry* **2005**, *44*, 1154–1162.
- (11) Saxena, A.; Viragh, C.; Frazier, D. S.; Kovach, I. M.; Maxwell, D. M.; Lockridge, O.; Doctor, B. P. *Biochemistry* **1998**, *37*, 15086–15096.
- (12) Heilbronn, E. *Biochem. Pharmacol.* **1963**, *12*, 25–36.
- (13) Heilbronn, E. *Biochim. Biophys. Acta* **1962**, *58*, 222–230.
- (14) Barak, D.; Ordentlich, A.; Kaplan, D.; Barak, R.; Mizrahi, D.; Kronman, C.; Segall, Y.; Velan, B.; Shafferman, A. *Biochemistry* **2000**, *39*, 1156–1161.
- (15) Elhanany, E.; Ordentlich, A.; Dgany, O.; Kaplan, D.; Segall, Y.; Barak, R.; Velan, B.; Shafferman, A. *Chem. Res. Toxicol.* **2001**, *14*, 912–918.
- (16) Ekstrom, F.; Akfur, C.; Tunemalm, A. K.; Lundberg, S. *Biochemistry* **2006**, *45*, 74–81.

- (17) Worek, F.; Aurbek, N.; Koller, M.; Becker, C.; Eyer, P.; Thiermann, H. *Biochem. Pharmacol.* **2007**, *73*, 1807–1817.
- (18) Nachon, F.; Nicolet, Y.; Viguié, N.; Masson, P.; Fontecilla-Camps, J. C.; Lockridge, O. *Eur. J. Biochem.* **2002**, *269*, 630–637.

described.<sup>18</sup> The active-site concentration of highly purified enzyme was determined using diisopropyl fluorophosphate as the titrant.<sup>19</sup>

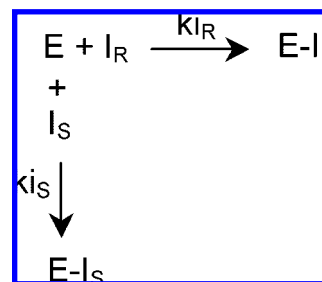
**Production of Recombinant hAChE.** The recombinant L544Stop mutant of human AChE (monomeric) was inserted into a pGS vector carrying the glutamine synthetase gene marker. CHO-K1 cells were maintained in serum-free Ultraculture Medium (Bio-Whittaker). Cells were transfected using DNA–calcium phosphate precipitation. Transfected clones were selected by incubation in media containing methionine sulfoximide. When cell death subsided, individual clones were manually transferred to 24 well plates. Clones with high expression of AChE were expanded and transferred to roller bottles for large-scale protein production. The used growth media contained up to 30 mg of hAChE per liter. Protein was precipitated from the media by ammonium sulfate. The pellets were dialyzed against 20 mM Tris-HCl buffer, pH 7.4, and loaded onto an affinity column (Sephacrose-4B/procainamide). Human AChE was eluted with 20 mM Tris-HCl buffer, pH 7.4, containing 1 M NaCl, 0.5 M tetramethylammonium iodide, and 1 mM decamethonium chloride. The enzyme was dialyzed against 20 mM Tris-HCl buffer, pH 7.4, and further purified by ion-exchange chromatography (monoQ; Amersham Bioscience) on a fast protein liquid chromatography system (Pharmacia). Fractions containing high hAChE activity were pooled and concentrated using a Centricon-30 ultrafiltration microconcentrator (30 000 MW cutoff, from Amicon). The concentration of the pure, homogeneous hAChE was determined from its absorbance at 280 nm using  $\epsilon_{1 \text{ mg/mL}} = 1.7$ .<sup>20</sup>

**Inhibition of hChEs by Tabun.** Phosphorylation rates were determined by incubating the ChE with different concentrations of tabun in 50 mM sodium phosphate buffer, pH 7.0, containing 5% 2-propanol and 1 mg/mL bovine serum albumin (BSA) and measuring the enzyme residual activity of aliquots at various times after initiation of inhibition at 25 °C. Human ChE activities were assayed according to Ellman<sup>21</sup> with 1 mM butyrylthiocholine for hBChE and 0.75 mM acetylthiocholine (ATC) for hAChE in the presence of 1 mg/mL BSA, 0.5 mM 5,5'-dithiobis(2-nitrobenzoic acid), and 50 mM sodium phosphate buffer, pH 7.0, at 25 °C using a Uvikon943 spectrophotometer. The stability of tabun under the assay conditions was verified by ionometry (measurement of CN<sup>−</sup> release) and by testing the invariant ability of tabun solution to inhibit hBChE as a function of time. No significant spontaneous hydrolysis of tabun was observed after more than 10 h of incubation. Analysis of the kinetic data was performed using GOSA-fit, a fitting software based on a simulated annealing algorithm (BioLog, Toulouse, France; <http://www.bio-log.biz>).

Cholinesterases are well-known to favor one stereoisomer over another. Therefore, it is prudent to analyze the tabun inhibition kinetics as if the ChE were behaving in a stereoselective manner. The rate of dissociation of the ChE–tabun adduct is slow relative to its rate of formation; therefore, the phosphorylation reaction can be treated as an irreversible process for analytical purposes.

Irreversible inhibition by a racemic inhibitor (*R,S*) can be described by Scheme 1. The apparent bimolecular phosphorylation rate constants ( $k_i = k_{iR} + k_{iS}$ , see Scheme 1) determined under pseudo-first-order conditions ( $[\text{tabun}] > 20[\text{hChE}]$ ) were computed from the slopes of  $\ln E$  vs time plots at different tabun concentrations.

Determination of inhibition enantioselectivity was performed under second-order conditions. The concentration of hBChE was 31.5 nM, while that of tabun ranged between 25 and 200 nM. The concentration of hAChE was 7.4 nM, while that of tabun ranged between 5 and 150 nM. Assuming that the enzymes were enantioselective, with one enantiomer much more efficient than the other (i.e.,  $k_{iR} \gg k_{iS}$ ), the fraction of enzyme inhibited by the lowest active

Scheme 1<sup>a</sup>

<sup>a</sup> E is the enzyme,  $I_R$  is the *R* enantiomer,  $I_S$  is the *S* enantiomer,  $E-I_R$  and  $E-I_S$  are the conjugates, and  $k_{iR}$  and  $k_{iS}$  are the bimolecular rate constants.

enantiomer is negligible, and the concentration of residual active enzyme follows eq 1 (derived from Scheme 1) as a function of time:

$$E = E_0 \frac{E_0 - I_0/n}{E_0 - (I_0/n) e^{(I_0/n - E_0)k_{iR}}} \quad (1)$$

where  $E$  is the concentration of residual active enzyme at time  $t$ ,  $E_0$  the concentration of enzyme at time  $t = 0$ ,  $I_0$  the concentration of racemic inhibitor at  $t = 0$ ,  $n$  the number of enantiomers, and  $k_{iR}$  the bimolecular rate constant of the most active enantiomer (taken to be enantiomer *R* in this case).

#### Tabun-Inhibited hBChE Samples for Mass Spectrometry.

Human BChE was reacted with tabun in H<sub>2</sub><sup>18</sup>O. Oxygen-18 was used so that the mechanism of dealkylation during aging could be more clearly defined. Evidence from the crystal structure of aged tabun-inhibited hBChE indicates that aging involves dealkylation of the ethoxy moiety. This reaction requires hydrolysis of the P–O–C linkage. In principle, such a hydrolysis could occur by cleavage of the P–O bond or the O–C bond. In the former case, a hydroxyl from water would replace the ethoxy. In the latter case, a hydroxyl from water would add to the ethyl, leaving the original oxygen on the phosphorus. By using H<sub>2</sub><sup>18</sup>O, the site of cleavage can be distinguished. If hydrolysis is at the O–C bond, the mass of the phosphorus component will reflect the presence of the original <sup>16</sup>O. If the hydrolysis is at the P–O bond, the phosphorus component will gain an <sup>18</sup>O from the medium and its mass will increase by 2 amu. This strategy was employed by Li et al. to characterize the aging reactions for a variety of hBChE–OP adducts.<sup>22</sup>

For the inhibition reaction, 10  $\mu$ L of recombinant hBChE (13 mg/mL in 15 mM 2-(*N*-morpholino)ethanesulfonic acid (MES) buffer at pH 6.5) was mixed with 90 mL of H<sub>2</sub><sup>18</sup>O, 1 mL of 1 M Tris buffer at pH 8.5, and 1 mL of tabun (10 mg/mL in 2-propanol). Samples for analysis of the non-aged adduct were frozen to  $-80$  °C shortly after preparation. Samples for analysis of the aged adduct were incubated at room temperature for 2 days, after which the preparation was stored at  $-80$  °C until use. Final concentrations of hBChE and tabun were 15 and 720 mM, respectively. Unlabeled hBChE was treated in the same manner, except that the tabun was omitted.

To prepare peptides for MS, frozen samples were thawed and 50 mL of sample was mixed with 50 mL of 25 mM ammonium bicarbonate buffer at pH 8.3. The mixture was concentrated to about 20 mL by centrifugation at 6700g using a Microcon YM-3 ultrafiltration microconcentrator (3000 MW cutoff, from Millipore). The process was repeated five times to remove the H<sub>2</sub><sup>18</sup>O and excess tabun and to change the buffer. The product was diluted to 50 mL with 25 mM ammonium bicarbonate, mixed with porcine trypsin (0.5 mg/mL from Promega) to a final hBChE/trypsin ratio of 30:1 (w/w), and incubated overnight at room temperature with constant,

(19) Amitai, G.; Moorad, D.; Adani, R.; Doctor, B. P. *Biochem. Pharmacol.* **1998**, *56*, 293–299.

(20) Rosenberry, T. L.; Scoggin, D. M. *J. Biol. Chem.* **1984**, *259*, 5643–5652.

(21) Ellman, G. L.; Courtney, K. D.; Andres, V.; Featherstone, R. M. *Biochem. Pharmacol.* **1961**, *7*, 88–95.

(22) Li, H.; Schopfer, L. M.; Nachon, F.; Froment, M. T.; Masson, P.; Lockridge, O. *Toxicol. Sci.* **2007**, *100*, 136–145.

gentle mixing. Peptides were concentrated and washed using ZipTips (Millipore), as described in the sections on MALDI-TOF mass spectrometry and Q-Trap mass spectrometry.

**MALDI-TOF Mass Spectrometry.** MALDI-TOF MS experiments were performed on an Applied Biosystems Voyager DE-PRO mass spectrometer equipped with a 337 nm pulsed nitrogen laser (Framingham, MA). Peptides that had been adsorbed onto a reverse-phase C-18 ZipTip were eluted into a microcentrifuge tube with 15  $\mu$ L of 60% acetonitrile and 0.1% trifluoroacetic acid (TFA). One microliter of eluant was mixed 1:1 (v/v) with  $\alpha$ -cyano-4-hydroxycinnamic acid (matrix, 10 mg/mL in 50% acetonitrile and 0.3% TFA) on the MALDI target plate and allowed to dry at room temperature. Mass spectra were acquired in positive-ion, linear mode under delayed extraction conditions, using an acceleration voltage of 20 kV. Laser intensity was adjusted so that the most intense ion in the spectrum did not exceed 80% of the maximum, saturated intensity value. Laser positioning on the sample spot was monitored with a video camera. Spectra shown are the average of 500 laser shots collected from multiple locations on the target spot. Calibration for the mass spectra was performed internally by reference to hBChE tryptic fragments. The sequence of hBChE (accession no. gi:158429457) was obtained from the NCBI database. The reference masses of the tryptic hBChE peptides were obtained using the MS-Digest feature of ProteinProspector version 4.0.6 (<http://prospector.ucsf.edu/>).

**Q-Trap Mass Spectrometry.** The amino acid sequence of the aged peptide from tabun-inhibited hBChE was determined by collision-induced dissociation in a QTrap 2000, hybrid, tandem-quadrupole, linear-ion trap mass spectrometer equipped with a nanospray interface (Applied Biosystems). The spectrometer was calibrated daily on selected fragments from the MSMS spectrum of [Glu]fibrinopeptide B. Tryptic peptides from tabun-inhibited hBChE (25  $\mu$ L total volume) were subjected to ZipTip cleanup to remove salts before they were delivered into the QTrap. Ten microliters of an 80% acetonitrile and 0.1% formic acid solution was used to elute the peptides from the ZipTip. Two 25- $\mu$ L aliquots were cleaned and the eluents combined. Eight microliters of the peptide solution was introduced into the mass spectrometer by static infusion using an Econo12 emitter (New Objective, Woburn, MA). The ion spray voltage was 1300 V (which creates a voltage differential of 1300 V between the emitter and the curtain plate). The emitter position was optimized to obtain maximum signal intensity. All mass spectra were collected in the enhanced mode, i.e., using the ion trap, and by convention are referred to as enhanced spectra. Enhanced product ion (EPI) spectra were obtained using low-energy collision-induced dissociation. The collision cell was pressurized to 40  $\mu$ Torr with pure nitrogen. The collision energy was 40 V. The trap fill time for each EPI scan was 20 ms. A total of 200 EPI scans were accumulated to generate the final EPI spectrum. The EPI spectra were manually analyzed to determine the sequence of the peptide.

#### Crystals of Non-aged Tabun-Inhibited hBChE Conjugate.

The mother liquor was 0.1 M MES buffer, pH 6.5, with 2.1 M ammonium sulfate. The tabun stock solution was 10 mM in 2-propanol. The tabun-hBChE conjugate was prepared by soaking crystals for 10 min in 0.1 M MES buffer, pH 6.5, with 2.1 M ammonium sulfate containing 1 mM tabun. The crystals were washed with a cryoprotectant solution (0.1 M MES buffer with 2.1 M ammonium sulfate, containing 20% glycerol) and then flash-cooled in liquid nitrogen.

**Crystallization of Aged Tabun-hBChE Conjugate.** The purified enzyme (9 mg/mL) was inhibited in the presence of 1 mM tabun in 10 mM Tris-HCl buffer, pH 7.4. The reaction mixture was incubated for 1 day at 4  $^{\circ}$ C. The inhibited enzyme was crystallized using the hanging drop method as described.<sup>23</sup> Crystals grew in 1 week at 20  $^{\circ}$ C. The length of time between phosphorylation

and data collection was sufficiently long (>1 week) to achieve completion of the aging reaction.

**X-ray Data Collection and Structure Solution of Tabun-hBChE Conjugate.** Diffraction data were collected at the European Synchrotron Radiation Facility (ESRF, Grenoble, France), at the ID14-eh2 beam line using  $\lambda = 0.932$   $\text{\AA}$  wavelength with ADSC Quantum 4 for non-aged conjugate, and at the ID23-2 beam line using  $\lambda = 0.873$   $\text{\AA}$  wavelength with MAR-Research CCD detector for aged conjugate. All data sets were processed with XDS. The structures were solved by use of the CCP4 suite.<sup>24</sup> An initial solution model was determined by molecular replacement with MolRep,<sup>25</sup> starting from the recombinant hBChE structure (PDB entry 1P0I) from which all ligands (butyrate, glycerol, ions) and glycan chains were removed. For all diffraction data sets, the model was refined as follows: an initial rigid-body refinement with REFMAC5<sup>26</sup> was followed by iterative cycles of model building with Coot,<sup>27</sup> and then restrained refinement was carried out with REFMAC5 and Phenix.<sup>28</sup> The bound ligands and their descriptions were built using the Dundee PRODRG2.5 server including energy minimization using GROMOS96.1 force field.

**Updated Refinement of Aged and Non-aged Tabun-Inhibited mAChE.** Coordinates and structure factors of non-aged (PDB entry 2C0Q) and aged (PDB entry 2C0P) tabun-inhibited mouse AChE were retrieved from the Protein Data Bank. The models were refined by iterative cycles of model building with Coot and restrained refinement with REFMAC5 and Phenix.

## Results

**Inhibition of Human Cholinesterases by Tabun.** The bimolecular rate constants,  $k_i$ , for inhibition of hAChE and hBChE by racemic tabun are respectively  $(3.0 \pm 0.4) \times 10^6$  and  $(2.0 \pm 0.2) \times 10^6$   $\text{M}^{-1} \cdot \text{min}^{-1}$  (data not shown). These values are in agreement with reported literature values.<sup>29</sup>

The time dependence of the inhibition of hAChE and hBChE by tabun, under second-order conditions, is shown in Figure 2. Both human ChEs are enantioselective. Fitting the AChE data to eq 1 yields  $k_{iR} = (6.9 \pm 0.2) \times 10^6$   $\text{M}^{-1} \cdot \text{min}^{-1}$  and  $n = 2.1 \pm 0.1$ . This corresponds to enantioselectivity of hAChE for one enantiomer of tabun. For hBChE, fitting yields  $k_{iR} = (6.0 \pm 0.4) \times 10^6$   $\text{M}^{-1} \cdot \text{min}^{-1}$  and  $n = 2.7 \pm 0.1$ . The latter  $n$  value also suggests an enantioselectivity of hBChE. However, the fact that more than 2 equiv of tabun was required to achieve full enzyme inhibition is puzzling. The value  $n = 2.7$  was systematically found for inhibition of both highly purified tetrameric plasma BChE and monomeric recombinant BChE. Because both tabun and BChE preparations were accurately titrated, and because no spontaneous hydrolysis of tabun was observed in buffer, a tentative hypothesis is that hydrolysis of tabun was promoted by a BChE nucleophile group other than Ser198. This requires further investigations.

**Mass Spectrometry Analysis of Tabun-hBChE Adducts.** The initial reaction of hBChE with tabun is expected to result in formation of a covalent adduct with loss of the CN moiety from tabun. This would cause the mass of the singly charged, active-

(23) Nicolet, Y.; Lockridge, O.; Masson, P.; Fontecilla-Camps, J. C.; Nachon, F. *J. Biol. Chem.* **2003**, *278*, 41141–41147.

(24) Collaborative-Computational-Project 4. *Acta Crystallogr. D. Biol. Crystallogr.* **1994**, *50*, 760–763.

(25) Vagin, A.; Teplyakov, A. *J. Appl. Crystallogr.* **1997**, *30*, 1022–1025.

(26) Murshudov, G. N.; Vagin, A. A.; Dodson, E. J. *Acta Crystallogr. D. Biol. Crystallogr.* **1997**, *53*, 240–255.

(27) Emsley, P.; Cowtan, K. *Acta Crystallogr. D. Biol. Crystallogr.* **2004**, *60*, 2126–2132.

(28) Adams, P. D.; Grosse-Kunstleve, R. W.; Hung, L. W.; Ioerger, T. R.; McCoy, A. J.; Moriarty, N. W.; Read, R. J.; Sacchettini, J. C.; Sauter, N. K.; Terwilliger, T. C. *Acta Crystallogr. D. Biol. Crystallogr.* **2002**, *58*, 1948–1954.

(29) Raveh, L.; Grunwald, J.; Marcus, D.; Papier, Y.; Cohen, E.; Ashani, Y. *Biochem. Pharmacol.* **1993**, *45*, 2465–2474.

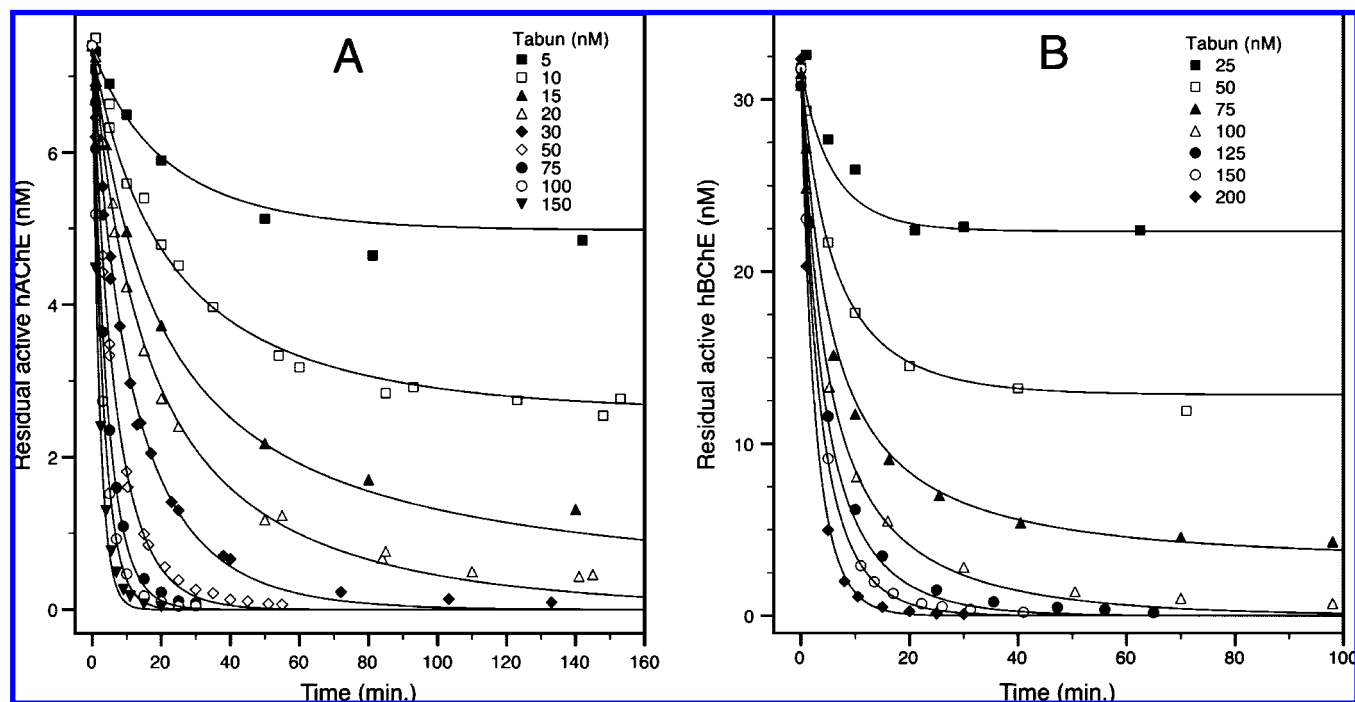


**Figure 2.** Irreversible inhibition of hAChE (A) and hBChE (B) by racemic tabun under second-order conditions. Human ChEs were inhibited by various concentrations of tabun, and the residual active concentration of enzyme was monitored as a function of time.

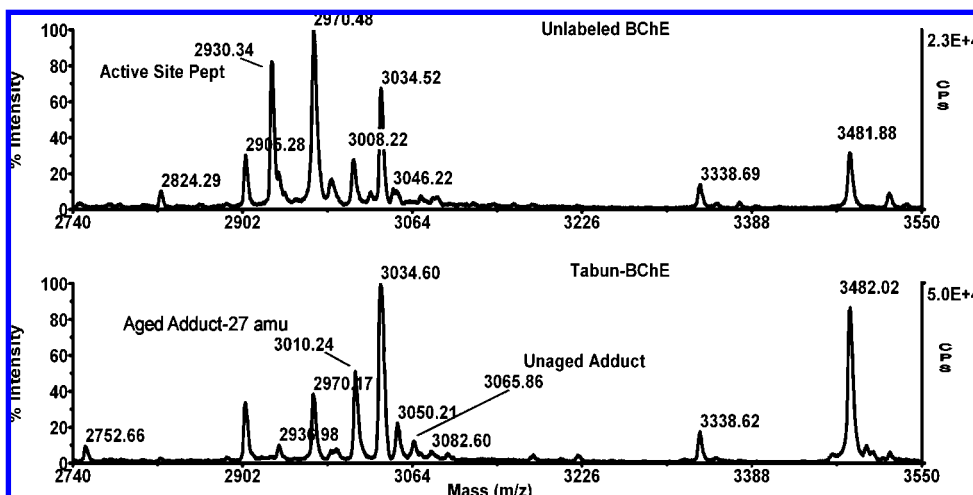


**Figure 3.** Mass spectra of tryptic digests of hBChE with and without tabun. Spectra were taken in linear mode on a MALDI-TOF mass spectrometer. Peptides were prepared and MALDI-TOF mass spectra were taken as described in the methods section. The upper panel is for unlabeled hBChE. It was internally calibrated using the average masses for hBChE peptides at 3482.07 (residues 148–180) and 3034.59 amu (residues 428–452). The lower panel is for the aged tabun–hBChE adduct. The peak labeled “Aged Adduct-27 amu” is the peak for tabun–hBChE after loss of the dimethylamine and ethoxy groups. It was internally calibrated using the hBChE peptides at 3482.07 (residues 148–180), 3050.59 (residues 428–452 with one oxidized methionine), and 3034.59 amu (residues 428–452). Calibration was performed using peak height as a weighting factor.

site, tryptic peptide to increase by 135 amu, from 2930.3 to 3065.3 amu (average masses). This transformation is evident in the MALDI-TOF mass spectra shown in Figure 3, where the tryptic digest of unlabeled hBChE (upper panel) shows a prominent peak at 2930.34 amu and no mass at 3065 amu, while the tryptic digest of the non-aged tabun–hBChE adduct (lower panel) shows no mass at 2930 amu and a distinct mass at 3065.86 amu.

Following its initial formation, the tabun–hBChE adduct will age. Aging would be expected to result in loss of either a dimethylamine or an ethoxy group. Such losses would lead to reduction in the mass of the active-site peptide adduct to either 3038.3 (for loss of dimethylamine) or 3037.3 amu (for loss of

ethoxy). Neither of these masses was detected in the MALDI-TOF mass spectra for the aged tabun–hBChE adduct. The large peak at 3034 amu (from hBChE peptide residues 428–452) could obscure peaks of small intensity at 3037 or 3038 amu. However, high-resolution, reflector-mode MALDI-TOF spectra showed that the peak at 3034 amu (average mass) was composed only of isotopes from a 3032 amu monoisotopic mass. There was no evidence in the isotopic pattern for additional mass at 3037 or 3038 amu. This finding was unexpected since the tabun–hBChE adduct had been allowed to age for several days before digestion and aged product should have been present.

Comparison of the two mass spectra in Figure 3 reveals a shift in the mass of the 3008 amu peak in unlabeled hBChE to

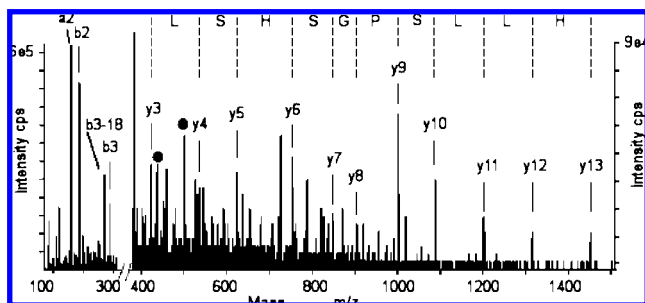


**Figure 4.** Tandem mass spectrum (MSMS) of the putative aged tabun-labeled active-site peptide from hBChE. An MSMS spectrum was taken of the 753.4  $m/z$ , quadruply charged form of the 3010 amu ion using the QTrap 2000 hybrid tandem-quadrupole, linear ion-trap mass spectrometer. The x-axis is divided into two intensity ranges. For masses from 400 to 1500  $m/z$ , the intensity of the data has been expanded 6.7-fold. The intensities for this region are given in counts per second (cps) on the scale to the right. For masses from 50 to 350  $m/z$ , the intensities are given in cps on the scale to the left. Selected y- and b-ions that are characteristic of hBChE active-site peptide are indicated. The amino acid sequence corresponding to the y-ion series is indicated by single-letter abbreviations for the amino acids. The spots indicate the 437.3 and 501.4 amu fragments; see the text for a description of these fragments.

3010 amu in the aged tabun–hBChE sample. The 3008 amu mass is consistent with the mass of a tryptic peptide from hBChE (residues 549–570 having one oxidized methionine). The 3010 amu mass appeared repeatedly in the spectra of aged tabun–hBChE. A mass of 3010 amu would be consistent with loss of both the dimethylamine and the ethoxy groups from the tabun adduct, leaving phosphate (added mass of 80 amu) attached to the active-site peptide.

Justification for the loss of both substituents can be made. The crystallography results indicate that the ethoxy group is lost through the aging process. Hydrolysis of dimethylamine from tabun is known to occur at low pH.<sup>30</sup> During preparation of peptides for positive-mode MALDI-TOF mass spectrometry, samples were routinely exposed to 0.1% TFA. Thus, loss of the dimethylamine could occur. The combination would have resulted in reduction of the tabun adduct to a phosphate adduct.

Confirmation of the identity of the 3010 amu mass was obtained by tandem mass spectrometry. Tryptic peptides from hBChE were infused into a QTrap 2000 tandem-quadrupole mass spectrometer. A mass equal to the quadruply charged form of the 3010 amu ion was observed at 753.4  $m/z$ . This mass was subjected to collision-induced dissociation in the mass spectrometer. The resulting MSMS mass spectrum was consistent with that of the active-site peptide from hBChE (Figure 4).

The sequence of the active-site peptide is SVTLFGESA-GAASVSLHLLSPGSHSLFTR, where the bold-type S at position 8 is the serine that is expected to be labeled. A singly charged, y-ion series identical to the C-terminal portion of the active-site peptide, HLLSPGSHSL(FTR), was clearly defined in the MSMS spectrum. Singly charged fragments from the N-terminal were also found (a2 at 159.1 amu for SV minus CO, b2 at 187.2 amu for SV, b3 at 288.1 amu for SVT, and b3 minus water at 270.1 amu). Most convincing, however, were two doubly charged masses, at 437.3 and 501.4  $m/z$ , which are consistent with phosphoserine fragments  $b9^{2+}$  (SVTLFGESA) and  $b11^{2+}$  (SVTLFGESAGA) that have lost 98 amu. Both fragments include the labeled serine. Loss of 98 amu from a phosphoserine is a commonly observed consequence of colli-

sion-induced dissociation. It represents loss of the phosphate (–80 amu) and transformation of the serine into dehydroalanine (–18 amu).

Thus, both the MALDI-TOF and tandem mass spectrometry results are consistent with the presence of a phosphoserine-containing, active-site peptide in the aged form of tabun-labeled hBChE. The most logical scenario to explain this species is loss of the ethoxy ligand through aging and loss of the dimethylamine ligand through acid-catalyzed hydrolysis during preparation of the sample for mass spectrometry. Only evidence of deamination was found in earlier mass spectrometry studies on human AChE.<sup>14,15</sup> This suggests that only the product of the acid-catalyzed deamination could be observed under those experimental conditions.

This analysis of aged tabun–hBChE utilizes an added mass of 80 amu for phosphate, which is the mass expected if natural abundance oxygen-16 is present for all of the oxygens on the phosphorus. If aging had involved release of the dimethylamine, then one of the phosphorus oxygens should have been derived from the  $H_2^{18}O$  in the medium, making the added mass of the phosphate 82 amu. Similarly, if aging involved release of the ethoxy moiety via P–O bond cleavage, then the added mass would have been 82 amu. It follows that the added mass is consistent with elimination of the ethoxy moiety during aging via O–C bond cleavage.

**X-ray Structure of Non-aged Tabun-Inhibited hBChE.** Data were collected from tetragonal crystals of space group  $I422$  and refined to 2.1 Å. Data and refinement statistics are shown in Table 1. There is no significant displacement of residue side chains compared to the native enzyme (PDB entry 1POI). A strong peak of positive electronic density ( $19\sigma$ ) within covalent bond distance of the catalytic serine was observed in the initial  $|F_o| - |F_c|$  map. This confirms that inhibitor was bound to the active-site serine after 5 min of soaking. The structure was refined as a conjugate of the P(R) enantiomer of tabun (Figure 5A). The phosphorus atom is found at covalent bonding distance of 1.65 Å from the Ser198O $\gamma$  atom. O2 of the phosphoramidate moiety is at hydrogen-bonding distance from the main-chain amide nitrogen of residues forming the oxyanion hole, Gly116 (2.9 Å), Gly117 (2.8 Å), and Ala199 (2.9 Å). The ethoxy moiety is pointing toward the top of the active-site gorge, with O3 at hydrogen-bonding distance from His438N $\epsilon$ 2 (3.2 Å). The dimethylamino moiety is located in the acyl-binding pocket with the two methyl groups pointing toward the top of the gorge. Despite the fact that the P–N distance was refined to 1.8 Å, there is still a residual peak of positive density ( $4\sigma$ ) above the two methyl groups. This density could correspond to low occupancy of the butyrate-like molecule that is always found in the native enzyme structure.<sup>23</sup> The C1 methyl group of the dimethylamine is interacting with Leu286C $\delta$ 2 and Phe398CZ (both at 3.5 Å) and the C2 methyl group is at 3.2 Å from Gly117C $\alpha$  and 3.8 Å from Trp231C $\epsilon$ 3. There is a peak of positive density in the initial  $|F_o| - |F_c|$  map ( $5.4\sigma$ ) close to Trp82 that could not be reasonably modeled. A similarly shaped density was found in the choline-binding pocket in several structures of native hBChE. In those structures, it was modeled as glycerol (1POI or 1XLV).<sup>10,23</sup> This unknown ligand appears to be stacked against Trp82 and seems to interact with Glu197O $\epsilon$ 2, a water molecule from the cluster along Trp430 and Tyr440, and the water molecule H-bonded to Thr120.

**X-ray Structure of Aged Tabun-Inhibited hBChE.** Data were collected from a crystal of aged tabun-inhibited hBChE and were refined to 2.3 Å. A strong peak of positive electronic density

(30) Larsson, L. *Acta Chim Scand* **1958**, *12*, 783–785.

**Table 1.** Data Collection and Refinement Statistics

	tabun-hBChE		tabun-mAChE	
	non-aged (3DJY)	aged (3DKK)	non-aged (3DL4)	aged (3DL7)
space group	I422	I422	P212121	P212121
unit cell axes, <i>a</i> , <i>b</i> , <i>c</i> (Å)	156.58, 127.74	155.24, 127.47	79.62, 112.94, 226.16	79.02, 110.88, 226.38
no. of measured reflections	305 954	236 247	n.d. <sup>d</sup>	n.d. <sup>d</sup>
unique reflections	45 888	34 165	71 021	69 074
resolution (Å)	55.4–2.1 (2.2–2.1)	28.2–2.3 (2.4–2.3)	29.2–2.5 (2.6–2.5)	29.0–2.5 (2.6–2.5)
completeness (%)	99.0 (99.6)	98.2 (93.0)	99.6 (100.0)	99.3 (99.0)
<i>R</i> <sub>merge</sub> <sup>a</sup> (%)	6.3 (50.5)	6.6 (42.7)	9.0 (59.0)	7.0 (51.0)
<i>I</i> /σ( <i>I</i> )	22.0 (4.4)	27.6 (5.1)	14.4 (3.3)	17.6 (7.5)
redundancy	6.7 (7.0)	6.9 (7.3)	6.2 (6.2)	7.4 (7.5)
Refinement Statistics				
<i>R</i> -factor <sup>b</sup> ( <i>R</i> -free <sup>c</sup> )	21.2 (24.8)	19.6 (24.6)	19.6 (24.5)	18.8 (22.7)
no. of atoms				
protein	4213	4192	8444	8403
solvent	285	275	133	439
others	154	154	168	72
mean <i>B</i> -factor (Å <sup>2</sup> )	39.8	40.1	47.2	49.6
rms from ideality				
bond length (Å)	0.017	0.022	0.014	0.013
angles (deg)	1.764	2.068	1.501	1.461
chiral (Å <sup>3</sup> )	0.123	0.140	0.105	0.097

<sup>a</sup>  $R_{\text{merge}} = (\sum |I - \langle I \rangle|) / \sum I$ , where *I* is the observed intensity and  $\langle I \rangle$  is the average intensity obtained from multiple observations of symmetry-related reflections after rejections. <sup>b</sup>  $R\text{-factor} = \sum |F_o - |F_c|| / \sum |F_o|$ , where *F*<sub>o</sub> and *F*<sub>c</sub> are observed and calculated structure factors. <sup>c</sup> *R*-free set uses 5% of randomly chosen reflections defined by Brunger et al.<sup>38</sup> <sup>d</sup> Structure factors come from the PDB: 2C0Q (non-aged) and 2C0P (aged).

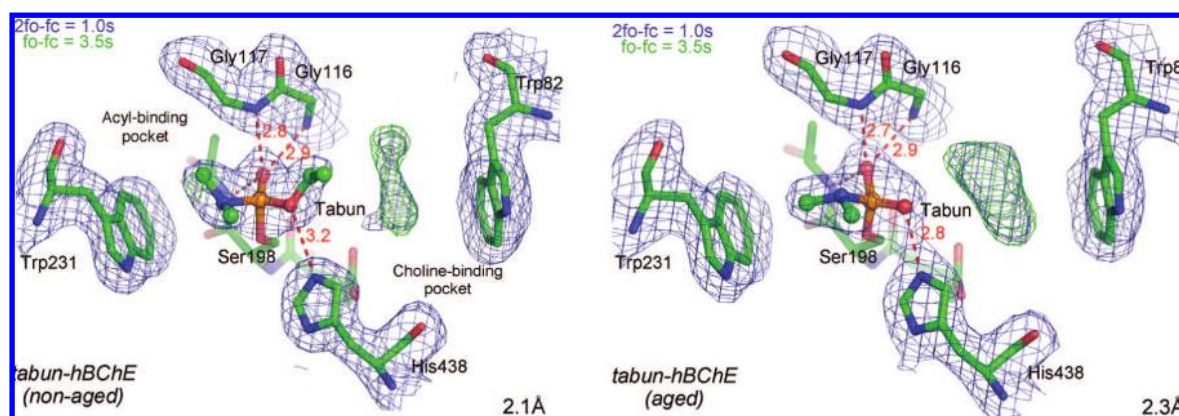


**Figure 5.** Active site of non-aged and aged tabun-hBChE conjugates. Key residues are represented as sticks with carbon atoms in green, nitrogen atoms in blue, phosphorus in orange, and oxygen atoms in red. Hydrogen bonds are represented by red dashes. Electron density  $2|F_o| - |F_c|$  is represented by a blue mesh, contoured at  $1.0\sigma$ , and  $|F_o| - |F_c|$  is represented by green/red mesh contoured at  $3.5\sigma$ .

( $13\sigma$ ) within covalent bond distance of the catalytic serine in the initial  $|F_o| - |F_c|$  map confirms the presence of the bound inhibitor. The refined structure clearly shows that aging proceeds through O-dealkylation of the P(R) enantiomer of tabun (Figure 5B). The phosphorus atom is found at a covalent bonding distance of 1.62 Å from the Ser198O $\gamma$  atom. O2 of the phosphoramidate moiety is at hydrogen-bonding distance from the main-chain amide nitrogens of the residues forming the oxyanion hole, Gly116 (2.9 Å), Gly117 (2.7 Å), and Ala199 (2.7 Å). As a result of the loss of the ethoxy substituent, the O3 moiety of the phosphorus is negatively charged and forms a strong salt bridge with His438N $\epsilon$ 2 (2.8 Å). The dimethylamino moiety is located in the acyl-binding pocket, but in contrast to the non-aged form, the two methyl groups point downward from Phe398. The C2 methyl group interacts with the indole ring of Trp231, about 3.5 Å from each aromatic carbon of the six-atom ring, while C1 is at least 3.7 Å from Phe398, Phe329, and Leu286. The P–N distance was refined to 1.7 Å. The peak of positive density that was close to Trp82 in the non-aged tabun-hBChE  $|F_o| - |F_c|$  map is still present but is much stronger ( $9.1\sigma$ ). It is likely that the occupancy of this ligand is

higher because there is no steric hindrance from the ethoxy, and there is a possibility for stronger H-bond interactions with the negatively charged O3 of the phosphoramidate.

#### Updated Refinement of Non-aged Tabun-Inhibited mAChE.

The original geometry of the aged and non-aged tabun moiety was based on calculations using the monomer library sketcher of the CCP4 program suite.<sup>24</sup> However, a careful examination of the crystal structure of non-aged tabun-inhibited mAChE reveals questionable geometry for the phosphoramidate adduct in both monomers (PDB code 2C0Q). For example, the N–P–Ser203O $\gamma$  angle was refined to 83°, which is at odds with the angle of 103° determined using the GROMOS96.1 force field analysis. The 103° value is in better agreement with the tetrahedral shape of the adduct. In addition, the P and N atoms and the two methyl groups were modeled as strictly coplanar, whereas molecular modeling based on GROMOS96.1 force field indicates an  $sp^3$  orbital hybridization of N. However, quantum mechanics computation at the BP86/TZVP level indicates a hybridization of N between  $sp^2$  and  $sp^3$ . This mixed hybridization is supported by two small-molecule structures in

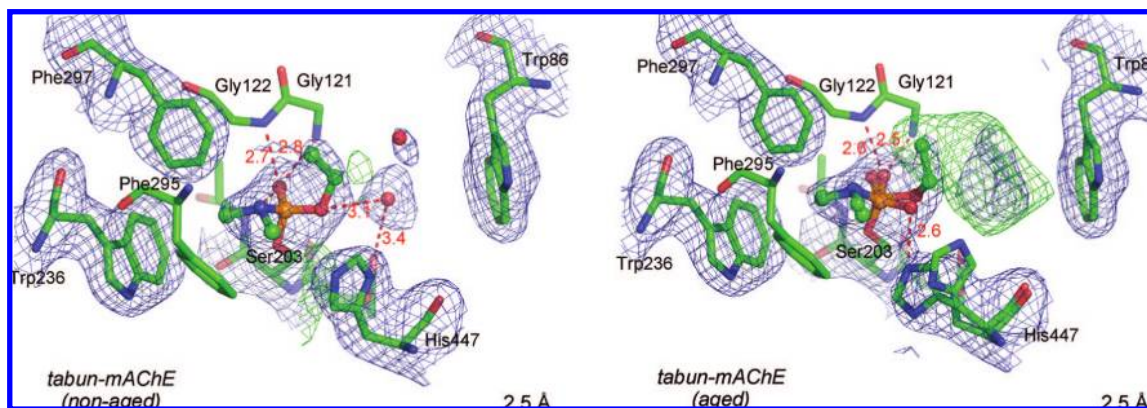


**Figure 6.** Active site of non-aged and aged tabun-mAChE conjugates. Key residues are represented as sticks, with carbon atoms in green, nitrogen atoms in dark blue, phosphorus in orange, and oxygen atoms in red. Hydrogen bonds are represented by red dashes. Electron density  $2|F_o| - |F_c|$  is represented by a blue mesh, contoured at  $1.0\sigma$ , and  $|F_o| - |F|$  is represented by green/red mesh contoured at  $3.5\sigma$ .

the Cambridge Structural Database (QOQWO<sup>31</sup> and ZEX-BAF<sup>32</sup>) in which dimethylamino groups are attached to phosphorus. Because of these ambiguities, a new refinement was made using better constraints for tabun (Figure 6A).

In the new refinement, the methyl groups of the dimethylamine are pointing downward, in a conformation similar to that found in aged tabun-inhibited hAChE. The C2 methyl group interacts with Trp236C $\zeta$ 3 (3.5 Å) and Phe295C $\epsilon$ 1, whereas C1 is 3.4 Å from Phe295C $\zeta$ . As previously reported, the imidazolium ring of His447 has shifted toward Phe338. There is a residual peak of density (4.5 $\sigma$ ) in the  $|F_o| - |F|$  map between Ser203 and Glu334 of both monomers that suggests some low-occupancy conformations of His447. Two water molecules were added to explain residual density close to Trp86 at the bottom of the gorge. The remainder of the gorge is apparently free of ligands. There is a noteworthy “blob” of density (up to 5.4 $\sigma$ ) close to Trp286, which indicates that the peripheral anionic site is occupied by an unknown ligand (data not shown).

**Updated Refinement of Aged Tabun-Inhibited mAChE.** In the original refinement (PDB code 2C0P), the modeled tabun-mAChE adduct underwent aging through displacement of the dimethylamine moiety from the acyl-binding pocket, while the ethoxy substituent was left intact in the choline-binding pocket, pointing toward the top of the gorge. The actual electronic density shows that the dimethylamine group is still attached to the phosphorus atom. While there is clearly some electron density in the  $2|F_o| - |F|$  map corresponding to an ethoxy substituent in monomer A, there appears to be none in monomer B. In addition, a peak of positive density next to His447 in both monomers suggests that His447 may adopt an alternate conformation. There were large “blobs” of unexplained density in the  $|F_o| - |F|$  map stretching from the peripheral site (Trp286) to the choline-binding site (Trp86), hinting that the whole gorge is occupied by unknown ligands. This material has perturbed the conformation of Tyr337. On the basis of these observations, it was concluded that an improved model should be built.

For monomer A, the presence of electronic density in the choline binding site indicated that the aged conjugate underwent incomplete dealkylation. Accordingly, both aged and non-aged forms of the tabun conjugates were included in the new model.

They were assigned an occupancy of 0.5 each, based on *B*-factor values, though a large uncertainty exists on this ratio (Figure 6B). The position and the array of interactions in the non-aged tabun adduct in monomer A are similar to those in the non-aged structure of mAChE. In the aged form, the phosphorus atom is found at a covalent bonding distance of 1.6 Å from the Ser203O $\gamma$  atom. O2 of the phosphoramidate moiety is at hydrogen-bonding distance from the main-chain amide nitrogens of the residues forming the oxyanion hole, Gly121 (2.8 Å), Gly122 (2.6 Å), and Ala204 (2.8 Å). The dimethylamino moiety is still located in the acyl-binding pocket, with the two methyl groups pointing downward. The C2 methyl group is interacting with the indole ring of Trp236, CH2 (3.5 Å), whereas C1 is 3.5 Å from Phe295C $\zeta$  and 3.3 Å from Phe338C $\zeta$ . The electron density of His447 is not clearly defined and was modeled as two conformers, despite features indicating that there is more likely a continuum of conformations between the two average positions. In the first conformer, His447N $\epsilon$ 2 forms a salt bridge with O3 of the phosphorus (2.6 Å), and His447N $\delta$ 1 is strongly H-bonded to Glu334O $\epsilon$ 1 (2.5 Å). The second conformer is similar to the conformation of the non-aged conjugate. These two models highlight the fact that dealkylation is accompanied by a shift of the phosphoramidate moiety toward His447N $\epsilon$ 2 (0.7 Å shift for O3). In addition, nearby residues Tyr337 and Phe338 are extremely perturbed. Their side chains were refined to occupancies of 0.6 and 0.8, respectively. The perturbation of the Tyr337 conformation, in particular, appears to be related to the presence of an unknown ligand close to Trp86. This is indicated by the strong unexplained positive electron density in the  $|F_o| - |F|$  map (peak at 8.8 $\sigma$ ). We tried to fit this electron density to (1) components of the crystallization buffer, polyethylene glycol monomethyl ether 750, HEPES; and (2) procainamide, the ligand that was used for the last affinity chromatography purification step,<sup>16</sup> without success.

For monomer B, at first sight the weak electron density for the ethyl substituent suggested that complete dealkylation of the conjugate had occurred. However, it became apparent during the refinement process that the weak residual density was better explained by modeling both aged and non-aged forms of the tabun adduct into the structure. For example, when the adduct was modeled solely as the aged form, a peak of positive density in the  $|F_o| - |F|$  map developed between His447N $\epsilon$ 2 and O3. This indicated that the refinement software was placing O3 too far away from the imidazolium. This would arise if the software was trying to fit density corresponding to trace amounts

(31) Gholivand, K.; Tadjarodi, A.; Taeb, A.; Garivani, G.; Ng, S. W. *Acta Crystallogr.* **2001**, E57, o472–o473.

(32) Shih, Y.-E.; Wang, F.-C.; Maa, S.-H.; Liu, L.-K. *Bull. Inst. Chem. Acad. Sin.* **1994**, 41, 9.

of the ethoxy substituent. Accordingly, models for both the aged and non-aged forms of the tabun adduct were refined into the structure with occupancies of 0.6 and 0.4, respectively. This ratio was based on a *B*-factor value of about 41 Å<sup>2</sup>. The position and the array of interactions in the non-aged and aged tabun adducts are similar to those in monomer A: the two methyl groups point downward and make contacts with Trp236, Phe295, and Phe338, and there is a slight shift of the phosphoramidate toward His447NE2 (0.6 Å for O3). His447 is again perturbed and, consequently, is modeled as two alternate conformations displaying average positions like those in monomer A. Nearby residues, Phe338 and Tyr337, are extremely perturbed and were refined with partial occupancy. This perturbation, at least that of Tyr337, is related to the presence of an unknown ligand in the active site, which is indicated by strong positive peaks in the  $|F_o| - |F|$  maps (7.2σ).

## Discussion

The kinetics for inhibition of hBChE and hAChE by tabun show that both enzymes are enantioselective. This is in agreement with a previous study showing that (–)-tabun reacts about 6.3 times faster than (+)-tabun with electric eel AChE.<sup>33</sup> However, for hBChE and hAChE, the enantioselectivity may be larger than 1 order of magnitude.

Assuming in-line substitution, the X-ray structure of non-aged tabun–hBChE reveals that the enzyme is mainly inhibited by P(*R*)-tabun with the dimethylamine group located in the acyl-binding pocket. Stereoselectivity may result from preferred H-bonding of His438 to the ethoxy substituent and interaction of Trp231 with the dimethylamine moiety. The same considerations apply for the structure of non-aged tabun–mAChE,<sup>16</sup> the refinement of which was improved in the present study. The X-ray structure of aged tabun–hBChE also showed enantioselectivity for P(*R*)-tabun; i.e., the electron density shows that the dimethylamine moiety is located in the acyl-binding pocket. The same enantioselectivity was found in the updated refinements of aged tabun–mAChE and from the structure of aged tabun–TcAChE.<sup>34</sup> These observations provide structural evidence that there is a selectivity of cholinesterases for the P(*R*) enantiomer of tabun. This has important implications for the aging pathway. Combining the enantioselectivity results from the solution kinetics with those from the X-ray crystal structures suggests that (–)-tabun is P(*R*)-tabun.

The first X-ray structure of an aged tabun–cholinesterase was made with mouse AChE (PDB code 2C0P).<sup>16</sup> This structure was determined following 4 weeks of aging, which, with an aging half-time of a few hours, should have been sufficient to complete the reaction. Still, an incomplete dealkylation led to an adduct model with the ethoxy group present in the choline-binding pocket and the *N*-dimethyl group substituted by hydroxyl.

That model implied that aging occurs through nucleophilic attack by water on the P–N bond and subsequent scission of that bond. However, the conformation of the adduct in the active site was peculiar. First, the oxygen arising from loss of the dimethylamine was located in the acyl-binding pocket with no possibility for stabilization through formation of a salt bridge. Previous structural data for aged AChEs indicated that the

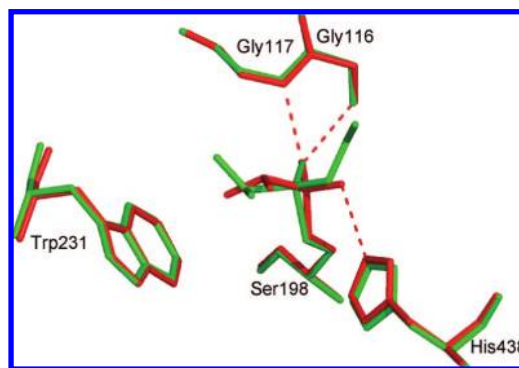


**Figure 7.** Superimposition of active sites of the non-aged (green) and aged (red) tabun–hBChE conjugates.

phosphorus oxygen resulting from aging was stabilized by formation of a salt bridge with His447.<sup>9,10,23,34,35</sup> Second, there were no groups in the acyl pocket that could promote aging. It is generally accepted that the active site of cholinesterase accelerates the aging process. This acceleration is generally thought to involve the histidine from the catalytic triad and the tryptophan from the choline-binding pocket. If the aging process for tabun required similar assistance, the dimethylamine moiety would have been located in the choline-binding pocket. Since the de-dimethylamidated moiety was located in the acyl-binding pocket in the mAChE model, there would have been a rearrangement of the substituents around the phosphorus after aging. Such motions are doubtful in a constrained active-site pocket like that of mAChE. All of these factors suggest that the aged tabun–mAChE model requires refinement.

The new model for aged tabun–mAChE shows unambiguously that the ethoxy substituent underwent dealkylation. The X-ray structure of aged tabun–hBChE and the structure of aged tabun–TcAChE<sup>34</sup> both support this interpretation. The negatively charged phosphoryl oxygen that results from aging forms a salt bridge with the catalytic imidazolium in each case. There is no doubt that aging of these three phosphoramidated cholinesterases proceeds through the classic aging pathway worked out for phosphonylated human AChE.<sup>10,22,35,36</sup> In that mechanism, the imidazolium stabilizes a developing negative charge on the C–O<sup>δ−</sup> oxygen, and a water molecule activated by Glu202 (197 in hBChE) attacks the carbocationic center that appears on the C<sup>δ+</sup>–O carbon, thus leading to scission of the C–O bond, release of the alkoxy moiety, and subsequent formation of the salt bridge between the phosphorus O3-oxygen and the imidazolium.

This mechanism can be extended to tabun–hAChE via the following logical argument. Knowing that (1) dealkylation of tabun–ChE conjugates occurs in three different ChEs, (2) residues lining the active-site gorge of mAChE and hAChE are identical, and (3) hAChE is enantioselective for tabun stereoisomers, we can reasonably state that aging of tabun–hAChE proceeds through dealkylation of the ethoxy substituent.

The formation of the salt bridge between the phosphorus O3-oxygen and the imidazolium of His438 in aged tabun–hBChE induces a small rearrangement of the phosphoramidyl-serine, while the active-site residues, notably His438, do not move (Figure 7). His438 is stabilized by a strong hydrogen bond with

(33) Degenhardt, C.; Van Den Berg, G.; De Jong, L.; Benschop, H. *J. Am. Chem. Soc.* **1986**, *108*, 8290–8291.

(34) Millard, C. B.; Olson, M. A.; Carlacchi, L.; Ordentlich, A.; Barak, D.; Shafferman, A.; Silman, I.; Sussman, J. L. Presented at the International Meeting on Cholinesterases, Perugia, Italy, Sept 26–30, 2004.

(35) Millard, C.; Koellner, G.; Ordentlich, A.; Shafferman, A.; Silman, I.; Sussman, J. L. *J. Am. Chem. Soc.* **1999**, *121*, 9883–9884.

(36) Shafferman, A.; Ordentlich, A.; Barak, D.; Stein, D.; Ariel, N.; Velan, B. *Biochem. J.* **1997**, *324*, 996–998 (Pt 3)

Glu335 and interactions with Phe398 that restrict its mobility (data not shown). The phosphoramidate moiety has to tilt toward His438N $\epsilon$ 2 in order to promote formation of the salt bridge. There is also a significant reinforcement of the interactions between the phosphoryl oxygen and the oxyanion hole in the aged form of tabun–hBChE. This is likely related to an increase in electron density in the oxyanion hole oxygen linked to the delocalization of the new negative charge on the phosphorus O2-oxygen. Similar observations were made during the aging of soman–hBChE (Weik, M., personal communication) and echothiophate–hBChE.<sup>10</sup> These features, taken together, are thought to raise the activation energy needed for the dephosphorylation reaction, thus rendering oxime-mediated reactivation virtually impossible after aging.

Interestingly, as a result of aging, the phosphoramidate tilts so that the dimethylamine moiety is less constrained and the two methyls point toward Trp231 to better fill in the acyl-binding pocket.

By contrast to hBChE, the catalytic histidine of AChEs (His447 in hAChE) is mobile. This was shown in NMR studies of the short strong hydrogen bond of aged TcAChE<sup>37</sup> and in crystal structure studies on non-aged VX–TcAChE.<sup>35</sup> It was suggested that this mobility was related to the lack of aromatic trapping.<sup>38</sup> Indeed, AChEs lack the aromatic residue equivalent to Phe398 in hBChE that provides stabilization for His438. A valine is found at the equivalent position in mAChE, hAChE, and TcAChE. The mobility of His447 is again illustrated in non-aged tabun–mAChE, as described by Ekstrom et al.<sup>16</sup> and reaffirmed in the present study. His447 and Phe338 shift in concert to avoid unfavorable contacts with the phosphoramidate moiety. Surprisingly, His447 adopts a continuum of conformations in the aged form. This was unexpected because the dealkylation and subsequent formation of a salt bridge normally releases the steric constraints on His447 and stabilizes the imidazolium into a well-defined conformation. The continuum of conformations could be due to the partial dealkylation, and to the coexistence of non-aged and aged conformations (Figure 8). The presence of an unknown ligand interfering with Tyr337 and indirectly with Phe338 might also contribute to the conformational disturbance of His447. Despite the conformational heterogeneity, the phosphoramidate moiety tips slightly toward His437 when the His occupies its usual triad position. This leads to formation of the salt bridge as observed in other aged AChE-OP conjugates.<sup>9,35</sup>

Nonaged cholinesterases inhibited by tabun are known to be resistant to most oxime reactivators.<sup>6</sup> It is acknowledged that oximes based on pyridinium aldoxime like HI-6 are too bulky to achieve a favorable orientation of the reactive group in the narrow active site of hAChE.<sup>39–41</sup> A smaller nucleophile capable of slipping in between the aromatic residues would be highly desirable to improve the efficiency of oxime reactivators. However, limited accessibility of the active site might not be the sole cause for the poor reactivation of tabun–ChE con-

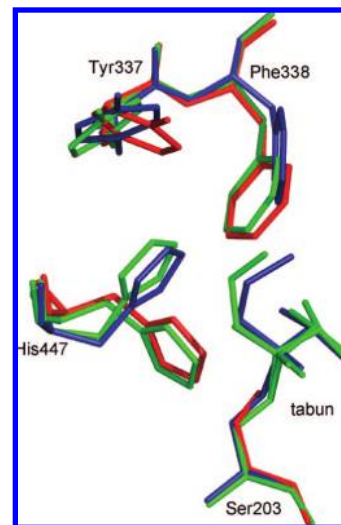


**Figure 8.** Superimposition of active sites of apo (red), non-aged (blue), and aged (green; two conformations, reflecting partial dealkylation of the tabun, are shown) tabun–mAChE conjugates. This figure highlights the conformational heterogeneity of His447, Tyr337, and Phe338.

jugates. The reactivation rate for tabun–hBChE is slow despite the fact that the active site is wide. This suggests that reactivation might be limited by the chemistry of the reaction. Partial delocalization of electron density from the nitrogen lone pair in the P–N bond on the phosphorus atom could reduce its electrophilicity, making it less susceptible to nucleophiles. Quantum mechanics/molecular mechanics (QM/MM) studies of the reactivation reaction based on tabun–mAChE and tabun–hBChE X-ray structures could clarify this point.

Finally, the X-ray structures of tabun–ChEs provide a template on which to design mutants of human cholinesterases that can spontaneously and more efficiently reactivate from OP inhibition. G117H hBChE<sup>42</sup> is a model for such mutations, but more efficient variants are needed. The mutagenesis strategy based on computational design (QM/MM) that was successfully implemented for designing a mutant of hBChE with improved cocaine hydrolase activity<sup>43</sup> could be applied to the design of more active hBChE mutants capable of hydrolyzing OPs.

Efficient BChE-based catalytic bioscavengers would provide a great improvement in prophylaxis, decontamination, and treatment of organophosphate poisoning.

**Acknowledgment.** This work was supported by DGA grant 03co10-05/PEA 01 08 7 to P.M. and by DGA/PEA 08co501 and ANR-06-BLAN-0163 to F.N.

JA804941Z

- (37) Massiah, M. A.; Viragh, C.; Reddy, P. M.; Kovach, I. M.; Johnson, J.; Rosenberry, T. L.; Mildvan, A. S. *Biochemistry* **2001**, *40*, 5682–5690.
- (38) Kaplan, D.; Barak, D.; Ordentlich, A.; Kronman, C.; Velan, B.; Shaffer, A. *Biochemistry* **2004**, *43*, 3129–3136.

- (39) Wong, L.; Radic, Z.; Bruggemann, R. J.; Hosea, N.; Berman, H. A.; Taylor, P. *Biochemistry* **2000**, *39*, 5750–5757.
- (40) Kovarik, Z.; Radic, Z.; Berman, H. A.; Simeon-Rudolf, V.; Reiner, E.; Taylor, P. *Biochemistry* **2004**, *43*, 3222–3229.
- (41) Luo, C.; Leader, H.; Radic, Z.; Maxwell, D. M.; Taylor, P.; Doctor, B. P.; Saxena, A. *Biochem. Pharmacol.* **2003**, *66*, 387–392.
- (42) Millard, C. B.; Lockridge, O.; Broomfield, C. A. *Biochemistry* **1995**, *34*, 15925–15933.
- (43) Pan, Y.; Gao, D.; Yang, W.; Cho, H.; Yang, G.; Tai, H. H.; Zhan, C. G. *Proc. Natl. Acad. Sci. U.S.A.* **2005**, *102*, 16656–16661.

## Five Tyrosines and Two Serines in Human Albumin Are Labeled by the Organophosphorus Agent FP-Biotin

Shi-Jian Ding,<sup>†</sup> John Carr,<sup>†</sup> James E. Carlson,<sup>‡</sup> Larry Tong,<sup>§</sup> Weihua Xue,<sup>§</sup> Yifeng Li,<sup>†</sup> Lawrence M. Schopfer,<sup>§</sup> Bin Li,<sup>§</sup> Florian Nachon,<sup>||</sup> Oluwatoyin Asojo,<sup>†</sup> Charles M. Thompson,<sup>⊥</sup> Steven H. Hinrichs,<sup>†</sup> Patrick Masson,<sup>||</sup> and Oksana Lockridge<sup>\*,§</sup>

Department of Pathology and Microbiology, University of Nebraska Medical Center, Omaha, Nebraska 68198, Applied Biosystems, Framingham, Massachusetts 01701, Eppley Institute, University of Nebraska Medical Center, Omaha, Nebraska 68198, Centre de Recherches d Service de Santé des Armées, Unité d'Enzymologie, BP87, 38702 La Tronche Cedex, France, and Department of Biomedical and Pharmaceutical Sciences, University of Montana, Missoula, Montana 59812

Received April 23, 2008

Tyrosine 411 of human albumin is an established site for covalent attachment of 10-fluoroethoxyphosphinyl-*N*-biotinamidopentyldecanamide (FP-biotin), diisopropylfluorophosphate, chlorpyrifos oxon, soman, sarin, and dichlorvos. This work investigated the hypothesis that other residues in albumin could be modified by organophosphorus agents (OP). Human plasma was aggressively treated with FP-biotin; plasma proteins were separated into high and low abundant portions using a proteome partitioning antibody kit, and the proteins were digested with trypsin. The FP-biotinylated tryptic peptides were isolated by binding to monomeric avidin beads. The major sites of covalent attachment identified by mass spectrometry were Y138, Y148, Y401, Y411, Y452, S232, and S287 of human albumin. Prolonged treatment of pure human albumin with chlorpyrifos oxon labeled Y138, Y150, Y161, Y401, Y411, and Y452. To identify the most reactive residue, albumin was treated for 2 h with DFP, FP-biotin, chlorpyrifos oxon, or soman, digested with trypsin or pepsin, and analyzed by mass spectrometry. The most reactive residue was always Tyr 411. Diethoxyphosphate-labeled Tyr 411 was stable for months at pH 7.4. These results will be useful in the development of specific antibodies to detect OP exposure and to engineer albumin for use as an OP scavenger.

### Introduction

Organophosphorus agents are used in agriculture as pesticides and are stocked by the military as chemical warfare agents. These chemicals are toxic to insects, fish, birds, and mammals. Seizures, respiratory arrest, and death are explained by a cascade of reactions that begins with inhibition of acetylcholinesterase. Although acetylcholinesterase in red blood cells and butyrylcholinesterase in plasma are established biomarkers of organophosphorus ester (OP)<sup>1</sup> exposure, additional biomarkers are being sought. Albumin has the potential to serve as a new biomarker of OP exposure (1, 2). Albumin has been reported to covalently bind diisopropylfluorophosphate (DFP), sarin, soman, cyclosarin, tabun, 10-fluoroethoxyphosphinyl-*N*-biotinamido pentyldecanamide (FP-biotin), chlorpyrifos oxon (CPO), and dichlorvos (2–6) and to hydrolyze CPO, paraoxon (7, 8), and *O*-hexyl *O*-2,5-dichlorophenyl phosphoramidate (9). Mass spectrometry has identified tyrosine 411 of human albumin as the site for covalent attachment of OP nerve agents and OP pesticides (6). A second site for covalent attachment of soman

was suggested by experiments that found more fluoride ion released than could be accounted for by one site in albumin (3). Pretreatment of albumin with decanoate, a lipid that binds to the Tyr 411 subdomain, inhibited incorporation of 91% of <sup>3</sup>H-DFP, leaving open the possibility that 9% of the <sup>3</sup>H-DFP bound to other sites (10). Crystallization trials of CPO-labeled human albumin yielded gelatinous soft amorphous crystals, further suggesting the likelihood that more than one site was labeled and that labeling was not uniform. The goal of this study was to determine if sites in addition to Tyr 411 could make a covalent bond with OP and to identify the labeled residues.

Our starting premise was that OP bound exclusively to Tyr 411 of human albumin. For certain studies, we wanted 100% labeling on Tyr 411. Therefore, we treated albumin with excess CPO. The sample was checked by mass spectrometry to confirm the site of OP labeling, and to our surprise, we found several CPO-labeled peptides.

Our studies with human plasma were initiated with the goal of identifying OP-labeled proteins in human plasma. We had expected to identify several FP-biotin-labeled proteins. However, we found only FP-biotin-labeled albumin. The albumin was covalently modified on five tyrosines and two serines. FP-biotin was used for studies with plasma because biotinylated peptides are readily purified by binding to immobilized avidin beads (1, 11).

### Experimental Procedures

**Materials.** FP-biotin (MW 592.32) was custom synthesized in the laboratory of Dr. Charles M. Thompson at the University of Montana (Missoula, MT) (12). FP-biotin was dissolved in methanol and stored at –80 °C. CPO (ChemService Inc. West Chester, PA;

\* To whom correspondence should be addressed. Tel: 402-559-6032. Fax: 402-559-4651. E-mail: olockrid@unmc.edu.

<sup>†</sup> Department of Pathology and Microbiology, University of Nebraska Medical Center.

<sup>‡</sup> Applied Biosystems.

<sup>§</sup> Eppley Institute, University of Nebraska Medical Center.

<sup>||</sup> Unité d'Enzymologie.

<sup>⊥</sup> University of Montana.

<sup>1</sup> Abbreviations: CPO, chlorpyrifos oxon; DFP, diisopropylfluorophosphate; FP-biotin, 10-fluoroethoxyphosphinyl-*N*-biotinamido pentyldecanamide; OP, organophosphorus ester; LC/MS/MS, liquid chromatography tandem mass spectrometry; MALDI-TOF-TOF, matrix-assisted laser desorption tandem time-of-flight mass spectrometry.

MET-674B) was dissolved in ethanol and stored at  $-80^{\circ}\text{C}$ . DFP, a liquid with a concentration of 5.73 M, was from Sigma (D0879). Soman from CEB (Vert-le-Petit, France) was dissolved in isopropanol. A Proteome Partitioning Kit, ProteomeLab IgY-12 High Capacity in Spin Column format contained IgY antibodies directed against the 12 most abundant proteins in human plasma (Beckman Coulter #A24331 S0510903) including albumin, IgG, fibrinogen, transferrin, IgA, IgM, HDL (apo A-I and apo A-II), haptoglobin,  $\alpha$ -1-antitrypsin,  $\alpha$ -1-acid glycoprotein, and  $\alpha$ -2-macroglobulin. Cibacron blue 3GA agarose (Sigma, C1535) bound 10–20 mg of human albumin per mL of gel. Porcine trypsin (Promega, Madison, WI; V5113 sequencing grade modified trypsin) at a concentration of  $0.4\text{ }\mu\text{g}/\mu\text{L}$  in 50 mM acetic acid was stored at  $-80^{\circ}\text{C}$ . Pepsin (Sigma, St. Louis, MO; P6887 from porcine gastric mucosa) was dissolved in 10 mM HCl to make a 1 mg/mL solution and stored at  $-80^{\circ}\text{C}$ . Monomeric avidin agarose beads (#20228) were from Pierce Co. NeutrAvidin agarose beads (#29202) were from Thermo Scientific (Rockford, IL). Human plasma (EDTA anticoagulant) was from an adult male, who had fasted overnight before donating blood. Fatty acid free human albumin (Fluka 05418) was from Sigma/Aldrich.

**Procedures for FP-Biotin-Labeled Plasma. Separation of Low and High Abundance Proteins in Human Plasma.** Two hundred microliters of human plasma were fractionated into low and high abundance proteins by processing 20  $\mu\text{L}$  of plasma at a time on the Beckman Coulter Proteome IgY Spin column depletion kit. The yield of high abundance proteins was 4800  $\mu\text{g}$  in 400  $\mu\text{L}$ . Of this, 123  $\mu\text{L}$  was labeled with FP-biotin, 123  $\mu\text{L}$  was used as a negative control, and the remainder was used for determination of protein concentration.

**High Abundance Proteins Labeled with FP-Biotin, Digested with Trypsin, and Purified on Monomeric Avidin.** The high abundance fraction of plasma had albumin as its major component. A 123  $\mu\text{L}$  aliquot of the high abundance fraction was treated with 1.25  $\mu\text{L}$  of 20 mM FP-biotin for 48 h at  $37^{\circ}\text{C}$  at pH 8.0. The final FP-biotin concentration was 200  $\mu\text{M}$ . Excess FP-biotin was removed by dialysis against  $2 \times 4\text{ L}$  of 10 mM ammonium bicarbonate.

Proteins, in 8 M urea, were reduced with 5 mM dithiothreitol and alkylated with 40 mM iodoacetamide. The samples were diluted to reduce the concentration of urea to 2 M. Proteins were digested with a 1:50 ratio of trypsin to protein at  $37^{\circ}\text{C}$  overnight. The trypsin was inactivated by heating the sample in a boiling water bath for 10 min. It was necessary to inactivate trypsin because trypsin could have destroyed the avidin protein used in the next step. FP-biotinylated peptides were purified by binding to 0.5 mL of monomeric avidin beads. Nonspecifically bound peptides were washed off with high salt buffers. The column was washed with water to remove salts, and FP-biotinylated peptides were eluted with 10% acetic acid. The eluate was dried in a vacuum centrifuge in preparation for mass spectrometry. The negative control was human plasma treated with everything except FP-biotin.

**Depletion of Albumin on Cibacron Blue, Labeling with FP-Biotin, Digestion with Trypsin, and Purification on NeutrAvidin.** An albumin-depleted plasma sample was prepared by binding 0.6 mL of human plasma to 2 mL of Cibacron Blue and collecting the protein that eluted in 10 mL of 10 mM TrisCl, pH 8.0, containing 0.3 M NaCl. About 70% of the albumin was removed from the plasma sample by this procedure. The protein was desalted, concentrated to 0.5 mL, and labeled with 100  $\mu\text{M}$  FP-biotin at  $37^{\circ}\text{C}$  for 16 h in 10 mM ammonium bicarbonate. The labeled protein was denatured in 8 M urea, reduced with dithiothreitol, carbamidomethylated with iodoacetamide, and desalted on a spin column. The yield was 2000  $\mu\text{g}$  in 500  $\mu\text{L}$ . The entire sample was digested with 40  $\mu\text{g}$  of trypsin (Promega) at  $37^{\circ}\text{C}$  overnight. The FP-biotinylated tryptic peptides were bound to 0.1 mL of NeutrAvidin beads, washed with high salt buffers and water, and eluted with 45% acetonitrile and 0.1% formic acid.

**Mass Spectrometry on QSTAR Elite and QTRAP 2000.** Five micrograms of the high abundance FP-biotinylated peptides purified with monomeric avidin beads was analyzed on the QSTAR elite liquid chromatography tandem mass spectrometry (LC/MS/MS)

system with ProteinPilot 2.0 software at the Applied Biosystems laboratories (Framingham, MA).

A second 5  $\mu\text{g}$  aliquot from the same protein preparation, a negative control sample, and the NeutrAvidin purified peptides were analyzed by LC/MS/MS on the QTRAP 2000 mass spectrometer (Applied Biosystems) at the University of Nebraska Medical Center with Analyst 1.4.1 software. The digest was dried in a vacuum centrifuge and dissolved in 5% acetonitrile and 0.1% formic acid to make  $0.5\text{ }\mu\text{g}/\mu\text{L}$ . A 10  $\mu\text{L}$  aliquot was injected into the HPLC nanocolumn (#218MS3.07515 Vydac C18 polymeric rev-phase, 75  $\mu\text{m}$  i.d.  $\times$  150 mm long; P.J. Cobert Assoc, St. Louis, MO). Peptides were separated with a 90 min linear gradient from 0 to 60% acetonitrile at a flow rate of  $0.3\text{ }\mu\text{L}/\text{min}$  and electrosprayed through a nanospray fused silica emitter (360  $\mu\text{m}$  o.d., 75  $\mu\text{m}$  i.d., 15  $\mu\text{m}$  taper, New Objective) directly into the QTRAP 2000, a hybrid quadrupole linear ion trap mass spectrometer. An ion spray voltage of 1900 V was maintained between the emitter and the mass spectrometer. Information-dependent acquisition was used to collect MS, enhanced MS, and MS/MS spectra for the three most intense peaks in each cycle, having a charge of +1 to +4, a mass between 400 and 1700  $m/z$ , and an intensity >10000 counts per s. All spectra were collected in the enhanced mode, that is, using the trap function. Precursor ions were excluded for 30 s after one MS/MS spectrum had been collected. The collision cell was pressurized to 40  $\mu\text{Torr}$  with pure nitrogen. Collision energies between 20 and 40 eV were determined automatically by the software, based on the mass and charge of the precursor ion. The mass spectrometer was calibrated on selected fragments from the MS/MS spectrum of Glu-Fibrinopeptide B. MS/MS spectra were submitted to Mascot for identification of labeled peptides and amino acids (13). MASCOT identified FP-biotinylated Y\*LYEIAR (score 17), HPY\*FYAPELFFAK (score 14), and MPCAEDY\*LSVVLNQLCVLHEK (score 15) but none of the other FP-biotinylated peptides. The others were identified by manually searching the MS/MS data files using the Extracted Ion Chromatogram feature of the Analyst software. The scores were low because the software did not recognize the characteristic fragments of FP-biotin at 227, 312, and 329. It also did not recognize the 591 ion of FP-biotin or the FP-biotin-tyrosine immonium ions at 708 and 691 or fragments containing dehydroalanine in place of serine. The ions that Mascot did not recognize were often very intense.

The MASCOT modification file is an open source software called UNIMOD. The FP-biotin modification on serine, threonine, and tyrosine was introduced according to the instructions found on the Web site <http://www.unimod.org>. Access to the modification is freely available to all MASCOT users in the Variable Modifications menu under the name FP-biotin. Fragments of FP-biotin are not part of the MASCOT modification file. Peptides yielding FP-biotin fragments at 227, 312, and 329 amu were identified using the Extracted Ion Chromatogram feature of ABI's Analyst software. Neutral loss of fragments of FP-biotin were identified by manual inspection of MS/MS spectra.

**Mass Spectrometry by Matrix-Assisted Laser Desorption Tandem Time-of-Flight Mass Spectrometry (MALDI-TOF-TOF) 4800.** A 0.5  $\mu\text{L}$  aliquot of essentially salt-free samples was spotted on a MALDI target plate, air-dried, and overlaid with 0.5  $\mu\text{L}$  of 10 mg/mL  $\alpha$ -cyano-4-hydroxy cinnamic acid in 50% acetonitrile and 0.1% trifluoroacetic acid. MS spectra were acquired using a MALDI-TOF-TOF 4800 (Applied Biosystems), with a laser power of 3000 V, in positive reflector mode. Each spectrum was the average of 500 laser shots. The mass spectrometer was calibrated against des-Arg-Bradykinin (904.468 Da), angiotensin 1 (1296.685 Da), Glu-Fibrinopeptide B (1570.677 Da), and neurotensin (1672.918 Da) (Cal Mix 1 from Applied Biosystems).

**Procedures for Pure Albumin. Percent OP-Labeled Tyr 411 Monitored by MALDI-TOF.** A 5  $\mu\text{L}$  aliquot of 10 mg/mL albumin was diluted with 5  $\mu\text{L}$  of 1% trifluoroacetic acid and digested with 2  $\mu\text{L}$  of 1 mg/mL porcine pepsin for 1–2 h at  $37^{\circ}\text{C}$ . The digest was diluted with 50% acetonitrile and 0.1% trifluoroacetic acid to give a final protein concentration of about 0.5 mg/mL. A 0.5  $\mu\text{L}$  aliquot was spotted on the MALDI target plate, dried, and

overlaid with 0.5  $\mu\text{L}$  of 10 mg/mL  $\alpha$ -cyano-4-hydroxy cinnamic acid. MS spectra were acquired with the laser set at 3000 V and were saved to Data Explorer. When the saved spectrum was opened in Data Explorer, the cluster areas appeared in an output window. Percent OP-labeled Tyr 411 was calculated by dividing the cluster area of the labeled peptide by the sum of the cluster areas for the unlabeled and labeled peaks. The unlabeled peptides were  $^{409}\text{VRYT-KKVPQVSTPTL}^{423}$  (1717.0 amu) and  $^{408}\text{LVRYTKKVPQVSTPTL}^{423}$  (1830.1 amu). After covalent bond formation with CPO, these masses increased by 136 amu to become 1853.0 and 1966.1 amu. After covalent bond formation with FP-biotin, these masses increased by 572.3 to become 2289.3 and 2402.4 amu.

**Prolonged Treatment of Albumin with CPO.** At the time that we prepared CPO-labeled human albumin, we knew that Tyr 411 was labeled by CPO and had no reason to suspect that other residues might also be labeled. CPO dissolved in ethanol was added to an albumin solution in 10 mM ammonium bicarbonate, pH 8.3, and 0.01% sodium azide in six additions over a 1 month period.

The labeling efficiency was poor when the albumin concentration was 500 mg/mL, so the albumin was diluted to 35 mg/mL, and then to 5 mg/mL, and finally to 1 mg/mL. The final ratio was 7.7  $\mu\text{mol}$  of albumin to 146  $\mu\text{mol}$  of CPO. During the 1 month labeling time, the decision to add more CPO was based on the percent Tyr 411 labeled. No further additions of CPO were made after 85% of the Tyr 411 had been labeled. The labeled albumin was dialyzed against 10 mM potassium phosphate, pH 7.0, and 0.01% azide and processed for LC/MS/MS analysis in the QTRAP mass spectrometer.

**Identification of the Most Reactive Residues.** The conditions reported to label 1 mol of albumin with 1 mol of DFP were used (10). Human albumin (1.8 mg/mL) in 10 mM TrisCl, pH 8.0, was treated with a 20-fold molar excess of DFP for 2 h at room temperature. The reaction was stopped by the addition of solid urea to 8 M and boiling for 10 min in the presence of 10 mM dithiothreitol. Free sulfhydryl groups were alkylated with iodoacetamide. The carbamidomethylated albumin was dialyzed against  $2 \times 4$  L of 10 mM ammonium bicarbonate and digested with trypsin. Tryptic peptides were subjected to LC/MS/MS on the QTRAP 2000.

The experiment was repeated with FP-biotin, soman, and CPO. A 15  $\mu\text{M}$  solution of albumin in 10 mM TrisCl pH 8.0 was treated with 150  $\mu\text{M}$  FP-biotin or 150  $\mu\text{M}$  soman or 150  $\mu\text{M}$  CPO for 2 h at 22  $^{\circ}\text{C}$ . Samples with intact disulfides were digested with pepsin and analyzed by MALDI-TOF. Carbamidomethylated tryptic peptides were analyzed by LC/MS/MS. Tryptic peptides labeled with FP-biotin were also purified on monomeric avidin beads eluted with 50% acetonitrile and 0.1% formic acid and analyzed by MALDI-TOF-TOF.

**Stability of CPO-Labeled Tyr 411.** The stability of CPO-labeled Tyr 411 in human albumin was tested at pH 1.5, 7.4, and 8.3 after incubation for up to 7 months at 22 and  $-80^{\circ}\text{C}$ . Albumin labeled on 97% of Tyr 411 with diethoxyphosphate was prepared by incubating 1 mg/mL human albumin (15.6  $\mu\text{M}$ ) in 10 mM TrisCl, pH 8.0, and 0.01% sodium azide with 118  $\mu\text{M}$  CPO for 2.5 days at 22  $^{\circ}\text{C}$ . Excess CPO was removed by dialysis of the 8.5 mL solution against  $2 \times 4$  L of 10 mM ammonium bicarbonate, pH 8.3, and 0.01% azide.

**pH 1.5.** The pH of 2.6 mL of the dialyzed CPO-albumin was adjusted to pH 1.5 by adding 2.6 mL of 1% trifluoroacetic acid. Half of the sample was stored at room temperature, and half was divided into 40  $\mu\text{L}$  aliquots and stored at  $-80^{\circ}\text{C}$ .

**pH 7.4.** The pH was adjusted to pH 7.4 by dialyzing 3.3 mL of the CPO-albumin preparation against 4.5 L of 10 mM potassium phosphate, pH 7.4, and 0.01% azide. To avoid freeze-thaw artifacts, samples intended for storage at  $-80^{\circ}\text{C}$  were divided into 20  $\mu\text{L}$  aliquots so that each tube was thawed only once.

**pH 8.3.** The pH of 2.6 mL of CPO-albumin was brought to pH 8.3 by dialysis against 10 mM ammonium bicarbonate and 0.01% sodium azide, pH 8.3. Samples to be stored at  $-80^{\circ}\text{C}$  were divided into 65 tubes each containing 20  $\mu\text{L}$ .

After various times, a tube was removed from  $-80^{\circ}\text{C}$  storage, and the entire contents were digested with pepsin. Samples stored

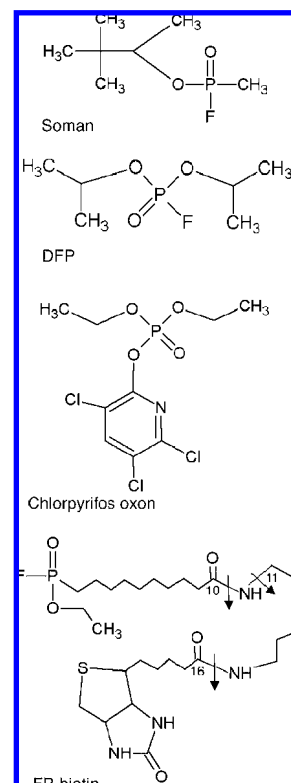


**Figure 1.** Structures of organophosphorus agents. Covalent binding to tyrosine or serine results in loss of the fluoride ion from soman, DFP, and FP-biotin and of the aromatic ring from CPO, so that the added mass is 162.2 for soman, 164.1 for DFP, 136.0 for CPO, and 572.3 for FP-biotin. The arrows in FP-biotin indicate fragmentation sites. A 227 amu ion is produced by cleavage between carbon 16 and the adjacent nitrogen. A 329 amu ion is produced by cleavage between carbon 10 and the adjacent nitrogen. The 312 amu ion is produced by loss of the amine from the 329 ion.

at room temperature were also digested with pepsin. The digests were analyzed by MALDI-TOF, and % labeled Tyr 411 was calculated from cluster areas as described above.

The sample stored at  $-80^{\circ}\text{C}$  in pH 7.4 buffer was analyzed by LC/MS/MS to determine whether sites in addition to Tyr 411 were labeled. The CPO-albumin was denatured, reduced, carbamidomethylated, and digested with trypsin in preparation for LC/MS/MS. The diethoxyphosphate group was found on Tyr 411 and Tyr 138.

## Results

**FP-Biotin Labeled Albumin in Human Plasma.** The structures of the organophosphorus agents are shown in Figure 1. Five tyrosines and two serines in human albumin were labeled with FP-biotin including Tyr 138, Tyr 148, Tyr 401, Tyr 411, Tyr 452, Ser 232, and Ser 287 (Table 1).

Supporting MS/MS spectra for these assignments are in Figures 2–6. A peptide labeled with FP-biotin had ions at 227, 312, and 329 atomic mass units (amu) resulting from fragmentation of FP-biotin (12). Two ions characteristic of covalent binding of FP-biotin to the hydroxyl group of tyrosine are the immonium ion of tyrosine-FP-biotin at 708 amu and its partner ion at 691 amu, produced by loss of  $\text{NH}_3$ . The 708 and 691 amu masses are prominent in Figure 2A,B but barely visible in Figure 3A,B. An additional complexity in Figure 2A is the presence of ions that had lost a 329 or 226 amu fragment from FP-biotin.

The masses in Figure 2A are consistent with the sequence YTK where the added mass of 572 amu from FP-biotin is on Tyr. The complete y-ion series is present (y1, 147.0 amu, Lys;

**Table 1.** FP-Biotinylated Human Albumin Tryptic Peptides Identified by LC/MS/MS<sup>a</sup>

start-end	<i>M<sub>r</sub></i>	sequence	FP-biotinylated
138-144	1499.8	Y*LYEIAR	Y138
146-159	2315.2	HPY*FYAPELLFFAK	Y148
226-233	1452.7	AEFAEVS*K	S232
287-313	3546.6	S*HCIAEVENDEMPADLP <sup>+</sup> LAAD-FVESK	S287
390-402	2230.0	QNCELFEQLGEY*K	Y401
411-413	983.5	Y*TK	Y411
446-466	3090.5	MPCAEDY*LSVVLNQLC <sup>+</sup> VLHEK	Y452

<sup>a</sup>Residue numbers in accession # gi: 3212456 are for the mature albumin protein and do not include the 24 amino acid signal peptide. The added mass from FP-biotin is 572.3 amu. Cysteines were carbamidomethylated, thus adding a mass of 57 amu.

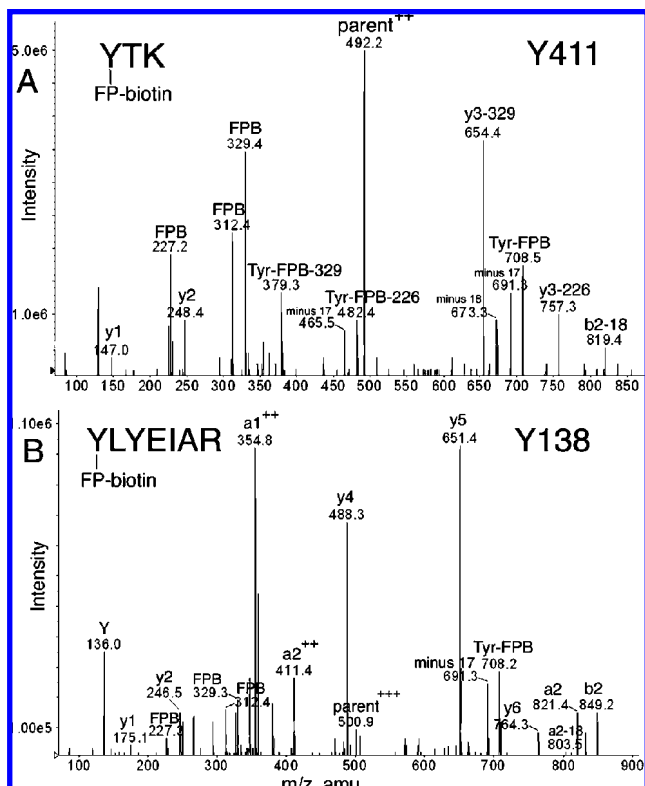


**Figure 2.** MS/MS spectra of albumin peptides labeled with FP-biotin on Tyrosine. (A) Tyr 411 in peptide YTK and (B) Tyr 138 in peptide YLYEIAR are covalently modified by FP-biotin. The characteristic fragments of FP-biotin at 227.2, 312.4, and 329.3 amu are present. Ions characteristic of FP-biotin modification on tyrosine are the immonium ion at 708 amu and the immonium ion minus 17 at 691 amu. Support for modification of the first tyrosine rather than the second in YLYEIAR is the mass of ions a2, b2, and a2<sup>+</sup>. The doubly charged parent ion in panel A had a mass of 492.2 amu. The triply charged parent ion in panel B had a mass of 500.9 m/z.

y2, 248.4 amu, LysThr; and the doubly charged, FP-biotinylated parent ion). Peaks at 227.2, 312.4, 329.4, 691.3, and 708.5 amu are indicative of the presence of FP-biotinylated tyrosine. The remaining major peaks are consistent with various FP-biotinylated tyrosine fragments missing pieces of the FP-biotin moiety.

Peptide YLYEIAR has two tyrosines. A y-ion series (y1–y6) indicates that the FP-biotin label is on the N-terminal Tyr. Additional evidence for labeling on Tyr 138 rather than on Tyr 140 was the presence of the a2 ion at 821.4 amu, the b2 ion at 849.2 amu, the a1<sup>+</sup> ion at 354.8, and the a2<sup>+</sup> ion at 411.4 m/z (Figure 2B). If the FP-biotin had been attached to Tyr 140, the masses would have been a2 = 249, b2 = 277, a1<sup>+</sup> = 68, and a2<sup>+</sup> = 125 amu. Peaks at 226.3, 312.4, and 329.3 are fragments of FP-biotin. Masses at 708.2 and 691.3 amu for FP-

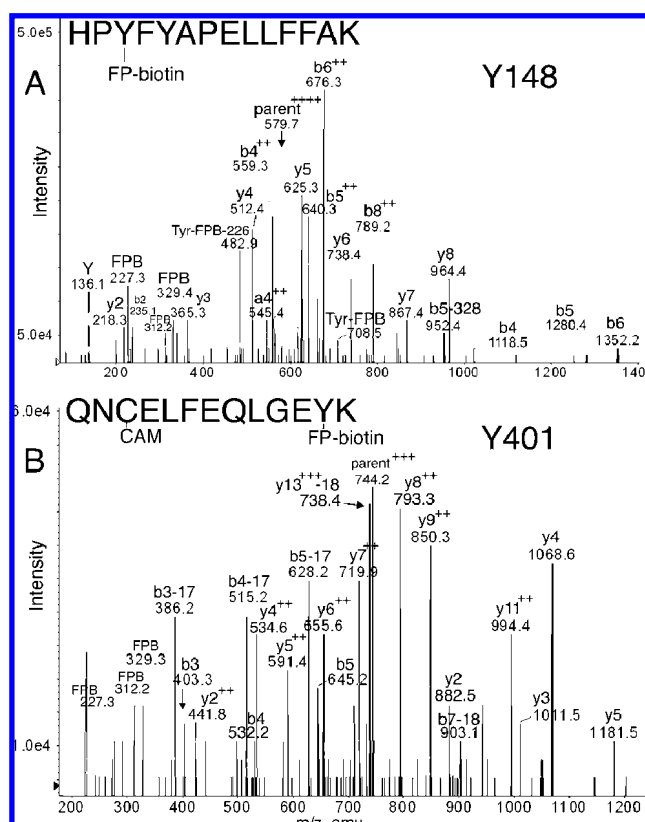


**Figure 3.** MS/MS spectra of albumin peptides labeled with FP-biotin on Tyrosine. (A) Tyr 148 in peptide HPYFYAPELLFFAK is labeled with FP-biotin. The quadruply charged parent ion has a mass of 579.7 m/z. The FP-biotin tyrosine immonium ion is at 708.5; after neutral loss of 226, its mass is 482.9. (B) Tyr 401 in peptide QNCELFEQLGEYK is covalently modified by FP-biotin. The triply charged parent ion in B has a mass of 744.2 m/z.

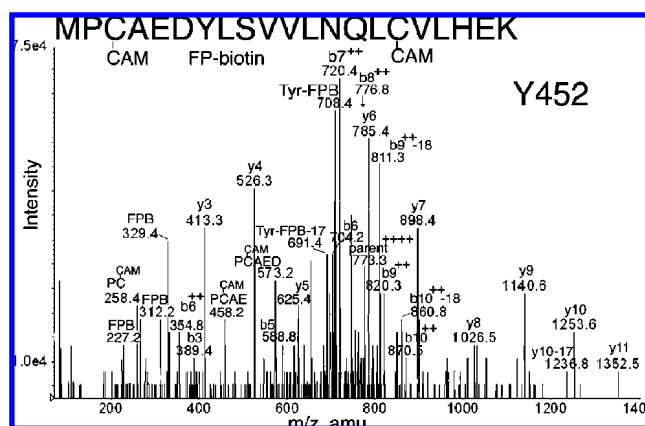


**Figure 4.** MS/MS spectrum of albumin peptide labeled with FP-biotin on tyrosine 452. The quadruply charged parent ion has a mass of 773.3 m/z. The carbamidomethylated cysteine is indicated as CAM. Internal fragmentation at proline yielded the 458.2 ion for PC(CAM)AE and the 573.2 ion for PC(CAM)AED. The characteristic fragments of FP-biotin at 227.2, 312.2, and 329.4 are present. The FP-biotin-tyrosine immonium ion is at 708.4 amu. After loss of an amine, the FP-biotin tyrosine immonium ion has a mass of 691.4 amu.

biotinylated tyrosine confirm the presence of FP-biotinylated tyrosine in the peptide. Analysis of the missed cleavage peptide KYLYEIAR supports labeling on Tyr 138 (data not shown).

Peptide HPYFYAPELLFFAK in Figure 3A also has two tyrosines. Evidence for labeling on Tyr 148 rather than on Tyr 150 is the presence of the b4 ion at 1118.5 amu, the a4<sup>+</sup> ion at 545.4 amu, and the b4<sup>+</sup> ion at 559.3 m/z. The total mass of the b4 fragment (1117.6 amu) is equal to the fragment HPYF

(545 amu) plus the added mass from FP-biotin (572 amu). Of the four residues in the b4 fragment, Tyr 148 is the most reasonable candidate for labeling. Fragment masses for b5 and b6 also support labeling of Tyr 148 rather than Tyr 150. An extensive y-ion series (y2–y8) supports the assignment of this peptide. Masses at 227.3, 312.2, and 329.4 indicate the presence of FP-biotin. Masses at 691.2 and 708.5 amu indicate the presence of FP-biotinylated tyrosine. A similar analysis was made for peptides RHPYFYAPELLFFAK and HPYFYAPELLFFAKR, which differ from HPYFYAPELLFFAK by virtue of missed cleavages (data not shown).

Peptide QNCELFEQLGEYK in Figure 3B is FP-biotinylated on Tyr 401 as demonstrated by the y2 ion at 882.5 amu, the y3 ion at 1011.5 amu, the y4 ion at 1068.5 amu, and the y5 ion at 1181.8 amu. The y2 mass is equal to the sum of Lys (147 amu), Tyr (163 amu), and the added mass of FP-biotin (572 amu). A variety of larger, multiply charged y-ion fragments support the labeling assignment. Prominent b-ion fragments confirm the identity of the peptide. Fragments at 227.2, 312.2, and 329.3 amu indicate the presence of FP-biotin in the peptide.

Peptide MPCAEDYLSVVLNQLCVLHEK in Figure 4 is FP-biotinylated on Tyr 452. The best evidence in support of this interpretation is the doubly charged mass at 720.4 *m/z*, which is consistent with the b7 ion plus the added mass from FP-biotin. The b7 ion consists of MPCAEDY. Of these residues, only Tyr 452 is a reasonable candidate for FP-biotinylation. The b8<sup>+</sup>, b9<sup>+</sup>, and b10<sup>+</sup> ions support this interpretation. The y-series (y3–y11) supports identification of this peptide. Masses at 227.2, 312.2, and 329.4 indicate the presence of FP-biotin. Masses at 691.4 and 708.4 amu indicate the presence of FP-biotinylated tyrosine in this peptide. A missed cleavage form of this peptide, RMPCAEDYLSVVLNQLCVLHEK, was also analyzed, and the results support labeling of Tyr 452 (data not shown).

Peptide SHCIAEVENDEMPADLPSLAADFVESK in Figure 5A is FP-biotinylated on Ser 287. Existence of an FP-biotinylated serine is indicated by the major peak at 591.4 amu. This is a characteristic mass from FP-biotin that appears as the result of  $\beta$ -type elimination of FP-biotin from a serine adduct (Figure 5B), during collision-induced dissociation in the mass spectrometer (12). The complementary peptide fragment arising from this fragmentation contains a dehydroalanine in place of serine. The masses of a b-series ( $\Delta$ b5– $\Delta$ b12) containing a dehydroalanine residue support the elimination of FP-biotin from serine. Of the residues in the b5 fragment (SHCIA), serine at position 287 is a candidate for FP-biotinylation. The cysteine might have been considered a target for labeling, but the overall mass of the fragment is consistent with carbamidomethylation on the cysteine. A y-ion series (y4–y15) supports the identification of the peptide. Additional support for the presence of FP-biotin in the peptide comes from characteristic masses at 312.1 and 329.2 amu. The absence of the characteristic mass at 227 amu is common for FP-biotinylated serine.

The MS/MS spectrum for peptide AEFAEVSK labeled by FP-biotin on Ser 232 is in Figure 6. The b- and y-ion masses support the assigned sequence. Peaks not assigned by Protein Pilot included six dehydroalanine fragments as well as the 591 amu ion of FP-biotin and the 227, 312, and 329 amu fragments of FP-biotin. These additional peaks strongly support the conclusion that Ser 232 of albumin was labeled by FP-biotin. This labeled peptide was detected by the sensitive QSTAR elite mass spectrometer but not by the QTRAP 2000 mass spectrometer. No FP-biotinylated peptides were found in the control plasma that had not been treated with FP-biotin.

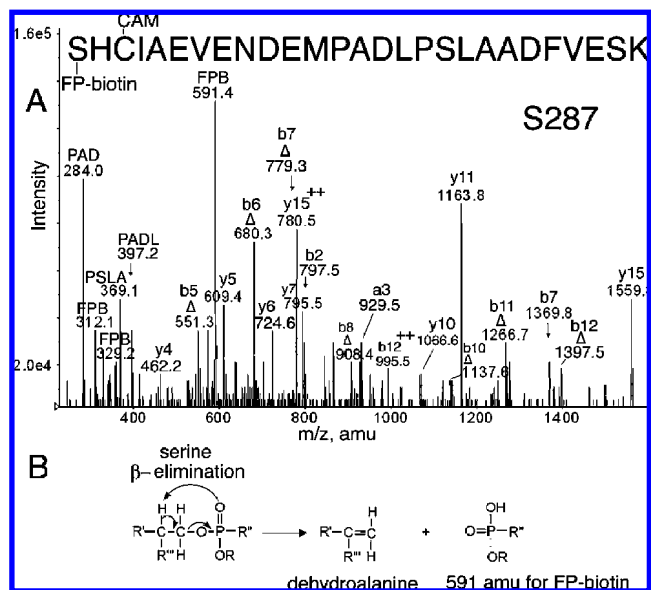


**Figure 5.** (A) MS/MS spectrum of albumin peptide labeled with FP-biotin on Ser 287. The triply charged parent ion has a mass of 1183.8 *m/z*. The carbamidomethylated (CAM) peptide carried the FP-biotin on Ser 287. The evidence for modification on serine is the presence of a b-ion series for the dehydroalanine form of the peptide, designated  $\Delta$ . The 591.4 amu ion is FP-biotin released from serine where the fluoride ion has been replaced by a hydroxyl group. Release of the entire OP accompanied by formation of dehydroalanine is a characteristic of OP bound to serine. Internal fragmentation at proline yielded masses at 284.0 for PAD, 369.1 for PSLA, and 397.2 for PADL. (B) Scheme for  $\beta$ -elimination of the OP label from serine. Fragmentation in the mass spectrometer eliminates the OP from serine and simultaneously converts serine to dehydroalanine.

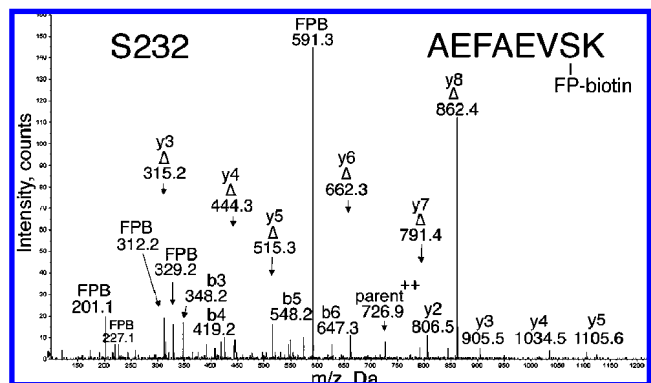


**Figure 6.** MS/MS spectrum of albumin peptide labeled with FP-biotin on Ser 232. This spectrum was acquired on the QSTAR elite mass spectrometer. The doubly charged parent ion is at 726.9 amu. The peak at 591.3 is FP-biotin released from serine, carrying a hydroxyl group in place of fluoride. Four y-ions (y2, y3, y4, and y5) carry FP-biotin on serine, whereas six y-ions ( $\Delta$ y3– $\Delta$ y8) have lost FP-biotin as well as a molecule of water, thus converting serine to dehydroalanine.

**Search for Other FP-Biotin-Labeled Proteins in Human Plasma.** The present method identified 7 FP-biotin-labeled albumin peptides but no FP-biotin-labeled peptides from any other protein. A Western blot hybridized with Streptavidin Alexafluor-680 showed many FP-biotinylated bands in human plasma treated with FP-biotin under our conditions (data not shown). One such protein is FP-biotinylated plasma butyrylcholinesterase (1, 14). However, the FP-biotinylated butyrylcholinesterase peptide was not found with the present methods. FP-biotinylated peptides from proteins other than albumin are difficult to detect in the presence of the overwhelmingly high concentration of albumin. Even after depletion of albumin with Cibacron Blue, the concentration of albumin was still too high

**Table 2. CPO-Labeled Human Albumin Peptides<sup>a</sup>**

start–end	<i>M<sub>r</sub></i>	sequence	CPO-labeled
139–144	1234.6	K(CONH <sub>2</sub> )Y*LYEIAR	Y138
146–159	1877.9	HPYFY*APELLFFAK	Y150
161–174	1797.8	Y*KAAFTECCQAADK	Y161
390–402	1791.8	QNCELFEQLGEY*K	Y401
411–413	547.2	Y*TK	Y411
446–466	2653.2	MPCAEDY*LSVVLNQLCVLHEK	Y452

<sup>a</sup> Peptide KYLYEIAR was carbamylated on the N-terminal Lys by degradation products in urea, adding a mass of 43. Chorpypifos oxon adds a mass of 136 to the labeled tyrosine.

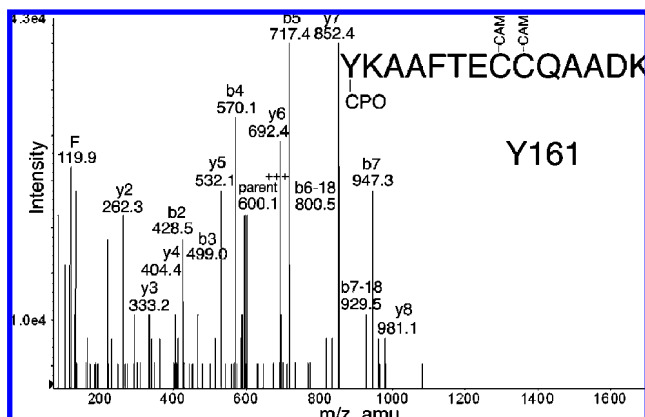


**Figure 7.** MS/MS spectrum of albumin peptide labeled with CPO on Tyr 161. The b2 and b3 ions support labeling on tyrosine.

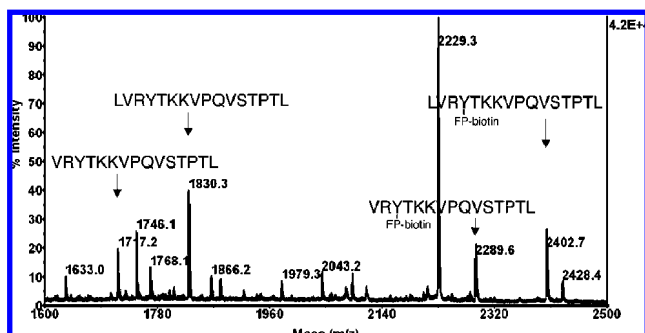


**Figure 8.** MALDI-TOF spectrum of pepsin-digested albumin to show labeling of Tyr 411 by FP-biotin. Pepsin digestion of albumin yields two unlabeled peptides at 1717.2 (VRYTKKVPQVSTPTL) and 1830.3 (LVRYTKKVPQVSTPTL) amu, both containing Tyr 411. Both peptides have a mass shift of 572.3 after reaction with FP-biotin, yielding the peaks at 2289.6 and 2402.7 amu. The FP-biotin is covalently bound to Tyr 411. About 50% of the Tyr 411 is labeled as calculated from cluster areas of the labeled and unlabeled peaks.

to allow detection of other FP-biotinylated peptides. Human plasma contains 5 mg of butyrylcholinesterase and 50000 mg albumin per L. In experiments not described in this report, we found OP-labeled butyrylcholinesterase in human plasma only after the butyrylcholinesterase had been purified by binding to procainamide affinity gel, thus eliminating more than 95% of the albumin.

**Albumin Residues Labeled by CPO.** Prolonged labeling of pure human albumin with CPO resulted in labeling of six tyrosines: Y138, Y150, Y161, Y401, Y411, and Y452 (Table 2). Four of these sites were also labeled by FP-biotin (Y138, Y401, Y411, and Y452). The HPYFYAPELLFFAK peptide was labeled on Tyr 150 by CPO, whereas it was labeled on Tyr 148 by FP-biotin. A new peptide YKAAFTECCQAADK was labeled by CPO (Figure 7) and not by FP-biotin. Labeling on tyrosine is supported by the b ion series. The identity of the peptide is supported by the y2–y8 ions. Additional MS/MS

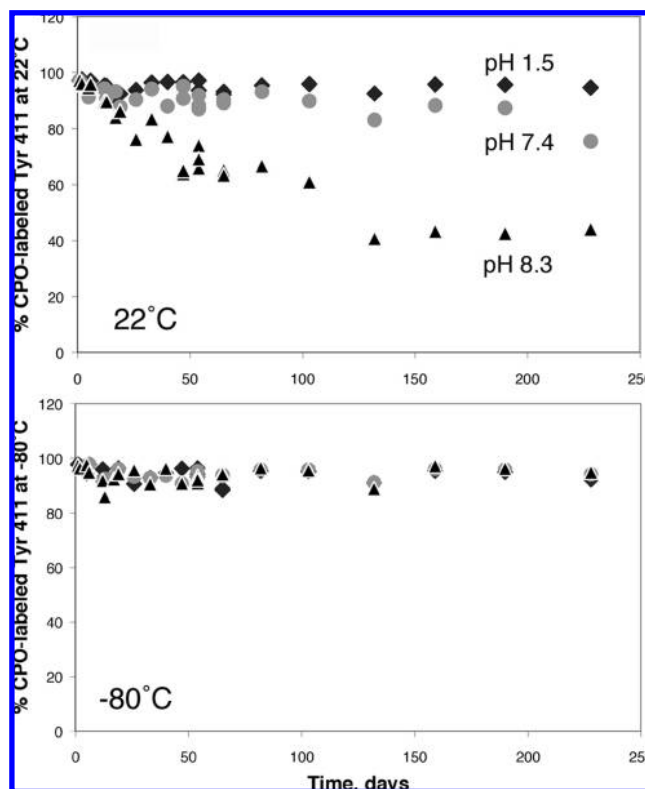


**Figure 9.** Stability of the diethoxyphosphate adduct of human albumin on Tyr 411. Albumin was treated with CPO to achieve 97% labeling of Tyr 411. Excess CPO was removed by dialysis. The pH of the dialyzed albumin was adjusted to 1.5, 7.4, and 8.3. CPO-albumin samples were stored at 22 and –80 °C. After various times of storage, samples were digested with pepsin and % labeling of Tyr 411 was calculated from cluster areas of labeled and unlabeled peptides in the MALDI-TOF mass spectrometer. CPO-labeled Tyr 411 was stable at pH 1.5 and 7.4 when CPO-albumin was stored at 22 °C (top panel), and it was stable at all pH values when CPO-albumin was stored at –80 °C (bottom panel). Storage of CPO-albumin at pH 8.3 at 22 °C resulted in release of half of the diethoxyphosphate group from Tyr 411 after 3.6 months.

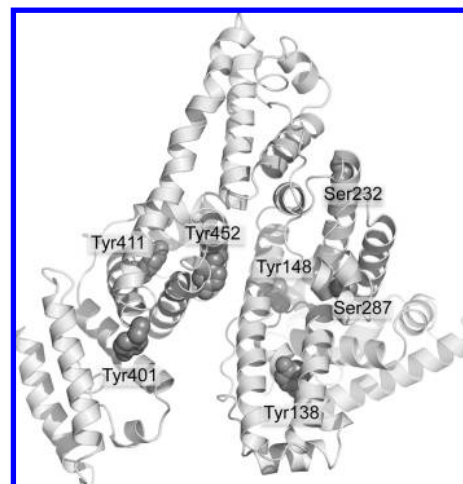


**Figure 10.** Crystal structure of human albumin showing surface location of Tyr 138, Tyr 148, Tyr 401, Tyr 411, Tyr 452, Ser 232, and Ser 287. The residues are shown as space-filled structures. The picture was made with PyMol software using the structure in PDB code 1bm0 (28).

spectra for CPO-labeled peptides are in the Supporting Information (Figures S1–S5).

**Tyr 411 Reacts Most Readily with OP.** The finding that seven tyrosines and two serines make a covalent bond with OP led to the question of which amino acid reacts most readily

with OP. To answer this question, we duplicated the conditions reported to label one molar equivalent of human albumin with DFP (10). MALDI-TOF analysis of pepsin-digested, DFP-treated human albumin suggested that 80% of Tyr 411 was labeled with DFP. MS/MS analysis of a tryptic digest of carbamidomethylated DFP-treated albumin confirmed that Tyr 411 in peptide Y\*TK was labeled. In addition, less than 10% of peptide EFNAETFTFHADICT\*LS\*EK was labeled (on residues T515 and S517).

Albumin treated with FP-biotin for 2 h and digested with pepsin had 52% of its Tyr 411 labeled in peptide VRY\*TKKV-PQVSTPTL as calculated by MALDI-TOF mass spectrometry (Figure 8). The carbamidomethylated, trypsin-digested preparation analyzed by LC/MS/MS confirmed that Tyr 411 in peptide Y\*TK was labeled with FP-biotin. Peptide HPY\*FYAPELLF-FAK was labeled on Tyr 148 with FP-biotin but to less than 10%. A third method to identify FP-biotinylated peptides was purification on monomeric avidin beads followed by MALDI-TOF-TOF analysis. This method yielded only one FP-biotinylated peptide, the Y\*TK peptide labeled on Tyr 411.

Soman-treated albumin (150  $\mu$ M soman for 2 h) analyzed by MALDI-TOF and LC/MS/MS yielded only one labeled peptide. The soman was on Tyr 411.

Albumin treated with CPO for 2 h before digestion with pepsin or trypsin and analyzed by MALDI-TOF and LC/MS/MS was labeled on Tyr 411. Approximately 30% of the Tyr 411 sites were labeled in peptides VRY\*TKKV-PQVSTPTL and LVRY\*TKKV-PQVSTPTL. In addition, less than 5% of Thr 566 in peptide ET\*CFAEEGKK and less than 5% of Thr 236 and Thr 239 in peptide LVT\*DLT\*KVHTECHGDLLECADDR were labeled. We conclude that Tyr 411 is the most OP reactive residue in human albumin.

Support for the conclusion that Tyr 411 is the most OP reactive residue in albumin comes from ref 2. Williams incubated the albumin fraction of human plasma with radiolabeled sarin, digested with trypsin, purified the radiolabeled peptides by HPLC, and analyzed by LC/MS/MS. A single radiolabeled peptide was isolated. Its sequence was YTK with the isopropyl methylphosphonyl group on tyrosine.

**Unstable OP-Ser and OP-Thr but Stable OP-Tyr.** It was noted that serine and threonine residues were labeled in addition to tyrosine when samples had been incubated at pH 8.0–8.3 for 2–48 h but were not found in samples incubated at pH 8.3 for a month. In contrast, OP-labeled tyrosines were found even after 1 month of incubation at pH 8.3. Our stability study of CPO-labeled albumin confirmed that the Tyr 411 adduct was stable (Figure 9). Incubation at pH 7.4 and 22 °C resulted in almost no loss of the CPO label on Tyr 411 after 7 months. In contrast, about half of the label was lost after 3.6 months at pH 8.3 and 22 °C. The CPO-labeled Tyr 411 was stable at pH 1.5 and 22 °C and was stable at all pH values when the labeled albumin was stored at –80 °C. These results suggest that OP-labeled serine and threonine adducts are unstable as compared to OP-labeled tyrosine.

**Surface Location of OP Reactive Residues.** The crystal structure in Figure 10 shows the five tyrosines and two serines that become labeled by FP-biotin. These residues are located on the surface of the albumin molecule where they are available for reaction with OP.

Human albumin has 18 tyrosines and 24 serines but only five tyrosines and two serines made a covalent bond with FP-biotin. Their special reactivity may be explained by a nearby arginine or lysine that stabilizes the ionized hydroxyl of tyrosine or serine.

## Discussion

**Many OP-Reactive Residues in Human Albumin.** Although Tyr 411 is the most OP reactive residue in human albumin, an additional eight amino acids were labeled when the OP concentration was high and the reaction time was prolonged. The reaction with FP-biotin at pH 8.0 resulted in the labeling of five tyrosines and two serines in albumin. CPO labeled six tyrosines (two of which were different from those labeled by FP-biotin) and no serines. We agree with Means and Wu (10) that about 90% of the label is on Tyr 411 and 10% is on other residues.

The  $pK_a$  of the tyrosine hydroxyl group is 10.1 and of the serine hydroxyl group is approximately 16, based on comparison to ethanol (15). In the absence of special activation, less than 1% of the tyrosines and less than 0.000001% of the serines would be expected to be ionized at pH 8.0. Ionized forms react preferentially with OP, so the reactivity of tyrosine and especially of serine with OP would be expected to be poor at pH 8. The special reactivity of Tyr 411 suggests that the  $pK_a$  of this particular tyrosine has been lowered. Means and Wu identified an OP reactive residue in albumin that had a  $pK_a$  of 8.3 (10). It is likely that Tyr 411 corresponds to that residue.

**Albumin as an OP Scavenger.** Our results show that albumin is an OP scavenger, undergoing a covalent reaction with OP. As such, albumin contributes to detoxication of OP. A significant amount of OP can be bound by albumin because the concentration of albumin in serum is high ( $\approx$ 0.6 mM), even though the rate of reaction with OP is slow (3).

Tyrosines with an abnormally low  $pK_a$  are involved directly or indirectly in the catalytic activity of numerous enzymes including glutathione S-transferase (16), asparaginase (17),  $\beta$ -lactamases (18), and old yellow enzyme (19). Lowering the  $pK_a$  of tyrosines in albumin by modifying their environment, either by mutagenesis or by chemical modification of vicinal residues, would increase the reactivity of albumin with OP. Specific nitration of tyrosine by tetranitromethane was found to lower the  $pK_a$  of tyrosine to 6.8 (20). Another nitration reagent of tyrosine, peroxydinitrite, was found to increase the catalytic activity of a few enzymes (21). Thus, specific nitration of tyrosine residues in albumin could also lead to a gain in reactivity of this protein, increasing its scavenging properties.

**No Aging of OP-Tyrosine Adducts.** When soman or DFP are bound to acetylcholinesterase or butyrylcholinesterase, the OP loses an alkyl group in a process called aging (22–25). An aged soman-labeled peptide would have an added mass of 78 rather than 162; an aged DFP-labeled peptide would have an added mass of 122 rather than 164; an aged CPO-labeled peptide would have an added mass of 108 rather than 136. Masses corresponding to aged OP-labeled peptides were not found in MS scans. We conclude that albumin OP adducts on tyrosine do not age.

Support for this conclusion comes from the work of others (2, 26). Human albumin covalently labeled with soman or sarin and treated with sodium fluoride to release the OP yielded intact soman and sarin. Soman-tyrosine adducts isolated from nerve agent-treated guinea pigs contained the pinacolyl group of soman.

The absence of aging is a special advantage for OP-albumin as a biomarker because it allows for a more precise identification of the OP. In contrast, soman and sarin exposure cannot be distinguished when the biomarker is cholinesterase, where aging of OP adducts occurs rapidly.

**OP Labeling of Albumin in Living Animals.** Guinea pigs treated with the nerve agents soman, sarin, cyclosarin, or tabun

have nerve agent-labeled albumin in their blood (2). The OPs are bound to tyrosine. The tabun-tyrosine and soman-tyrosine adducts were detected in blood 7 days postexposure, indicating that the adducts are stable. The adducts had not undergone aging and had not been released from tyrosine by treatment of the guinea pigs with oxime. These are characteristic features of OP adducts on albumin. Mice treated with a nontoxic dose of FP-biotin by intraperitoneal injection had FP-biotinylated albumin in blood and muscle (1). These examples show that OP binds covalently to albumin under physiological conditions and that OP-albumin adducts could therefore be useful as biomarkers of OP exposure (27). Low OP doses make a covalent bond with Tyr 411 of albumin.

**Significance.** Our results suggest that OP exposure could be monitored by mass spectrometry of OP-albumin adducts or with antibodies against OP-albumin adducts. The surface location of the OP-binding sites in albumin suggests that these epitopes may be available for reaction with antibodies. This is in distinct contrast with acetylcholinesterase and butyrylcholinesterase where the OP binding site is buried deep within the molecule, making it unavailable to antibodies. Antibodies to OP-albumin would be primarily against OP-labeled Tyr 411 because Tyr 411 is the most reactive residue at low OP concentrations. The common OP pesticides yield either diethoxyphosphate or dimethoxyphosphate adducts. Therefore, only two antibodies would be needed for detection of exposure to common OP pesticides. The studies described here support investigation into whether albumin could be engineered to become a more efficient OP scavenger.

**Acknowledgment.** Mass spectra were obtained with the support of the Mass Spectrometry & Proteomics core facility at the University of Nebraska Medical Center. This work was supported by U.S. Army Medical Research and Materiel Command W81XWH-07-2-0034 (to O.L.), W81XWH-06-1-0102 (to S.H.H.), NIH CounterACT U01 NS058056-02 (to O.L.), NIH Eppley Cancer Center Grant P30CA36727, NIH Grant U01 ES016102, and NIH CounterACT U44 NS058229 (to C.M.T.), DGA/PEA 08co501 (to F.N.), and DGA Grant 03co010-05/PEA01 08 7 (to P.M.).

**Supporting Information Available:** MS/MS spectra for CPO-labeled peptides (Figures S1–S5). This material is available free of charge via the Internet at <http://pubs.acs.org>.

## References

- (1) Peeples, E. S., Schopfer, L. M., Duysen, E. G., Spaulding, R., Voelker, T., Thompson, C. M., and Lockridge, O. (2005) Albumin, a new biomarker of organophosphorus toxicant exposure, identified by mass spectrometry. *Toxicol. Sci.* **83**, 303–312.
- (2) Williams, N. H., Harrison, J. M., Read, R. W., and Black, R. M. (2007) Phosphorylated tyrosine in albumin as a biomarker of exposure to organophosphorus nerve agents. *Arch. Toxicol.* **81**, 627–639.
- (3) Li, B., Nachon, F., Froment, M. T., Verdier, L., Debouzy, J. C., Brasme, B., Gillon, E., Schopfer, L. M., Lockridge, O., and Masson, P. (2008) Binding and hydrolysis of soman by human serum albumin. *Chem. Res. Toxicol.* **21**, 421–431.
- (4) Schwartz, M. (1982) A serine protease activity of human serum albumin towards 4-methylumbelliferyl-guanidinobenzoate (MUGB) and diisopropyl fluorophosphate (DFP): Implications for the use of MUGB reactivity in amniotic fluid in prenatal diagnosis of cystic fibrosis. *Clin. Chim. Acta* **124**, 213–223.
- (5) Hagag, N., Birnbaum, E. R., and Darnall, D. W. (1983) Resonance energy transfer between cysteine-34, tryptophan-214, and tyrosine-411 of human serum albumin. *Biochemistry* **22**, 2420–2427.
- (6) Li, B., Schopfer, L. M., Hinrichs, S. H., Masson, P., and Lockridge, O. (2007) Matrix-assisted laser desorption/ionization time-of-flight mass spectrometry assay for organophosphorus toxicants bound to human albumin at Tyr411. *Anal. Biochem.* **361**, 263–272.
- (7) Sultatos, L. G., Basker, K. M., Shao, M., and Murphy, S. D. (1984) The interaction of the phosphorothioate insecticides chlorpyrifos and parathion and their oxygen analogues with bovine serum albumin. *Mol. Pharmacol.* **26**, 99–104.
- (8) Ortigoza-Ferado, J., Richter, R. J., Hornung, S. K., Motulsky, A. G., and Furlong, C. E. (1984) Paraaxon hydrolysis in human serum mediated by a genetically variable arylesterase and albumin. *Am. J. Hum. Genet.* **36**, 295–305.
- (9) Sogorb, M. A., and Vilanova, E. (2002) Enzymes involved in the detoxification of organophosphorus, carbamate and pyrethroid insecticides through hydrolysis. *Toxicol. Lett.* **128**, 215–228.
- (10) Means, G. E., and Wu, H. L. (1979) The reactive tyrosine residue of human serum albumin: Characterization of its reaction with diisopropylfluorophosphate. *Arch. Biochem. Biophys.* **194**, 526–530.
- (11) Kidd, D., Liu, Y., and Cravatt, B. F. (2001) Profiling serine hydrolase activities in complex proteomes. *Biochemistry* **40**, 4005–4015.
- (12) Schopfer, L. M., Champion, M. M., Tamblin, N., Thompson, C. M., and Lockridge, O. (2005) Characteristic mass spectral fragments of the organophosphorus agent FP-biotin and FP-biotinylated peptides from trypsin and bovine albumin (Tyr410). *Anal. Biochem.* **345**, 122–132.
- (13) Perkins, D. N., Pappin, D. J., Creasy, D. M., and Cottrell, J. S. (1999) Probability-based protein identification by searching sequence databases using mass spectrometry data. *Electrophoresis* **20**, 3551–3567.
- (14) Schopfer, L. M., Voelker, T., Bartels, C. F., Thompson, C. M., and Lockridge, O. (2005) Reaction kinetics of biotinylated organophosphorus toxicant, FP-biotin, with human acetylcholinesterase and human butyrylcholinesterase. *Chem. Res. Toxicol.* **18**, 747–754.
- (15) Ballinger, P., and Long, F. A. (1960) Acid ionization constants of alcohols. II. Acidities of some substituted methanols and related compounds. *J. Am. Chem. Soc.* **82**, 795–798.
- (16) Atkins, W. M., Wang, R. W., Bird, A. W., Newton, D. J., and Lu, A. Y. (1993) The catalytic mechanism of glutathione S-transferase (GST). Spectroscopic determination of the pKa of Tyr-9 in rat alpha 1-1 GST. *J. Biol. Chem.* **268**, 19188–19191.
- (17) Derst, C., Wehner, A., Specht, V., and Rohm, K. H. (1994) States and functions of tyrosine residues in *Escherichia coli* asparaginase II. *Eur. J. Biochem.* **224**, 533–540.
- (18) Lamotte-Brasseur, J., Dubus, A., and Wade, R. C. (2000) pK(a) calculations for class C beta-lactamases: The role of Tyr-150. *Proteins* **40**, 23–28.
- (19) Kohli, R. M., and Massey, V. (1998) The oxidative half-reaction of Old Yellow Enzyme. The role of tyrosine 196. *J. Biol. Chem.* **273**, 32763–32770.
- (20) Cuatrecasas, P., Fuchs, S., and Anfinsen, C. B. (1968) The tyrosyl residues at the active site of staphylococcal nuclease. Modifications by tetranitromethane. *J. Biol. Chem.* **243**, 4787–4798.
- (21) Ji, Y., Neverova, I., Van Eyk, J. E., and Bennett, B. M. (2006) Nitration of tyrosine 92 mediates the activation of rat microsomal glutathione S-transferase by peroxynitrite. *J. Biol. Chem.* **281**, 1986–1991.
- (22) Michel, H. O., Hackley, B. E., Jr., Berkowitz, L., List, G., Hackley, E. B., Gillilan, W., and Pankau, M. (1967) Ageing and dealkylation of soman (pinacolylmethylphosphonofluoridate)-inactivated eel cholinesterase. *Arch. Biochem. Biophys.* **121**, 29–34.
- (23) Millard, C. B., Kryger, G., Ordentlich, A., Greenblatt, H. M., Harel, M., Raves, M. L., Segall, Y., Barak, D., Shafferman, A., Silman, I., and Sussman, J. L. (1999) Crystal structures of aged phosphorylated acetylcholinesterase: nerve agent reaction products at the atomic level. *Biochemistry* **38**, 7032–7039.
- (24) Nachon, F., Asojo, O. A., Borgstahl, G. E., Masson, P., and Lockridge, O. (2005) Role of water in aging of human butyrylcholinesterase inhibited by echothiophate: The crystal structure suggests two alternative mechanisms of aging. *Biochemistry* **44**, 1154–1162.
- (25) Jansz, H. S., Brons, D., and Warringa, M. G. (1959) Chemical nature of the DFP-binding site of pseudocholinesterase. *Biochim. Biophys. Acta* **34**, 573–575.
- (26) Adams, T. K., Capacio, B. R., Smith, J. R., Whalley, C. E., and Korte, W. D. (2004) The application of the fluoride reactivation process to the detection of sarin and soman nerve agent exposures in biological samples. *Drug Chem. Toxicol.* **27**, 77–91.
- (27) Carter, W. G., Tarhoni, M., Rathbone, A. J., and Ray, D. E. (2007) Differential protein adduction by seven organophosphorus pesticides in both brain and thymus. *Hum. Exp. Toxicol.* **26**, 347–353.
- (28) Sugio, S., Kashima, A., Mochizuki, S., Noda, M., and Kobayashi, K. (1999) Crystal structure of human serum albumin at 2.5 Å resolution. *Protein Eng.* **12**, 439–446.

TX800144Z

# Nerve Agent Analogues That Produce Authentic Soman, Sarin, Tabun, and Cyclohexyl Methylphosphonate-Modified Human Butyrylcholinesterase

Cynthia Gilley,<sup>†</sup> Mary MacDonald,<sup>†</sup> Florian Nachon,<sup>‡</sup> Lawrence M. Schopfer,<sup>§</sup> Jun Zhang,<sup>†</sup>  
John R. Cashman,<sup>†</sup> and Oksana Lockridge<sup>\*,§</sup>

Human BioMolecular Research Institute, 5310 Eastgate Mall, San Diego, California 92121, Département de Toxicologie, Centre de Recherches du Service de Santé des Armées, 24 avenue des Maquis du Grésivaudan, 38700 La Tronche, France, and Eppley Institute, University of Nebraska Medical Center, Omaha, Nebraska 68198-6805

Received March 6, 2009

The goal was to test 14 nerve agent model compounds of soman, sarin, tabun, and cyclohexyl methylphosphonofluoridate (GF) for their suitability as substitutes for true nerve agents. We wanted to know whether the model compounds would form the identical covalent adduct with human butyrylcholinesterase that is produced by reaction with true nerve agents. Nerve agent model compounds containing thiocholine or thiomethyl in place of fluorine or cyanide were synthesized as *Sp* and *Rp* stereoisomers. Purified human butyrylcholinesterase was treated with a 45-fold molar excess of nerve agent analogue at pH 7.4 for 17 h at 21 °C. The protein was denatured by boiling and was digested with trypsin. Aged and nonaged active site peptide adducts were quantified by matrix-assisted laser desorption/ionization time-of-flight (MALDI-TOF) mass spectrometry of the tryptic digest mixture. The active site peptides were isolated by HPLC and analyzed by MALDI-TOF-TOF mass spectrometry. Serine 198 of butyrylcholinesterase was covalently modified by all 14 compounds. Thiocholine was the leaving group in all compounds that had thiocholine in place of fluorine or cyanide. Thiomethyl was the leaving group in the GF thiomethyl compounds. However, sarin thiomethyl compounds released either thiomethyl or isopropyl, while soman thiomethyl compounds released either thiomethyl or pinacolyl. Thiocholine compounds reacted more rapidly with butyrylcholinesterase than thiomethyl compounds. Labeling with the model compounds resulted in aged adducts that had lost the *O*-alkyl group (*O*-ethyl for tabun, *O*-cyclohexyl for GF, isopropyl for sarin, and pinacolyl for soman) in addition to the thiocholine or thiomethyl group. The nerve agent model compounds containing thiocholine and the GF thiomethyl analogue were found to be suitable substitutes for true soman, sarin, tabun, and GF in terms of the adduct that they produced with human butyrylcholinesterase. However, the soman and sarin thiomethyl compounds yielded two types of adducts, one of which was thiomethyl phosphonate, a modification not found after treatment with authentic soman and sarin.

## Introduction

The nerve agents soman, sarin, tabun, and GF are among the most toxic chemicals known (1). Minute quantities can be lethal to humans, as demonstrated in the Tokyo subway attack with sarin where 12 persons died and about 5000 were injured (2). The great toxicity of these agents has led to restriction of their use for investigational purposes, so that only military laboratories have access to these compounds. Nonmilitary research laboratories must use nerve agent simulants, such as diisopropylfluorophosphate, or nerve agent model compounds. We chose to use nerve agent model compounds, whose design suggested that they would yield the same covalently modified protein as the true nerve agents. Stereoselective isomers were synthesized because it is known that the cholinesterases react preferentially with specific stereoisomers of nerve agents (3–6). The present work tested the hypothesis that model compounds of soman, sarin, tabun, and GF would react with human butyrylcholinest-

erase to yield adducts identical to those produced by reaction with true nerve agents. This information will determine the choice of model compounds that will yield suitable nerve agent modified proteins for use in the evaluation of biological targets of nerve agents.

Chromogenic nerve agent analogues containing *p*-nitrophenol or fluorescent 3-chloro-7-oxy-4-methylcoumarin as the leaving group have been synthesized (7, 8). They make adducts identical to those of authentic nerve agents. Therefore, these analogues are useful for screening large enzyme libraries for nerve agent hydrolase activity. Other fluorescent analogues have been synthesized for use in the search for variants of paraoxonase that detoxify nerve agents more rapidly than wild-type paraoxonase (9).

Nerve agent simulants that have no possibility of making an adduct identical to that of a nerve agent include demeton (*S*-2-ethylthioethyl *O,O*-dimethyl phosphorothioate), an analogue of VX; diisopropylfluorophosphate, an analogue of sarin; and dipinacolyl methylphosphonate, an analogue of soman. The first two can be used as substitutes for nerve agents when characterizing organophosphorus hydrolases (10). The third, a nontoxic soman analogue, is used for immunoassay screening of antibodies (11).

\* To whom correspondence should be addressed. Tel: 402-559-6032. Fax: 402-559-4651. E-mail: olockrid@unmc.edu.

<sup>†</sup> Human BioMolecular Research Institute.

<sup>‡</sup> Centre de Recherches du Service de Santé des Armées.

<sup>§</sup> University of Nebraska Medical Center.

## Materials and Methods

**Materials.** Nerve agent model compounds were synthesized at the Human BioMolecular Research Institute (San Diego, CA) (12). The model compounds were dissolved in dimethylsulfoxide to make 100 mM solutions and used immediately. Human butyrylcholinesterase was purified from outdated human plasma by ion exchange chromatography at pH 4.0 followed by affinity chromatography on procainamide-Sepharose, and anion exchange at pH 7 on a Protein-Pak DEAE 8HR 1000 Å, 10 mm × 100 mm HPLC column (Waters/Millipore) (13). The purified butyrylcholinesterase had an activity of 540 units/mL (with 1 mM butyrylthiocholine at 25 °C, pH 7.0) and a protein concentration of 0.75 mg/mL. Sequencing grade modified trypsin (V5113, Promega, Madison, WI) in 50 mM acetic acid at a concentration of 0.4 µg/µL was stored at -80 °C. α-Cyano-4-hydroxycinnamic acid (70990, Fluka, via Sigma, St. Louis, MO) was recrystallized from ethanol, dried, and stored at -20 °C.

**Inhibition of Butyrylcholinesterase.** A 0.25 mL aliquot of butyrylcholinesterase (0.19 mg = 2.2 nmol) in pH 7.4 phosphate-buffered saline was treated with 1 µL of 100 mM nerve agent analogue at 21 °C for 17 h. The molar ratio of butyrylcholinesterase to nerve agent was 1:45.

**Butyrylcholinesterase Activity Assay.** The assay contained 1 mL butyrylthiocholine, 0.5 mM 5,5-dithiobis(2-nitrobenzoic acid) in 2 mL of 0.1 M potassium phosphate, pH 7.0, at 25 °C, and 1 µL of butyrylcholinesterase. The absorbance increase at 412 nm was recorded on a Gilford spectrophotometer interfaced to MacLab 200 (ADInstruments Pty Ltd., Castle Hill, Australia) and a Macintosh computer. The activity was calculated from the extinction coefficient of 13600 M<sup>-1</sup> cm<sup>-1</sup>. Units of activity are µmol substrate hydrolyzed per min.

**Digestion with Trypsin.** The nerve agent-treated BChE was denatured in a boiling water bath for 10 min. The cooled solution received 2 µL of 1 M ammonium bicarbonate to raise the pH to about 8.3 and 10 µL of 0.4 µg/µL trypsin. Digestion was overnight at 37 °C.

**HPLC.** Digests were centrifuged to remove a pellet and injected into a Phenomenex C18 column, 100 mm × 4.6 mm, on a Waters 625 LC system. Peptides were eluted with a 60 min gradient starting with 100% buffer A (0.1% trifluoroacetic acid in water) and ending with 60% buffer B (acetonitrile containing 0.09% trifluoroacetic acid) at a flow rate of 1 mL per min. One milliliter fractions were collected.

**Matrix-Assisted Laser Desorption/Ionization Time-of-Flight (MALDI-TOF)-TOF Mass Spectrometer.** The digest before HPLC separation, as well as each HPLC fraction, was analyzed in the MS mode on the MALDI-TOF-TOF 4800 mass spectrometer (Applied Biosystems, Foster City, CA). A 0.5 µL aliquot was spotted on an Opti-TOF 384 Well Insert (P/N 1016629, Applied Biosystems), dried, and overlaid with 0.5 µL of α-cyano-4-hydroxycinnamic acid (10 mg/mL in 50% acetonitrile and 0.1% trifluoroacetic acid). MS spectra were acquired using delayed extraction in reflector mode with a laser intensity of 3500 V. Each spectrum was the sum of 500 laser shots. All other settings on the instrument were default settings. Default settings included a bin size of 0.5 ns, a final detector voltage of 1.905, and a delay extraction time of 500 ns. The instrument was calibrated with Glu-Fibrinopeptide standards. Spectra were saved to Data Explorer where an output window listed the cluster area for each peak.

The peptide sequence and the identity of the modified amino acid were determined by fragmenting the parent ions in the MS/MS mode of the MALDI-TOF-TOF mass spectrometer. The acquisition method was the factory method MS/MS, 1 kv positive. Default settings included a precursor mass window of ±10 Da and a random pattern of shots. The metastable suppressor was On, and the timed ion selector was enabled. The y ions and b ions were assigned with the aid of the Proteomics Toolkit, a free online fragment ion calculator (<http://db.systemsbio.org>).

**Quantitation of Phosphorylated Peptides.** Relative amounts of phosphorylated peptides before and after aging were calculated

from cluster areas displayed in the output window of Data Explorer. This method of quantitation assumed that the unaged and aged peptides ionize with similar efficiencies. Each sample served as its own internal control because the two peptides whose cluster areas were compared were in the same MALDI spot in the same MALDI-TOF spectrum. They had the same amino acid sequence and the same net charge. The phosphonate in the aged sample, although negatively charged at neutral pH, had no charge in 0.1% trifluoroacetic acid, the solvent for the MALDI matrix. Thus, the net charge on both peptides was the same. The validity of calculating labeled and unlabeled peptide quantities from cluster areas in the same MALDI spot was confirmed by amino acid composition analysis for peptides labeled by reaction with *p*-nitrophenyl acetate (14).

**Safety Consideration.** Nerve agent model compounds are less toxic than authentic nerve agents. To ensure the safety of personnel, only small quantities that would not intoxicate a human were in one vial. Vials were opened in a fume hood. Empty vials and pipet tips were detoxified in 0.1 M sodium hydroxide. Personal protective equipment was worn.

## Results

**Inhibition of Butyrylcholinesterase Activity.** Purified human butyrylcholinesterase (0.75 mg/mL) was treated with a 45 M excess of the nerve agent model compounds listed in Table 1. A 1 µL aliquot was removed after various times to measure enzyme inhibition. After 3 h of incubation at 21 °C, pH 7.4, inhibition levels were 90–99.9% for the thiocholine model compounds (1–8 in Table 1) and for the thiomethyl GF model compounds (9 and 10). However, inhibition levels for the thiomethyl sarin and soman model compounds (11–14) were about 80% for the *Sp* isomers and about 40% for the *Rp* model compounds. The incubations were continued for a total of 17 h at which time all samples were inhibited at least 85%. The least inhibited sample was the one treated with the thiomethyl soman *Rp* analogue 14, which was inhibited about 85%. In summary, the most rapidly reacting inhibitors were the thiocholine model compounds. The most slowly reacting inhibitors were the thiomethyl *Rp* model compounds of sarin and soman.

**Mass Spectrometry of Tryptic Digests To Identify Nerve Agent Adducts on Butyrylcholinesterase.** After 17 h of treatment with nerve agent model compounds, the butyrylcholinesterase samples were denatured by boiling and were digested with trypsin. The digests were spotted on a MALDI plate, and the masses of the labeled active site peptides were determined by MALDI-TOF mass spectrometry.

Table 1 shows the structures of the 14 nerve agent model compounds and the peptide masses observed for the labeled active site tryptic peptides of human butyrylcholinesterase. The amino acid sequence of the 29-residue active site tryptic peptide of human butyrylcholinesterase is SerValThrLeuPheGlyGluSerAlaGlyAlaAlaSerValSerLeuHisLeuLeuSerProGlySerHisSerLeuPheThrArg. The active site serine is residue 8 in the peptide, which corresponds to residue 198 in the mature protein and to residue 226 in accession #P06276, where numbering includes the 28 amino acid signal peptide. The active site serine was covalently modified by the nerve agent model compounds.

Nerve agent model compounds 1 and 2 have thiocholine in place of the cyanide in tabun, while model compounds 3–8 have thiocholine in place of the fluorine atom in GF, sarin, and soman. MALDI-TOF mass spectrometry showed that the reaction of butyrylcholinesterase with nerve agent model compounds 1–8 resulted in covalent binding of the nerve agent to serine 198 and simultaneous release of thiocholine. This reaction is illustrated in Figure 1 with the sarin thiocholine analogue.

**Table 1. Structures of Nerve Agent Model Compounds and Masses of the Butyrylcholinesterase Tryptic Peptide after Labeling and Aging**

#	Structure	analog of	isomer	adduct mass (abundance, %)	mass of aged adduct (abundance, %)
1		tabun	<i>Sp</i>	3063.5 (50±5%)	3036 (50±5%)
2		tabun	<i>Rp</i>	3063.5 (54±2%)	3036 (46±2%)
3		GF	<i>Sp</i>	3088.5 (44±2%)	3006.5 (56±2%)
4		GF	<i>Rp</i>	3088.5 (86±3%)	3006.5 (14±3%)
5		sarin	<i>Sp</i>	3048.5 (74±3%)	3006.5 (26±3%)
6		sarin	<i>Rp</i>	3048.5 (99±1%)	3006.5 (1±1%)
7		soman	<i>Sp</i>	3090.5 (26±4%)	3006.5 (74±4%)
8		soman	<i>Rp</i>	3090.5 (78±5%)	3006.5 (22±5%)
9		GF	<i>Sp</i>	3088.5 (40±1%)	3006.5 (60±1%)
10		GF	<i>Rp</i>	3088.5 (38±2%)	3006.5 (62±2%)
11		sarin	<i>Sp</i>	3048.5 (79±3%) 3036.5 (5±1%)	3006.5 (16±1%)
12		sarin	<i>Rp</i>	3048.5 (76±2%) 3036.5 (13±2%)	3006.5 (11±3%)
13		soman	<i>Sp</i>	3090.5 (26±2%) 3036.5 (19±2%)	3006.5 (55±1%)
14		soman	<i>Rp</i>	3090.5 (8±2%) 3036.5 (70±5%)	3006.5 (22±3%)

<sup>a</sup> Numbers in parentheses (%) indicate the relative abundance of each type of adduct after 17 h of reaction at pH 7.4 and 21 °C for four replicates ± standard deviation. The monoisotopic mass of the singly charged unlabeled peptide is 2928.5 amu. Accession number P06276 for human butyrylcholinesterase.

The mass of the tryptic peptide became 3063.5 after the addition of 135 amu from the tabun analogue (**1** and **2** in Table 1), 3088.5 after the addition of 160 amu from the GF analogue (**3** and **4**), 3048.5 after the addition of 120 amu from the sarin

analogue (**5** and **6**), and 3090.5 after the addition of 162 amu from the soman analogue (**7** and **8**). These masses are consistent with release of thiocholine from model compounds **1–8** upon covalent bond formation with butyrylcholinesterase. The same

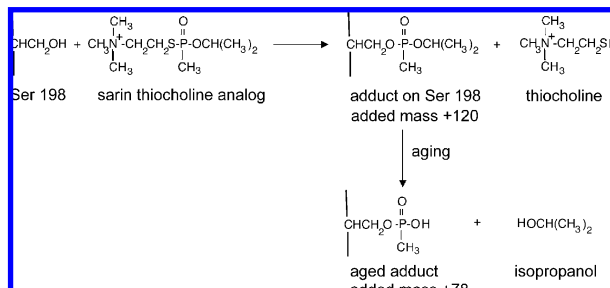


**Figure 1.** Covalent binding of the sarin nerve agent model compounds **5** or **6** to human butyrylcholinesterase. The active site serine (Ser198) forms an initial adduct with an added mass of +120 amu. Thiocholine is released in this step. This is followed by a dealkylation reaction called “aging”, which releases isopropanol.

adducts form when butyrylcholinesterase is treated with authentic tabun, GF, sarin, and soman.

Mass spectrometry also showed that the adducts for compounds **3–8** in Table 1 underwent a dealkylation reaction in which sarin lost isopropyl, GF lost *O*-cyclohexyl, and soman lost pinacolyl alcohols. The aged products all had the same monoisotopic mass of 3006.5, consistent with the structure shown in Figure 1 for the methylphosphonyl adduct whose added mass is 78 amu. The result for aging of the tabun adduct was unclear (**1** and **2** in Table 1). The aged product appeared to have a mass of 3036 amu, which does not allow one to distinguish between 3036.5 amu for loss of the dimethylamine and 3035.5 amu for loss of the *O*-ethyl group. However, the crystal structure of the aged tabun adduct of human butyrylcholinesterase showed that aging resulted in loss of *O*-ethyl (*15*). Because the crystal structure is definitive, we conclude that aging of the tabun adduct results in loss of the *O*-ethyl group.

The thiomethyl model compounds of GF (**9** and **10** in Table 1) made a butyrylcholinesterase adduct with an added mass of 160 amu, which means that the thiomethyl group was released during covalent bond formation with serine 198. Both isomers formed the same adduct, although the *Sp* isomer reacted more rapidly than the *Rp* isomer.

The thiomethyl model compounds of sarin (**11** and **12** in Table 1) released either thiomethyl or isopropyl to form adducts with an added mass of +120 or +108. For example, for the thiomethyl sarin *Rp* isomer **12**, it was estimated that about 76% had an added mass of 120 amu (to give 3048.5) representing loss of thiomethyl, while 13% had an added mass of 108 amu (to give 3036.5) representing loss of isopropyl. The remaining 11% was the aged adduct with a monoisotopic mass of 3006.5 amu.

Similarly, the thiomethyl model compounds of soman (**13** and **14** in Table 1) formed adducts that released either the thiomethyl or the pinacolyl group. For the thiomethyl *Sp* soman isomer **13**, it was estimated that 26% had a mass of 3090.5 representing loss of the thiomethyl group, 19% had a mass of 3036.5 representing loss of pinacolyl, and 55% had a mass of 3006.5 representing loss of both thiomethyl and pinacolyl groups. In contrast, the thiomethyl *Rp* soman isomer **14** formed a majority of 3036.5 amu adduct (70%), representing loss of pinacolyl. Only 22% of the thiomethyl *Rp* soman adduct had aged to 3006.5 amu.

We conclude that the initial adducts with the thiomethyl model compounds of sarin and soman differ from those produced by authentic sarin and soman because 5–70% retained the thiomethyl group on the phosphorus atom. In contrast, all of the thiocholine model compounds yield adducts that are indistinguishable from those produced by authentic nerve agents.

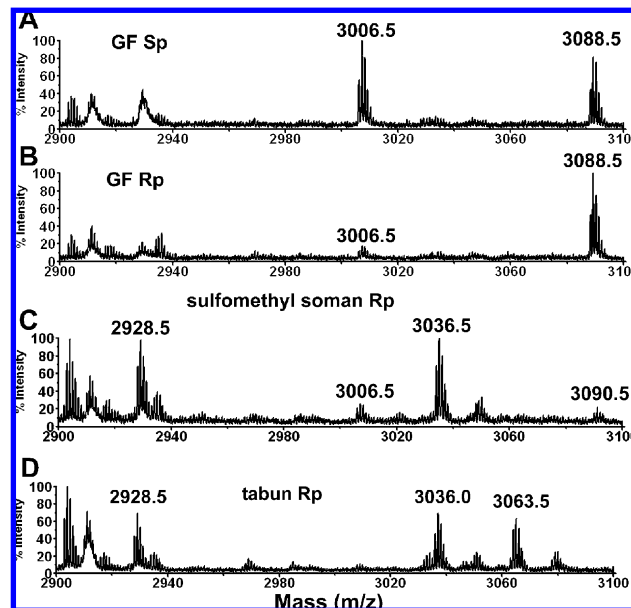


**Figure 2.** MALDI-TOF spectra of tryptic digests of human butyrylcholinesterase inhibited with (A) GF thiocholine *Sp* isomer, (B) GF thiocholine *Rp* isomer, (C) thiomethyl soman *Rp* isomer, and (D) tabun thiocholine *Rp* isomer. The inhibition reaction proceeded at 21 °C for 17 h in pH 7.4 buffer with a 45-fold molar excess of nerve agent analogue. Each MALDI spot contained 0.5  $\mu$ L of 8.8 pmol/ $\mu$ L butyrylcholinesterase digest. The laser intensity was 3500 V.

**Quantitation of Types of Adducts.** Values for the relative abundance of the adducts in Table 1 were calculated from cluster areas in MALDI-TOF spectra of trypsin-digested nerve agent analogue-inhibited butyrylcholinesterase. The calculation assumes that the peptides ionize with similar efficiencies when serine carries the nonaged or aged nerve agent. Examples of MALDI-TOF spectra are in Figure 2. Panels A and B compare the MALDI-TOF spectra of the tryptic digests of butyrylcholinesterase inhibited with the GF *Sp* thiocholine isomer and the GF *Rp* thiocholine isomer (**3** and **4** in Table 1). The peak clusters at 3088.5 are isotopes of the active site peptide labeled on serine with cyclohexyl methylphosphonate. The peak clusters at 3006.5 are isotopes of the labeled active site peptide that has lost the cyclohexyl group as a result of aging. The peak areas for 3006.5 and 3088.5 are approximately equal for GF *Sp* in Figure 2A, showing that about 56% of the labeled butyrylcholinesterase has aged. In contrast, 86% of the labeled peptide in Figure 2B has a mass of 3088.5 and 14% has a mass of 3006.5, indicating that the GF *Rp* isomer yielded low amounts of aged butyrylcholinesterase.

The MALDI-TOF spectrum of Figure 2C shows a prominent peak at 3036.5 for the tryptic peptide of butyrylcholinesterase labeled with the thiomethyl soman *Rp* isomer. About 70% of the labeled peptide is the thiomethyl methylphosphonate adduct with mass 3036.5. This is an unusual adduct that is not found by reaction with authentic soman. The peaks at 3090.5 for the pinacolyl methylphosphonate adduct and at 3006.5 for the aged adduct represent 8 and 22% of the labeled peptide. The unlabeled active site peptide has a monoisotopic mass of 2928.5 amu for the singly charged ion.

Figure 2D shows peaks for the nonaged tabun adduct at 3063.5 and aged tabun adduct at 3036.0. About 46% of the labeled peptide is the nonaged adduct and 54% the aged adduct.

**Verification of Peptide Identities.** The masses in Table 1 are consistent with the interpretation that they are the nerve agent analogue labeled tryptic peptides of human butyrylcholinesterase. However, these masses do not provide irrefutable proof

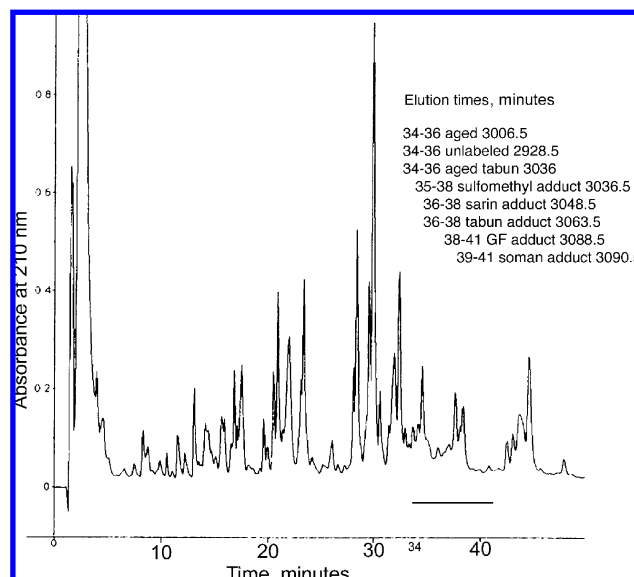


**Figure 3.** Reverse phase HPLC of trypsin-digested human butyrylcholinesterase labeled with thiomethyl sarin *Rp*. The 0.18 mg of labeled human butyrylcholinesterase (2.2 nmol) was digested with trypsin and loaded onto a 100 mm  $\times$  4.6 mm Phenomenex C18 column. Peptides were eluted with a 60 min gradient, from 0 to 60% acetonitrile and 0.1% trifluoroacetic acid at a flow rate of 1 mL/min. A 0.5  $\mu$ L aliquot from each 1 mL fraction was examined in the MALDI-TOF mass spectrometer to identify the fraction that contained the active site peptide. The inset summarizes the elution times for unlabeled peptide and for peptides labeled with tabun, GF, sarin, or soman.

of the peptide identities. Absolute proof was obtained from MS/MS spectra of peptides that had been purified by reverse phase HPLC. Figure 3 shows an HPLC trace monitored at 210 nm for a tryptic digest of butyrylcholinesterase labeled with thiomethyl sarin *Rp* (**11** in Table 1). The aged peptide of mass 3006.5 amu and the unlabeled peptide of mass 2928.5 amu eluted between 34 and 35 min. The thiomethyl phosphonate adduct of mass 3036.5 eluted between 35 and 37 min. The isopropyl phosphonate adduct of mass 3048.5 eluted between 36 and 38 min.

HPLC traces for the other labeled butyrylcholinesterase digests were nearly identical in appearance to the trace in Figure 3. There were no distinguishing peaks that could be assigned to labeling by a particular nerve agent analogue. Although the labeled active site peptides eluted between 34 and 41 min, they coeluted with other peptides. The presence of the other peptides explains why the HPLC traces are not unique for each type of label. The inset to Figure 3 shows that the heavier masses tended to elute later than the lighter masses.

MS/MS spectra were acquired for 0.5  $\mu$ L aliquots of the HPLC fractions by using the MS/MS mode of the MALDI-TOF-TOF mass spectrometer. The eight spectra in Figure 4 are for the active site tryptic peptide of human butyrylcholinesterase. The spectrum in panel A is for the unlabeled peptide, while the spectra in panels B–H are for the peptides labeled on serine 198 (serine 8 in the peptide) by various phosphonates. No distinction is made between the adducts formed by *Sp* and *Rp* isomers because they yielded the same adduct masses.

The unlabeled peptide in Figure 4A has a singly charged parent ion of mass 2928.5 amu. The y ion series supports the amino acid sequence SVTLFGESAGAASVSLHLLSPGSHSLFTR. The most prominent peak, y9 with mass 1001.1, represents cleavage between serine and proline to yield the y9 ion PGSHSLFTR, consistent with the fact that peptide bonds on the N-terminal side of proline are particularly susceptible to

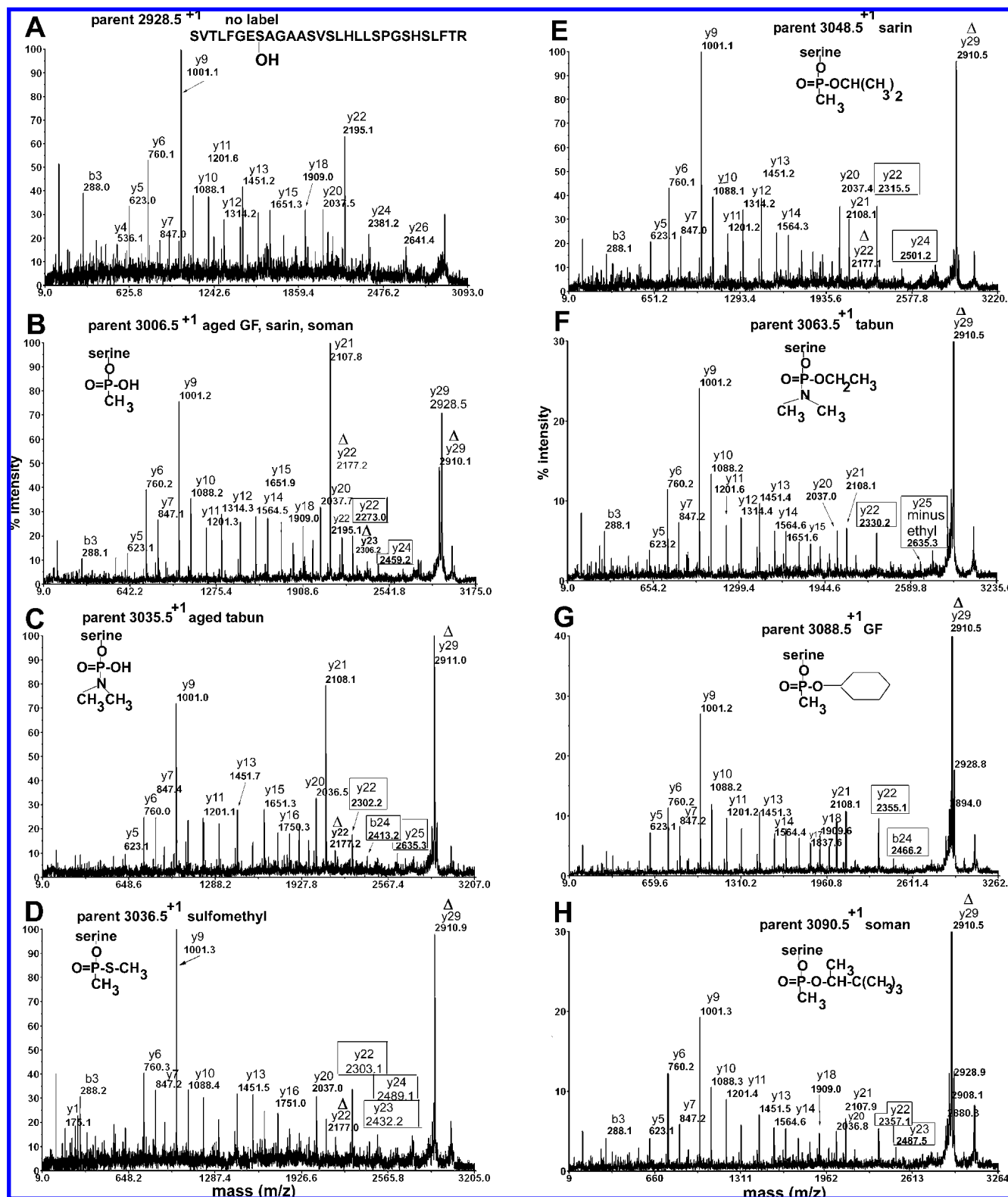
collision-induced dissociation (16). The mass at 2195.1 amu represents cleavage on the N-terminal side of the active site serine to yield the y22 ion SAGAASVSLHLLSPGSHSLFTR.

Figure 4B shows the MS/MS spectrum for the singly charged parent ion of mass 3006.5 where the active site serine is labeled with methylphosphonate. The same derivative was produced by aging of butyrylcholinesterase inhibited by GF, sarin, and soman. The alkyl group that distinguishes GF, sarin, and soman has been enzymatically removed during the aging process to yield an adduct of mass 3006.5 amu. The peak at 2910.1 amu is the  $\Delta$ y29 ion. This ion is consistent with the loss of the organophosphorus agent and loss of a molecule of water from the parent ion to yield dehydroalanine in place of the phosphorylated active site serine. The  $\Delta$ y29 ion is prominent in Figure 4B–H, showing that all organophosphorus agents, regardless of their identity, are easily released from serine in the MS/MS mode of the mass spectrometer. Similarly, the  $\Delta$ y23 ion at 2306.2 contains dehydroalanine in place of serine. Support for our assignment of dehydration at the active site serine and not at one of the other serine residues in the  $\Delta$ y23 ion comes from the fact that the masses of the y21 and smaller y ions are consistent with peptides that contain normal serines. Figure 4B has two types of y22 ions. The y22 ion at 2195.1 has the same mass as the y22 ion in the spectrum for unlabeled peptide in Figure 4A. Its presence in Figure 4B suggests that some of the organophosphorus agent was released from serine without concomitant loss of a molecule of water, so that the serine remained serine. The other y22 ion at 2273.0 amu has the methylphosphonate intact on the active site serine. The y24 ion at 2459.2 amu also carries intact methylphosphonate. These ions provide additional proof for modification of the active site serine by methylphosphonate.

Figure 4C shows the MS/MS spectrum for the singly charged parent ion of mass 3035.5 where the active site serine is labeled with dimethylaminephosphonate. The modification is the result of aging of tabun-labeled butyrylcholinesterase with release of *O*-ethyl. Two types of y22 ions are present. The  $\Delta$ y22 ion at 2177.2 amu has lost the organophosphorus agent and a molecule of water and therefore contains dehydroalanine in place of the active site serine. The y22 ion at 2302.2 amu retains the organophosphorus agent. Similarly, the b24 ion at 2413.2 and the y25 ion at 2635.3 retain the organophosphorus agent. Ions that retain the organophosphorus agent provide additional proof of the mass of the modifying agent.

Figure 4D shows the MS/MS spectrum for the singly charged parent ion of mass 3036.5 where the active site serine is labeled with thiomethyl methylphosphonate. This unusual modification was produced by reaction of butyrylcholinesterase with thiomethyl sarin and thiomethyl soman model compounds. To create this adduct, thiomethyl sarin released the isopropyl group or thiomethyl soman released the pinacolyl group, leaving the thiomethyl group on phosphorus. The thiomethyl derivative is not observed with authentic nerve agents. The y22 ion at 2303.1, the y24 ion at 2489.1, and the y23 ion at 2432.2 amu retain the thiomethyl methylphosphonate on serine. The majority of the organophosphorus agent has been released from serine to yield the dehydroalanine ions  $\Delta$ y29 at 2910.9 and  $\Delta$ y22 at 2177.0. The thiomethyl sarin and soman model compounds also produced the alternative adducts shown in Figure 4E,H.

Figure 4E shows the MS/MS spectrum for the singly charged parent ion of mass 3048.5 where the active site serine is labeled with *O*-isopropyl methylphosphonate by thiomethyl sarin and thiocholine sarin model compounds, compounds **5**, **6**, **11**, and **12**. In this spectrum, most of the label has been released to



**Figure 4.** MS/MS spectra acquired on the MALDI-TOF-TOF mass spectrometer for peptide SVTLFGESAGAASVSLHLLSPGSHSLFTR of human butyrylcholinesterase. (A) No label, (B) methylphosphonate adduct produced by aging of GF, sarin, and soman adducts, (C) aged tabun adduct, (D) thiomethyl methylphosphonate adduct produced by reaction with thiomethyl sarin and soman model compounds, (E) nonaged sarin adduct, (F) nonaged tabun adduct, (G) nonaged GF adduct, and (H) nonaged soman adduct. The Δ symbol designates masses that are consistent with loss of the phosphonate and a molecule of water. The boxed masses designate fragments that retain the phosphonate.

produce the Δy29 dehydroalanine ion. However, the y22 ion at 2315.5 and the y24 ion at 2501.2 indicate that a portion of the peptides retain the *O*-isopropyl methylphosphonate on the active site serine.

Figure 4F shows the MS/MS spectrum for the singly charged parent ion of mass 3063.5 where the active site serine is labeled

with *O*-ethyl, *N*-dimethylphosphonoamidate by tabun model compounds, compounds **1** and **2**. The y22 ion at 2330.2 retains the phosphoamidate on the active site serine. The y25 ion at 2635.3 has lost *O*-ethyl but retains dimethylaminephosphonate.

Figure 4G shows the MS/MS spectrum for the singly charged parent ion of mass 3088.5 where the active site serine is labeled

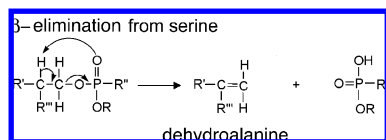


**Figure 5.**  $\beta$ -Elimination converts serine to dehydroalanine and releases the organophosphorus agent from serine.

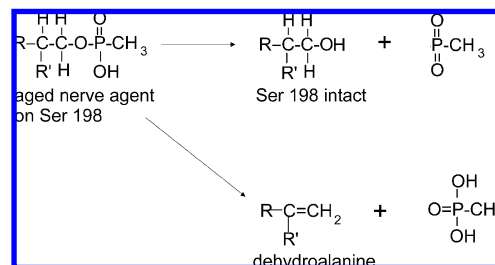
with *O*-cyclohexyl, methylphosphonate by thiocholine GF and thiomethyl GF model compounds, compounds **3**, **4**, **9**, and **10**. The  $y_{22}$  ion at 2355.1 and the  $b_{24}$  ion at 2466.2 retain phosphonate on the active site serine.

Figure 4H shows the MS/MS spectrum for the singly charged parent ion of mass 3090.5 where the active site serine is labeled with *O*-pinacolyl methyl phosphonate by thiocholine soman and thiomethyl soman model compounds, compounds **7**, **8**, **13**, and **14**. This spectrum was taken from a sample labeled with compound **8** (the *Rp* thiocholine analog of soman). The pinacolyl group is still present on this parent ion because the *Rp* analogue did not undergo aging. The  $y_{22}$  ion at 2357.1 and the  $y_{23}$  ion at 2487.5 retain the phosphonate on the active site serine and thus support the parent ion mass in providing proof that the modifying agent was the soman analogue.

**$\beta$ -Elimination To Release Organophosphorus Agent.** The  $\Delta y_{29}$  ion in Figure 4B–H has 29 amino acids but no active site serine and no organophosphorus agent. The masses are consistent with the interpretation that serine was converted to dehydroalanine during a  $\beta$ -elimination reaction that released the organophosphorus agent. Sequence analysis of the modified active site peptide indicates that the conversion to dehydroalanine occurs only on the serine that had been modified with organophosphorus agent. None of the other six serines in this peptide was converted to dehydroalanine. The likely mechanism to explain the loss of organophosphorus agent plus loss of a molecule of water is illustrated in Figure 5. The mass spectrometer promotes  $\beta$ -elimination by excitation of peptide ions during MS/MS acquisition. An analogous  $\beta$ -elimination occurs in the test tube when the sample pH is raised to pH 11 or higher.

**Two Mechanisms To Release Organophosphorus Agent in the Mass Spectrometer.** Figure 4B shows one example of the MS/MS spectrum of the aged adduct for GF, sarin, and soman. We have a total of 12 MS/MS spectra for parent ion 3006.5 for compounds **3**–**14**. Comparison of the 12 MS/MS spectra shows a pattern of fragment ions suggesting two mechanisms of fragmentation for aged adducts. All MS/MS spectra of parent ion 3006.5 have peaks at 2928.5 and 2910.5 amu, which are of comparable high intensity. The  $y_{29}$  ion at 2928.5 is the active site peptide from which the nerve agent has been released while leaving the serine structure intact. The  $\Delta y_{29}$  ion at 2910.5 is the dehydroalanine form of the active site peptide produced by  $\beta$ -elimination. Another consistent feature is that all spectra have a  $y_{22}$  ion at 2195.2 in which the active site serine is intact but has lost the organophosphorus agent. The  $y_{22}$  ion at 2195.2 is always accompanied by a  $\Delta y_{22}$  ion at 2177.2, representing loss of water from the active site serine, although the intensity of this peak is always less than that of the 2195.2 peak. Figure 6 illustrates the two mechanisms of fragmentation for the aged butyrylcholinesterase adduct.

The nonaged adducts all fragment to give an intense  $\Delta y_{29}$  ion at 2910.5 indicative of formation of dehydroalanine in the process of losing the phosphonate (Figure 4C–H). In some cases, a weak  $\Delta y_{22}$  ion at 2177.2 is also observed (Figure 4C–E), which supports formation of dehydroalanine. However, only weak  $y_{29}$  ions at 2928.5 amu are seen for the nonaged adducts (Figure 4G,H). The 2928.5 ion is never as intense as



**Figure 6.** Aged adducts fragment via two mechanisms. In one mechanism, the aged phosphonate group is released from serine while leaving the serine structure intact. The competing pathway releases the organophosphonate and a molecule of water to yield dehydroalanine in place of serine.

the  $\Delta y_{29}$  ion, indicating that the  $\beta$ -elimination mechanism is the dominant mechanism for release of nonaged organophosphonate from serine. Consistent with the low intensity of the 2928.5 ion, a  $y_{22}$  ion at 2195.2 amu was never detected. It is concluded that the nonaged adduct preferentially fragments by the  $\beta$ -elimination mechanism, whereas the aged adduct fragments by two mechanisms. Dephosphorylation to yield serine rather than dehydroalanine is probably promoted by the hydroxyl group on the phosphorus atom in the aged adduct.

Loss of phosphate from phosphoserine-containing peptides also occurs via two routes: one involving loss of 98 amu (formation of dehydroalanine) and the other involving loss of 80 amu. Unlike the case for organophosphorus agents, the pathway leading to dehydroalanine is always much more active than the other. The greater intensity for the 98 amu pathway has, in fact, become diagnostic for the presence of phosphoserine (17).

## Discussion

**Adducts Produced by Authentic Nerve Agents.** Fidler et al. treated purified human butyrylcholinesterase with authentic soman[methyl- $^{14}\text{C}$ ] and reported the fragmentation spectrum of the tryptic peptide in Figure 1 of their paper (18). The parent ion was the aged soman adduct (3008.3 amu for the  $^{14}\text{C}$  methylphosphonate derivative). Their mass spectrum acquired on a Q-TOF Micromass instrument is consistent with our mass spectrum acquired on a MALDI-TOF-TOF mass spectrometer. Both mass spectrometers show a major peak at 2910 amu. This mass is consistent with the dehydroalanine form of the peptide, representing loss of the methylphosphonate and a molecule of water from the parent ion. Precedent for facile loss of phosphorus compounds from serine in the MALDI mass spectrometer comes from studies on phosphoserine-containing peptides, which readily lose 98 Da (phosphate plus water) (17, 19). In the case of nerve agent-labeled butyrylcholinesterase, a few  $y$  ions retain methylphosphonic acid on the active site serine, yielding a set of parallel  $y$  ions, some with the organophosphorus agent and some in the dehydroalanine form. Both types of mass spectrometers yield these parallel sets of ions for the 29-residue tryptic peptide.

Fidler et al. used pepsin to digest sarin-treated butyrylcholinesterase and found a nonaged parent ion mass consistent with addition of sarin and loss of fluorine (18). Their MS/MS spectrum for the nonaged parent ion shows that  $\beta$ -elimination occurs with the nonaged sarin adduct. A parallel set of ions retaining the methylphosphonate label was not seen with the 9-residue peptic peptide; the collision energy for the short peptide converted all of the organophosphorus-labeled serine to dehydroalanine.

Tsuge et al. studied chymotryptic peptides of human butyrylcholinesterase treated with soman, sarin, and VX (20). The b ions in their MS/MS spectra lost the organophosphorus agent and a molecule of water yielding identical sets of b ions for nonaged sarin, nonaged VX, nonaged soman, and aged soman adducts. The nerve agent was identified from the mass of the parent ion, which is unique for each nerve agent. In conclusion, the adducts and MS/MS spectra that we produced with nerve agent model compounds yielded results identical to those produced with authentic nerve agents.

A general principle for fragmentation of organophosphorus-labeled serine adducts can be derived from these studies. The energy of fragmentation can produce a population of ions that has lost the organophosphorus agent and a molecule of water, yielding dehydroalanine in place of the active site serine. Aged as well as nonaged organophosphorus-labeled serine adducts degrade to dehydroalanine in the mass spectrometer. However, not all of the labeled serine will lose the label during fragmentation. This behavior is the same as the well-established behavior of phosphoserine-containing peptides (17, 19, 21).

**Stereoselectivity.** *Rp* and *Sp* nerve agent model compounds gave similar butyrylcholinesterase adducts. Because of the long incubation times between butyrylcholinesterase and the nerve agent model compounds, we did not expressly study the stereoselectivity of adduct formation. However, our data suggest that phosphorylation of butyrylcholinesterase is stereoselective, in agreement with the literature for related nerve agents (3–6). Stereoselectivity is most clearly illustrated in the case of the slowly phosphorylating thiomethyl agents (i.e., 11–14). After 3 h of reaction, 80% of the butyrylcholinesterase was labeled by the *Sp* isomers, while only 40% was labeled by the *Rp*. The percentage of inhibition showed a clear preference for *Sp* > *Rp*. Presumably, evaluation of incubations run for a much shorter time would have shown stereoselective adduct formation for the faster reacting compounds. However, the object of the present study was to quantify the extent of protein adduction, and thus, exhaustive covalent labeling was done. Kinetic studies are the best way to show stereoselectivity of inhibition, and those studies have been done in an accompanying report (12).

***Rp* Stereoisomers Do Not Undergo Aging.** Crystal structure studies of organophosphorus adducts of butyrylcholinesterase and acetylcholinesterase have resulted in an understanding of the mechanism of aging (15, 22, 23). The mechanism requires that the alkyl group that is to undergo aging be positioned close to His 438 and Glu 199 in the choline pocket (22). These residues catalyze the dealkylation reaction called “aging”. Placement of the *Sp* and *Rp* isomers into the active site of butyrylcholinesterase shows that the alkyl group is correctly positioned for dealkylation in the *Sp* isomer but not in the *Rp* isomer. In the *Rp* isomer the alkyl group projects toward the acyl-binding pocket, a location not accessible for interaction with His 438 and Glu 199. The *Rp* stereoisomer is therefore not capable of undergoing dealkylation. The crystal structure results are in conflict with the results in Table 1 where substantial aging is observed for all *Rp* isomers except sarin *Rp* 6. The following discussion rationalizes the mass spectrometry results.

The compounds can be divided into four functionally distinct groups.

1. The tabun adducts (1 and 2) constitute a special case because deamination might occur when the dimethylamino group projects toward the choline pocket. Thus, aging could occur by removal of either dimethylamine (28 amu minus a proton to give a 27 amu loss) or ethyl (29 amu minus a proton to

give a 28 amu loss). If deamination is taken as a valid aging pathway, then either the *Rp* or the *Sp* isomer could age.

2. The *Sp* form of the thiocholine analogue of sarin (5) showed 26% aging, while the *Rp* form (6) showed only 1% aging (well within experimental error of zero). Therefore, this enantiomeric pair behaved as predicted from the geometry of the active site of BChE. Namely, the *Sp* form aged while the *Rp* form did not.
3. Both the *Sp* and the *Rp* forms of the thiomethyl analogue of sarin (11 and 12) yielded two types of initial covalent adduct: one from the release of the thiomethyl moiety (3048.5 amu) and another from the release of the isopropoxy (3036.5 amu). For the *Sp* form, initial release of the thiomethyl would leave the isopropoxy moiety in the choline-binding site, suitably oriented to support aging. For the *Rp* form, initial release of the isopropoxy would leave the thiomethyl in the choline-binding site, suitably oriented to support aging. Therefore, aging of both the *Sp* and the *Rp* forms can be rationalized. The behavior of the thiomethyl model compounds of soman (13 and 14) can be rationalized in the same manner.
4. That leaves only three of the seven enantiomeric pairs for which aging of the *Rp* form is unexplained. These are the thiocholine analogue of cyclosarin (3 and 4), the thiocholine analogue of soman (7 and 8), and the thiomethyl analogue of cyclosarin (9 and 10). In all three cases, the thioalkyl moiety was released from both enantiomers in the initial covalent reaction. No masses were found that would be consistent with release of the alkoxy moiety in the initial covalent reaction. Therefore, the argument that can be made for enantiomeric pairs 11/12 and 13/14 is not applicable for enantiomeric pairs 3/4, 7/8, and 9/10. In these cases, the most logical explanation for aged masses is contamination of the *Rp* preparation by the *Sp* form. The contamination by the *Sp* isomer would need to be no more than 1%. This small amount of contamination could lead to high amounts of aged product because the *Sp* isomers react with butyrylcholinesterase much faster than the *Rp* isomers.

In conclusion, adducts of human butyrylcholinesterase with the *Rp* stereoisomer of cyclosarin, sarin, and soman do not age.

***Rp* Stereoisomer Useful for Identifying the Poison.** The conclusion that adducts with the *Rp* stereoisomer do not age has application to mass spectral diagnosis of exposure to nerve agents. Nerve agents used in war are a mixture of stereoisomers. The *Sp* stereoisomer will yield an aged adduct that is identical for soman, sarin, and GF and is not distinguishable by mass spectrometry. In contrast, the *Rp* stereoisomer will produce a butyrylcholinesterase adduct that will not age. The nonaged butyrylcholinesterase adduct will retain the pinacolyl group of soman, the isopropyl group of sarin, or the cyclohexyl group of GF. The nonaged masses allow identification of the poison to which a person was exposed. However, only a small percentage of the butyrylcholinesterase will have been inhibited by the *Rp* form. Because of the difference in rates of reaction, exposure to a nerve agent mixture of stereoisomers will result in preferential inhibition by the *Sp* form.

**MALDI-TOF Is Useful for Aging Studies.** A MALDI-TOF mass spectrum of a nerve agent-labeled butyrylcholinesterase tryptic digest shows the unlabeled active site peptide as well as the nerve agent-labeled peptide and the aged peptide, all in one spectrum. This allows quantitation of the relative cluster areas and therefore estimation of the amount of each type of adduct present. This approach has been successfully applied to aging studies on both butyrylcholinesterase and acetylcholinesterase, labeled with a variety of organophosphorus agents (24, 25).

Previously, aging could be estimated only from enzyme activity assays where the proportion of enzyme that could not be reactivated with oximes was defined as aged enzyme (26, 27).

## Conclusion

The thiocholine nerve agent model compounds react with human butyrylcholinesterase to yield adducts indistinguishable from those produced by authentic nerve agents. The MALDI-TOF spectra of tryptic digests of nerve agent-labeled human butyrylcholinesterase show the presence of unmodified peptides, adducted peptides, and aged peptides. Two of the three thiomethyl compounds yielded unanticipated adducts. None of the thiocholine compounds yielded evidence of new or unanticipated adducts. Accordingly, the thiocholine-containing nerve agent model compounds appear to give the same adducts as authentic nerve agents. Therefore, they are suitable substitutes for nerve agents in work that aims to study biological effects of nerve agent-modified proteins.

**Acknowledgment.** Supported by NIH Grant U01 NS058038-03 (to J.C.), U01 NS058056-03 (to O.L.), U54NS058183 (to J.Z.), NIH Cancer Center Support Grant P30CA036727, U.S. Army Medical Research & Materiel Command W81XWH-07-2-0034 (to O.L.), U.S. Army Medical Research Institute of Chemical Defense V91ZLK-06-R-0029 (to J.Z.), French Procurement Agency DGA/PEA 08co501 (to F.N.), and Agence Nationale pour la Recherche ANR-06-BLAN-0163 (to F.N.).

## References

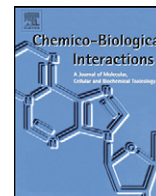
- (1) Munro, N. (1994) Toxicity of the organophosphate chemical warfare agents GA, GB, and VX: Implications for public protection. *Environ. Health Perspect.* 102, 18–37.
- (2) Ohbu, S., Yamashina, A., Takasu, N., Yamaguchi, T., Murai, T., Nakano, K., Matsui, Y., Mikami, R., Sakurai, K., and Hinojara, S. (1997) Sarin poisoning on Tokyo subway. *South Med. J.* 90, 587–593.
- (3) Saxena, A., Viragh, C., Frazier, D. S., Kovach, I. M., Maxwell, D. M., Lockridge, O., and Doctor, B. P. (1998) The pH dependence of dealkylation in soman-inhibited cholinesterases and their mutants: Further evidence for a push-pull mechanism. *Biochemistry* 37, 15086–15096.
- (4) Hosea, N. A., Berman, H. A., and Taylor, P. (1995) Specificity and orientation of trigonal carboxyl esters and tetrahedral alkylphosphonyl esters in cholinesterases. *Biochemistry* 34, 11528–11536.
- (5) Millard, C. B., Lockridge, O., and Broomfield, C. A. (1998) Organophosphorus acid anhydride hydrolase activity in human butyrylcholinesterase: synergy results in a somanase. *Biochemistry* 37, 237–247.
- (6) De Bisschop, H. C., Michiels, K. W., Vlamincx, L. B., Vansteenkiste, S. O., and Schacht, E. H. (1991) Phosphorylation of purified human, canine and porcine cholinesterase by soman. Stereoselective aspects. *Biochem. Pharmacol.* 41, 955–959.
- (7) Briseno-Roa, L., Hill, J., Notman, S., Sellers, D., Smith, A. P., Timperley, C. M., Wetherell, J., Williams, N. H., Williams, G. R., Fersht, A. R., and Griffiths, A. D. (2006) Analogues with fluorescent leaving groups for screening and selection of enzymes that efficiently hydrolyze organophosphorus nerve agents. *J. Med. Chem.* 49, 246–255.
- (8) Li, W. S., Lum, K. T., Chen-Goodspeed, M., Sogorb, M. A., and Raushel, F. M. (2001) Stereoselective detoxification of chiral sarin and soman analogues by phosphotriesterase. *Bioorg. Med. Chem.* 9, 2083–2091.
- (9) Amitai, G., Adani, R., Yacov, G., Yishay, S., Teitlboim, S., Tveria, L., Limanovich, O., Kushnir, M., and Meshulam, H. (2007) Asymmetric fluorogenic organophosphates for the development of active organophosphate hydrolases with reversed stereoselectivity. *Toxicology* 233, 187–198.
- (10) Grimsley, J. K., Calamini, B., Wild, J. R., and Mesecar, A. D. (2005) Structural and mutational studies of organophosphorus hydrolase reveal a cryptic and functional allosteric-binding site. *Arch. Biochem. Biophys.* 442, 169–179.
- (11) Lenz, D. E., Brimfield, A. A., Hunter, K. W., Jr., Benschop, H. P., de Jong, L. P., van Dijk, C., and Clow, T. R. (1984) Studies using a monoclonal antibody against soman. *Fundam. Appl. Toxicol.* 4, S156–S164.
- (12) Barakat, N. H., Zheng, X., Gilley, C. B., MacDonald, M., Okolotowicz, K., Cashman, J. R., Vyas, S., Beck, J. M., Hadad, C. M., and Zhang, J. (2009) Chemical synthesis of two series of nerve agent model compounds and their stereoselective interaction with human acetylcholinesterase and human butyrylcholinesterase. *Chem. Res. Toxicol.* DOI: 10.1021/tx900096j.
- (13) Lockridge, O., Schopfer, L. M., Winger, G., and Woods, J. H. (2005) Large scale purification of butyrylcholinesterase from human plasma suitable for injection into monkeys; a potential new therapeutic for protection against cocaine and nerve agent toxicity. *J. Med. CBR Def. 3*.
- (14) Lockridge, O., Xue, W., Gaydess, A., Grigoryan, H., Ding, S. J., Schopfer, L. M., Hinrichs, S. H., and Masson, P. (2008) Pseudo-esterase activity of human albumin: slow turnover on tyrosine 411 and stable acetylation of 82 residues including 59 lysines. *J. Biol. Chem.* 283, 22582–22590.
- (15) Carletti, E., Li, H., Li, B., Ekstrom, F., Nicolet, Y., Loiodice, M., Gillon, E., Froment, M. T., Lockridge, O., Schopfer, L. M., Masson, P., and Nachon, F. (2008) Aging of cholinesterases phosphorylated by tabun proceeds through O-dealkylation. *J. Am. Chem. Soc.* 130, 16011–16020.
- (16) Breci, L. A., Tabb, D. L., Yates, J. R., and Wysocki, V. H. (2003) Cleavage N-terminal to proline: Analysis of a database of peptide tandem mass spectra. *Anal. Chem.* 75, 1963–1971.
- (17) Annan, R. S., and Carr, S. A. (1996) Phosphopeptide analysis by matrix-assisted laser desorption time-of-flight mass spectrometry. *Anal. Chem.* 68, 3413–3421.
- (18) Fiddler, A., Hulst, A. G., Noort, D., de Ruiter, R., van der Schans, M. J., Benschop, H. P., and Langenberg, J. P. (2002) Retrospective detection of exposure to organophosphorus anti-cholinesterases: Mass spectrometric analysis of phosphorylated human butyrylcholinesterase. *Chem. Res. Toxicol.* 15, 582–590.
- (19) Qin, J., and Chait, B. T. (1997) Identification and characterization of posttranslational modifications of proteins by MALDI ion trap mass spectrometry. *Anal. Chem.* 69, 4002–4009.
- (20) Tsuge, K., and Seto, Y. (2006) Detection of human butyrylcholinesterase-nerve gas adducts by liquid chromatography-mass spectrometric analysis after in gel chymotryptic digestion. *J. Chromatogr., B: Anal. Technol. Biomed. Life Sci.* 838, 21–30.
- (21) Tholey, A., Reed, J., and Lehmann, W. D. (1999) Electrospray tandem mass spectrometric studies of phosphopeptides and phosphopeptide analogues. *J. Mass Spectrom.* 34, 117–123.
- (22) Nachon, F., Asojo, O. A., Borgstahl, G. E., Masson, P., and Lockridge, O. (2005) Role of water in aging of human butyrylcholinesterase inhibited by echothiophate: The crystal structure suggests two alternative mechanisms of aging. *Biochemistry* 44, 1154–1162.
- (23) Millard, C. B., Kryger, G., Ordentlich, A., Greenblatt, H. M., Harel, M., Raves, M. L., Segall, Y., Barak, D., Shafferman, A., Silman, I., and Sussman, J. L. (1999) Crystal structures of aged phosphorylated acetylcholinesterase: nerve agent reaction products at the atomic level. *Biochemistry* 38, 7032–7039.
- (24) Li, H., Schopfer, L. M., Nachon, F., Froment, M. T., Masson, P., and Lockridge, O. (2007) Aging pathways for organophosphate-inhibited human butyrylcholinesterase, including novel pathways for isomathion, resolved by mass spectrometry. *Toxicol. Sci.* 100, 136–145.
- (25) Jennings, L. L., Malecki, M., Komives, E. A., and Taylor, P. (2003) Direct analysis of the kinetic profiles of organophosphate-acetylcholinesterase adducts by MALDI-TOF mass spectrometry. *Biochemistry* 42, 11083–11091.
- (26) Worek, F., Diepold, C., and Eyer, P. (1999) Dimethylphosphoryl-inhibited human cholinesterases: Inhibition, reactivation, and aging kinetics. *Arch. Toxicol.* 73, 7–14.
- (27) Masson, P., Froment, M. T., Bartels, C. F., and Lockridge, O. (1997) Importance of aspartate-70 in organophosphate inhibition, oxime reactivation and aging of human butyrylcholinesterase. *Biochem. J.* 325 (1), 53–61.

TX900090M



Contents lists available at ScienceDirect

## Chemico-Biological Interactions

journal homepage: [www.elsevier.com/locate/chembioint](http://www.elsevier.com/locate/chembioint)

## Covalent binding of the organophosphorus agent FP-biotin to tyrosine in eight proteins that have no active site serine

Hasmik Grigoryan<sup>a</sup>, Bin Li<sup>a</sup>, Erica K. Anderson<sup>a</sup>, Weihua Xue<sup>a</sup>,  
 Florian Nachon<sup>b</sup>, Oksana Lockridge<sup>a</sup>, Lawrence M. Schopfer<sup>a,\*</sup>

<sup>a</sup> Eppley Institute, University of Nebraska Medical Center, 986805 Nebraska Medical Center, Omaha, NE 68198-6805, United States

<sup>b</sup> Unité d'Enzymologie, Département de Toxicologie, Centre de Recherches du Service de Santé des Armées (CRSSA),  
 24 avenue des Maquis du Grésivaudan, 38702 La Tronche, France

## ARTICLE INFO

## Article history:

Received 28 February 2009

Received in revised form 23 March 2009

Accepted 24 March 2009

Available online 2 April 2009

## Keywords:

FP-biotin

Organophosphorus agent

Tyrosine

Non-cholinesterase

Mass spectrometry

## ABSTRACT

Organophosphorus (OP) esters are known to bind covalently to the active site serine of enzymes in the serine hydrolase family. It was a surprise to find that proteins with no active site serine are also covalently modified by OP. The binding site in albumin, transferrin, and tubulin was identified as tyrosine. The goal of the present work was to determine whether binding to tyrosine is a general phenomenon. Fourteen proteins were treated with a biotin-tagged organophosphorus agent called FP-biotin. The proteins were digested with trypsin and the labeled peptides enriched by binding to monomeric avidin. Peptides were purified by HPLC and fragmented by collision induced dissociation in a tandem ion trap mass spectrometer. Eight proteins were labeled and six were not. Tyrosine was labeled in human alpha-2-glycoprotein 1 zinc-binding protein (Tyr 138, Tyr 174 and Tyr 181), human kinesin 3C motor domain (Tyr 145), human keratin 1 (Tyr 230), bovine actin (Tyr 55 and Tyr 200), murine ATP synthase beta (Tyr 431), murine adenine nucleotide translocase 1 (Tyr 81), bovine chymotrypsinogen (Tyr 201) and porcine pepsin (Tyr 310). Only 1–3 tyrosines per protein were modified, suggesting that the reactive tyrosine was activated by nearby residues that facilitated ionization of the hydroxyl group of tyrosine. These results suggest that OP binding to tyrosine is a general phenomenon. It is concluded that organophosphorus-reactive proteins include not only enzymes in the serine hydrolase family, but also proteins that have no active site serine. The recognition of a new OP-binding motif to tyrosine suggests new directions to search for mechanisms of long-term effects of OP exposure. Another application is in the search for biomarkers of organophosphorus agent exposure. Previous searches have been limited to serine hydrolases. Now proteins such as albumin and keratin can be considered.

© 2009 Elsevier Ireland Ltd. All rights reserved.

## 1. Introduction

Organophosphorus agents (OP) are used as insecticides, fuel additives, plasticizers, lubricants, flame retardants, and chemical warfare agents [1,2]. These compounds are toxic to insects, fish, birds and mammals. Exposure can lead to a variety of symptoms culminating in seizures, respiratory arrest and death in acute cases [3]. The traditional targets for organophosphorus agents have long been considered to be the active site serine residues in acetylcholinesterase and butyrylcholinesterase. It is generally accepted that covalent inhibition of acetylcholinesterase is responsible for

most of the clinically relevant symptoms observed upon high dose exposure to OP [3]. However, evidence has been accumulating over the past several years that suggests cholinesterases are not the only clinically relevant targets for OP, especially during low-dose exposure [1,2,4,5].

Investigations in several laboratories have been directed at identifying other proteins with which OP can react covalently. In addition to a variety of serine hydrolases [2,6], reactions of OP with other classes of enzymes and with receptors have been reported [2,7]. Results from our laboratory have demonstrated that non-enzymatic proteins such as transferrin [8], serum albumin [9–11] and tubulin [12] can be covalently modified by OP. For these latter proteins, the reactive amino acid is tyrosine.

Reaction of the organophosphorus agent diisopropylfluorophosphate (DFP) with a tyrosine residue in human serum albumin (and in bovine serum albumin) was reported by Sanger in 1963 [13]. Between 1965 and 1971, DFP was shown to react with tyrosine residues on bromelain [14], papain [15], and lysozyme [16].

\* Corresponding author. Tel.: +1 402 559 6014; fax: +1 402 559 4651.

E-mail addresses: [hgrigoryan@berkeley.edu](mailto:hgrigoryan@berkeley.edu) (H. Grigoryan), [binli@unmc.edu](mailto:binli@unmc.edu) (B. Li), [ericaanderson@mail.unomaha.edu](mailto:ericaanderson@mail.unomaha.edu) (E.K. Anderson), [weihuaxue@gmail.com](mailto:weihuaxue@gmail.com) (W. Xue), [fnachon@crssa.net](mailto:fnachon@crssa.net) (F. Nachon), [olockrid@unmc.edu](mailto:olockrid@unmc.edu) (O. Lockridge), [lmshopf@unmc.edu](mailto:lmshopf@unmc.edu) (L.M. Schopfer).

These findings were consistent with the known reactivity of tyrosine with organophosphorus agents [17]. Interest in the reaction of OP with protein-bound tyrosyl residues appears to have waned after 1970. However, starting in 1999, a resurgence of interest was re-kindled with the recognition that serum albumin provided an alternative to butyrylcholinesterase as a biological marker for exposure to OP [18]. Researchers responsible for this work took advantage of improvements in mass spectrometry that simplified the identification of post-translational modifications on proteins. Subsequent studies on serum albumin (1) identified Tyr411 as the most reactive tyrosine residue on human serum albumin, confirming Sanger's assignment [9]; (2) demonstrated that multiple tyrosine residues from albumin could react with OP [19]; and (3) showed that OP-labeled tyrosine could be detected in rodents that had been treated with sub-lethal doses of OP [11] including nerve agents [20].

To our knowledge, reaction of OP with tyrosyl residues has not been confirmed for any proteins other than those mentioned. If this reaction is wide spread, as we suspect, then it opens a new arena for investigation when considering intoxication due to OP exposure. Reactions with tyrosine could be responsible for intoxication that is not consistent with inhibition of acetylcholinesterase. Demonstrating that tyrosine residues from a wide variety of proteins will react with OP is an essential step for the development of this concept.

In this work, we have expanded the list of proteins that react with OP at tyrosine to include: human alpha-2-glycoprotein 1 zinc, human kinesin 3C, human keratin 1, bovine actin, murine ATP synthase beta, murine adenine nucleotide translocase 1, bovine chymotrypsinogen and porcine pepsin. We suggest that covalent reaction of OP with tyrosine is a general phenomenon that can be expected to occur for a large number of proteins.

Our findings may have application to diagnosis and treatment of OP exposure. Proteins that have no active site serine may serve as biomarkers of exposure. In the future it may be possible to develop antibodies to the new OP-labeled biomarkers to use for screening OP exposure. The recognition of a new OP-binding motif to tyrosine suggests new directions to search for mechanisms of long-term effects of OP exposure.

## 2. Materials and methods

### 2.1. Materials

Human alpha-2-glycoprotein 1 zinc was isolated from plasma. Human kinesin KIF3C motor domain was from Cytoskeleton Inc. (Denver, CO #KF01). Human epidermal keratin (#K0253), bovine actin (#A3653), bovine DNase (#D4527), porcine pepsin (#P6887), chicken lysozyme (#L6876), bovine RNase A (#R5125), bovine insulin (#I5500), diisopropylfluorophosphate (#D0879) and iodoacetamide (#I6125) were from Sigma (St. Louis, MO). Human IgG was from Fluka/Sigma (St. Louis, MO, #56834). ATP synthase beta and adenine nucleotide translocase 1 were isolated from a mouse heart membrane preparation. Porcine gelatin was from USB (Cleveland, OH, #16045). Chymotrypsinogen was found as a component of the bovine DNase preparation. Sequencing grade modified trypsin (#V5113, porcine, reductively methylated, TPCK treated) was from Promega (Madison, WI). Dithiothreitol was from Fisher Biotech (Fair Lawn, NJ, #BP172-25, electrophoresis grade). Alpha-cyano-4-hydroxy cinnamic acid (CHCA) from Fluka (#70990) was recrystallized before use then dissolved to 10 mg/ml in 50% acetonitrile, 0.1% trifluoroacetic acid. NeutrAvidin agarose beads were from Thermo Scientific (Rockford, IL, #29202). Monomeric avidin agarose beads were from Pierce (Rockford, IL, #20228).

FP-biotin was custom synthesized in the laboratory of Dr. Charles M. Thompson at the University of Montana (Missoula, MT) [22].

Stock solutions of FP-biotin were made in dimethylsulfoxide and stored at  $-80^{\circ}\text{C}$ .

### 2.2. Sample preparation for mass spectrometry

Proteins were either purchased and were therefore relatively pure, or they were isolated from crude extracts. All pure proteins except kinesin were treated with FP-biotin by the following protocol. One mg/ml protein (approximately 10–25  $\mu\text{M}$ ) was dissolved in 10 mM ammonium bicarbonate, pH 8.3, containing 0.01% sodium azide. FP-biotin was added to a final concentration of 120  $\mu\text{M}$  and the solution was incubated at  $37^{\circ}\text{C}$  for 24 h. Negative controls were processed in the same manner as labeled samples except that FP-biotin was omitted. Samples were boiled for 10 min, reduced with 10 mM dithiothreitol for 2 h at  $60^{\circ}\text{C}$ , alkylated with 50 mM iodoacetamide for 1 h at room temperature in the dark, and dialyzed against 4 l of 10 mM ammonium bicarbonate pH 8.3 for 24 h at  $8^{\circ}\text{C}$  (with one change), and then digested with sequencing grade trypsin at a ratio of 1:100 ( $\mu\text{g}$  trypsin: $\mu\text{g}$  sample) for 24 h at  $37^{\circ}\text{C}$ . Digests were used directly for MALDI TOF TOF analysis or dried and resuspended in 5% acetonitrile, 0.1% formic acid for QTrap analysis.

Kinesin motor domain (1 mg or 13.3 nanomoles) was dissolved in 1 ml of 80 mM PIPES buffer pH 7.0 containing 0.5 mM EGTA, 2 mM  $\text{MgCl}_2$ , 0.2 M NaCl and 20  $\mu\text{M}$  ATP. FP-biotin (260 nanomoles) was added. The protein did not fully dissolve. The mixture was incubated at  $37^{\circ}\text{C}$  for 48 h, with occasional mixing. The protein was denatured in 8 molar urea in the presence of 10 mM dithiothreitol and boiled for 3 min. The resultant solution was clear. Sulfhydryl groups were alkylated with 90 mM iodoacetamide at  $37^{\circ}\text{C}$  for 3 h. The protein solution was freed of unbound FP-biotin and salts by dialysis against 4 l of 25 mM ammonium bicarbonate, pH 8.5 for 36 h at  $4^{\circ}\text{C}$  (with three changes). There were some particles in the preparation after dialysis. The preparation was then digested with trypsin (at a ratio of 50–1,  $\mu\text{g}$  protein to  $\mu\text{g}$  trypsin) for 11 h at  $37^{\circ}\text{C}$  before a second aliquot of trypsin was added for another 14 h of digestion. Trypsin was inactivated by reaction with 1  $\mu\text{l}$  of 5.73 M diisopropylfluorophosphate overnight. Labeled peptides were enriched by extraction with monomeric avidin beads (1 ml, settled volume) equilibrated in 10 mM ammonium bicarbonate, pH 8.5. Loaded beads were washed with 10 ml of 1 M potassium phosphate, pH 7.5; 10 ml of 0.1 M Tris acetate, pH 8.6; and 30 ml of water before elution with 10% acetic acid. The digest was examined with the MALDI TOF TOF 4800 mass spectrometer. Peptides that showed characteristic masses for FP-biotin under MSMS conditions were further purified by reverse phase HPLC (Phenomenex Prodigy 5 micron ODS column) using an acetonitrile/trifluoroacetic acid gradient. Fractions containing masses consistent with the putative FP-biotinylated peptides were dried, resuspended in 50% acetonitrile/0.1% formic acid, and infused into the QTrap 2000 mass spectrometer for improved MSMS fragmentation.

The FP-biotinylated tryptic peptide from human alpha-2-glycoprotein 1 zinc-binding protein was isolated from human plasma by extraction with NeutrAvidin Agarose beads as described [19].

Mouse heart membrane was prepared in 5 mM HEPES buffer, pH 7.4, from 5 mouse hearts as described [7]. The membrane preparation (at 2 mg/ml protein) was incubated with 100  $\mu\text{M}$  FP-biotin at  $37^{\circ}\text{C}$  overnight, then it was denatured with 8 M urea, reduced with 10 mM dithiothreitol for 1 h at  $37^{\circ}\text{C}$ , alkylated with 40 mM iodoacetamide for 1 h at  $37^{\circ}\text{C}$  in the dark, and dialyzed against 10 mM ammonium bicarbonate buffer. Tryptic digestion was accomplished by incubation at  $37^{\circ}\text{C}$  overnight with Promega sequencing grade trypsin, at a trypsin to protein ratio of 1–37 (weight to weight). FP-biotinylated peptides were extracted from the digest with NeutrAvidin Agarose beads (1 ml settled volume) in 8 mM sodium phosphate buffer, pH 7.0, containing 155 mM sodium chloride (PBS).

Beads were washed with 5–10 ml of PBS and then with 10 ml of water. Peptides were eluted with 50% acetonitrile/water containing 0.15% trifluoroacetic acid. It had been anticipated that this procedure would yield FP-biotinylated muscarinic receptor. However, the FP-biotinylated proteins identified in the preparation were ATP synthase beta and adenine nucleotide translocase I.

### 2.3. MALDI TOF TOF analysis

Generally, 0.5–1 µl of sample (approximately 20 pmole/µl for pure proteins, assuming no losses during processing) was air dried onto a 384-well Opti-TOF sample plate (Applied Biosystems, Foster City, CA, #1016491) and then overlaid with 1 µl of CHCA (10 mg/ml). Mass spectra and collision induced MSMS spectra were collected in positive ion reflector mode on a MALDI TOF TOF 4800 mass spectrometer (Applied Biosystems). The final spectrum was the average of 500 laser shots. The mass spectrometer was calibrated before each use with CalMix 5 (Applied Biosystems).

### 2.4. QTrap analysis

For analysis using on-line HPLC separation of sample before introduction into the mass spectrometer, a 1 ml sample from the tryptic digest was dried by SpeedVac and re-dissolved in 0.4 ml of 5% acetonitrile containing 0.1% formic acid to yield approximately 3–5 pmole of peptide/µl, assuming no losses during processing. Ten microliters of this solution (30–50 pmole, assuming no losses during handling) were injected onto an HPLC nanocolumn (218MS3.07515 Vydac C18 polymeric reverse phase, 75 µm I.D.—150 mm long; P.J. Cobert Assoc, St. Louis, MO). Peptides were separated with a 90 min linear gradient from 5 to 60% acetonitrile at a flow rate of 0.3 µl/min and electrosprayed through a fused silica emitter (360 µm O.D., 75 µm I.D., 15 micron taper, New Objective, Woburn, MA) directly into the QTRAP 2000, a hybrid quadrupole linear ion trap mass spectrometer (Applied Biosystems). An ion-spray voltage of 1900 V was maintained between the emitter and the mass spectrometer. Information dependent acquisition was used to collect MS, high resolution MS, and MSMS spectra. All spectra were collected in the enhanced mode, using the trap function. The three most intense MS peaks in each cycle with mass between 400 and 1700 *m/z*, charge of +1 to +4, and intensities greater than 10,000 cps were selected for high resolution MS and MSMS analysis. Precursor ions were excluded for 30 s after one MSMS spectrum had been collected. The collision cell was pressurized to 40 µTorr with pure nitrogen, and collision energies between 20 and 40 eV were determined automatically by the software based on the mass and charge of the precursor ion. The mass spectrom-

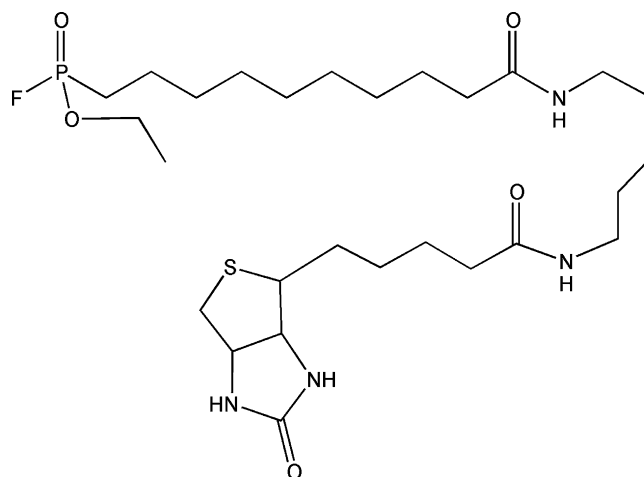


**Fig. 1.** The structure of FP-biotin, 10-(fluoroethoxyphosphinyl)-N-(biotinamido)decanamide.

ter was calibrated on selected fragments from the MSMS spectrum of Glu-fibrinopeptide B.

The MSMS data were submitted to Mascot (Matrix Science, London, UK, <http://www.matrixscience.com>) for identification of labeled peptide [23]. The added mass of the FP-biotin (572 amu) has been incorporated into the UNIMOD database (<http://www.unimod.org>) for use as a variable modification in the Mascot algorithm. In addition, the MSMS chromatograms were searched with an extracted ion chromatographic protocol (Analyst 1.4.1 software, Applied Biosystems) for fragment ions at 329, 312 and 227 amu which are characteristic of the FP-biotin label [24]. Sequences of peptides identified by either procedure were confirmed manually.

## 3. Results

The structure of FP-biotin is shown in Fig. 1. FP-biotin was used for these studies for two reasons. First, MSMS fragmentation creates fragments that are characteristic of FP-biotin. Characteristic fragments are found at 329, 312 and 227 amu (for fragmentation of FP-biotin at its internal amide linkages) [24]. In addition, tyrosine-FP-biotin immonium ion fragments are found at 708 amu (for the singly charged immonium ion), 691 amu (for the immonium ion less amine), 355 amu (for the doubly charged immonium ion) and 346 amu (for the doubly charged immonium ion less amine). These ions provide a convenient, positive identification for the labeled peptides. They also can be used as target masses when the mass

**Table 1**  
FP-biotin labeled peptides.

Species	Protein	Accession number gi	Peptide sequence <sup>a</sup>	Tyr	FP-biotin characteristic ions				
					329	312	227	691	708
Human	Alpha-2-glycoprotein 1 zinc	52790422	WEAEPVY*VQR	174	X	X	X	X	X
	Alpha-2-glycoprotein 1 zinc	52790422	AY*LEECPATLR	181	X	X	–	X	X
	Alpha-2-glycoprotein 1 zinc	52790422	YY*YDGKDYIEFNK	138	X	X	X	X	X
	Kinesin 3C	41352705	ASY*LEIYQEEIR	145	X	X	X	X	X
	Keratin 1	119395750	THNLEPY*FESFINNLR	230	X	X	–	X	X
Bovine	Actin	62287933	DSY*VGDEAQS	55	X	–	–	X	X
	Actin	62287933	GY*SFVTTAER	200	X	X	X	X	X
	Chymotrypsinogen	194674931	Y*TNANTPDR	201	X	X	X	X	X
Mouse	ATP Synthase beta	20455479	ILQDY*K	431	X	X	X	X	X
	Adenine Nucleotide Translocase 1	902008	Y*FPTQALNFAFK	81	X	X	X	X	X
Porcine	Pepsin	13096225	QYY*TVFDR	310	X	X	X	X	X

<sup>a</sup> The asterisk (\*) indicates the labeled tyrosine. The residue number of the labeled tyrosine in the protein sequence is given. X indicates the presence of FP-biotin characteristic ions in MSMS spectra of the labeled peptide.

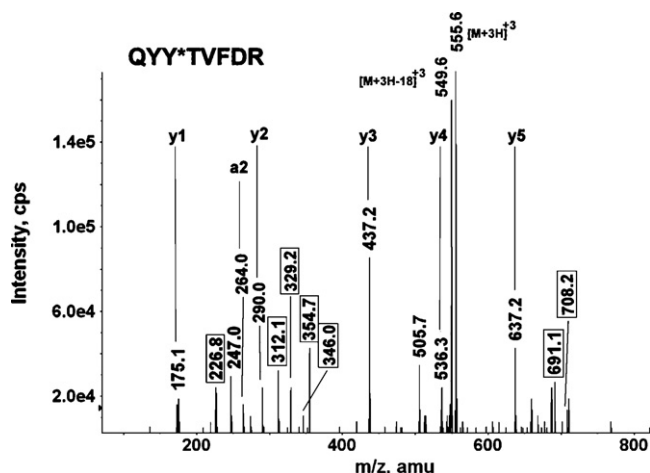


**Fig. 2.** The MSMS spectrum of peptide QYY\*TVFDR from porcine pepsin (where Y\* is the labeled tyrosine). The boxed masses identify the non-sequence, characteristic fragments from FP-biotin. The triply charged parent ion has a mass of 555.6 amu.

spectra from crude mixtures are searched for the labeled peptides using extracted ion techniques. Second, avidin agarose can be used to concentrate and enrich the biotinylated-peptides from crude mixtures.

In the current study, eleven peptides from eight proteins were found to be labeled (see Table 1). The parent ion mass of each peptide was consistent with a covalent reaction of FP-biotin with some residue on that peptide (added mass of 572 amu). As it turned out, each peptide was labeled on tyrosine. The labeled residue for each peptide was confirmed by manual analysis of the MSMS spectra, with the assistance of the MS-Product algorithm for assignment of internal fragments (University of California, San Francisco, <http://prospector2.ucsf.edu>). Four representative MSMS spectra are presented.

Fig. 2 shows the MSMS spectrum of QYY\*TVFDR from porcine pepsin where FP-biotin is on Tyr 310. A 5-residue y-ion sequence could be extracted which included the C-terminal arginine. The labeled tyrosine was part of an unresolved three amino acid y-ion fragment at the N-terminus. This three amino acid fragment contained two tyrosines. Fortunately, masses consistent with the unlabeled a2-ion (QY=264.0 amu) and its deaminated consort at 247.0 amu appeared in the spectrum. Thus, by a process of elimination the label could be assigned to the tyrosine in position three

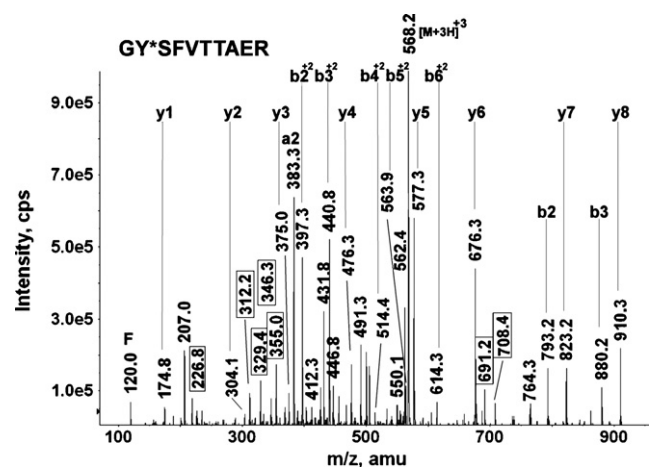


**Fig. 3.** The MSMS spectrum of peptide GY\*SFVTTAER from bovine actin (where Y\* is the labeled tyrosine). The boxed masses identify the non-sequence, characteristic fragments from FP-biotin. The triply charged parent ion has a mass of 568.2 amu.

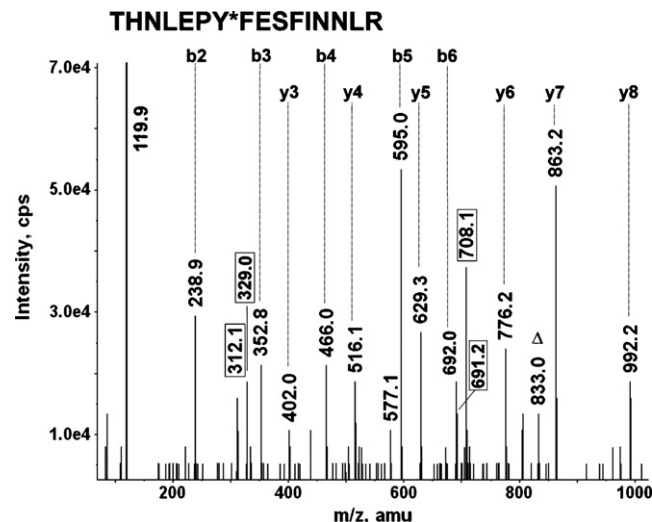


**Fig. 4.** The MSMS spectrum of peptide THNLEPY\*FESFINNLR from human keratin 1 (where Y\* is the labeled tyrosine). The boxed masses identify the non-sequence, characteristic fragments from FP-biotin. The mass marked with a triangle (833.0 amu) is the N-terminus of a proline internal fragment. The triply charged parent ion has a mass of 642.6 amu which does not appear in the spectrum.

from the N-terminus. The majority of the remaining masses in the spectrum could be assigned to dehydration/deamination products or internal fragments. Characteristic fragments from FP-biotin appeared at 226.8, 312.1, 329.2, 708.2, 691.1, 354.7 and 346.0 amu.

Fig. 3 shows the MSMS spectrum of GY\*SFVTTAER from bovine actin where FP-biotin is on Tyr 200. The peptide was identified by an eight amino acid y-ion sequence. The labeled tyrosine appeared in all b-ions, for example in the singly charged b2-ion at 793.2 amu and in the doubly charged b2-ion at 397.3 amu. The majority of the remaining masses in the spectrum could be assigned to dehydration/deamination products or internal fragments. Characteristic fragments from the internal amide bonds of FP-biotin appeared at 226.8, 312.2, 329.4, 708.4, 691.2, 355.0 and 346.3 amu.

Fig. 4 shows the MSMS spectrum of THNLEPY\*FESFINNLR from human keratin 1 where FP-biotin is on Tyr 230. The peptide was identified by an eight amino acid y-ion sequence and a six amino acid b-ion sequence. The label was found as part of the Pro Tyr pair (833.0 amu) at the N-terminus of the proline internal fragment. The majority of the remaining masses in the spectrum could be assigned to dehydration/deamination products or internal

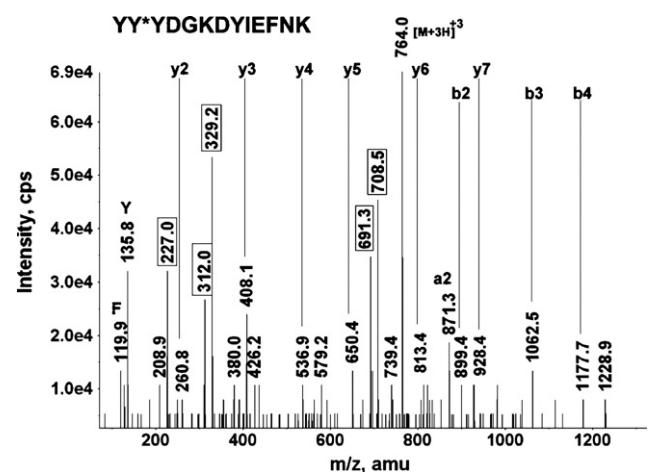


**Fig. 5.** The MSMS spectrum of peptide YY\*YDGKDYIEFNK from alpha-2-glycoprotein 1 zinc-binding protein (where Y\* is the labeled tyrosine). The boxed masses identify the non-sequence, characteristic fragments from FP-biotin. The triply charged parent ion has a mass of 764.0 amu.

fragments. Characteristic fragments from the internal amide bonds of FP-biotin appeared at 312.1, 329.0, 708.1 and 691.2 amu.

Fig. 5 shows the MSMS spectrum of YY\*YDGDYIEFNK from human alpha-2-glycoprotein 1 zinc-binding protein where FP-biotin is on Tyr 138. Though the signal-to-noise ratio was low, the peptide could still be identified by a seven amino acid y-ion sequence and a four amino acid b-ion sequence. The minimum signal-to-noise ratio for the sequence peaks had an acceptable value of three. The label was found as part of a trimer at the N-terminus that consisted of three tyrosines. Analysis of the b-ion sequence demonstrated that the label was on the b2-ion (899.4 amu) and therefore had to be on one of the first two N-terminal tyrosines. Though the b2 peak had low intensity, its identity was confirmed by the a2-ion at 871.4 amu which was substantially more intense. Since it could not be determined which tyrosine actually carried the label, the second tyrosine was arbitrarily marked as labeled. Characteristic fragments from the internal amide bonds of FP-biotin appeared at 227.0, 312.0, 329.2, 708.5 and 691.3 amu.

Labeled amino acids in the seven remaining peptides were identified using similar analyses of their MSMS spectra. The label was found as one of the sequence fragments in peptide WEAEPVY\*VQR. The labeled amino acid was found as part of the b2-ion in peptides AY\*LEEECPATLR and Y\*FPTQALNFAFK. For both sequences, the only reasonable candidate for labeling was the tyrosine. For peptide ILQDY\*K, the labeled tyrosine was part of the y2-ion at the C-terminus. Again, the only reasonable candidate for labeling was the tyrosine. If the lysine had been labeled, it would not have been recognized for cleavage by trypsin. The labeled tyrosine was part of a y-ion dimer at the N-terminus of peptide Y\*TNANTPDR and as part of an unresolved three amino acid y-ion fragment at the N-terminus of two sequences (ASY\*LEIQEEIR and DSY\*VGDEAQS). In principle, either serine or threonine might have been labeled rather than tyrosine in all three peptides. However, there are three lines of evidence to indicate that the label is on tyrosine rather than serine or threonine. First, there was no evidence for the 591 amu fragment that is characteristic of a serine label (and presumably of a threonine label) [24]. Second, OP-labeled serine (like phosphoserine) readily loses the OP-label in the mass spectrometer, under the CID conditions employed in these experiments. This fragmentation leaves a dehydroalanine residue in its stead. A similar loss for OP-threonine would be predicted to yield dehydro-threonine. The masses of the observed fragments were consistent with the presence of both the intact serine (or threonine) and the OP label. No masses consistent with the loss of OP and the presence of either dehydroalanine or dehydro-threonine were detected. Third, masses for both tyrosine-FP-biotin immonium ions and tyrosine-FP-biotin immonium ions minus amine were detected in all three MSMS spectra, indicating the presence of FP-biotinylated tyrosine. For these reasons, the label was assigned to tyrosine in each case.

Non-sequence fragments characteristic of FP-biotinylated tyrosine at 329, 312, 691, 708 and 355 amu masses appeared in all 7 MSMS spectra and the 346 amu mass in 5 spectra. The presence of these ions in the MSMS spectra confirmed the presence of FP-biotin on the peptides.

Not all of the proteins that we treated with FP-biotin yielded labeled peptides. Proteins for which we could find no FP-biotinylated peptides included porcine gelatin, bovine RNase, bovine DNase I, human IgG, chicken lysozyme, and bovine insulin.

## 4. Discussion

### 4.1. General phenomenon

We have previously demonstrated that tyrosine in transferrin, serum albumin and tubulin (both alpha and beta) react in vitro

with a variety of organophosphorus agents (FP-biotin, chlorpyrifos-oxon, diisopropylfluorophosphate, dichlorvos, soman, and sarin) [8–10,12,19]. In addition, SDS PAGE experiments have demonstrated the presence of at least 50 FP-biotin reactive proteins in mouse brain supernatant, again in vitro [25]. Many of these latter proteins were identified as members of the serine hydrolase family. Such proteins are the expected targets for FP-biotin [26]. However, many were not members of that family [25].

The current experiments clearly demonstrate that the organophosphorus agent FP-biotin is capable of reacting with tyrosines on a variety of non-serine hydrolase proteins. By inference, other OP should react with these tyrosines as well.

With the addition of these proteins to those that have already been identified, it stands to reason that the reaction of protein-bound tyrosine with FP-biotin is a widespread phenomenon. On the other hand, not all tyrosines in a protein are reactive nor do all proteins contain reactive tyrosines.

### 4.2. Only certain tyrosines react with OP

The question of what determines the selectivity for the reaction of some tyrosines with FP-biotin arises. In order for a tyrosine to react with FP-biotin, it must satisfy two criteria. First, the phenolic oxygen of the tyrosine must be exposed to the medium. The necessity for this criterion is self-evident.

Second, the phenolic oxygen must be capable of nucleophilic attack. Reactions of OP typically involve attack by a nucleophile on the phosphorous to displace the most labile of the OP ligands [27]. For tyrosine to serve as a nucleophile, it must be deprotonated at the pH of the reaction. Ashbolt and Rydon [17] have demonstrated that tyrosine alone can react with diisopropylfluorophosphate (13 mM diisopropylfluorophosphate, 3 mM tyrosine, at pH 7.8 and 37 °C for 24 h). Despite the fact that the concentration of OP in their experiments was 100-fold higher than in ours they demonstrated the potential of tyrosine to react with OP.

The high concentrations of OP used by Ashbolt and Rydon were necessary because of the low reactivity of tyrosine under their conditions. This low reactivity can be attributed to the  $pK_a$  of tyrosine. The  $pK_a$  of tyrosine is 10.1 [28]. At pH 8.3, where our reactions were conducted, only 1% of the typical tyrosine would be deprotonated. To promote a nucleophilic reaction of protein-bound tyrosine with OP, some mechanism for increasing the amount of deprotonated tyrosine would be advantageous. A simple way to accomplish this objective would be to lower the  $pK_a$  value of the tyrosine.

It has been demonstrated that interactions between histidine and cysteine provide a viable method for lowering the  $pK_a$  of cysteine in proteins. Decreases of 4–5 pH units have been reported [29,30]. It has been proposed that the decrease in cysteine  $pK_a$  is due to through-space, charge–charge interactions [31]. Lowered  $pK_a$  values for tyrosine in human transferrin [32] and UDP-galactose 4-epimerase [33] also have been reported. The decrease in  $pK_a$  was ascribed to interaction with nearby positively charged residues. In the case of UDP-galactose 4-epimerase, NAD<sup>+</sup> was implicated. For human transferrin, four tyrosines were found to have  $pK_a$  values around 7. Neighboring lysines were implicated. We suggest that this sort of process may be involved in activating the FP-biotin reactive tyrosines in the peptides described in this paper.

### 4.3. Labeled peptides are hard to find; knowing what to look for helps

Our ultimate goal is to identify the proteins that are modified by low-dose exposure in an animal, and eventually in humans. Organophosphorus pesticides have no tag to help identify the labeled peptide. The task is to find a labeled peptide based on

its mass, starting from a mixture of 30,000 proteins which upon digestion with trypsin will yield at least a million peptides. This is a very difficult assignment. The work we are doing with pure proteins aims to make it possible. By knowing what we are looking for, we can reduce the complexity of the starting material. For example, the most OP-reactive protein in human plasma is butyrylcholinesterase. By purifying butyrylcholinesterase from plasma before beginning a search for the labeled peptide, one can successfully find the labeled peptide and identify the modifying agent [34,35].

Covalent modification of butyrylcholinesterase and acetylcholinesterase does not explain cognitive impairment and depression following pesticide exposure [36–38]. Therefore we are searching for unknown proteins modified by OP. When we first identified FP-biotinylated albumin in mice treated with a nontoxic dose of FP-biotin [11], and identified Tyr 411 of human albumin as the site modified by OP [9], we thought the OP-tyrosine adduct on albumin was an exception. Only with study of additional proteins has it become clear that covalent binding of OP to tyrosine is common. This principle allows us to expand our search. One way we have applied this principle is by adding OP-bound tyrosine as a variable modification in the UNIMOD database (<http://www.unimod.org>) of the Mascot search engine (<http://www.matrix-science.com>); all Mascot users can now search for OP-tyrosine adducts.

Knowing the exact mass of candidate OP-labeled peptides helps us find the labeled peptide. Even after a protein has been partially purified from plasma or from brain, there are still thousands of peptides in the tryptic digest. In a mixture of peptides some peptides dominate in a process called ion suppression, making it impossible for other ions to ionize in the mass spectrometer. Often, the labeled peptide cannot be found. An example of the ion suppression problem and the difficulty of finding a labeled peptide is the fact that we could not find the labeled peptide in pure chicken lysozyme even though it is known that tyrosine in chicken lysozyme is labeled by OP [21]. The solution to the problem of ion suppression is to fractionate the peptides. We separate the peptides offline by HPLC and check each fraction by MALDI-TOF to identify the fraction that includes the mass of interest. This step requires that we know the mass we are looking for. This is where our studies with pure proteins are very helpful. The partially purified peptide is then subjected to LC/MS/MS which adds another liquid chromatography purification step before the peptide is fragmented in the mass spectrometer. We search the data for labeled peptides using Mascot software, but we also search the data manually for peptides that Mascot might have missed. Mascot generally does not report peptides that contain fewer than 5 amino acids in its search results. For example, the OP-labeled tryptic peptide of bovine albumin YTR, was not reported by Mascot but it was found by manual examination of the data [24]. This step requires that we know what we are looking for. In conclusion, the information obtained from a study of pure proteins labeled with OP is the basis for *in vivo* studies that aim to identify proteins modified by OP.

#### 4.4. *In vivo* studies

The issue that we currently have under investigation is whether reaction of OP with proteins occurs *in vivo* at OP concentrations low enough that signs of cholinergic toxicity do not appear. We have already demonstrated that albumin and carboxylesterase from mouse plasma together with nine other unidentified proteins can be labeled *in vivo* by FP-biotin, at concentrations that do not significantly inhibit acetylcholinesterase [11]. The reactive residue on albumin is tyrosine [9,20], while that on carboxylesterase is the active site serine [39]. *In vivo* studies in guinea pigs treated with soman and tabun identified OP-tyrosine adducts on albumin [20]. *In vivo* studies to search for other proteins modified by OP are

underway. The work with pure proteins in this report will aid in the identification of proteins modified *in vivo*.

#### 4.5. Significance

Our findings may have application to diagnosis of OP exposure. Proteins that have no active site serine may serve as biomarkers of exposure. In the future it may be possible to develop antibodies to new OP-labeled biomarkers to use for screening OP exposure. The recognition of a new OP-binding motif to tyrosine suggests new directions to search for mechanisms to explain cognitive deficits and depression associated with exposure to OP.

#### Conflict of interest

The authors declare that there are no conflicts of interest.

#### Acknowledgements

Mass spectra were obtained with the support of the Mass Spectrometry and Proteomics core facility at the University of Nebraska Medical Center. FP-biotin was generous gift from Dr. Charles M. Thompson at the University of Montana (Missoula, MT). This work was supported by the U.S. Army Medical Research and Materiel Command [grant number W81XWH-07-2-0034 to OL]; the National Institutes of Health [grant numbers U01 NS058056-03 to OL, P30CA36727 to Eppley Cancer Center]; and the Direction Générale de l'Armement of the French Ministry of Defense [grant numbers DGA 08co501, ANR-06-BLAN-0163 to F.N.].

#### References

- [1] C.N. Pope, Organophosphorus pesticides: do they all have the same mechanism of toxicity? *J. Toxicol. Environ. Health B Crit. Rev.* 2 (1999) 161–181.
- [2] J.E. Casida, G.B. Quistad, Organophosphate toxicology: safety aspects of nonacetylcholinesterase secondary targets, *Chem. Res. Toxicol.* 17 (2004) 983–998.
- [3] T.C. Marrs, Organophosphate poisoning, *Pharmacol. Ther.* 58 (1993) 51–66.
- [4] J.E. Casida, G.B. Quistad, Serine hydrolase targets of organophosphorus toxicants, *Chem. Biol. Interact.* 157–158 (2005) 277–283.
- [5] V.C. Moser, Comparisons of the acute effects of cholinesterase inhibitors using a neurobehavioral screening battery in rats, *Neurotoxicol. Teratol.* 17 (1995) 617–625.
- [6] D. Kidd, Y. Liu, B.F. Cravatt, Profiling serine hydrolase activities in complex proteomes, *Biochemistry* 40 (2001) 4005–4015.
- [7] J.A. Bomser, J.E. Casida, Diethylphosphorylation of rat cardiac M2 muscarinic receptor by chlorpyrifos oxon *in vitro*, *Toxicol. Lett.* 119 (2001) 21–26.
- [8] B. Li, L.M. Schopfer, H. Grigoryan, C.M. Thompson, S.H. Hinrichs, P. Masson, O. Lockridge, Tyrosines of human and mouse transferrin covalently labeled by organophosphorus agents: a new motif for binding to proteins that have no active site serine, *Toxicol. Sci.* 107 (2009) 144–155.
- [9] B. Li, L.M. Schopfer, S.H. Hinrichs, P. Masson, O. Lockridge, Matrix-assisted laser desorption/ionization time-of-flight mass spectrometry assay for organophosphorus toxicants bound to human albumin at Tyr411, *Anal. Biochem.* 361 (2007) 263–272.
- [10] B. Li, F. Nachon, M.T. Froment, L. Verdier, J.C. Debouzy, B. Brasme, E. Gillon, L.M. Schopfer, O. Lockridge, P. Masson, Binding and hydrolysis of soman by human serum albumin, *Chem. Res. Toxicol.* 21 (2008) 421–431.
- [11] E.S. Peeples, L.M. Schopfer, E.G. Duysen, R. Spaulding, T. Voelker, C.M. Thompson, O. Lockridge, Albumin, a new biomarker of organophosphorus toxicant exposure, identified by mass spectrometry, *Toxicol. Sci.* 83 (2005) 303–312.
- [12] H. Grigoryan, L.M. Schopfer, C.M. Thompson, A.V. Terry, P. Masson, O. Lockridge, Mass spectrometry identifies covalent binding of soman, sarin, chlorpyrifos oxon, diisopropyl fluorophosphate, and FP-biotin to tyrosines on tubulin: a potential mechanism of long term toxicity by organophosphorus agents, *Chem. Biol. Interact.* 175 (2008) 180–186.
- [13] F. Sanger, Amino-acid sequences in the active centers of certain enzymes, *Proc. Chem. Soc.* 5 (1963) 76–83.
- [14] T. Murachi, T. Inagami, M. Yasui, Evidence for alkylphosphorylation of tyrosyl residues of stem bromelain by diisopropylphosphorofluoridate, *Biochemistry* 4 (1965) 2815–2825.
- [15] I.M. Chaiken, E.L. Smith, Reaction of a specific tyrosine residue of papain with diisopropylfluorophosphate, *J. Biol. Chem.* 244 (1969) 4247–4250.
- [16] K. Kato, T. Murachi, Chemical modification of tyrosyl residues of hen egg-white lysozyme by diisopropylphosphorofluoridate, *J. Biochem.* 69 (1971) 725–737.

- [17] R.F. Ashbolt, H.N. Rydon, The action of diisopropyl phosphorofluoridate and other anticholinesterases on amino acids, *Biochem. J.* 66 (1957) 237–242.
- [18] R.M. Black, J.M. Harrison, R.W. Read, The interaction of sarin and soman with plasma proteins: the identification of a novel phosphorylation site, *Arch. Toxicol.* 73 (1999) 123–126.
- [19] S.J. Ding, J. Carr, J.E. Carlson, L. Tong, W. Xue, Y. Li, L.M. Schopfer, B. Li, F. Nachon, O. Asojo, C.M. Thompson, S.H. Hinrichs, P. Masson, O. Lockridge, Five tyrosines and two serines in human albumin are labeled by the organophosphorus agent FP-biotin, *Chem. Res. Toxicol.* 21 (2008) 1787–1794.
- [20] N.H. Williams, J.M. Harrison, R.W. Read, R.M. Black, Phosphorylated tyrosine in albumin as a biomarker of exposure to organophosphorus nerve agents, *Arch. Toxicol.* 81 (2007) 627–639.
- [21] T. Murachi, T. Miyake, N. Yamasaki, Alkylphosphorylation of hen egg-white lysozyme by diisopropylphosphorofluoridate, *J. Biochem.* 68 (1970) 239–244.
- [22] L.M. Schopfer, T. Voelker, C.F. Bartels, C.M. Thompson, O. Lockridge, Reaction kinetics of biotinylated organophosphorus toxicant, FP-biotin, with human acetylcholinesterase and human butyrylcholinesterase, *Chem. Res. Toxicol.* 18 (2005) 747–754.
- [23] D.N. Perkins, D.J. Pappin, D.M. Creasy, J.S. Cottrell, Probability-based protein identification by searching sequence databases using mass spectrometry data, *Electrophoresis* 20 (1999) 3551–3567.
- [24] L.M. Schopfer, M.M. Champion, N. Tamblyn, C.M. Thompson, O. Lockridge, Characteristic mass spectral fragments of the organophosphorus agent FP-biotin and FP-biotinylated peptides from trypsin and bovine albumin (Tyr410), *Anal. Biochem.* 345 (2005) 122–132.
- [25] H. Li, L. Schopfer, R. Spaulding, C.M. Thompson, O. Lockridge, Identification of organophosphate-reactive proteins by tandem mass spectrometry, *Chem. Biol. Interact.* 157–158 (2005) 383–384.
- [26] Y. Liu, M.P. Patricelli, B.F. Cravatt, Activity-based protein profiling: the serine hydrolases, *Proc. Natl. Acad. Sci. U.S.A.* 96 (1999) 14694–14699.
- [27] S.J. Benkovic, K.J. Schray, Chemical basis of biological phosphoryl transfer, *The Enzymes* (ed. P.D. Boyer) 8 (1973) 201–238.
- [28] D.I. Hitchcock, The solubility of tyrosine in acid and alkali, *J. Gen. Physiol.* 6 (1924) 747–757.
- [29] Z.Y. Zhang, J.E. Dixon, Active site labeling of the Yersinia protein tyrosine phosphatase: the determination of the  $pK_a$  of the active site cysteine and the function of the conserved histidine 402, *Biochemistry* 32 (1993) 9340–9345.
- [30] S.D. Lewis, F.A. Johnson, J.A. Shafer, Effect of cysteine-25 on the ionization of histidine-159 in papain as determined by proton nuclear magnetic resonance spectroscopy. Evidence for a his-159–Cys-25 ion pair and its possible role in catalysis, *Biochemistry* 20 (1981) 48–51.
- [31] F.A. Johnson, S.D. Lewis, J.A. Shafer, Perturbations in the free energy and enthalpy of ionization of histidine-159 at the active site of papain as determined by fluorescence spectroscopy, *Biochemistry* 20 (1981) 52–58.
- [32] X. Sun, H. Sun, R. Ge, M. Richter, R.C. Woodworth, A.B. Mason, Q.Y. He, The low  $pK_a$  value of iron-binding ligand Tyr188 and its implication in iron release and anion binding of human transferrin, *FEBS Lett.* 573 (2004) 181–185.
- [33] Y. Liu, J.B. Thoden, J. Kim, E. Berger, A.M. Gulick, F.J. Ruzicka, H.M. Holden, P.A. Frey, Mechanistic roles of tyrosine 149 and serine 124 in UDP-galactose 4-epimerase from *Escherichia coli*, *Biochemistry* 36 (1997) 10675–10684.
- [34] H. Li, I. Ricordel, L. Tong, L.M. Schopfer, F. Baud, B. Megarbane, E. Maury, P. Masson, O. Lockridge, Carbofuran poisoning detected by mass spectrometry of butyrylcholinesterase adduct in human serum, *J. Appl. Toxicol.* (2008).
- [35] A. Fidler, A.G. Hulst, D. Noort, R. de Ruiter, M.J. van der Schans, H.P. Benschop, J.P. Langenberg, Retrospective detection of exposure to organophosphorus anti-cholinesterases: mass spectrometric analysis of phosphorylated human butyrylcholinesterase, *Chem. Res. Toxicol.* 15 (2002) 582–590.
- [36] K. Steenland, R.B. Dick, R.J. Howell, D.W. Chrislip, C.J. Hines, T.M. Reid, E. Lehman, P. Laber, E.F. Krieg Jr., C. Knott, Neurologic function among termiticide applicators exposed to chlorpyrifos, *Environ. Health Perspect.* 108 (2000) 293–300.
- [37] F. Kamel, L.S. Engel, B.C. Gladen, J.A. Hoppin, M.C. Alavanja, D.P. Sandler, Neurologic symptoms in licensed pesticide applicators in the agricultural health study, *Hum. Exp. Toxicol.* 26 (2007) 243–250.
- [38] C. Beseler, L. Stallones, J.A. Hoppin, M.C. Alavanja, A. Blair, T. Keefe, F. Kamel, Depression and pesticide exposures in female spouses of licensed pesticide applicators in the agricultural health study cohort, *J. Occup. Environ. Med.* 48 (2006) 1005–1013.
- [39] C.D. Fleming, C.C. Edwards, S.D. Kirby, D.M. Maxwell, P.M. Potter, D.M. Cerasoli, M.R. Redinbo, Crystal structures of human carboxylesterase 1 in covalent complexes with the chemical warfare agents soman and tabun, *Biochemistry* 46 (2007) 5063–5071.



## Mass spectral characterization of organophosphate-labeled lysine in peptides

Hasmik Grigoryan, Bin Li, Weihua Xue, Marine Grigoryan, Lawrence M. Schopfer \*, Oksana Lockridge

*Eppley Institute, University of Nebraska Medical Center, Omaha, NE 68198, USA*

### ARTICLE INFO

#### Article history:

Received 2 June 2009

Available online 9 July 2009

#### Keywords:

Mass spectrometry

Organophosphate esters

Chlorpyrifos oxon

Diisopropylfluorophosphate

Serum albumin

Keratin

Tubulin

Actin

Transferrin

### ABSTRACT

Organophosphate (OP) esters bind covalently to the active site serine of enzymes in the serine hydrolase family. Recently, mass spectrometry identified covalent binding of OPs to tyrosine in a wide variety of proteins when purified proteins were incubated with OPs. In the current work, manual inspection of tandem mass spectrometry (MS/MS) data led to the realization that lysines also make a covalent bond with OPs. OP-labeled lysine residues were found in seven proteins that had been treated with either chlorpyrifos oxon (CPO) or diisopropylfluorophosphate (DFP): human serum albumin (K212, K414, K199, and K351), human keratin 1 (K211 and K355), human keratin 10 (K163), bovine tubulin alpha (K60, K336, K163, K394, and K401), bovine tubulin beta (K58), bovine actin (K113, K291, K326, K315, and K328), and mouse transferrin (K296 and K626). These results suggest that OP binding to lysine is a general phenomenon. Characteristic fragments specific for CPO-labeled lysine appeared at 237.1, 220.0, 192.0, 163.9, 128.9, and 83.9 amu. Characteristic fragments specific for DFP-labeled lysine appeared at 164.0, 181.2, and 83.8 amu. This new OP-binding motif to lysine suggests new directions to search for mechanisms of long-term effects of OP exposure and in the search for biomarkers of OP exposure.

© 2009 Elsevier Inc. All rights reserved.

Organophosphate (OP)<sup>1</sup> agents include pesticides and chemical warfare agents [1,2]. The intended target of these agents is the active site serine of acetylcholinesterase (AChE, EC 3.1.1.7). Inhibition of AChE explains the acute symptoms that are observed on exposure to high doses of OPs [3,4]. However, chronic exposure to OPs at doses too low to generate cholinergic symptoms has been implicated in a variety of adverse effects, including memory loss, learning disability, fatigue, depression, and Parkinson's disease [5–9]. These symptoms may appear after exposures too low to significantly inhibit AChE [10]. These observations suggest that there are clinically relevant targets for OPs in addition to AChE.

Reactions of OPs with a variety of serine hydrolases in vitro have long been known. Targets include, but are not limited to, fatty acid amide hydrolase, acyl peptide hydrolase, carboxylesterase, phosphoglucomutase, and trypsin [2,11–13]. Enzymes without a serine active site, such as lysyl oxidase and the M2 muscarinic receptor, also react with OPs [2,14]. Results from electrospray ionization mass spectrometry (ESI–MS) have demonstrated that OPs can react with tyrosines on proteins such as transferrin [15], serum albumin [16–21], and tubulin [22]. Although there has been

a renewed interest in the reaction of tyrosine with OPs recently, reaction of tyrosines from human serum albumin and bovine serum albumin with the OP agent diisopropylfluorophosphate (DFP) was reported by Sanger in 1963 [23]. Between 1965 and 1971, DFP was shown to react with tyrosine residues on bromelain [24], papain [25], and lysozyme [26]. We enlarged the group of proteins for which tyrosine serves as an OP target to include kinesin 3C, alpha 2-glycoprotein 1 zinc, pro-apolipoprotein A-I, keratin, actin, ATP synthase, adenine nucleotide translocase I, chymotrypsinogen, and pepsin [27]. Reaction of free tyrosine with OPs was demonstrated by Ashbolt and Rydon [28]. Taken together, these observations firmly establish tyrosine as a target for OPs in proteins.

In the course of our investigations into OP labeling of tyrosine, we found that the  $\epsilon$ -amine of lysine was also labeled. This finding was quite unexpected because it has long been known that the phosphoramidate bond, such as that in  $\epsilon$ -N-phospho-lysine, is sensitive to hydrolysis, especially at pH values below 8.0 [29]. The pH sensitivity is of particular importance for our experiments because, as is the general practice when preparing peptide samples for ESI–MS, we used solvents containing 0.1% formic acid. Despite the unexpected nature of the observations, we found OP-labeled lysine in seven proteins. To our knowledge, there are no previous reports of proteins containing an OP-labeled lysine.

Mass spectrometry (MS) is an excellent tool for identifying markers of protein modification. Three mass spectral features can be used for the identification of protein modification. First is the mass of the parent ion that must be consistent with the mass of

\* Corresponding author. Fax: +1 402 559 4651.

E-mail address: [lmshopf@unmc.edu](mailto:lmshopf@unmc.edu) (L.M. Schopfer).

<sup>1</sup> Abbreviations used: OP, organophosphate; AChE, acetylcholinesterase; DFP, diisopropylfluorophosphate; ESI–MS, electrospray ionization–mass spectrometry; MS, mass spectrometry; MS/MS, tandem mass spectrometry fragmentation; CID, collision-induced dissociation; CPO, chlorpyrifos oxon; TPCK, N-tosyl-L-phenylalanine chloromethyl ketone; MWCO, molecular weight cutoff; HPLC, high-performance liquid chromatography; pseudo-MS<sup>3</sup>, fragmentation of a fragment from MS/MS.

a known peptide plus the mass of the modification. Second is the presence of a gap in the amino acid sequence from a tandem mass spectrometry (MS/MS) spectrum that is consistent with the mass of a modified amino acid. Third is the presence of fragments in the MS/MS spectrum that are characteristic of the modification. We employed tandem quadrupole ESI-MS in conjunction with collision-induced dissociation (CID) to study peptides containing OP-labeled lysine. All three mass spectral features were found.

This presentation has four goals. The first is to document the existence of OP-labeled lysine in proteins. The second is to identify the OP-labeled peptides and the specific OP-labeled lysine residues. The third is to describe the characteristic fragment ions for the OP-labeled lysine along with the frequency at which each ion appears and the relative intensity of the signals for each characteristic fragment. The fourth goal is to establish that OPs react with lysine in a number of proteins.

Here we report on the reaction of seven proteins from three species (human serum albumin, human keratin 1, human keratin 10, bovine tubulin alpha, bovine tubulin beta, bovine actin, and mouse transferrin) with two OP agents (chlorpyrifos oxon [CPO] and DFP). In all cases, the mass of the parent ion in the MS spectrum was consistent with the presence of the OP label. Manual analysis of the MS/MS spectra from the labeled peptides typically revealed gaps in the *b* and/or *y* ion series that were consistent with the mass of OP-modified lysine. These gaps confirmed the presence of the OPs and yielded the location of the labeled residue in the peptide sequence. Finally, characteristic fragments that are diagnostic for the presence of OP-labeled lysine were identified for each OP.

## Materials and methods

### Materials

Purified human serum albumin (essentially fatty acid free, cat. no. 05418), bovine actin (cat. no. 3653), human epidermal keratin (cat. no. K0253), DFP (cat. no. D0879), iodoacetamide (cat. no. I6125), Glu-fibrinopeptide B (cat. no. F3261), and mouse transferrin (cat. no. T0523) were obtained from Sigma-Aldrich-Fluka (St. Louis, MO, USA). Dithiothreitol (electrophoresis grade, cat. no. BP172-25) was obtained from Fisher Biotech (Fair Lawn, NJ, USA). Modified porcine trypsin (*N*-tosyl-L-phenylalanine chloromethyl ketone [TPCK] treated, reductively methylated, sequencing grade, cat. no. V5113) was purchased from Promega (Madison, WI, USA). Bovine brain tubulin (> 99% pure, cat. no. TL238) was obtained from Cytoskeleton (Denver, CO, USA). CPO (cat. no. MET-674B) was obtained from Chem Service (West Chester, PA, USA).

### Labeling

Reaction of human serum albumin with DFP was performed as follows. Serum albumin (8.8 mg) was dissolved in 5 ml of 10 mM Tris-HCl (pH 8.0, to yield 1.76 mg protein/ml or  $2.6 \times 10^{-5}$  M protein) and treated with 26.5  $\mu$ l of 0.1 M DFP in isopropanol (final concentration of  $5.3 \times 10^{-4}$  M) for 2 h at room temperature. The protein was denatured in 8 M urea, reduced with 10 mM dithiothreitol (with boiling for 10 min in a water bath), alkylated with 90 mM iodoacetamide (for 1 h at 37 °C in the dark), and dialyzed against 10 mM ammonium bicarbonate at 4 °C overnight using Spectra/Por Dialysis Membrane (molecular weight cutoff [MWCO] = 12,000–14,000, cat. no. 132700, Spectrum Medical Industries, Los Angeles, CA, USA). Then 500  $\mu$ l of the mixture was digested with trypsin (1:50 [w/w] ratio) overnight at 37 °C. The tryptic digest was dried in a Jouan SpeedVac (model RC10-10,

Thermo Fisher Scientific, Waltham, MA, USA) and redissolved in 5% acetonitrile/95% water/0.1% formic acid to make a final solution of 7 pmol albumin peptides per microliter that was used for ESI-MS.

Reaction of human albumin with CPO was performed in an analogous manner using 15  $\mu$ M albumin and 150  $\mu$ M CPO [19].

Reaction of tubulin with CPO was performed as described by Grigoryan and coworkers [30]. Bovine tubulin was dissolved in 200  $\mu$ l of 15 mM ammonium bicarbonate (pH 8.3) to give a concentration of 0.6 mg tubulin/ml or 12  $\mu$ M. This was treated with 500  $\mu$ M CPO (10  $\mu$ l of a 10-mM CPO stock solution in dimethyl sulfoxide) for 24 h at 37 °C. The tubulin was denatured by heating for 10 min in boiling water, and then the denatured protein was dialyzed against 4 L of ammonium bicarbonate (pH 8.3) using a Slide-A-Lyzer dialysis cassette (MWCO = 7000, cat. no. 66370, Pierce, Rockford, IL, USA). Dialyzed tubulin (60  $\mu$ g) was digested with 1.5  $\mu$ g of sequencing-grade trypsin for 16 h at 37 °C. The tryptic peptides were dried in a SpeedVac and redissolved in 5% acetonitrile/water plus 0.1% formic acid to a final concentration of approximately 2 pmol/ $\mu$ l, which was used for mass spectral analysis.

Reaction of actin with CPO was performed as described by Schopfer and coworkers [31]. Bovine actin was dissolved in 130  $\mu$ l of 10 mM ammonium bicarbonate (pH 8.3) to give a final concentration of 2.5 mg actin/ml or 48  $\mu$ M. This was reacted with 240  $\mu$ M CPO (3  $\mu$ l of a 10-mM CPO stock solution in dimethyl sulfoxide) at 37 °C for 24 h. The actin was denatured, reduced, alkylated, dialyzed, digested with trypsin, dried, and resuspended in 5% acetonitrile/0.1% formic acid for mass spectral analysis as described for tubulin.

Reaction of keratin with CPO was performed as described by Schopfer and coworkers [31]. Here 100  $\mu$ l of a mixture of denatured human keratins at 1 mg protein/ml (in 5 mM Tris, 8 M urea, 1 mM  $\beta$ -mercaptoethanol, and 0.1% azide, pH 8.4) was renatured by dialysis against 25 mM Tris-Cl (pH 7.5) and then treated with 2 mM CPO (25  $\mu$ l of a 10-mM CPO stock solution in dimethyl sulfoxide) at 37 °C for 24 h. The keratin was then processed as described for actin.

Reaction of transferrin with CPO was performed as described by Li and coworkers [15]. Here 100  $\mu$ l of mouse transferrin at 1 mg transferrin/ml was treated with 0.5 mM CPO (5  $\mu$ l of a 10-mM CPO stock solution in ethanol) at 37 °C for 16 h. The transferrin was denatured in 8 M urea and then reduced, alkylated, dialyzed, digested with trypsin (at a transferrin-to-trypsin ratio of 50:1 by weight), dried, and resuspended in 5% acetonitrile/0.1% formic acid for mass spectral analysis.

### Quadrupole MS

For quadrupole MS, 5 to 10  $\mu$ l of a tryptic digest (30–50 pmol) was injected onto a high-performance liquid chromatography (HPLC) nanocolumn (218MS3.07515 Vydac C18 polymeric reverse phase, 75  $\mu$ m i.d.  $\times$  150 mm long, P. J. Cobert Associates, St. Louis, MO, USA). Peptides were separated with a 90-min linear gradient from 5 to 60% acetonitrile at a flow rate of 0.3  $\mu$ l/min and electrosprayed through a fused silica emitter (360  $\mu$ m o.d., 75  $\mu$ m i.d., 15  $\mu$ m taper, New Objective, Woburn, MA, USA) directly into the QTRAP 2000 (a hybrid quadrupole linear ion trap mass spectrometer, Applied Biosystems, Foster City, CA, USA). An ion spray voltage of 1900 V was maintained between the emitter and the orifice. Information-dependent acquisition was used to collect MS, high-resolution MS, and MS/MS spectra. All spectra were collected in the enhanced mode using the trap function. The three most intense MS peaks in each cycle, having masses between 200 and 1700 *m/z*, charge of +1 to +4, and intensities greater than 10,000 cps, were selected for high-resolution MS and MS/MS analysis. Precursor ions

were excluded for 30 s after one MS/MS spectrum had been collected. MS/MS fragmentation was obtained by low-energy CID. The collision cell was pressurized to 40  $\mu$ Torr with pure nitrogen. Collision energies between 20 and 40 eV were determined automatically by the software based on the mass and charge of the precursor ion. The mass spectrometer was calibrated on selected fragments from the MS/MS spectrum of human Glu-fibrinopeptide B.

## Results

### OP-labeled peptides

A lysine from each of 22 peptides was found to have reacted with either CPO or DFP. Those 22 peptides came from seven different proteins: 5 peptides from human serum albumin, 2 peptides from human keratin 1, 1 peptide from human keratin 10, 6 peptides from bovine tubulin alpha, 1 peptide from bovine tubulin beta, 5 peptides from bovine actin, and 2 peptides from mouse transferrin (see Table 1).

When CPO reacts with lysine, the mass added to the peptide is 136 amu (for diethoxyphosphate). When DFP reacts with lysine, the mass added to the peptide is 164 amu (for diisopropoxyphosphate). Most of the peptides in Table 1 exhibited a parent ion mass equal to the mass of the amino acid sequence plus the mass added from the OP adduct (to within 0.2 amu). In five instances, the mass of the peptide was equal to the mass of the amino acid sequence plus twice the mass of the OP adduct. In the latter instances, a label was found on both a tyrosine and a lysine. The sequence of each peptide was confirmed by manual analysis of the CID MS/MS spectrum. The "MS Product" algorithm (a component of Protein Prospector, version 5.2.2, University of California, San Francisco, <http://prospector.ucsf.edu>) was used to help identify fragments from the MS/MS spectra. The Mascot database algorithm (Matrix Science, London, UK, <http://www.matrixscience.com>) was also used in the identification of labeled peptides [32]. The masses for OP-labeled lysine have been added to the Unimod protein modifi-

cation database (<http://www.unimod.org>) to facilitate the use of Mascot in searches for OP-modified residues. They are listed as O-diethylphosphate (for CPO) and diisopropylphosphate (for DFP). The precise location of the labeled amino acid could generally be established from the observed sequence. Finally, characteristic nonsequence masses that supported the proposed labeling were identified (see Table 2).

### Reaction of OPs with lysine

Reaction of an OP with a lysine (in a protein) would be expected to proceed via nucleophilic attack of the  $\epsilon$ -amino group from the lysine on the phosphorus of the OP. This reaction would result in the addition of a single organophosphorus moiety to the  $\epsilon$ -amino group of the lysine (Fig. 1).

The OPs used in the following work were CPO and DFP (see Fig. 2 for structures). The groups that are displaced from the OPs as a consequence of nucleophilic attack are the O-(3,5,6-trichloro-2-pyridinyl) of CPO and the fluoride of DFP. The resulting adducts are diethoxyphospho-lysine and diisopropoxyphospho-lysine, respectively.

### CID fragmentation of $\epsilon$ -N-modified lysine from peptides

When peptides containing  $\epsilon$ -N-modified lysine are subjected to low-energy CID, a sequence of reactions ensues, yielding prominent characteristic fragment ions corresponding to (i) a modified  $\alpha$ -amino-caprolactam (at 129 amu plus the mass of the modification), (ii) a modified lysine immonium ion (at 101 amu plus the mass of the modification), (iii) a modified lysine immonium ion minus  $\text{NH}_3$  (at 84 amu plus the added mass of the modification), and (iv) a lysine immonium ion minus the modification and minus  $\text{NH}_3$  (at 84 amu). Fig. 3 illustrates the sequence of structures involved in this fragmentation process. Details of the process were worked out by Fenaille and coworkers using MS/MS and pseudo-MS<sup>3</sup> (fragmentation of a fragment from MS/MS) analysis of peptides containing lysine modified on the  $\epsilon$ -amine with hexanal

**Table 1**  
OP-labeled lysine-containing peptides observed in tryptic digests.

	Species	Protein	Peptide <sup>a</sup>	Residue number <sup>b</sup>	gi number <sup>c</sup>	Peptide mass <sup>d</sup>	OP <sup>e</sup>
1	Human	Serum albumin	AFK*AWAVAR	K212	28592	1155.4	CPO
2	Human	Serum albumin	K*VPQVSTPTLVEVSR	K414	28592	1775.5	CPO
3	Human	Serum albumin	Y*TKK*VPQVSTPTLVEVSR	K414 Y411	28592	2307.4	CPO
4	Human	Serum albumin	LK*CASLQK	K199	28592	1083.4	CPO
5	Human	Serum albumin	LAK*TYETTLEK	K351	28592	1461.0	DFP
6	Human	Keratin 1	FLEQQNQVLQTK*WELLQQVDTSTR	K211	119395750	3069.1	CPO
7	Human	Keratin 1	SLDLDSIIAEVK*AQYEDIQK	K355	119395750	2486.5	CPO
8	Human	Keratin 10	LASYLDK*VR	K163	47744568	1200.7	CPO
9	Bovine	Tubulin alpha	DVNAAIATIK*TK	K336	73586894	1380.8	CPO
10	Bovine	Tubulin alpha	LSVDY*GK*K	K163 Y161	73586894	1181.6	CPO
11	Bovine	Tubulin alpha	LDHK*FDLMYAK	K394	73586894	1517.0	CPO
12	Bovine	Tubulin alpha	FDLMY*AK*R	K401 Y399	73586894	1315.6	CPO
13	Bovine	Tubulin alpha	Y*AK*R	K401 Y399	73586894	809.4	CPO
14	Bovine	Tubulin alpha	TIGGGDDSFNTFFSETGAGK*HVPR	K60	73586894	2633.4	CPO
15	Bovine	Tubulin beta	K*Y*VPR	K58 Y59	75773583	934.0	CPO
16	Bovine	Actin	VAPEEHPTLLTEAPLNPK*ANR	K113	62287933	2433.7	CPO
17	Bovine	Actin	DLTDYLMK*ILTER	K291	62287933	1746.4	CPO
18	Bovine	Actin	EITALAPSTMK*IK	K326	62287933	1538.4	CPO
19	Bovine	Actin	MQK*EITALAPSTMK	K315	62287933	1684.3	CPO
20	Bovine	Actin	IK*IIAPPER	K328	62287933	1172.5	CPO
21	Mouse	Transferrin	DLLFK*DSAFGLLR	K296	21363012	1631.4	CPO
22	Mouse	Transferrin	STTK*DLLFR	K626	21363012	1217.0	CPO

<sup>a</sup> K\* indicates the labeled lysine. Y\* indicates a labeled tyrosine in the same peptide.

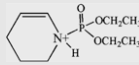
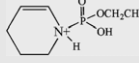
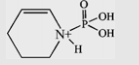
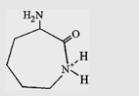
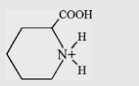
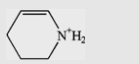
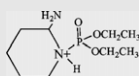
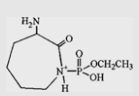
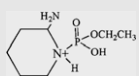
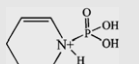
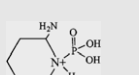

<sup>b</sup> Numbering is for the mature sequence except for the keratins that are numbered from the gene sequence.

<sup>c</sup> The gi number is the NCBI accession number for the protein from PubMed.

<sup>d</sup> The peptide masses are the measured, singly charged average masses  $[\text{M}+\text{H}]^{1+}$  for the labeled peptides. Peptides containing cysteine are carbamidomethylated.

<sup>e</sup> CPO indicates chlorpyrifos oxon. DFP indicates diisopropylfluorophosphate.

**Table 2**  
OP-labeled lysine characteristic ions.

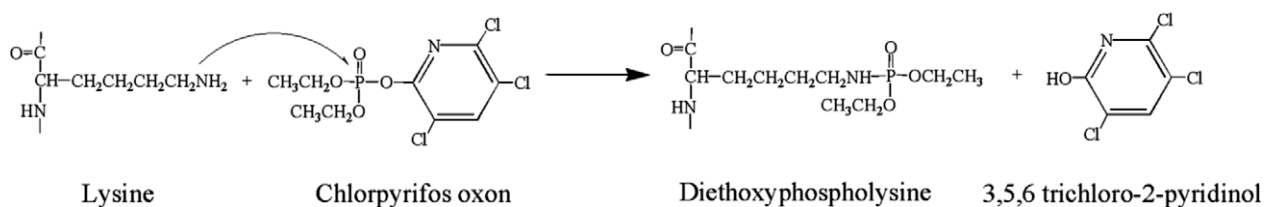
Mass amu <sup>a</sup>	Name	Structure	Percentage <sup>b</sup>	Relative intensity <sup>c</sup>
<i>CPO (21 tryptic peptides analyzed)</i>				
220.0	Diethoxyphospho-Lys immonium minus NH <sub>3</sub>		95	6–100
192.0	Monoethoxyphospho-Lys immonium minus NH <sub>3</sub>		85	4–38
163.9	Phospho-Lys immonium minus NH <sub>3</sub>		75	5–26
128.9	α-Amino caprolactam		30	4–13
129.9	Pipecolic acid		10	10–15
83.9	Lys immonium minus NH <sub>3</sub>		50	4–27
237.1	Diethoxyphospho-Lys immonium		50	3–18
237.0	Monoethoxyphospho α-amino caprolactam		–	–
209.1	Monoethoxyphospho-Lys immonium		10	2–5
<i>DFP (1 tryptic peptide analyzed)</i>				
164.0	Phospho-Lys immonium minus NH <sub>3</sub>		100	42
181.2	Phospho-Lys immonium		100	8
83.8	Lys immonium minus NH <sub>3</sub>		100	8

Note. All masses are for the protonated dehydro form of the amino acid.

<sup>a</sup> Mass is given as the average of all measurements.

<sup>b</sup> Percentage refers to the fraction of the tryptic peptides that exhibited this mass.

<sup>c</sup> Relative intensity refers to the intensity of the mass relative to the most intense peak in the MS/MS spectrum. This value is generally given as a range in percentage.

**Fig. 1.** Illustration of the reaction of lysine with OPs using CPO as an example for the OP.

[33]. Their proposed sequence of steps is consistent with the process described by Yalcin and Harrison for CID fragmentation of

unmodified lysine-containing peptides [34]. CID fragmentation of OP-labeled lysine would be expected to follow the pathway de-

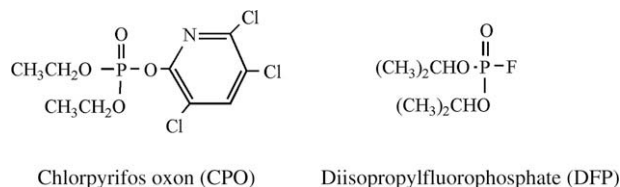


Fig. 2. OP structures.

scribed in Fig. 3. This is essentially what is observed. We found fragment masses that are consistent with these structures from peptides containing OP-modified lysine (where the OP is either CPO or DFP) (see Table 2).

An alternative fragmentation pathway that leads to pipecolic acid (130 amu) has also been reported [33,34]. This mass was occasionally observed in the CID of peptides containing OP-labeled lysine.

#### Characteristic fragments from OP-labeled lysine

##### CPO

When CPO reacts with lysine, the added mass is 136 amu (for diethoxyphosphate). Under CID conditions, there is a relatively facile gas-phase elimination of one or both of the ethylene side chains (28 amu each) from the diethoxyphosphate [31], resulting in a monoethoxyphosphate adduct (added mass = 108 amu) or a phosphate adduct (added mass = 80 amu). This side chain elimination explains the lysine-related masses observed during CID fragmentation of CPO-modified lysine-containing peptides (see Table 2).

CID fragmentation of peptides containing diethoxyphosphate-modified lysine yields nonsequence characteristic ions at 237, 220, 209, 192, 164, 130, 129, and 84 amu. These masses correspond to the diethoxyphosphate adduct of the lysine immonium ion ( $136 + 101 = 237$  amu), the diethoxyphosphate adduct of the lysine immonium ion minus  $\text{NH}_3$  ( $136 + 84 = 220$  amu), the monoethoxyphosphate adduct of the lysine immonium ion ( $108 + 101 = 209$  amu), the monoethoxyphosphate adduct of the lysine immonium ion minus  $\text{NH}_3$  ( $108 + 84 = 192$  amu), the phosphate adduct of the lysine immonium ion minus  $\text{NH}_3$  ( $80 + 84 = 164$  amu), pipecolic acid (130 amu),  $\alpha$ -amino-caprolactam (129 amu), and the lysine immonium ion minus  $\text{NH}_3$  and minus all vestiges of the diethoxyphosphate label (84 amu). Table 2 lists these fragments, shows their structures, indicates the frequency with which they appeared in the 21 MS/MS spectra of CPO-modified peptides, and indicates their intensities relative to the most intense mass in each spectrum.

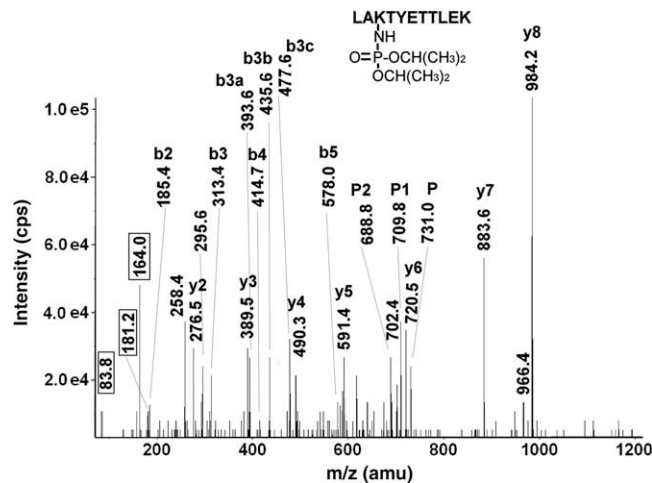


Fig. 4. CID mass spectrum of the diisopropoxyphosphate-labeled, human serum albumin, tryptic peptide LAK<sup>TYET</sup>LEK. The doubly charged parent ion at 731.0 amu is designated by the letter P. Sequential neutral loss of isopropylene (42 amu) from the diisopropoxyphosphate parent ion is designated by P1 (709.8 amu) and P2 (688.3 amu). Sequential neutral loss of isopropylene from the b3 ion is indicated by b3c (diisopropoxyphosphate form at 477.6 amu), b3b (monoisopropoxyphosphate form at 435.6 amu), and b3a (phosphate form at 363.6 amu). The values enclosed in the boxes are the masses of the characteristic fragments for diisopropoxyphosphate-labeled lysine. Lys351 is covalently modified by DFP.

As indicated in Table 2, the 237-amu mass could be interpreted as either the diethoxyphospho-lysine immonium ion or the monoethoxyphospho  $\alpha$ -amino-caprolactam. If the latter interpretation were correct, one might expect to see ions consistent with the diethoxyphospho  $\alpha$ -amino-caprolactam (at 265 amu). No peak at 265 amu appeared in any of the 21 MS/MS spectra, suggesting that the  $\alpha$ -amino-caprolactam interpretation is incorrect. Conversely, masses for both the diethoxyphospho-lysine immonium ion (237 amu) and the monoethoxyphospho-lysine immonium ion (209 amu) were detected (see Table 2), suggesting that the lysine immonium ion interpretation is correct. Modified immonium ions are most often the source of characteristic fragments [35].

The most prevalent characteristic ion was the diethoxyphospho-lysine immonium ion minus  $\text{NH}_3$  (220 amu), appearing in 95% of the MS/MS spectra (20 of 21). This is consistent with the results of Fenaille and coworkers, who found the modified lysine immonium ion minus  $\text{NH}_3$  to be a prominent mass in MS/MS spectra of hexanal-modified lysine-containing peptides [33]. Although the intensity of the 220-amu ion varied from 6 to 100% of the most intense ion in the spectrum, its intensity was generally around 30%.

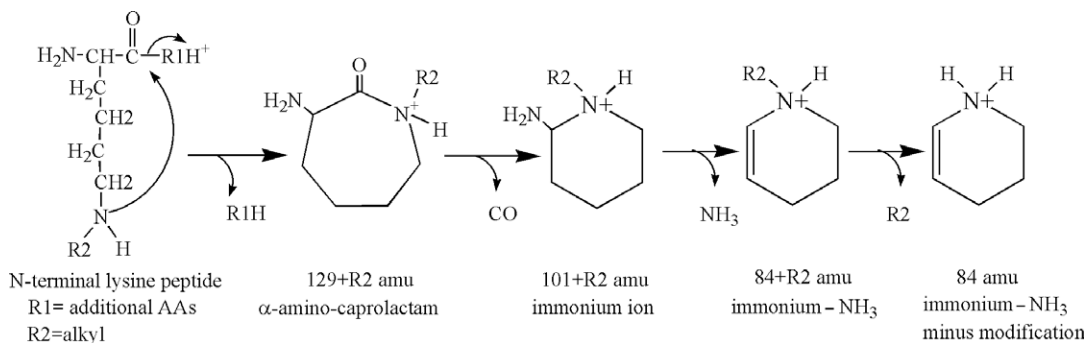
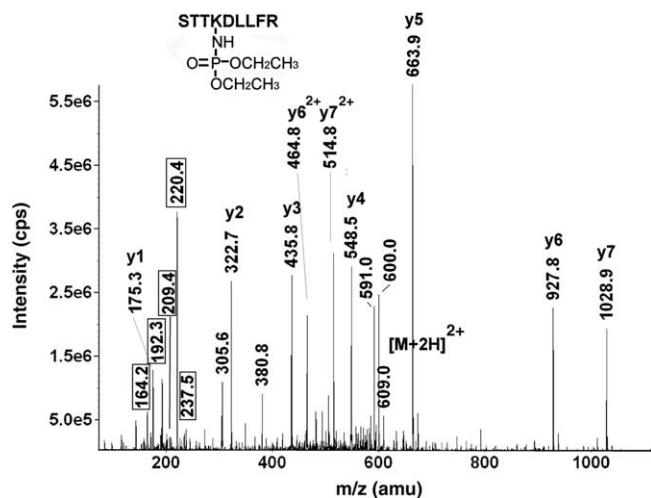


Fig. 3. CID fragmentation of  $\epsilon$ -N-modified lysine. The mass of R2 for DFP can be +164 for diisopropoxyphosphate or +80 for DFP that has lost both isopropyl groups. The mass of R2 for CPO can be +136 for diethoxyphosphate, +108 for monoethoxyphosphate, or +80 for CPO that has lost both ethoxy groups. The immonium ion minus  $\text{NH}_3$  is indicated as immonium -  $\text{NH}_3$ .



**Fig. 5.** CID mass spectrum of the diethoxyphosphate-labeled, mouse transferrin, tryptic peptide STTK\*DLLFR. The values enclosed in the boxes are the masses of the characteristic fragments for diethoxyphosphate-labeled lysine. The parent ion is marked by  $[M+2H]^{2+}$ . Lys626 is labeled by CPO.

On three occasions it was the most intense ion in the spectrum. The two next most common characteristic ions were also modified derivatives of the lysine immonium ion minus  $NH_3$ : monoethoxyphospho-lysine immonium ion minus  $NH_3$  (192.0 amu) and phospho-lysine immonium ion minus  $NH_3$  (163.9 amu). The lysine immonium ion (without modification, 83.9 amu) and the diethoxyphospho-lysine immonium ion (237.1 amu) also were frequently present. Occasionally, masses for the  $\alpha$ -amino caprolactam (128.9 amu), pipecolic acid (129.9 amu), and monoethoxyphospho-lysine immonium ion (209.1 amu) appeared.

Once identified, the characteristic ions for the diethoxyphosphate adduct were particularly useful in that they provided a convenient way to identify diethoxyphosphate-labeled lysine in other peptides.

#### DFP

Only human serum albumin was treated with DFP, and only one labeled peptide was found, namely LAK\*TYETTLK. Because no other proteins were treated with DFP, it is entirely possible that other DFP-labeled peptides may be found in the future.

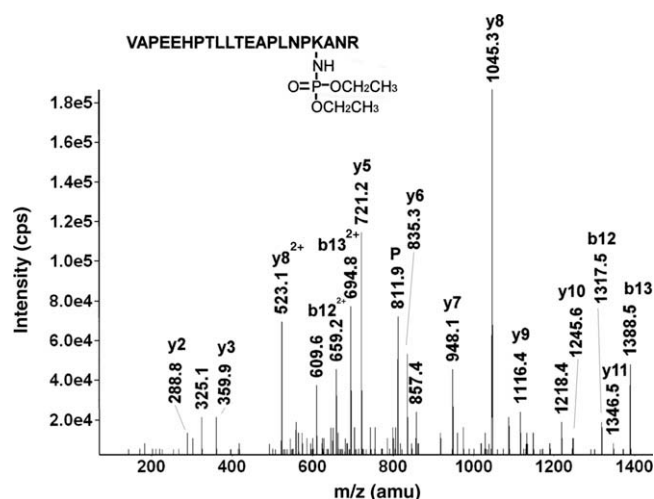


**Fig. 6.** CID mass spectrum of the diethoxyphosphate-labeled, bovine actin, tryptic peptide VAPEEHPTLLTEAPLNPK\*ANR. The parent ion is marked by the letter P. There are no characteristic fragments for diethoxyphosphate-labeled lysine. Lys113 is covalently modified by CPO.

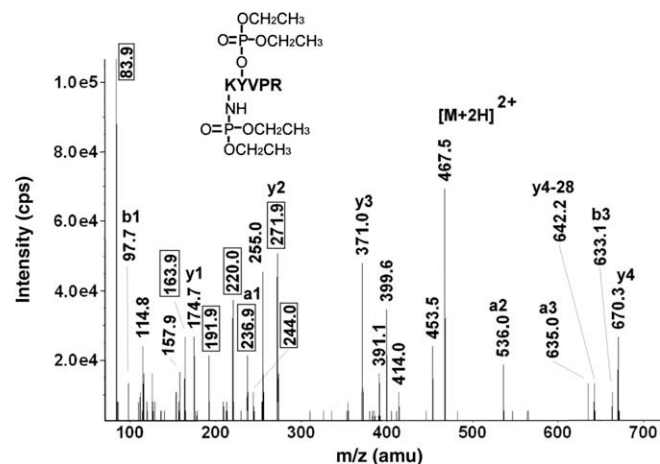


**Fig. 7.** CID mass spectrum of the diethoxyphosphate-labeled, bovine tubulin beta, tryptic peptide K\*Y\*VPR. The values enclosed in the boxes are the masses of the characteristic fragments for diethoxyphosphate-labeled lysine and diethoxyphosphate-labeled tyrosine. The parent ion is marked by  $[M+2H]^{2+}$ . Lys58 and Tyr59 are labeled by CPO.

When DFP reacts with lysine, the added mass is 164 amu (for diisopropoxyphosphate). Under CID conditions, gas-phase elimination of the isopropylene side chains (42 amu) is even more facile than elimination of ethylene is for the diethoxyphospho adducts [31]. Isopropylene elimination is so easy that there is no evidence for characteristic ions that retain a side chain.

CID fragmentation of the peptide containing the diisopropoxyphosphate-modified lysine yielded nonsequence characteristic ions at 181, 164, and 84 amu. These masses correspond to the phospho-lysine immonium ion ( $80 + 101 = 181$  amu), the phospho-lysine immonium ion minus  $NH_3$  ( $80 + 84 = 164$  amu), and the lysine immonium ion minus  $NH_3$  and minus all vestiges of the diisopropoxyphosphate label (84 amu). Table 2 lists these fragments, shows their structures, and indicates their intensities relative to the most intense mass in the spectrum. Because only one diisopropoxyphospho peptide was identified, the frequency with which they appear in the MS/MS spectra is set at 100%.

#### Illustration of CID fragmentation for peptides containing OP-labeled lysine adducts

Figs. 4–7 show representative MS/MS fragmentation spectra for peptides containing OP-labeled lysine. There is a spectrum for the diisopropoxyphospho adduct (Fig. 4), a spectrum for a peptide carrying a single diethoxyphosphate adduct on lysine that yielded characteristic fragments (Fig. 5), a spectrum for a diethoxyphosphate adduct on lysine that did not yield characteristic fragments (Fig. 6), and a spectrum for a peptide carrying a diethoxyphosphate adduct on lysine and another diethoxyphosphate adduct on tyrosine that yielded fragments characteristic of both labeled amino acids (Fig. 7).

Fig. 4 shows the MS/MS spectrum of the diisopropoxyphosphate-labeled peptide LAK\*TYETTLK from human serum albumin. It is labeled on the lysine that is three residues from the N terminus. That this lysine was not cleaved during the tryptic digestion supports the proposal that it is labeled. The parent ion is doubly charged with an  $m/z$  of 731.0, which includes the mass of the amino acid sequence plus an added mass of 164 amu for the diisopropoxyphosphate.

The spectrum is complicated by the facile loss of isopropylene (42 amu) from the diisopropoxyphosphate [31]. This neutral loss fragmentation accounts for the doubly charged peaks at 709.8

and 688.3 amu, designated P1 and P2, respectively. These are associated with the parent ion (at 731.0 amu, designated P) and are consistent with the loss of first one isopropylene group and then both isopropylene groups from the diisopropoxyphosphate adduct of the parent ion.

A similar phenomenon occurs for the *b*3 ion. This ion appears in four forms, designated *b*3, *b*3a, *b*3b, and *b*3c. The mass of the *b*3c fragment (477.6 amu) is consistent with the N-terminal three amino acids, LAK, plus the mass of diisopropoxyphosphate. Fragment *b*3b is 42 amu smaller (at 435.6 amu), consistent with the loss of one isopropylene group. Fragment *b*3a (at 393.6 amu) is smaller by yet another 42 amu. Finally, the *b*3 fragment (at 313.4 amu) is 80 amu smaller than *b*3a, indicative of the loss of the phospho moiety. All of the masses of these *b*3 fragments are consistent with diisopropoxyphosphate labeling of the lysine at position 3.

The *b* series, without any added mass, continues from *b*3 to *b*5. In addition, there is a *y* series that extends from *y*2 to *y*8. None of the residues in this series shows any indication of being labeled. The *y* series includes residues *y*7 and *y*8, which carry the two other potentially reactive groups, namely threonine and tyrosine. The fact that their masses do not include the adduct mass indicates that they are not labeled. Most of the other major peaks in the spectrum are consistent with loss of water from the sequence ions or with characteristic fragments. The foregoing observations—the parent ion mass, the neutral losses from the parent ion, the sequence data, and the neutral loss from the *b*3 fragment—clearly identify this peptide as being labeled by diisopropoxyphosphate on lysine.

Having established the identity of the label, we can turn to the nonsequence fragments in the CID spectrum to identify masses that are characteristic of this particular label. Three such masses appear in Fig. 4. They are enclosed in boxes for emphasis. The most intense of these masses is at 164.0 amu. It is consistent with phospho-lysine immonium ion minus NH<sub>3</sub>. The phospho-lysine immonium ion is also present (at 181.2 amu), as is the lysine immonium ion at 83.6 amu. Structures for these compounds are given in Table 2.

Fig. 5 shows the MS/MS spectrum of the diethoxyphosphate-labeled peptide STTK\*DLLFR from mouse transferrin. It is labeled on the lysine that is four residues from the N terminus. That this lysine was not cleaved during the tryptic digestion supports the proposal that it is labeled. The parent ion is doubly charged with an *m/z* of 609.0, which includes the mass of the amino acid sequence plus an added mass of 136 amu for the diethoxyphosphate.

A *y* ion series from *y*1 to *y*7 is present. The delta mass for the diethoxyphosphate-lysine adduct appears in the sequence between *y*5 and *y*6. This delta mass is 263.9 amu, consistent with the expected value for lysine (128.0 amu) plus diethoxyphosphate (136.0 amu). Unlike the diisopropoxyphosphate adduct, neutral loss is not evident from either the parent ion or the sequence ions. This is similar to our experience with modified tyrosine [31]. The masses at 464.8 and 514.8 amu are consistent with doubly charged forms of *y*6 and *y*7. Most other significant masses could be assigned as fragments due to loss of ammonia from sequence ions, to loss of water from the parent ion, to internal fragments, or to characteristic ions. The parent ion mass and the sequence data, including the *y*5–*y*6 interval for diethoxyphospho-lysine, clearly identify this peptide as being labeled on lysine by diethoxyphosphate.

Nonsequence characteristic fragments appeared at 237.5 amu (diethoxyphospho-lysine immonium ion), 220.4 amu (diethoxyphospho-lysine immonium ion minus NH<sub>3</sub>), 209.4 amu (monoethoxyphospho-lysine immonium ion), 192.3 amu (monoethoxyphospho-lysine immonium ion minus NH<sub>3</sub>), and 164.2 amu (phospho-lysine immonium ion minus NH<sub>3</sub>). Although neutral loss of ethylene (28 amu) from neither the parent ion nor the sequence ions was observed, neutral loss from the immonium ion seems to

be more facile. A similar observation was made for diethoxyphospho-tyrosine [31]. Structures of the characteristic ions are given in Table 2.

Fig. 6 shows the MS/MS spectrum of the diethoxyphosphate-labeled peptide VAPEEHPTLLTEAPLNPK\*ANR from bovine actin. It is labeled on the lysine that is four residues from the C terminus. That this lysine was not cleaved during the tryptic digestion supports the proposal that it is labeled. The parent ion is triply charged with an *m/z* of 811.9, which includes the mass of the amino acid sequence plus an added mass of 136 amu for the diethoxyphosphate.

A *y* ion series from *y*2 to *y*11 is present. There is a gap in the sequence at *y*4, which is the position of the proposed lysine adduct. The delta mass for this gap is too large for simply the lysine adduct. However, it is consistent with the interval between *y*3 and *y*5 (361.3 amu), which would include lysine plus diethoxyphosphate plus proline (128 + 136 + 97 = 361 amu). This places the diethoxyphospho adduct on either lysine or proline. Because proline is not a viable candidate for labeling, it may be concluded that the label resides on lysine. In addition to the *y* series, there are strong peaks for the *b*12 and *b*13 fragments, both the singly charged forms (at 1317.5 and 1388.5 amu) and the doubly charged forms (at 659.2 and 694.8 *m/z*). Most other major peaks can be assigned to internal fragments.

The parent mass and the sequence data, including the *y*3–*y*5 interval for diethoxyphospho-lysine and proline, clearly identify this peptide as being labeled by diethoxyphosphate on lysine. However, there is no evidence for characteristic ions in the MS/MS spectrum. This was the only peptide of the 21 CPO-labeled peptides we analyzed that did not show any characteristic fragments.

Fig. 7 shows the MS/MS spectrum of the diethoxyphosphate-labeled peptide K\*Y\*VPR from bovine tubulin beta. This peptide is doubly labeled, once on the N-terminal lysine and again on the neighboring tyrosine. In support of the foregoing statement, the parent ion mass is 467.5 *m/z* (doubly charged), which includes the mass of the amino acid sequence plus two times the added mass of 136 amu for the two diethoxyphosphate labels. The N-terminal lysine and the neighboring tyrosine are the only reasonable candidates for labeling in this peptide. Simultaneous labeling of both lysine and tyrosine occurred in four other peptides (Table 1): Y\*AK\*R, LSVDY\*GK\*K, and FDLMY\*AK\*R (all three from bovine tubulin alpha) and Y\*TKK\*VPQVSTPTLVEVSR (from human serum albumin). Thus, double labeling is not an isolated phenomenon. Labeling of two tyrosines in a single peptide was observed for two peptides from mouse transferrin [31].

A complete *y* ion series for K\*Y\*VPR is present in Fig. 7. The interval between *y*3 and *y*4 (299.3 amu) is consistent with a diethoxyphosphate-labeled tyrosine (163 + 136 = 299 amu). The addition of 264.0 amu to *y*4 (670.3 amu) yields the singly charged parent ion mass of 934.0 amu. The mass for diethoxyphosphate-labeled lysine is 264.0 amu (128 + 136 amu). There is a neutral loss from *y*4 of 28 amu (to give the peak at 642.2 amu), most likely due to dissociation of ethylene from the diethoxyphosphate adduct on tyrosine. A similar loss of 28 amu from *b*3 (to give the peak at 635.0 amu) is more difficult to interpret given that *b* ions readily lose CO (28 amu) to yield *a* ions. Alternatively, the 28-amu loss could again reflect loss of ethylene. The 635.0-amu mass has been designated *a*3 in Fig. 7.

Characteristic ions for diethoxyphospho-lysine appear at 220.0, 191.9, 163.9, and 83.9 amu. In addition, there is a mass at 236.9 amu, which could be interpreted as the diethoxyphospho-lysine immonium ion or the *a*1 ion. There is a significant peak at 244.0 amu, consistent with the monoethoxyphospho-tyrosine immonium ion [31]. A more commonly observed characteristic ion for CPO-labeled tyrosine is the diethoxyphospho-tyrosine immonium ion at 272 amu [31]. Although an intense peak exists at 271.9 amu, its interpretation is complicated by the possibility

of a proline-arginine internal fragment (nominal mass = 272 amu). Support for the existence of the internal fragment is the 97.7-amu mass, consistent with the N-terminal proline expected from such an internal fragment. At a minimum, the 271.9-amu mass is a combination of the proline-arginine internal fragment and the diethoxyphospho-tyrosine immonium characteristic ion.

A final complication in this MS/MS spectrum is a group of doubly charged fragments (at 453.5, 414.0, 399.6, and 391.1  $m/z$ ) in the vicinity of the parent ion. The 453.5- $m/z$  fragment is 28 amu smaller than the parent ion, making it tempting to assign 453.5 to a neutral loss of ethylene from the parent ion. Similarly, the 399.6- $m/z$  fragment is 136 amu smaller than the parent, making it reasonable to assign 399.6 to a neutral loss of the entire diethoxyphosphate group, that is,  $\text{HPO}(\text{OCH}_2\text{CH}_2)_2$ . However, a neutral loss of this sort has not been seen before for either diethoxyphospho-tyrosine or diethoxyphospho-lysine adducts. The  $m/z$  of 414.0 is still more confusing. Being 108 amu smaller than the parent, it would appear to be due to neutral loss of monoethoxyphosphate where the second ethylene remains attached to the peptide; however, we can conceive of no mechanism to accommodate such an interpretation. The 391.1  $m/z$  is a simple loss of 17 amu ( $\text{NH}_3$ ) from 399.6  $m/z$ . One might attribute these masses to contaminants or some other sort of artifact except that an analogous pattern of peaks is seen in the MS/MS spectrum of  $\text{Y}^*\text{AK}^*\text{R}$  (data not shown).

The parent ion mass, the sequence data (including the  $y3$ – $y4$  and  $y4$ –parent ion intervals), and the characteristic fragments strongly argue that this peptide is doubly labeled by CPO, carrying diethoxyphosphate groups on both lysine and tyrosine.

## Discussion

Reaction of OPs with tyrosine in a variety of proteins has been thoroughly documented [31]. We have now found a comparable reaction between OPs and lysine. Table 1 lists 22 peptides from seven proteins that are labeled on lysine. Involvement of this many different proteins strongly suggests that the reaction is commonplace. Nonetheless, we are aware of no other reports of OPs reacting with lysine on protein.

Analysis of the MS/MS spectra for 4 of the 22 peptides was presented. Comparable data exist for the remaining 18 peptides. These data firmly establish the existence of this reaction. A useful list of ions that are characteristic of diethoxyphospho-lysine and diisopropoxyphospho-lysine are given in Table 2. We found the characteristic ions for diethoxyphospho-lysine to be especially helpful in finding unknown peptides that were labeled.

Until recently, investigations into the reaction of OPs with biological targets have been confined largely to studies on serine hydrolases where the OPs react with the active site serine [2,11,12]. Early work did demonstrate that OPs could react with selected tyrosines on some proteins [23–26]. These studies laid the groundwork for the possibility that reaction of OPs with proteins other than AChE could be clinically relevant. As a result of increased interest in the hypothesis that there are clinically relevant targets for OPs other than AChE, the reaction of OPs with tyrosine in proteins has been revisited [18,20,21,31]. The observation of OP-reactive lysine described in the current article enlarges the field of targets that must be considered when searching for potential clinically significant OP targets.

## Acknowledgments

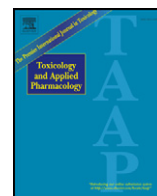
This work was supported by the U.S. Army Medical Research and Materiel Command (W81XWH-07-2-0034 to O.L.), the National Institutes of Health (U01 NS058056 to O.L. and P30CA36727 to Eppley Cancer Center), the Direction Générale de l'Armement of the

French Ministry of Defense (DGA 03co010-05/PEA01 08 7 and DGA/PEA 08co501), and the Agence Nationale pour la Recherche (ANR-06-BLAN-0163). Mass spectra were obtained with the support of the Mass Spectrometry and Proteomics Core Facility at the University of Nebraska Medical Center.

## References

- [1] C.N. Pope, Organophosphorus pesticides: do they all have the same mechanism of toxicity?, *J. Toxicol. Environ. Health B* 2 (1999) 161–181.
- [2] J.E. Casida, G.B. Quistad, Organophosphate toxicology: safety aspects of nonacetylcholinesterase secondary targets, *Chem. Res. Toxicol.* 17 (2004) 983–998.
- [3] D.M. Maxwell, K.M. Brecht, I. Koplovitz, R.E. Sweeney, Acetylcholinesterase inhibition: does it explain the toxicity of organophosphorus compounds?, *Arch. Toxicol.* 80 (2006) 756–760.
- [4] M.A. Brown, K.A. Brix, Review of health consequences from high-, intermediate-, and low-level exposure to organophosphorus nerve agents, *J. Appl. Toxicol.* 18 (1998) 393–408.
- [5] M.B. Abou-Donia, Organophosphorus ester-induced chronic neurotoxicity, *Arch. Environ. Health* 58 (2003) 484–497.
- [6] R.M. Salvi, D.R. Lara, E.S. Ghisolfi, L.V. Portela, R.D. Dias, D.O. Souza, Neuropsychiatric evaluation in subjects chronically exposed to organophosphate pesticides, *Toxicol. Sci.* 72 (2003) 267–271.
- [7] C. Beseler, L. Stallones, J.A. Hoppin, M.C. Alavanja, A. Blair, T. Keefe, F. Kamel, Depression and pesticide exposures in female spouses of licensed pesticide applicators in the agricultural health study cohort, *J. Occup. Environ. Med.* 48 (2006) 1005–1013.
- [8] F. Kamel, L.S. Engel, B.C. Gladen, J.A. Hoppin, M.C. Alavanja, D.P. Sandler, Neurologic symptoms in licensed pesticide applicators in the Agricultural Health Study, *Hum. Exp. Toxicol.* 26 (2007) 243–250.
- [9] D.B. Hancock, E.R. Martin, G.M. Mayhew, J.M. Stajich, R. Jewett, M.A. Stacy, B.L. Scott, J.M. Vance, W.K. Scott, Pesticide exposure and risk of Parkinson's disease: a family-based case-control study, *BMC Neurol.* 8 (2008) 6.
- [10] A.K. Srivastava, B.N. Gupta, V. Bihari, N. Mathur, L.P. Srivastava, B.S. Pangtey, R.S. Bharti, P. Kumar, Clinical, biochemical, and neurobehavioural studies of workers engaged in the manufacture of quinalphos, *Food Chem. Toxicol.* 38 (2000) 65–69.
- [11] D.E. Koshland, Correlation of structure and function in enzyme action, *Science* 142 (1963) 1533–1541.
- [12] D. Kidd, Y. Liu, B.F. Cravatt, Profiling serine hydrolase activities in complex proteomes, *Biochemistry* 40 (2001) 4005–4015.
- [13] P.G. Richards, M.K. Johnson, D.E. Ray, Identification of acylpeptide hydrolase as a sensitive site for reaction with organophosphorus compounds and a potential target for cognitive enhancing drugs, *Mol. Pharmacol.* 58 (2000) 577–583.
- [14] J.A. Bomser, J.E. Casida, Diethylphosphorylation of rat cardiac M2 muscarinic receptor by chlorpyrifos oxon in vitro, *Toxicol. Lett.* 119 (2001) 21–26.
- [15] B. Li, L.M. Schopfer, H. Grigoryan, C.M. Thompson, S.H. Hinrichs, P. Masson, O. Lockridge, Tyrosines of human and mouse transferrin covalently labeled by organophosphorus agents: a new motif for binding to proteins that have no active site serine, *Toxicol. Sci.* 107 (2009) 144–155.
- [16] B. Li, L.M. Schopfer, S.H. Hinrichs, P. Masson, O. Lockridge, Matrix-assisted laser desorption/ionization time-of-flight mass spectrometry assay for organophosphorus toxicants bound to human albumin at Tyr411, *Anal. Biochem.* 361 (2007) 263–272.
- [17] B. Li, F. Nachon, M.T. Froment, L. Verdier, J.C. Debouzy, B. Brasme, E. Gillon, L.M. Schopfer, O. Lockridge, P. Masson, Binding and hydrolysis of soman by human serum albumin, *Chem. Res. Toxicol.* 21 (2008) 421–431.
- [18] E.S. Peeples, L.M. Schopfer, E.G. Duysen, R. Spaulding, T. Voelker, C.M. Thompson, O. Lockridge, Albumin, a new biomarker of organophosphorus toxicant exposure, identified by mass spectrometry, *Toxicol. Sci.* 83 (2005) 303–312.
- [19] S.-J. Ding, J. Carr, J.E. Carlson, L. Tong, W. Xue, Y. Li, L.M. Schopfer, B. Li, F. Nachon, O. Asojo, C.M. Thompson, S.H. Hinrichs, P. Masson, O. Lockridge, Five tyrosines and two serines in human albumin are labeled by the organophosphorus agent FP-biotin, *Chem. Res. Toxicol.* 21 (2008) 1787–1794.
- [20] N.H. Williams, J.M. Harrison, R.W. Read, R.M. Black, Phosphylated tyrosine in albumin as a biomarker of exposure to organophosphorus nerve agents, *Arch. Toxicol.* 81 (2007) 627–639.
- [21] R.M. Black, J.M. Harrison, R.W. Read, The interaction of sarin and soman with plasma proteins: the identification of a novel phosphorylation site, *Arch. Toxicol.* 73 (1999) 123–126.
- [22] H. Grigoryan, L.M. Schopfer, C.M. Thompson, A.V. Terry, P. Masson, O. Lockridge, Mass spectrometry identifies covalent binding of soman, sarin, chlorpyrifos oxon, diisopropyl fluorophosphate, and FP-biotin to tyrosines on tubulin: a potential mechanism of long term toxicity by organophosphorus agents, *Chem. Biol. Interact.* 175 (2008) 180–186.
- [23] F. Sanger, Amino-acid sequences in the active centers of certain enzymes, *Proc. Chem. Soc.* 5 (1963) 76–83.
- [24] T. Murachi, T. Inagami, M. Yasui, Evidence for alkylphosphorylation of tyrosyl residues of stem bromelain by diisopropylphosphorofluoridate, *Biochemistry* 4 (1965) 2815–2825.

- [25] I.M. Chaiken, E.L. Smith, Reaction of a specific tyrosine residue of papain with diisopropylfluorophosphate, *J. Biol. Chem.* 244 (1969) 4247–4250.
- [26] K. Kato, T. Murachi, Chemical modification of tyrosyl residues of hen egg-white lysozyme by diisopropylphosphorofluoridate, *J. Biochem.* 69 (1971) 725–737.
- [27] H. Grigoryan, B. Li, E.K. Anderson, W. Xue, F. Nachon, O. Lockridge, L.M. Schopfer, Covalent binding of the organophosphorus agent FP-biotin to tyrosine in eight proteins that have no active site serine, *Chem. Biol. Interact.* 180 (2009) 492–498.
- [28] R.F. Ashbolt, H.N. Rydon, The action of diisopropyl phosphorofluoridate and other anticholinesterases on amino acids, *Biochem. J.* 66 (1957) 237–242.
- [29] R.A. Smith, R.M. Halpern, B.B. Bruegger, A.K. Dunlap, O. Fricke, Chromosomal protein phosphorylation on basic amino acids, *Methods Cell Biol.* 19 (1978) 153–159.
- [30] H. Grigoryan, L.M. Schopfer, E. Peeples, E. Duysen, O. Lockridge, Mass spectrometry identifies multiple organophosphorylated sites on tubulin, *Toxicol. Appl. Pharm.* (2009), doi:10.1016/j.taap.2009.07.020.
- [31] L.M. Schopfer, H. Grigoryan, B. Li, F. Nachon, P. Masson, O. Lockridge, Mass spectral characterization of organophosphate-labeled tyrosine-containing peptides: characteristic mass fragments and a new binding motif for organophosphates, *J. Chromatogr. B* (2009), in press.
- [32] D.N. Perkins, D.J. Pappin, D.M. Creasy, J.S. Cottrell, Probability-based protein identification by searching sequence databases using mass spectrometry data, *Electrophoresis* 20 (1999) 3551–3567.
- [33] F. Fenaille, J.-C. Tabet, P.A. Guy, Study of peptides containing modified lysine residues by tandem mass spectrometry: precursor ion scanning of hexanal-modified peptides, *Rapid Commun. Mass Spectrom.* 18 (2004) 67–76.
- [34] T. Yalcin, A.G. Harrison, Ion chemistry of protonated lysine derivatives, *J. Mass Spectrom.* 31 (1996) 1237–1243.
- [35] C.W. Hung, A. Schlosser, J. Wei, W.D. Lehmann, Collision-induced reporter fragmentations for identification of covalently modified peptides, *Anal. Bioanal. Chem.* 389 (2007) 1003–1016.



## Nanoimages show disruption of tubulin polymerization by chlorpyrifos oxon: Implications for neurotoxicity

Hasmik Grigoryan, Oksana Lockridge\*

University of Nebraska Medical Center, Eppley Institute for Cancer Research, 986805 Nebraska Medical Center, Omaha, NE 68198-6805, USA

### ARTICLE INFO

#### Article history:

Received 29 May 2009

Revised 15 July 2009

Accepted 15 July 2009

Available online 22 July 2009

#### Keywords:

Nanoimages

Tubulin polymerization

Chlorpyrifos oxon

Mass spectrometry

### ABSTRACT

Organophosphorus agents cause cognitive deficits and depression in some people. We hypothesize that the mechanism by which organophosphorus agents cause these disorders is by modification of proteins in the brain. One such protein could be tubulin. Tubulin polymerizes to make the microtubules that transport cell components to nerve axons. The goal of the present work was to measure the effect of the organophosphorus agent chlorpyrifos oxon on tubulin polymerization. An additional goal was to identify the amino acids covalently modified by chlorpyrifos oxon in microtubule polymers and to compare them to the amino acids modified in unpolymerized tubulin dimers. Purified bovine tubulin (0.1 mM) was treated with 0.005–0.1 mM chlorpyrifos oxon for 30 min at room temperature and then polymerized by addition of 1 mM GTP to generate microtubules. Microtubules were visualized by atomic force microscopy. Chlorpyrifos oxon-modified residues were identified by tandem ion trap electrospray ionization and matrix-assisted laser desorption/ionization mass spectrometry of tryptic peptides. Nanoimaging showed that low concentrations (0.005 and 0.01 mM) of chlorpyrifos oxon yielded short, thin microtubules. A concentration of 0.025 mM stimulated polymerization, while high concentrations (0.05 and 0.1 mM) caused aggregation. Of the 17 tyrosines covalently modified by chlorpyrifos oxon in unpolymerized tubulin dimers, only 2 tyrosines were labeled in polymerized microtubules. The two labeled tyrosines in polymerized tubulin were Tyr 103 in EDAANNY\*R of alpha tubulin, and Tyr 281 in GSQQY\*R of beta tubulin. In conclusion, chlorpyrifos oxon binding to tubulin disrupts tubulin polymerization. These results may lead to an understanding of the neurotoxicity of organophosphorus agents.

© 2009 Elsevier Inc. All rights reserved.

### Introduction

Exposure to organophosphorus pesticides has been linked to memory loss, learning disability, fatigue, depression, and Parkinson's disease (Abou-Donia, 2003; Salvi et al., 2003; Beseler et al., 2006; Kamel et al., 2007; Hancock et al., 2008). These symptoms may appear after exposures too low to significantly inhibit acetylcholinesterase (Srivas-tava et al., 2000). A mechanism to explain the low dose toxicity of organophosphorus agents is needed. Tubulin has been implicated in neurodegenerative diseases (Gendron and Petrucelli, 2009) and may also have a role in low dose organophosphorus agent effects. Behavioral studies in rats treated with low doses of chlorpyrifos, followed by a wash out period before testing cognitive function in a water-maze hidden platform task, revealed memory impairment (Terry et al., 2007). In vitro tests of tubulin function in a turbidity assay showed that very low doses of chlorpyrifos oxon inhibited tubulin polymerization (Prendergast et al., 2007). Mice treated with a biotin labeled organophosphorus agent called FP-biotin have FP-biotin labeled tubulin in the brain (Grigoryan

et al., 2009). In vitro studies with purified bovine brain tubulin have identified tyrosine in tubulin as the site of covalent attachment of FP-biotin, chlorpyrifos oxon, soman, sarin, and diisopropylfluorophosphate (Grigoryan et al., 2008). One tyrosine is labeled rapidly in bovine tubulin, while an additional 16 tyrosines can be labeled at least partially with a 40-fold molar excess of chlorpyrifos oxon in a 24 h reaction at 37 °C (Grigoryan et al., 2009).

In the present study we tested the ability of tubulin to polymerize into microtubules after tubulin dimers had been treated with various concentrations of chlorpyrifos oxon. Microtubules are part of the cytoskeletal system that maintains the morphology of neurons including axonal and dendritic processes (Gendron and Petrucelli, 2009). Microtubules serve as highways for transport of mitochondria, synaptic vesicles, components of ion channels, receptors, and scaffolding proteins to and from synaptic sites. Synapses are highly vulnerable to impairments in transport. Perturbations to microtubule transport could cause malfunctions in neurotransmission and signal propagation and lead to synaptic degradation (Gendron and Petrucelli, 2009). Drugs that inhibit tubulin polymerization, for example colchicine, trigger apoptosis (Yeste-Velasco et al., 2008). Thus, the ability of tubulin to polymerize is very important for the life of a cell. We tested the hypothesis that modification of tubulin by chlorpyrifos oxon would affect tubulin polymerization. Tubulin polymers were visualized by atomic force microscopy. It was found that substoichiometric concentrations of

Abbreviations: CPO, chlorpyrifos oxon; PEM buffer, 80 mM PIPES, 2 mM magnesium chloride and 0.5 mM EGTA, pH 7.0; MS, mass spectrometry; MALDI TOF TOF, matrix-assisted laser desorption ionization time of flight mass spectrometry.

\* Corresponding author. Fax: +1 402 559 4651.

E-mail address: [olockrid@unmc.edu](mailto:olockrid@unmc.edu) (O. Lockridge).

chlorpyrifos oxon yielded short, thin microtubules. In contrast, stoichiometric concentrations of chlorpyrifos oxon resulted in clumping of tubulin. The nanoimaging study leads to the conclusion that chlorpyrifos oxon disrupts tubulin polymerization.

## Materials and methods

**Materials.** Bovine brain tubulin (TL238) >99% pure, purchased from Cytoskeleton, Inc (Denver, CO), contains dimers of alpha beta tubulin. Chlorpyrifos oxon (MET-674B, Chem. Service Inc., West Chester, PA) was diluted into dimethylsulfoxide and stored at  $-80^{\circ}\text{C}$ . Guanosine 5'-triphosphate sodium salt hydrate (GTP, G8877)  $\geq 95\%$  HPLC pure powder; 1,4-piperazinediethanesulfonic acid (PIPES, P6757) >99% pure powder; and colchicine (C9754)  $\geq 95\%$  HPLC pure powder were from Sigma (St Louis, MO). Sequencing grade modified porcine trypsin (V5113) was from Promega (Madison, WI). Slide-A-Lyzer 7K dialysis cassettes (No. 66370) were from Pierce Biotechnology Inc. (Rockford, IL). Alpha-cyano-4-hydroxycinnamic acid, and Cal Mix 5 were from Applied Biosystems (MDS Sciex, Foster City, CA). All other chemicals were of analytical grade.

**Tubulin polymerization for nanoimaging.** Tubulin was treated with chlorpyrifos oxon for 30 min before it was polymerized. Each tube contained 0.05 ml of 5 mg/ml tubulin (0.1 mM) in PEM buffer (80 mM PIPES, 2 mM magnesium chloride and 0.5 mM EGTA, pH 7.0) and 0, 0.005, 0.01, 0.025, 0.05, or 0.1 mM chlorpyrifos oxon. After 30 min at room temperature, samples were stored on ice for a brief period while GTP was added. Tubulin polymerization was initiated by addition of GTP to a concentration of 1 mM and continued for 2 h at  $37^{\circ}\text{C}$ . Samples were turbid after 2 h, confirming that tubulin had polymerized. A control to show the effect of inhibition of tubulin polymerization was tubulin incubated with 0.025 mM colchicine and 1 mM GTP (Skoufias and Wilson, 1992). A control to show the background from unpolymerized tubulin was tubulin in PEM buffer without GTP.

**Nanoimages of microtubules.** Samples for atomic force microscopy were fixed with 0.25% glutaraldehyde and diluted 10-fold before deposition of 5–7  $\mu\text{l}$  onto freshly cleaved mica. The freshly cleaved mica had been treated with a 0.167 mM aqueous solution of 1-(3-aminopropyl) silatrane. This chemical treatment of the mica surface allows the sample to be deposited in a wide range of ionic strengths and pH. The negatively charged microtubules do not adsorb to untreated mica because untreated mica is negatively charged. After 2 min the samples were thoroughly rinsed with deionized water (Labconco Co., Kansas City, MO) and dried under argon gas flow. Images were acquired in air using a MFP-3D AFM microscope (Asylum Research, Santa Barbara, CA) operated in tapping mode. Pictures were acquired on average from 7 different  $20 \times 20 \mu\text{m}$  areas. Image processing and microtubule characterization were performed using Femtoscan software (Advanced Technology Center, Moscow, Russia) (Lushnikov et al., 2006).

### Mass spectrometry to identify sites modified by chlorpyrifos oxon.

Bovine brain tubulin (0.5 mg/ml) in PEM buffer pH 7.0 containing 1 mM GTP and 20% glycerol was polymerized in an Eppendorf Thermomixer R thermoblock (Westbury, NY) for 3 h at  $37^{\circ}\text{C}$ . After 3 hours the sample was turbid, an indication that the tubules had polymerized. Chlorpyrifos oxon was added to a final concentration of 0.5 mM and incubation was continued at  $37^{\circ}\text{C}$  for 24 h. Two control samples were 1) tubulin treated with chlorpyrifos oxon while the tubulin was an unpolymerized dimer, and 2) tubulin not treated with chlorpyrifos oxon. Protein was denatured by boiling in a water bath for 10 min. Excess chlorpyrifos oxon was removed by dialysis against 4 l of 10 mM ammonium bicarbonate (pH 8.3) at  $4^{\circ}\text{C}$  overnight. Tubulin (250  $\mu\text{g}$ ) was digested with 2.5  $\mu\text{g}$  of Promega trypsin at  $37^{\circ}\text{C}$  overnight. One microliter of tryptic digest was spotted on a 384 well Opti-TOF sample plate (# 1016491,

Applied Biosystems, Foster City, CA), air dried and overlaid with 1  $\mu\text{l}$  of 10 mg/ml alpha-cyano-4-hydroxycinnamic acid dissolved in 50% acetonitrile, 0.1% trifluoroacetic acid. Mass spectra were acquired in positive ion reflector mode on a MALDI TOF 4800 mass spectrometer (Applied Biosystems). The final spectrum was the average of 500 laser shots. The mass spectrometer was calibrated before each use with CalMix 5 (Applied Biosystems).

Tryptic digests were also analyzed by LCMSMS in a QTRAP 2000 tandem ion trap electrospray mass spectrometer (Applied Biosystems) as previously described (Lockridge et al., 2008).

**Statistical analysis of microtubule parameters.** The width of untreated and chlorpyrifos oxon treated microfibrils was measured using Femtoscan software (Advanced Technology Center, Moscow, Russia) (Lushnikov et al., 2006). On average 15–70 different fibrils from each sample were analyzed from at least 4–5 different areas. A one-way ANOVA was performed to determine statistical significance between the chlorpyrifos oxon treated groups compared to the control group. SPSS software (Microsoft Corp.) was used for this analysis.

## Results

### Concentration dependent effect of chlorpyrifos oxon on tubulin polymerization

The effect of chlorpyrifos oxon on tubulin polymerization was evaluated by acquiring nanoimages of microtubules formed in the absence and in the presence of chlorpyrifos oxon. Five different concentrations of chlorpyrifos oxon were used. In addition, images were collected of unpolymerized tubulin and of tubules whose polymerization was inhibited by 0.025 mM colchicine. The results are illustrated at different magnifications in Fig. 1 ( $20 \times 20 \mu\text{m}$ ) and Fig. 2 ( $2 \times 2 \mu\text{m}$ ).

Fig. 1A shows unpolymerized tubulin, prepared in the absence of GTP. The background is full of small particles.

Fig. 1B shows microtubules polymerized in the presence of 1 mM GTP without chlorpyrifos oxon. These microtubules are straight, well structured, and individually separated. They appear uniform in width and are long (average length  $10.4 \pm 1 \mu\text{m}$ ). The background has fewer small particles than Fig. 1A. The average number of microtubules in a  $20 \times 20 \mu\text{m}$  area was  $60.7 \pm 6$ . See Table 1.

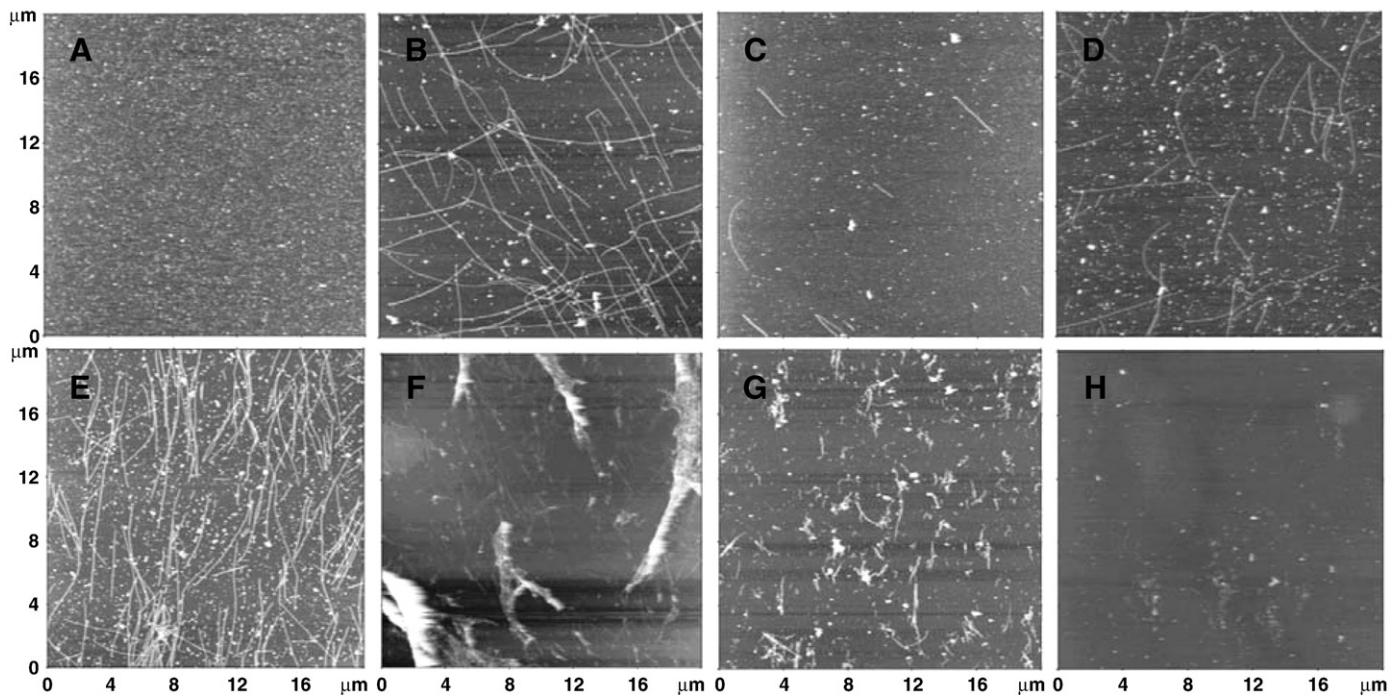
Fig. 1C shows the effect of pretreatment of 0.1 mM tubulin with 0.005 mM chlorpyrifos oxon. There is a drastic reduction in the number of microtubules, and in their length (average length  $4.3 \pm 0.4 \mu\text{m}$ ). The average number of tubules in a  $20 \times 20 \mu\text{m}$  area was  $8.3 \pm 0.8$ , indicating that 0.005 mM chlorpyrifos oxon inhibited tubulin polymerization 7.3-fold.

Fig. 1D shows the effect of pretreatment of 0.1 mM tubulin with 0.010 mM chlorpyrifos oxon. Microtubule density and length are reduced compared to Fig. 1B where tubulin had not been treated with chlorpyrifos oxon. However, there are more microtubules than were found after treatment with 0.005 mM chlorpyrifos oxon, and they are longer (average length  $6 \pm 0.6 \mu\text{m}$ ). The average number of tubules in a  $20 \times 20 \mu\text{m}$  area was  $49.6 \pm 5$  indicating 0.010 mM chlorpyrifos oxon inhibited polymerization only 1.2-fold.

Fig. 1E shows that pretreatment with 0.025 mM chlorpyrifos oxon stimulates microtubule polymerization. The density of microtubules is 2-fold greater than in Fig. 1B, with an average of 135 tubules in a  $20 \times 20 \mu\text{m}$  area. Microtubules were not well separated, they were clustered, and they were longer than those formed in the absence of chlorpyrifos oxon, on average being longer than  $20 \mu\text{m}$ .

Fig. 1F shows that pretreatment with 0.050 mM chlorpyrifos oxon causes microtubules to clump. The structures also seem to be more fragile, with the blurred images likely being the result of deformation induced by the atomic force microscope probe.

Fig. 1G shows that pretreatment of 0.1 mM tubulin with 0.1 mM chlorpyrifos oxon causes further degradation of the microtubules.



**Fig. 1.** Effect of chlorpyrifos oxon on tubulin polymerization visualized by atomic force microscopy. (A) 0.1 mM bovine tubulin in PEM buffer, no GTP; (B) 0.1 mM tubulin polymerized with 1 mM GTP, no chlorpyrifos oxon; (C) 0.1 mM tubulin pretreated with 0.005 mM chlorpyrifos oxon before polymerization with GTP; (D) pretreated with 0.010 mM chlorpyrifos oxon before polymerization; (E) pretreated with 0.025 mM chlorpyrifos oxon before polymerization; (F) pretreated with 0.050 mM chlorpyrifos oxon before polymerization; (G) 0.1 mM tubulin pretreated with 0.1 mM chlorpyrifos oxon before polymerization; (H) polymerized in the presence of 0.025 mM colchicine. The dimensions of each panel are  $20 \times 20 \mu\text{m}$ . Images are presented in height trace mode.

Fig. 1H shows a nearly blank background for microtubules polymerized in the presence of 0.025 mM colchicine. Colchicine is a potent inhibitor of tubulin polymerization (Skoufias and Wilson, 1992).

Fig. 2 shows images comparable to those in Fig. 1, after 10-fold magnification. Such magnification provides better images for analysis

of detailed structural differences, including measurement of width. It is tempting to propose that the globules in Fig. 2A are tubulin dimers. This interpretation is based on the similarity of the size of these particles to those in Fig. 2H, where polymerization has been precluded by the presence of colchicine.

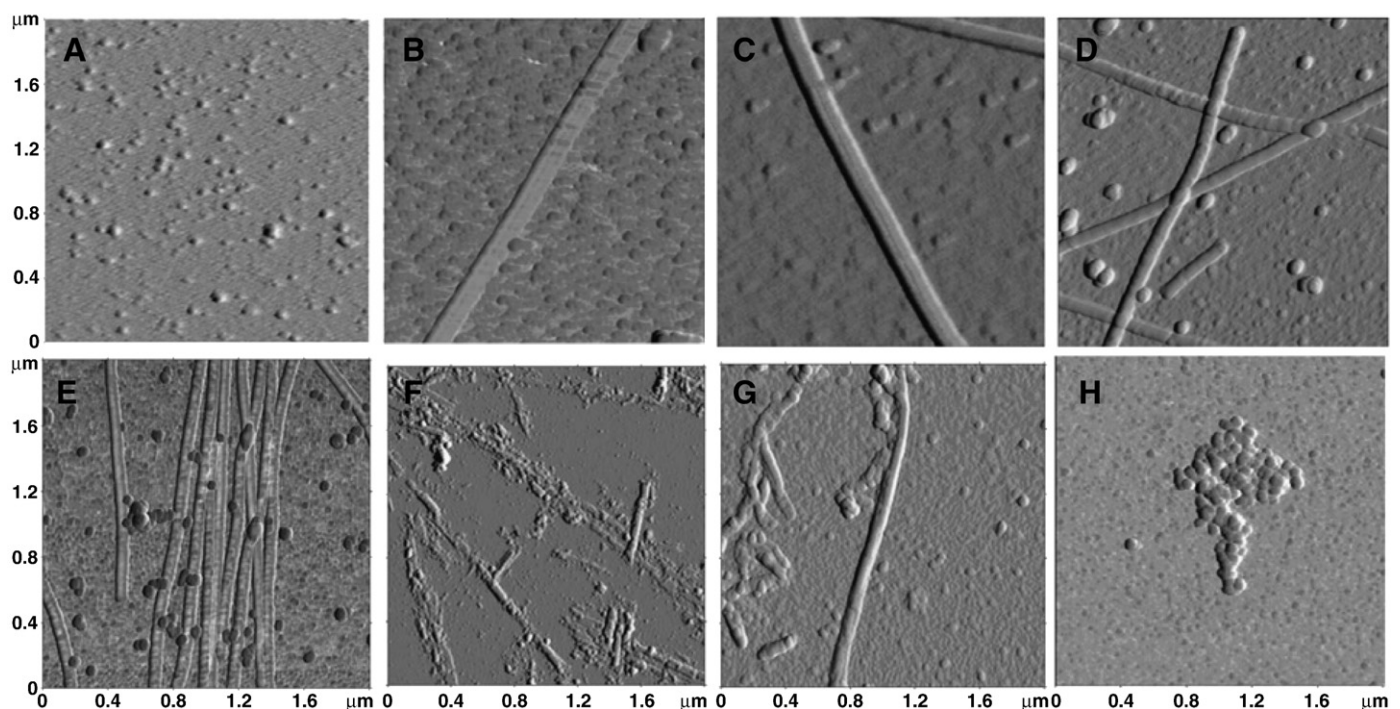


**Fig. 2.** Ten times magnified view of polymerized tubulin. Samples are the same as in Fig. 1. (A) no GTP, no chlorpyrifos oxon; (B) control with GTP, no chlorpyrifos oxon; (C) 0.005 mM chlorpyrifos oxon; (D) 0.010 mM chlorpyrifos oxon; (E) 0.025 mM chlorpyrifos oxon; (F) 0.050 mM chlorpyrifos oxon; (G) 0.100 mM chlorpyrifos oxon; (H) 0.025 mM colchicine. The dimensions of each panel are  $2 \times 2 \mu\text{m}$ . Images are presented in phase trace mode.

**Table 1**

Microtubule length, density, and width as a function of chlorpyrifos oxon (CPO) concentration during polymerization of 0.1 mM bovine tubulin.

[CPO], mM	Length, $\mu\text{m}$	Number of tubules in $20 \times 20 \mu\text{m}$ area	Width, nm
0 (Control)	$10.4 \pm 1$	$60.7 \pm 6$	$84.2 \pm 20$
0.005	$4.3 \pm 0.4$	$8.3 \pm 0.8$	$75.2 \pm 7$
0.010	$6 \pm 0.6$	$49.6 \pm 5$	$72.1 \pm 8$
0.025	$>20$	135	$65.1 \pm 4.9$
0.050	Clumps	Clumps	Clumps
0.100	Clumps	Clumps	Clumps

A one-way ANOVA on the width of fibrils at each concentration of chlorpyrifos oxon demonstrated statistically significant differences  $p=0.04$  for the 0.01 mM treated group and  $p=0.002$  for the 0.025 mM group compared to control.

The control microtubules in Fig. 2B show an average width of  $84.2 \pm 20$  nm. The average width of microtubules prepared from tubules pretreated with 0.005 mM chlorpyrifos oxon was  $75.2 \pm 7$  nm (Fig. 2C), and those pretreated with 0.010 mM chlorpyrifos oxon was  $72.1 \pm 8$  nm (Fig. 2D). Pretreatment of 0.1 mM tubulin with 0.025 mM chlorpyrifos oxon resulted in abnormal polymerization (Fig. 2E) and a further reduction in the average width to  $65.1 \pm 4.9$  nm. Thus pretreatment of tubulin with chlorpyrifos oxon reduced the width of microtubules compared to that for control microtubules.

The picture dramatically changed when 0.1 mM tubulin was incubated with 0.05 and 0.10 mM chlorpyrifos oxon (Figs. 2F and G). Under those conditions, the most prominent structures are large aggregates. In addition there are finely elongated shapes that suggest that narrow microtubules may have been formed, but then have been degraded during sample preparation. In Fig. 2G the tubules are fragmented. The widths of clumps and fragments of tubules were not measured.

No microtubules are present in Fig. 2H for the sample treated with 0.025 mM colchicine. Only small aggregates and particles are present. The nanoimages confirm that colchicine is a potent inhibitor of tubulin polymerization.

Figs. 1 and 2 define a triphasic process which implies the binding of at least three molecules of chlorpyrifos oxon to tubulin. The initial binding results in a decrease in polymerization, the second binding causes an increase, and the third results in destruction of the microtubules. We have previously demonstrated that as many as 17 tubulin tyrosines can be labeled by chlorpyrifos oxon.

#### Sites in polymerized microtubules modified by chlorpyrifos oxon

The above nanoimaging study showed that chlorpyrifos oxon binding to tubulin interfered with tubulin polymerization. In a previous

work we had identified 17 tyrosines in the unpolymerized tubulin  $\alpha\beta$ -dimer that are covalently modified by treatment with a 40-fold molar excess of chlorpyrifos oxon (Grigoryan et al., 2008, 2009). Those labeled sites are listed in Table 2. In the present study we tested the hypothesis that some of these chlorpyrifos oxon binding sites would be blocked in polymerized tubulin and therefore would be unavailable for reaction with chlorpyrifos oxon.

The polymerized microtubules were incubated with 0.5 mM chlorpyrifos oxon at 37 °C for 24 h. To show the difference in site availability, tubulin that had not been polymerized was also treated with 0.5 mM chlorpyrifos oxon. Another control was tubulin not treated with chlorpyrifos oxon and not polymerized.

Covalent binding of chlorpyrifos oxon to tubulin was determined in two ways. First, the masses of tryptic peptides from the tubulin chlorpyrifos oxon reaction mixture were compared to masses of tryptic peptides from unreacted tubulin using the MALDI TOF TOF 4800 mass spectrometer. Labeled peptides gained 136 amu following reaction with chlorpyrifos oxon due to formation of a diethoxyphosphate adduct. MALDI analysis was performed to obtain an estimate of the extent of labeling. The relative intensities of the labeled and unlabeled peptides were taken as a measure of the extent of labeling. This estimate assumes that the diethoxyphosphate label did not significantly affect the ionization properties of the peptide. Second, the labeled peptides were isolated and fragmented in the QTRAP 2000 mass spectrometer after online liquid chromatography separation. We have found that such LCMSMS analysis with the QTRAP mass spectrometer revealed more labeled peptides than the MALDI, and that the fragmentation spectra were more readily analyzed. Fragmentation spectra were manually analyzed to confirm the sequence of the peptide and to identify the labeled amino acid.

An example of the MALDI TOF TOF analysis is given in Fig. 3. Fig. 3A shows the MALDI mass spectrum of tubulin that has not been treated with chlorpyrifos oxon. The peak at 1023.5 amu is consistent with the unlabeled peptide EDAANNYAR of alpha tubulin. The peak at 1039.6 amu is consistent with the unlabeled YLTVAAVFR from beta tubulin. Fig. 3B shows the MALDI mass spectrum of tubulin treated with chlorpyrifos oxon, but not polymerized. The unlabeled peaks at 1023.5 and 1039.6 amu are present, but in addition two new peaks have appeared. The new peaks at 1059.6 and 1075.6 amu correspond to chlorpyrifos oxon labeled EDAANNY\*AR and Y\*LTVAAVFR peptides. The added mass of + 136 amu from chlorpyrifos oxon was shown to be on the tyrosine (Y\*), indicated by an asterisk, by subsequent fragmentation in the QTRAP mass spectrometer. Comparison of the relative peak heights for the labeled and unlabeled peptides suggests that 30%

**Table 2**

Chlorpyrifos oxon-labeled tryptic peptides from bovine alpha1 and beta2 tubulin identified by mass spectrometry.

Tubulin chain	Peptide	CPO labeled tyrosine in tubulin dimer	CPO labeled tyrosine in polymerized microtubules	Contact type in crystal structure
Alpha	TGTY*R	83	103	Lateral Longitudinal GTP binding Longitudinal
	EDAANNY*AR	103		
	GHY*TIGK	108		
	LSVDY*GK	161		
	NLDIERPTY*TNLNR	224		
	FDGALNVDLTFQTNLVPY*PR	262		
	IHFPLATY*APVISAEL	272		
	VGINY*QPPTVVPGGDLAK	357		
	FDLMY*AK	399		
	INVVY*YNEATGGK	50		
Beta	INVVY*NEATGGK	51	281	Longitudinal Lateral Lateral  Lateral Lateral
	Y*VPR	59		
	GHY*TEGAELVDSVLDVVR	106		
	EEY*PDR	159		
	GSQQY*R	281		
	Y*LTVAAVFR	310		
	NSSY*FVEWIPNNVK	340		

Numbering of the organophosphorylated residues corresponds to accession numbers gi 15988311 for alpha and gi 15988312 for beta tubulin. The crystal structure of the bovine tubulin heterodimer (Protein Data Bank code 1jff) identifies residues involved in contacts in the microtubule (Nogales et al., 1999). Chlorpyrifos oxon (CPO) labeled residues in the tubulin dimer were identified by mass spectrometry in previous publications (Grigoryan et al., 2008, in press), while those in polymerized microtubules are reported in the present work.

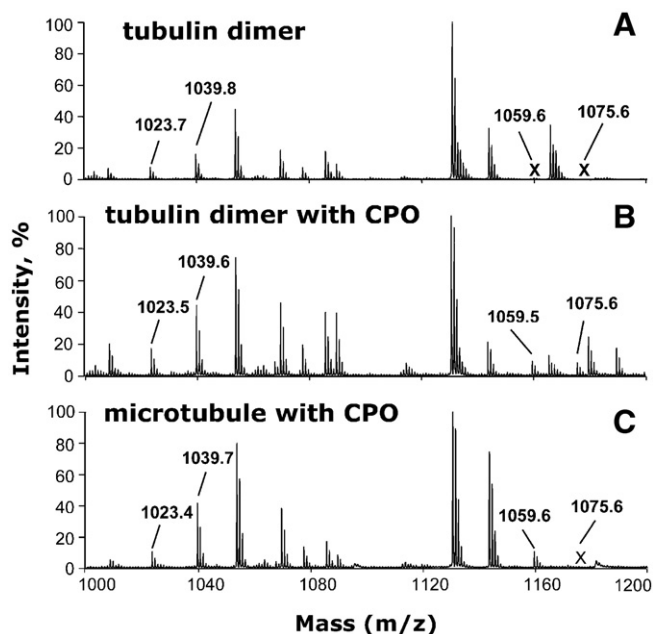


**Fig. 3.** MS spectra showing chlorpyrifos oxon-labeled and unlabeled tubulin tryptic peptides. (A) Control tubulin dimer without chlorpyrifos oxon (CPO); (B) tubulin dimer treated with 0.5 mM CPO; (C) polymerized microtubules treated with 0.5 mM CPO. Peaks at 1023.5 and 1039.6 amu correspond to unlabeled EDAANNYAR and YLTVAAVFR peptides from alpha and beta tubulin, respectively. Peaks at 1059.6 and 1075.6 amu correspond to CPO labeled (+136 amu added mass from CPO) EDAANNY\*AR and Y\*LTVAAVFR peptides. The labeled peak at 1059.5 amu is present in panels B and C. The labeled peak at 1075.6 amu is present only in panel B. The letter X in panels A and C indicates absent peaks.

of peptide EDAANNYAR and 15% of peptide YLTVAAVFR were labeled. Fig. 3C shows the MS spectrum of microtubules that had been treated with chlorpyrifos oxon after the tubulin had polymerized. The unlabeled peaks at 1023.5 and 1039.6 amu are present in Fig. 3C. One labeled peak, at 1059.6 amu is present, but there is no peak at 1075.6 amu. This shows that tyrosine 103 in peptide EDAANNY\*AR was labeled in polymerized microtubules, but that tyrosine 310 in peptide YLTVAAVFR was not. The relative peak heights of the unlabeled and labeled EDAANNY\*AR are similar, suggesting that 50% of peptide EDAANNYAR was labeled.

The identity of the labeled residue was determined from tandem MSMS spectra acquired in the QTRAP 2000 mass spectrometer. Peptides were partially separated by liquid chromatography on a C18 reverse phase column before being electrosprayed into the mass spectrometer. This method confirmed the list of 17 labeled peptides given in Table 2 for tubulin treated with chlorpyrifos oxon before polymerization (Grigoryan et al., 2008, 2009). Only 2 labeled peptides were identified when polymerized tubulin was treated with chlorpyrifos oxon. The first, EDAANNY\*AR, was described above in the section on MALDI analysis. The second was GSQQY\*R where tyrosine 281 had an added mass of +136 (Table 2). MSMS spectra for each labeled residue can be found in previous publications (Grigoryan et al., 2008, 2009).

Table 2 indicates residues involved in contacts between protofilaments in the crystal structure (Nogales et al., 1999). Eight of the chlorpyrifos oxon labeled tyrosines are involved in contacts, suggesting that modification of these tyrosines alters the conformation of tubulin dimers and therefore accounts for the abnormal polymer structures observed in Fig. 1. Only 2 of the 17 tyrosines were available for covalent binding by chlorpyrifos oxon when polymerized microtubules were treated with chlorpyrifos oxon, suggesting that the other 15 tyrosines were buried in the polymer structure and therefore involved in microtubule contacts.

## Discussion

### Nanoimaging to measure effect of organophosphorus agents on tubulin polymerization

The classical way to measure tubulin polymerization is by increase in turbidity. This method was not satisfactory for measurement of the effect of chlorpyrifos oxon because all concentrations of chlorpyrifos oxon showed similar increases in turbidity. A lack of concentration-dependence has been reported by others (Prendergast et al., 2007). However, nanoimaging revealed pronounced concentration-dependent effects of chlorpyrifos oxon on tubulin polymerization. This is the first report to use atomic force microscopy to measure the effect of an organophosphorus agent on tubulin polymerization.

### Thin, short microtubules

Microtubules grow by elongation of open sheets that later close into a cylinder. Lateral interactions between adjacent protofilaments govern the stability of microtubules. The finding of thin microtubules in chlorpyrifos oxon treated samples suggests that protofilaments were lost. A normal microtubule contains 13 protofilaments, but the thin microtubules probably contain fewer. This explanation was offered for the thin microtubules observed in mice deficient in crystallin chaperones (Xi et al., 2006), and seems applicable to the thin microtubules observed in our study.

The width of wild-type mouse microtubules measured by electron microscopy is  $27 \pm 3$  nm (Xi et al., 2006) and the width of bovine microtubules measured in fluid tapping mode atomic force microscopy is also  $27 \pm 3$  nm (Wagner et al., 2004). In contrast, the width of wild-type bovine microtubules measured by atomic force microscopy of dried samples in our experiments was 84 nm. The width of porcine microtubules measured by scanning force microscopy was 70–100 nm (Vater et al., 1995), similar to the values we obtained. The larger widths of microtubules in the latter experiments are explained by collapse and flattening of the hollow tube structure during drying of the sample.

Abnormally short microtubules, such as those observed after treatment with 0.005 or 0.01 mM chlorpyrifos oxon, suggest that these chlorpyrifos oxon-modified microtubules may be fragile and break along their length. Alternatively, adducts formed with chlorpyrifos oxon may partially block polymerization. At 0.01 mM chlorpyrifos oxon, the only tyrosine found to be significantly labeled was Tyr 83, in the alpha tubulin peptide TGT\*YR. About 12% of Tyr 83 was covalently modified (Grigoryan et al., 2009). Tyrosine 83 is not known to be involved in lateral or longitudinal contacts in the crystal structure (Nogales et al., 1999), but it did not appear to be labeled in microtubules. This observation suggests that its accessibility is changed upon polymerization and that labeling this residue might alter the capacity of tubulin to change shape during polymerization, thereby inhibiting polymerization. Alternatively, since excess chlorpyrifos oxon was not removed before polymerization, the possibility cannot be ruled out that the short microtubules that are generated upon treatment with 0.005 and 0.01 mM chlorpyrifos oxon are due to noncovalent binding of chlorpyrifos oxon to tubulin. Excess chlorpyrifos oxon was not removed prior to polymerization because dialyzed tubulin did not polymerize.

### Stimulation of polymerization

Pretreatment of 0.1 mM tubulin with 0.025 mM chlorpyrifos oxon, yielded a higher than normal number of microtubules. This is opposite to the effect seen at lower concentrations of chlorpyrifos oxon. We speculate that the additional sites bound by chlorpyrifos oxon at the higher concentration had a stabilizing effect on microtubule structure, similar to that of taxol (Derry et al., 1995).

## Aggregation

When 0.1 mM tubulin was pretreated with 0.05 and 0.1 mM chlorpyrifos oxon, the microtubules clumped into aggregates. At these concentrations of chlorpyrifos oxon, alpha tubulin is covalently modified on about 40% of Tyr 83, 7% of Tyr 224, and 5% of Tyr 272, while beta tubulin is covalently modified on 10% of Tyr 59, 2% of Tyr 106, and 20% of Tyr 281 (Grigoryan et al., 2009). Some of these residues are involved in contacts between protofilaments and in GTP binding (Table 1), suggesting that their modification resulted in structurally altered polymers. The nanoimages suggest that binding of chlorpyrifos oxon destabilized the structure of the tubules.

These high concentrations of chlorpyrifos oxon are not going to be found in living mammalian species. High concentrations are mainly useful for finding labeled peptides in the mass spectrometer.

## Defective tubulin assembly in neurodegenerative diseases

Disruption of microtubule polymerization in neuronal axons has been implicated as a mechanism leading to neurodegenerative diseases (Gendron and Petrucelli, 2009). Alzheimer disease brains have defective microtubule assembly (Iqbal et al., 1986). We hypothesize that the neurotoxicity of organophosphorus agents may be linked to disruption in microtubule function.

## Modification of microtubule associated proteins

Covalent binding of organophosphorus agents to tyrosine in a variety of proteins has been found (Grigoryan et al., 2009). Therefore reaction of chlorpyrifos oxon with other proteins involved in tubulin polymerization may also occur. Prendergast et al. have shown that chlorpyrifos oxon treatment of rat brain slices causes a marked decrease in the concentration of microtubule associated protein-2 and results in neuron injury (Prendergast et al., 2007). Since this protein promotes tubulin polymerization, it is reasonable to propose that microtubule associated protein-2, as well as other microtubule associated proteins such as kinesin (Gearhart et al., 2007) may be modified by chlorpyrifos oxon. Thus, disruption of microtubule function may involve chlorpyrifos oxon modification of several proteins including tubulin and proteins associated with microtubules.

## Acknowledgments

Nanoimages were obtained with the support of Dr. Luda S. Shlyakhtenko, co-director, and Dr. Yuri L. Lyubchenko, director of the Nanoimaging Core Facility at the University of Nebraska Medical Center in the Department of Pharmaceutical Sciences. The Nanoimaging Core Facility is supported by grants from NIH (SIG program), the UNMC Program of Excellence (POE) and the Nebraska Research Initiative (NRI). Mass spectra were obtained with the support of the Mass Spectrometry and Proteomics core facility at the University of Nebraska Medical Center. We thank Ellen G. Duysen for help with statistical analysis. This study was also supported by the U.S. Army Medical Research and Materiel Command W81XWH-07-2-0034, the National Institutes of Health U01 NS058056 and P30CA36727, and DGA/PEA grants 08co501 and ANR-06-BLAN-0163.

## References

- Abou-Donia, M.B., 2003. Organophosphorus ester-induced chronic neurotoxicity. Arch. Environ. Health 58, 484–497.
- Beseler, C., Stallones, L., Hoppin, J.A., Alavanja, M.C., Blair, A., Keefe, T., Kamel, F., 2006. Depression and pesticide exposures in female spouses of licensed pesticide applicators in the agricultural health study cohort. J. Occup. Environ. Med. 48, 1005–1013.
- Derry, W.B., Wilson, L., Jordan, M.A., 1995. Substoichiometric binding of taxol suppresses microtubule dynamics. Biochemistry 34, 2203–2211.
- Gearhart, D.A., Sickles, D.W., Buccafusco, J.J., Prendergast, M.A., Terry Jr., A.V., 2007. Chlorpyrifos, chlorpyrifos-oxon, and diisopropylfluorophosphate inhibit kinesin-dependent microtubule motility. Toxicol. Appl. Pharmacol. 218, 20–29.
- Gendron, T.F., Petrucelli, L., 2009. The role of tau in neurodegeneration. Mol. Neurodegener. 4, 13.
- Grigoryan, H., Schopfer, L.M., Thompson, C.M., Terry, A.V., Masson, P., Lockridge, O., 2008. Mass spectrometry identifies covalent binding of soman, sarin, chlorpyrifos oxon, diisopropyl fluorophosphate, and FP-biotin to tyrosines on tubulin: a potential mechanism of long term toxicity by organophosphorus agents. Chem. Biol. Interact. 175, 180–186.
- Grigoryan, H., Li, B., Anderson, E.K., Xue, W., Nachon, F., Lockridge, O., Schopfer, L.M., 2009. Covalent binding of the organophosphorus agent FP-biotin to tyrosine in eight proteins that have no active site serine. Chem. Biol. Interact. 180, 492–498.
- Grigoryan, H., Schopfer, L.M., Peeples, E.S., Duysen, E.G., Grigoryan, M., Thompson, C.M., Lockridge, O., 2009. Mass spectrometry identifies multiple organophosphorylated sites in tubulin: dynamics of chlorpyrifos oxon binding. Toxicol. Appl. Pharmacol. 240, 149–158.
- Hancock, D.B., Martin, E.R., Mayhew, G.M., Stajich, J.M., Jewett, R., Stacy, M.A., Scott, B.L., Vance, J.M., Scott, W.K., 2008. Pesticide exposure and risk of Parkinson's disease: a family-based case-control study. BMC Neurol. 8, 6.
- Iqbal, K., Grundke-Iqbal, I., Zaidi, T., Merz, P.A., Wen, G.Y., Shaikh, S.S., Wisniewski, H.M., Alafuzoff, I., Winblad, B., 1986. Defective brain microtubule assembly in Alzheimer's disease. Lancet 2, 421–426.
- Kamel, F., Engel, L.S., Gladen, B.C., Hoppin, J.A., Alavanja, M.C., Sandler, D.P., 2007. Neurologic symptoms in licensed pesticide applicators in the Agricultural Health Study. Hum. Exp. Toxicol. 26, 243–250.
- Lockridge, O., Xue, W., Gaydess, A., Grigoryan, H., Ding, S.J., Schopfer, L.M., Hinrichs, S.H., Masson, P., 2008. Pseudo-esterase activity of human albumin: slow turnover on tyrosine 411 and stable acetylation of 82 residues including 59 lysines. J. Biol. Chem. 283, 22582–22590.
- Lushnikov, A.Y., Potaman, V.N., Oussatcheva, E.A., Sinden, R.R., Lyubchenko, Y.L., 2006. DNA strand arrangement within the Sfil-DNA complex: atomic force microscopy analysis. Biochemistry 45, 152–158.
- Nogales, E., Whittaker, M., Milligan, R.A., Downing, K.H., 1999. High-resolution model of the microtubule. Cell 96, 79–88.
- Prendergast, M.A., Self, R.L., Smith, K.J., Ghayoumi, L., Mullins, M.M., Butler, T.R., Buccafusco, J.J., Gearhart, D.A., Terry Jr., A.V., 2007. Microtubule-associated targets in chlorpyrifos oxon hippocampal neurotoxicity. Neuroscience 146, 330–339.
- Salvi, R.M., Lara, D.R., Ghisolfi, E.S., Portela, L.V., Dias, R.D., Souza, D.O., 2003. Neuropsychiatric evaluation in subjects chronically exposed to organophosphate pesticides. Toxicol. Sci. 72, 267–271.
- Skoufias, D.A., Wilson, L., 1992. Mechanism of inhibition of microtubule polymerization by colchicine: inhibitory potencies of unliganded colchicine and tubulin–colchicine complexes. Biochemistry 31, 738–746.
- Srivastava, A.K., Gupta, B.N., Bihari, V., Mathur, N., Srivastava, L.P., Pangtey, B.S., Bharti, R.S., Kumar, P., 2000. Clinical, biochemical and neurobehavioural studies of workers engaged in the manufacture of quinalphos. Food Chem. Toxicol. 38, 65–69.
- Terry Jr., A.V., Gearhart, D.A., Beck Jr., W.D., Truan, J.N., Middlemore, M.L., Williamson, L.N., Bartlett, M.G., Prendergast, M.A., Sickles, D.W., Buccafusco, J.J., 2007. Chronic, intermittent exposure to chlorpyrifos in rats: protracted effects on axonal transport, neurotrophin receptors, cholinergic markers, and information processing. J. Pharmacol. Exp. Ther. 322, 1117–1128.
- Vater, W., Fritzsche, W., Schaper, A., Bohm, K.J., Unger, E., Jovin, T.M., 1995. Scanning force microscopy of microtubules and polymorphic tubulin assemblies in air and in liquid. J. Cell Sci. 108 (Pt. 3), 1063–1069.
- Wagner, O.I., Ascano, J., Tokito, M., Leterrier, J.F., Janmey, P.A., Holzbaur, E.L., 2004. The interaction of neurofilaments with the microtubule motor cytoplasmic dynein. Mol. Biol. Cell 15, 5092–5100.
- Xi, J.H., Bai, F., McGaha, R., Andley, U.P., 2006. Alpha-crystallin expression affects microtubule assembly and prevents their aggregation. FASEB J. 20, 846–857.
- Yeste-Velasco, M., Alvira, D., Sureda, F.X., Rimbau, V., Forsby, A., Pallas, M., Camins, A., Folch, J., 2008. DNA low-density array analysis of colchicine neurotoxicity in rat cerebellar granular neurons. Neurotoxicology 29, 309–317.



## Mass spectrometry identifies multiple organophosphorylated sites on tubulin

Hasmik Grigoryan<sup>a</sup>, Lawrence M. Schopfer<sup>a</sup>, Eric S. Peebles<sup>a</sup>, Ellen G. Duysen<sup>a</sup>, Marine Grigoryan<sup>a</sup>, Charles M. Thompson<sup>b</sup>, Oksana Lockridge<sup>a,\*</sup>

<sup>a</sup> University of Nebraska Medical Center, Eppley Institute for Cancer Research, 986805 Nebraska Medical Center, Omaha, NE 68198-6805, USA

<sup>b</sup> University of Montana, Department of Biomedical and Pharmaceutical Sciences, Missoula, MT 59812, USA

### ARTICLE INFO

#### Article history:

Received 3 June 2009

Revised 17 July 2009

Accepted 17 July 2009

Available online 24 July 2009

#### Keywords:

Mass spectrometry

Tubulin

Chlorpyrifos oxon

Tyrosine

### ABSTRACT

Acute toxicity of organophosphorus poisons (OP) is explained by inhibition of acetylcholinesterase in nerve synapses. Low-dose effects are hypothesized to result from modification of other proteins, whose identity is not yet established. The goal of the present work was to obtain information that would make it possible to identify tubulin as a target of OP exposure. Tubulin was selected for study because live mice injected with a nontoxic dose of a biotinylated organophosphorus agent appeared to have OP-labeled tubulin in brain as determined by binding to avidin beads and mass spectrometry. The experiments with live mice were not conclusive because binding to avidin beads could be nonspecific. To be convincing, it is necessary to find and characterize the OP-labeled tubulin peptide. The search for OP-labeled tubulin peptides was begun by identifying residues capable of making a covalent bond with OP. Pure bovine tubulin (0.012 mM) was treated with 0.01–0.5 mM chlorpyrifos oxon for 24 h at 37 °C in pH 8.3 buffer. The identity of labeled amino acids and percent labeling was determined by mass spectrometry. Chlorpyrifos oxon bound covalently to tyrosines 83, 103, 108, 161, 224, 262, 272, 357, and 399 in bovine alpha tubulin, and to tyrosines 50, 51, 59, 106, 159, 281, 310, and 340 in bovine beta tubulin. The most reactive were tyrosine 83 in alpha and tyrosine 281 in beta tubulin. In the presence of 1 mM GTP, percent labeling increased 2-fold. Based on the crystal structure of the tubulin heterodimer (PDB 1jff) tyrosines 83 and 281 are well exposed to solvent. In conclusion seventeen tyrosines in tubulin have the potential to covalently bind chlorpyrifos oxon. These results will be useful when searching for OP-labeled tubulin in live animals.

© 2009 Elsevier Inc. All rights reserved.

### Introduction

Although some organophosphorus compounds (OP) have been banned or severely restricted ([www.epa.gov](http://www.epa.gov)) they still comprise more than 50% of all pesticides used worldwide, causing much of the human population to be exposed. An especially high percentage of exposure is reported for farmers and workers dealing with pesticides in El Salvador, Peru and Southern Spain (Azaroff, 1999; Roldan-Tapia et al., 2006).

**Abbreviations:** AChE, acetylcholinesterase; CPO, chlorpyrifos oxon; CREB, calcium/cyclic AMP response element binding protein; FP-biotin, 10-Fluoroethoxyphosphinyl-N-biotinamidopentyldecanamide; GTP, guanosine-5'-triphosphate; PVDF, polyvinylidene difluoride; MS, mass spectrometry; MS/MS, tandem mass spectrometry; LC/MS/MS, liquid chromatography tandem mass spectrometry; MALDI-TOF/TOF, matrix-assisted laser desorption/ionization time of flight mass spectrometry; OP, organophosphorus compounds; QTRAP, a tandem quadrupole linear-ion trap mass spectrometer.

\* Corresponding author. Fax: +1 402 559 4651.

E-mail addresses: [hgrigoryan@berkeley.edu](mailto:hgrigoryan@berkeley.edu) (H. Grigoryan), [lmschopf@unmc.edu](mailto:lmschopf@unmc.edu) (L.M. Schopfer), [eppebles@phoenixchildrens.com](mailto:eppebles@phoenixchildrens.com) (E.S. Peebles), [edyusen@unmc.edu](mailto:edyusen@unmc.edu) (E.G. Duysen), [marinegrig@yahoo.com](mailto:marinegrig@yahoo.com) (M. Grigoryan), [charles.thompson@umontana.edu](mailto:charles.thompson@umontana.edu) (C.M. Thompson), [olockrid@unmc.edu](mailto:olockrid@unmc.edu) (O. Lockridge).

The acute toxicity of OP is due to inhibition of acetylcholinesterase (EC 3.1.1.7, AChE). Inhibition of greater than 50% of an individual's AChE produces an acute "cholinergic syndrome" initiated by accumulation of the neurotransmitter acetylcholine at cholinergic synapses (McDonough and Shih, 1997; Brown and Brix, 1998; Pope, 1999). Respiratory failure due to inhibition of AChE can cause death (Brown and Brix, 1998; Eddleston et al., 2006). In addition to the acute toxicity that occurs with high doses of OP, low-dose exposure has been implicated in insomnia, fatigue, inability to concentrate, memory deficits, depression, and generalized weakness (Stephens et al., 1995; Salvi et al., 2003; Roldan-Tapia et al., 2006; Kamel et al., 2007). Low-dose exposure is defined as a dosage that causes minimal inhibition of AChE and no obvious cholinergic symptoms.

The idea that AChE is the only physiologically important target for OP exposure was undisputed for many decades. However, toxicologists demonstrated that signs of toxicity in animals depended on the identity of the OP (Moser, 1995; Pope, 1999). For example, a low dose of fenthion decreased motor activity in rats by 86% but did not alter the tail-pinch response, whereas a low dose of parathion did not lower motor activity but did decrease the tail-pinch response. This led to the conclusion that OP have other biological actions in addition to their cholinesterase-inhibitory properties.

A variety of enzymes have been shown to react with OP, not all of which contain the serine hydrolase active site that is a hallmark of OP targets (Casida and Quistad, 2004). These findings re-enforce the proposal that non-cholinesterase targets may contribute to the toxicity of OP.

#### Possible non-cholinesterase targets

Cytoskeletal proteins including tubulin have been implicated in the neurotoxicity of OP (Abou-Donia, 2003). Rats treated with subthreshold doses of chlorpyrifos oxon had impaired axonal transport in the nervous system, indicative of structural damage to the kinesin motor protein whose task is to transport cell components along microtubules (Gearhart et al., 2007; Terry et al., 2007). Studies on organotypic slice cultures of rat hippocampus suggested that chlorpyrifos oxon produces a progressive decrease in neuronal viability that may be associated with impaired microtubule synthesis and/or function (Prendergast et al., 2007). Furthermore, the polymerization of pure bovine brain tubulin was inhibited by low doses of chlorpyrifos oxon (0.1–10  $\mu$ M) (Prendergast et al., 2007). These studies suggest that the function of cytoskeletal proteins, including tubulin, may be adversely affected by OP.

Tubulin was selected for study because tubulin appeared to be labeled by the organophosphorus ester, FP-biotin, when mice were treated with a low dose that did not inhibit acetylcholinesterase. The evidence for labeling of tubulin was indirect. In efforts to provide direct evidence of labeling *in vivo*, we need to know the identity of the potentially modified residues. For this purpose we undertook the mass spectrometry study of purified bovine tubulin presented here.

#### Materials and methods

**Materials.** Bovine tubulin (TL238)>99% pure, isolated from bovine brain, was from Cytoskeleton, Inc (Denver, CO). This tubulin preparation contains both alpha and beta tubulin (MW is approximately 50 kDa for each). Chlorpyrifos oxon (MET-674B from ChemService Inc, West Chester, PA) was dissolved in dimethyl sulfoxide and stored at  $-80^{\circ}\text{C}$ . 10-Fluoroethoxyphosphiny-N-biotinamidopentyldecanamide (FP-biotin) was custom synthesized in the laboratory of Dr. Charles M. Thompson at the University of Montana, Missoula, MT (Schopfer et al., 2005a). Sequencing grade modified porcine trypsin (V5113) was from Promega (Madison, WI). Slide-A-Lyzer 7K dialysis cassettes (No. 66370) were from Pierce Biotechnology Inc. (Rockford, IL), PVDF (polyvinylidene difluoride) membrane (Immun-Blot #162-0177), Coomassie blue G250 (Bio-Safe), and broad range biotinylated SDS PAGE molecular weight markers (#161-0319) were from BioRad Laboratories (Hercules, CA). Performa Spin Columns (#73328) with 0.8 ml capacity, packed with a gel-filtration matrix were from Edge Bio-Systems (Gaithersburg, MD). Avidin–Agarose (A-9207) was from Sigma (St. Louis, MO), Streptavidin Alexa-680 (S-21378) was from Molecular Probes (Eugene, OR). All other chemicals were of analytical grade.

**Detection of FP-biotinylated proteins from mouse brain supernatant.** *In vitro* studies were performed as follows. Mouse brain was homogenized in 10 volumes of 50 mM potassium phosphate buffer pH 7.0 and centrifuged at 100,000  $\times$ g. The clear supernatant (1.4 mg protein/ml) was reacted with 10  $\mu$ M FP-biotin at  $25^{\circ}\text{C}$  for 5 h in 50 mM TrisCl buffer, pH 8.0, containing 5 mM EDTA. The reaction was stopped by passage over a G-25 gel-filtration column to separate the excess FP-biotin from the protein, followed by boiling in 0.5% SDS for 3 min. The FP-biotinylated proteins were enriched by binding to avidin beads, and analyzed by mass spectrometry as described (Peebles et al., 2005).

**Mice treated with FP-biotin.** Animal work was carried out in accordance with the Guide for the Care and Use of Laboratory Animals as

adopted by the National Institutes of Health. Two mice in strain 129Sv were injected intraperitoneally with 5.5 mg/kg FP-biotin (9.3  $\mu$ M) dissolved in ethanol. Mice were euthanized 120 min later by inhalation of carbon dioxide. Blood was washed out by intracardial perfusion with 0.1 M phosphate buffered saline. Brains were homogenized in 10 volumes of 50 mM TrisCl pH 8.0 containing 5 mM EDTA, and centrifuged for 10 min to partially clarify the suspension. FP-biotinylated proteins were isolated by adsorption onto Avidin–Agarose beads (Peebles et al., 2005). The boiled beads were loaded on an SDS PAGE gel where proteins were visualized with Coomassie blue. Coomassie-stained bands were excised, digested with trypsin, and the peptides identified by tandem quadrupole LC/MS/MS mass spectrometry. Proteins from a separate SDS PAGE gel were transferred to a PVDF membrane and hybridized with the fluorescent probe, Streptavidin Alexa-680.

**Chlorpyrifos oxon-labeled tryptic peptides from bovine tubulin.** Bovine tubulin (0.6 mg/ml or 12  $\mu$ M in terms of tubulin monomer) dissolved in 15 mM ammonium bicarbonate (pH 8.3) was treated with a 40-fold molar excess (0.5 mM) of chlorpyrifos oxon. The reaction mixture was incubated at  $37^{\circ}\text{C}$  for 24 h. The protein was denatured by incubating in a boiling water bath for 10 min. Excess chlorpyrifos oxon was removed by dialysis against 10 mM ammonium bicarbonate at  $4^{\circ}\text{C}$  for 12 h. Sixty  $\mu$ g of dialyzed tubulin was digested with 1.5  $\mu$ g of Promega trypsin at  $37^{\circ}\text{C}$  for 16 h.

**Tubulin labeling by different concentrations of chlorpyrifos oxon.** A 0.05 ml aliquot of 0.6 mg/ml bovine tubulin, in 15 mM ammonium bicarbonate pH 8.3, was treated with 0.01; 0.05; 0.1; 0.25 and 0.5 mM chlorpyrifos oxon. The reaction mixtures were incubated at  $37^{\circ}\text{C}$  for 24 h. Tubulin was denatured in a boiling water bath for 10 min. Excess chlorpyrifos oxon was removed by dialysis against 10 mM ammonium bicarbonate at  $4^{\circ}\text{C}$  for 12 h. Thirty  $\mu$ g of dialyzed tubulin was digested with 0.75  $\mu$ g of Promega trypsin at  $37^{\circ}\text{C}$  overnight.

**Time course for labeling of bovine tubulin by chlorpyrifos oxon.** Bovine tubulin, 0.3 mg dissolved in 0.5 ml of 15 mM ammonium bicarbonate pH 8.3, was treated with a 40-fold molar excess (0.5 mM) of chlorpyrifos oxon at  $37^{\circ}\text{C}$  for 1, 3, 6.5, 10, and 24 h. At each time point 0.1 ml of reaction mixture was removed for analysis of chlorpyrifos oxon-labeled peptides. Samples were immediately centrifuged (Sorvall MC 12 V benchtop microcentrifuge) through a Performa Spin Column to remove excess chlorpyrifos oxon (2 min at 3000 rpm) and the pass-thru was frozen at  $-70^{\circ}\text{C}$ . After all samples were collected, each was digested with 1.5  $\mu$ g of Promega trypsin at  $37^{\circ}\text{C}$  for 16 h.

**GTP effect on OP binding to tubulin.** One tenth ml of 0.6 mg/ml tubulin, dissolved in 15 mM ammonium bicarbonate (pH 8.3) containing 1 mM GTP, was treated with a 40-fold molar excess of chlorpyrifos oxon or 8-fold molar excess of FP-biotin dissolved in dimethylsulfoxide. The reaction mixtures were incubated at  $37^{\circ}\text{C}$  for 24 h. The tubulin was denatured by boiling in a water bath for 10 min. Excess OP was removed by dialysis against 10 mM ammonium bicarbonate at  $4^{\circ}\text{C}$  overnight. The 60  $\mu$ g of dialyzed tubulin was digested with 1.5  $\mu$ g of Promega trypsin at  $37^{\circ}\text{C}$  overnight.

**MALDI-TOF/TOF mass spectrometry.** The MALDI-TOF/TOF 4800 mass spectrometer (Applied Biosystems, Foster City, CA) was used for analysis of tryptic peptides from the tubulin heterodimer. One  $\mu$ l of a tryptic digest was spotted on a 384 well Opti-TOF plate (P/N 1016491, Applied Biosystems) and air dried. The spot was overlaid with 1  $\mu$ l of 10 mg/ml alpha-cyano-4-hydroxycinnamic acid matrix dissolved in 50% acetonitrile, 0.1% trifluoroacetic acid and allowed to air dry. Mass spectra were collected in positive ion reflector mode. The

final spectrum was the average of 500 laser shots. Masses were calibrated using CalMix 5 (Applied Biosystems).

**Percent labeled peptide estimated from MALDI-TOF peak areas.** MALDI-TOF spectra are saved as DATA EXPLORER files. The DATA EXPLORER file has an output window that lists the area for each peak in an MS spectrum. Percentage of chlorpyrifos oxon labeling was calculated from the isotope cluster areas of peaks corresponding to unlabeled and labeled peptides. Cluster areas for both labeled and unlabeled masses were taken from the same MALDI spectrum where the unlabeled peptide served as the internal control. The percentage labeling was calculated by dividing the cluster area for the labeled mass by the sum of the cluster areas for the labeled and the unlabeled masses. This method assumes that addition of the organophosphate does not significantly alter the intrinsic properties of the peptide (i.e. charge state, peptide size, peptide hydrophobicity, or secondary structure) which are considered to be responsible for the signal intensity in MALDI-TOF mass spectrometry (Pashkova et al., 2004). This ratio method has proven to be valid in kinetic studies of modified peptides and in the quantitative determination of other peptide modifications (Tang et al., 1996; Jennings et al., 2003; Li et al., 2007b; Sun and Lynn, 2007; Lockridge et al., 2008).

**LC/MS/MS mass spectrometry.** Tryptic peptides of chlorpyrifos oxon treated tubulin were dried in a vacuum centrifuge (SpeedVac from Jouan, RC10-10) and dissolved in 5% acetonitrile, and 0.1% formic acid. A 10  $\mu$ l aliquot was subjected to HPLC using a nanocolumn (#218MS3.07515 Vydac C18 polymeric rev-phase, 75  $\mu$ m I.D.  $\times$  150 mm long; P.J. Cobert Assoc, St. Louis, MO). Peptides were separated with a 90 min linear gradient from 0% to 60% acetonitrile at a flow rate of 0.3  $\mu$ l/min and electrosprayed through a fused silica emitter (360  $\mu$ m O.D., 75  $\mu$ m I.D., 15  $\mu$ m taper, New Objective) directly into the QTRAP 2000 (Applied Biosystems, Foster City, CA), a hybrid quadrupole linear-ion trap mass spectrometer. An ion-spray voltage of 1900 V was maintained between the emitter and the mass spectrometer. Information-dependent acquisition was used to collect MS, high resolution MS and MS/MS spectra for the 3 most intense peaks in each cycle, having a charge of +1 to +4, a mass between 200 and 1700 m/z, and an intensity >10,000 cps. All spectra were collected in the enhanced mode, using the trap function. Precursor ions were excluded for 30 s after one MS/MS spectrum had been collected. The collision cell was pressurized to 40  $\mu$ Torr with pure nitrogen and collision energies between 20 and 40 eV were determined automatically by the software based on the mass and charge of the precursor ion. The mass spectrometer was calibrated on selected fragments from the MS/MS spectrum of Glu-Fibrinopeptide B. The MS/MS data were processed using Analyst 1.4.1 software.

Initial identification of peptide sequences was obtained using the Mascot search engine licensed to the University Nebraska Medical Center (<http://www.matrixscience.com> (Perkins et al., 1999). Mascot used the NCBI database version Dec 29, 2005. To make it possible to search for chlorpyrifos oxon labeled and FP-biotin labeled Ser, Thr, Tyr, and Lys we introduced these modifications into the UNIMOD database according to the instructions on the web site <http://www.unimod.org>. Access to the modifications is freely available to all Mascot users in the Variable Modifications menu under the names O-diethylphosphate (for chlorpyrifos oxon), and FP-biotin. The search parameters included a variable modification for oxidized methionine, a fixed modification for carbamidomethylated cysteine, and charge states +1, +2, and +3. One missed cleavage was allowed for digestion by trypsin. The peptide tolerance was  $\pm 1.2$  Da. The MS/MS tolerance was  $\pm 0.6$  Da. The sequences of labeled peptides that were identified by Mascot were further checked manually with the aid of MS/MS Fragment Ion Calculator from Systems Biology (<http://db.systemsbio.org>).

## Results

### Preliminary detection of FP-biotinylated tubulin

Preliminary screening for OP-targets other than AChE was conducted with the biotinylated organophosphorus agent FP-biotin, whose structure is shown in Fig. 1. FP-biotin was employed because the biotin moiety provided a convenient way for enriching and extracting OP-reactive proteins from crude mixtures (Kidd et al., 2001; Nomura et al., 2005; Peebles et al., 2005; Schopfer et al., 2005a, 2005b; Ding et al., 2008; Grigoryan et al., 2008; Nomura et al., 2008; Tuin et al., 2009).

In vitro labeling of mouse brain supernatant (100,000  $\times$ g) with 10  $\mu$ M FP-biotin, was followed by binding to avidin beads, SDS gel electrophoresis, transfer of proteins to PVDF membrane, and staining with Streptavidin Alexa-680. This sensitive, fluorescent dye revealed as many as 55 separate bands from a single SDS PAGE gel lane for FP-biotinylated mouse brain supernatant (Fig. 2, lane B). In the absence of FP-biotin, no more than four bands were normally detected.

Coomassie staining is less sensitive than staining with Streptavidin Alexa-680; twenty-two bands were detected in the Coomassie-stained lane shown in Fig. 2C. Proteins identified by mass spectrometry from tryptic, in-gel digests of these bands included serine hydrolases, dehydrogenases, a phosphatase, a monooxygenase, peroxidase, heat shock proteins, albumin, and tubulin. See Table 1. In addition, two endogenously biotinylated enzymes (pyruvate carboxylase and propionyl CoA-carboxylase) were identified.

An intensely stained band at 55 kDa from the SDS PAGE gel contained tubulin as the major component. Both the alpha and beta subunits of tubulin were found through probability-based searching of the NCBI database using the Mascot algorithm (Perkins et al., 1999). The MOWSE scores showed high confidence in the identification. The band at 55 kDa did not appear in brain preparations that had not been treated with FP-biotin (Fig. 2A).

Of the 36 proteins in Table 1, only 11 have an active site serine as indicated by Yes in the column headed by GX SXG. Proteins that have an active site serine are expected to covalently bind organophosphorus agents on serine. However, the 25 proteins without the consensus sequence GX SXG bind organophosphorus agent at unknown sites.

### Mice treated with FP-biotin

Similar analyses were conducted on brain supernatant from mice that had been injected intraperitoneally with 5.5 mg/kg FP-biotin.

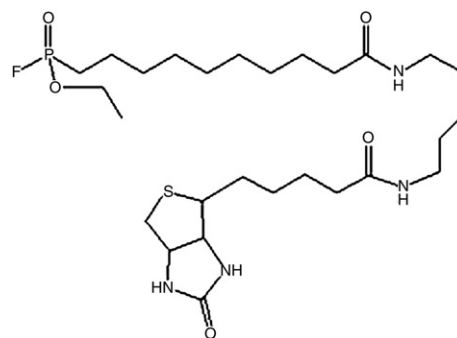


**Fig. 1.** Structure of FP-biotin. The second order rate constant for the reaction of FP-biotin with human butyrylcholinesterase is  $1.6 \times 10^8 \text{ M}^{-1} \text{ min}^{-1}$  and for the reaction with human acetylcholinesterase is  $1.8 \times 10^7 \text{ M}^{-1} \text{ min}^{-1}$ . These rates are comparable to the rates of reaction with chlorpyrifos oxon which are  $1.7 \times 10^9 \text{ M}^{-1} \text{ min}^{-1}$  for human butyrylcholinesterase and  $1.0 \times 10^7 \text{ M}^{-1} \text{ min}^{-1}$  for human acetylcholinesterase (Schopfer et al., 2005b).

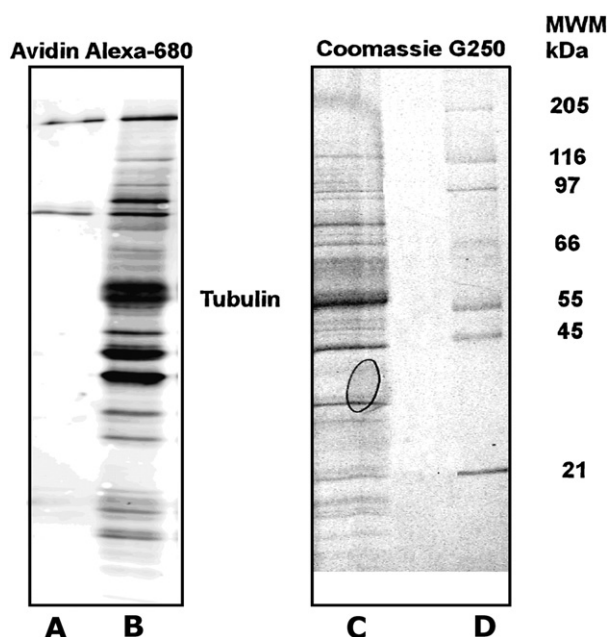


**Fig. 2.** Preliminary detection of FP-biotinylated tubulin in mouse brain. Mouse brain supernatant was treated with 10  $\mu$ M FP-biotin. Excess FP-biotin was separated by gel filtration. FP-biotinylated proteins were extracted by binding to Avidin-Agarose beads. The Avidin-Agarose beads were washed with 0.2% SDS, boiled in SDS gel loading buffer, and the extract and beads loaded on an SDS PAGE gradient gel (10–20%). Proteins in lanes A and B were transferred to PVDF membrane and stained with Streptavidin Alexa-680. Lane A shows endogenously biotinylated proteins that appear in the absence of FP-biotinylation. Lane B shows 55 FP-biotinylated bands including an intense band for FP-biotinylated tubulin. Lanes C and D were stained with Coomassie blue. Lane C is the same sample as in lane B at a 20-fold higher concentration. Lane D contains molecular weight marker proteins. The molecular weight values for the marker proteins are shown to the right of the panel (MWM/kDa). The oval in lane C is an air bubble.

These animals showed no signs of cholinergic toxicity and no AChE inhibition (Peeples et al., 2005). Proteins that bound to avidin beads were separated by SDS gel electrophoresis, digested with trypsin, and analyzed by mass spectrometry. A gel band at about 55 kDa contained tubulin as the primary component. Alpha tubulin gave a MOWSE score of 322, which was based on 9 peptides, 6 of which scored in the identity range and 3 in the homology range. Beta tubulin gave a MOWSE score of 217, which was based on 4 peptides, 3 of which scored in the identity range and 1 in the homology range.

Mascot clearly identified tubulin as the major component in the avidin-bound material extracted from the brain of a mouse that had been treated with FP-biotin. However, the FP-biotin-labeled peptides for neither alpha nor beta tubulin were found. Identification of the labeled peptide is essential to confirm that tubulin truly reacts with OP. This question is particularly important in the case of tubulin, because this protein does not carry the serine hydrolase active site, which is the traditionally accepted target for OP.

#### *Chlorpyrifos oxon-labeled tryptic peptides from bovine tubulin identified by mass spectrometry*

In an effort to find an OP-labeled peptide from tubulin, the reaction of pure bovine tubulin with a different OP was studied. The OP chosen for these more focused studies was chlorpyrifos oxon. Chlorpyrifos oxon was chosen because it is the active metabolite of chlorpyrifos, a commercially used pesticide that is more relevant than FP-biotin in terms of human exposure. The chlorpyrifos oxon studies complement those from the more exotic FP-biotin and address the question of whether the FP-biotin results are relevant to real-world exposure situations. Though FP-biotin is very convenient for finding unknown

**Table 1**

Proteins in mouse brain homogenates that bind FP-biotin.

Protein name	Accession #	MOWSE	kDa	GXSXG
Fatty acid synthase	gi: 28461372	49	270	Yes
Puromycin-sensitive aminopeptidase	gi: 6679491	174	103	No
Formyltetrahydrofolate dehydrogenase	gi: 27532959	426	97	No
Heat shock protein 90-beta	gi: 123681	352	84	No
Prolyl endopeptidase	gi: 6755152	827	81	Yes
Acylpeptide hydrolase	gi: 22122789	254	80	Yes
RIKEN D030028o16	gi: 22122431	372	73	No
Serum albumin precursor	gi: 5915682	270	67	No
RIKEN 4931406N15	gi: 28076969	173	70	No
Heat shock protein 8	gi: 13242237	154	71	Yes
Acetylcholinesterase	gi: 28279461	64	68	Yes
Protein phosphatase 2	gi: 8394027	70	65	No
Fatty acid amide hydrolase	gi: 30354073	72	64	Yes
Dihydropyrimidinase-like 2	gi: 6753676	62	61	No
Dihydropyrimidinase-like 3	gi: 6681219	59	62	No
Dihydropyrimidinase-like 5	gi: 12746424	43	61	Yes
Esterase 1	gi: 6679689	91	61	Yes
D-3-phosphoglycerate dehydrogenase	gi: 3122875	195	51	No
Tubulin	gi: 20455323	5320	50	No
Tubulin alpha1	gi: 6755901	576	50	No
Tubulin alpha6	gi: 74186501	327	50	No
Tubulin beta	gi: 21746161	453	50	No
Tubulin beta2	gi: 13542680	106	50	No
Tubulin beta5	gi: 7106439	423	50	No
Acyl-CoA hydrolase	gi: 19923052	296	38	No
Glyceraldehyde-3-phosphate dehydrogenase	gi: 6679937	275	36	No
Lactate dehydrogenase 1	gi: 6754524	337	36	No
Esterase 10	gi: 12846304	261	35	Yes
Platelet-activating factor acetylhydrolase alpha2	gi: 6679199	65	25	No
Tyrosine 3-monooxygenase/tryptophan 5-monooxygenase activation protein	gi: 6756039	354	28	No
Platelet-activating factor acetylhydrolase alpha1	gi: 6679201	273	26	No
Platelet-activating factor alpha1	gi: 44890813	110	26	No
Platelet-activating factor 1b2	gi: 1373363	158	25	No
Lysophospholipase 1	gi: 6678760	206	25	Yes
Lysophospholipase 2	gi: 7242156	160	25	Yes
Peroxisomal oxidin 1	gi: 6754976	245	22	No

The accession number is unique to each protein in the NCBI database in PubMed. The accession number typed into the Protein subsection of PubMed or into Google brings up the protein sequence, the species, and the references. The MOWSE score is the statistical probability that the identification is correct. A score greater than 34 is significant. A score greater than 69 is significant with  $p < 0.05$ . kDa indicates the protein molecular weight in kilodaltons. GXSXG is the consensus sequence for the active site serine. Yes indicates proteins that have this motif.

proteins that react with OP, it is subject to the criticism that it is an atypical OP and that its reactions may not reflect the selectivity that can be expected for commonly used OP.

Initial analysis of the tryptic digest of chlorpyrifos oxon treated bovine tubulin was made on the MALDI-TOF/TOF 4800 mass spectrometer. The MS peaks from the labeled preparation were compared with theoretical mass lists of tryptic peptides from unlabeled tubulin (alpha1, gi 73586894 and beta2 gi 75773583 NCBI database). Alpha1 and beta2 are the most abundant tubulin isotypes in the brain. Therefore we took these isotypes for generation of the theoretical mass lists by Protein Prospector. The list of theoretical masses was generated with Protein Prospector software (UCSF, [www.prospector.ucsf.edu](http://www.prospector.ucsf.edu)). Peaks from the labeled preparation whose mass was equal to that of an unlabeled peptide plus the added mass from chlorpyrifos oxon (136 amu) were considered to be candidates for chlorpyrifos oxon-modified peptides.

Labeling did not reach 100% under the experimental conditions employed. Therefore, masses for both labeled and unlabeled peptides appeared in the same mass spectrum. A MALDI-TOF MS spectrum showing some unlabeled peptides and their corresponding chlorpyrifos oxon-labeled candidates is shown in Fig. 3.

Not all labeled peptides could be detected in the MALDI mass spectrometer and MS/MS fragmentation in the MALDI mass

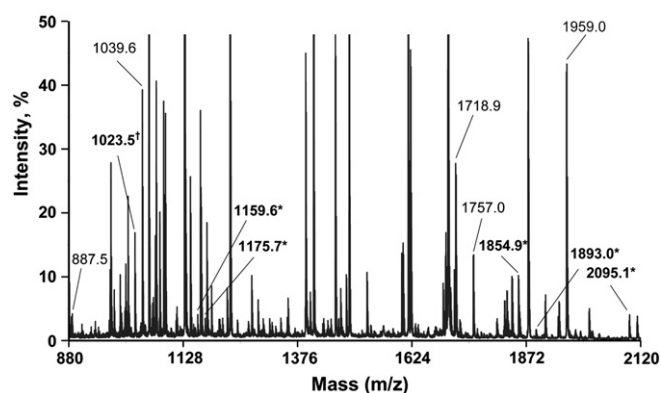


**Fig. 3.** MALDI-TOF MS spectrum of tryptic peptides from bovine tubulin treated with a 40-fold molar excess of chlorpyrifos oxon (0.5 mM). Singly-charged, unlabeled peptides with masses of 887.5, 1023.5, 1039.5, 1159.5, 1718.9, 1757.0, and 1959.0 amu are shown in regular font. Corresponding candidates for chlorpyrifos oxon-labeled peptides (plus 136 amu) with masses of 1023.5, 1159.5, 1175.7, 1854.9, 1893.0, and 2095.1 amu are shown in bold and marked with an asterisk. The mass at 1023.5 m/z coincides with both the unlabeled peptide EDAANNYAR and the chlorpyrifos oxon-labeled peptide FDLMYAK.

spectrometer was not always sufficient to fully characterize the labeled peptides. Complementary MS/MS spectra for the candidate peptides were obtained via LC/MS/MS in the tandem, quadrupole, linear-ion trap, QTRAP 2000 mass spectrometer, using electrospray ionization to introduce the sample.

MS/MS data from the QTRAP 2000 were submitted to the Mascot search engine for identification of chlorpyrifos oxon-labeled peptides. The Mascot results were checked manually to confirm the sequences of putative, chlorpyrifos oxon-labeled peptides and to identify the covalently modified amino acid residue. In total, 16 labeled peptides and 17 amino acid residues were identified (one peptide carried two labels). Each labeled peptide was covalently attached to an O-diethyl

phosphate fragment. Nine tyrosines were from alpha tubulin and 8 tyrosines were from beta tubulin. Four of the tyrosines (59, 83, 159 and 281) had been identified and reported previously (Grigoryan et al., 2008). Representative MS/MS spectra of labeled peptides are shown in Fig. 4.

Theoretical fragment ion masses for each labeled peptide were calculated using the MS/MS Fragment Ion Calculator from Systems Biology (<http://db.systemsbio.net>) and compared to the observed data. Extensive y-ion series were identified for each peptide. A delta mass corresponding to the labeled tyrosine fits into the sequence ions for the y-series of each peptide.

Characteristic, non-sequence fragments at 216, 244, and/or 272 m/z were found for each peptide. The mass at 216 m/z is consistent with the immonium ion of phosphotyrosine, the mass at 244 m/z is consistent with the immonium ion of O-monoethylphosphotyrosine, and the mass at 272 m/z is consistent with the immonium ion of O-diethylphosphotyrosine. These characteristic ions provide additional evidence that the chlorpyrifos oxon is bound to tyrosine in these peptides. In Fig. 4, the characteristic ion masses are enclosed in boxes (Schopfer et al., 2009).

The scheme for the reaction of chlorpyrifos oxon with tyrosine is presented in Fig. 5.

#### No aging

Aging is a secondary, enzymatically catalyzed reaction that occurs with OP-labeled acetyl- and butyrylcholinesterase. It results in the loss of one alkoxy side-chain from the phosphorus atom. For example, aging of chlorpyrifos oxon-modified acetylcholinesterase would result in loss of ethylene from one ethoxy group (28 amu). Chlorpyrifos oxon-labeled tyrosine did not lose an ethylene group from the phosphate. If aging had occurred the added mass from chlorpyrifos oxon modification would have been +108 rather than +136. No peptides with an added mass of +108 were found.

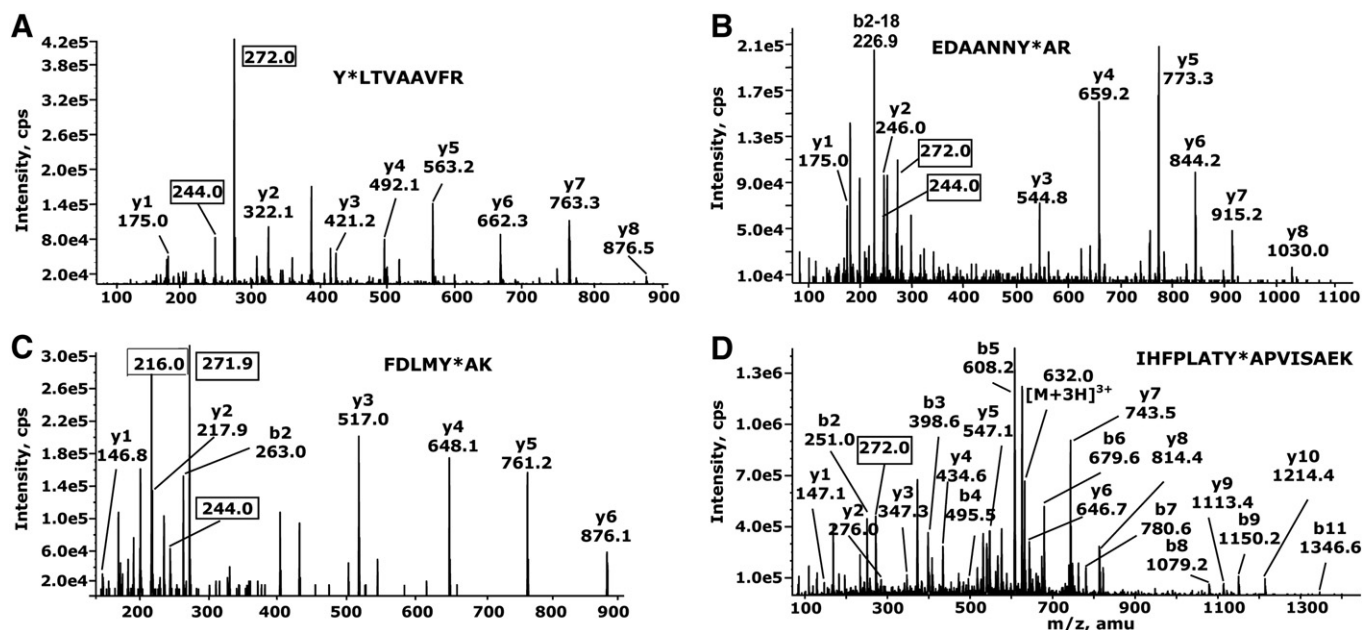


**Fig. 4.** MS/MS spectra of chlorpyrifos oxon-labeled peptides from bovine tubulin obtained by LC/MS/MS on the QTRAP 2000 mass spectrometer. Panel (A) peptide Y<sub>310</sub>LTVAAVFR from beta tubulin; (B) peptide EDAANNY<sub>103</sub>AR from alpha tubulin; (C) peptide, FDLMY<sub>399</sub>AK from beta tubulin; (D) peptide IHFLPATY<sub>272</sub>APVISAIEK from alpha tubulin. In panels A–C, singly-charged y-ion series derived from doubly-charged parent ions at 588.43 (A), 580.23 (B) and 512.32 (C) m/z are indicated. For IHFLPATY<sub>272</sub>APVISAIEK, in panel D, singly-charged y and b-ion series derived from a triply-charged parent ion at 632.01 m/z are marked. In all cases the masses of the y and b-ions are consistent with O-diethylphosphate attached to tyrosine (marked by an asterisk in the peptide sequence). Masses enclosed in a box are the immonium ion of phosphotyrosine (216), the immonium ion of O-monoethylphosphotyrosine (244), and the immonium ion of O-diethylphosphotyrosine (272). Peaks that are not labeled include internal fragments and masses that have lost a molecule of water or ammonia.



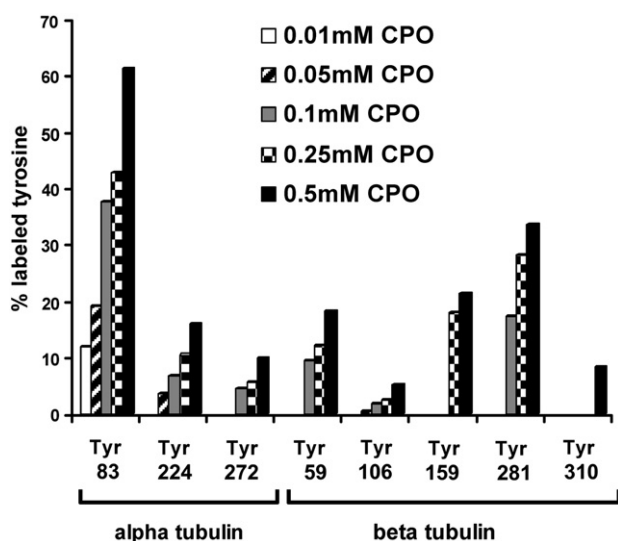


**Fig. 6.** Reactivity of chlorpyrifos oxon with various tyrosines from tubulin. Bars represent the percentage of chlorpyrifos oxon-modified tyrosine in 3 peptides from alpha tubulin and 5 peptides from beta tubulin. Twelve  $\mu$ M tubulin was incubated with various concentrations of chlorpyrifos oxon at 37 °C for 24 h (pH 8.3).

beta tubulin, tyrosine 281 exhibited the largest amount of labeling, with 34% labeling at 0.5 mM chlorpyrifos oxon. Residues 224, 272, 59, 106, 159 and 310 were substantially less reactive than 83 and 281. Reaction with 0.5 mM chlorpyrifos oxon resulted in 17%, 10%, 19%, 5%, 22% and 8.3% labeling of these tyrosines, respectively. Tyr 83 showed 3–12-fold higher reactivity than all other tyrosines. Tyrosines 106 and 310 from beta tubulin were the least reactive. The difference in the reactivity between tyrosines can be rationalized by their location in the crystal structure of the tubulin heterodimer and by the effect of neighboring amino acids.

#### Kinetics of the chlorpyrifos oxon reaction with tubulin tyrosines

Progress curves for chlorpyrifos oxon binding to tyrosine were obtained by plotting the percentage of labeled peptide against the corresponding incubation time. Fig. 7 shows that the progress curves are linear ( $R^2 = 0.7-1$ ).

The initial velocity for each tyrosine was taken from the slope of the plot. No significant labeling was observed for any peptide during the first hour of incubation. Tyr 272 is not depicted in Fig. 7 because it showed labeling only after 24 h of incubation. Tyr 83 yielded the

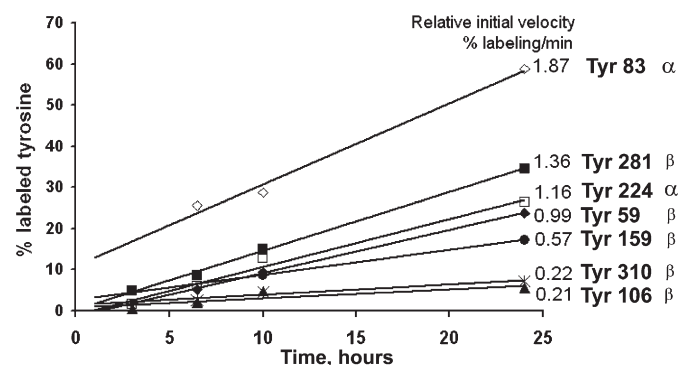


**Fig. 7.** Progress curves for chlorpyrifos oxon binding to tyrosines from bovine tubulin. The percentage of labeled peptides was calculated after 3, 6.5, 10 and 24 h of incubation at 37 °C. Experimental data for alpha tubulin (tyrosines 83 and 224) are presented with empty symbols for TGT<sub>83</sub>R and NLDIERPT<sub>224</sub>TNLNR. Data for beta tubulin (tyrosines 281, 59, 159, 310 and 106) are shown with filled symbols for GSQY<sub>281</sub>R, Y<sub>59</sub>VPR, EY<sub>159</sub>PDR, Y<sub>310</sub>LTVAAVFR and GHY<sub>106</sub>TEGAELVDSVLDVVR. The values of the initial velocities are presented next to each curve. Each point is the average of 3 trials, with an error of approximately 10%.

fastest rate at 1.87% labeling/min, but no labeling was detected until the 6.5 h time point. At that time it was found to be 25% labeled. Thereafter, the rate of labeling was rapid. This observation suggests that there might have been a reorientation of tyrosine 83 within the structure of tubulin. Tyr 83 reacted with chlorpyrifos oxon 1.5–9 times faster than other tyrosines. Tyrosine 281 showed the second fastest rate at 1.36% labeling/min. These findings are consistent with the reactivity measurements described above.

Bovine alpha tubulin (accession # 73586894) has 19 tyrosines, of which 9 can be labeled by chlorpyrifos oxon. Bovine beta tubulin (accession # 75773583) has 16 tyrosines of which 8 can be labeled. About half of the tyrosines are reactive and half are unreactive.

In summary, Tyr 83 from alpha and Tyr 281 from beta bovine tubulin were more reactive toward chlorpyrifos oxon than the other tyrosines that became labeled. They both showed a higher percentage of labeling: Tyr 83 and Tyr 281 were labeled 61% and 34%, respectively, after 24 h of incubation at 37 °C (Fig. 6). And, they reacted with chlorpyrifos oxon more rapidly than the other tyrosines, being labeled at a rate of 1.87 and 1.36% labeled peptide/min, respectively (Fig. 7).

#### Effect of GTP on the reaction of chlorpyrifos oxon with tubulin

Tubulin dimers are incorporated into microtubules only after they have bound GTP to the exchangeable GTP binding site on beta tubulin. The binding of GTP alters the structure of the tubulin dimer. It was of interest to determine whether the structural change induced by GTP binding was reflected in the amount of chlorpyrifos oxon covalently bound to tubulin. The effect of GTP on chlorpyrifos oxon binding to tubulin was determined by incubation of 0.012 mM bovine tubulin heterodimer with 0.5 mM chlorpyrifos oxon at 37 °C for 24 h in the presence and absence of 1 mM GTP. Tryptic peptides were analyzed in the MALDI-TOF/TOF 4800 mass spectrometer. Fig. 8 presents the MS spectra of pairs of unlabeled and chlorpyrifos oxon-labeled tryptic peptides without (panel A) and with GTP (panel B). The presence of 1 mM GTP increased the extent of tubulin organophosphorylation. The peak intensities of chlorpyrifos oxon-labeled peptides were increased about 2-fold in the presence of GTP relative to the intensities of the unlabeled peaks.

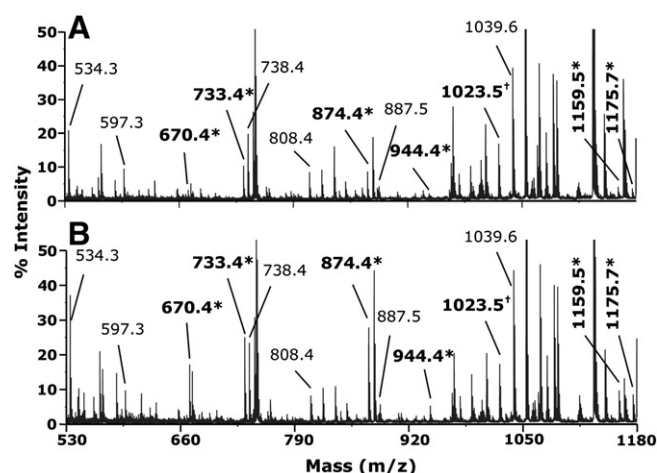


**Fig. 8.** Effect of GTP on extent of chlorpyrifos oxon labeling. MS spectra were acquired on the MALDI-TOF mass spectrometer. (A) labeled in the absence of GTP; (B) labeled in the presence of 1 mM GTP. Unlabeled peptides are indicated by regular font and labeled peptides (+136 amu added mass from chlorpyrifos oxon) are indicated in bold and marked by asterisks. Seven pairs of peptides are represented. Their masses and amino acid sequences are listed in Table 2. The peak at 1023.5 m/z corresponds to the unlabeled EDANNYAR and the chlorpyrifos oxon-labeled FDLMY\*AK peptides. The peak height of each labeled peptide compared to the unlabeled peptide is higher in panel B (with GTP) than in panel A (without GTP).

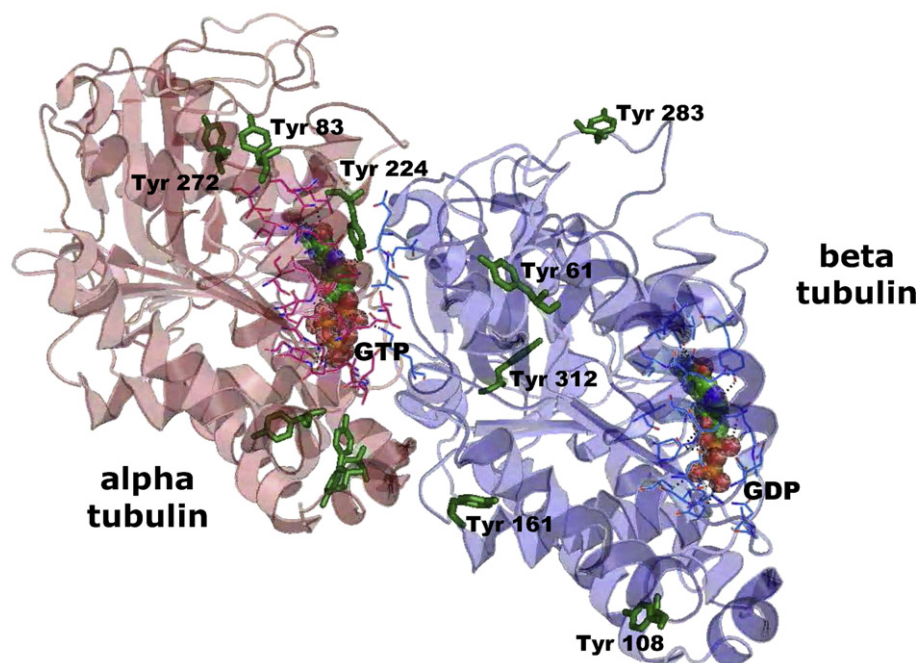


**Fig. 9.** Crystal structure of the bovine brain tubulin heterodimer with subunit alpha in red and beta in blue (Protein Data Bank number, 1jff). Eight chlorpyrifos oxon-labeled tyrosines (3 in alpha and 5 in beta tubulin) are shown as solid green sticks. GTP in the GTP non-exchangeable binding site in alpha tubulin and GDP in the exchangeable binding site in beta tubulin are shown as balls surrounded by amino acid residues that directly interact with these nucleotides. Amino acid numbers correspond to the numbers in pdb 1jff. These numbers are high compared to the numbers in the protein sequence because a gap of two residues was introduced in the numbers of the beta tubulin crystal structure (Nogales et al., 1999). The structure was drawn with PyMol software [www.pymol.sourceforge.net](http://www.pymol.sourceforge.net).

#### *Location of chlorpyrifos oxon-labeled tyrosines in the crystal structure of the tubulin heterodimer*

Tyrosines of bovine tubulin differed in their sensitivity toward chlorpyrifos oxon. To explain these differences, the location of modified tyrosines was of interest. The crystal structure of bovine brain tubulin heterodimer, reported by Nogales et al. (Protein Data Bank number, 1jff) is shown in Fig. 9 (Nogales et al., 1999). The 8 tyrosines for which reactivity data were obtained are indicated. Nogales et al. introduced gaps into the numbers of the beta tubulin amino acid sequence, which explains why the numbers in the crystal structure are higher than the numbers in the protein database.

The phenolic oxygen of Tyr 272 in alpha tubulin and Tyr 108 (Y106) and Tyr 312 (Y310) in beta tubulin face the inside of the protein. As a consequence, it can be assumed that access of chlorpyrifos oxon to these tyrosines was limited, which is consistent with the relatively low percentage of chlorpyrifos oxon labeling observed for these tyrosines (see Fig. 6). Tyrosines 61 (59), 83, 161 (159), 224 and 283 (281) are exposed on the surface of tubulin. Tyr 224, in addition to being exposed to solvent, makes a  $\pi$ - $\pi$  interaction with the guanine moiety of the GTP molecule. Tyrosine 83 and Tyr 283 (281) are exposed on the surface of the tubulin dimer making them readily available for reaction with chlorpyrifos oxon, which would contribute to their high reactivity.

## Discussion

#### *Tubulin labeled in living mice*

Living mice treated with a nontoxic dose of FP-biotin appeared to have FP-biotin labeled tubulin in their brains. The evidence for OP-labeled tubulin in mice is not complete because the OP-labeled peptide was not identified. The following observations led to the idea that tubulin was labeled by FP-biotin. 1) Avidin beads bound tubulin from brains of FP-biotin treated mice, but not from brains of untreated

mice. 2) A protein of 55 kDa contained covalently bound FP-biotin as visualized on a blot hybridized with Streptavidin Alexa-680. Mass spectrometry identified the major component of this 55 kDa SDS gel band as tubulin. The data presented in this report are intended to aid the search for OP-labeled tubulin peptides, to provide the proof that is currently missing.

#### *OP-labeled tyrosines in bovine tubulin*

In preparation for renewed attempts to find the OP-labeled tubulin peptide in mouse brain, we set out to identify the potentially labeled sites. For this purpose we studied the labeling of highly purified bovine tubulin by chlorpyrifos oxon. We identified tyrosine as the site of covalent binding by OP and identified the specific tyrosines that are most reactive with OP, i.e. Tyr 83 from alpha tubulin and Tyr 281 from beta tubulin.

#### *OP-target tyrosines are conserved in bovine, mouse, and human tubulin*

The NCBI database shows up to 8 alpha and 8 beta tubulin sequences in bovine, mouse, and human species. Their amino acid sequences are highly conserved. For example, alignment of accession numbers 73586894 (bovine alpha), 55977479 (mouse alpha) and 17986283 (human alpha) shows 98% sequence identity with all tyrosines conserved. Alignment of accession numbers 75773583 (bovine beta), 33859488 (mouse beta), and 4507729 (human beta) shows 97% identity with all tyrosines conserved. It can therefore be proposed that the tyrosines modified by OP in bovine tubulin are likely to be modified in mouse and human tubulin.

#### *Tyrosine as a motif for OP binding to proteins*

The presence of the consensus sequence GXSGX defines a protein as a member of the serine hydrolase family. These proteins make a covalent bond with OP on the active site serine. However, the majority

of proteins that bound FP-biotin covalently in Table 1 do not have the consensus sequence GXSGX. Except for albumin and tubulin, where OP make a covalent bond with tyrosine (Li et al., 2007a; Grigoryan et al., 2008), the site of covalent attachment of FP-biotin is unknown. The most extensive data are for OP labeling of albumin. Several laboratories agree that albumin is covalently modified by OP both in vitro and in vivo (Adams et al., 2004; Peoples et al., 2005; Carter et al., 2007; Williams et al., 2007; Ding et al., 2008; Tarhoni et al., 2008).

#### Non-acetylcholinesterase mechanisms of OP toxicity

Tubulin dimers polymerize to form microtubules. Microtubules are part of the cytoskeletal system that maintains the morphology of neurons including axonal and dendritic processes (Gendron and Petrucelli, 2009). Microtubules serve as tracks for transport of mitochondria, synaptic vesicles, components of ion channels, receptors, and scaffolding proteins to and from synaptic sites. Synapses are highly vulnerable to impairments in transport. Perturbations to microtubule transport could cause malfunctions in neurotransmission and signal propagation and lead to synaptic degradation (Gendron and Petrucelli, 2009). Drugs that inhibit tubulin polymerization, for example colchicine, trigger apoptosis (Yeste-Velasco et al., 2008). Thus, the ability of tubulin to polymerize is very important for the life of a cell.

Microtubule function is also disrupted by hyperphosphorylation. It has been reported that aberrant phosphorylation of cytoskeletal proteins results in destabilization of microtubules and neurofilaments, leading to their aggregation. Consequently, normal function of the axons of central and peripheral nervous systems is disrupted (Abou-Donia, 1995; Abou-Donia, 2003). Organophosphorylation occurs on many of the same tyrosines that are phosphorylated (Table 2). It is reasonable to suggest that, like hyperphosphorylation, organophosphorylation of tubulin on multiple sites could impede tubulin polymerization and normal functioning of microtubules.

It has also been reported that dichlorvos, tri-*o*-cresyl phosphate, and diisopropyl phosphofluoridate induce hyperphosphorylation of cytoskeletal proteins (Suwita et al., 1986; Gupta and Abou-Donia, 1994; Choudhary et al., 2001). Phosphorylation is mediated by the microtubule associated endogenous cAMP dependent protein kinases and  $\text{Ca}^{2+}$ /Calmodulin kinase. This could provide an alternate means by which organophosphates could disrupt the function of microtubules.

These observations make disruption of tubulin function a very likely source of toxicity related to low-dose exposure to OP. However, disruption of other systems is also possible.

Hyperphosphorylation of CREB, induced by OP has been proposed as a mechanism of OP toxicity (Schuh et al., 2002). CREB is the nuclear transcription factor that controls cell differentiation. CREB is critical to synaptic plasticity and transcription-dependent forms of memory. Exposure to OP has been correlated with increased phosphorylation of CREB and it has been suggested that the increased phosphorylation alters the function of CREB. Alteration in the function of CREB could explain the memory impairment following OP exposure. It is not known whether the hyperphosphorylated CREB is a result of the direct action of OP on CREB or an indirect effect from OP-modification of proteins involved in phosphorylation or dephosphorylation of CREB.

The developmental neurotoxicity of chlorpyrifos may be due to disruption of the adenylyl cyclase cell signaling cascade (Song et al., 1997). Perturbation of the synthesis of the second messenger cyclic AMP affects cell replication and differentiation. The serotonergic signal transduction system has also been implicated in chlorpyrifos neurotoxicity. Abnormal levels of serotonin may alter the differentiation and architectural organization of the developing brain (Aldridge et al., 2003). Either of these effects could be the consequence of direct

reaction of chlorpyrifos oxon with tyrosine in critical proteins of these systems.

Direct action of chlorpyrifos on muscarinic receptors causes M2 receptor dysfunction and bronchoconstriction in the absence of AChE inhibition. This mechanism is proposed to explain symptoms of asthma including airway hyperreactivity and wheezing following OP exposure (Lein and Fryer, 2005). Covalent binding of 3H-chlorpyrifos oxon to M2 muscarinic acetylcholine receptors in rat heart has been demonstrated, though the modified amino acid has not been identified (Bomser and Casida, 2001).

Some OP inhibit neuronal  $\alpha\beta 2$  nicotinic acetylcholine receptors at low concentrations that have no effect on AChE activity (Smulders et al., 2004). The desensitized receptors may contribute to neurological and neurobehavioral deficits.

Though we have demonstrated a clear reaction of OP with tubulin, it is likely that disruption of some or all of these other systems is involved in low-dose OP neurotoxicity. The dominant mechanism would depend on the identity of the OP, the developmental age of the exposed individual, the health of the organs that metabolize and dispose of OP, and genetic factors, for example the genotype of enzymes involved in OP metabolism.

#### Acknowledgments

Mass spectra were obtained with the support of the Mass Spectrometry and Proteomics core facility at the University of Nebraska Medical Center. This study was supported by the U.S. Army Medical Research and Materiel Command W81XWH-07-2-0034, the National Institutes of Health U01 NS058056, U01 ES016102, and P30CA36727, and DGA/PEA grants 08co501 and ANR-06-BLAN-0163.

#### References

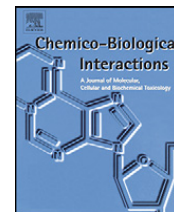
- Abou-Donia, M.B., 1995. Involvement of cytoskeletal proteins in the mechanisms of organophosphorus ester-induced delayed neurotoxicity. *Clin. Exp. Pharmacol. Physiol.* 22, 358–359.
- Abou-Donia, M.B., 2003. Organophosphorus ester-induced chronic neurotoxicity. *Arch. Environ. Health* 58, 484–497.
- Adams, T.K., Capacio, B.R., Smith, J.R., Whalley, C.E., Korte, W.D., 2004. The application of the fluoride reactivation process to the detection of sarin and soman nerve agent exposures in biological samples. *Drug Chem. Toxicol.* 27, 77–91.
- Aldridge, J.E., Seidler, F.J., Meyer, A., Thillai, I., Slotkin, T.A., 2003. Serotonergic systems targeted by developmental exposure to chlorpyrifos: effects during different critical periods. *Environ. Health Perspect.* 111, 1736–1743.
- Azaroff, L.S., 1999. Biomarkers of exposure to organophosphorus insecticides among farmers' families in rural El Salvador: factors associated with exposure. *Environ. Res.* 80, 138–147.
- Bomser, J.A., Casida, J.E., 2001. Diethylphosphorylation of rat cardiac M2 muscarinic receptor by chlorpyrifos oxon in vitro. *Toxicol. Lett.* 119, 21–26.
- Brown, M.A., Brix, K.A., 1998. Review of health consequences from high-, intermediate- and low-level exposure to organophosphorus nerve agents. *J. Appl. Toxicol.* 18, 393–408.
- Carter, W.G., Tarhoni, M., Rathbone, A.J., Ray, D.E., 2007. Differential protein adduction by seven organophosphorus pesticides in both brain and thymus. *Hum. Exp. Toxicol.* 26, 347–353.
- Casida, J.E., Quistad, G.B., 2004. Organophosphate toxicology: safety aspects of non-acetylcholinesterase secondary targets. *Chem. Res. Toxicol.* 17, 983–998.
- Choudhary, S., Joshi, K., Gill, K.D., 2001. Possible role of enhanced microtubule phosphorylation in dichlorvos induced delayed neurotoxicity in rat. *Brain Res.* 897, 60–70.
- Ding, S.J., Carr, J., Carlson, J.E., Tong, L., Xue, W., Li, Y., Schopfer, L.M., Li, B., Nachon, F., Asojo, O., Thompson, C.M., Hinrichs, S.H., Masson, P., Lockridge, O., 2008. Five tyrosines and two serines in human albumin are labeled by the organophosphorus agent FP-biotin. *Chem. Res. Toxicol.* 21, 1787–1794.
- Eddleston, M., Mohamed, F., Davies, J.O., Eyer, P., Worek, F., Sherif, M.H., Buckley, N.A., 2006. Respiratory failure in acute organophosphorus pesticide self-poisoning. *Qjm* 99, 513–522.
- Gearhart, D.A., Sickles, D.W., Buccafusco, J.J., Prendergast, M.A., Terry Jr., A.V., 2007. Chlorpyrifos, chlorpyrifos-oxon, and diisopropylfluorophosphate inhibit kinesin-dependent microtubule motility. *Toxicol. Appl. Pharmacol.* 218, 20–29.
- Gendron, T.F., Petrucelli, L., 2009. The role of tau in neurodegeneration. *Mol. Neurodegener.* 4, 13.
- Grigoryan, H., Schopfer, L.M., Thompson, C.M., Terry, A.V., Masson, P., Lockridge, O., 2008. Mass spectrometry identifies covalent binding of soman, sarin, chlorpyrifos oxon, diisopropyl fluorophosphate, and FP-biotin to tyrosines on tubulin: a potential mechanism of long term toxicity by organophosphorus agents. *Chem. Biol. Interact.* 175, 180–186.

- Guo, A., Villen, J., Kornhauser, J., Lee, K.A., Stokes, M.P., Rikova, K., Possemato, A., Nardone, J., Innocenti, G., Wetzel, R., Wang, Y., MacNeill, J., Mitchell, J., Gygi, S.P., Rush, J., Polakiewicz, R.D., Comb, M.J., 2008. Signaling networks assembled by oncogenic EGFR and c-Met. *Proc. Natl. Acad. Sci. U. S. A.* 105, 692–697.
- Gupta, R.P., Abou-Donia, M.B., 1994. In vivo and in vitro effects of diisopropyl phosphorofluoridate (DFP) on the rate of hen brain tubulin polymerization. *Neurochem. Res.* 19, 435–444.
- Jennings, L.L., Malecki, M., Komives, E.A., Taylor, P., 2003. Direct analysis of the kinetic profiles of organophosphate-acetylcholinesterase adducts by MALDI-TOF mass spectrometry. *Biochemistry* 42, 11083–11091.
- Kamel, F., Engel, L.S., Gladen, B.C., Hoppin, J.A., Alavanja, M.C., Sandler, D.P., 2007. Neurologic symptoms in licensed pesticide applicators in the Agricultural Health Study. *Hum. Exp. Toxicol.* 26, 243–250.
- Kidd, D., Liu, Y., Cravatt, B.F., 2001. Profiling serine hydrolase activities in complex proteomes. *Biochemistry* 40, 4005–4015.
- Lein, P.J., Fryer, A.D., 2005. Organophosphorus insecticides induce airway hyperreactivity by decreasing neuronal M2 muscarinic receptor function independent of acetylcholinesterase inhibition. *Toxicol. Sci.* 83, 166–176.
- Ley, S.C., Verbi, W., Pappin, D.J., Druker, B., Davies, A.A., Crumpton, M.J., 1994. Tyrosine phosphorylation of alpha tubulin in human T lymphocytes. *Eur. J. Immunol.* 24, 99–106.
- Li, B., Schopfer, L.M., Hinrichs, S.H., Masson, P., Lockridge, O., 2007a. Matrix-assisted laser desorption/ionization time-of-flight mass spectrometry assay for organophosphorus toxicants bound to human albumin at Tyr411. *Anal. Biochem.* 361, 263–272.
- Li, H., Schopfer, L.M., Nachon, F., Froment, M.T., Masson, P., Lockridge, O., 2007b. Aging pathways for organophosphate-inhibited human butyrylcholinesterase, including novel pathways for isomalathion, resolved by mass spectrometry. *Toxicol. Sci.* 100, 136–145.
- Lockridge, O., Xue, W., Gaydess, A., Grigoryan, H., Ding, S.J., Schopfer, L.M., Hinrichs, S.H., Masson, P., 2008. Pseudo-esterase activity of human albumin: slow turnover on tyrosine 411 and stable acetylation of 82 residues including 59 lysines. *J. Biol. Chem.* 283, 22582–22590.
- McDonough Jr., J.H., Shih, T.M., 1997. Neuropharmacological mechanisms of nerve agent-induced seizure and neuropathology. *Neurosci. Biobehav. Rev.* 21, 559–579.
- Moser, V.C., 1995. Comparisons of the acute effects of cholinesterase inhibitors using a neurobehavioral screening battery in rats. *Neurotoxicol. Teratol.* 17, 617–625.
- Nogales, E., Whittaker, M., Milligan, R.A., Downing, K.H., 1999. High-resolution model of the microtubule. *Cell* 96, 79–88.
- Nomura, D.K., Blankman, J.L., Simon, G.M., Fujioka, K., Issa, R.S., Ward, A.M., Cravatt, B.F., Casida, J.E., 2008. Activation of the endocannabinoid system by organophosphorus nerve agents. *Nat. Chem. Biol.* 4, 373–378.
- Nomura, D.K., Leung, D., Chiang, K.P., Quistad, G.B., Cravatt, B.F., Casida, J.E., 2005. A brain detoxifying enzyme for organophosphorus nerve poisons. *Proc. Natl. Acad. Sci. U. S. A.* 102, 6195–6200.
- Pashkova, A., Moskovets, E., Karger, B.L., 2004. Coumarin tags for improved analysis of peptides by MALDI-TOF MS and MS/MS. 1. Enhancement in MALDI MS signal intensities. *Anal. Chem.* 76, 4550–4557.
- Peebles, E.S., Schopfer, L.M., Duysen, E.G., Spaulding, R., Voelker, T., Thompson, C.M., Lockridge, O., 2005. Albumin, a new biomarker of organophosphorus toxicant exposure, identified by mass spectrometry. *Toxicol. Sci.* 83, 303–312.
- Perkins, D.N., Pappin, D.J., Creasy, D.M., Cottrell, J.S., 1999. Probability-based protein identification by searching sequence databases using mass spectrometry data. *Electrophoresis* 20, 3551–3567.
- Pope, C.N., 1999. Organophosphorus pesticides: do they all have the same mechanism of toxicity? *J. Toxicol. Environ. Health B Crit. Rev.* 2, 161–181.
- Prendergast, M.A., Self, R.L., Smith, K.J., Ghayoumi, L., Mullins, M.M., Butler, T.R., Buccafusco, J.J., Gearhart, D.A., Terry Jr., A.V., 2007. Microtubule-associated targets in chlorpyrifos oxon hippocampal neurotoxicity. *Neuroscience* 146, 330–339.
- Rikova, K., Guo, A., Zeng, Q., Possemato, A., Yu, J., Haack, H., Nardone, J., Lee, K., Reeves, C., Li, Y., Hu, Y., Tan, Z., Stokes, M., Sullivan, L., Mitchell, J., Wetzel, R., MacNeill, J., Ren, J.M., Yuan, J., Bakalarski, C.E., Villen, J., Kornhauser, J.M., Smith, B., Li, D., Zhou, X., Gygi, S.P., Gu, T.L., Polakiewicz, R.D., Rush, J., Comb, M.J., 2007. Global survey of phosphotyrosine signaling identifies oncogenic kinases in lung cancer. *Cell* 131, 1190–1203.
- Roldan-Tapia, L., Nieto-Escamez, F.A., del Aguila, E.M., Laynez, F., Parron, T., Sanchez-Santed, F., 2006. Neuropsychological sequelae from acute poisoning and long-term exposure to carbamate and organophosphate pesticides. *Neurotoxicol. Teratol.* 28, 694–703.
- Rush, J., Moritz, A., Lee, K.A., Guo, A., Goss, V.L., Spek, E.J., Zhang, H., Zha, X.M., Polakiewicz, R.D., Comb, M.J., 2005. Immunoaffinity profiling of tyrosine phosphorylation in cancer cells. *Nat. Biotechnol.* 23, 94–101.
- Salvi, R.M., Lara, D.R., Ghisolfi, E.S., Portela, L.V., Dias, R.D., Souza, D.O., 2003. Neuropsychiatric evaluation in subjects chronically exposed to organophosphate pesticides. *Toxicol. Sci.* 72, 267–271.
- Schopfer, L.M., Champion, M.M., Tamblyn, N., Thompson, C.M., Lockridge, O., 2005a. Characteristic mass spectral fragments of the organophosphorus agent FP-biotin and FP-biotinylated peptides from trypsin and bovine albumin (Tyr410). *Anal. Biochem.* 345, 122–132.
- Schopfer, L.M., Grigoryan, H., Li, B., Nachon, F., Masson, P., Lockridge, O., 2009. Mass spectral characterization of organophosphate-labeled, tyrosine-containing peptides: characteristic mass fragments and a new binding motif for organophosphates. *J. Chromatogr. B.*
- Schopfer, L.M., Voelker, T., Bartels, C.F., Thompson, C.M., Lockridge, O., 2005b. Reaction kinetics of biotinylated organophosphorus toxicant, FP-biotin, with human acetylcholinesterase and human butyrylcholinesterase. *Chem. Res. Toxicol.* 18, 747–754.
- Schuh, R.A., Lein, P.J., Beckles, R.A., Jett, D.A., 2002. Noncholinesterase mechanisms of chlorpyrifos neurotoxicity: altered phosphorylation of Ca<sup>2+</sup>/cAMP response element binding protein in cultured neurons. *Toxicol. Appl. Pharmacol.* 182, 176–185.
- Smulders, C.J., Bueters, T.J., Vailati, S., van Kleef, R.G., Vijverberg, H.P., 2004. Block of neuronal nicotinic acetylcholine receptors by organophosphate insecticides. *Toxicol. Sci.* 82, 545–554.
- Song, X., Seidler, F.J., Saleh, J.L., Zhang, J., Padilla, S., Slotkin, T.A., 1997. Cellular mechanisms for developmental toxicity of chlorpyrifos: targeting the adenylyl cyclase signaling cascade. *Toxicol. Appl. Pharmacol.* 145, 158–174.
- Stephens, R., Spurgeon, A., Calvert, I.A., Beach, J., Levy, L.S., Berry, H., Harrington, J.M., 1995. Neuropsychological effects of long-term exposure to organophosphates in sheep dip. *Lancet* 345, 1135–1139.
- Sun, J., Lynn, B.C., 2007. Development of a MALDI-TOF-MS method to identify and quantify butyrylcholinesterase inhibition resulting from exposure to organophosphate and carbamate pesticides. *J. Am. Soc. Mass Spectrom.* 18, 698–706.
- Suwita, E., Lapadula, D.M., Abou-Donia, M.B., 1986. Calcium and calmodulin stimulated in vitro phosphorylation of rooster brain tubulin and MAP-2 following a single oral dose of tri-o-cresyl phosphate. *Brain Res.* 374, 199–203.
- Tang, X., Sadeghi, M., Olumee, Z., Vertes, A., Braatz, J.A., McIlwain, L.K., Dreifuss, P.A., 1996. Detection and quantitation of beta-2-microglobulin glycosylated end products in human serum by matrix-assisted laser desorption/ionization mass spectrometry. *Anal. Chem.* 68, 3740–3745.
- Tarhoni, M.H., Lister, T., Ray, D.E., Carter, W.G., 2008. Albumin binding as a potential biomarker of exposure to moderately low levels of organophosphorus pesticides. *Biomarkers* 13, 343–363.
- Terry Jr., A.V., Gearhart, D.A., Beck Jr., W.D., Truan, J.N., Middlemore, M.L., Williamson, L. N., Bartlett, M.G., Prendergast, M.A., Sickles, D.W., Buccafusco, J.J., 2007. Chronic, intermittent exposure to chlorpyrifos in rats: protracted effects on axonal transport, neurotrophin receptors, cholinergic markers, and information processing. *J. Pharmacol. Exp. Ther.* 322, 1117–1128.
- Tuin, A.W., Mol, M.A., van den Berg, R.M., Fidler, A., van der Marel, G.A., Overkleeft, H.S., Noort, D., 2009. Activity-based protein profiling reveals broad reactivity of the nerve agent sarin. *Chem. Res. Toxicol.*
- Wandossell, F., Serrano, L., Avila, J., 1987. Phosphorylation of alpha-tubulin carboxyl-terminal tyrosine prevents its incorporation into microtubules. *J. Biol. Chem.* 262, 8268–8273.
- Williams, N.H., Harrison, J.M., Read, R.W., Black, R.M., 2007. Phosphorylated tyrosine in albumin as a biomarker of exposure to organophosphorus nerve agents. *Arch. Toxicol.* 81, 627–639.
- Yeste-Velasco, M., Alvira, D., Sureda, F.X., Rimbau, V., Forsby, A., Pallas, M., Camins, A., Folch, J., 2008. DNA low-density array analysis of colchicine neurotoxicity in rat cerebellar granular neurons. *Neurotoxicology* 29, 309–317.
- Zheng, H., Hu, P., Quinn, D.F., Wang, Y.K., 2005. Phosphotyrosine proteomic study of interferon alpha signaling pathway using a combination of immunoprecipitation and immobilized metal affinity chromatography. *Mol. Cell Proteomics* 4, 721–730.



Contents lists available at ScienceDirect

## Chemico-Biological Interactions

journal homepage: [www.elsevier.com/locate/chembioint](http://www.elsevier.com/locate/chembioint)

# Mass spectrometry identifies covalent binding of soman, sarin, chlorpyrifos oxon, diisopropyl fluorophosphate, and FP-biotin to tyrosines on tubulin: A potential mechanism of long term toxicity by organophosphorus agents

Hasmik Grigoryan<sup>a</sup>, Lawrence M. Schopfer<sup>a</sup>, Charles M. Thompson<sup>b</sup>, Alvin V. Terry<sup>c</sup>, Patrick Masson<sup>d</sup>, Oksana Lockridge<sup>a,\*</sup>

<sup>a</sup> Eppley Institute, University of Nebraska Medical Center, 986805 Nebraska Medical Center, Omaha, NE 68198-6805, USA

<sup>b</sup> Department of Biomedical and Pharmaceutical Sciences, University of Montana, Missoula, MT 59812, USA

<sup>c</sup> Department of Pharmacology and Toxicology, Medical College of Georgia, 1120 Fifteenth St., Augusta, GA 30912-2450, USA

<sup>d</sup> Centre de Recherches du Service de Santé des Armées, Département de Toxicologie, Unité d'Enzymologie, BP 87, 38702 La Tronche cédex, France

## ARTICLE INFO

## Article history:

Available online 22 April 2008

## Keywords:

Tubulin  
Organophosphate  
Tyrosine  
Nerve agent  
Mass spectrometer

## ABSTRACT

Chronic low dose exposure to organophosphorus poisons (OP) results in cognitive impairment. Studies in rats have shown that OP interfere with microtubule polymerization. Since microtubules are required for transport of nutrients from the nerve cell body to the nerve synapse, it has been suggested that disruption of microtubule function could explain the learning and memory deficits associated with OP exposure. Tubulin is a major constituent of microtubules. We tested the hypothesis that OP bind to tubulin by treating purified bovine tubulin with sarin, soman, chlorpyrifos oxon, diisopropylfluorophosphate, and 10-fluoroethoxyphosphinyl-*N*-biotinamidopentyldecanamide (FP-biotin). Tryptic peptides were isolated and analyzed by mass spectrometry. It was found that OP bound to tyrosine 83 of alpha tubulin in peptide TGTyr, tyrosine 59 in beta tubulin peptide YVPR, tyrosine 281 in beta tubulin peptide GSQQYR, and tyrosine 159 in beta tubulin peptide EEYPDR. The OP reactive tyrosines are located either near the GTP binding site or within loops that interact laterally with protofilaments. It is concluded that OP bind covalently to tubulin, and that this binding could explain cognitive impairment associated with OP exposure.

© 2008 Elsevier Ireland Ltd. All rights reserved.

## 1. Introduction

Acute toxicity from organophosphorus poisons (OP) is mainly due to inhibition of acetylcholinesterase [1]. However, low dose exposure that causes minimal inhibition

of AChE and no obvious cholinergic symptoms has been linked to memory loss, sleep disorder, depression, learning and language impairment, and decreased motor skills in humans [2–4]. Rats treated with low doses of chlorpyrifos have behavioral deficits in a water-maze hidden platform task and in prepulse inhibition [5]. The mechanism to explain cognitive deficits from low dose exposure is thought to be inhibition of fast axonal transport [5]. Axonal transport was impaired in sciatic nerves isolated from chlorpyrifos treated rats [5,6]. Transport of nutrients to nerve endings is accomplished via microtubules that serve as the highway on which kinesin molecules

**Abbreviations:** amu, atomic mass units; CPO, chlorpyrifos oxon; DFP, diisopropyl fluorophosphate; FP-biotin, 10-fluoroethoxyphosphinyl-*N*-biotinamidopentyldecanamide; FPB, FP-biotin; OP, organophosphorus poisons; CID, collision induced dissociation.

\* Corresponding author. Tel.: +1 402 559 6032; fax: +1 402 559 4651.

E-mail address: [olockrid@unmc.edu](mailto:olockrid@unmc.edu) (O. Lockridge).

carry their cargo [7]. When microtubule function is disrupted, neurons lose viability. Microtubules are polymers of alpha and beta tubulin. Prendergast et al. have shown that polymerization of tubulin is inhibited by low doses of chlorpyrifos and diisopropyl fluorophosphate (DFP) [8]. The goal of the present work was to identify the amino acid residues modified by reaction of tubulin with OP. Mass spectrometry identified four covalent binding sites, all of them tyrosines.

## 2. Materials and methods

### 2.1. Materials

Bovine tubulin (TL238) >99% pure, isolated from bovine brain, was from Cytoskeleton, Inc. (Denver, CO). This tubulin preparation contains both alpha and beta-tubulin. Chlorpyrifos oxon (MET-674B) was from Chem Service Inc. (West Chester, PA). 10-Fluoroethoxyphosphinyl-*N*-biotinamidopentyldecanamide (FP-biotin) was custom synthesized in the laboratory of Dr. Charles M. Thompson at the University of Montana, Missoula, MT [9]. Diisopropylfluorophosphate (D0879) was from Sigma-Aldrich (St. Louis, MO). The nerve agents sarin and soman were from CEB (Vert-le-Petit, France). Sequencing grade modified porcine trypsin (V5113) was from Promega (Madison, WI). Slide-A-Lyzer 7K dialysis cassettes (No. 66370) and ImmunoPure immobilized monomeric avidin (#20228) were from Pierce Biotechnology Inc. (Rockford, IL).

### 2.2. OP-labeled tubulin tryptic peptides

Bovine tubulin (2 mg/ml) was dissolved in either 50 mM ammonium bicarbonate pH 8.3 or in 80 mM PIPES, 0.5 mM EGTA, 0.25 mM MgCl<sub>2</sub> buffer pH 6.9, or in 10 mM Tris-Cl pH 8.0. The 0.5 ml of 2 mg/ml tubulin (40 μM) was treated with a 20-fold molar excess of FP-biotin dissolved in dimethyl sulfoxide, or a 200-fold molar excess of diisopropyl fluorophosphate (DFP), or a 20-fold molar excess of chlorpyrifos oxon (CPO) dissolved in dimethyl sulfoxide, or a 5-fold molar excess of soman and sarin dissolved in isopropanol. The reaction mixtures were incubated at 37 °C for 16–24 h. The proteins were denatured by boiling in a water bath for 10 min. Excess OP was removed by dialysis against 10 mM ammonium bicarbonate. The 1 mg of dialyzed tubulin was digested with 0.02 mg of Promega trypsin at 37 °C for 16 h.

### 2.3. Purification of FP-biotinylated peptides on monomeric avidin beads

The trypsin-digested, FP-biotinylated tubulin was boiled for 10 min to denature trypsin. This prevented digestion of avidin protein by trypsin. The digest was loaded on a 1 ml column of monomeric avidin beads. The column was washed with 20 ml of 1 M Tris-Cl pH 8.5 to wash off unbound peptides, followed by 20 ml of 0.1 M Tris-Cl pH 8.5, and 20 ml of 10 mM ammonium bicarbonate. Salts were washed off with 20 ml water, before the peptides were eluted with 10 ml of 10% acetic acid. One millilitre fractions were collected.

### 2.4. HPLC purification

Peptides intended for infusion on the Q-Trap mass spectrometer were purified by reverse phase HPLC. The advantage of offline HPLC purification was the large amount of peptide sample that could be loaded on the C18 column (Phenomenex Prodigy 5 micron ODS size 100 × 4.60 mm). Peptides from a 1 mg tubulin digest were eluted with a gradient that started with 100% of 0.1% trifluoroacetic acid and increased to 60% acetonitrile/40% 0.1% trifluoroacetic acid in 60 min on a Waters 625 LC system. Fractions of 1 ml were collected, analyzed by MALDI-TOF mass spectrometry, and dried in a SpeedVac.

### 2.5. MALDI-TOF mass spectrometry

The MALDI-TOF-TOF 4800 mass spectrometer (Applied Biosystems) was used for analysis of tryptic peptides prior to more rigorous analysis with the Q-Trap. This mass spectrometer was also used for analysis of tryptic peptides. A 0.5 μl sample was spotted on a 384 well Opti-TOF plate (P/N 1016491, Applied Biosystems) and the air dried spot was overlaid with 0.5 μl of 10 mg/ml α-cyano-4-hydroxycinnamic acid dissolved in 50% acetonitrile, 0.1% trifluoroacetic acid. Mass spectra were collected in positive ion reflector mode on a MALDI-TOF-TOF 4800 mass spectrometer (Applied Biosystems, Foster City, CA). The final spectrum was the average of 500 laser shots. Masses were calibrated using CalMix 5 (Applied Biosystems).

### 2.6. Q-Trap 4000 mass spectrometry

Peptides from selected HPLC fractions were dissolved in 100 μl of 50% acetonitrile, 0.1% formic acid and infused into the Q-Trap 4000 linear ion trap mass spectrometer (Applied Biosystems) via a nanospray source, using a continuous flow head, a flow rate of 0.30 μl/min, and an ion spray potential of 1900 V. Spray was through a distal coated silica tip emitter FS360-75-15-D (New Objective, Woburn, MA). Mass spectra were obtained using the trap function at 4000 amu/s with dynamic fill to determine the filling time for the trap. One hundred to 350 spectra were averaged. Peptide fragmentation also employed the trap. MS/MS spectra were obtained by collision induced dissociation (CID) at a nitrogen gas pressure of 40 μTorr and a collision energy of 30–60 V. The spectrometer was calibrated on selected fragments from the MS/MS spectrum of [Glu]-fibrinopeptide B.

## 3. Results

### 3.1. Strategy for identifying labeled residues in tubulin

The strategy is to first use FP-biotin to label the tubulin. FP-biotinylated peptides are easy to find because the biotin tag gives a signature fragmentation pattern. Masses of 227, 312, and 329 amu are always present in the MS/MS scan of an FP-biotin labeled peptide [9]. We use the MS/MS function of the MALDI-TOF-TOF mass spectrometer to screen for FP-biotin labeled peptides. Then we use the Q-Trap 4000 mass spectrometer to fragment the peptides for de novo

**Table 1**

Theoretical masses of bovine tubulin tryptic peptides covalently labeled by OP

Tubulin chain	Sequence	Mass (m/z)	+120 sarin	+136 CPO	+162 soman	+164 DFP	+572 FP-biotin
Alpha	TGTyr	597.3	717.3	733.3	759.3	761.3	1169.3
Beta	YVPR	534.3	654.3	670.3	696.3	698.3	1106.3
Beta	GSQQYR	738.4	858.4	874.4	900.4	902.4	1310.4
Beta	EEYPDR	808.3	928.3	944.3	970.3	972.3	1380.3

Accession # gi: 73586894 for alpha-tubulin and gi: 75773583 for beta-tubulin in the NCBI nr database.

sequencing to identify the site of covalent attachment of FP-biotin.

In a second phase, the protein is labeled with other OP. In the first round of screening for peptides labeled with these other OP, the assumption is made that the sites labeled by FP-biotin are also labeled by other OP. This assumption allows one to calculate theoretical OP-peptide masses and to look for the presence of these masses in the HPLC-fractionated, tryptic digest using the MALDI-TOF-TOF mass spectrometer. However, this assumption may not hold for all OP. Therefore a second strategy is used. Peptide masses observed in the MS scan for OP-labeled peptides are compared with theoretical masses for unlabeled peptides. The list of theoretical masses is generated with Protein Prospector software (UCSF). This free software is available at <http://prospector.ucsf.edu>. Candidates for OP-labeled peptides are chosen when their masses are equal to the sum of the known peptide mass and the added mass from the OP. These putative, OP-labeled peptides are further tested by CID fragmentation in the Q-Trap 4000 mass spectrometer, followed by manual de novo sequencing to identify the site of covalent, OP attachment.

### 3.2. Four tubulin peptides are labeled by OP

The structures of the OP studied in the present report are shown in Fig. 1. A portion of each OP and the phenolic proton from the labeled tyrosine are displaced when the OP makes a covalent bond with tubulin, so that the mass added to tubulin is less than the mass of the OP. The added masses are 120 amu for sarin, 136 amu for CPO, 162 amu for soman, 164 amu for DFP, and 572 amu for FP-biotin. The leaving group is fluoride ion for sarin, soman, DFP and FP-biotin, and is 3,5,6-trichloro-2-(O)-pyridine for CPO.

Fig. 2 shows the tubulin tryptic peptides that are targets for OP-labeling, before (panel A) and after treatment with OP (panels B–F). The peaks at 534.4, 597.4, 738.5 and 808.5 m/z in panel A are unlabeled peptides with the sequences YVPR, TGTyr, GSQQYR, and EEYPDR. After treatment of tubulin with OP, new peaks appear whose masses correspond to some of the expected, theoretical masses for OP-labeled peptides (Table 1).

Unlabeled active site peptides were present in each digest, indicating that modification by OP was incomplete. The relative amount of labeled and unlabeled peptide was calculated from isotope cluster areas. The results are summarized in Table 2. FP-biotin, DFP, and CPO reacted with all four peptides, whereas sarin and soman reacted with only one peptide. Soman and sarin concentrations were signifi-

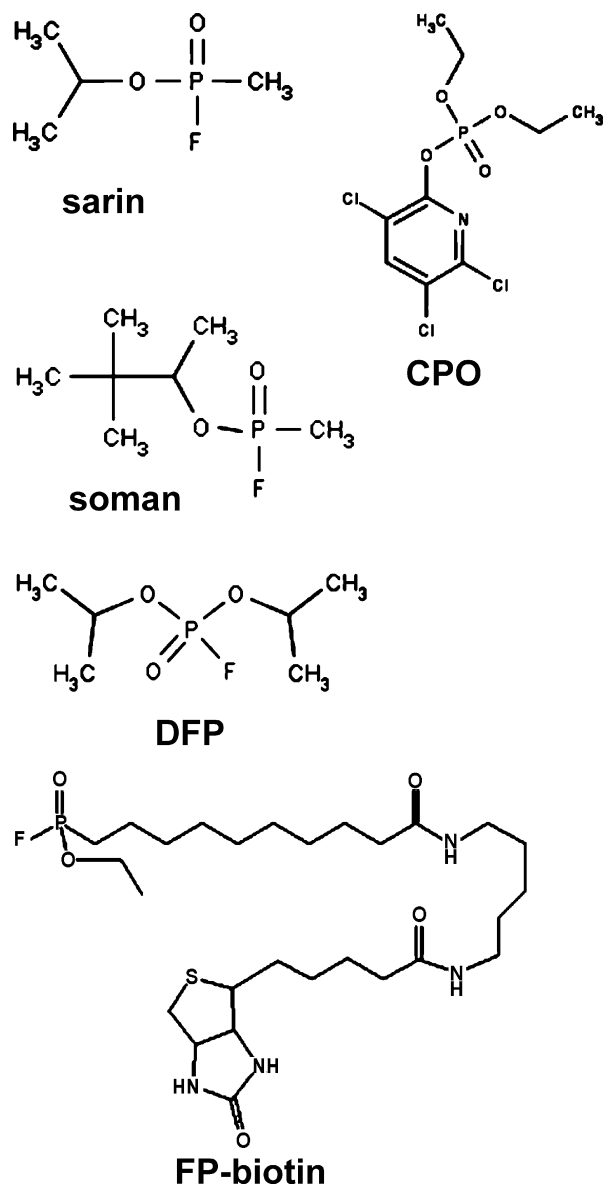


**Fig. 1.** OP structures.

**Table 2**

Percent of each peptide labeled by OP

Sequence	% labeled				
	Sarin	CPO	Soman	DFP	FP-biotin
TGTyr		43		7	70
YVPR		19	2	6	54
GSQQYR	54	23		13	66
EEYPDR		21		12	62

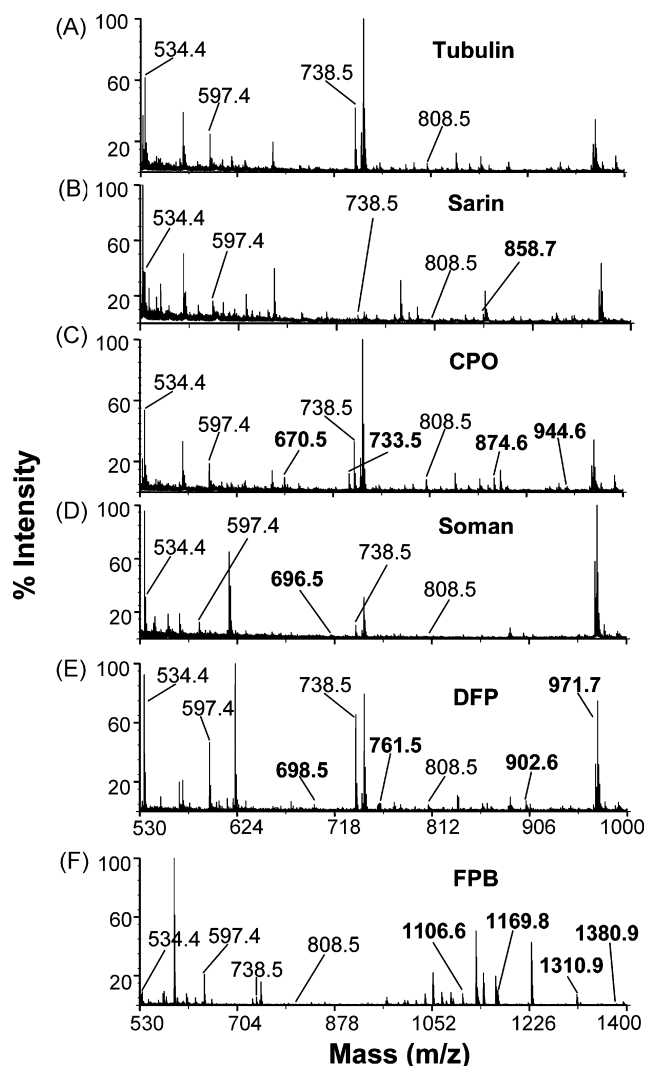


**Fig. 2.** Mass spectra of tryptic peptides of bovine tubulin, before and after labeling with OP. Peptides from (A) control bovine tubulin, (B) sarin treated tubulin, (C) CPO treated tubulin, (E) DFP treated tubulin, (D) soman treated tubulin, (F) FP-biotin treated tubulin. OP-labeled peptide masses are in bold. One peptide was labeled with sarin and soman; four peptides were labeled with CPO, DFP, and FP-biotin.

cantly lower than the concentrations of the other OP during the labeling reaction, which might explain why fewer peptides were labeled.

### 3.3. Tyrosine covalently modified by OP

Collision induced fragmentation in the Q-Trap mass spectrometer conclusively identified the amino acid sequence of each labeled peptide and the residue covalently modified by OP. The MS/MS spectra in Figs. 3–6 show the

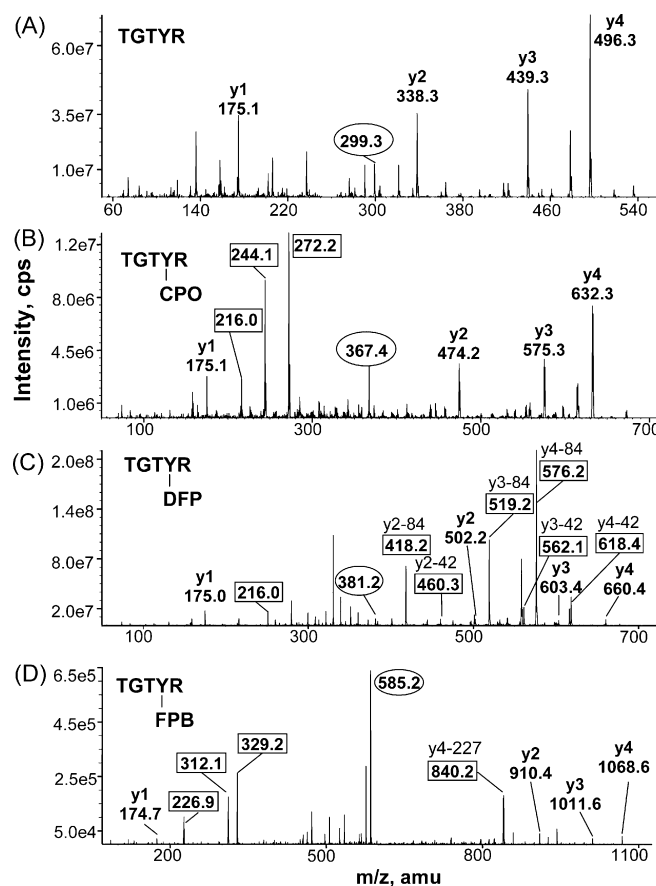


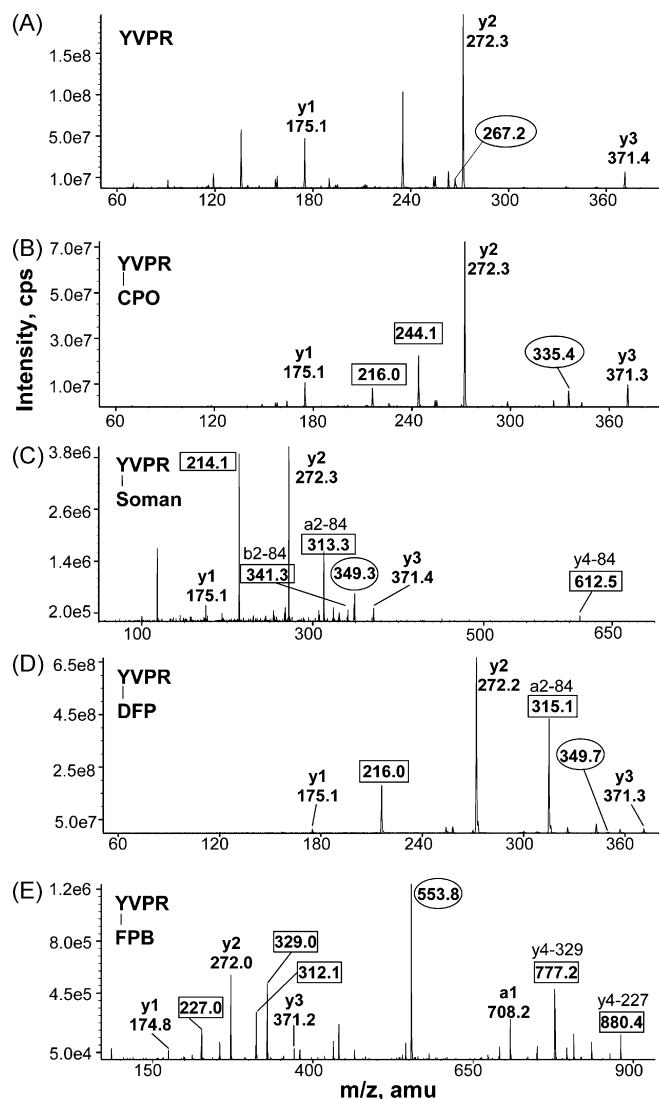
**Fig. 3.** MS/MS spectra of the TGTyr peptide of alpha tubulin. (A) Singly charged y ions derived from the doubly-charged, unlabeled parent ion at 299.3 m/z are shown. (B) CPO-labeled TGTyr has a doubly charged parent ion of 367.4 m/z. The y ion masses are consistent with diethylphosphate attached to tyrosine. The mass at 244 m/z is phosphotyrosine, the mass at 216 m/z is the immonium ion of phosphotyrosine, and the mass at 272 m/z is monoethylphosphotyrosine. (C) DFP-labeled TGTyr has a doubly charged parent ion of 381.2 m/z. The y ion masses are consistent with diisopropylphosphate attached to tyrosine. Masses enclosed in boxes are y ions that have lost one (42 amu) or both (84 amu) isopropyl groups. The ion at 216 m/z is the immonium ion of phosphotyrosine. (D) FP-biotin labeled TGTyr has a doubly charged parent ion of 585.2 m/z. The y ion masses are consistent with FP-biotin attached to tyrosine. The ions at 227, 312, and 329 m/z are fragments of FP-biotin. The ion at 840.2 m/z is the y4 ion that has lost 227 amu from FP-biotin.

y ions of each unlabeled peptide (panel A), and the same peptide after covalent modification by sarin, CPO, soman, DFP, and FP-biotin (panels B–F). The masses exactly fit the indicated sequence and fit the interpretation that the OP is attached to tyrosine (Table 3).

Ions at 214, 216, 244, and 272 m/z provide additional evidence that the OP bind to tyrosine (see the figure legends for details).

**Table 3**  
OP-labeled tyrosines in bovine tubulin

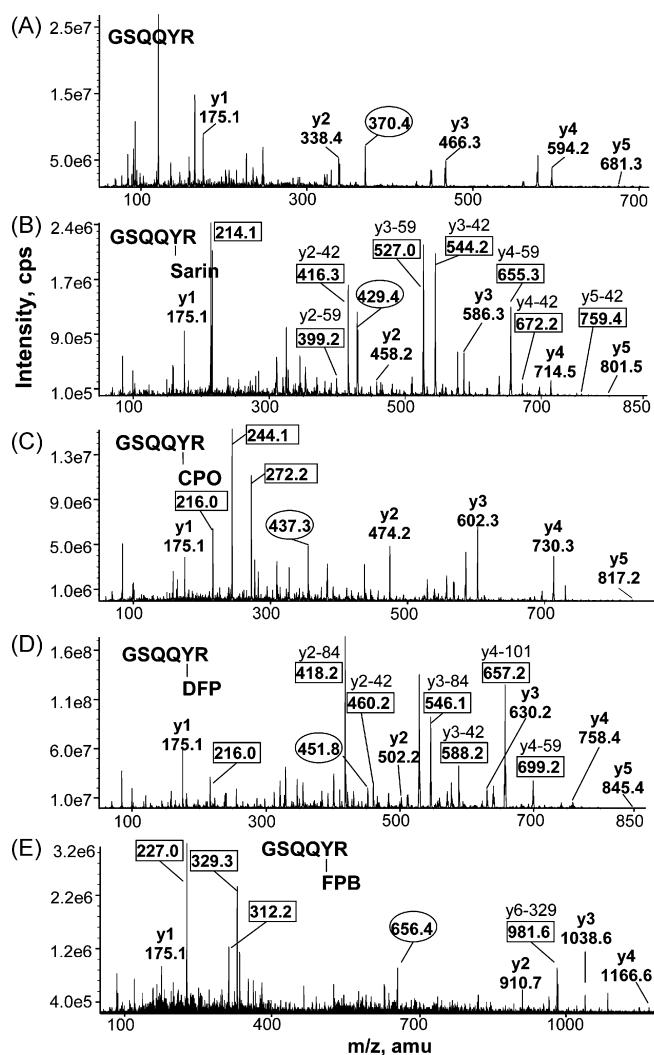
Tubulin chain	Sequence	OP-labeled tyrosine	Location in crystal structure
Alpha	TGTyr	Tyr 83	Loop between H2 and S3
Beta	YVPR	Tyr 59	Part of the loop between H1–S2; makes lateral contact between protofilaments [10]
Beta	GSQQYR	Tyr 281	Part of the M loop between S7 and H9; makes lateral contact between protofilaments [10]
Beta	EEYPDR	Tyr 159	At the C-terminus of helix H4: residues 157–176 bind ribose of GTP [11]



**Fig. 4.** MS/MS spectra of the YVPR peptide of beta tubulin. (A) Singly charged y ions derived from the doubly charged, unlabeled parent ion at 267.2 m/z are shown. (B) CPO-labeled YVPR has a doubly charged parent ion of 335.4 m/z. The y ion masses are consistent with diethylphosphate attached to tyrosine. The 216 m/z ion is the immonium ion of phosphotyrosine. The 244.1 m/z ion is phosphotyrosine. (C) Soman labeled YVPR had a doubly charged parent ion at 214 m/z. The 214 m/z ion is the immonium ion of methylphosphotyrosine. Loss of the pinacolyl group of soman reduces the mass of the singly charged parent ion by 84 amu to yield the 612 m/z ion. Loss of the pinacolyl group also yields the b2 ion at 341 m/z, and the a2 ion at 313.3 m/z. (D) DFP-labeled YVPR has a doubly charged parent ion at 349.7 m/z. The a2 ion has lost both isopropyl groups (84 amu) to yield 315.1 m/z. (E) FP-biotin labeled YVPR has a doubly charged parent ion at 553.8 m/z. Ions at 227, 312, and 329 m/z are fragments of FP-biotin. The ions at 777.2 and 880.4 m/z are the parent ion that has lost 329 or 227 amu from FP-biotin, respectively.

### 3.4. Fragmentation patterns characteristic of a particular OP

The data from Figs. 3–6 reveal CID fragmentation patterns that are characteristic of particular OP. For example, DFP-peptides readily release one or both isopropyl to yield y ions missing either 42 or 84 amu. CPO-labeled peptides yield intense peaks at 216, 244 and 272 m/z that are consistent with phosphotyrosine immonium ion, phosphotyrosine and monoethylphosphotyrosine, respectively.



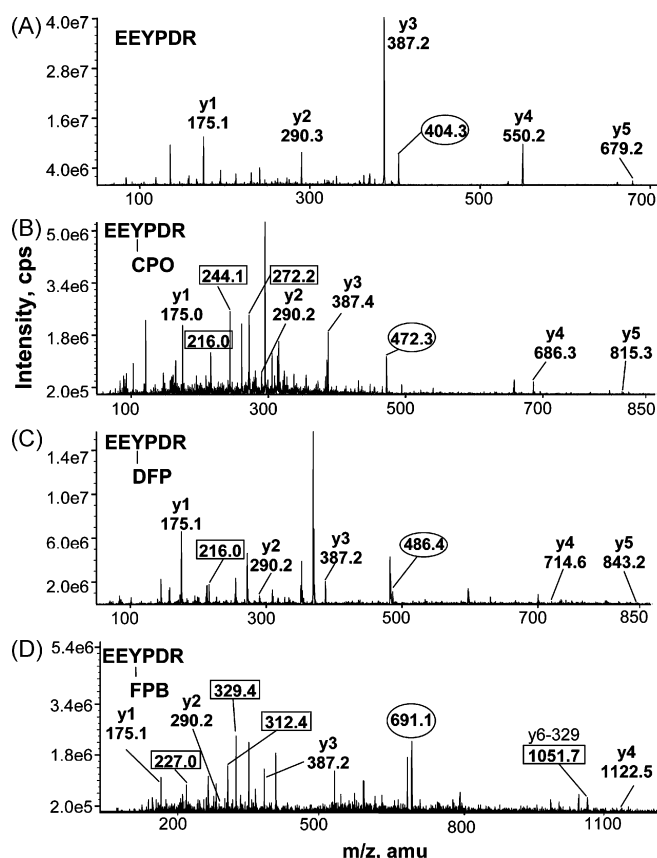


**Fig. 6.** MS/MS spectra of the EEYPDR peptide of beta tubulin. (A) Singly charged y ions derived from the doubly charged, unlabeled parent at 404.3 m/z are shown. (B) CPO-EEYPDR has a doubly charged parent ion at 472.3 m/z. The immonium phosphotyrosine ion is at 216 m/z. Phosphotyrosine is at 244 m/z and monoethylphosphotyrosine is at 272 m/z. (C) DFP-EEYPDR has a doubly charged parent ion at 486.4 m/z and an immonium phosphotyrosine ion at 216 m/z. (D) FP-biotin EEYPDR has a doubly charged parent ion at 691.1 m/z. Fragment ions of FP-biotin are present at 227, 312, and 329 m/z. The singly charged parent ion that has lost 329 amu from FP-biotin is at 1051.7 m/z.

In no case was the entire OP released from tyrosine. The phosphate group remained bound to tyrosine during CID fragmentation. This contrasts with OP bound to serine where the fragmentation process releases the entire bound OP, leaving no trace of the OP behind, and yielding dehydroAlanine in place of the OP-labeled serine [12].

### 3.5. No aging

When soman, sarin, or DFP are bound to acetylcholinesterase or butyrylcholinesterase they rapidly lose an alkyl group in a process called aging [13–15]. An aged soman labeled peptide would have an added mass of 78 amu rather than 162; an aged sarin labeled peptide would have an added mass of 78 amu rather than 120; an aged DFP labeled peptide would have an added mass of 122 amu rather than 164 in the MS spectrum. No evidence of aging was found in OP labeled tubulin peptides as no masses representing aged OP-peptides were found in MS scans. We conclude that tubulin OP adducts on tyrosine do not age.

## 4. Discussion

### 4.1. Tyrosine as a motif for OP labeling

The literature overwhelmingly supports the fact that OP bind covalently to an active site serine within the consensus sequence GXSG. Enzymes are defined as serine hydrolases when their activity is inhibited by OP. On the other hand, covalent binding of OP to tyrosine has previously been reported only for albumin [16–19], papain [20] and bromelain [21]. Our previous mass spectrometry work identified the OP binding site in human albumin as Tyr 411, and in bovine albumin as Tyr 410 [9,16]. The present report of OP binding to tyrosine in alpha and beta tubulin is novel. No covalent attachment site for OP binding to tubulin has previously been reported.

No obvious consensus binding site can be deduced from the four peptides reported here, though each target peptide contains a positively charged arginine within three residues of the labeled tyrosine which may serve to reduce the  $pK_a$  of the tyrosine hydroxyl group, and thereby activate it.

### 4.2. Significance of OP-labeling of tubulin

The crystal structure of tubulin shows that each of the OP-labeled tyrosines is located in a region where protofilaments interact laterally, or bind GTP [10,11]. OP-binding to tubulin could therefore alter tubulin conformation or GTP binding. A change in tubulin conformation or GTP binding could explain the observation of Prendergast et al. that CPO inhibits tubulin polymerization [8]. When tubulin does not polymerize, microtubules do not form, and nutrient transportation from the nerve cell body to the nerve synapse is disrupted. It is concluded that OP bind covalently to tubulin, and that this binding could explain the axonal transport deficits and cognitive impairment previously associated with OP exposure [5,6].

## Acknowledgements

Supported by U.S. Army Medical Research and Materiel Command W81XWH-07-2-0034 (to OL), W81XWH-06-1-0102, Epplery Cancer Center grant P30CA36727, DGA grant 03co010-05/PEA 01 08 7 to (PM), NIH/NIEHS) 1 R01 ES012241-01A1 (to AT), and NIH ES016102 (to CMT).

## References

- [1] D.M. Maxwell, K.M. Brecht, I. Koplovitz, R.I. Sweeney, Acetylcholinesterase inhibition: does it explain the toxicity of organophosphorus compounds? *Arch. Toxicol.* 80 (2006) 756–760.
- [2] L. Roldan-Tapia, T. Parron, F. Sanchez-Santed, Neuropsychological effects of long-term exposure to organophosphate pesticides, *Neurotoxicol. Teratol.* 27 (2005) 259–266.
- [3] R. Stephens, A. Spurgeon, I.A. Calvert, J. Beach, L.S. Levy, H. Berry, J.M. Harrington, Neuropsychological effects of long-term exposure to organophosphates in sheep dip, *Lancet* 345 (1995) 1135–1139.
- [4] L. London, A.J. Flisher, C. Wesseling, D. Mergler, H. Kromhout, Suicide and exposure to organophosphate insecticides: cause or effect? *Am. J. Ind. Med.* 47 (2005) 308–321.
- [5] A.V. Terry Jr., D.A. Gearhart, W.D. Beck Jr., J.N. Truan, M.L. Middlemore, L.N. Williamson, M.G. Bartlett, M.A. Prendergast, D.W. Sickles, J.J. Buccafusco, Chronic, intermittent exposure to chlorpyrifos in rats: protracted effects on axonal transport, neurotrophin receptors,

- cholinergic markers, and information processing, *J. Pharmacol. Exp. Ther.* 322 (2007) 1117–1128.
- [6] A.V. Terry Jr., J.D. Stone, J.J. Buccafusco, D.W. Sickles, A. Sood, M.A. Prendergast, Repeated exposures to subthreshold doses of chlorpyrifos in rats: hippocampal damage, impaired axonal transport, and deficits in spatial learning, *J. Pharmacol. Exp. Ther.* 305 (2003) 375–384.
- [7] D.A. Gearhart, D.W. Sickles, J.J. Buccafusco, M.A. Prendergast, A.V. Terry Jr., Chlorpyrifos, chlorpyrifos-oxon, and diisopropylfluorophosphate inhibit kinesin-dependent microtubule motility, *Toxicol. Appl. Pharmacol.* 218 (2007) 20–29.
- [8] M.A. Prendergast, R.L. Self, K.J. Smith, L. Ghayoumi, M.M. Mullins, T.R. Butler, J.J. Buccafusco, D.A. Gearhart, A.V. Terry Jr., Microtubule-associated targets in chlorpyrifos oxon hippocampal neurotoxicity, *Neuroscience* 146 (2007) 330–339.
- [9] L.M. Schopfer, M.M. Champion, N. Tamblyn, C.M. Thompson, O. Lockridge, Characteristic mass spectral fragments of the organophosphorus agent FP-biotin and FP-biotinylated peptides from trypsin and bovine albumin (Tyr410), *Anal. Biochem.* 345 (2005) 122–132.
- [10] J. Lowe, H. Li, K.H. Downing, E. Nogales, Refined structure of alpha beta-tubulin at 3.5 Å resolution, *J. Mol. Biol.* 313 (2001) 1045–1057.
- [11] E. Nogales, S.G. Wolf, K.H. Downing, Structure of the alpha beta tubulin dimer by electron crystallography, *Nature* 391 (1998) 199–203.
- [12] A. Fidder, A.G. Hulst, D. Noort, R. de Ruiter, M.J. van der Schans, H.P. Benschop, J.P. Langenberg, Retrospective detection of exposure to organophosphorus anti-cholinesterases: mass spectrometric analysis of phosphorylated human butyrylcholinesterase, *Chem. Res. Toxicol.* 15 (2002) 582–590.
- [13] H.O. Michel, B.E. Hackley Jr., L. Berkowitz, G. List, E.B. Hackley, W. Gillilan, M. Pankau, Ageing and dealkylation of Soman (pinacolylmethylphosphonofluoridate)-inactivated eel cholinesterase, *Arch. Biochem. Biophys.* 121 (1967) 29–34.
- [14] C.B. Millard, G. Kryger, A. Ordentlich, H.M. Greenblatt, M. Harel, M.L. Raves, Y. Segall, D. Barak, A. Shafferman, I. Silman, J.L. Sussman, Crystal structures of aged phosphorylated acetylcholinesterase: nerve agent reaction products at the atomic level, *Biochemistry* 38 (1999) 7032–7039.
- [15] F. Nachon, O.A. Asojo, G.E. Borgstahl, P. Masson, O. Lockridge, Role of water in aging of human butyrylcholinesterase inhibited by echothiophate: the crystal structure suggests two alternative mechanisms of aging, *Biochemistry* 44 (2005) 1154–1162.
- [16] B. Li, L.M. Schopfer, S.H. Hinrichs, P. Masson, O. Lockridge, Matrix-assisted laser desorption/ionization time-of-flight mass spectrometry assay for organophosphorus toxicants bound to human albumin at Tyr411, *Anal. Biochem.* 361 (2007) 263–272.
- [17] G.E. Means, H.L. Wu, The reactive tyrosine residue of human serum albumin: characterization of its reaction with diisopropylfluorophosphate, *Arch. Biochem. Biophys.* 194 (1979) 526–530.
- [18] N.H. Williams, J.M. Harrison, R.W. Read, R.M. Black, Phosphorylated tyrosine in albumin as a biomarker of exposure to organophosphorus nerve agents, *Arch. Toxicol.* 81 (2007) 627–639.
- [19] B. Li, F. Nachon, M.-T. Froment, L. Verdier, J.-C. Debouzy, E. Gillon, B. Brasme, L. Schopfer, O. Lockridge, P. Masson, Binding and hydrolysis of soman by human serum albumin, *Chem. Res. Toxicol.* 21 (2008) 421–431.
- [20] I.M. Chaiken, E.L. Smith, Reaction of a specific tyrosine residue of papain with diisopropylfluorophosphate, *J. Biol. Chem.* 244 (1969) 4247–4250.
- [21] T. Murachi, T. Inagami, M. Yasui, Evidence for alkylphosphorylation of tyrosyl residues of stem bromelain by diisopropylphosphorofluoridate, *Biochemistry* 4 (1965) 2815–2825.

# Mice Treated with Chlorpyrifos or Chlorpyrifos Oxon Have Organophosphorylated Tubulin in the Brain and Disrupted Microtubule Structures, Suggesting a Role for Tubulin in Neurotoxicity Associated with Exposure to Organophosphorus Agents

Wei Jiang,\* Ellen G. Duysen,\* Heidi Hansen,\* Luda Shlyakhtenko,† Lawrence M. Schopfer,\* and Oksana Lockridge\*<sup>1</sup>

\*Eppley Institute, University of Nebraska Medical Center, Omaha, Nebraska 68198-5950; and †Department of Pharmaceutical Sciences, University of Nebraska Medical Center, Omaha, Nebraska 68198-6025

<sup>1</sup> To whom correspondence should be addressed. Fax: (402) 559-4651. E-mail: olockrid@unmc.edu.

Received November 30, 2009; accepted January 22, 2010

Exposure to organophosphorus (OP) agents can lead to learning and memory deficits. Disruption of axonal transport has been proposed as a possible explanation. Microtubules are an essential component of axonal transport. *In vitro* studies have demonstrated that OP agents react with tubulin and disrupt the structure of microtubules. Our goal was to determine whether *in vivo* exposure affects microtubule structure. One group of mice was treated daily for 14 days with a dose of chlorpyrifos that did not significantly inhibit acetylcholinesterase. Beta-tubulin from the brains of these mice was diethoxyphosphorylated on tyrosine 281 in peptide GSQQY<sub>281</sub>RALTVP<sub>ELTQ</sub>MFDSK. A second group of mice was treated with a single sublethal dose of chlorpyrifos oxon (CPO). Microtubules and cosedimenting proteins from the brains of these mice were visualized by atomic force microscopy nanoimaging and by Coomassie blue staining of polyacrylamide gel electrophoresis bands. Proteins in gel slices were identified by mass spectrometry. Nanoimaging showed that microtubules from control mice were decorated with many proteins, whereas microtubules from CPO-treated mice had fewer associated proteins, a result confirmed by mass spectrometry of proteins extracted from gel slices. The dimensions of microtubules from CPO-treated mice (height  $8.7 \pm 3.1$  nm and width  $36.5 \pm 15.5$  nm) were about 60% of those from control mice (height  $13.6 \pm 3.6$  nm and width  $64.8 \pm 15.9$  nm). A third group of mice was treated with six sublethal doses of CPO over 50.15 h. Mass spectrometry identified diethoxyphosphorylated serine 338 in peptide NS<sub>338</sub>NFVEWIPNNVK of beta-tubulin. In conclusion, microtubules from mice exposed to chlorpyrifos or to CPO have covalently modified amino acids and abnormal structure, suggesting disruption of microtubule function. Covalent binding of CPO to tubulin and to tubulin-associated proteins is a potential mechanism of neurotoxicity.

**Key Words:** chlorpyrifos; tubulin; mass spectrometry; nanoimaging; neurotoxicity.

for treatment of Schistosomiasis. The acute toxicity that occurs with high doses of OP is due to inhibition of acetylcholinesterase (AChE). Some people who survive acute exposure describe neurological symptoms that last long after the acute symptoms have abated. The sarin attack in the Tokyo subway occurred in 1995, but 5 years later, some victims of this attack still suffered from blurred vision, easy fatigability, difficulty in concentration, and insomnia (Kawada *et al.*, 2005; Yanagisawa *et al.*, 2006). Magnetic resonance imaging revealed structural changes in the brains of exposed subjects (Yamasue *et al.*, 2007). These long-lasting symptoms could be the consequence of seizure activity and anoxia initiated by acute inhibition of AChE (McDonough and Shih, 1997).

Low doses of OP that do not inhibit AChE have also been associated with neurological dysfunction, including clinically significant extrapyramidal symptoms, anxiety, depression (Salvi *et al.*, 2003), memory loss, and learning disability (Srivastava *et al.*, 2000). The mechanism of low-dose toxicity is not understood. One hypothesis to explain long-lasting neurotoxicity from low doses of OP involves OP modification of proteins in the axonal transport system (Gearhart *et al.*, 2007; Gupta *et al.*, 1997; Prendergast *et al.*, 2007; Terry *et al.*, 2007). The transport system moves organelles from the cell nucleus to the axon termini and back to the nucleus. Hundreds of proteins are present in the axoplasm of neurons (Rishal *et al.*, 2010), suggesting the involvement of a great many proteins in this transport process.

Indirect evidence supports the hypothesis that organophosphorylation of key proteins in the axonal transport system disrupts the transport mechanism in neurons (Gearhart *et al.*, 2007; Terry *et al.*, 2007). Such a disruption could result in loss of synaptic contacts, slow dying back of axon structures, and finally in neuron cell death as has been described by Morfini *et al.* (2009) to explain neurodegenerative diseases, including Parkinson's, Alzheimer's disease, and amyotrophic lateral sclerosis.

Organophosphorus (OP) agents are used as pesticides, in jet engine oil as a flame retardant, as chemical warfare agents, and

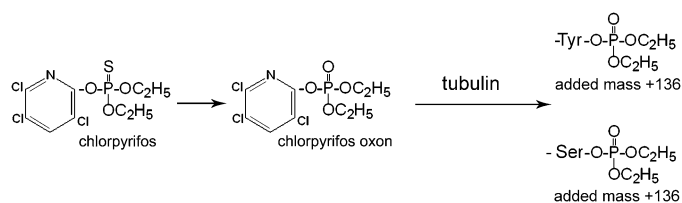


**FIG. 1.** Chlorpyrifos is bioactivated to CPO by cytochrome P450. Results presented below show that the oxon reacts with tubulin by donating its diethoxyphosphate group to tyrosine 281 and to serine 338 of beta-tubulin in mouse brain. Each diethoxyphosphate group adds a mass of 136 amu to tubulin. The 3,5,6-trichloro-2-(O)-pyridine group is released from CPO and excreted.

Rats treated chronically with low doses of chlorpyrifos have decreased rates of axonal transport measured in sciatic nerves *ex vivo*, implicating OP modification of tubulin, kinesin, and microtubule-associated proteins in this dysfunction (Gearhart *et al.*, 2007; Terry *et al.*, 2007). The present report focuses on tubulin in brain because *in vitro* experiments have shown that OP modification of tubulin disrupts polymerization of tubulin into microtubules (Grigoryan and Lockridge, 2009; Prendergast *et al.*, 2007). Disruption of tubulin polymerization has been shown to result in neuron dysfunction, cellular apoptosis, and tissue damage (Conde and Caceres, 2009; Tierno *et al.*, 2009).

Mass spectrometry analysis of a variety of proteins treated with OP *in vitro* identified covalent binding of OP to tyrosine and lysine residues (Grigoryan *et al.*, 2008, 2009a,b,c). The results suggest that almost any protein can be modified by OP. Previously, OP adducts were thought to form only with the active site serine of enzymes in the serine hydrolase superfamily. *In vivo* studies have identified OP-tyrosine adducts in the blood of guinea pigs treated with nerve agents and have shown that the adducts are detectable 24 days after exposure at a time when OP-serine adducts of butyrylcholinesterase (BChE) are no longer detectable (Read *et al.*, 2010).

In the present report, we treated mice with the pesticide chlorpyrifos as well as with its active metabolite, chlorpyrifos oxon (CPO). The pesticide chlorpyrifos is relatively harmless to man and rodents because it is rapidly detoxified and excreted. However, a portion of the chlorpyrifos is bioactivated through oxidative desulfuration catalyzed by cytochrome P450 enzymes to form CPO, the toxic agent that inhibits AChE (Sams *et al.*, 2004; Tang *et al.*, 2001) (see Fig. 1).

Our goal was to identify alterations in microtubule structure following *in vivo* treatment of mice with chronic low doses of chlorpyrifos and with sublethal doses of CPO. This is the first report to identify structural deficits in microtubules of animals treated *in vivo* with OP and furthermore to provide mass spectrometry evidence for OP labeling of tubulin in mice treated *in vivo* with chlorpyrifos or CPO.

## MATERIALS AND METHODS

**Materials.** Chlorpyrifos and CPO (PS-674 and MET-674B; ChemService Inc., West Chester, PA) were stored at  $-80^{\circ}\text{C}$ . Guanosine 5'-triphosphate

(GTP) sodium salt hydrate (G8877)  $\geq 95\%$  HPLC pure powder and 1,4-piperazinediethanesulfonic acid (PIPES, P6757)  $> 99\%$  pure powder were from Sigma (St Louis, MO). Sequencing grade-modified trypsin (V5113) was from Promega (Madison, WI). Alpha-cyano-4-hydroxycinnamic acid was from Applied Biosystems (MDS Sciex; Foster City, CA). All other chemicals were of analytical grade.

**Animal.** All animal work was conducted in accordance with the Guide for the Care and Use of Laboratory Animals as adopted by the National Institutes of Health. Formal approval to conduct the experiments was obtained from the Institutional Animal Care and Use Committee of the University of Nebraska Medical Center. Adult wild-type mice of strain 129Sv were used in all trials. Mice were bred at the University of Nebraska Medical Center.

Adult female mice treated for 14 days with a low dose of chlorpyrifos ( $n = 4$ ) ( $85.6 \pm 11.2$  days of age) weighed an average of  $19.8 \pm 3.2$  g, while female control mice ( $n = 4$ ) ( $90.1 \pm 5.8$  days of age) weighed an average of  $18.2 \pm 1.4$  g. Adult male mice treated with a single sublethal dose of CPO ( $n = 3$ ) (72 days of age) weighed an average of  $24.6 \pm 1.4$  g, and control male mice ( $n = 3$ ) (72 days of age) weighed an average of  $23.8 \pm 1.9$  g. Two female mice were treated with six sublethal doses of CPO over a period of 50.15 h (127 days of age, 23.0 g), and two control female mice (127 days of age, 22.6 g) were treated at the same time points with an equivalent volume of ethanol.

**Chronic low-dose treatment of mice ( $n = 4$ ) with chlorpyrifos.** Female mice ( $n = 4$ ) were injected sc with 3 mg/kg chlorpyrifos dissolved in 3% dimethyl sulfoxide/97% corn oil. Each mouse was treated for 14 consecutive days between 10 and 11 A.M. Surface body temperature, body weight, and observations were made every 5 min through 15 min and at 30-min postdosing. The axial body temperature was measured with a digital thermometer, Thermalert model TH-5, and a surface Microprobe MT-D, Type T thermocouple (Physitemp Instruments Inc., Clifton, NJ). Blood was collected (50  $\mu\text{l}$ ) via the saphenous vein prior to dosing each day. On day 15, 24 h after the final dose, the mice were decapitated, plasma was collected, and the brains placed on ice. Brains were weighed and processed according to the tubulin purification protocol. The tubulin was examined for OP modifications.

**Single-dose treatment of mice ( $n = 3$ ) with chlorpyrifos.** In three separate experiments, a mouse was injected ip with CPO dissolved in ethanol at a dose of 3.0 mg/kg delivered in 50  $\mu\text{l}$ . A control mouse was injected with ethanol only. Animals were observed for signs of toxicity following injection. About 30-min postinjection, the mice were euthanized and perfused with 50 ml of 0.1M PBS to remove blood from tissues. Tubulin from the brains of these animals was purified and used for nanoimaging and SDS gel electrophoresis. Proteins in the SDS bands were analyzed mass spectrally.

**Treatment of mice ( $n = 2$ ) with six doses of CPO.** To derive samples for mass spectral analysis of CPO-labeled tubulin, mice ( $n = 2$ ) were injected ip with CPO dissolved in ethanol at a dose of 2.5 mg/kg delivered in 50  $\mu\text{l}$ . Control mice ( $n = 2$ ) were injected with ethanol only. Each mouse received six injections at 0, 1, 22, 48, 50, and 50.15 h. Animals were observed for signs of toxicity after each injection. Mice were euthanized 5 min after the last dose by inhalation of carbon dioxide and then perfused via intracardial injection with 50 ml 0.1M PBS solution to remove blood from the tissues. Tubulin from the brains of these animals was examined for OP modifications.

**Enzyme activity assays.** AChE and BChE activities in mouse plasma and brain were measured with 1mM acetylthiocholine and 1mM butyrylthiocholine, respectively, as described (Peebles *et al.*, 2005). Carboxylesterase activity in mouse plasma was assayed with 2.5mM *p*-nitrophenyl acetate after incubating 3  $\mu\text{l}$  plasma for 5 min in 0.1M potassium phosphate (pH 7.0) containing 12.5mM EDTA, to inhibit paraoxonase, and 0.01mM eserine, to inhibit AChE and BChE. The reaction was started by adding 0.05 ml of 0.1M *p*-nitrophenyl acetate dissolved in methanol. The total reaction volume was 2.0 ml, and the temperature was  $25^{\circ}\text{C}$ . Absorbance increase at 400 nm was measured on a Gilford spectrophotometer and recorded on a computer interfaced to MacLab/200 (AD Instruments, Sydney, Australia). Activity in micromoles per minute was calculated from the extinction coefficient for *p*-nitrophenol of  $9000\text{M}^{-1}\text{cm}^{-1}$ .

**Tubulin purification and polymerization.** Tubulin from mouse brains was purified by two cycles of polymerization using the protocol of Shelanski *et al.* (1973). Brains from mice were collected and placed on ice. The brains were homogenized in four volumes of ice-cold PM buffer (80mM PIPES, 2mM magnesium chloride, and 0.5mM ethylene glycol tetraacetic acid (EGTA), pH 7.0) and centrifuged at  $17,000 \times g$  for 60 min at 4°C. The pellet was discarded, and the clear supernatant was transferred to a clean ultracentrifuge tube. The supernatant, in which no microtubules were present, was mixed with an equal volume of 8M glycerol containing 1.0mM GTP. The samples were incubated for 2 h at 37°C to assemble the microtubules. The solution was centrifuged for 60 min at  $100,000 \times g$  at 29°C to pellet the microtubules and remove the polymerization inducers glycerol and GTP. The pellet was suspended in 500  $\mu$ l PM buffer, depolymerized on ice for 30 min, and centrifuged for 1 h at 4°C to remove particulates. Tubulin in the supernatant was mixed with an equal volume of 8M glycerol containing 1.0mM GTP and incubated for 45 min at 37°C to assemble the microtubules for a second time. The sample was centrifuged for 60 min at 29°C to pellet the microtubules. The pellet was resuspended in 1 ml of PM buffer and maintained at room temperature to preserve the microtubules. The protein concentration of the final microtubule pellet ranged from 3 to 7  $\mu$ g/ $\mu$ l (depending on the preparation) as measured by absorbance at 280 nm using the NanoDrop spectrophotometer ND-1000 (NanoDrop Technologies Inc.; Thermo Scientific, Waltham, MA). Absorbance at 280 nm was compared to protein concentration estimated from the Pierce bicinchoninic acid protein assay. Both methods gave similar results. Bovine albumin was used as the standard for both assays.

**Atomic force microscopy of microtubules.** Atomic force microscopy nanoimages were acquired in the Nanoimaging Core Facility at the University of Nebraska Medical Center, codirected by L.S. A portion of the microtubule pellet, prepared by two cycles of assembly, was fixed immediately by addition of glutaraldehyde to 0.25%. The fixed microtubules were stored at 4°C for 12 h before an aliquot was diluted 10-fold with double-distilled water to a protein concentration of 0.5  $\mu$ g/ $\mu$ l. Ten microliters of the suspension was drawn from the bottom of the tube and placed in the center of a mica chip that had been treated with 1-(3-aminopropyl) silatrane. The detailed procedure for mica surface modification is given in Shlyakhtenko *et al.* (2003) and Lyubchenko and Shlyakhtenko (2009). The silatrane modification allows the sample to be deposited in a wide range of ionic strengths and pH. After 2-min incubation in a humid chamber, the samples were rinsed with deionized water and dried with argon gas flow. Images were acquired using an MFP-3DAtomic Force Microscope (Asylum Research, Santa Barbara, CA) operated in tapping mode. Pictures were taken from 15 different  $5 \times 5 \mu$ m areas on average. Image processing and measurement of microtubule height and width were performed using Femtoscanner software (Advanced Technology Center, Moscow, Russia).

**Off-line HPLC purification of peptides for determination of labeled proteins by mass spectrometry.** A portion of the microtubule pellet was denatured in 8M urea, reduced with 10mM dithiothreitol, and carbamidomethylated with 50mM iodoacetamide. The sample was diluted to 2M urea and then digested with trypsin at a ratio of 50:1 (wt/wt) at 37°C for 16 h. The salt concentration was reduced by dilution rather than by dialysis because dialysis resulted in loss of up to 95% of the tubulin protein due to sticking to the dialysis membrane. Peptides were desalted and separated by reverse phase HPLC on a  $100 \times 4.60$  mm Phenomenex C18 column eluted with a gradient from 0 to 60% (vol/vol) acetonitrile versus 0.1% (vol/vol) trifluoroacetic acid at a flow rate of 1 ml/min for 60 min on a Waters 625 LC system. Fractions of 1 ml were collected, dried by vacuum centrifugation, and redissolved in 50  $\mu$ l of 5% acetonitrile and 0.1% formic acid. Fractions that eluted between 5 and 40 min were analyzed by liquid chromatography-tandem mass spectrometry (LC-MS/MS) electrospray ionization. The CPO-labeled peptide in Figure 4 was in fraction 38, and the CPO-labeled peptide in Figure 7 was in fraction 30. Details on the method for searching mass spectrometry data to identify labeled peptides are in the "Materials and Methods" section entitled Q-Trap 4000 and LTQ-Orbitrap mass spectrometry. In brief, the mass spectrometry data were compared to the National Center for Biotechnology Information (NCBI)

nonredundant database using Mascot software. Diethoxyphosphate was used as a variable modification for Ser, Thr, Tyr, and Lys. Each identified peptide was manually examined to verify that the tandem mass spectral fragmentation (MS/MS) spectrum supported the Mascot assignment.

**Polyacrylamide gel electrophoresis of proteins in the microtubule pellet, followed by in-gel digestion.** Two gradient polyacrylamide gels (4–30%) were cast in a Hoefer gel apparatus to make  $15 \times 11$ -cm gels, 0.75-mm thick, with a single well that spanned the entire gel. Microtubule pellets from control and CPO-treated mouse brains in 400  $\mu$ l PM buffer were denatured by addition of 80  $\mu$ l of 6  $\times$  SDS gel loading buffer containing 0.2M Tris/Cl (pH 6.8), 10% SDS, 30% glycerol, 0.6M dithiothreitol, and 0.012% bromophenol blue. The samples were boiled for 3 min, and each was loaded onto a gel. About 2 mg of protein were loaded onto each gel. Electrophoresis was for 3000 V/h at 4°C. Gels were stained with Coomassie blue. Protein bands from the upper 75% of each gel were cut into slices. Gel slices were destained, dried, treated with trypsin, and the peptides extracted as previously described (Peebles *et al.*, 2005). The dry samples were dissolved in 80  $\mu$ l of 5% acetonitrile and 0.1% formic acid and placed in autosampler vials for analysis in the Q-Trap 4000 (MDS Sciex; Applied Biosystems) and the LTQ-Orbitrap (Thermo Scientific) mass spectrometers.

**Q-Trap 4000 and LTQ-Orbitrap mass spectrometry.** Peptides purified by off-line HPLC or extracted from gel slices were analyzed by LC-MS/MS in the Q-Trap 4000 linear ion trap mass spectrometer using a nanospray source with a continuous flow head, at a flow rate of 0.3  $\mu$ l/min (Li *et al.*, 2009). The four most intense peptides in each cycle of analysis were fragmented by collision-induced dissociation using pure nitrogen at 40  $\mu$  Torr and a collision energy of 20–50 V. Collision voltage was determined by the Analyst software based on the size and charge state of the peptide. The data were searched against the NCBI nonredundant database using Mascot v 1.9 (Matrix Science Ltd, London, UK) for tryptic peptides with an added mass of 136 Da from CPO (Perkins *et al.*, 1999). The CPO added mass was put into the UNIMOD public database of protein modifications (<http://www.unimod.org>) for use with Mascot. Mascot search parameters included peptides with one missed tryptic cleavage, carbamidomethylated cysteine as a fixed modification; diethoxyphosphorylated serine, threonine, tyrosine, and lysine; and oxidized methionine as variable modifications, a peptide mass tolerance of 1.2 Da and a fragment mass tolerance of 0.6 Da. The MS/MS fragmentation spectra of peptides identified by Mascot were manually confirmed with the aid of the MS-Product algorithm from Protein Prospector (v 5.3.2 from the University of California Mass Spectrometry Facility). Peptides extracted from gel slices were also analyzed in the LTQ-Orbitrap mass spectrometer as described (Wiederin *et al.*, 2009).

**Statistical analysis of microtubule nanoimaging parameters.** A two-independent sample *t*-test was performed to determine the statistical significance of differences in the dimensions of the microtubules between the treated and control groups. The data were normally distributed. SPSS software 16.0 (Microsoft Corp., Redmond, WA) was used for statistical analysis.

## RESULTS

### *Mice Treated Chronically with Low Doses of Chlorpyrifos*

**Nontoxic dose of chlorpyrifos.** Mice injected daily for 14 consecutive days with a nontoxic dose of chlorpyrifos (not the oxon), 3 mg/kg sc, showed no signs of toxicity with the exception of hunched posture, which persisted for less than 15 min after treatment. Their body temperature and body weight remained normal (see Fig. 2).

Plasma AChE activity dropped from 0.3 to 0.2 U/ml after the first two doses of chlorpyrifos but rebounded to 0.45 U/ml after 9–14 days of treatment (see Fig. 3A). In contrast, plasma BChE

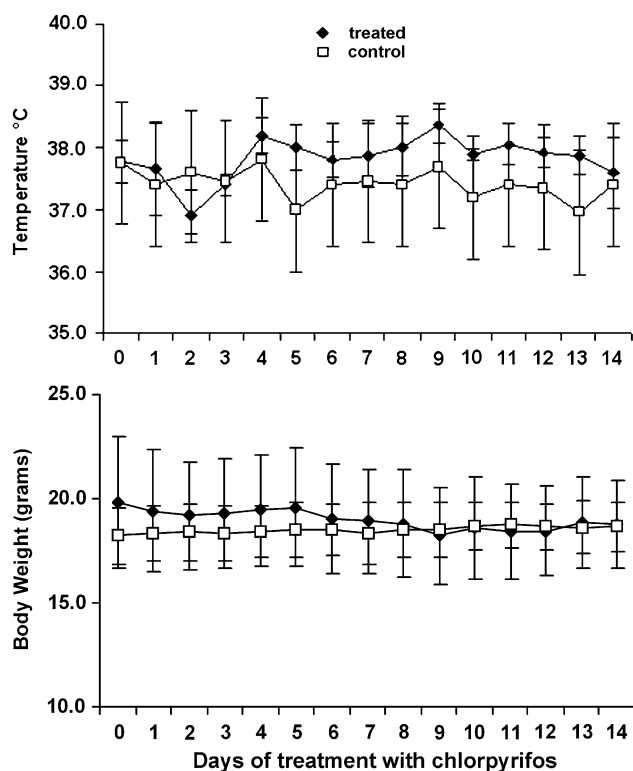


**FIG. 2.** Surface body temperature and body weight of mice treated daily for 14 days sc with 3 mg/kg chlorpyrifos (not the oxon). Values for control mice ( $n = 4$ ) treated with vehicle were indistinguishable from values for treated mice ( $n = 4$ ). Day 0 values are the temperature and body weight before treatment. Errors bars are SD.

activity steadily declined following each injection of chlorpyrifos (Fig. 3B). This result is consistent with the greater sensitivity of BChE to inhibition by CPO compared to that of AChE (Amitai *et al.*, 1998). Plasma carboxylesterase activity was unaffected (Fig. 3C). Since inhibition of BChE has no health consequences and since AChE activity was not inhibited by the 14th day of treatment, it is concluded that the dosing regimen was nontoxic.

**Mass spectrometry identifies CPO-modified tubulin.** Tubulin purified from the brains of mice treated with a daily low dose of chlorpyrifos was digested with trypsin and analyzed by LC-MSMS. The mass spectrometry data were searched for diethoxyphosphorylated peptides with an added mass of 136 amu on tyrosine, serine, threonine, or lysine. One modified peptide was found. Figure 4 shows the MSMS spectrum for peptide GSQQY<sub>281</sub>RALTVP<sub>ELT</sub>QQMFDSK from mouse beta-tubulin, covalently modified on tyrosine 281 by diethoxyphosphate. The triply charged parent ion has a mass-to-charge ratio of 854.8, which is consistent with the peptide sequence plus 136 amu from the diethoxyphosphate. The y5 to y11 ions and the internal fragments support the sequence. Internal fragments are at 157.0 (AL minus 28), 268.1 (ALT minus water), 286.2 (LTV minus 28), 367.1 (ALTV minus water),

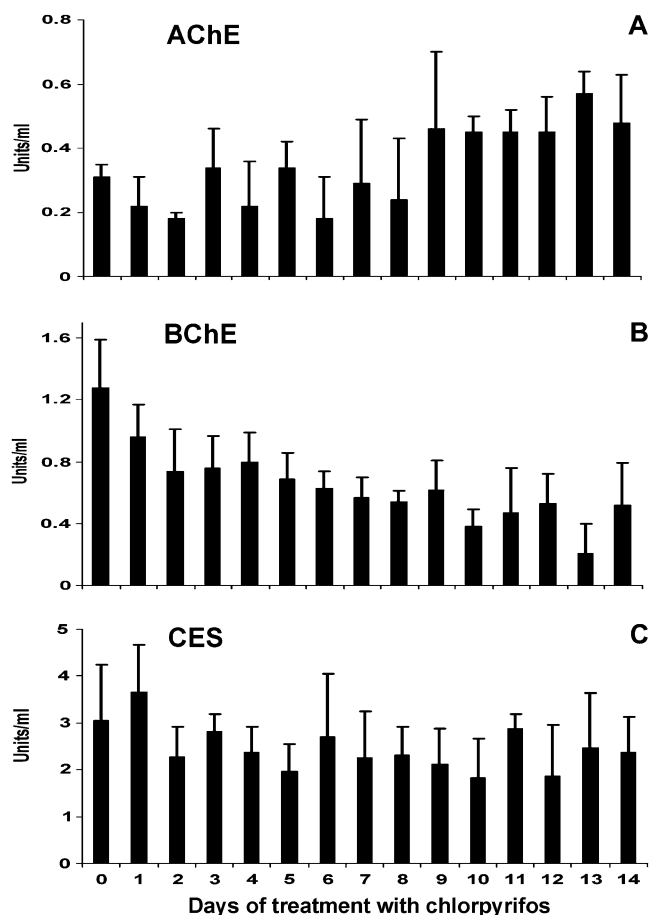


**FIG. 3.** Plasma esterase activity in mice ( $n = 4$ ) treated daily for 14 days with chlorpyrifos, 3 mg/kg sc. (A) Plasma AChE activity. (B) Plasma BChE activity. (C) Plasma carboxylesterase (CES) activity. Day 0 values are the activities before treatment was begun. Units of activity are micromoles substrate hydrolyzed per minute per microliter plasma. Error bars are SD for four mice.

423.0 (PELT minus water), 569.2 (PELTQ), 653.2 (LTVPEL), 697.2 (PELTQQ), 737.2 (QQMFDS), and 920.3 amu (YRALTVP diethoxyphosphorylated on Y).

Support for modification of tyrosine comes from the internal fragment at 920.3 amu, which corresponds to the sequence Y\*RALTVP where Y has an added mass of 136 amu. The threonine in peptide YRALTVP can be ruled out as the site of diethoxyphosphorylation because internal fragments that include this threonine (ALT minus water, LTV minus 28, ALTV minus water, and LTVPEL) do not have an added mass of 136 amu. The second threonine in peptide GSQQY<sub>281</sub>RALTVP<sub>ELT</sub>QQMFDSK can be ruled out because internal fragments that include this threonine (PELT minus water, PELTQ, and PELTQQ) do not have an added mass of 136 amu. The serine near the C-terminus can be ruled out based on the mass of the internal fragment QQMFDS. The serine near the N-terminal can be ruled out based on the mass of the doubly charged b4 ion. Precedent for the reactivity of this tyrosine in tubulin

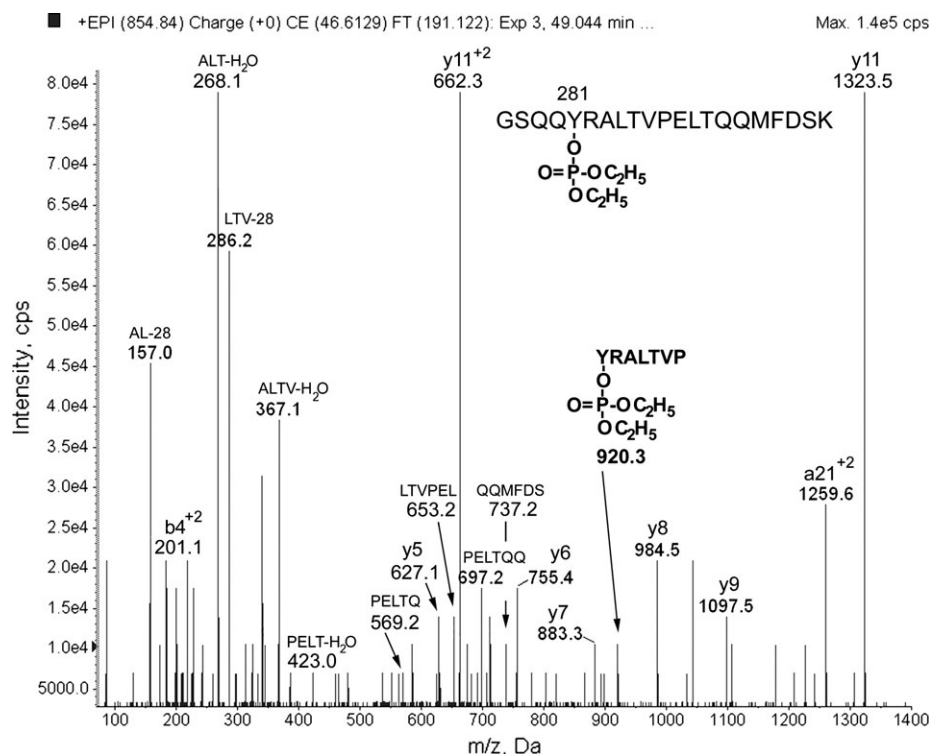


**FIG. 4.** Mouse beta-tubulin from brain, covalently modified after *in vivo* treatment with 14 daily low doses of chlorpyrifos that did not significantly inhibit AChE activity. The triply charged parent ion has a mass-to-charge ratio ( $m/z$ ) of 854.8. The masses of the  $y$  ions and the internal cleavage ions are consistent with the sequence GSQQY<sub>281</sub>RALTVP ELTQQMFDSK (accession number gi 21746161) where the diethoxyphosphorylated residue is tyrosine 281. The presence of the internal cleavage ion at 920.3 amu is direct evidence that the modification is on tyrosine.

comes from *in vitro* experiments where the homologous tyrosine in bovine beta-tubulin, GSQQY<sub>281</sub>R, was covalently labeled by CPO (Grigoryan *et al.*, 2009c).

#### Mice Treated with a Single Dose of CPO

**Signs of toxicity.** Mice treated ip with one dose of 3.0 mg/kg CPO and euthanized 30-min postdosing had toxic signs, including decreased body temperature (average reduction  $2.1^{\circ}\text{C} \pm 0.5$ ), reduced activity, piloerection, and hunched posture. BChE and AChE activities in the plasma were inhibited 70 and 62%, respectively. Tubulin from the brains of these mice was purified and polymerized to microtubules. The proteins in an aliquot of these microtubules were separated by SDS gel electrophoreses and identified by mass spectrometry. Another aliquot of the microtubule preparation was used for nanoimaging.

**CPO-treated mice have decreased levels of proteins that cosediment with microtubules.** Figure 5 shows the SDS gels stained with Coomassie blue from which gel slices were analyzed by mass spectrometry. The banding pattern and staining intensities are similar for the control and treated samples. The original goal of this experiment was to identify proteins modified by CPO. In anticipation that several proteins would be modified by CPO, gel slices from the upper 75% of

the gels were prepared for mass spectrometry. The criterion for a positive result was finding the labeled peptide and finding an MSMS spectrum that supported the presence of diethoxyphosphate in the peptide. Labeled peptides are extremely difficult to find. The LC-MSMS analysis identified the proteins in the gel slices but did not identify any labeled peptides. However, the mass spectrometry analysis showed the surprising result that the set of proteins was not identical in the two gels. The microtubules from the CPO-treated mice were missing the six proteins listed at the bottom of Table 1. The missing proteins were well represented in the control microtubule sample but were undetectable in microtubules prepared from CPO-treated mice.

The Coomassie-stained bands in the gels in Figure 5 appeared identical, yet mass spectrometry analysis of the proteins in the gels revealed missing proteins in the microtubules from the CPO-treated mouse. This result can be explained by the fact that any gel slice contains multiple proteins. Coomassie blue staining reports the aggregate composition of the band, favoring the most abundant proteins, but mass spectrometry identifies the individual proteins in a gel band.

The mass spectrometry results in Table 1 are supported by the atomic force microscopy nanoimages in Figure 6. Microtubules prepared from control mouse brain in Figure 6A are

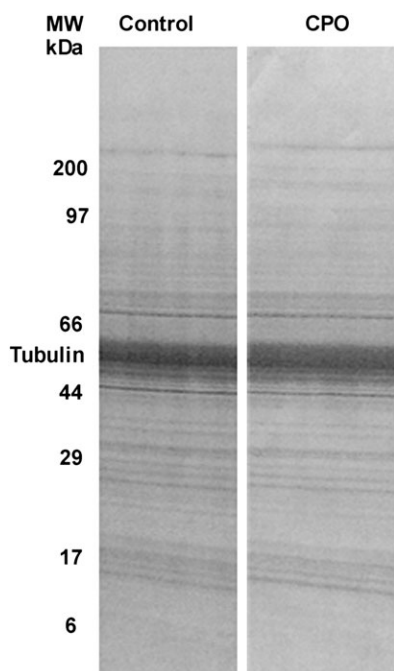


**FIG. 5.** Coomassie blue-stained SDS gels. Tubulin isolated from the brains of control and CPO-treated mice was polymerized to microtubules. The microtubule preparations were denatured and loaded on the gels. Each 15-cm wide gel was loaded with 2 mg of protein. A representative 1.5-cm portion of each gel is shown. The upper 75% of each gel was sliced horizontally. Proteins were extracted from the gel slices, digested with trypsin, and analyzed by mass spectrometry.

decorated with many proteins. In contrast, microtubules prepared from the CPO-treated mouse brain in Figure 6B have few attached proteins.

The microtubules from CPO-treated animals (in Fig. 6B) appeared to be thinner than those from untreated animals (in Fig. 6A). The difference was quantified by measuring the width and height of 100 microtubules at three to four positions along each tubule for a total of 700 measurements. Figure 6C shows that the average width was  $64.8 \pm 15.9$  nm for the control and  $36.5 \pm 15.5$  nm for the CPO-treated microtubules. The average height was  $13.6 \pm 3.6$  nm for the control and  $8.7 \pm 3.1$  nm for the CPO-treated microtubules.

The atomic force microscopy nanoimaging and the mass spectrometry experiments to identify proteins that cosediment with microtubules were conducted by two researchers, each finding similar results. It is unlikely that the missing proteins were removed during purification as both control and CPO-treated samples were handled identically, and the tubulin was not exposed during the purification process to the high-salt conditions, which remove microtubule-associated proteins (Friden and Wallin, 1991).

#### *Mice Treated with Six Sublethal Doses of CPO*

**Signs of toxicity.** Mice treated ip with six doses of 2.5 mg/kg CPO showed no toxic signs after injections at 0, 1, 22, 48, and

**TABLE 1**  
**Proteins Identified in Control and CPO-Treated Mouse Brain Microtubules**

Protein	Molecular weight (kDa)	Accession number	Control Mowse score	CPO Mowse score
Plectin 1 isoform 6	534	gi 41322931	78	110
Dynein, cytoplasmic, heavy chain 1	527	gi 148686723	1254	589
Titin	300	gi 123232572	112	68
Microtubule-associated protein 1A	300	gi 122065442	913	841
Microtubule-associated protein 1B	271	gi 6678946	1066	1573
Microtubule-associated protein 2	199	gi 126741	4982	4769
Microtubule-associated protein 4	121	gi 148677083	423	271
mKIAA0325 protein	230	gi 28972155	1424	790
Neurofilament protein	115	gi 200022	964	295
Mtap4 protein	114	gi 29747932	432	308
Stop protein	96	gi 2769587	324	383
Ulip2 protein	62	gi 1915913	362	148
Neurofilament L	61	gi 387492	504	499
Tubulin beta 3	50	gi 12963615	600	672
Tubulin beta 1	50	gi 124430500	89	160
Tubulin beta 5	50	gi 7106439	826	803
Tubulin beta 6	50	gi 27754056	686	467
Tubulin alpha isotype m-alpha 2	50	gi 202210	923	522
Tubulin alpha 1C	50	gi 6678469	920	672
Tubulin alpha 1B	50	gi 34740335	571	550
Tubulin alpha 1a	50	gi 6678465	909	403
Alpha-tubulin	50	gi 74182829	256	330
Tubulin alpha 8	50	gi 8394493	502	125
Microtubule-associated protein tau	76	gi 13432200	739	374
Beta-tubulin	42	gi 202229	412	440
Tubulin polymerization-promoting protein	24	gi 33469051	401	417
Cytoskeleton-associated protein 5	218	gi 123227410	915	0
Myosin Va	215	gi 148694358	2097	0
Heat-shock protein 84 kDa	84	gi 309317	123	0
Dynein, cytoplasmic, 1 light intermediate chain	57	gi 22122795	422	0
Alpha-internexin	56	gi 94730353	543	0
Microtubule-associated protein 2 isoform 1	53	gi 90186270	396	0

*Note.* Accession number is the identifying number in the NCBI nonredundant protein database. Mowse scores are assigned by Mascot software to indicate the probability that the assignment is correct. They are the sum of the scores for all of the peptides associated with a particular protein. A score of 69 or higher is considered to be a definitive assignment ( $p < 0.05$ ).

50 h. Following the injection at 50.15 h, CPO-treated mice had hunched posture, piloerection, decreased activity, ataxic gait, decrease in body temperature (average reduction  $4.2^\circ\text{C} \pm 1.8$ ), and lacrimation. Mice were euthanized 5 min after the 50.15-h

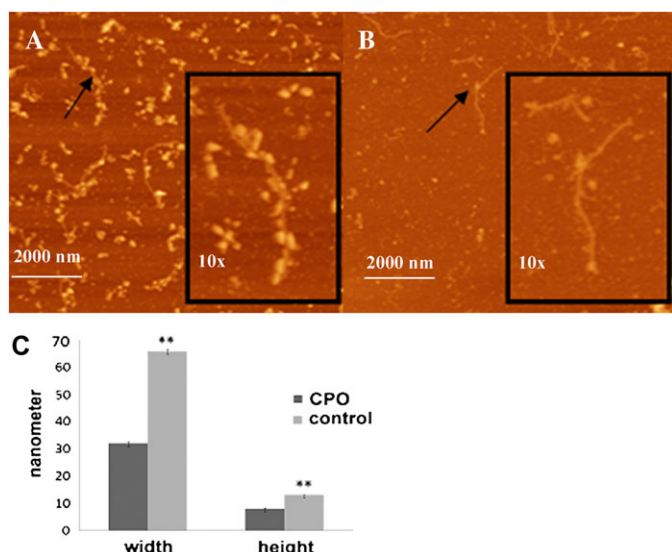


**FIG. 6.** Atomic force microscopy nanoimages of microtubules from purified mouse brain tubulin. (A) Microtubules from a control mouse. Microtubules are highly decorated with associated proteins. (B) Microtubules from a mouse treated ip with CPO (3 mg/kg). Microtubules show fewer associated proteins. Arrows indicate microtubules that are shown as magnified images in the box inserts. Mice were injected, and microtubules from both a control ( $n = 3$ ) and a CPO ( $n = 3$ )-treated animal were prepared and imaged on three different occasions by two different investigators. All three trials gave similar results. (C) Width and height comparison for microtubules from CPO-treated and control groups. \*\*Statistically significant difference ( $p = 0.001$ ).

dosing. BChE and AChE plasma activities were completely inhibited 5 min after the 50.15-h injection. At this same time point, BChE and AChE activities in the brain were inhibited

50 and 46%, respectively. Brains from these mice were the source of the tubulin that yielded the CPO-labeled peptide in Figure 7.

**Second tubulin peptide labeled by CPO** Collision-induced fragmentation identified a second tubulin peptide covalently modified by CPO. The MSMS fragmentation spectrum in Figure 7 shows peptide NS<sub>338</sub>NFVEWIPNNVK of beta-tubulin to be covalently modified on serine 338 by CPO. The masses of y and b ions exactly fit the indicated sequence. Internal fragments are at 430 (EWI), 538.3 (IPNNV), 584.3 (S<sub>338</sub>NFV with diethoxyphosphate on S), and 740 amu (VEWIPN). Support for labeling on serine comes from the internal fragment at 584.3 amu, which corresponds to the sequence S<sub>338</sub>NFV, where S has an added mass of 136 Da. In addition, the parent ion mass requires the presence of an extra 136 amu component, and there are no other nucleophilic residues in this peptide that could reasonably support reaction with CPO.

## DISCUSSION

### Tubulin Peptides Labeled by CPO in Living Mice

Living mice treated with a nontoxic dose of chlorpyrifos or a sublethal dose of CPO have CPO-labeled tubulin in their brains. The identification of two diethoxyphosphorylated tubulin residues (tyrosine 281 and serine 338) is direct evidence that CPO covalently reacts with tubulin in mouse brain.

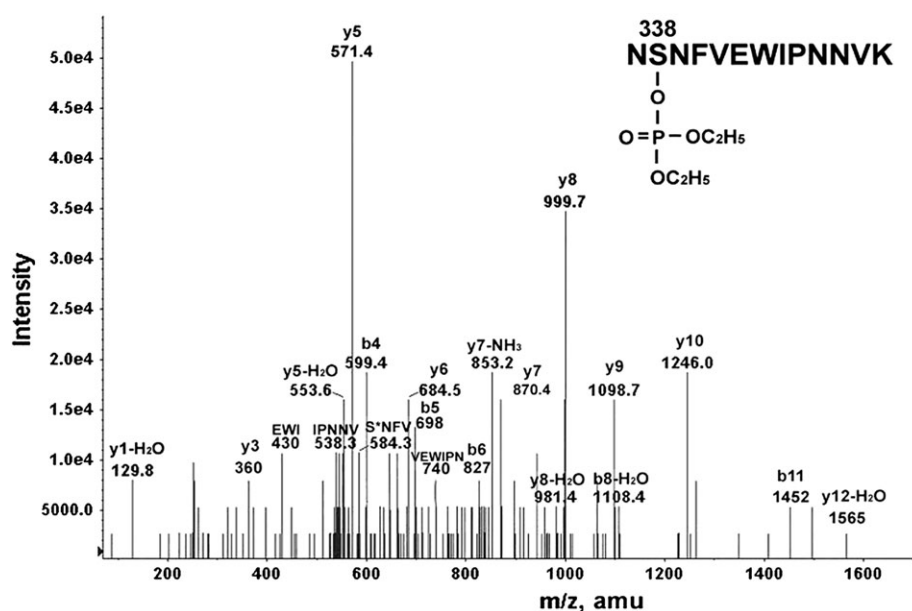


**FIG. 7.** MSMS fragmentation spectrum of the NS<sub>338</sub>NFVEWIPNNVK peptide labeled by CPO on serine 338 of mouse beta-tubulin (accession number gi 91855). The doubly charged parent ion has a mass-to-charge ratio ( $m/z$ ) of 849.0. The spectrum was acquired in the Q-Trap 4000 mass spectrometer. Mice had been treated with sublethal doses of CPO six times over a period of 50.15 h.

TABLE 2  
CPO-Labeled Beta-Tubulin Peptides

Species	Sequence	Accession number	Labeled amino acid	Reference
Mus musculus	GSQQY <sub>281</sub> RALTVPELTQQMFDSK	gi 21746161	Tyr 281	Present work
Bovine	GSQQY <sub>281</sub> RALTVPELTQQMFDAK	gi 75773583	Tyr 281	Grigoryan <i>et al.</i> (2009c)
Homo sapiens	GSQQY <sub>281</sub> RALTVPELTQQMFDSK	gi 4507729	Unknown	
Mus musculus	NS <sub>338</sub> NFVEWIPNNVK	gi 91855	Ser 338	Present work
Bovine	NSSY <sub>340</sub> FVEWIPNNVK	gi 75773583	Tyr 340	Grigoryan <i>et al.</i> (2009c)
Homo sapiens	NSSYFVEWIPNNVK	gi 4507729	Unknown	

In previous studies with purified bovine tubulin, 17 peptides from bovine alpha- and beta-tubulin were found to have been labeled with CPO on tyrosine and lysine. Tyrosine 281 was the most reactive residue in beta-tubulin (Grigoryan *et al.*, 2009c). However, no serine was found to be organophosphorylated by CPO in bovine tubulin (Grigoryan *et al.*, 2009c). When live mice were treated with chlorpyrifos or CPO, the labeled tubulin residues were tyrosine 281 and serine 338. No other residues were found to be organophosphorylated in mouse tubulin. It is possible that more sensitive methods will detect additional labeled residues in the future.

Table 2 compares the amino acid sequences of bovine and mouse tubulin peptides that include tyrosine 281 and serine 338. The sequence of peptide GSQQY<sub>281</sub>RALTVPELTQQMFDSK is conserved in both species, bovine differing from mouse by virtue of a single conservative change (alanine to serine) at the second position from the C-terminus. Tyrosine 281 is present in both bovine and mouse tubulin. Both bovine beta-tubulin peptide NSSY<sub>440</sub>FVEWIPNNVK and mouse beta-tubulin peptide NS<sub>338</sub>NFVEWIPNNVK have serine at position 338, but only bovine tubulin has tyrosine at position 340. Both peptides are labeled by CPO. The label in bovine tubulin is on tyrosine 440. The difference in target at this locus could reflect the greater nucleophilicity of tyrosine compared to serine.

Seventeen sites on bovine tubulin were labeled with CPO *in vitro*, while only two sites were labeled on mouse tubulin *in vivo*. The larger overall number of labeling sites for bovine tubulin *in vitro* could be partly explained by the fact that the pure bovine tubulin purchased from Cytoskeleton Inc. had been depleted of microtubule-associated proteins before it was treated with CPO. Tyrosine sites available for reaction *in vitro* may be unavailable *in vivo*. The tyrosines might be protected by interaction with other proteins or might already be phosphorylated by kinases (Westermann and Weber, 2003). Prior phosphorylation could mask other potential serine residue targets *in vivo*.

The homologous sequences in human beta-tubulin are nearly identical to those in bovine and mouse beta-tubulin. Sites of labeling on human tubulin are unknown, but they would be expected to be similar to those identified here.

*Thin Microtubules and Decreased Proteins on Tubulin Isolated from CPO-treated mice*

Thirty-two proteins are listed in Table 1. Eleven of these are forms of tubulin. Two are large proteins (plectin 1 isoform 6 and Titin) with Mowse scores of about 100. These proteins are frequently identified in database searches and may be considered as nonspecific identifications. The remaining 19 proteins appear to copurify with the microtubules. These proteins are recognized as being involved in axonal transport (Maccioni and Cambiazo, 1995; Park *et al.*, 2008; Sakamoto *et al.*, 2008).

Six proteins in Table 1 were undetectable in microtubules prepared from CPO-treated mice. These were heat-shock protein 84 kDa, alpha-internexin, Myosin Va, dynein cytoplasmic 1 light intermediate chain, cytoskeleton-associated protein 5, and microtubule-associated protein 2 isoform 1. Heat-shock proteins function as molecular chaperones, able to direct folding of cytoskeletal proteins, such as alpha/beta/gamma-tubulin, actin, and centractin (Liang and MacRae, 1997). Internexin is among the five major types of intermediate filament proteins expressed in mature neurons. Alpha-internexin, which is highly expressed during mammalian nervous system development, can coassemble with neurofilament proteins and plays a key role in axonal outgrowth (Lariviere and Julien, 2004). Myosin is involved in fast axonal/dendritic transport and can form a complex with kinesin, a microtubule-based motor. This complex allows long-range movement of vesicles within axons and dendrites on microtubules (Langford, 2002). The formation and maintenance of neuronal synapses are dependent on the active transport of material between the cell body and the axon terminal. Cytoplasmic dynein is one of the motors for microtubule-based axonal transport, and it takes part in regulating the dynamic behavior of microtubules (Hestermann *et al.*, 2002; Susalka and Pfister, 2000). Cytoskeleton-associated protein 5 plays a major role in organizing spindle poles. Microtubule-associated protein 2 isoform 1 is a low-molecular weight alternatively spliced variant that is more abundant in embryonic brain than in adult brain (Tucker *et al.*, 1988). Thus, the proteins that are missing from microtubules in CPO-treated mouse brain are related to microtubule assembly, structure, stability, and

function. Dissociation of these proteins from the microtubules could account for the abnormally thin microtubules in CPO-treated mice.

Our observation of a decrease in microtubule cosedimenting proteins in response to exposure to CPO is supported by other reports. Prendergast *et al.* (2007) found that CPO treatment of organotypic hippocampal slice cultures from rat brain results in dramatically reduced levels of microtubule-associated protein 2a and 2b. The fluorescence intensity from bound antibody was reduced up to 85% following 3 days of treatment with 1–10  $\mu$ M CPO. However, levels of  $\alpha$ -tubulin were not altered by CPO exposure, suggesting that the general structure of the microtubules was not destroyed. A proteomic analysis of cultured N2a neuroblastoma cells found that treatment with 10  $\mu$ M diazinon (an OP agent) increased the levels of some proteins, decreased the levels of others, but left tubulin levels unchanged (Harris *et al.*, 2009). It was suggested that diazinon exposure interferes with cytoskeletal networks, disrupting the structure and function of microtubules, microfilaments, and neurofilaments. Reduced levels of the cytoskeletal protein microtubule-associated protein 1B were found in differentiating rat C6 glioma cells following treatment with CPO, thus demonstrating a potent perturbation effect of CPO on the microtubule network (Sachana *et al.*, 2008).

#### *Mechanisms of OP Toxicity Independent of AChE Inhibition*

Microtubules are polymers of tubulin dimers that serve in a structural capacity in neurons and as tracks for transporting cell components from the nucleus to the axons and from the axons back to the nucleus. Microtubule-associated proteins bind to tubulin and serve a wide range of functions, including stabilizing, destabilizing, cross-linking, and facilitating interactions between microtubules and other proteins in the cell. Protein binding to microtubules is regulated through phosphorylation. For example, tubulin phosphorylated by calmodulin-dependent protein kinase is not capable of binding to microtubule-associated protein 2 or of polymerizing to microtubules (Wandosell *et al.*, 1986). Detachment of microtubule-associated proteins from the microtubule is regulated by microtubule affinity-regulating kinase. Phosphorylation of the associated proteins and subsequent detachment causes destabilization and destruction of the microtubule. Hyperphosphorylation of the tau protein causes disassembly of microtubules, a phenomenon seen in Alzheimer's disease (Alonso *et al.*, 1994).

Phosphorylation of tubulin and tubulin-associated proteins following challenge with OP agents has been studied *in vitro*, in brain extracts, and *in vivo*, in rats and hens. Choudhary *et al.* (2001) found in rats that dichlorvos induced hyperphosphorylation of tubulin and microtubule-associated protein 2, resulting in destabilization of the microtubule assembly. An increase in phosphorylation of microtubule-associated protein 2 was measured in the brain of hens following a single *in vivo* challenge with diisopropylfluorophosphate (DFP) (Abou-Donia *et al.*, 1993). An increase in the phosphorylation of

tubulin, myelin basic protein, and tau was found following *in vitro* DFP treatment of brain extracts (Gupta and Abou-Donia, 1999). The DFP-treated hen had decreased concentrations of tau protein as well as decreased tubulin polymerization (Gupta and Abou-Donia, 1994).

We propose that the reduction in microtubule cosedimenting proteins for microtubules purified from CPO-treated mice resulted from direct organophosphorylation of tubulin by CPO and perhaps from organophosphorylation of the associated proteins as well. It is also possible that enhanced phosphorylation of tubulin and microtubule-associated proteins by kinases such as CaM kinase II was triggered by CPO exposure (Gupta and Abou-Donia, 1999) and that this contributed to the dissociation of some of the microtubule-associated proteins that we observed. We further propose that the dissociation of these vital microtubule-associated proteins resulted in impaired microtubule structure as demonstrated by the significant reduction in their width and height. Such structural alterations imply disruption of microtubule function. These results support a noncholinergic mechanism for OP neurotoxicity in which long-lasting neurotoxicity is due to OP modification of proteins involved in axonal transport.

The question was raised how disruption of axonal transport provides a better explanation of long-lasting neurotoxicity after OP exposure when it is likely that both the persistence of microtubule disruption and of AChE inhibition are short lived? To address this question, we offer the hypothesis developed by Scott Brady and his associates to explain neurodegenerative diseases (Morfini *et al.*, 2009). Their hypothesis is that alterations in phosphorylation-dependent intracellular signaling mechanisms result in alterations of axonal transport. Dysregulation of axonal transport causes axons to lose connectivity to synapses and to slowly die back. The consequence is a slow neurodegeneration. The abnormality that initiates these events in diseases such as Alzheimer's and Huntington's is a mutation. We propose that phosphorylation abnormalities can also be initiated by covalent binding of OP. The present work demonstrates covalent binding by OP. Other workers have shown that treatment with OP leads to hyperphosphorylation of neurofilaments, tau, calcium/cyclic AMP response element binding protein, tubulin, and microtubule-associated protein 2 (Choudhary *et al.*, 2001; Gupta and Abou-Donia, 1999; Gupta *et al.*, 1997; Schuh *et al.*, 2002) and to disruption of adenylyl cyclase signaling and serotonin-mediated signal transduction (Aldridge *et al.*, 2003; Song *et al.*, 1997). Thus, we propose a mechanism in which low-dose exposure to OP disrupts axonal transport for a sufficient length of time to initiate an irreversible degradation of the neuron, which in turn leads to permanent loss of neuronal function.

#### FUNDING

U.S. Army Medical Research and Materiel Command (W81XWH-07-2-0034); the National Institutes of Health

(NIH) (U01 NS058056 and P30CA36727); NIH (SIG program), the UNMC Program of Excellence, the Nebraska Research Initiative; Mass spectra were obtained with the support of the Mass Spectrometry; Proteomics Core Facility at the University of Nebraska Medical Center.

## ACKNOWLEDGMENTS

Nanoimages were obtained with the support of L.S., codirector, and Dr Yuri L. Lyubchenko, director of the Nanoimaging Core Facility at the University of Nebraska Medical Center in the Department of Pharmaceutical Sciences. The Nanoimaging Core.

## REFERENCES

- Abou-Donia, M. B., Viana, M. E., Gupta, R. P., and Anderson, J. K. (1993). Enhanced calmodulin binding concurrent with increased kinase-dependent phosphorylation of cytoskeletal proteins following a single subcutaneous injection of diisopropyl phosphorofluoridate in hens. *Neurochem. Int.* **22**, 165–173.
- Aldridge, J. E., Seidler, F. J., Meyer, A., Thillai, I., and Slotkin, T. A. (2003). Serotonergic systems targeted by developmental exposure to chlorpyrifos: effects during different critical periods. *Environ. Health Perspect.* **111**, 1736–1743.
- Alonso, A. C., Zaidi, T., Grundke-Iqbal, I., and Iqbal, K. (1994). Role of abnormally phosphorylated tau in the breakdown of microtubules in Alzheimer disease. *Proc. Natl. Acad. Sci. U.S.A.* **91**, 5562–5566.
- Amitai, G., Moorad, D., Adani, R., and Doctor, B. P. (1998). Inhibition of acetylcholinesterase and butyrylcholinesterase by chlorpyrifos-oxon. *Biochem. Pharmacol.* **56**, 293–299.
- Choudhary, S., Joshi, K., and Gill, K. D. (2001). Possible role of enhanced microtubule phosphorylation in dichlorvos induced delayed neurotoxicity in rat. *Brain Res.* **897**, 60–70.
- Conde, C., and Caceres, A. (2009). Microtubule assembly, organization and dynamics in axons and dendrites. *Nat. Rev. Neurosci.* **10**, 319–332.
- Friden, B., and Wallin, M. (1991). Dependency of microtubule-associated proteins (MAPs) for tubulin stability and assembly; use of estramustine phosphate in the study of microtubules. *Mol. Cell. Biochem.* **105**, 149–158.
- Gearhart, D. A., Sickles, D. W., Buccafusco, J. J., Prendergast, M. A., and Terry, A. V., Jr. (2007). Chlorpyrifos, chlorpyrifos-oxon, and diisopropyl-fluorophosphate inhibit kinesin-dependent microtubule motility. *Toxicol. Appl. Pharmacol.* **218**, 20–29.
- Grigoryan, H., Li, B., Anderson, E. K., Xue, W., Nachon, F., Lockridge, O., and Schopfer, L. M. (2009a). Covalent binding of the organophosphorus agent FP-biotin to tyrosine in eight proteins that have no active site serine. *Chem. Biol. Interact.* **180**, 492–498. PMID:2700782.
- Grigoryan, H., Li, B., Xue, W., Grigoryan, M., Schopfer, L. M., and Lockridge, O. (2009b). Mass spectral characterization of organophosphate-labeled lysine in peptides. *Anal. Biochem.* **394**, 92–100.
- Grigoryan, H., and Lockridge, O. (2009). Nanoimages show disruption of tubulin polymerization by chlorpyrifos oxon: implications for neurotoxicity. *Toxicol. Appl. Pharmacol.* **240**, 143–148. NIHMS:134468.
- Grigoryan, H., Schopfer, L. M., Peeples, E. S., Duysen, E. G., Grigoryan, M., Thompson, C. M., and Lockridge, O. (2009c). Mass spectrometry identifies multiple organophosphorylated sites on tubulin. *Toxicol. Appl. Pharmacol.* **240**, 149–158.
- Grigoryan, H., Schopfer, L. M., Thompson, C. M., Terry, A. V., Masson, P., and Lockridge, O. (2008). Mass spectrometry identifies covalent binding of soman, sarin, chlorpyrifos oxon, diisopropyl fluorophosphate, and FP-biotin to tyrosines on tubulin: a potential mechanism of long term toxicity by organophosphorus agents. *Chem. Biol. Interact.* **175**, 180–186.
- Gupta, R. P., Abdel-Rahman, A., Wilmarth, K. W., and Abou-Donia, M. B. (1997). Alteration in neurofilament axonal transport in the sciatic nerve of the diisopropyl phosphorofluoridate (DFP)-treated hen. *Biochem. Pharmacol.* **53**, 1799–1806.
- Gupta, R. P., and Abou-Donia, M. B. (1994). In vivo and in vitro effects of diisopropyl phosphorofluoridate (DFP) on the rate of hen brain tubulin polymerization. *Neurochem. Res.* **19**, 435–444.
- Gupta, R. P., and Abou-Donia, M. B. (1999). Tau phosphorylation by diisopropyl phosphorofluoridate (DFP)-treated hen brain supernatant inhibits its binding with microtubules: role of Ca<sup>2+</sup>/Calmodulin-dependent protein kinase II in tau phosphorylation. *Arch. Biochem. Biophys.* **365**, 268–278.
- Harris, W., Sachana, M., Flaskos, J., and Hargreaves, A. J. (2009). Proteomic analysis of differentiating neuroblastoma cells treated with sub-lethal neurite inhibitory concentrations of diazinon: identification of novel biomarkers of effect. *Toxicol. Appl. Pharmacol.* **240**, 159–165.
- Hestermann, A., Rehberg, M., and Graf, R. (2002). Centrosomal microtubule plus end tracking proteins and their role in Dictyostelium cell dynamics. *J. Muscle Res. Cell. Motil.* **23**, 621–630.
- Kawada, T., Katsumata, M., Suzuki, H., Li, Q., Inagaki, H., Nakada, A., Shimizu, T., Hirata, K., and Hirata, Y. (2005). Insomnia as a sequela of sarin toxicity several years after exposure in Tokyo subway trains. *Percept. Mot. Skills.* **100**, 1121–1126.
- Langford, G. M. (2002). Myosin-V, a versatile motor for short-range vesicle transport. *Traffic* **3**, 859–865.
- Lariviere, R. C., and Julien, J. P. (2004). Functions of intermediate filaments in neuronal development and disease. *J. Neurobiol.* **58**, 131–148.
- Li, B., Schopfer, L. M., Grigoryan, H., Thompson, C. M., Hinrichs, S. H., Masson, P., and Lockridge, O. (2009). Tyrosines of human and mouse transferrin covalently labeled by organophosphorus agents: a new motif for binding to proteins that have no active site serine. *Toxicol. Sci.* **107**, 144–155. PMID:2638647.
- Liang, P., and MacRae, T. H. (1997). Molecular chaperones and the cytoskeleton. *J. Cell. Sci.* **110**(Pt 13), 1431–1440.
- Lyubchenko, Y. L., and Shlyakhtenko, L. S. (2009). AFM for analysis of structure and dynamics of DNA and protein-DNA complexes. *Methods* **47**, 206–213.
- Maccioni, R. B., and Cambiazo, V. (1995). Role of microtubule-associated proteins in the control of microtubule assembly. *Physiol. Rev.* **75**, 835–864.
- McDonough, J. H., Jr, and Shih, T. M. (1997). Neuropharmacological mechanisms of nerve agent-induced seizure and neuropathology. *Neurosci. Biobehav. Rev.* **21**, 559–579.
- Morfini, G. A., Burns, M., Binder, L. I., Kanaan, N. M., LaPointe, N., Bosco, D. A., Brown, R. H., Jr, Brown, H., Tiwari, A., Hayward, L., et al. (2009). Axonal transport defects in neurodegenerative diseases. *J. Neurosci.* **29**, 12776–12786.
- Park, H., Kim, M., and Fygenson, D. K. (2008). Tau-isoform dependent enhancement of taxol mobility through microtubules. *Arch. Biochem. Biophys.* **478**, 119–126.
- Peeples, E. S., Schopfer, L. M., Duysen, E. G., Spaulding, R., Voelker, T., Thompson, C. M., and Lockridge, O. (2005). Albumin, a new biomarker of organophosphorus toxicant exposure, identified by mass spectrometry. *Toxicol. Sci.* **83**, 303–312.
- Perkins, D. N., Pappin, D. J., Creasy, D. M., and Cottrell, J. S. (1999). Probability-based protein identification by searching sequence databases using mass spectrometry data. *Electrophoresis* **20**, 3551–3567.

- Prendergast, M. A., Self, R. L., Smith, K. J., Ghayoumi, L., Mullins, M. M., Butler, T. R., Buccafusco, J. J., Gearhart, D. A., and Terry, A. V., Jr. (2007). Microtubule-associated targets in chlorpyrifos oxon hippocampal neurotoxicity. *Neuroscience* **146**, 330–339.
- Read, R. W., Riches, J. R., Stevens, J. A., Stubbs, S. J., and Black, R. M. (2010). Biomarkers of organophosphorus nerve agent exposure: comparison of phosphorylated butyrylcholinesterase and phosphorylated albumin after oxime therapy. *Arch. Toxicol.* **84**, 25–36.
- Rishal, I., Michaelievski, I., Rozenbaum, M., Shinder, V., Medzihradsky, K. F., Burlingame, A. L., and Fainzilber, M. (2010). Axoplasm isolation from peripheral nerve. *Dev. Neurobiol.* **70**, 126–133.
- Sachana, M., Flaskos, J., Sidiropoulou, E., Yavari, C. A., and Hargreaves, A. J. (2008). Inhibition of extension outgrowth in differentiating rat C6 glioma cells by chlorpyrifos and chlorpyrifos oxon: effects on microtubule proteins. *Toxicol. In Vitro* **22**, 1387–1391.
- Sakamoto, T., Uezu, A., Kawauchi, S., Kuramoto, T., Makino, K., Umeda, K., Araki, N., Baba, H., and Nakanishi, H. (2008). Mass spectrometric analysis of microtubule co-sedimented proteins from rat brain. *Genes Cells* **13**, 295–312.
- Salvi, R. M., Lara, D. R., Ghisolfi, E. S., Portela, L. V., Dias, R. D., and Souza, D. O. (2003). Neuropsychiatric evaluation in subjects chronically exposed to organophosphate pesticides. *Toxicol. Sci.* **72**, 267–271.
- Sams, C., Cocker, J., and Lennard, M. S. (2004). Biotransformation of chlorpyrifos and diazinon by human liver microsomes and recombinant human cytochrome P450s (CYP). *Xenobiotica* **34**, 861–873.
- Schuh, R. A., Lein, P. J., Beckles, R. A., and Jett, D. A. (2002). Noncholinesterase mechanisms of chlorpyrifos neurotoxicity: altered phosphorylation of Ca<sup>2+</sup>/cAMP response element binding protein in cultured neurons. *Toxicol. Appl. Pharmacol.* **182**, 176–185.
- Shelanski, M. L., Gaskin, F., and Cantor, C. R. (1973). Microtubule assembly in the absence of added nucleotides. *Proc. Natl. Acad. Sci. U.S.A.* **70**, 765–768.
- Shlyakhtenko, L. S., Gall, A. A., Filonov, A., Cerovac, Z., Lushnikov, A., and Lyubchenko, Y. L. (2003). Silatrane-based surface chemistry for immobilization of DNA, protein-DNA complexes and other biological materials. *Ultramicroscopy* **97**, 279–287.
- Song, X., Seidler, F. J., Saleh, J. L., Zhang, J., Padilla, S., and Slotkin, T. A. (1997). Cellular mechanisms for developmental toxicity of chlorpyrifos: targeting the adenylyl cyclase signaling cascade. *Toxicol. Appl. Pharmacol.* **145**, 158–174.
- Srivastava, A. K., Gupta, B. N., Bihari, V., Mathur, N., Srivastava, L. P., Pangtey, B. S., Bharti, R. S., and Kumar, P. (2000). Clinical, biochemical and neurobehavioural studies of workers engaged in the manufacture of quinalphos. *Food Chem. Toxicol.* **38**, 65–69.
- Susalka, S. J., and Pfister, K. K. (2000). Cytoplasmic dynein subunit heterogeneity: implications for axonal transport. *J. Neurocytol.* **29**, 819–829.
- Tang, J., Cao, Y., Rose, R. L., Brimfield, A. A., Dai, D., Goldstein, J. A., and Hodgson, E. (2001). Metabolism of chlorpyrifos by human cytochrome P450 isoforms and human, mouse, and rat liver microsomes. *Drug Metab. Dispos.* **29**, 1201–1204.
- Terry, A. V., Jr., Gearhart, D. A., Beck, W. D., Jr., Truan, J. N., Middlemore, M. L., Williamson, L. N., Bartlett, M. G., Prendergast, M. A., Sickles, D. W., and Buccafusco, J. J. (2007). Chronic, intermittent exposure to chlorpyrifos in rats: protracted effects on axonal transport, neurotrophin receptors, cholinergic markers, and information processing. *J. Pharmacol. Exp. Ther.* **322**, 1117–1128.
- Tierno, M. B., Kitchens, C. A., Petrik, B., Graham, T. H., Wipf, P., Xu, F. L., Saunders, W. S., Raccor, B. S., Balachandran, R., Day, B. W., et al. (2009). Microtubule binding and disruption and induction of premature senescence by disorazole C(1). *J. Pharmacol. Exp. Ther.* **328**, 715–722.
- Tucker, R. P., Binder, L. I., Viereck, C., Hemmings, B. A., and Matus, A. I. (1988). The sequential appearance of low- and high-molecular-weight forms of MAP2 in the developing cerebellum. *J. Neurosci.* **8**, 4503–4512.
- Wandosell, F., Serrano, L., Hernandez, M. A., and Avila, J. (1986). Phosphorylation of tubulin by a calmodulin-dependent protein kinase. *J. Biol. Chem.* **261**, 10332–10339.
- Westermann, S., and Weber, K. (2003). Post-translational modifications regulate microtubule function. *Nat. Rev. Mol. Cell Biol.* **4**, 938–947.
- Wiederin, J., Rozek, W., Duan, F., and Ciborowski, P. (2009). Biomarkers of HIV-1 associated dementia: proteomic investigation of sera. *Proteome Sci.* **7**, 8.
- Yamasue, H., Abe, O., Kasai, K., Suga, M., Iwanami, A., Yamada, H., Tochigi, M., Ohtani, T., Rogers, M. A., Sasaki, T., et al. (2007). Human brain structural change related to acute single exposure to sarin. *Ann. Neurol.* **61**, 37–46.
- Yanagisawa, N., Morita, H., and Nakajima, T. (2006). Sarin experiences in Japan: acute toxicity and long-term effects. *J. Neurol. Sci.* **249**, 76–85.

# Binding and Hydrolysis of Soman by Human Serum Albumin

Bin Li,<sup>†</sup> Florian Nachon,<sup>‡,§</sup> Marie-Thérèse Froment,<sup>‡,§</sup> Laurent Verdier,<sup>#</sup>  
Jean-Claude Debouzy,<sup>‡,△</sup> Bernardo Brasme,<sup>‡,⊥</sup> Emilie Gillon,<sup>‡,§</sup> Lawrence M. Schopfer,<sup>†</sup>  
Oksana Lockridge,<sup>†</sup> and Patrick Masson<sup>\*,‡,§</sup>

University of Nebraska Medical Center, Eppley Institute, Omaha, Nebraska 68198-6805, Centre de Recherches du Service de Santé des Armées, Département de Toxicologie, Unité d'Enzymologie, Unité de Biophysique, Service de Biospectroscopie, BP 87, 38702 La Tronche cedex, France, 3, and Département Analyse Chimique, Centre d'Etudes du Bouchet, BP 3, 91710 Vert-le-Petit, France

Received September 15, 2007

Human plasma and fatty acid free human albumin were incubated with soman at pH 8.0 and 25 °C. Four methods were used to monitor the reaction of albumin with soman: progressive inhibition of the aryl acylamidase activity of albumin, the release of fluoride ion from soman, <sup>31</sup>P NMR, and mass spectrometry. Inhibition (phosphorylation) was slow with a bimolecular rate constant of  $15 \pm 3 \text{ M}^{-1} \text{ min}^{-1}$ . MALDI-TOF and tandem mass spectrometry of the soman–albumin adduct showed that albumin was phosphorylated on tyrosine 411. No secondary dealkylation of the adduct (aging) occurred. Covalent docking simulations and <sup>31</sup>P NMR experiments showed that albumin has no enantiomeric preference for the four stereoisomers of soman. Spontaneous reactivation at pH 8.0 and 25 °C, measured as regaining of aryl acylamidase activity and decrease of covalent adduct (pinacolyl methylphosphonylated albumin) by NMR, occurred at a rate of  $0.0044 \text{ h}^{-1}$ , indicating that the adduct is quite stable ( $t_{1/2} = 6.5 \text{ days}$ ). At pH 7.4 and 22 °C, the covalent soman–albumin adduct, measured by MALDI-TOF mass spectrometry, was more stable ( $t_{1/2} = 20 \text{ days}$ ). Though the concentration of albumin in plasma is very high (about 0.6 mM), its reactivity with soman (phosphorylation and phosphotriesterase activity) is too slow to play a major role in detoxification of the highly toxic organophosphorus compound soman. Increasing the bimolecular rate constant of albumin for organophosphates is a protein engineering challenge that could lead to a new class of bioscavengers to be used against poisoning by nerve agents. Soman-albumin adducts detected by mass spectrometry could be useful for the diagnosis of soman exposure.

## 1. Introduction

Albumin is an abundant protein that represents 50–60% of the total protein in human plasma and body fluids. Its concentration in plasma is about 0.6 mM. Albumin displays both an esterase activity (1) and an aryl acylamidase activity (2, 3). The topology of the esterase/amidase active site of albumin has been probed by site-directed mutagenesis (4) and X-ray structure determination of several drug–albumin complexes (5). Tyr411 was determined to be the catalytic nucleophile in these reactions.

Albumin is also known to bind organophosphates (OPs<sup>1</sup>) and carbamates (6–8) and to react with them (9–11). OPs and certain carbamates are actually hydrolyzed by albumin through transient phosphorylation/alkylation of its active site (12–17). The residue that reacts with OPs was proven to be a tyrosine (9–11, 14, 18). DF<sup>32</sup>P-labeling of human albumin followed by peptide sequencing showed that the labeled tyrosine is in the tetrapeptide

sequence Arg-Tyr-Thr-Lys (9). Arg and Tyr were subsequently identified as Arg 410 and Tyr 411, the key residues of the esteratic site of HSA (4). Recently, DFP-inhibition of the aryl acylamidase (AAA) activity of FAF-HSA confirmed that Tyr 411 is also the nucleophilic pole of the albumin AAA activity (2). Finally, MALDI-TOF mass spectrometry provided direct evidence that the OPs chlorpyrifos-oxon, dichlorvos, DFP, and sarin bind covalently to human albumin at Tyr 411 (19).

In the present work, we investigated the reaction of human albumin with soman. MALDI-TOF and quadrupole tandem MS/MS mass spectrometry of the soman–albumin adduct showed that Tyr411 was phosphorylated. Unlike soman adducts of butyrylcholinesterase, the albumin–soman adduct did not age, that is, lose its pinacolyl chain. Covalent docking simulations and <sup>31</sup>P NMR experiments indicated that there was no enantiomeric preference of albumin for the stereoisomers of soman. Kinetic parameters of albumin phosphorylation by soman and subsequent dephosphorylation were determined.

Our results could have application for the detection of soman exposure in humans. Mass spectrometry could be used to detect soman–albumin adducts. In addition, antibodies to the soman–albumin adduct could be generated for use in a rapid antibody-based assay of soman exposure. Lastly, mutants of albumin could lead to a new class of scavengers against OP poisoning.

## 2. Experimental Procedures

**2.1. Chemicals.** Fatty acid-free human albumin (FAF-HSA) and porcine pepsin were from Sigma Chemical Co. (Saint Quentin

\* To whom correspondence should be addressed. Patrick Masson, CRSSA, Département de Toxicologie, Unité d'Enzymologie, BP 87, 38702 La Tronche cedex, France. Tel: +33 (0)4 76 63 69 59. Fax: +33 (0)4 76 63 69 62. E-mail: pmasson@unmc.edu.

<sup>†</sup> Eppley Institute.

<sup>‡</sup> Centre de Recherches du Service de Santé des Armées.

<sup>§</sup> Département de Toxicologie, Unité d'Enzymologie.

<sup>#</sup> Centre d'Etudes du Bouchet.

<sup>△</sup> Unité de Biophysique.

<sup>⊥</sup> Service de Biospectroscopie.

<sup>1</sup> Abbreviations: AAA, aryl acylamidase; AChE, acetylcholinesterase; BuChE, butyrylcholinesterase; DFP, diisopropylfluorophosphate; FAF-HSA, fatty acid-free human serum albumin; HSA, human serum albumin; MP, methylphosphonate; PMP, pinacolyl methylphosphonate; o-NTFAC, *N*-(*o*-nitrophenyl)trifluoroacetamide; OP, organophosphorus ester.

Fallavier, France). o-NTFNAC was a gift from Dr. Sultan Darvesh (Dalhousie University, Halifax, Canada). Racemic soman (pinacolyl methylfluorophosphate) dissolved in isopropanol was from CEB (Vert-le-Petit, France). All other chemicals were of biochemical grade.

The concentration of racemic soman in the stock solution was determined by programmed temperature gas chromatography after hydrolysis into methylpinacolyl phosphonic acid and derivatization with pentafluorobenzyl bromide (20). It was 4.73 mg/mL (26 mM).  $^{31}\text{P}$  NMR spectra of 2 mM soman in deuterated dimethylsulfoxide were recorded at 27 °C on a Bruker spectrometer (AM400, 9.4 T). The spectra showed that the four stereoisomers are present in nearly equimolar amounts. Soman has two chiral centers. The absolute configuration of the four diastereoisomers is known.  $\text{P}_\text{S}$ ,  $\text{P}_\text{R}$ ,  $\text{C}_\text{S}$ , and  $\text{C}_\text{R}$  correspond to the old notation P<sup>+</sup>, C<sup>+</sup>, and C<sup>−</sup>, respectively. Thus, isomers  $\text{P}_\text{S}\text{C}_\text{S} = \text{P}^+\text{C}^+$ ,  $\text{P}_\text{S}\text{C}_\text{R} = \text{P}^+\text{C}^-$ ,  $\text{P}_\text{R}\text{C}_\text{R} = \text{P}^-\text{C}^-$ , and  $\text{P}_\text{R}\text{C}_\text{S} = \text{P}^-\text{C}^+$ . Stereoisomers  $\text{P}_\text{S}\text{C}_\text{S}$  and  $\text{P}_\text{S}\text{C}_\text{R}$  are the most active toward the biological target acetylcholinesterase (21).

**2.2. Aryl Acylamidase Enzymatic Assay of Albumin.** The AAA activity of albumin was assayed with o-NTFNAC (2 mM) as the substrate in 60 mM Tris/HCl buffer at pH 8.0 at 25 °C. A 60 mM stock solution of o-NTFNAC was prepared in 50% water/acetonitrile (v/v). Because isopropanol is the solvent for soman, isopropanol was also added to the buffer in the control assay for the AAA activity of albumin in the absence of soman. The final concentration of acetonitrile in the assay was 3.3% and that of isopropanol was 2%. The release of the phenolic product (o-nitroaniline) was monitored for 5 min at 430 nm ( $\epsilon = 3954 \text{ M}^{-1} \text{ cm}^{-1}$ ) according to Darvesh et al. (22). Because of the low enzymatic activity of albumin with o-NTFNAC (3), high concentrations of FAF-HSA were used in assays (0.075 mM final). Measured rates were corrected for spontaneous hydrolysis of o-NTFNAC.

**2.3. Mass Spectrometry (MALDI-TOF and Quadrupole MS/MS) of the Soman–Albumin Adduct from Human Plasma.** One hundred microliters of human plasma was mixed with 2.3  $\mu\text{L}$  of stock soman (26 mM in isopropanol) to give a reaction mixture containing 600  $\mu\text{M}$  soman (in 2.3% isopropanol). The mixture was incubated at room temperature for 3–7 days before processing. No buffer was added to the plasma during this step. The pH of a 10  $\mu\text{L}$  aliquot was reduced to pH 2.3 by adding 10  $\mu\text{L}$  of 1% trifluoroacetic acid. Proteins were digested with 0.5  $\mu\text{g}$  of pepsin for 2 h at 37 °C. At pH 2.3, selective proteolysis at the C-terminal side of the leucine and phenylalanine residues is expected. There was no need to denature the proteins or to reduce and alkylate the disulfide bonds because the peptides of interest were released without these added steps. Peptides were separated on a C18 reverse phase column on a Waters 625 LC system with a 40 min gradient starting with 85% buffer A (0.1% trifluoroacetic acid in water), 15% buffer B (acetonitrile containing 0.07% trifluoroacetic acid), and ending with 65% buffer A and 35% buffer B. One milliliter fractions were reduced in volume to 200  $\mu\text{L}$  in a vacuum centrifuge, and 1  $\mu\text{L}$  was analyzed by MALDI-TOF with a 2,5-dihydroxybenzoic acid matrix. Mass spectra were acquired with the Applied Biosystems Voyager DE-PRO MALDI-TOF mass spectrometer in linear positive ion mode. The spectrometer was calibrated using standard peptides (Applied Biosystems Mixture 1). A control plasma sample was identically treated, except that it was incubated with 3.1% isopropanol rather than with soman.

MS/MS spectra were acquired on a Q-Trap 2000 triple quadrupole linear ion trap mass spectrometer (Applied Biosystems, MDS Sciex, Foster City, CA) with a nano electrospray ionization source. Samples were infused into the mass spectrometer at 0.35  $\mu\text{L}/\text{min}$  via a fused silica emitter (360  $\mu\text{m}$  o.d., 20  $\mu\text{m}$  i.d., 15  $\mu\text{m}$  taper, New Objective, Woburn, MA) using a Harvard syringe pump to drive a 25  $\mu\text{L}$  Hamilton syringe equipped with an inline 0.25  $\mu\text{m}$  filter. Samples were sprayed with 50% acetonitrile and 0.1% formic acid. Mass spectra were calibrated using fragment ions generated from collision-induced dissociation of Glu fibrinopeptide B (Sigma). Enhanced product ion scans were obtained with a collision energy of  $50 \pm 5 \text{ V}$  and a pure nitrogen gas pressure of  $4 \times 10^{-5} \text{ Torr}$ .

The final enhanced product ion scan was the average of 105 scans. Ions were identified by manual sequencing.

**2.4.  $^{31}\text{P}$  NMR Spectroscopy.**  $^{31}\text{P}$  NMR spectra for the reaction between albumin (0.78 mM or 1.3 mM) and soman (1.3 mM) in 60 mM Tris/HCl buffer at pH 8.0 were recorded at 27 °C on a Bruker AM400NB spectrometer operating at 162 MHz. The spectra were acquired using successive 8 acquisition blocks of 5,000 accumulated scans (acquisition time: 3 h/spectrum) using 30 kHz spectral width, 32,000 acquisition points, and a composite pulse proton decoupling (CPD mode). The external reference for chemical shifts was 85% (w/v)  $\text{H}_3\text{PO}_4$ . Spectra were compared to the spectrum of soman in buffer and the spectrum of methyl pinacolyl phosphonate (MPP) in the presence and absence of albumin. MPP was made by the complete hydrolysis of soman in 5 N sodium hydroxide.

**2.5. Kinetic Studies of the Reaction of Albumin with Soman.**  
**2.5.1. Residual AAA Activity.** FAF-HSA (780  $\mu\text{M}$ ) was incubated with 120 to 1300  $\mu\text{M}$  concentrations of racemic soman in 60 mM Tris/HCl buffer at pH 8.0 at 25 °C. The time dependence of the inhibition of albumin by soman was monitored by following the residual AAA activity of albumin. Measurements of the AAA residual activity were performed on 100  $\mu\text{L}$  aliquots of reaction mixture, using the sampling method (23).

**2.5.2. Monitoring the Release of Fluoride from Soman.** The release of fluoride, that is, the leaving group of soman, upon the reaction of soman with albumin and spontaneous hydrolysis was monitored by ionometry using a thermostatted ionometer (Radiometer IONcheck 45) equipped with an ion-selective electrode for fluoride (ISE 301F). FAF-HSA (780  $\mu\text{M}$ ) was incubated with 520, 780, and 1300  $\mu\text{M}$  concentrations of racemic soman in 60 mM Tris/HCl buffer at pH 8.0 at 25 °C, and the concentration of released fluoride was assayed. The spontaneous hydrolysis of soman was determined under the same conditions.

**2.5.3. Kinetic  $^{31}\text{P}$  NMR Spectroscopy.** To follow the phosphorylation reaction, 1.33 mM FAF-HSA was incubated with 1.35 mM soman in 60 mM Tris/HCl buffer at pH 8.0 at 25 °C in the presence of deuterated DMSO (10% v/v final). The successive spectra were recorded every 20 min (800 scans) over 4 h. Concentrations of the different species were plotted as a function of time. To follow the reactivation of phosphorylated albumin, 1.3 mM FAF-HSA was reacted with one equivalent of racemic soman in 60 mM Tris/HCl buffer at pH 8.0. Then, the phosphorylated albumin solution was maintained at 25 °C, and spectra were recorded every 2 h over 60 h. Kinetic constants for the spontaneous hydrolysis of soman, phosphorylation of albumin, and reactivation of albumin (dephosphorylation) were determined by fitting data against the numeric solution of differential equations that describe Scheme 1, using Mathematica 5 (Wolfram Research).

**2.5.4. Kinetic Mass Spectrometry.** The stability of the covalent soman–albumin adduct was measured on a MALDI-TOF-TOF 4800 mass spectrometer (Applied Biosystems). Human albumin was labeled by incubating a 1 mg/mL solution (15  $\mu\text{M}$ ) in 10 mM Tris/HCl at pH 8.0 with 200  $\mu\text{M}$  soman for 24 h at room temperature. After this time, the concentration of active soman was negligible as determined by measuring the inhibition of human butyrylcholinesterase. The albumin solution was diluted to 0.1 mg/mL with 0.01% sodium azide in water and the pH adjusted to 7.4. The 200  $\mu\text{L}$  solution was stored at 22 °C. Every 2 or 3 days, a 10  $\mu\text{L}$  aliquot was acidified with 10  $\mu\text{L}$  of 1% trifluoroacetic acid and digested with 2  $\mu\text{L}$  of 1 mg/mL porcine pepsin (dissolved in 10 mM HCl). The digest was incubated at 37 °C for 1–4 h, and then 0.5  $\mu\text{L}$  was spotted on a MALDI target plate. The dry spot was overlaid with 0.5  $\mu\text{L}$  of 10 mg/mL  $\alpha$ -cyano-4-hydroxycinnamic acid in 50% acetonitrile and 0.1% trifluoroacetic acid. MS scans in reflector mode were acquired at 3000 V by summing 500 laser shots per scan. The percent label on Tyr 411 was calculated from cluster areas. Peptide masses acquired in reflector mode are monoisotopic, which makes their mass about 1 amu lower than the average mass acquired in linear mode.

**2.6. Molecular Modeling.** **2.6.1. Noncovalent Docking.** Docking calculations were carried out using two programs: (1) Autodock, version 3.0.5, with the Lamarckian genetic algorithm (LGA (24)) and (2) Gold, version 3.1 (CCDC Software, Ltd). Docking with Autodock employed the following procedure. The molecular models of the four diastereoisomers of soman were built and minimized with the MM2 force field of Chem3D (Cambridge soft.). The structure of HSA was prepared from the crystal structure of its complex with indoxyl sulfate (pdb code 2bxh) or warfarin (pdb code 2bxd) to take into account the heterogeneity of conformation of Val433. Molecules of water and ligands were removed from the model. Soman and HSA were further prepared using Autodock Tools 1.4 (25). The 3D affinity grid box was designed to include the full pocket near Tyr411. The number of grid points in the *x*-, *y*-, and *z*-axes was 60, 60, and 60 with grid points separated by 0.375 Å. Docking calculations were set to 100 runs. At the end of the calculation, Autodock performed cluster analysis. Docking solutions with ligand all-atom root-mean-square deviation (rmsd) within 1.0 Å of each other were clustered together and ranked by the lowest energy representative. The lowest-energy solution was accepted as the one most representative of the soman–HSA complex. Docking with Gold employed the following procedure. Protein structures were protonated and minimized by conjugate gradients using Gromacs 3.3 (26, 27) and the parameter set 53A6 (28). Ligands were built into the Sybyl 7.2 package (Tripos Inc.). The Mopac-PM3 (29) semiempirical method was chosen for geometry optimization and calculation of atomic charges. The cavity was defined as residues having atoms up to 15 Å from the Tyr411 hydroxyl group. We used long search settings for the Gold GA: 40 docking with parameters corresponding to the default 200% search efficiency settings. The final selection of conformers was based on the two scoring functions, Goldscore (30) and Chemscore (31).

**2.6.2. Covalent Docking.** This simulation was carried out using Gold, version 3.1 with GA settings similar to those for noncovalent docking. We used the same proteins as before, and the results were scored using both Goldscore and Chemscore functions. The fluorine atom from each of the four soman stereoisomers was replaced by a hydroxyl group, and the phosphorus stereochemistry was inverted to get the right configuration when the phosphorus atom binds to the Tyr411 Oγ. The highest score isomers were chosen as the ones giving the lowest  $\Delta H_f$  when estimating the energy of the system with Mopac-PM3. To reduce the number of atoms in our system, we removed residues having all atoms further than 5 Å from any soman atoms.

### 3. Results

**3.1. Mass Spectrometry to Identify the Covalent Binding of Soman to Tyrosine 411.** Peptic digests of soman-labeled and control human plasma were separated by HPLC. Matched fractions from the two preparations were examined by MALDI-TOF mass spectrometry. MALDI-TOF signals for soman–albumin and control albumin peptides are shown in Figure 1. A peptide with mass 1880 amu is present in fraction 21 from the soman-labeled preparation (Figure 1, panel B). This mass is consistent with the peptide (L)VRY\*TKKVPQVSTPTL(V) (1718 amu, from residues 409–423 of the mature albumin sequence) with an added mass of 162 amu from soman. A peptide with mass 1993 amu is present in fraction 23 from the soman-labeled preparation (Figure 1, panel D). This mass is consistent with the peptide (L)LVRY\*TKKVPQVSTPTL(V) (1831 amu, from residues 408–423 of the mature albumin sequence, representing a missed peptic cleavage) with an added mass of 162 amu from soman. The parallel fractions from control human plasma do not have peptides of these masses (Figure 1, panels A and C). However, other prominent peaks are present at identical masses in both the control and soman-labeled spectra (compare panels A to B, and C to D), confirming that the fractions are matched with regard to HPLC elution and relative mass spectral

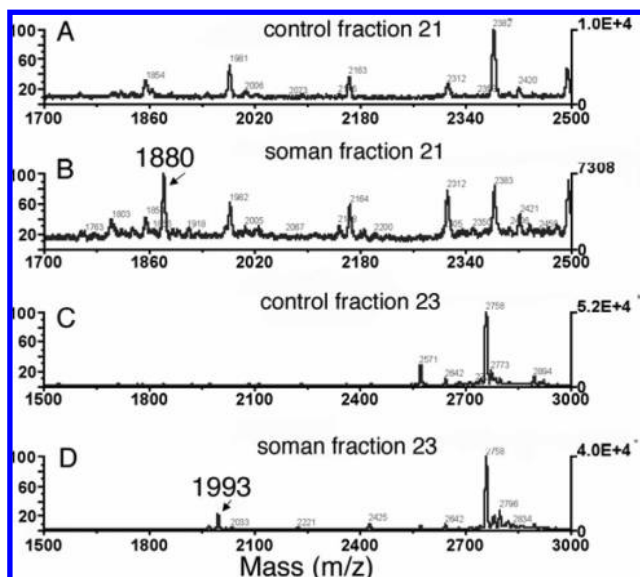


**Figure 1.** MALDI-TOF mass spectra of peptic peptides from the soman–albumin adduct. Panels A and C, control human plasma digested with pepsin and fractionated by HPLC, but not treated with soman. Panels B and D, human plasma treated with soman before digestion with pepsin and fractionation by HPLC. Soman-labeled albumin peptides of 1880 and 1993 amu include 162 amu from soman.

sensitivity. Tyr411 is present in both peptides (indicated by the star), supporting the proposal that soman binds covalently to Tyr411 of human albumin in plasma. Peptides with an added mass of 162 from soman, but not with an added mass of 78 were found. This indicates that the soman adduct does not lose the pinacolyl group when soman is bound to albumin. Thus, the soman–albumin adduct does not age.

An additional experiment was performed to demonstrate by a second mass spectrometry method that soman was covalently bound to Tyr 411 of human albumin. HPLC fraction 21 containing the soman-labeled albumin peptide at 1880 *m/z* was infused into the Q-Trap, quadrupole mass spectrometer. The enhanced mass spectrum showed a peak at 940.7 *m/z*, which is consistent with the doubly charged form of the 1880 peptide. This peptide was subjected to collision-induced dissociation. The resulting enhanced product ion spectrum yielded amino acid sequence information consistent with the sequence VRYT-KKVPQVSTPTL, with soman covalently bound to tyrosine (see Figure 2).

The prominent peak at 898.6 *m/z* is a doubly charged ion, 42 mass units less than the parent ion at 940.7 *m/z*. This is consistent with the loss of the pinacolyl group (84 mass units) from the doubly charged parent to form a doubly charged product retaining methylphosphonic acid. A comparable 42 amu loss from the parent ion was seen in the enhanced product ion spectrum of the LVRYTKKVPQVSTPTL peptide (data not shown). Preferential loss of the pinacolyl group seems to be a characteristic feature of soman-labeled peptides when they are fragmented in the mass spectrometer, as the soman-labeled butyrylcholinesterase peptide also lost the pinacolyl group during the collision process (32, 33).

The 940.7 *m/z* parent ion in Figure 2 included the pinacolyl group of soman. This is a significant point because it demonstrates that soman had not lost the pinacolyl group while bound to intact albumin protein or during digestion and HPLC separation. The pinacolyl group only dissociated when the peptide was subjected to collision-induced dissociation in the

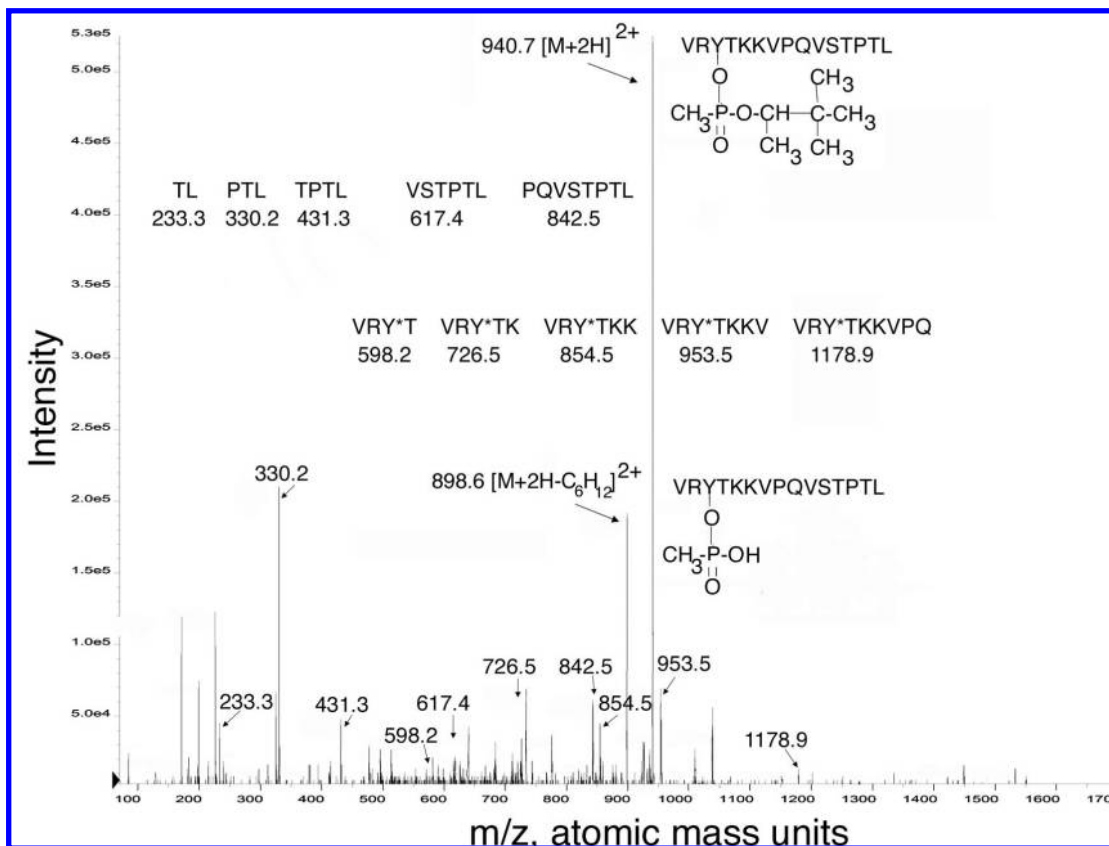


**Figure 2.** Product ion spectrum of the soman-labeled human albumin peptic peptide. The doubly charged parent ion at 940.7  $m/z$  yielded fragments consistent with the sequence VRY\*TKKVPQVSTPTL, where \* indicates soman covalently bound to tyrosine 411. The accession number for human albumin is GI:28592. In this resource, Tyr 411 is given as Tyr 435 because the numbering begins with the 24-amino acid signal peptide.

mass spectrometer. The presence of the pinacolyl group in the parent ion demonstrates that soman did not age when bound to albumin.

At least four separate ion series from the VRYTKKVPQVSTPTL peptide could be extracted from the spectrum in Figure 2. Only the y and b ion series are indicated in the Figure for the sake of clarity.

The peptide [VRY\*T]KKV[PQ] was seen as part of the b-ion series. The masses of all five observed fragments were consistent with the indicated amino acid sequence plus 78 amu for the added mass of a methyl phosphonic acid. The only residue in this sequence capable of forming a methyl phosphonic acid adduct is the tyrosine, establishing this as the modified amino acid in the peptide. The presence of a 78 amu added mass on the observed fragments, rather than 162 amu, indicates that the pinacolyl group is dissociated from the peptide, in the collision chamber, prior to the onset of backbone fragmentation.

The peptide [PQ][VS]TP[TL] was seen as part of the y-ion series. The masses of the observed fragments were consistent with only the amino acids, unencumbered with any adduct mass. Thus, the potentially phosphorylated serine was not labeled, supporting the assignment of the tyrosine as the modified amino acid.

The complete amino acid sequence of peptide VRY\*TKKV PQVSTPTL was represented by these two ions. These results confirm the conclusion that soman covalently binds to Tyr 411 of human albumin.

### 3.2. Kinetics for the Phosphorylation of Albumin by Soman and for the Reactivation of Phosphorylated Albumin.

**3.2.1. Phosphorylation of Albumin by Soman.** Because of the low reactivity of albumin with esters, aryl amides (1, 3),

and DFP (10), a low soman phosphorylation rate was expected. Therefore, the phosphorylation of albumin by soman was carried out under second-order conditions (3, 34), that is, the initial concentrations of soman,  $[S]_0$ , and albumin,  $[A]_0$ , were not very different. As a result, the concentrations of the uncomplexed forms of both reactants varied with time during the reaction.

Albumin (0.78 mM) was phosphorylated by sub and super-stoichiometric amounts of racemic soman (0.32 to 1.3 mM) that inhibited albumin's aryl acylamidase activity. Reaction was monitored by following albumin's aryl acylamidase (AAA) activity. Inspection of the inhibition time courses (Figure 3) indicated that less albumin was inhibited by soman than would have been expected from a stoichiometric reaction with the total amount of soman in the reaction. For example, in the presence of a 2-fold excess of soman, 100% inactivation of the AAA activity of albumin was never reached. The titration plot (not shown) for 0.78 mM albumin incubated with different concentrations of soman (0.38, 0.65, 0.81, and 1.30 mM) confirmed this observation. This suggests either that a large part of soman spontaneously hydrolyzed in the nucleophilic Tris/HCl buffer at pH 8.0 or that albumin reacted stereoselectively with specific stereoisomers of soman.

#### 3.2.2. Determination of Fluoride Released during the Reaction of Soman with Albumin.

In an effort to decide whether the substoichiometric reaction of soman with albumin was due to a competing spontaneous hydrolysis of soman or to a stereoselective reaction of albumin with soman, ionometric measurements of fluoride released from soman in the presence and absence of albumin were performed (Figure 4). It was found that spontaneous hydrolysis of soman in 60 mM Tris/HCl buffer at pH 8.0 at 25 °C was high. The rate constant for hydrolysis

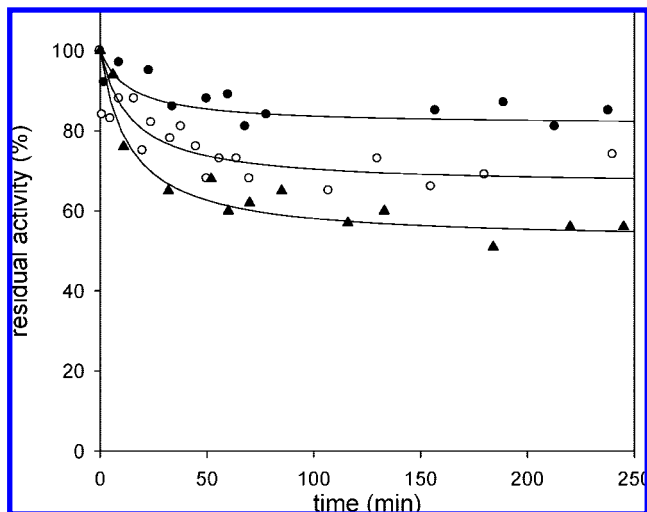


**Figure 3.** Progressive inhibition of the AAA activity of FAF-HSA ( $[E] = 0.78$  mM) by different concentrations of racemic soman ( $\bullet$ , 0.324 mM;  $\circ$ , 0.520 mM;  $\blacktriangle$ , 0.780 mM) in 60 mM Tris/HCl buffer at pH 8.0 at 25 °C. A plot of % residual AAA activity of albumin vs time. The progress curves reach a plateau after consumption of the reactive soman.

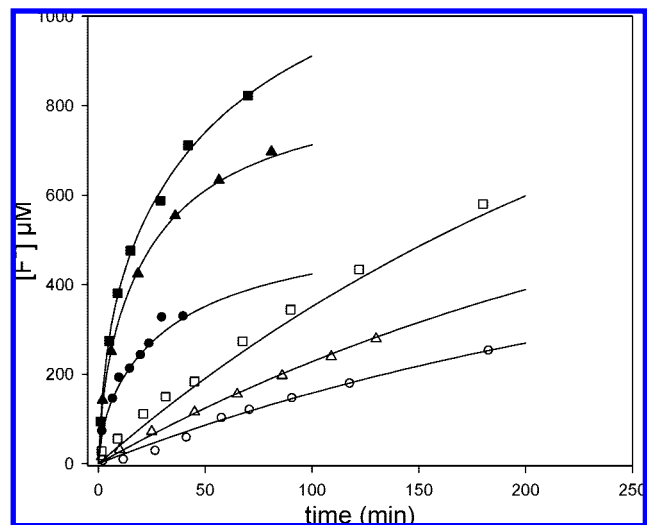


**Figure 4.** Time course of fluoride ions released from soman, in the presence and absence of FAF-HSA. Soman ( $[S]_0 = \bullet\circ$ , 0.52,  $\blacktriangle$ , 0.78,  $\blacksquare$ , 1.3 mM) was incubated with albumin ( $[E] = 0.78$  mM) (filled symbols), or soman was incubated by itself through spontaneous hydrolysis (open symbols on continuous curves). Both reactions were in 60 mM Tris/HCl at pH 8.0.

of soman ( $k_{h0}$ ) was  $0.00342 \pm 0.00007 \text{ min}^{-1}$ . In the presence of albumin, the rate of fluoride release was significantly higher. Semiquantitative analysis of progress curves shows not only that spontaneous hydrolysis of soman occurred at rates comparable to the phosphorylation rates of albumin but also that albumin itself provides a physicochemical environment that enhances the spontaneous hydrolysis of soman. The following is an example of this semiquantitative analysis.

The filled squares in Figure 4 describe the release of fluoride after mixing 1.3 mM soman with 0.78 mM FAF-HSA. After 100 min of incubation, 0.3 mM albumin was inhibited (see Figure 3) so that the phosphorylation of albumin accounts for 0.3 mM of released fluoride. Over this time period, about 0.9 mM fluoride was released. Spontaneous hydrolysis of 1.3 mM soman ( $\square$  in Figure 4) accounts for about 0.35 mM of released fluoride. This leaves about 0.25 mM fluoride unaccounted for. Thus, the release of this extra fluoride suggests that the hydrolysis of soman at pH

8.0 is faster in the presence of albumin than in buffer alone. However, dephosphorylation of the Tyr411 adduct is far too slow ( $0.0044 \pm 0.0008 \text{ h}^{-1}$ ; see section 3.2.5) to account for this albumin-dependent hydrolysis of soman. Thus, this suggests that this catalysis takes place at a different site. However, only one soman adduct on albumin was detected by MALDI-TOF. This finding is consistent with reports on the phosphorylation of bovine serum albumin by FP-biotin (18) and the phosphorylation of human serum albumin by diisopropylfluorophosphate (9). Therefore, it may be hypothesized that albumin-mediated hydrolysis of soman occurs via a mechanism that does not involve a covalent intermediate. Nevertheless, this catalytic effect is extremely weak, about 2 times higher than spontaneous hydrolysis, and may be tentatively regarded as a nonenzymatic, physicochemical interfacial reaction. However, we cannot rule out the existence of a second active center.

**3.2.3. Is There Enantioselectivity in the Reaction of Albumin with Soman?** Racemic soman is an equimolar mixture of four stereoisomers. Though experiments on the release of fluoride argue against the enantioselectivity of albumin for certain soman isomers, the possibility that albumin's reaction with soman is stereoselective was tested directly using  $^{31}\text{P}$  NMR. Each of the intact isomers of soman (Ps- and Pr-) generates a doublet in  $^{31}\text{P}$  NMR (Figure 5, panel A). Soman completely hydrolyzed in 5 N sodium hydroxide gives methylphosphonate (MP) (Figure 5, panel B); the hydrolysis of soman at pH 8.0 gives pinacolyl methylphosphonate PMP (Figure 5, panel D) (35).

The reaction between 1.3 mM racemic soman and 0.78 mM albumin was monitored over 24 h by recording  $^{31}\text{P}$  NMR spectra. Initial spectra showed the progressive disappearance of the intact soman peaks with the concomitant appearance of three broader resonance peaks, of 80 Hz line width (Figure 5, panel C). After 2 h of incubation, signals for intact soman had vanished. At this point in the reaction, the spectrum of the products was compared to a spectrum of methylpinacolyl phosphonate (MPP). MPP, created under mild conditions of hydrolysis, showed a peak at 23.74 ppm. That peak was unaffected by the presence of albumin (Figure 5, panel D). The most prominent peak in the soman/albumin reaction mixture (the 23.74 ppm peak, f, in Figure 5, panel C) can therefore be assigned to MPP. For longer reaction times (up to 24 h), the MPP peak increased at the expense of the other two peaks in Figure 5, panel C. This strongly suggests that peaks e and d (at 25.59 and 27.56 ppm) correspond to the Ps- and Pr-covalent adducts of soman bound to albumin and that there is a slow, spontaneous release of MPP from the of phosphonylated albumin. Such a release can be described as reactivation.

The fact that after 2 h of reaction between albumin and soman, adduct peaks d and e have the same intensity indicates that albumin reacted with the same probability with both the Ps- and Pr- soman enantiomers. Thus, there is no enantiomeric preference of albumin for the soman isomers.

**3.2.4. Effect of MPP on Phosphorylation of Albumin by Soman.** Because a large part of soman was hydrolyzed into MPP in Tris buffer at pH 8.0 during the time course of the phosphorylation reaction (Figure 5, panel C), we tested the hypothesis that MPP could compete with soman for noncovalent binding to the Tyr411 site and thereby slow down the phosphorylation reaction. We found that phosphorylation of (0.75 mM) albumin by soman (1.3 mM) in the presence of 1.3 mM MPP caused no change in the progressive inhibition of the AAA activity of albumin. Thus, MPP does not compete with soman.

**3.2.5. Spontaneous Reactivation of Soman-Inhibited Albumin Monitored by  $^{31}\text{P}$  NMR and MALDI-TOF.** Fluoride has been shown to promote dephosphorylation of albumin (36).

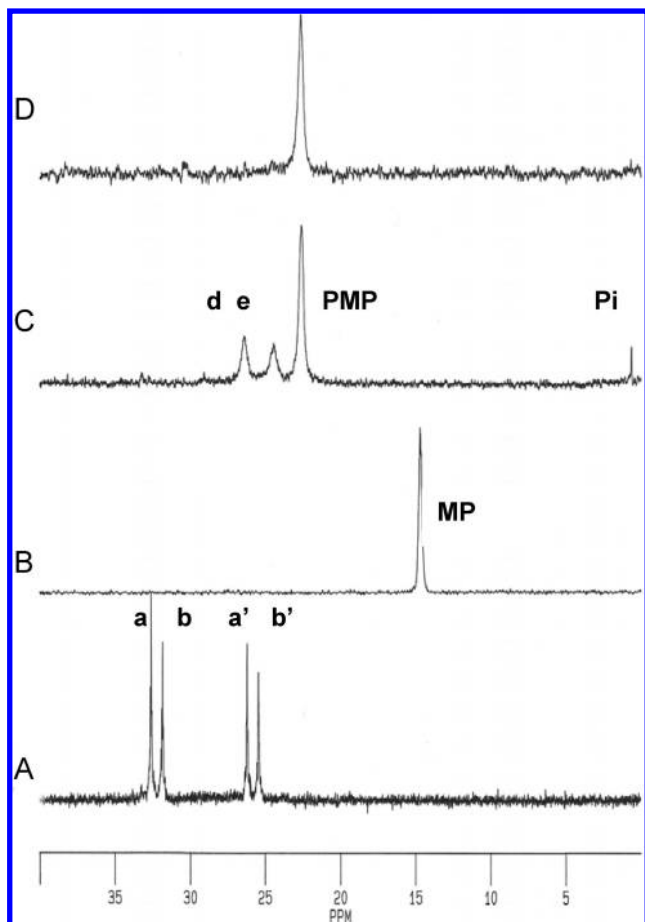


**Figure 5.**  $^{31}\text{P}$  NMR spectra of soman in the presence and absence of albumin. Panel A shows 2 mM racemic soman in dimethylsulfoxide- $d_6$ . The four stereoisomers are indistinguishable. The four resonance peaks correspond to the two doublets of the two pairs of diastereoisomers (35). Panel B shows methyl phosphonate (MP) (a product of soman hydrolysis in 5 N NaOH). Panel C shows 1.3 mM racemic soman after reaction (2 h) with 0.78 mM albumin, in 60 mM Tris/HCl at pH 8; d and e correspond to the  $P_R$  and  $P_S$  adducts of albumin, and f is the product of the spontaneous hydrolysis of soman and methyl pinacolyl phosphonate (MPP). Panel D shows 1.3 mM methyl pinacolyl phosphonate (MPP) in the presence of 1.3 mM albumin. The observed peak is that of uncomplexed MPP (35).

However, because of the low nucleophilicity of fluoride ion, it seems unlikely that reactivation was mediated by the fluoride ions released during the phosphorylation step ( $[\text{F}^-] \leq 1.3 \text{ mM}$  for the highest soman concentration used). Following the reactivation rate by measuring the recovery of the AAA activity was not accurate; therefore,  $^{31}\text{P}$  NMR spectral kinetics was used instead.

FAF-HSA (1.3 mM) was inhibited by 1.3 mM soman (10% isopropanol, final). We followed the decrease of the integrated area of the NMR peaks corresponding to the soman–albumin adduct (peaks d + e in Figure 5, panel C) from 10 to 60 h (Figure 6). Because no soman was left after 10 h of incubation, because of its spontaneous hydrolysis ( $\text{S} \rightarrow \text{S}'' + \text{F}^-$ ) and to its reaction with albumin (see Scheme 1), the change in the concentration of the soman–albumin conjugate ( $\text{A-S}'$ ) was due only to reactivation ( $k_r$ ). It was assumed that the process was uncompromised and followed pseudo-first-order kinetics (eq 1):

$$[\text{A-S}']_t = [\text{A-S}']_{10\text{h}} \cdot e^{-k_r(t-10)} \quad (1)$$

The relative intensity at  $t = 10 \text{ h}$  was  $0.54 \pm 0.01$ ; this is equivalent to  $0.700 \pm 0.015 \text{ mM}$  of conjugate. Fitting the data from Figure 6 to eq 1 provided the reactivation constant,  $k_r =$

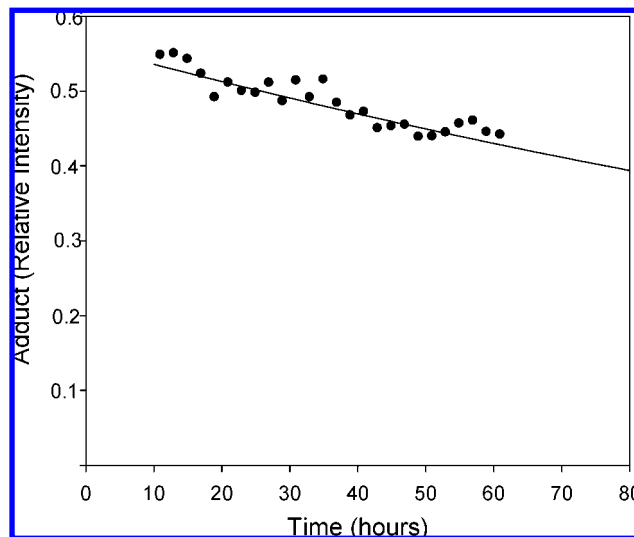
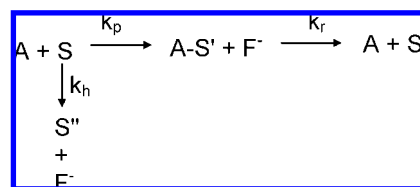


**Figure 6.** Reactivation kinetics by  $^{31}\text{P}$  NMR. Each point represents the integrated area of the NMR peaks (d + e). The areas, in turn, correspond to the relative amounts of adduct. The line is from a fit of the data to eq 1.

**Scheme 1**



$0.0044 \pm 0.0008 \text{ h}^{-1} = 0.000073 \pm 0.000013 \text{ min}^{-1} = 0.74 \pm 0.13 \text{ week}^{-1}$ . Thus the half-time for decay of the soman–albumin adduct at pH 8.0 and  $25^\circ\text{C}$  is about 1 week.

The stability of the soman–albumin adduct was also measured by mass spectrometry. Soman-labeled albumin was digested with pepsin to release labeled and unlabeled Tyr411 peptides after various periods of incubation. The peptide masses and the area of each peak were determined by MALDI-TOF in reflector mode. Figure 7A shows a scan, after 24 h, where the highest peaks at 1992.1 and 1879.0 have soman bound to Tyr411 in peptides LVRYTKKVPQVSTPTL and VRYTKKVPQVSTPTL. At a later time point after the adduct had been incubated at pH 7.4 and  $22^\circ\text{C}$  for 768 h, the unlabeled peptides at 1717.0 and 1830.1 have a higher intensity than the labeled peptides (Figure 7B). The % label on Tyr411 was calculated from cluster areas and plotted in Figure 7C as a function of time. The half-life for decay of the soman–albumin adduct at pH 7.4 and  $22^\circ\text{C}$  was 20 days. The time course in Figure 7C is first order for nearly two half-lives, supporting the proposal that reactivation is a simple first order process. The difference in rate constants obtained from the mass spectrometry and the NMR experiments is consistent with expectation for the difference in pH.

**3.2.6. Progressive Binding of Soman to Tyr411 of Albumin Monitored by  $^{31}\text{P}$  NMR Kinetics.** The complete reaction path of albumin (A) with soman (S) can be depicted by Scheme 1, which includes the competing spontaneous hydrolysis of soman, second-order phosphorylation of albumin, followed by hydrolytic dephosphorylation (reactivation of the AAA activity of albumin).

In Scheme 1,  $k_p$  is the rate constant of phosphorylation,  $k_r$  is the rate constant of dephosphorylation (spontaneous reactivation of phosphorylated albumin  $\text{A-S}'$ ), and  $k_h$  is the rate of the

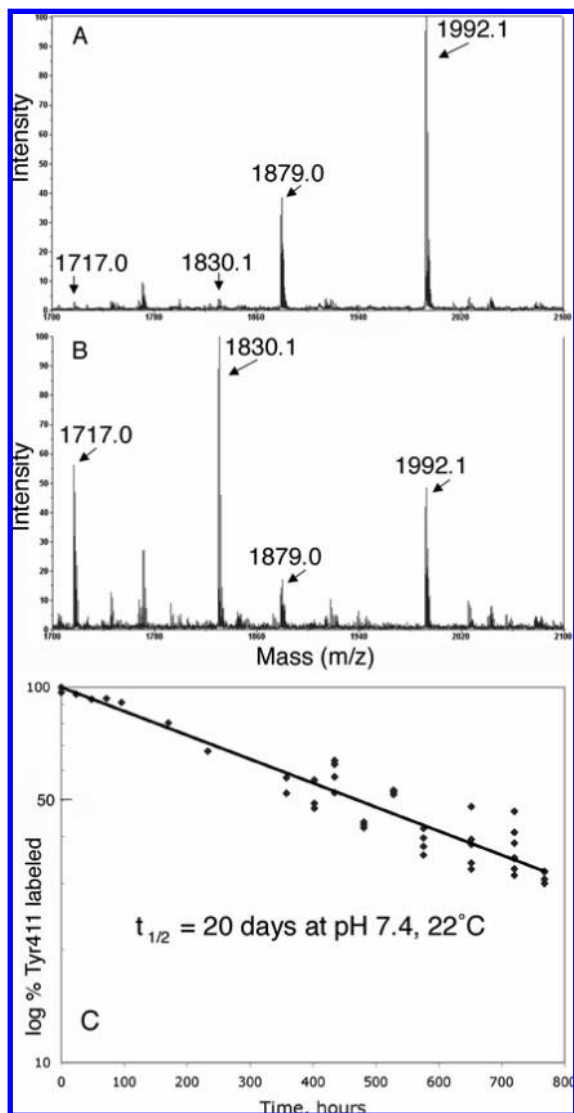


**Figure 7.** Stability of the soman–albumin adduct calculated from mass spectrometer data. Panels A and B are MALDI-TOF spectra of pepsin-digested, soman-labeled human albumin after 24 and 768 h incubation, respectively, at pH 7.4 and 22 °C. Panel C is a plot of % Tyr411 labeled by soman, as a function of time of incubation of the soman–albumin adduct. The soman–albumin adduct decays with a half-life of 20 days.

spontaneous hydrolysis of soman.  $F^-$  is the fluoride leaving group and  $S''$  the hydrolysis product, methyl pinacolyl phosphonate (MPP). It follows then that the concentration of all species as a function of time is described by a system of differential equations (eq 2) as follows:

$$\begin{aligned}
 \frac{d[A]}{dt} &= -k_p \cdot [A][S] + k_r \cdot [AS'] \\
 \frac{d[S]}{dt} &= -k_p \cdot [A][S] + k_h \cdot [S] \\
 \frac{d[AS']}{dt} &= -\frac{d[A]}{dt} \\
 \frac{d[S'']}{dt} &= -k_r \cdot [AS'] + k_h \cdot [S] \\
 \frac{d[F^-]}{dt} &= -\frac{d[S]}{dt}
 \end{aligned} \quad (2)$$

Because the concentration of soman and albumin are of the same order of magnitude and because the rates of spontaneous hydrolysis of soman and phosphorylation of albumin are of the

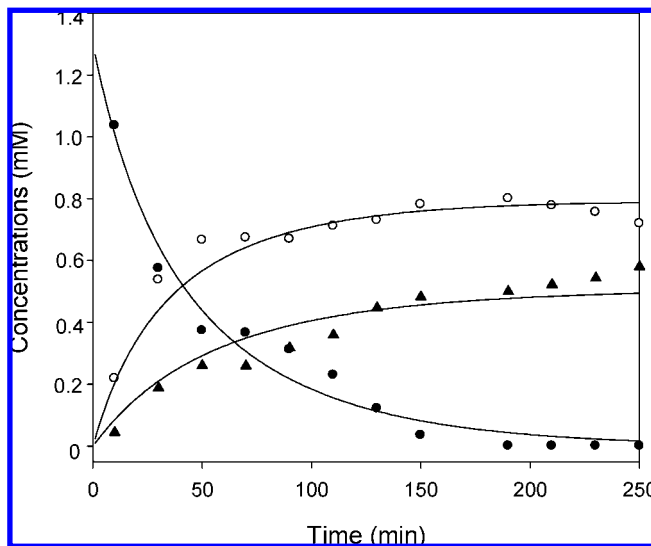


**Figure 8.** Time course of the reaction between 1.3 mM soman and 1.3 mM albumin monitored by  $^{31}\text{P}$  NMR: ●, soman; ○, adduct; ▲, MPP. The points were measured data. The lines are from numerical fitting of the data to eq 2.

same order of magnitude, it is not possible to make assumptions allowing a simple integration of the system. However, a numerical solution of the system can be obtained using mathematical software such as Mathematica.

Following the residual AAA activity of albumin allows only the measurement of  $d[A]/dt = -d[AS']/dt$ , while measuring the release of  $F^-$  gives only  $d[F^-]/dt = d[S]/dt$ . However, following the reaction kinetics by  $^{31}\text{P}$  NMR gives  $d[S]/dt = -d[F^-]/dt$ ,  $d[AS']/dt = -d[A]/dt$ , and  $d[S'']/dt$  in one single experiment (Figure 8).  $k_r$  was measured separately under the same experimental conditions ( $k_r = 0.0044 \pm 0.0008 \text{ h}^{-1}$ ; see section 3.2.4 and Figure 6).

Fitting the numerical solution of the differential equation system against  $^{31}\text{P}$  NMR data gave  $k_p = 15 \pm 3 \text{ M}^{-1} \text{ min}^{-1}$  and  $k_h = 0.0076 \pm 0.005 \text{ min}^{-1}$ . Thus, the rate constant for spontaneous hydrolysis of soman in the presence of albumin ( $k_h$ ) is about 2 times the rate for the spontaneous hydrolysis of soman in the absence of albumin ( $k_{h0} = 0.00342 \pm 0.00007 \text{ min}^{-1}$ , from section 3.2.2). This value for  $k_h$  is in agreement with the estimate for  $k_h$  made from the measurement of  $[F^-]$  release, as described in section 3.2.2.

**3.3. Molecular Modeling.** The crystal structure of HSA with numerous ligands has been described (5). A comparison between these structures shows that Val433 located in the pocket containing Tyr411 might adopt two different conformations depending on the occupant of the pocket. These alternate conformations change the diameter of the pocket and may affect the binding of soman in the pocket. Therefore, we docked soman with both representative crystal structures: 2bxd displaying a narrower pocket in absence of ligand and 2bxh displaying a wider pocket that develops when indoxyl sulfate is bound. The four diastereoisomers of soman were docked in both structures.

**3.3.1. Noncovalent Docking by Autodock.** Key values from the noncovalent docking results are summarized in Table 1. All four stereoisomers of soman bind better to HSA when the pocket is narrowed by the conformational change of Val433 (2bxd). A narrower pocket provides more stabilizing van der Waals interactions between soman and the residues of the pocket. Therefore, it is expected that the actual conformation of HSA when in complex with soman is similar to that of 2bxd. For 2bxd, the estimated affinity constants for all four stereoisomers

**Table 1. Non Covalent Docking of Soman in the Tyr411 Pocket of HSA Performed by Autodock**

soman isomer	HSA pdb structure	docked energy (kcal.mol <sup>-1</sup> )	estimated $K_d$ ( $\mu$ M)
$P_S C_R$	2bxd	-5.69	148
	2bxh	-5.56	167
$P_S C_S$	2bxd	-5.76	115
	2bxh	-5.48	206
$P_R C_R$	2bxd	-5.69	147
	2bxh	-5.50	176
$P_R C_S$	2bxd	-5.73	128
	2bxh	-5.42	226

are virtually identical:  $K_d = 134 \pm 16 \mu\text{M}$  (Table 1). The pocket seems to be large enough to accommodate all enantiomers of soman (Figure 9). Soman binds with the pinacolyl group stacked against the disulfide bridge formed by Cys392-Cys438. The pinacolyl group makes many hydrophobic contacts with the side chains of Val433, Ile388, Ala449, Phe395, Phe403 and the main chain of Gly434. The binding conformation of soman is largely dictated by its carbon stereocenter. Indeed,  $P_S C_S$  and  $P_R C_S$  display the same binding conformation (rmsd = 0.07 Å), except that the positions of the fluoride and phosphonate oxygen are inverted as a result of the difference in stereochemistry at the phosphorus. The same applies to the  $P_S C_R$  and  $P_R C_R$  stereoisomers (rmsd = 0.13 Å). This inversion between the fluoride and phosphonate oxygen does not cost much energy of binding because of the lack of specific interactions between these atoms and residues of the pocket. The phosphorus atom is separated from the hydroxyl of Tyr411 by a distance ranging from 6.80 Å ( $C_R$  enantiomers) to 7.24 Å ( $C_S$  enantiomers). This distance is not suitable for a nucleophilic attack of Tyr411 on the phosphorus and explains the slow reactivity of soman toward HSA. It looks like soman may randomly react with Tyr411 on its way in/out of the pocket.

**3.3.2. Noncovalent Docking by Gold.** In order to check the dependency of the results on the software, to test the robustness of the models obtained by Autodock, and also to generate as many conformers as possible, we decided to repeat the docking simulations using another software, Gold, version 3.1. Gold gave us the possibility of using two scoring functions, Goldscore (force-field-based like Autodock) and Chemscore (empirical, i.e., optimized on a test set of protein-ligand complexes). We performed the docking simulations using both the 2bxh and the 2bxd protein structures. Our results did not show any significant

difference between the structures; therefore, we describe here only the results obtained with the minimized 2bxh protein.

We docked the four enantiomers of soman with the minimized 2bxh protein using Gold/Goldscore. The best conformers obtained were similar to the ones obtained by Autodock. The pinacolyl moiety is located at essentially the same place obtained by Autodock (Figure 9); the difference is only a small translation of Tyr411 in the direction of the phosphorus atom ( $P\text{-OH}_{Y411}$  distances vary from 6.37 to 6.67 Å). As described for Autodock, the rotation of the P (O, F, Me) moiety is relatively free; this is not surprising because of the lack of specific interactions of these atoms with residues of the active site pocket. Again, the phosphorus atom is at a position that does not permit easy phosphorylation of Tyr411. The scores obtained were in the same range for all enantiomers:  $P_S C_S = 39.93$ ,  $P_S C_R = 40.09$ ,  $P_R C_R = 41.28$ , and  $P_R C_S = 38.16$ . We obtained very similar results in terms of conformers and energies when we used Autodock or Gold with either 2bxh or 2bxd, which clearly shows the robustness of the models in Figure 9.

The Chemscore function is empirical. It can potentially generate different binding modes because contributions of intermolecular interactions are not the same as those with Goldscore or Autodock. The docking using Gold/Chemscore gave different kinds of conformers than Goldscore, but with very small changes in energy. Within the different clusters, some models displayed a phosphorus atom close to Tyr411 ( $P\text{-OH}_{Y411}$  distances:  $P_R C_R = 4.33$  Å,  $P_R C_S = 3.51$  Å,  $P_S C_S = 3.98$  Å, and  $P_S C_R = 3.41$  Å). The enantiomers with  $P_R$  configuration have a P-F in a favorable position for a nucleophilic attack ( $\text{OH}_{Y411}\text{-P-F}$  angle:  $P_R C_R = 155^\circ$ ,  $P_R C_S = 138^\circ$ ,  $P_S C_S = 42^\circ$ , and  $P_S C_R = 45^\circ$ ). Chemscore docking simulation generated a prephosphorylation complex (fluorine opposite  $\text{OH}_{Y411}$  and hydrogen bonding between  $\text{P}=\text{O}$  and  $\text{OG}_{S489}$ ) for the two  $P_R$  enantiomers. These results suggest that the prephosphorylation step would be energetically more favorable for the  $P_R$  than for the  $P_S$  enantiomers. To compare these models with the previous ones, we rescored the prephosphorylation complexes with conformers  $P_R C_R$  and  $P_S C_S$  by the Goldscore function and obtained 10.78 and 27.07, respectively. Compared to the Gold/Goldscore results (41.28 and 38.16), the rescoring clearly indicates that the ligand positions in the prephosphorylation complexes are not energetically favorable. Therefore, the Chemscore results do not contradict the previous conclusions obtained from the Autodock and Gold/Goldscore dockings.

These docking results may explain why the reactivity of soman with HSA is so poor. First, the binding affinity is weak ( $K_d = 134 \mu\text{M}$ ). Second, the phosphorus does not bind in a position that is favorable for reaction with Tyr411. The docking results also suggest that a higher bimolecular rate constant is probable in the case of  $P_R$  enantiomers. But because of the poor reactivity and the limited measurement accuracy, an increased reactivity of the  $P_R$  enantiomers was not experimentally observed.

**3.3.3. Covalent Docking by Gold.** The noncovalent docking of soman to the HSA protein showed a low enantioselectivity. In order to confirm this finding, we covalently docked the four enantiomers of soman to the 2bxh form of albumin and compared energies (or scores). We used the software Gold, version 3.1, which permits covalent docking. As done before, dockings were scored by the functions Goldscore and Chemscore. To discriminate the conformers obtained by Gold/Goldscore or Gold/Chemscore dockings, we calculated the energies of soman-protein complexes using mopac-pm3, a

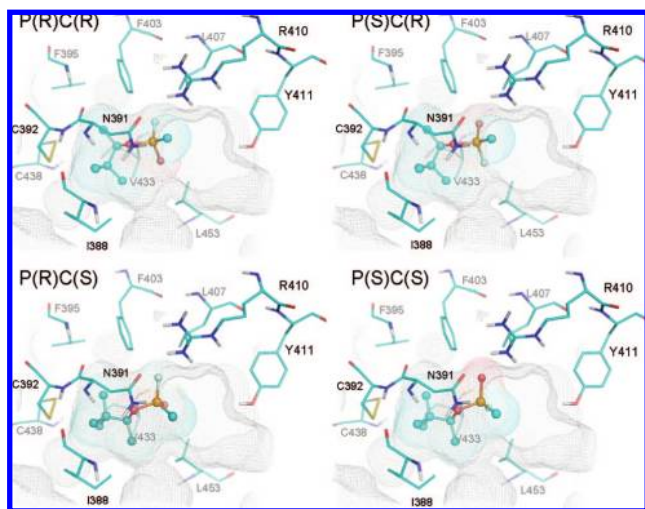


**Figure 9.** Models of soman noncovalently docked into albumin. The various stereoisomers of soman were docked in the estero-amidase active center (Tyr411) of HSA using Autodock software.

**Table 2. Covalent Docking of Soman in HSA Performed by Gold<sup>a</sup>**

soman isomer	Goldscore/ $\Delta H_f$	Chemscore/ $\Delta H_f$
P <sub>S</sub> C <sub>R</sub>	11.68/489.8	15.95/519.3
P <sub>S</sub> C <sub>S</sub>	16.88/483.2	17.43/514.7
P <sub>R</sub> C <sub>R</sub>	15.67/529.0	16.46/497.8
P <sub>R</sub> C <sub>S</sub>	12.88/480.4	14.55/539.8

<sup>a</sup> Scores (Goldscore and Chemscore) have no units. Enthalpies of formation ( $\Delta H_f$ ) are in kcal·mol<sup>-1</sup>.

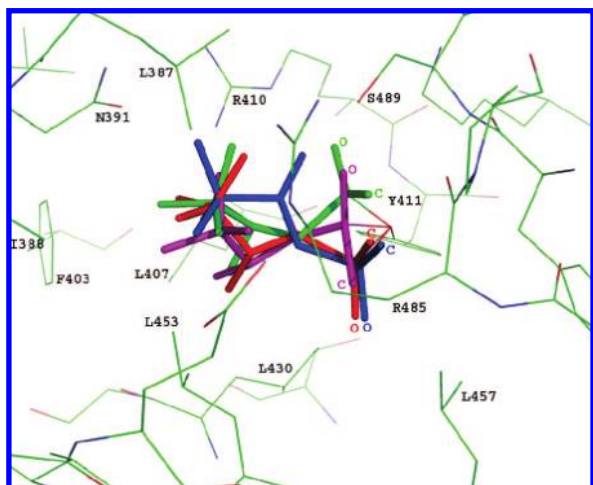


**Figure 10.** Models of soman covalently docked into albumin. Various enantiomers of soman were docked into Tyr 411 of HSA (form 2bxh) using Gold software, version 3.1. P<sub>S</sub>C<sub>S</sub> (blue), P<sub>S</sub>C<sub>R</sub> (red), P<sub>R</sub>C<sub>R</sub> (magenta), and P<sub>R</sub>C<sub>S</sub> (green).

semiempirical method, and selected those with the lowest  $\Delta H_f$ . The results are summarized in Table 2.

The four models are superimposed in Figure 10. The position of the tertiary butyl group is well conserved for all enantiomers (it points to Leu387, Ile388, Asn391, and Phe403), while the P = O points to Leu430 and Leu457 for P<sub>S</sub>C<sub>R</sub> or P<sub>S</sub>C<sub>S</sub> enantiomers, Ser489 (hydrogen bonding with OH) for P<sub>R</sub>C<sub>R</sub>, and R410 for P<sub>R</sub>C<sub>S</sub>. The conformers P<sub>S</sub>C<sub>S</sub> and P<sub>S</sub>C<sub>R</sub> are nearly perfect mirror images, the only difference being the position of the CH<sub>3</sub> bond to the asymmetric carbon that points to Leu430 for C<sub>R</sub> and Arg410 for C<sub>S</sub>. In the case of P<sub>R</sub>, there are more differences between the two enantiomers because the P<sub>R</sub>C<sub>R</sub> enantiomer is the only one that allows hydrogen bonding with Ser489 without having too many disfavored van der Waals interactions. (Arg410 constrains the position of the CH<sub>3</sub> bond to C\*.) The mopac-pm3  $\Delta H_f$  values are in the same order of magnitude ( $\sim 490 \pm 10$  kcal·mol<sup>-1</sup>), showing no thermodynamic enantioselectivity.

## 4. Discussion

### 4.1. Roles for Albumin and Albumin/Soman Adducts in the Monitoring of and Protection against Soman Exposure.

**4.1.1. Scavenging OP.** The reaction of albumin with soman was found to be slow ( $k_p = 15 \pm 3$  M<sup>-1</sup> min<sup>-1</sup> at pH 8.0). This is in agreement with the slow rate of reaction of albumin with the nerve agent simulant, DFP (75 M<sup>-1</sup> min<sup>-1</sup> at pH 8.2) (10). Combined with the high concentration of albumin present in plasma (0.6 mM), the apparent pseudo-first-order rate constant for the reaction of albumin with soman would be 0.009 min<sup>-1</sup> ( $t_{1/2} = 77$  min). Thus, despite its high concentration in blood, stoichiometric scavenging of soman by albumin is not expected to play a major role in protection against acute poisoning. Regardless of the low reactivity, significant amounts of OPs are bound to albumin upon in vivo exposure. For example, when

mice were injected with small amounts of the organophosphonate, FP-biotin (10-fluoroethoxyphosphinyl-*N*-biotinamido pentyldecanamide), amounts that produced no toxic signs, albumin was the most abundantly labeled protein in plasma (46), making it the dominant stoichiometric scavenger. In vitro pretreatment of plasma with a variety of organophosphates (malaoxon, paraoxon, chlorpyrifos oxon, methyl paraoxon, dichlorvos, diisopropylfluorophosphate, diazoxon, and echothiophate) reduced the subsequent reaction of FP-biotin with albumin, indicating that all of these other OPs also react with albumin (46). This strongly suggests that albumin will also be a scavenger for these OPs in vivo.

Although albumin displays a low reactivity toward OPs compared to that of cholinesterases and other known secondary biological targets of OPs (37), the large quantity of albumin in blood circulation and lymph may provide a substantial reservoir for sequestering OPs. We also found that phosphorylated albumin slowly self-reactivates. Though the catalytic OPase activity is associated with HSA, and Tyr411 is slow and thus toxicologically insignificant, it may be hypothesized that mutants of albumin capable of hydrolyzing OPs at high rate could be used for the detoxification of soman in vivo.

**4.1.2. Biomarker.** Phosphorylated albumin may prove to be a useful biological marker of soman exposure (11). The sensitive mass spectrometry methods used by Black et al. (11) and further developed in the present article could prove useful for the diagnosis of soman exposure. In particular, it has been shown that soman tyrosine adducts can be detected at least up to 7 days post exposure in guinea pigs (38). Advantages of a soman–albumin biomarker include its stability and the absence of aging. The half-life for spontaneous reactivation is estimated to be about 1 week at pH 8.0 and 25 °C, and 20 days at pH 7.4 and 22 °C, making the soman–albumin adduct suitable for retrospective studies. The absence of aging means that soman exposure can be unambiguously identified because the soman–albumin adduct does not lose the diagnostic pinacolyl group. Our finding that soman–albumin adducts do not age confirms the reports that there is no loss of alkoxy groups from soman–, sarin–, or DFP–albumin adducts (11, 19, 36). In addition, it has recently been shown that OP–albumin conjugates do not appear to be reactivatable by oximes used as antidotes of OP poisoning. Therefore, the detection of Tyr411 adducts in plasma may be possible, even though individuals exposed to OPs have received effective oxime therapy (38).

Another potential method of monitoring for soman exposure is through the use of antibodies. The information presented in this work raises interesting possibilities regarding the generation of antibodies to the soman–albumin adduct. The noteworthy aspect of the soman–albumin adduct in this regard is that Tyr411 is located on the surface of albumin. A soman–albumin adduct at Tyr411 therefore becomes a viable target for antibodies, unlike the soman adducts of cholinesterases, which are buried in a deep gorge well below the enzyme's surface. In addition, the surface location for the soman–albumin adduct suggests that people exposed to soman might normally produce antibodies against the soman–albumin adduct. This in turn suggests the possibility of monitoring exposure to soman by looking for those antibodies, long after the exposure incident has passed and long after the antigen has disappeared.

**4.2. Perspectives: Would Mutant Albumins Be Good OP Scavengers?** **4.2.1. Stoichiometric Scavenging.** The bimolecular rate constant for the phosphorylation of albumin,  $k_p$ , 15 M<sup>-1</sup> min<sup>-1</sup>, is about  $6 \times 10^6$  times slower than that for the inhibition of acetylcholinesterase and butyrylcholinesterase by

soman ( $\sim 9 \times 10^7 \text{ M}^{-1} \text{ min}^{-1}$ ). Because the concentration of soman in the most severe cases of poisoning would be far less than that of albumin in plasma, for example,  $<11 \text{ nM}$  (39), the reaction between albumin and soman would be pseudo-first-order. The pseudo-first-order rate expression can be rearranged (eq 3) so that the time,  $t$ , needed for a stoichiometric scavenger to reduce a concentration of a toxicant such as soman from  $[S]_0$  to  $[S]_t$  can be easily determined.

$$t = \frac{\ln([S]_0/[S]_t)}{k_p \cdot [E]} \quad (3)$$

Since the concentration of albumin in plasma is about 0.6 mM, it would take about 8.5 h to reduce the soman concentration by 100-fold ( $\ln [S]_0/[S]_t = 4.6$ ). Because, red blood cell acetylcholinesterase, plasma butyrylcholinesterase, and plasma paraoxonase react much faster than albumin with soman, the contribution of albumin to soman detoxification would take place only after the saturation of these enzymes (36).

**4.2.2. Catalytic Scavenging.** If we assume that the turnover of soman by albumin fits a Michael mechanism with a high  $K_m$ , then phosphorylation could appear to be second-order under our experimental conditions. If in addition,  $k_r < k_p$ , which is the case for the soman/albumin turnover, then  $k_{cat}/K_m$  is equal to  $k_p$ . Under these conditions,  $k_p$  defines the catalytic efficiency. Thus, the catalytic efficiency for the hydrolysis of soman by albumin, at Tyr411, is  $15 \text{ M}^{-1} \text{ min}^{-1}$ . This value is about 4 to 5 orders of magnitude lower than that for the hydrolysis of soman by *Pseudomonas diminuta* phosphotriesterase ( $6 \times 10^5 \text{ M}^{-1} \text{ min}^{-1}$ ) (40) or allozyme Q192 of human paraoxonase ( $2.6 \times 10^6 \text{ M}^{-1} \text{ min}^{-1}$ ) (41). Eq 4 gives the time needed for a catalytic scavenger to drop the concentration of a toxicant from  $[S]_0$  to  $[S]_t$ .

$$t = \frac{\ln([S]_0/[S]_t)}{(k_{cat}/K_m) \cdot [E]} \quad (4)$$

Thus, taking the estimated  $k_{cat}/K_m$  value, the time needed for the catalytic activity of albumin (0.6 mM) to decrease the soman concentration in blood by 100-fold would be about 9 h. It is therefore obvious that the reaction of soman at Tyr411 of HSA does not contribute significantly to the catalytic turnover of soman molecules in plasma. However, the in vitro observation that pure FAF-HSA promotes the hydrolysis of soman at a second site ( $k_h = 0.0076 \text{ min}^{-1}$ ) with a rate 100 times higher than the turnover at Tyr411 is important. The in vivo toxicological relevance of this chemical activity has to be demonstrated, but if proved, this process could contribute to the degradation of soman and other nerve agents in human plasma.

**4.2.3. Mutant Albumin.** Could mutants of recombinant human albumin be made into productive stoichiometric or catalytic scavengers for prophylaxis and treatment of OP poisoning? HSA is a nonglycosylated protein. Scaled-up production of recombinant human albumin (rHSA) in *Pichia pastoris* has been made possible for pharmaceutical purposes (42). This product exhibits good pharmacokinetics and biodistribution (43). Thus, rHSA would appear to be an ideal candidate for protein engineering.

To address the scavenger issue of rHSA, we have to first determine how much improvement in reactivity would be desired. As a reference, the reactivity of the currently accepted OP scavengers, serum butyrylcholinesterase and red cell acetylcholinesterase, were used. Comparison was made on the basis of the first-order rate constants. For the reaction of natural HSA with soman in plasma, the apparent pseudofirst order rate

constant,  $k_p \cdot [E]$ , is  $0.009 \text{ min}^{-1}$ . The sum of the first-order reaction rate constants for the reaction of soman with erythrocyte AChE and plasma BuChE is  $4.5 \text{ min}^{-1}$ . This number was arrived at by taking the concentration of AChE in blood to be about 2.5 nM, the concentration of BuChE to be 50 nM, and  $k_2/K_d$  to be about  $9 \times 10^7 \text{ M}^{-1} \text{ min}^{-1}$  for both enzymes. Thus, in blood, cholinesterases react with soman about 500 times faster than albumin does.

For an injected, mutated albumin to be used as a stoichiometric scavenger, it should react at least 500 times faster than the endogenous albumin to be competitive with the cholinesterases. There is a limit to the amount of plasma-derived albumin that can be put into the human body, that is, 25 g/100 mL (Albu Rx25) by slow infusion or 500 mg in 2 mL by intravenous injection. Injected into a human of 70 kg (3 L of plasma), 500 mg would give a final plasma concentration of mutant albumin of 166 mg/L ( $2.55 \times 10^{-6} \text{ M}$ ). To react faster than cholinesterases, the bimolecular rate constant of this amount of mutant albumin should be at least  $1.8 \times 10^6 \text{ M}^{-1} \text{ min}^{-1}$ . Compared to endogenous albumin ( $15 \text{ M}^{-1} \text{ min}^{-1}$ ), this is an efficiency improvement of about 5 orders of magnitude. Though there are few examples of evolved enzymes, showing enhancement of such a magnitude, site-directed mutagenesis and/or directed evolution can lead to dramatic improvement in the catalytic activity of enzymes. Improvements of 4 orders of magnitude for the glyphosate tolerance protein (44) and 5 orders of magnitude for  $\alpha$ -lytic protease (45) have been reported. Therefore, improving the reactivity of albumin against OPs for the purpose of making a stoichiometric scavenger would be a challenge, but it is possible.

In addition, the observed catalysis of soman hydrolysis on the albumin surface at a site different from Tyr 411 could also be improved. Work is in progress to identify this area on the albumin surface. Thus, stoichiometric and catalytic bioscavengers based on modified human albumins have to be considered as possible candidates.

**Acknowledgment.** We thank D. S. Darvesh (Department of Medicine, Dalhousie University, Halifax, Canada) for the gift of o-NTFAC. Mass spectra were obtained with the support of the Protein Structure core Facility at the University of Nebraska Medical Center. This work was supported by U.S. Army Medical Research and Materiel Command W81XWH-07-2-0034, Eppley Cancer Center grant P30CA36727, and NIH grant 1 U01 NS058056-02 (to O.L.), and DGA grant 03co010-05/PEA 01 08 7 (to P.M.).

## References

- (1) Sakurai, Y., Ma, S. F., Watanabe, H., Yamaotsu, N., Hirono, S., Kurono, Y., Kragh-Hansen, U., and Ottagiri, M. (2004) Esterase-like activity of serum albumin: characterization of its structural chemistry using p-nitrophenyl esters as substrates. *Pharm. Res.* 21, 285–292.
- (2) Manoharan, I., and Boopathy, R. (2006) Diisopropylfluorophosphate-sensitive aryl acylamidase activity of fatty acid free human serum albumin. *Arch. Biochem. Biophys.* 452, 186–188.
- (3) Masson, P., Froment, M.-T., Darvesh, S., Schopfer, L. M., and Lockridge, O. (2007) Aryl acylamidase activity of human serum albumin with o-nitrotrifluoroacetanilide as the substrate. *J. Enzyme Inhib. Med. Chem.* 22, 463–469.
- (4) Watanabe, H., Tanase, S., Nakajou, K., Maruyama, T., Kragh-Hansen, U., and Ottagiri, M. (2000) Role of arg-410 and tyr-411 in human serum albumin for ligand binding and esterase-like activity. *Biochem. J.* 349, 813–819.
- (5) Ghuman, J., Zunsain, P. A., Petitpas, I., Bhattacharya, A. A., Ottagiri, M., and Curry, S. (2005) Structural basis of the drug-binding specificity of human serum albumin. *J. Mol. Biol.* 353, 38–52.

- (6) Mourik, J., and de Jong, L. P. (1978) Binding of the organophosphates parathion and paraoxon to bovine and human serum albumin. *Arch. Toxicol.* 41, 43–48.
- (7) Maliwal, B. P., and Guthrie, F. E. (1981) Interaction of insecticides with human serum albumin. *Mol. Pharmacol.* 20, 138–144.
- (8) Silva, D., Cortez, C. M., Cunha-Bastos, J., and Louro, S. R. (2004) Methyl parathion interaction with human and bovine serum albumin. *Toxicol. Lett.* 147, 53–61.
- (9) Sanger, F. (1963) Amino-acid sequences in the active centers of certain enzymes. *Proc. Chem. Soc.* 5, 76–83.
- (10) Means, G. E., and Wu, H. L. (1979) The reactive tyrosine residue of human serum albumin: characterization of its reaction with diisopropylfluorophosphate. *Arch. Biochem. Biophys.* 194, 526–530.
- (11) Black, R. M., Harrison, J. M., and Read, R. W. (1999) The interaction of sarin and soman with plasma proteins: the identification of a novel phosphorylation site. *Arch. Toxicol.* 73, 123–126.
- (12) De Bisschop, H. C., De Meerleer, W. A., Van Hecke, P. R., and Willems, J. L. (1987) Stereoselective hydrolysis of soman in human plasma and serum. *Biochem. Pharmacol.* 36, 3579–3585.
- (13) Sogorb, M. A., Monroy, A., and Vilanova, E. (1998) Chicken serum albumin hydrolyzes dichlorophenyl phosphoramidates by a mechanism based on transient phosphorylation. *Chem. Res. Toxicol.* 11, 1441–1446.
- (14) Sogorb, M. A., Carrera, V., and Vilanova, E. (2004) Hydrolysis of carbaryl by human serum albumin. *Arch. Toxicol.* 78, 629–634.
- (15) Sogorb, M. A., Diaz-Alejo, N., Escudero, M. A., and Vilanova, E. (1998) Phosphotriesterase activity identified in purified serum albumins. *Arch. Toxicol.* 72, 219–226.
- (16) Sogorb, M. A., and Vilanova, E. (2002) Enzymes involved in the detoxification of organophosphorus, carbamate and pyrethroid insecticides through hydrolysis. *Toxicol. Lett.* 128, 215–228.
- (17) Sogorb, M. A., Alvarez-Escalante, C., Carrera, V., and Vilanova, E. (2007) An in vitro approach for demonstrating the critical role of serum albumin in the detoxication of the carbamate carbaryl at in vivo toxicologically relevant concentrations. *Arch. Toxicol.* 81, 113–119.
- (18) Schopfer, L. M., Champion, M. M., Tamblin, N., Thompson, C. M., and Lockridge, O. (2005) Characteristic mass spectral fragments of the organophosphorus agent FP-biotin and FP-biotinylated peptides from trypsin and bovine albumin (Tyr410). *Anal. Biochem.* 345, 122–132.
- (19) Li, B., Schopfer, L. M., Hinrichs, S. H., Masson, P., and Lockridge, O. (2007) Matrix-assisted laser desorption/ionization time-of-flight mass spectrometry assay for organophosphorus toxicants bound to human albumin at Tyr411. *Anal. Biochem.* 361, 263–272.
- (20) Riches, J., Morton, I., Read, R. W., and Black, R. M. (2005) The trace analysis of alkyl alkylphosphonic acids in urine using gas chromatography-ion trap negative ion tandem mass spectrometry. *J. Chromatogr., B* 816, 251–258.
- (21) Ordentlich, A., Barak, D., Kronman, C., Benschop, H. P., De Jong, L. P., Ariel, N., Barak, R., Segall, Y., Velan, B., and Shafferman, A. (1999) Exploring the active center of human acetylcholinesterase with stereoisomers of an organophosphorus inhibitor with two chiral centers. *Biochemistry* 38, 3055–3066.
- (22) Darvesh, S., McDonald, R. S., Darvesh, K. V., Mataija, D., Mothana, S., Cook, H., Carneiro, K. M., Richard, N., Walsh, R., and Martin, E. (2006) On the active site for hydrolysis of aryl amides and choline esters by human cholinesterases. *Bioorg. Med. Chem.* 14, 4586–4599.
- (23) Kitz, R., and Wilson, I. B. (1962) Esters of methanesulfonic acid as irreversible inhibitors of acetylcholinesterase. *J. Biol. Chem.* 237, 3245–3249.
- (24) Morris, G. M., Goodsell, D. S., Halliday, R. S., Huey, R., Hart, W. E., Belew, R. K., and Olson, A. J. (1998) Automated docking using a Lamarckian genetic algorithm and an empirical binding free energy function. *J. Comput. Chem.* 19, 1639–1662.
- (25) Sanner, M. F. (1999) Python: a programming language for software integration and development. *J. Mol. Graphics* 17, 57–61.
- (26) Berendsen, H. J. C., van der Spoel, D., and van Drunen, R. (1995) Gromacs: a message-passing parallel molecular dynamics implementation. *Comput. Phys. Commun.* 91, 43–56.
- (27) Lindahl, E., Hess, B., and van der Spoel, D. (2001) Gromacs 3.0: a package for molecular simulation and trajectory analysis. *J. Mol. Model.* 7, 306–317.
- (28) Oostenbrink, C., Villa, A., Mark, A. E., and van Gunsteren, W. F. (2004) A biomolecular force field based on the free enthalpy of hydration and solvation: the GROMOS force-field parameter sets 53A5 and 53A6. *J. Comput. Chem.* 25, 1656–1676.
- (29) Stewart, J. J. P. (1989) Optimization of parameters for semiempirical methods I. Method. *J. Comput. Chem.* 10, 209–220.
- (30) Jones, G., Willett, P., Glen, R. C., Leach, A. R., and Taylor, R. (1997) Development and validation of a genetic algorithm for flexible docking. *J. Mol. Biol.* 267, 727–748.
- (31) Eldridge, M. D., Murray, C. W., Auton, T. R., Paolini, G. V., and Mee, R. P. (1997) Empirical scoring functions: I. The development of a fast empirical scoring function to estimate the binding affinity of ligands in receptor complexes. *J. Comput.-Aided Mol. Des.* 11, 425–445.
- (32) Tsuge, K., and Seto, Y. (2006) Detection of human butyrylcholinesterase-nerve gas adducts by liquid chromatography-mass spectrometric analysis after in gel chymotryptic digestion. *J. Chromatogr., B* 838, 21–30.
- (33) Fidler, A., Hulst, A. G., Noort, D., de Ruiter, R., van der Schans, M. J., Benschop, H. P., and Langenberg, J. P. (2002) Retrospective detection of exposure to organophosphorus anti-cholinesterases: mass spectrometric analysis of phosphorylated human butyrylcholinesterase. *Chem. Res. Toxicol.* 15, 582–590.
- (34) Frost, A. A., and Pearson, R. G. (1965) *Kinetics and Mechanisms: A Study of Homogeneous Chemical Reactions*, 2nd ed., John Wiley & Sons, New York.
- (35) Segall, Y., Waysbort, D., Barak, D., Ariel, N., Doctor, B. P., Grunwald, J., and Ashani, Y. (1993) Direct observation and elucidation of the structures of aged and nonaged phosphorylated cholinesterases by 31P NMR spectroscopy. *Biochemistry* 32, 13441–13450.
- (36) Adams, T. K., Capacio, B. R., Smith, J. R., Whalley, C. E., and Korte, W. D. (2004) The application of the fluoride reactivation process to the detection of sarin and soman nerve agent exposures in biological samples. *Drug Chem. Toxicol.* 27, 77–91.
- (37) Casida, J. E., and Quistad, G. B. (2004) Organophosphate toxicology: safety aspects of nonacetylcholinesterase secondary targets. *Chem. Res. Toxicol.* 17, 983–998.
- (38) Williams, N. H., Harrison, J. M., Read, R. W., and Black, R. M. (2007) Phosphorylated tyrosine in albumin as a biomarker of exposure to organophosphorus nerve agents. *Arch. Toxicol.* 81, 627–639.
- (39) Sweeney, R. E., and Maxwell, D. M. (2003) A theoretical expression for the protection associated with stoichiometric and catalytic scavengers in a single compartment model of organophosphorus poisoning. *Math. Biosci.* 181, 133–143.
- (40) Dumas, D. P., Durst, H. D., Landis, W. G., Raushel, F. M., and Wild, J. R. (1990) Inactivation of organophosphorus nerve agents by the phosphotriesterase from *Pseudomonas diminuta*. *Arch. Biochem. Biophys.* 277, 155–159.
- (41) Davies, H. G., Richter, R. J., Keifer, M., Broomfield, C. A., Sowalla, J., and Furlong, C. E. (1996) The effect of the human serum paraoxonase polymorphism is reversed with diazoxon, soman and sarin. *Nat. Genet.* 14, 334–336.
- (42) Kobayashi, K. (2006) Summary of recombinant human serum albumin development. *Biologicals* 34, 55–59.
- (43) Matsushita, S., Chuang, V. T., Kanazawa, M., Tanase, S., Kawai, K., Maruyama, T., Suenaga, A., and Otogiri, M. (2006) Recombinant Human Serum Albumin Dimer has High Blood Circulation Activity and Low Vascular Permeability in Comparison with Native Human Serum Albumin. *Pharm. Res.* 23, 882–891.
- (44) Castle, L. A., Siehl, D. L., Gorton, R., Patten, P. A., Chen, Y. H., Bertain, S., Cho, H. J., Duck, N., Wong, J., Liu, D., and Lassner, M. W. (2004) Discovery and directed evolution of a glyphosate tolerance gene. *Science* 304, 1151–1154.
- (45) Bone, R., Fujishige, A., Kettner, C. A., and Agard, D. A. (1991) Structural basis for broad specificity in alpha-lytic protease mutants. *Biochemistry* 30, 10388–10398.
- (46) Peeples, E. S., Schopfer, L. M., Duysen, E. G., Spaulding, R., Voelker, T., Thompson, C. M., and Lockridge, O. (2005) Albumin, a new biomarker of organophosphorus toxicant exposure, identified by mass spectrometry. *Toxicol. Sci.* 83, 303–312.

TX700339M

# Dichlorvos, chlorpyrifos oxon and Aldicarb adducts of butyrylcholinesterase, detected by mass spectrometry in human plasma following deliberate overdose

Bin Li,<sup>a</sup> Ivan Ricordel,<sup>b</sup> Lawrence M. Schopfer,<sup>a</sup> Frédéric Baud,<sup>c</sup> Bruno Mégarbane,<sup>c</sup> Patrick Masson<sup>d</sup> and Oksana Lockridge<sup>a\*</sup>

**ABSTRACT:** The goal of this study was to develop a method to detect pesticide adducts in tryptic digests of butyrylcholinesterase in human plasma from patients poisoned by pesticides. Adducts to butyrylcholinesterase in human serum may serve as biomarkers of pesticide exposure because organophosphorus and carbamate pesticides make a covalent bond with the active site serine of butyrylcholinesterase. Serum samples from five attempted suicides (with dichlorvos, Aldicarb, Baygon and an unknown pesticide) and from one patient who accidentally inhaled dichlorvos were analyzed. Butyrylcholinesterase was purified from 2 ml serum by ion exchange chromatography at pH 4, followed by procainamide affinity chromatography at pH 7. The purified butyrylcholinesterase was denatured, digested with trypsin and the modified peptide isolated by HPLC. The purified peptide was analyzed by multiple reaction monitoring in a QTRAP 4000 mass spectrometer. This method successfully identified the pesticide-adducted butyrylcholinesterase peptide in four patients whose butyrylcholinesterase was inhibited 60–84%, but not in two patients whose inhibition levels were 8 and 22%. It is expected that low inhibition levels will require analysis of larger serum plasma volumes. In conclusion, a mass spectrometry method for identification of exposure to live toxic pesticides has been developed, based on identification of pesticide adducts on the active site serine of human butyrylcholinesterase. Copyright © 2010 John Wiley & Sons, Ltd.

**Keywords:** dichlorvos; Aldicarb; chlorpyrifos oxon; mass spectrometry; butyrylcholinesterase; pesticide poisoning biomarker

## INTRODUCTION

Butyrylcholinesterase is highly reactive with organophosphorus pesticides (OP) and carbamates. These poisons make a covalent bond with the active site serine, thus inhibiting the activity of butyrylcholinesterase. The inhibited butyrylcholinesterase in human plasma and serum is an indicator of exposure to cholinesterase inhibitors such as OP and carbamates. However, measurement of inhibition levels does not distinguish between exposure to pesticides and exposure to Alzheimer drugs such as tacrine and donepezil (Darvesh *et al.*, 2003).

A sensitive method for detection of nerve agent exposure is GC–mass spectrometry of the nerve agent released by treatment of plasma with 2 M potassium fluoride (Jakubowski *et al.*, 2004; Van Der Schans *et al.*, 2004). Another method used electrospray ionization in a Q-TOF mass spectrometer to identify the sarin-adducted butyrylcholinesterase peptide isolated from victims of the Tokyo subway attack (Fidder *et al.*, 2002). The key step in the analysis by Fidder *et al.* is the microscale purification of butyrylcholinesterase (BChE) from 0.5 to 1 ml plasma samples. A high level of purification of BChE from plasma is required before the mass spectrometer can detect the modified peptide. It is difficult to obtain sufficient quantities of purified BChE from 1–2 ml of human serum, where the BChE concentration is 4 µg ml<sup>-1</sup>, corresponding to 50 nM, considering that the protein concentration in human serum is 50,000 µg ml<sup>-1</sup>.

A method similar to that introduced by Fidder *et al.* has been adapted in the present report to analyze blood samples from patients suspected to have been poisoned by pesticides. Our method introduces two additional purification steps, thus resulting in high-quality MSMS spectra. In addition, we use multiple reaction monitoring for detection of the modified BChE peptide. Multiple reaction monitoring of carbofuran-labeled BChE purified from patients exposed to carbofuran has been previously reported by us (Li *et al.*, 2009).

\*Correspondence to: O. Lockridge, Eppley Institute, University of Nebraska Medical Center, Omaha, NE 68198-5950, USA.  
E-mail: olockrid@unmc.edu

<sup>a</sup>Eppley Institute, University of Nebraska Medical Center, Omaha, NE 68198-5950, USA

<sup>b</sup>Institut National de Police Scientifique, Laboratoire de toxicologie de la préfecture de police, 2 Place Mazas, 75012 Paris, France

<sup>c</sup>Service de Réanimation Médicale et Toxicologique and Université Paris-Diderot, Hôpital Lariboisière, 2 Rue Ambroise Paré, 75010 Paris, France

<sup>d</sup>Centre de Recherches du Service de Santé des Armées, 24 avenue des maquis du Grésivaudan, 38702 La Tronche, France

## METHODS

### Serum

Serum samples from five attempted suicides and one accidentally poisoned individual were provided by Dr Ivan Ricordel, Paris Police. The samples were shipped on dry ice and stored at  $-80^{\circ}\text{C}$ .

### BChE Activity assay

BChE activity was measured with 1 mM butyrylthiocholine in 0.1 M potassium phosphate pH 7.0 in the presence of 0.5 mM dithiobisnitrobenzoic acid by measuring the increase in absorbance at 412 nm at  $25^{\circ}\text{C}$ . The reaction rate in delta absorbance per min was converted to  $\mu\text{moles per minute}$  using the extinction coefficient  $E = 13\,600\text{ M}^{-1}\text{ cm}^{-1}$  (Ellman *et al.*, 1961). One unit of activity is defined as one micromole of substrate hydrolyzed per minute.

### Purification of BChE from Dichlorvos-poisoned Serum by Ion Exchange at pH 4 and Procainamide Affinity Gel

The purification method that was developed for 70–100 L of serum was scaled down to process small clinical serum samples (Lockridge *et al.*, 2005). Two milliliters of the strong anion exchanger Q-Sepharose fast flow (catalog no. 17-0510-04, Amersham BioSciences, Piscataway, NJ, USA) were washed with binding buffer (20 mM sodium acetate, 1 mM EDTA, pH 4.0) until the supernatant reached pH 4.0 and the conductivity was 0.3 mSi. Then 1.5–2 ml serum, diluted 20-fold with binding buffer to reduce the salt concentration, was added to the equilibrated Q-Sepharose in a 50 ml plastic tube. The tube was gently rocked at  $4^{\circ}\text{C}$  for 4–16 h. Binding to Q-Sepharose was monitored by measuring BChE activity in the supernatant. After 85–90% of the BChE had bound, the gel was packed into a 10 ml column, and washed with binding buffer until the absorbance of the eluant had dropped to 0.04 at 280 nm. About 15 ml of binding buffer was needed for the wash step. BChE was eluted with 6 ml of 0.05 M NaCl in 20 mM sodium acetate and 1 mM EDTA, pH 4.0. Fractions of 1 ml were collected. Fractions with BChE activity were pooled and further purified on a procainamide affinity column. Q-Sepharose purified the BChE about 70-fold.

Procainamide-Sepharose gel, custom made by Dr Yacov Ashani (Grunwald *et al.*, 1997), had procainamide attached through a six-carbon spacer to Sepharose 4B at a ratio of 34  $\mu\text{mol}$  of procainamide per ml gel. A 0.4 ml aliquot of procainamide gel was packed into a 1.5 ml microfuge spin column and equilibrated with 2 ml of 20 mM potassium phosphate pH 7.0 buffer. The partially purified BChE was loaded on the column by gravity flow. The column was washed four times with 1 ml of 20 mM potassium phosphate pH 7.0 buffer. Washing buffer was removed by briefly centrifuging the column. Contaminating proteins were eluted by washing four times with 1 ml of 0.2 M NaCl in 20 mM potassium phosphate pH 7.0 buffer. BChE was eluted twice with 1 ml of 1 M sodium chloride in 20 mM potassium phosphate pH 7.0. The affinity column increased the purity of BChE about 10-fold. BChE purity was increased 700-fold after Q-Sepharose and procainamide gel purification.

### Purification of BChE from Carbamate (Aldicarb, Baygon), and Unknown Organophosphate-poisoned Sera by Procainamide Affinity Gel

Purification speed was critical for carbamate-poisoned samples because the carbamates, Aldicarb and Baygon, are easily released from intact BChE. A one-step purification method on procainamide affinity gel was chosen because this step took 15 min from thawing the serum to elution (Li *et al.*, 2009). In contrast, ion exchange purification took at least 6 h. A 1.5–2 ml aliquot of serum was allowed to flow through a 0.4 ml column of pre-equilibrated procainamide gel by gravity. Wash steps used brief centrifugation to speed up the process. BChE was loaded and eluted by gravity flow.

### Trypsin Digestion of Purified BChE

Following purification, the BChE was immediately boiled for 10 min. This denaturation step prevented decarbamylation of the active site serine and unfolded the BChE protein. The BChE (in 2 ml) was digested with 20  $\mu\text{l}$  of 0.4  $\mu\text{g}\,\mu\text{l}^{-1}$  porcine trypsin (V5113, Promega) for 18 h at  $37^{\circ}\text{C}$ .

### HPLC Purification of the Tryptic BChE Peptides

The modified active site peptide of BChE was purified using a Phenomenex Prodigy, 5  $\mu\text{m}$   $\text{C}_{18}$  column on a Waters HPLC system. Peptides were eluted with a 60 min gradient starting at 0.1% trifluoroacetic acid, and ending at 60% acetonitrile, 0.1% trifluoroacetic acid, at a flow rate of 1  $\text{ml min}^{-1}$ . One milliliter fractions were collected. A 1  $\mu\text{l}$  aliquot from each 1 ml fraction was analyzed by MALDI-TOF mass spectrometry (Applied Biosystems) to identify fractions containing the unlabeled BChE active site peptide. The unlabeled active site peptide of mass 2928.5 amu was detectable by MALDI-TOF and was used as a marker to estimate the elution position of the modified peptide. The modified BChE peptide was not detectable by MALDI-TOF when the starting material was 2 ml serum. However, the elution position could be estimated from previous studies with 0.2 mg of highly purified BChE covalently modified on Serine 198 by various agents. The unlabeled active site peptide elutes between 32 and 36% acetonitrile, while covalently modified active site peptides elute between 32 and 41% acetonitrile (Gilley *et al.*, 2009; Li *et al.*, 2009). HPLC fractions were dried in a vacuum centrifuge and dissolved in 50  $\mu\text{l}$  of 5% of acetonitrile and 0.1% formic acid in preparation for analysis on the QTRAP 4000 mass spectrometer. If the offline HPLC purification step was omitted, OP-adducted BChE peptide was not detected in the mass spectrometer.

### Multiple Reaction Monitoring on the QTRAP 4000 Mass Spectrometer

A 5  $\mu\text{l}$  aliquot of HPLC-purified, tryptic BChE peptides were injected onto a Vydac  $\text{C}_{18}$  polymeric reverse-phase nanocolumn for a second phase of HPLC separation. Peptides were separated with a 90 min linear gradient from 0 to 60% acetonitrile and 0.1% formic acid and electrosprayed through a fused silica emitter directly into the QTRAP 4000, a hybrid quadrupole linear ion trap mass spectrometer (Applied Biosystems). The mass spectrometer was calibrated on selected fragments from the MSMS spectrum of Glu-Fibrinopeptide B. The MSMS data were collected and pro-

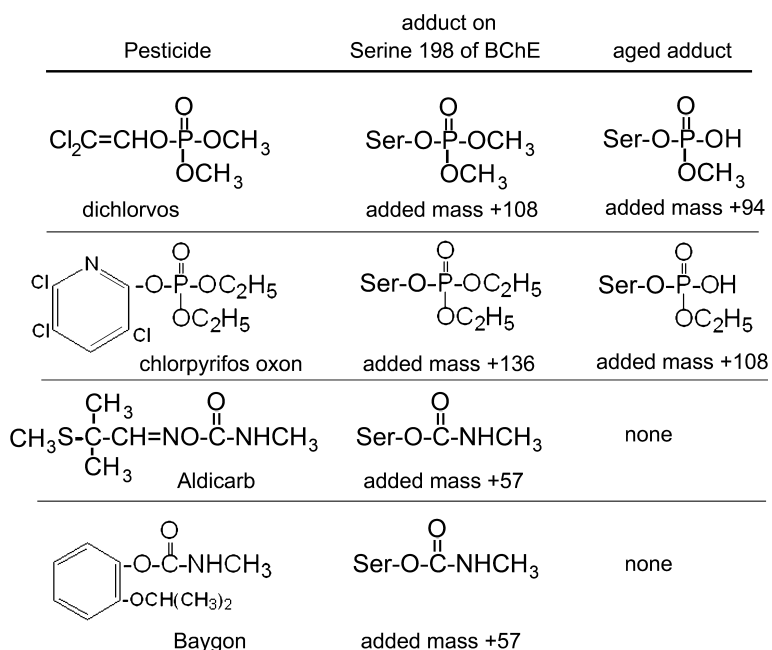


**Figure 1.** Structures of pesticides and the adducts formed by covalent binding to Serine 198 of human BChE. Dichlorvos and aged chlorpyrifos oxon adducts have the same added mass of +108. Aldicarb and Baygon give the same BChE adduct with an added mass of +57. The unlabeled active site peptide of BChE produced by digestion with trypsin has a monoisotopic mass of 2928.5 amu.

**Table 1.** BChE activity in sera from poisoned individuals and from controls

Poison	Time between poisoning and blood draw	Days in hospital	BChE activity (units ml <sup>-1</sup> )	Inhibition of BChE (%)	Labeled BChE peptide found
Dichlorvos	10 h	11	0.41	84	Yes
Dichlorvos	9 h	2	0.50	80	Yes
Dichlorvos	11 h	1	2.30	8	No
Aldicarb	7 h	3	0.07	97	Yes
Baygon	22 h	3	1.96	22	No
Unknown OP	Unknown	Unknown	0.95	62	Yes
None	None	None	2.50	0	No

The name of the poison was established from the reports of family members who found bottles of pesticide in the home. The unknown OP was identified in the present work as chlorpyrifos oxon from mass spectrometry of the BChE adduct.

cessed using Analyst 1.4.1 software (Applied Biosystems). The QTRAP 4000 was operated in multiple reaction monitoring (MRM) mode. Details of the MRM method can be found in the Results and Discussion sections.

## RESULTS

### Pesticide Structures and the Adducts they Form with BChE

The structures of the OP and carbamate pesticides (the suspect poisons) are shown in Fig. 1. The poisons make a covalent bond with the active site serine of BChE to make the adducts shown in the middle column of Fig. 1. The initial OP adducts release an alkyl group in a process called 'aging' to yield the structures shown in the right-hand column of Fig. 1. The entries for the carbamate adducts are listed as 'none' in the column labeled 'aged adduct' because carbamate adducts do not age. The mass added from each pesticide is large compared with the error tolerance of 1 amu in the QTRAP mass spectrometer.

The aging reaction is catalyzed by amino acid residues in the active site of BChE including His 438 and Glu 197 (Nachon *et al.*, 2005). Dimethoxyphosphate adducts age with a half-life of 3.9 h, whereas diethoxyphosphate adducts age with a half-life of 11.6 h at pH 7.0, 25 °C (Masson *et al.*, 1997; Worek *et al.*, 1999). The carbamate adducts spontaneously reactivate with a half-life of about 2 h (Li *et al.*, 2009), but they do not age.

### BChE Inhibition Levels in Patient Sera

Table 1 shows that three patients were poisoned with dichlorvos (2,2-dichlorovinyl dimethyl phosphate), one with Aldicarb (2-methyl-2-(methylthio)propionaldehyde O-methylcarbamoyloxime), one with Baygon (isopropoxyphenyl methyl carbamate) and one with an unknown OP. The serum samples analyzed in this work came from blood drawn 7–22 h after the patients were poisoned. BChE activity in patient sera was inhibited 8–97%. The patient with the lowest level of inhibition (8%) was a 15-year-old female who accidentally inhaled

**Table 2.** Multiple reaction monitoring transitions for the BChE active site peptide

BChE active site peptide SVTLFGESAGAASVSLHLLSPGSHSLFTR	Charge	Parent ion $m/z$	Transition to y9	Transition to y10
Unlabeled BChE peptide	4	733.8	1001.5	1088.5
Dichlorvos labeled; added mass +108	4	760.3	1001.5	1088.5
Aged dichlorvos labeled; added mass +94	4	756.8	1001.5	1088.5
Aged chlorpyrifos oxon labeled; added mass +108	4	760.3	1001.5	1088.5
Aldicarb/Baygon labeled; added mass +57	4	747.6	1001.5	1088.5

Theoretical masses in the QTRAP mass spectrometer are listed. Masses of the quadruple-charged parent ions are average masses, while those of the singly charged y9 and y10 ions are monoisotopic masses. The monoisotopic mass of the single-charged unlabeled peptide is 2928.5 amu. The accession number for human butyrylcholinesterase in the NCBI nonredundant database is gi: 116353. This sequence includes 28 amino acids of the signal peptide, so that Serine198 is numbered Serine226.

dichlorvos. The other five patients drank the pesticide in attempted suicide. All patients survived. Patients whose BChE was inhibited 80% or more survived with the aid of mechanical ventilation and treatment with atropine and pralidoxime. The last column in Table 1 indicates that our mass spectrometry analysis identified the adducted BChE peptide in four of the six samples. The samples with minor BChE inhibition (8–22%) did not yield enough adducted BChE peptide from 2 ml serum for detection in the mass spectrometer.

#### Information for MRM to Detect BChE Adducts

The mass spectrometry method selected for detection of BChE adducts was the MRM method. This method instructs the mass spectrometer to look only for the specified masses and to ignore all other ions. This increases the sensitivity of detection by deleting background signals. To use MRM one must know the possible parent ion masses. The mass of the parent ion can be calculated from the structure of the pesticide and its known reaction with BChE. Organophosphorus and carbamate pesticides make a covalent bond with Serine 198 of BChE. After digestion with trypsin, the peptide that includes Serine 198 has the sequence SVTLFGES<sub>198</sub>AGAASVSLHLLSPGSHSLFTR (Lockridge *et al.*, 1987; Lockridge and La Du, 1986). A list of the 49 tryptic peptides of human BChE can be obtained from the Protein Prospector website of the University of California, San Francisco (<http://prospector.ucsf.edu/prospector/mshome.htm>), by searching for tryptic peptides in accession number gi116353 in the NCBI non-redundant database, after deleting the 28 amino acids in the signal peptide.

In addition one must know which product ion masses (called transition ions) are consistently intense in the MSMS spectrum. From our previous work with OP-labeled and carbamate-labeled pure BChE (Gilley *et al.*, 2009; Li *et al.*, 2009) we knew that the y9 ion at 1001.5 amu and the y10 ion at 1088.5 amu are reliable indicators of both the labeled and unlabeled BChE active site peptide. Therefore, the y9 and y10 ions were selected as MRM transition ions. Table 2 lists the masses of the quadruply charged parent ions and the transition ions used for MRM.

#### Detection of the Monomethoxyphosphate Adduct of BChE Produced by Exposure to Dichlorvos

An example of the signal detected by the MRM method for one of the patient samples is given in Fig. 2. The parent ion mass at 756.8

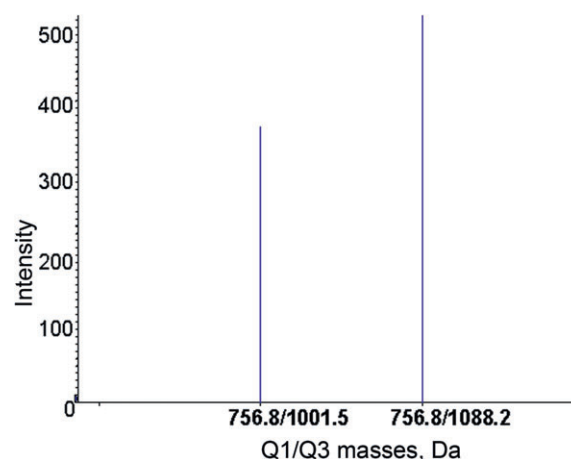


**Figure 2.** MRM transitions for the aged dichlorvos labeled tryptic BChE peptide. The quadruple-charged parent ion has a mass to charge ratio of 756.8  $m/z$  and yields single-charged product ions at 1001.5 and 1088.2 amu. Q1 is the mass of the parent ion. Q3 is the mass of the production.

$m/z$  and the product ion masses at 1001.5 and 1088.2 amu were found in this sample. These values correspond to the aged dichlorvos-adducted BChE tryptic peptide in Table 2.

The MRM hit automatically triggered acquisition of the MSMS spectrum shown in Fig. 3. The MSMS spectrum proves that the peptide has the amino acid sequence of the BChE active site tryptic peptide SVTLFGES<sub>198</sub>AGAASVSLHLLSPGSHSLFTR and that monomethoxyphosphate is covalently bound to the active site Serine 198. The singly charged y ion series from y4 to y15 and the doubly charged y ion series from y13<sup>+2</sup> to y22<sup>+2</sup> support the peptide sequence. The mass of the parent ion (756.6  $m/z$ ) is consistent with a monomethoxyphosphate adduct on this peptide and supports the conclusion that the patient was poisoned by dichlorvos.

Support for modification of Serine 198 by monomethoxyphosphate comes from the doubly charged y22 ion at 1145.2  $m/z$ ; this mass includes the mass of aged dichlorvos. Additional support for modification of Serine 198 are the seven ions marked with the symbol  $\Delta$  to indicate the presence of dehydroalanine in place of the active site serine. The collision energy in the mass spectrometer releases the organophosphorus agent plus a molecule of water from the OP-modified serine to produce dehydroalanine in place of serine (Fidder *et al.*, 2002). No serine other than Serine

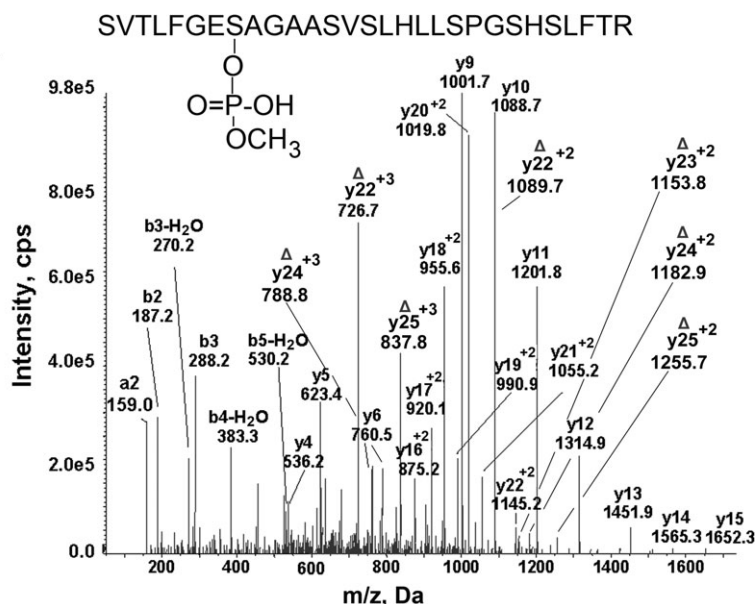


**Figure 3.** MSMS spectrum of the aged dichlorvos labeled tryptic peptide of BChE derived from serum of a dichlorvos-poisoned patient. The quadruple-charged parent ion has 756.6  $m/z$ . The y9 and y10 transition ions are present. In addition, a series of b and y ions are present that fit the masses of the active site tryptic peptide of BChE. The double-charged y22<sup>+2</sup> ion at 1145.2  $m/z$  carries the aged dichlorvos (monomethoxyphosphate) on Serine 198. The triple- and double-charged ions labeled with the symbol  $\Delta$  contain dehydroalanine in place of Serine 198. They have lost the OP plus a molecule of water during collision with gas molecules in the mass spectrometer. Facile loss of the organophosphorus agent plus a molecule of water to produce dehydroalanine is a characteristic feature of modified serine. The masses of the ions labeled with the symbol  $\Delta$  support the conclusion that the modified residue is Serine 198.

198 in peptide SVTLFGES<sub>198</sub>AGAASVSLHLLSPGSHSLFTR is modified. This conclusion is supported by the masses of the b and y ions in Fig. 3.

Human BChE covalently modified by dimethoxyphosphate ages with a half-life of 3.9 h (Worek *et al.*, 1999). The blood sample was drawn 10 h after exposure, a time interval that allowed greater than 75% (>2 half-lives) of the modified BChE to undergo aging. It is not surprising, therefore, that the modified BChE detected in Fig. 3 is the aged dichlorvos adduct.

The second dichlorvos-poisoned patient with 80% inhibition of plasma BChE, also yielded the MRM and MSMS spectra, shown in Figs 2 and 3, thus providing evidence that the poison was dichlorvos. However the patient whose plasma BChE was inhibited only 8% did not yield enough dichlorvos-adducted BChE for detection in the mass spectrometer. It is expected that very low levels of exposure will require more than 2 ml of plasma to confirm the diagnosis by mass spectrometry.

MRM is a valuable component of our method because it allows analysis to be directed at specific peptides that may be present in low yield. The ability to dismiss peptides that do not meet the MRM selection criteria allows the mass spectrometer to focus on just those peptides that are of interest. However, despite the sensitivity and selectivity of the MRM method, confirmation of the peptide's identity by analysis of its MSMS spectrum is essential to avoid false positive identifications, especially when dealing with unknown samples. Reliance on MRM identification alone, as is done in a clinical setting, requires that the target be very well characterized (including reproducible liquid chromatography elution times). The myriad of parent ion/product ion possibilities that exist when analyzing a sample from a patient who has been exposed to an unknown OP or carbamate is too complex to rely on MRM identification alone.

#### Identification of Aged CPO Adducted BChE Peptide in Serum from the Patient Poisoned with an Unknown Pesticide

Serum from the patient poisoned with an unknown pesticide had 40% of normal BChE activity. The fact that the pesticide inhibited the BChE activity suggested that the poison was either an OP or a carbamate. The sample was handled as if the poison were a carbamate. This meant the BChE purification was limited to use of the procainamide affinity column, followed by HPLC purification of the tryptic peptide. Omission of the pH 4 ion exchange chromatography step yields a less purified BChE. A lower fold purification is associated with interference by contaminating ions when the sample is analyzed in the mass spectrometer, and therefore a lower quality MSMS spectrum.

The MSMS spectrum triggered by the MRM method is shown in Fig. 4. The quadruple-charged parent ion at 760.1  $m/z$  and the y9 and y10 transition ions are present. According to Table 2 these values are consistent with either unaged dichlorvos or aged chlorpyrifos oxon adducts. We interpreted the adduct in Fig. 4 to be the aged chlorpyrifos oxon adduct because the aging of dichlorvos is so rapid (half-life 3.9 h) that finding the unaged dichlorvos-adducted BChE seemed unlikely.

The masses of the ions in Fig. 4 support the identity of the peptide as the active site peptide of BChE. As expected, the number and intensity of ions in Fig. 4 are not as high as those in Fig. 3 where the BChE peptide had undergone more extensive purification before the protein was denatured and digested.

#### Identification of Carbamate Adducted BChE Peptide in Patient Poisoned by Aldicarb

The MRM triggered MSMS spectrum of the adducted BChE peptide isolated from 2 ml serum of the patient poisoned with

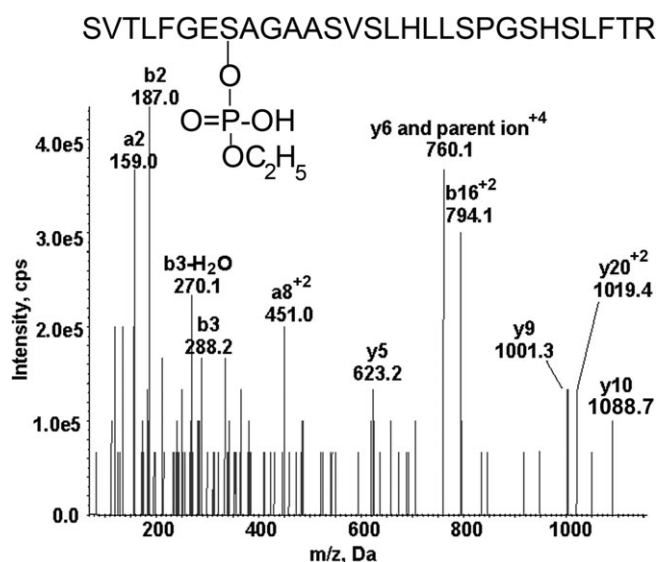


**Figure 4.** MSMS spectrum of the aged chlorpyrifos oxon labeled BChE tryptic peptide from serum taken from the patient exposed to an unknown poison. The quadruple-charged parent ion of 760.1 *m/z* is consistent with aged chlorpyrifos oxon labeled BChE peptide.

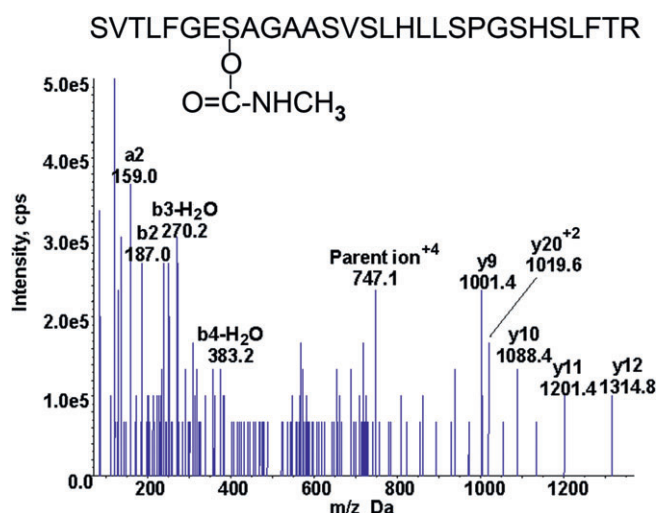


**Figure 5.** MSMS spectrum of the Aldicarb labeled BChE tryptic peptide from serum taken from the Aldicarb-poisoned patient. The quadruple-charged parent ion has a mass to charge ratio of 747.1 *m/z*.

Aldicarb is shown in Fig. 5. The mass of the parent ion and the masses of the y9 and y10 ions are consistent with the masses in Table 2 for the BChE active site peptide labeled with carbamate. The other ions whose masses are indicated in Fig. 5 support the assignment of the peptide as the BChE active site peptide. The ion series is incomplete as it is missing the covalently modified serine at y22 and b8. The BChE would need to be more highly purified to generate a more complete mass spectrum. This is a difficult task because of the instability of the carbamate adduct.

The instability of carbamate-adducted BChE is illustrated in Fig. 6, where a 10  $\mu$ l sample of serum from the patient poisoned with Aldicarb was assayed for BChE activity. The increase in absorbance at 412 nm was not linear with time. Rather it became faster as time elapsed, giving an upward curve. This behavior is charac-

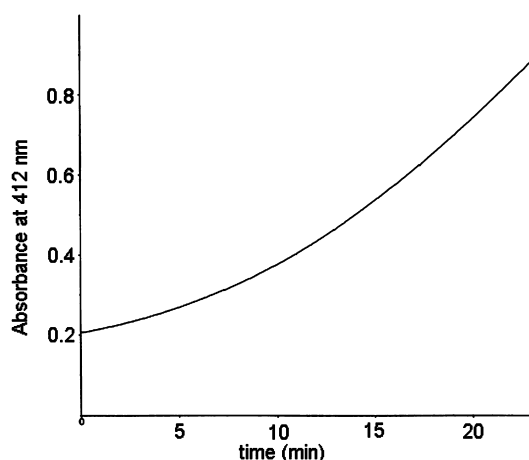


**Figure 6.** Spontaneous reactivation of Aldicarb-inhibited BChE. BChE activity in Aldicarb-poisoned sera was measured with 1 mM butyrylthiocholine in 1 ml of 0.1 M potassium phosphate pH 7.0 in the presence of 0.5 mM dithiobisnitrobenzoic acid by recording increase in absorbance at 412 nm. BChE activity was 0.07 units  $\text{mL}^{-1}$  at the beginning of the measurement and was 0.34 units  $\text{mL}^{-1}$  at 23 min.

teristic of an increase in enzyme activity with time. After 23 min the activity had increased 4.8-fold over the activity at time zero. The increase in BChE activity can be explained by spontaneous decarbamylation of the active site serine. Spontaneous reactivation is a problem because our goal is to detect covalently modified BChE. Denaturation of the BChE protein stops spontaneous reactivation as previously demonstrated for a carbofuran-poisoned plasma sample (Li *et al.*, 2009). To maximize the amount of carbamylated BChE peptide available for analysis it is important to freeze the serum or plasma sample immediately after the blood draw, to rapidly purify the BChE protein after the frozen plasma has thawed and to denature the BChE immediately after it has been purified.

## DISCUSSION

### Limitations of the Method

The major limitation of this mass spectrometry method is the need to purify BChE from plasma. Before it becomes practical to use mass spectrometry for detection of pesticide exposure, it will be necessary to devise a simple purification method that yields pure BChE in one step. Mass spectrometers are expensive and require highly skilled personnel to operate them, but mass spectrometers are already used in US hospitals for routine clinical assays. A clinician reviewer of this manuscript pointed out that a clinician will treat a patient based on the symptoms, and will not wait for information on the identity of the poison. We agree with this assessment, but point out that understanding the progress of the illness may require knowing the identity of the poison. For example Eddleston has found that patients poisoned with fenthion have few symptoms initially, but many more die from fenthion than from chlorpyrifos-poisoning (Eddleston *et al.*, 2005). Eddleston suggests that patients might benefit from management protocols developed for particular organophosphorus agents, a suggestion that requires knowing the identity of the poison.

Another limitation of the method is that it cannot distinguish between pesticide exposures that yield adducts with an identical

mass. For example, paraoxon-ethyl and chlorpyrifos oxon-ethyl both form diethoxyphosphate adducts with an added mass of +136. The reaction of BChE with Aldicarb, carbofuran, Baygon, carbaryl, aldoxycarb, formetanate, methiocarb, methomyl, oxamyl, propoxur, physostigmine and physostigmine results in identical adducts with an added mass of +57.

### Advantages of the Method

The adduct mass distinguishes classes of pesticides. OP pesticide adducts have masses that are distinct from masses of carbamate pesticide adducts and these are distinct from OP nerve agent adducts. The presence of a BChE adduct is proof that the person was exposed to live agent, as opposed to a metabolite or degradation product. Only the live agent is capable of binding covalently to BChE. The Centers for Disease Control and Prevention reported that 96% of the 1997 Americans in their study contained pesticide metabolites in their urine (Barr *et al.*, 2005). This information does not reveal whether Americans are exposed to live agent or simply to harmless pesticide degradation products.

Exposure to nerve agents, organophosphorus pesticides and carbamate pesticides can cause similar toxic symptoms and result in similar levels of butyrylcholinesterase inhibition. Our mass spectrometry method distinguishes between these classes of poison. Knowledge of the type of cholinesterase inhibitor to which a person was exposed could be useful to forensic toxicologists. It would aid in tracing the source of the inhibitor.

Epidemiologists have linked OP exposure to risk of Parkinson's and Alzheimer's Disease in old age (Baldi *et al.*, 2003; Hancock *et al.*, 2008). Gulf War Illness in veterans of the 1991 Persian Gulf War has been linked to OP exposure (Toomey *et al.*, 2009). Depression and cognitive impairment have also been linked to OP exposure (Beseler *et al.*, 2008). Laboratory evidence proving exposure to live agent would strengthen these associations.

### CONCLUSION

A mass spectrometry method to identify exposure to organophosphorus and carbamate pesticides has been developed. The method identifies pesticides covalently bound to butyrylcholinesterase in human blood. Success depends on achieving a high level of purification of butyrylcholinesterase from serum, thus enabling detection of the modified peptide. This is the first report to identify dichlorvos, chlorpyrifos oxon and Aldicarb adducts on butyrylcholinesterase in the blood of patients hospitalized for pesticide overdose.

### Acknowledgment

Supported by NIH grant U01 NS058056, NIH Cancer Center Support grant CA036727, US Army Medical Research and Materiel Command W81XWH-07-2-0034, French Procurement Agency DGA/PEA 08co501 and Agence Nationale pour la Recherche ANR-06-BLAN-0163. Mass spectra were obtained with the support of the Mass Spectrometry and Proteomics Core Facility at the University of Nebraska Medical Center.

### REFERENCES

- Baldi I, Lebaillly P, Mohammed-Brahim B, Letenneur L, Dartigues JF, Brochard P. 2003. Neurodegenerative diseases and exposure to pesticides in the elderly. *Am. J. Epidemiol.* **157**(5): 409–414.
- Barr DB, Allen R, Olsson AO, Bravo R, Caltabiano LM, Montesano A, Nguyen J, Udunka S, Walden D, Walker RD *et al.* 2005. Concentrations of selective metabolites of organophosphorus pesticides in the United States population. *Environ. Res.* **99**(3): 314–326.
- Beseler CL, Stallones L, Hoppin JA, Alavanja MC, Blair A, Keefe T, Kamel F. 2008. Depression and pesticide exposures among private pesticide applicators enrolled in the Agricultural Health Study. *Environ. Health Perspect.* **116**(12): 1713–1719.
- Darvesh S, Walsh R, Kumar R, Caines A, Roberts S, Magee D, Rockwood K, Martin E. 2003. Inhibition of human cholinesterases by drugs used to treat Alzheimer disease. *Alzheimer Dis. Assoc. Disord.* **17**(2): 117–126.
- Eddleston M, Eyer P, Worek F, Mohamed F, Senarathna L, von Meyer L, Juszcak E, Hittarage A, Azhar S, Dissanayake W *et al.* 2005. Differences between organophosphorus insecticides in human self-poisoning: a prospective cohort study. *Lancet* **366**(9495): 1452–1459.
- Ellman GL, Courtney KD, Andres V Jr, Feather-Stone RM. 1961. A new and rapid colorimetric determination of acetylcholinesterase activity. *Biochem. Pharmacol.* **7**: 88–95.
- Fidder A, Hulst AG, Noort D, de Ruiter R, van der Schans MJ, Benschop HP, Langenberg JP. 2002. Retrospective detection of exposure to organophosphorus anti-cholinesterases: mass spectrometric analysis of phosphorylated human butyrylcholinesterase. *Chem. Res. Toxicol.* **15**(4): 582–590.
- Gilley C, Macdonald M, Nachon F, Schopfer LM, Zhang J, Cashman JR, Lockridge O. 2009. Nerve agent analogues that produce authentic soman, sarin, tabun, and cyclohexyl methylphosphonate-modified human butyrylcholinesterase. *Chem. Res. Toxicol.* **22**(10): 1680–1688.
- Grunwald J, Marcus D, Papier Y, Raveh L, Pittel Z, Ashani Y. 1997. Large-scale purification and long-term stability of human butyrylcholinesterase: a potential bioscavenger drug. *J. Biochem. Biophys. Meth.* **34**(2): 123–135.
- Hancock DB, Martin ER, Mayhew GM, Stajich JM, Jewett R, Stacy MA, Scott BL, Vance JM, Scott WK. 2008. Pesticide exposure and risk of Parkinson's disease: a family-based case-control study. *BMC Neurol.* **8**: 6.
- Jakubowski EM, McGuire JM, Evans RA, Edwards JL, Hulet SW, Benton BJ, Forster JS, Burnett DC, Muse WT, Matson K *et al.* 2004. Quantitation of fluoride ion released sarin in red blood cell samples by gas chromatography-chemical ionization mass spectrometry using isotope dilution and large-volume injection. *J. Anal. Toxicol.* **28**(5): 357–363.
- Li H, Ricordel I, Tong L, Schopfer LM, Baud F, Megarbane B, Maury E, Masson P, Lockridge O. 2009. Carbofuran poisoning detected by mass spectrometry of butyrylcholinesterase adduct in human serum. *J. Appl. Toxicol.* **29**(2): 149–155.
- Lockridge O, La Du BN. 1986. Amino acid sequence of the active site of human serum cholinesterase from usual, atypical, and atypical-silent genotypes. *Biochem. Genet.* **24**(5–6): 485–498.
- Lockridge O, Bartels CF, Vaughan TA, Wong CK, Norton SE, Johnson LL. 1987. Complete amino acid sequence of human serum cholinesterase. *J. Biol. Chem.* **262**(2): 549–557.
- Lockridge O, Schopfer LM, Winger G, Woods JH. 2005. Large scale purification of butyrylcholinesterase from human plasma suitable for injection into monkeys; a potential new therapeutic for protection against cocaine and nerve agent toxicity. *J. Med. CBR Def* **3**: online publication.
- Masson P, Froment MT, Bartels CF, Lockridge O. 1997. Importance of aspartate-70 in organophosphate inhibition, oxime re-activation and aging of human butyrylcholinesterase. *Biochem. J.* **325**(Pt 1): 53–61.
- Nachon F, Asajo OA, Borgstahl GE, Masson P, Lockridge O. 2005. Role of water in aging of human butyrylcholinesterase inhibited by echothiophate: the crystal structure suggests two alternative mechanisms of aging. *Biochemistry* **44**(4): 1154–1162.
- Toomey R, Alpern R, Vasterling JJ, Baker DG, Reda DJ, Lyons MJ, Henderson WG, Kang HK, Eisen SA, Murphy FM. 2009. Neuropsychological functioning of U.S. Gulf War veterans 10 years after the war. *J. Int. Neuropsychol. Soc.* **15**(5): 717–729.
- Van Der Schans MJ, Polhuijs M, Van Dijk C, Degenhardt CE, Pleijssier K, Langenberg JP, Benschop HP. 2004. Retrospective detection of exposure to nerve agents: analysis of phosphofluoridates originating from fluoride-induced reactivation of phosphorylated BuChE. *Arch. Toxicol.* **78**(9): 508–524.
- Worek F, Diepold C, Eyer P. 1999. Dimethylphosphoryl-inhibited human cholinesterases: inhibition, reactivation, and aging kinetics. *Arch. Toxicol.* **73**(1): 7–14.

# Detection of Adduct on Tyrosine 411 of Albumin in Humans Poisoned by Dichlorvos

Bin Li,\* Ivan Ricordel,† Lawrence M. Schopfer,\* Frédéric Baud,‡ Bruno Mégarbane,‡ Florian Nachon,§ Patrick Masson,\*§ and Oksana Lockridge\*<sup>1</sup>

\*Eppley Institute, University of Nebraska Medical Center, Omaha, Nebraska 68198-5950; †Laboratoire de toxicologie de la préfecture de police, Institut National de Police Scientifique, 75012 Paris, France; ‡Department de Toxicologie, Service de Réanimation Médicale et Toxicologique and Université Paris-Diderot, Hôpital Lariboisière, 75010 Paris, France; and §Institut de Recherche Biomédicale des Armées—Centre de Recherches du Service de Santé des Armées, 38702 La Tronche, France

<sup>1</sup>To whom correspondence should be addressed at Eppley Institute, University of Nebraska Medical Center, Omaha, NE 68198-5950. Fax: (402) 559-4651. E-mail: olockrid@unmc.edu.

Received March 13, 2010; accepted April 12, 2010

Studies in mice and guinea pigs have shown that albumin is a new biomarker of organophosphorus toxicant (OP) and nerve agent exposure. Our goal was to determine whether OP-labeled albumin could be detected in the blood of humans exposed to OP. Blood from four OP-exposed patients was prepared for mass spectrometry analysis by digesting 0.010 ml of serum with pepsin and purifying the labeled albumin peptide by offline high performance liquid chromatography. Dimethoxyphosphate-labeled tyrosine 411 was identified in albumin peptides VRY<sub>411</sub>TKKVPQVSTPTL and LVRY<sub>411</sub>TKKVPQVSTPTL from two patients who had attempted suicide with dichlorvos. The butyrylcholinesterase activity in these serum samples was inhibited 80%. A third patient whose serum BChE activity was inhibited 8% by accidental inhalation of dichlorvos had undetectable levels of adduct on albumin. A fourth patient whose BChE activity was inhibited 60% by exposure to chlorpyrifos had no detectable adduct on albumin. This is the first report to demonstrate the presence of OP-labeled albumin in human patients. It is concluded that tyrosine 411 of human albumin is covalently modified in the serum of humans poisoned by dichlorvos and that the modification is detectable by mass spectrometry. The special reactivity of tyrosine 411 with OP suggests that other proteins may also be modified on tyrosine. Identification of other OP-modified proteins may lead to an understanding of neurotoxic symptoms that appear long after the initial OP exposure.

**Key Words:** organophosphorus toxicant; albumin; butyrylcholinesterase; mass spectrometry.

Organophosphorus toxicants (OP) are toxic chemicals used in agriculture, medicine, and warfare. Their acute toxicity is due to inhibition of acetylcholinesterase in the cholinergic nervous system by covalent modification of the active site serine.

The authors certify that all research involving human subjects was done under full compliance with all government policies and the Helsinki Declaration.

OP are also highly effective inhibitors of butyrylcholinesterase (BChE, accession number gi:116353), though inhibition of BChE has no known clinical sequelae. Carbamates also inhibit cholinesterases by covalently binding to the active site serine. Acylpeptide hydrolase in red blood cells is 10 times more reactive with dichlorvos, chlorpyrifos oxon, and diisopropylfluorophosphate than acetylcholinesterase and has the potential to serve as a biomarker of OP exposure (Quistad *et al.*, 2005; Richards *et al.*, 2000).

We have successfully used mass spectrometry to identify covalently labeled BChE peptides from patients poisoned with the OP, dichlorvos and chlorpyrifos, and with the carbamates, carbofuran and Aldicarb (Li *et al.*, 2009, 2010). To find these peptides, we had to develop methods for the purification of carbamate-labeled and OP-labeled BChE from 2 ml plasma or serum. We were then able to use mass spectrometry to demonstrate covalent binding of these poisons to serine 198 of human BChE, to identify the mass of the adduct on serine 198, and to deduce the type of pesticide to which the patient was exposed.

The purpose of the present work was to determine whether albumin is labeled in people who have been exposed to OP. Mice (Peeples *et al.*, 2005) and guinea pigs (Read *et al.*, 2010; Williams *et al.*, 2007) treated with OP *in vivo* have covalently bound OP on albumin. Mass spectrometry has identified tyrosine 411 of human albumin (accession number gi:122920512) as the residue that is covalently modified by dichlorvos, chlorpyrifos oxon, diisopropylfluorophosphate, soman, sarin, and fluorophosphinate-biotin when human albumin or plasma is treated *ex vivo* with these OP (Li *et al.*, 2007).

The rate of reaction of albumin with OP is slow compared with the rate of reaction of BChE with OP (Li *et al.*, 2008). However, there is a 10,000-fold higher concentration of albumin (0.6mM; 40,000 mg/l) compared with BChE (50nM; 4 mg/l); in human serum. This difference in concentration compensates for the slow reactivity, resulting in OP labeling of albumin

*in vivo*. The most reactive residue in human albumin is tyrosine 411, though other tyrosines are also labeled when conditions are maximized *in vitro* (Ding *et al.*, 2008; Means and Wu, 1979). Tyrosine 411 can be found in peptic peptides VRY<sub>411</sub>TKKVPQVSTPTL and LVRY<sub>411</sub>TKKVPQVSTPTL, which are related by a missed cleavage. The most reactive residue in BChE is serine 198 in the tryptic peptide SVTLFGES<sub>198</sub>AGAASVSLHLLSPGSHSLFTR.

The adducts on albumin and BChE after reaction with dichlorvos and chlorpyrifos oxon are shown in Figure 1. OP-albumin adducts are stable, whereas OP-BChE adducts lose an alkyl group in a process called “aging.” The present report is the first to identify OP-albumin adducts in humans exposed to OP.

## MATERIAL AND METHODS

### Materials

Pepsin (Sigma, St Louis, MO; catalog number P6887 from porcine gastric mucosa) 1 mg/ml in 10mM HCl was stored at  $-80^{\circ}\text{C}$ . Alpha-cyano 4-hydroxycinnamic acid (CHCA; Sigma; catalog number 70990) was recrystallized before use. A 10 mg/ml solution in 50% acetonitrile, 0.1% trifluoroacetic acid was stored at room temperature in the dark. Purified human serum albumin, essentially fatty acid free (Fluka via Sigma; catalog number 05418), butyrylthiocholine (catalog number B3253), and dithiobisnitrobenzoic acid (catalog number D8130) were from Sigma. Modified trypsin (Promega, Madison, WI; catalog number V5113) 0.4  $\mu\text{g}/\mu\text{l}$  in 50mM acetic acid was stored at  $-80^{\circ}\text{C}$ . Chlorpyrifos oxon 98% pure and dichlorvos 98% pure were from ChemService Inc. (West Chester, PA; catalog numbers MET-674B and PS-89, respectively).

**Human serum.** Serum samples from three attempted suicides and one accidentally poisoned individual were provided by Dr Ivan Ricordel, Paris Police in a protocol approved by the Institutional Review Board of the University of Nebraska Medical Center. The samples were shipped on dry ice

and stored at  $-80^{\circ}\text{C}$ . The name of the poison in three cases was established from the reports of family members who found bottles of dichlorvos pesticide in the home. The name of the poison in one case was unknown but was identified as chlorpyrifos (Li *et al.*, 2010).

The two patients who attempted suicide with dichlorvos had severe cholinergic symptoms, including bilateral myosis and hypersalivation. One patient was unconscious when admitted to the hospital. The other was drowsy without coma. The patient who accidentally inhaled dichlorvos had a brief period of respiratory difficulty and paresthesia in four limbs but no other symptoms. Nothing is known about the patient who attempted suicide with chlorpyrifos.

**BChE activity assay.** BChE activity was measured with 1mM butyrylthiocholine in 0.1M potassium phosphate pH 7.0 in the presence of 0.5mM dithiobisnitrobenzoic acid by measuring the increase in absorbance at 412 nm at  $25^{\circ}\text{C}$ . The reaction rate in delta absorbance per minute was converted to micromoles per minute using the extinction coefficient  $E = 13600/\text{M}\cdot\text{cm}$  (Ellman *et al.*, 1961). One unit of activity is defined as 1  $\mu\text{mol}$  of substrate hydrolyzed per minute.

**Pepsin digestion to release labeled albumin peptide.** From previous work, it was known that tyrosine 411 of human albumin is labeled by OP and that the labeled peptide is easily released by digestion with pepsin (Li *et al.*, 2007, 2008). It was also known that the labeled albumin peptide could be detected in the mass spectrometer if the peptide was isolated by offline high performance liquid chromatography (HPLC) before liquid chromatography tandem mass spectrometry (LCMSMS). A 0.01 ml aliquot of human serum was adjusted to pH 2.5 by addition of 0.01 ml of 1% trifluoroacetic acid and digested with 2.5  $\mu\text{g}$  of pepsin for 2 h at  $37^{\circ}\text{C}$ .

**Offline HPLC purification of the peptic albumin peptides from patient samples.** Peptides in the digested serum were purified by HPLC (Waters LC 625 system) on a Phenomenex Prodigy, 5  $\mu\text{C}18$  column  $100 \times 4.6\text{mm}$  eluted with a 60-min gradient starting at 0.1% trifluoroacetic acid in water and ending at 60% acetonitrile, 0.1% trifluoroacetic acid, at a flow rate of 1 ml/min. One-milliliter fractions were collected. A 1  $\mu\text{l}$  aliquot from each 1 ml fraction was analyzed by matrix assisted laser desorption ionization-time of flight (MALDI-TOF) mass spectrometry to identify fractions containing the unlabeled albumin tyrosine 411 peptides VRY<sub>411</sub>TKKVPQVSTPTL  $m/z$  1717 and LVRY<sub>411</sub>TKKVPQVSTPTL  $m/z$  1830. When starting with 10  $\mu\text{l}$  of serum

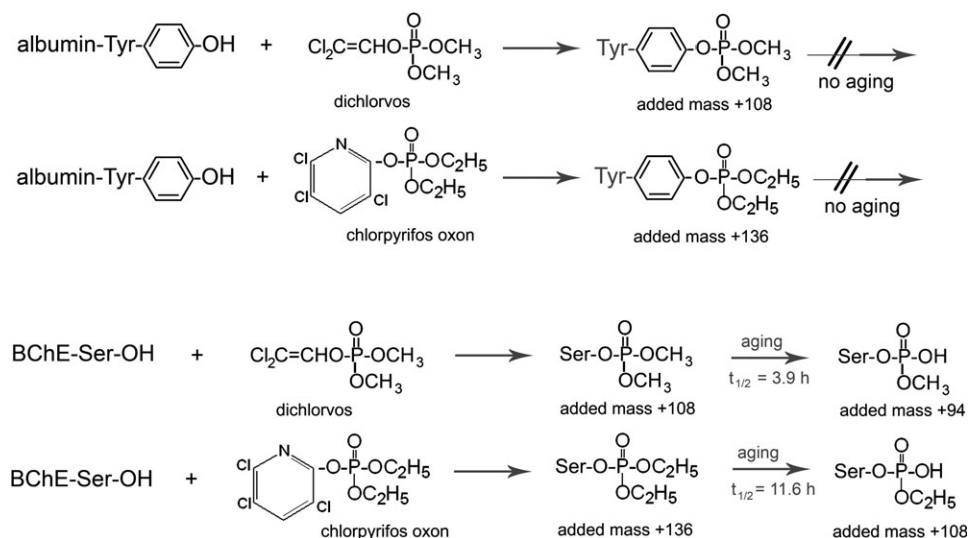


**FIG. 1.** Covalent binding of dichlorvos and chlorpyrifos oxon to albumin and BChE. Tyrosine 411 of human albumin makes a covalent bond with dichlorvos, adding a mass of 108 amu, and, with chlorpyrifos oxon, adding a mass of 136 amu. Adducts on tyrosine do not age. Serine 198 of human BChE makes covalent bonds with dichlorvos and chlorpyrifos oxon. The BChE adducts dealkylate during the aging process so that the added masses characteristically observed in the mass spectrometer are 94 and 108 amu. The dimethoxyphosphate adduct on human BChE ages with a half-time of 3.9 h (Worek *et al.*, 1999), whereas the diethoxyphosphate adduct ages with a half-time of 11.6 h (Masson *et al.*, 1997). The amino acid sequence of human BChE is in accession number gi:116353 in the National Center for Biotechnology Information nonredundant database and that of human albumin in accession number gi:122920512.

from a patient sample, the unlabeled peptides were detectable by MALDI-TOF but the labeled peptides were present at too low a level to be detectable. However, the elution position of the labeled peptides could be estimated from previous studies. The unlabeled albumin tyrosine 411 peptides eluted between 19–24% acetonitrile, whereas labeled peptides eluted 1–8 min later. HPLC fractions predicted to contain the labeled peptides were dried in a vacuum centrifuge and dissolved in 50  $\mu$ l of 5% of acetonitrile, 0.1% formic acid in preparation for analysis on the QTRAP 4000 mass spectrometer.

**Reaction of human plasma with chlorpyrifos oxon and dichlorvos.** Human plasma was treated with 0.1–1.5mM chlorpyrifos oxon or dichlorvos for 16 h at 37°C. A 10  $\mu$ l aliquot was mixed with 10  $\mu$ l of 1% trifluoroacetic acid before digestion with 1  $\mu$ l of 1 mg/ml pepsin. After 2-h incubation at 37°C, the digest was diluted 400-fold with 0.1% trifluoroacetic acid and 1  $\mu$ l was spotted on a matrix assisted laser desorption ionization (MALDI) plate.

The labeled and unlabeled albumin tyrosine 411 peptides were identified in the same MALDI-TOF mass spectrum. Unlabeled peptides had masses of 1717 and 1830 amu. Chlorpyrifos oxon-labeled peptides had masses of 1853 and 1966 amu. Dichlorvos-labeled peptides had masses of 1825 and 1938 amu. Relative quantities of labeled and unlabeled peptides were calculated by comparison of cluster areas using the Data Explorer software. This method of quantitation assumes that the labeled and unlabeled peptides ionize with similar efficiencies. Each sample serves as its own internal control because the peptides are in the same MALDI spot in the same MALDI spectrum.

**MALDI-TOF mass spectrometry.** A 1  $\mu$ l aliquot of essentially salt-free sample was spotted onto a 384 well Opti-TOF sample plate (#1016491; Applied Biosystems, Foster City, CA). After the spot was dry, it was overlaid with 1  $\mu$ l of CHCA matrix. Mass spectrometry spectra were acquired with a matrix assisted laser desorption ionization tandem time of flight 4800 mass spectrometer (Applied Biosystems), in positive reflector mode, with laser intensity at 4000 V, using delayed extraction, and default calibration. Spectra were saved to Data Explorer V4.9 software for analysis. Each spectrum was the sum of 500 laser shots. The mass spectrometer was calibrated with Cal Mix 5 (bradykinin, 2–9 clip; angiotensin I; Glu-fibrinopeptide B; adrenocorticotrophic hormone [ACTH], 1–17 clip; ACTH, 18–39 clip; and ACTH, 7–38 clip from Applied Biosystems Inc., Framingham, MA).

**Multiple reaction monitoring on the QTRAP 4000 mass spectrometer (Applied Biosystems).** Five microliter aliquots from selected fractions of HPLC-purified peptic peptides from patient sera were injected onto a Vydac C18 polymeric reverse-phase nanocolumn for a second phase of HPLC separation. Peptides were separated on a HPLC nanocolumn (#218MS3.07515 Vydac C18 polymeric rev-phase, 75  $\mu$ m i.d.  $\times$  150 mm long; P.J. Cobert Assoc, St Louis, MO) with a 90 min linear gradient from 0 to 60% acetonitrile, 0.1% formic acid, at 300 nl/min, and electrosprayed through a fused silica emitter (360  $\mu$ m o.d., 75  $\mu$ m i.d., 15  $\mu$ m taper, New Objective) directly into the QTRAP 4000, a hybrid quadrupole linear ion trap mass spectrometer. The mass spectrometer was calibrated on selected fragments from the tandem mass spectrometry (MSMS) spectrum of Glu-Fibrinopeptide B. The MSMS data were collected and processed using Analyst 1.4.1 software (Applied Biosystems).

The QTRAP 4000 was operated in multiple reaction monitoring (MRM) mode. The MRM algorithm screens ions entering the mass spectrometer for selected parent ion masses, fragments the selected parent ions when they appear, and examines the fragments for selected product ions. A signal is recorded when both the correct parent and the product ions are observed. Preliminary experiments showed that triply charged parent ions gave better signals in the QTRAP mass spectrometer than did doubly charged parent ions. For dichlorvos-labeled samples, a strong product ion fragment was observed at 748.8 amu ( $b_{12}$ )<sup>+2</sup> from parent peptide VRY<sub>411</sub>TKKVPQVSTPTL,  $[M + 3H]^{+3} = 609.4$  amu. A strong product ion was observed at 805.3 amu ( $b_{12}$ )<sup>+2</sup> from parent peptide LVRY<sub>411</sub>TKKVPQVSTPTL,  $[M + 3H]^{+3} = 647.4$  amu. These parent/product ion pairs were used in the MRM experiments on dichlorvos-labeled samples. The dwell time for collecting the MRM signals was 40 ms, collision energy was 30 V, and collision gas was pure nitrogen (40  $\mu$ Torr). Data were collected using an Information Directed Acquisition protocol that triggered the collection of an

enhanced product ion spectrum (MSMS) following the detection of a peptide of interest by the MRM algorithm. The enhanced product ion spectrum was taken using the trap function of the QTRAP mass spectrometer. Collision energy was 30 V, collision gas was pure nitrogen (40  $\mu$ Torr), scan rate was 4000 Da/s, and 10 enhanced product ion scans were summed for each spectrum.

**LCMSMS on the QTRAP 4000 mass spectrometer.** Samples that gave a positive result in the MRM method were also analyzed by LCMSMS. In addition, the LCMSMS method was used to test unfractionated pepsin-digested serum. The digested serum was diluted 2000-fold with 5% acetonitrile, 0.1% formic acid to reduce the protein concentration to 0.5  $\mu$ g/ $\mu$ l (~7 pmol albumin per  $\mu$ l). Protein concentration was estimated from absorbance at 280 nm in the NanoDrop spectrophotometer (Thermo Scientific, Wilmington, DE) relative to albumin standards. Five microliter of the diluted digest were separated on an HPLC nanocolumn and electrosprayed into the QTRAP 4000 mass spectrometer as described for the MRM experiment.

An information directed acquisition protocol triggered the collection of an enhanced resolution spectrum and an enhanced product ion spectrum on the four most intense ions entering the mass spectrometer having an m/z between 200 and 1500, a charge state of +2 to +4 and an intensity greater than 500,000 counts per second. After an ion was analyzed twice, it was excluded from analysis for 60 s. Collision energy was determined by the mass spectrometer based on mass and charge state of the ion. Collision gas was pure nitrogen (40  $\mu$ Torr), and the scan rate was 4000 Da/s. Because of the time required to obtain this series of scans, only one enhanced product ion scan was taken for each ion. An ion spray voltage of 1900 V was maintained between the emitter and the mass spectrometer. The mass spectrometer was calibrated using MSMS fragments of Glu-Fibrinopeptide B.

The MSMS data files were searched for spectra that included a singly charged mass of 330 amu. The 330 amu mass is the y3 ion in both labeled and unlabeled albumin peptides VRYTKKVPQVSTPTL and LVRYTKKVPQVSTPTL. The extracted ion chromatogram feature of the Analyst software (version 1.4) was used for the search. MSMS spectra were accepted if the other masses in the spectra matched the fragment masses for the albumin peptides. Predicted fragment masses, for comparison with the observed fragment masses, were calculated with the aid of the fragment ion calculator in the Proteomics Toolkit (<http://db.systemsbiology.net:8080/proteomicsToolkit/FragionServlet.html>).

**Infusion into the QTRAP 4000 mass spectrometer.** The MRM and LCMSMS protocols proved that the VRYTKKVPQVSTPTL and LVRYTKKVPQVSTPTL peptides had a mass 108 amu higher than the mass of the unlabeled peptides. However, the MSMS spectra did not show the b ion masses that proved the adduct was on tyrosine 411. To obtain proof that the reaction of dichlorvos with albumin resulted in covalent modification of tyrosine 411, we treated 0.1 ml of a 50 mg/ml solution of pure human albumin in 25mM NH<sub>4</sub>HCO<sub>3</sub> pH 8.5 with 1.5mM dichlorvos overnight. The albumin was digested with pepsin and the peptides purified by offline HPLC. Purified peptides were dried and dissolved in 50% acetonitrile, 25% methanol, and 1% acetic acid in preparation for infusion. Samples were infused into the QTRAP mass spectrometer because infusion allows one to sum hundreds of MSMS spectra into one final spectrum, whereas the MRM method sums ten spectra and the LCMSMS method only one MSMS spectrum. The improved signal-to-noise ratio after summing 500 MSMS spectra in the infusion method reveals low-intensity ions.

Initially, a mass spectrum was taken to identify the ions in the sample. Masses consistent with those expected for dichlorvos-labeled peptic peptides were then fragmented in the mass spectrometer. Collision gas was nitrogen (40  $\mu$ Torr), collision energy was optimized for maximum fragment information, and the scan rate was 4000 Da/s. The final spectrum was the sum of 500 MSMS spectra.

## RESULTS

### MRM for Detection of Dichlorvos-Albumin Adducts

Use of the MRM feature of the mass spectrometer requires one to know the masses of the parent and product ions that best

indicate the presence of the desired peptide. This information was obtained from MSMS spectra of dichlorvos-labeled pure human albumin peptic peptides. The MSMS spectra acquired in the QTRAP 4000 mass spectrometer showed that the parent ions were most readily detectable in the triply charged state. The b12 product ion (also called transition and daughter ion) in charge state + 2 was intense for the OP-labeled VRYT KKVPQVSTPTL peptide. The b13 product ion in charge state + 2 was intense for the OP-labeled LVRYTKKVPQVSTPTL peptide. Therefore, the triply charged parent ion masses and the doubly charged product ion masses listed in Table 1 were selected for MRM.

*Sera from Dichlorvos-Poisoned Patients Contain Dichlorvos Adducts on Tyrosine 411 of Albumin*

Albumin peptides partially purified from 0.010 ml patient serum were subjected to reverse-phase liquid chromatography followed by electrospray ionization and fragmentation in the triple quadrupole linear ion trap mass spectrometer. The mass spectrometer was programmed to search for the ion partners listed in Table 1. An example of an MRM hit is given in Figure 2, where two parent ions coeluted from the nanocolumn at the same time. Parent ion 609.4 m/z had product ion 748.8 m/z. Parent ion 647.4 had product ion 805.3. A positive MRM signal does not prove that the ion represents the peptide of interest. Proof comes from the MSMS spectrum, which is automatically acquired following the appearance of an MRM signal.

The MSMS spectrum for the triply charged parent ion at 609.4 m/z is given in Figure 3A. The mass of the parent ion is consistent with the peptide VRYTKKVPQVSTPTL plus an added mass from dichlorvos of 108 amu. The y and b ion series fit the predicted peptide sequence and appear with approximately the same relative intensities as the ions from a control sample of dichlorvos-labeled peptide (Figure 3B). These observations provide strong evidence that the 609.4 amu mass is dichlorvos-labeled albumin peptide VRYTKKVPQVSTPTL.

There is no direct proof in this spectrum that the dimethoxyphosphate is attached to tyrosine because there are

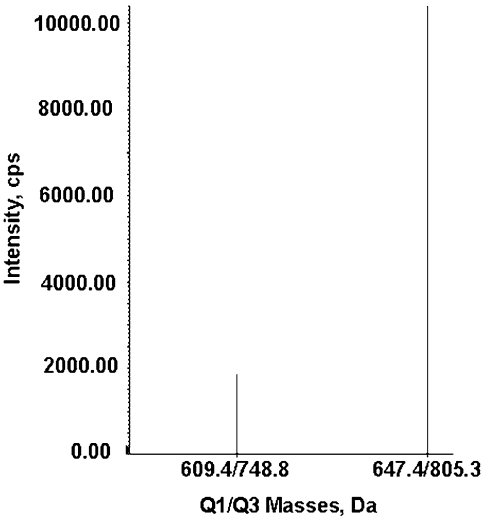
no signals for the b2 and b3 ions that define tyrosine 411. However, the masses of the remainder of the b ions in the spectrum (b<sub>7</sub>), (b<sub>10</sub>), (b<sub>11</sub>)<sup>+2</sup>, (b<sub>12</sub>)<sup>+2</sup>, and (b<sub>14</sub>)<sup>+2</sup> are all consistent with the presence of the label. Therefore, the labeled residue must reside on the VRYTKKVP portion of the peptide. There are four nucleophilic residues in that portion of the peptide that could theoretically react with dichlorvos: tyrosine, threonine, and two lysines. The interpretation that the OP is covalently bound to tyrosine relies on comparison with the MSMS spectrum of pure albumin treated with dichlorvos where the b2 ion at 256.2 amu carries no label but the b3 ion at 527.5 amu has a mass consistent with dimethoxyphosphorylation of tyrosine (Figure 3B).

The MSMS spectrum for the second dichlorvos-labeled peptide isolated from a poisoned patient is given in Figure 4. The triply charged parent ion has a mass of 647.4 m/z, consistent with the peptide LVRYTKKVPQVSTPTL plus an added mass of 108 from dichlorvos. The y and b ion series fit the predicted peptide sequence. The masses of all observed b ions are consistent with an added mass of 108 amu on tyrosine.

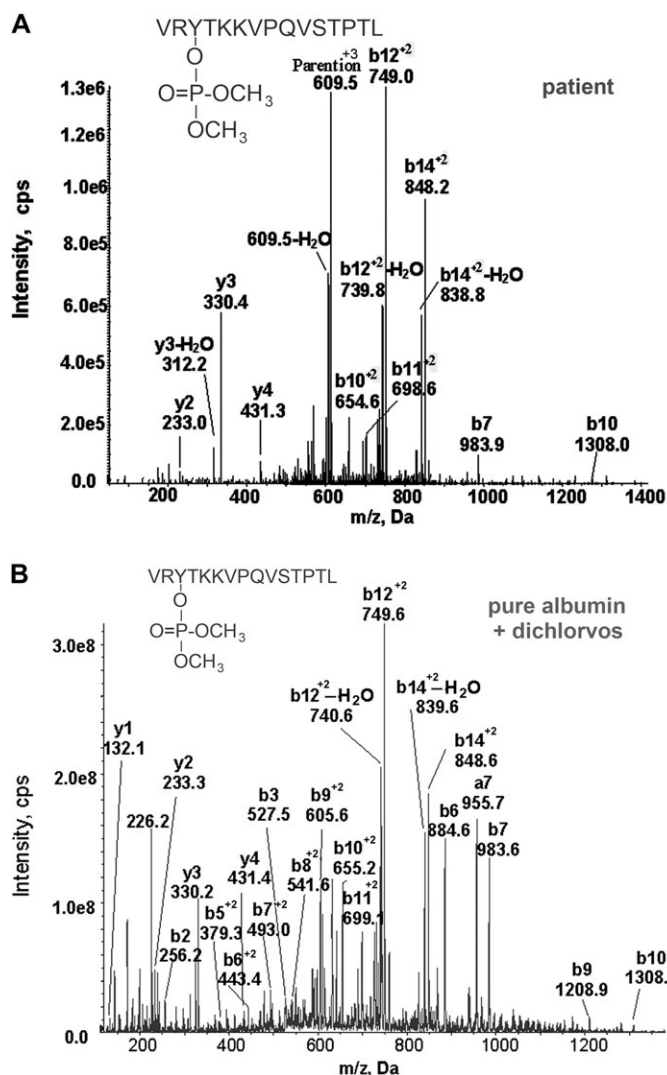
The patient samples were reanalyzed by LCMSMS without using the MRM feature of the QTRAP 4000. The output mass spectrometry spectra were manually searched for the dichlorvos-labeled parent ions 609.4 and 647.4 m/z. Both parent ions were found. They eluted from the nanocolumn at about 40 min. The MSMS spectra acquired from LCMSMS analysis supported an added mass of 108 on peptides VRYTKKVPQVSTPTL and LVRYTKKVPQVSTPTL. However, peak intensities were lower than MSMS spectra acquired

TABLE 1 MRM Transitions for the Albumin Peptides		
Albumin peptide	Parent ion, charge + 3 m/z	Product ion b12, charge + 2 m/z
VRYTKKVPQVSTPTL		
No label	573.3	694.8
Dichlorvos labeled; added mass + 108	609.4	748.8
Albumin peptide	Parent ion, charge + 3 m/z	Product ion b13, charge + 2 m/z
LVRYTKKVPQVSTPTL		
No label	611.1	751.4
Dichlorvos labeled; added mass + 108	647.4	805.3

*Note.* Average masses are listed. The accession number for human albumin in the NCBI nonredundant database is gi:122920512.



**FIG. 2.** MRM transitions for dichlorvos-labeled albumin peptides. Two parent ions eluted at the same time from the nanocolumn. The triply charged parent ion at 609.4 m/z has a product ion at 748.8 m/z. The triply charged parent ion at 647.4 m/z has a product ion at 805.3 m/z. Q1 is the mass of the parent ion. Q3 is the mass of the product ion. MRM spectra, such as this, for dichlorvos-labeled albumin were obtained from the blood of two humans poisoned by dichlorvos.



**FIG. 3.** MSMS spectra of dichlorvos-labeled albumin peptide VRY<sub>411</sub>TKKVPQVSTPTL where dimethoxyphosphate is on tyrosine 411. (A) MSMS spectrum of the dichlorvos-labeled albumin peptide from the serum of a patient poisoned with dichlorvos. The spectrum was acquired in conjunction with the MRM method and is the sum of 10 MSMS spectra. The triply charged parent ion shows an m/z of 609.5 in this spectrum. (B) MSMS spectrum of the dichlorvos-labeled peptide prepared by *in vitro* treatment of pure human albumin with dichlorvos. The spectrum is the sum of 500 MSMS spectra acquired during infusion of purified peptides. The mass at 226.2 m/z is the dimethoxyphosphotyrosine immonium ion minus water. Masses are average.

by MRM or by infusion. Peak intensities were 4 e4 for unfractionated digest analyzed by LCMSMS, 1.5 e5 for HPLC-purified digest analyzed by LCMSMS, 1.3 e6 and 1 e7 for HPLC-purified digest analyzed by MRM, and 3 e8 for infused sample. The difference in signal intensity is the result of being able to collect only one scan per MSMS spectrum in the LCMSMS protocol, as compared with 10 scans per MSMS spectrum in the MRM protocol and 500 scans per MSMS spectrum in the infusion protocol.

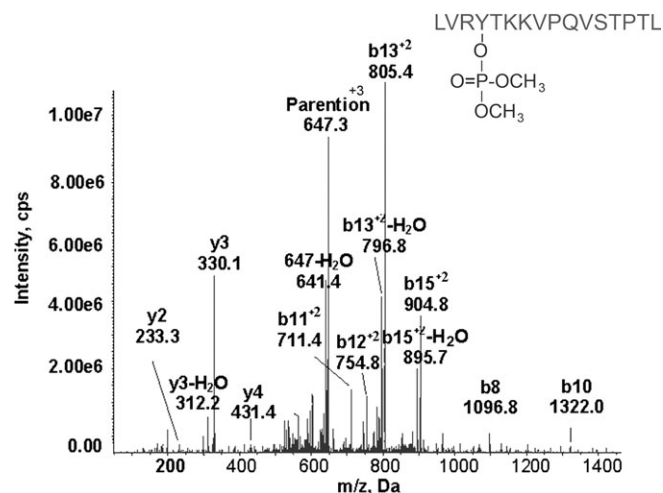


**FIG. 4.** MRM triggered MSMS spectrum of the dichlorvos-labeled albumin peptide, LVRY<sub>411</sub>TKKVPQVSTPTL. Serum from a patient poisoned with dichlorvos yielded the peptide modified on tyrosine 411 by dimethoxyphosphate. The triply charged parent ion has m/z 647.3.

### The Chlorpyrifos-Poisoned Patient

The pesticide sold for agricultural use is chlorpyrifos. Patients exposed to chlorpyrifos are analyzed for adducts from chlorpyrifos oxon because poison symptoms are caused by the oxon. Chlorpyrifos is a precursor of the active metabolite chlorpyrifos oxon. Chlorpyrifos undergoes oxidative desulfuration by liver cytochrome P450 enzymes to become the highly toxic chlorpyrifos oxon (Sams *et al.*, 2004; Tang *et al.*, 2001).

HPLC-purified peptides from a pepsin digest of serum from the patient poisoned with chlorpyrifos were analyzed on the QTRAP using LCMSMS and infusion methods. The diethoxyphosphate adduct on albumin was not observed.

In an effort to understand why no diethoxyphosphate albumin adducts were detected, the relative reactivity of albumin with dichlorvos and chlorpyrifos oxon was examined. Plasma was incubated with various concentrations of chlorpyrifos oxon and dichlorvos for 16 h at 37°C. Cluster areas of labeled and unlabeled peptides observed in MALDI-TOF mass spectra were used to calculate percent labeling of tyrosine 411 (see the "Materials and Methods" section on "Reaction of human plasma with chlorpyrifos oxon and dichlorvos" for quantitation details). Figure 5 shows that 60% of the tyrosine 411 residues in albumin were labeled when human plasma was treated with 0.2mM dichlorvos. In contrast, less than 1% labeling occurred with 0.2mM chlorpyrifos oxon. It was not until 1.5mM chlorpyrifos oxon was used in the reaction that a significant amount of albumin adduct was observed (about 30%). Thus, it appears that chlorpyrifos oxon is substantially less reactive than dichlorvos toward albumin. The decreased reactivity of chlorpyrifos oxon indicates that a lower fraction of labeled albumin would be expected from sera of chlorpyrifos oxon-poisoned individuals. This, in turn, argues that a volume of plasma larger than the 0.010 ml used in the present study

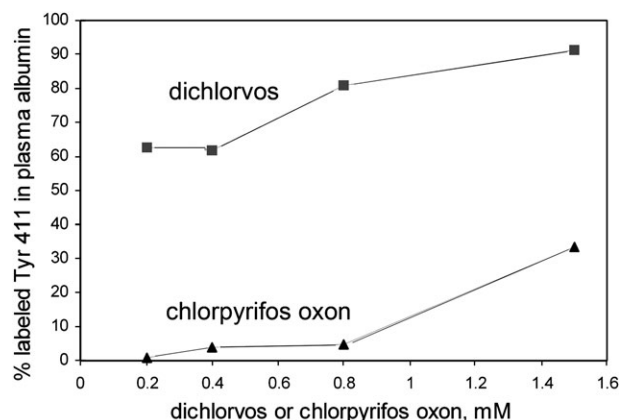


**FIG. 5.** Reactivity of tyrosine 411 in human albumin with dichlorvos and chlorpyrifos oxon. Percent labeling was calculated from cluster areas observed in the MALDI-TOF mass spectrometer of pepsin-digested plasma that had been treated with OP. The unlabeled peptides VRYTKKVPQVSTPTL and LVRYTKKVPQVSTPTL have masses of 1717 and 1830 amu. The dichlorvos-labeled peptides have masses of 1825 and 1938 amu. The chlorpyrifos oxon-labeled peptides have masses of 1853 and 1966 amu.

would need to be analyzed to detect the low level of albumin expected to have been modified by chlorpyrifos oxon.

## DISCUSSION

### *Comparison of Peptide Analyses for BChE and Albumin from Dichlorvos- and Chlorpyrifos-Poisoned Patients*

Sera from the group of patients described in this report were previously analyzed for BChE adducts (Li *et al.*, 2010). In those experiments, partially purified BChE was digested with trypsin and analyzed by mass spectrometry. Adducts on serine 198 were found. Table 2 summarizes the results for adducts on both BChE and albumin from the sera of four poisoned patients. The three patients who attempted suicide by drinking pesticides have low serum BChE activity, with inhibition levels from 62 to 84%. BChE in the accidental exposure case was only slightly inhibited (8%). OP adducts on BChE were found for all three samples where BChE inhibition was high but not for the sample where BChE inhibition was low.

Dichlorvos adducts on albumin were found for the two patients who ingested a relatively large dose of dichlorvos, based on BChE inhibition of 84 and 80%. No dichlorvos adduct was found on albumin for the patient whose BChE was inhibited 8%. No chlorpyrifos oxon adduct was found on albumin for the patient whose BChE was inhibited 62%. The absence of a detectable chlorpyrifos oxon adduct on albumin can be explained as follows. (1) Chlorpyrifos oxon added to plasma is less reactive with tyrosine 411 of albumin than dichlorvos. (2) Chlorpyrifos oxon is hydrolyzed by paraoxonase in plasma and is sequestered by albumin in noncovalent binding sites from which it can be extracted with pentane (Eyer *et al.*, 2009; Heilmair *et al.*, 2008). This diminishes the concentration of chlorpyrifos oxon available

**TABLE 2**  
Detection of OP Adducts on BChE and Albumin in Poisoned Patients

Pesticide	Time between poisoning and blood draw	BChE activity U/ml	Inhibition of BChE %	Labeled BChE peptide found	Labeled albumin peptide found
Dichlorvos	10 h	0.41	84	Yes	Yes
Dichlorvos	9 h	0.50	80	Yes	Yes
Dichlorvos	11 h	2.30	8	No	No
Unknown (chlorpyrifos) <sup>a</sup>	Unknown	0.95	62	Yes	No
Control—none	None	2.50	0	No	No

<sup>a</sup>Chlorpyrifos oxon was identified by mass spectrometry of the BChE adduct in a sample for which the poison was originally unknown. Results for BChE have been previously reported (Li *et al.*, 2010). Mass spectrometry analysis used 2 ml serum for detection of BChE adducts and 0.010 ml serum for detection of albumin adducts. The concentration of BChE in human plasma is 4 mg/l, whereas that of albumin is 40,000 mg/l. This difference in protein abundance explains the necessity of using a larger plasma sample for detection of BChE adducts.

for covalent reaction with tyrosine 411 of albumin. (3) The chlorpyrifos poison ingested by patients is converted to the toxic oxon by hepatic cytochrome P450 enzymes. There is a 10-fold variability in the efficiency of this step, as shown in studies that measured plasma levels of both the chlorpyrifos and the oxon (Eyer *et al.*, 2009). Patients with high CYP2B6 and CYP3A4 levels would produce more of the oxon and therefore might have detectable levels of OP-albumin adducts in 0.01 ml plasma. However, detection of albumin adducts in other patients is expected to require plasma volumes larger than 0.01 ml.

### *OP-Albumin Adduct in Poisoned Humans*

This is the first report to identify OP-albumin adducts in humans poisoned by OP. The amino acid modified by covalent attachment of dichlorvos is tyrosine 411. In previous work, we have found that many proteins can be modified by OP on tyrosine and that the OP-tyrosine adduct is stable and does not undergo aging (Li *et al.*, 2008; Schopfer *et al.*, 2010). Identification of the dichlorvos-albumin adduct in human serum required only 0.010 ml of serum because the exposure levels were high, as indicated by plasma BChE inhibition levels of 80%. It is anticipated that detection of OP-albumin adducts in people exposed to low doses will also be possible but that larger volumes of plasma will need to be processed in preparation for analysis by mass spectrometry. OP-albumin adducts have been found in the plasma of guinea pigs treated *in vivo* with the nerve agents tabun, soman, sarin, and cyclosarin (Read *et al.*, 2010; Williams *et al.*, 2007).

### *OP-Albumin as a Biomarker of Exposure*

Butyrylcholinesterase in human plasma reacts rapidly with a wide range of OP. Upon reaction with OP, the enzymatic

activity of BChE is inhibited. Loss of activity has long served as an indicator of OP exposure (Eddleston *et al.*, 2008; Namba *et al.*, 1971). However, use of BChE activity as a biomarker for OP exposure has major drawbacks. (1) The normal activity of BChE can vary widely so that only severe exposure can be confidently diagnosed (Eddleston *et al.*, 2008; Kalow and Staron, 1957). (2) Hepatocarcinoma and malnutrition can cause depression of BChE activity (Whittaker, 1980). (3) Other compounds, such as carbamates, can inhibit BChE activity (Li *et al.*, 2009) so that the true identity of the inhibitor is always in question. Consequently, efforts have shifted to the application of mass spectrometry for identification of the actual adducts formed upon reaction of BChE with inhibitors (Fidder *et al.*, 2002; Li *et al.*, 2009). Mass spectrometry provides a direct measure of the nature of the inhibitor attached to BChE. However, analysis of OP adducts on BChE as biomarkers for OP exposure also has drawbacks. The principal problem is that OP adducts on the active site serine of BChE are unstable. Instability arises from two sources. (1) Treatment with oximes releases the OP from serine, and oxime treatment is part of the normal medical response to OP poisoning. (2) Spontaneous dealkylation of the OP on BChE occurs via the aging process (Masson and Lockridge, 2010). Dealkylation reduces the information content of the resulting adduct. For example, aging converts adducts with soman, sarin, and cyclosarin to identical methylphosphonate structures, as indicated in Figure 6. The products of the aging of dichlorvos and chlorpyrifos oxon adducts on BChE are illustrated in Figure 1. To circumvent these drawbacks, new OP targets have been sought. Serum albumin is a promising candidate (Li *et al.*, 2007, 2008; Means and Wu, 1979; Noort *et al.*, 2009; Ortigoza-Ferado *et al.*, 1984; Read *et al.*, 2010; Sogorb *et al.*, 2008; Tarhoni *et al.*, 2008; Williams *et al.*, 2007; Yeung *et al.*, 2008).

The OP-albumin adduct has several advantages as a biomarker of OP exposure. (1) OP binds to tyrosine 411 on albumin, and tyrosine adducts are not reversed by oximes (Read *et al.*, 2010). (2) OP-tyrosine adducts do not age (Li *et al.*, 2007; Williams *et al.*, 2007). This means that exposure to soman can be distinguished from exposure to sarin and to cyclosarin. (3) The OP-albumin adduct persists longer in the blood than the OP-BChE adduct. Studies in guinea pigs treated with nerve agents found OP-tyrosine adducts 24 days after exposure to OP, at a time when OP-BChE adducts were undetectable (Read *et al.*, 2010).

The major drawback for use of albumin-OP adducts as a biomarker for exposure to OP is the slow reaction of OP with albumin (Li *et al.*, 2008). However, despite the low reactivity, OP-albumin adducts form *in vivo* and can be detected using mass spectral techniques, as has been demonstrated in this report.

The principal advantage of working with albumin is the stability of its OP-tyrosine adduct. Another significant factor is that the OP adduct is located on the surface of albumin, as opposed to the adduct on BChE that is located at the bottom of

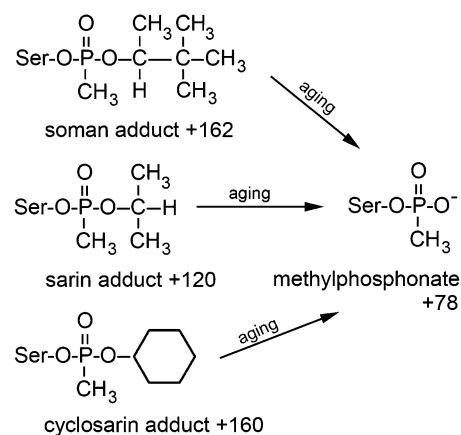


**FIG. 6.** Aging yields the identical methylphosphonate adduct on BChE. The reactions of soman, sarin, and cyclosarin with serine 198 of BChE yield distinct initial covalent adducts with added masses of + 162 for soman, + 120 for sarin, and + 160 for cyclosarin. These adducts age to the identical methylphosphonate structure with an added mass of + 78.

a deep pocket in the protein (Nachon *et al.*, 2005). A novel outgrowth of the stability and accessibility of the albumin adduct is the potential to develop antibodies to OP-tyrosine. Such antibodies could be used for detection of OP exposure.

#### *Hypothesis to Explain Neurotoxicity because of Chronic Low-Dose Exposure to OP*

It is generally agreed that acute toxicity because of exposure to OP comes from inhibition of acetylcholinesterase in the synapses and nerve muscle junctions (Miles *et al.*, 1998). However, inhibition of acetylcholinesterase does not explain all of the clinical sequelae that arise from exposure to OP, especially low-dose exposure. It has been proposed that excess acetylcholine or inhibition of serine hydrolases with greater OP reactivity than acetylcholinesterase may explain low-dose neurotoxicity (Pernot *et al.*, 2009; Richards *et al.*, 2000). Symptoms of low-dose toxicity are neurological in nature (e.g., headache, memory loss, anxiety, fatigue) (Ray and Richards, 2001; Salvi *et al.*, 2003). Investigation into the causes of this neurotoxicity is ongoing.

OP binding to albumin would not be expected to explain the neurotoxicity of OP but can serve as a model for what could be happening to other proteins. The special reactivity of tyrosine 411 in human albumin suggests that other proteins may have similarly reactive tyrosine residues. In fact, we have demonstrated that OP react with tyrosine on tubulin and that this reaction can disrupt the structure of microtubules *in vitro* and *in vivo* (Grigoryan and Lockridge, 2009; Jiang *et al.*, 2010). If the function of key proteins important for axonal transport (such as tubulin) is disrupted by OP, the neuron could lose synaptic connectivity and nerve function (Gearhart *et al.*, 2007; Terry *et al.*, 2007).

Epidemiologists have linked chronic low-dose OP exposure to Parkinson's disease, neurologic dysfunction, Gulf War illness, and depression (Beseler *et al.*, 2008; Hancock *et al.*, 2008; Kamel *et al.*, 2007; Toomey *et al.*, 2009). Disruption of axonal transport has been suggested as the mechanism to explain neurodegenerative diseases, including Parkinson's, Alzheimer disease, and amyotrophic lateral sclerosis (Morfini *et al.*, 2009). Our finding that tyrosine in albumin is covalently labeled by OP in clinically relevant human cases suggests that OP labeling of tyrosine in other proteins may also be occurring under these conditions. This concept provides a new direction in the search for a mechanism of OP-induced chronic neurotoxicity.

### FUNDING

The U.S. Army Medical Research and Materiel Command (W81XWH-07-2-0034 to O.L.); the National Institutes of Health (U01 NS058056 to O.L.) and CA36727; Délégation Générale pour l'Armement (DGA/PEA 03CO10-05/01 08 7 to P.M.) (DGA/PEA 08CO501 to F.N.); Agence Nationale de la Recherche (ANR-06-BLAN-0163 and ANR-09-BLAN-0192 to F.N.).

### ACKNOWLEDGMENTS

Mass spectra were obtained with the support of the Mass Spectrometry and Proteomics core facility at the University of Nebraska Medical Center.

### REFERENCES

- Beseler, C. L., Stallones, L., Hoppin, J. A., Alavanja, M. C., Blair, A., Keefe, T., and Kamel, F. (2008). Depression and pesticide exposures among private pesticide applicators enrolled in the Agricultural Health Study. *Environ. Health Perspect.* **116**, 1713–1719.
- Ding, S. J., Carr, J., Carlson, J. E., Tong, L., Xue, W., Li, Y., Schopfer, L. M., Li, B., Nachon, F., Asojo, O., *et al.* (2008). Five tyrosines and two serines in human albumin are labeled by the organophosphorus agent FP-biotin. *Chem. Res. Toxicol.* **21**, 1787–1794; PMID:2646670
- Eddleston, M., Eyer, P., Worek, F., Sheriff, M. H., and Buckley, N. A. (2008). Predicting outcome using butyrylcholinesterase activity in organophosphorus pesticide self-poisoning. *QJM* **101**, 467–474.
- Ellman, G. L., Courtney, K. D., Andres, V., Jr, and Feather-Stone, R. M. (1961). A new and rapid colorimetric determination of acetylcholinesterase activity. *Biochem. Pharmacol.* **7**, 88–95.
- Eyer, F., Roberts, D. M., Buckley, N. A., Eddleston, M., Thiermann, H., Worek, F., and Eyer, P. (2009). Extreme variability in the formation of chlorpyrifos oxon (CPO) in patients poisoned by chlorpyrifos (CPF). *Biochem. Pharmacol.* **78**, 531–537.
- Fidder, A., Hulst, A. G., Noort, D., de Ruiter, R., van der Schans, M. J., Benschop, H. P., and Langenberg, J. P. (2002). Retrospective detection of exposure to organophosphorus anti-cholinesterases: mass spectrometric analysis of phosphorylated human butyrylcholinesterase. *Chem. Res. Toxicol.* **15**, 582–590.
- Gearhart, D. A., Sickles, D. W., Buccafusco, J. J., Prendergast, M. A., and Terry, A. V., Jr. (2007). Chlorpyrifos, chlorpyrifos-oxon, and diisopropyl-fluorophosphate inhibit kinesin-dependent microtubule motility. *Toxicol. Appl. Pharmacol.* **218**, 20–29.
- Grigoryan, H., and Lockridge, O. (2009). Nanoimages show disruption of tubulin polymerization by chlorpyrifos oxon: implications for neurotoxicity. *Toxicol. Appl. Pharmacol.* **240**, 143–148.
- Hancock, D. B., Martin, E. R., Mayhew, G. M., Stajich, J. M., Jewett, R., Stacy, M. A., Scott, B. L., Vance, J. M., and Scott, W. K. (2008). Pesticide exposure and risk of Parkinson's disease: a family-based case-control study. *BMC Neurol.* **8**, 6.
- Heilmair, R., Eyer, F., and Eyer, P. (2008). Enzyme-based assay for quantification of chlorpyrifos oxon in human plasma. *Toxicol. Lett.* **181**, 19–24.
- Jiang, W., Duysen, E. G., Hansen, H., Shlyakhtenko, L., Schopfer, L. M., and Lockridge, O. (2010). Mice treated with chlorpyrifos or chlorpyrifos oxon have organophosphorylated tubulin in the brain and disrupted microtubule structures, suggesting a role for tubulin in neurotoxicity associated with exposure to organophosphorus agents. *Toxicol. Sci.* **115**, 183–193.
- Kalow, W., and Staron, N. (1957). On distribution and inheritance of atypical forms of human serum cholinesterase, as indicated by dibucaine numbers. *Can. J. Med. Sci.* **35**, 1305–1320.
- Kamel, F., Engel, L. S., Gladen, B. C., Hoppin, J. A., Alavanja, M. C., and Sandler, D. P. (2007). Neurologic symptoms in licensed pesticide applicators in the Agricultural Health Study. *Hum. Exp. Toxicol.* **26**, 243–250.
- Li, B., Nachon, F., Froment, M. T., Verdier, L., Debouzy, J. C., Brasme, B., Gillon, E., Schopfer, L. M., Lockridge, O., and Masson, P. (2008). Binding and hydrolysis of soman by human serum albumin. *Chem. Res. Toxicol.* **21**, 421–431.
- Li, B., Ricordel, I., Schopfer, L. M., Baud, F., Megarbane, B., Masson, P., and Lockridge, O. (2010). Dichlorvos, chlorpyrifos oxon, and aldicarb adducts of butyrylcholinesterase detected by mass spectrometry, in human plasma following deliberate overdose. *J. Appl. Toxicol.* Advance Access published on April 13, 2010; doi: 10.1002/jat.1526.
- Li, B., Schopfer, L. M., Hinrichs, S. H., Masson, P., and Lockridge, O. (2007). Matrix-assisted laser desorption/ionization time-of-flight mass spectrometry assay for organophosphorus toxicants bound to human albumin at Tyr411. *Anal. Biochem.* **361**, 263–272; PMID:1828685.
- Li, H., Ricordel, I., Tong, L., Schopfer, L. M., Baud, F., Megarbane, B., Maury, E., Masson, P., and Lockridge, O. (2009). Carbofuran poisoning detected by mass spectrometry of butyrylcholinesterase adduct in human serum. *J. Appl. Toxicol.* **29**, 149–155.
- Masson, P., Froment, M. T., Bartels, C. F., and Lockridge, O. (1997). Importance of aspartate-70 in organophosphate inhibition, oxime re-activation and aging of human butyrylcholinesterase. *Biochem. J.* **325**(Pt 1), 53–61.
- Masson, P., and Lockridge, O. (2010). Butyrylcholinesterase for protection from organophosphorus poisons: catalytic complexities and hysteretic behavior. *Arch. Biochem. Biophys.* **494**, 107–120.
- Means, G. E., and Wu, H. L. (1979). The reactive tyrosine residue of human serum albumin: characterization of its reaction with diisopropylfluorophosphate. *Arch. Biochem. Biophys.* **194**, 526–530.
- Miles, B. E., Chambers, J. E., Chen, W. L., Dettbarn, W., Ehrich, M., Eldefrawi, A. T., Gaylor, D. W., Hamernik, K., Hodgson, E., Karczmar, A. G., *et al.* (1998). Common mechanism of toxicity: a case study of organophosphorus pesticides. *Toxicol. Sci.* **41**, 8–20.
- Morfini, G. A., Burns, M., Binder, L. I., Kanaan, N. M., LaPointe, N., Bosco, D. A., Brown, R. H., Jr, Brown, H., Tiwari, A., Hayward, L., *et al.* (2009). Axonal transport defects in neurodegenerative diseases. *J. Neurosci.* **29**, 12776–12786.
- Nachon, F., Asojo, O. A., Borgstahl, G. E., Masson, P., and Lockridge, O. (2005). Role of water in aging of human butyrylcholinesterase inhibited by echothiophate: the crystal structure suggests two alternative mechanisms of aging. *Biochemistry* **44**, 1154–1162.

- Namba, T., Nolte, C. T., Jackrel, J., and Grob, D. (1971). Poisoning due to organophosphate insecticides. Acute and chronic manifestations. *Am. J. Med.* **50**, 475–492.
- Noort, D., Hulst, A. G., van Zuylen, A., van Rijssel, E., and van der Schans, M. J. (2009). Covalent binding of organophosphorothioates to albumin: a new perspective for OP-pesticide biomonitoring? *Arch. Toxicol.* **83**, 1031–1036.
- Ortigoza-Ferado, J., Richter, R. J., Hornung, S. K., Motulsky, A. G., and Furlong, C. E. (1984). Paraoxon hydrolysis in human serum mediated by a genetically variable arylesterase and albumin. *Am. J. Hum. Genet.* **36**, 295–305.
- Peebles, E. S., Schopfer, L. M., Duysen, E. G., Spaulding, R., Voelker, T., Thompson, C. M., and Lockridge, O. (2005). Albumin, a new biomarker of organophosphorus toxicant exposure, identified by mass spectrometry. *Toxicol. Sci.* **83**, 303–312.
- Pernot, F., Carpentier, P., Baille, V., Testylier, G., Beaup, C., Foquin, A., Filliat, P., Liscia, P., Coutan, M., Pierard, C., et al. (2009). Intrahippocampal cholinesterase inhibition induces epileptogenesis in mice without evidence of neurodegenerative events. *Neuroscience* **162**, 1351–1365.
- Quistad, G. B., Klintonberg, R., and Casida, J. E. (2005). Blood acylpeptide hydrolase activity is a sensitive marker for exposure to some organophosphate toxicants. *Toxicol. Sci.* **86**, 291–299.
- Ray, D. E., and Richards, P. G. (2001). The potential for toxic effects of chronic, low-dose exposure to organophosphates. *Toxicol. Lett.* **120**, 343–351.
- Read, R. W., Riches, J. R., Stevens, J. A., Stubbs, S. J., and Black, R. M. (2010). Biomarkers of organophosphorus nerve agent exposure: comparison of phosphorylated butyrylcholinesterase and phosphorylated albumin after oxime therapy. *Arch. Toxicol.* **84**, 25–36.
- Richards, P. G., Johnson, M. K., and Ray, D. E. (2000). Identification of acylpeptide hydrolase as a sensitive site for reaction with organophosphorus compounds and a potential target for cognitive enhancing drugs. *Mol. Pharmacol.* **58**, 577–583.
- Salvi, R. M., Lara, D. R., Ghisolfi, E. S., Portela, L. V., Dias, R. D., and Souza, D. O. (2003). Neuropsychiatric evaluation in subjects chronically exposed to organophosphate pesticides. *Toxicol. Sci.* **72**, 267–271.
- Sams, C., Cocker, J., and Lennard, M. S. (2004). Biotransformation of chlorpyrifos and diazinon by human liver microsomes and recombinant human cytochrome P450s (CYP). *Xenobiotica* **34**, 861–873.
- Schopfer, L. M., Grigoryan, H., Li, B., Nachon, F., Masson, P., and Lockridge, O. (2010). Mass spectral characterization of organophosphate-labeled, tyrosine-containing peptides: characteristic mass fragments and a new binding motif for organophosphates. *J. Chromatogr. B Analyt. Technol. Biomed. Life Sci.* **878**, 1297–1311.
- Sogorb, M. A., Garcia-Arguelles, S., Carrera, V., and Vilanova, E. (2008). Serum albumin is as efficient as paraxonase in the detoxication of paraoxon at toxicologically relevant concentrations. *Chem. Res. Toxicol.* **21**, 1524–1529.
- Tang, J., Cao, Y., Rose, R. L., Brimfield, A. A., Dai, D., Goldstein, J. A., and Hodgson, E. (2001). Metabolism of chlorpyrifos by human cytochrome P450 isoforms and human, mouse, and rat liver microsomes. *Drug Metab. Dispos.* **29**, 1201–1204.
- Tarhoni, M. H., Lister, T., Ray, D. E., and Carter, W. G. (2008). Albumin binding as a potential biomarker of exposure to moderately low levels of organophosphorus pesticides. *Biomarkers* **13**, 343–363.
- Terry, A. V., Jr, Gearhart, D. A., Beck, W. D., Jr, Truan, J. N., Middlemore, M. L., Williamson, L. N., Bartlett, M. G., Prendergast, M. A., Sickles, D. W., and Buccafusco, J. J. (2007). Chronic, intermittent exposure to chlorpyrifos in rats: protracted effects on axonal transport, neurotrophin receptors, cholinergic markers, and information processing. *J. Pharmacol. Exp. Ther.* **322**, 1117–1128.
- Toomey, R., Alpern, R., Vasterling, J. J., Baker, D. G., Reda, D. J., Lyons, M. J., Henderson, W. G., Kang, H. K., Eisen, S. A., and Murphy, F. M. (2009). Neuropsychological functioning of U.S. Gulf War veterans 10 years after the war. *J. Int. Neuropsychol. Soc.* **15**, 717–729.
- Whittaker, M. (1980). Plasma cholinesterase variants and the anaesthetist. *Anaesthesia* **35**, 174–197.
- Williams, N. H., Harrison, J. M., Read, R. W., and Black, R. M. (2007). Phosphorylated tyrosine in albumin as a biomarker of exposure to organophosphorus nerve agents. *Arch. Toxicol.* **81**, 627–639.
- Worek, F., Diepold, C., and Eyer, P. (1999). Dimethylphosphoryl-inhibited human cholinesterases: inhibition, reactivation, and aging kinetics. *Arch. Toxicol.* **73**, 7–14.
- Yeung, D. T., Smith, J. R., Sweeney, R. E., Lenz, D. E., and Cerasoli, D. M. (2008). A gas chromatographic-mass spectrometric approach to examining stereoselective interaction of human plasma proteins with soman. *J. Anal. Toxicol.* **32**, 86–91.

# Tyrosines of Human and Mouse Transferrin Covalently Labeled by Organophosphorus Agents: A New Motif for Binding to Proteins that Have No Active Site Serine

Bin Li,\* Lawrence M. Schopfer,\* Hasmik Grigoryan,\* Charles M. Thompson,† Steven H. Hinrichs,‡ Patrick Masson,§ and Oksana Lockridge\*<sup>1</sup>

\*Eppley Institute, University of Nebraska Medical Center, Omaha, Nebraska 68198-6805; †Department of Biomedical and Pharmaceutical Sciences, University of Montana, Missoula, Montana 59812; ‡Department of Pathology and Microbiology, University of Nebraska Medical Center, Omaha, Nebraska 68198; and §Centre de Recherches d Service de Santé des Armées, Unité d'Enzymologie, BP87, 38702 La Tronche Cedex, France

Received August 5, 2008; accepted September 26, 2008

The expectation from the literature is that organophosphorus (OP) agents bind to proteins that have an active site serine. However, transferrin, a protein with no active site serine, was covalently modified *in vitro* by 0.5mM 10-fluoroethoxyphosphinyl-N-biotinamido pentyldodecanamide, chlorpyrifos oxon, diisopropylfluorophosphate, dichlorvos, sarin, and soman. The site of covalent attachment was identified by analyzing tryptic peptides in the mass spectrometer. Tyr 238 and Tyr 574 in human transferrin and Tyr 238, Tyr 319, Tyr 429, Tyr 491, and Tyr 518 in mouse transferrin were labeled by OP. Tyrosine in the small synthetic peptide ArgTyrThrArg made a covalent bond with diisopropylfluorophosphate, chlorpyrifos oxon, and dichlorvos at pH 8.3. These results, together with our previous demonstration that albumin and tubulin bind OP on tyrosine, lead to the conclusion that OP bind covalently to tyrosine, and that OP binding to tyrosine is a new OP-binding residue. The OP-reactive tyrosines are activated by interaction with Arg or Lys. It is suggested that many proteins in addition to those already identified may be modified by OP on tyrosine. The extent to which tyrosine modification by OP can occur *in vivo* and the toxicological implications of such modifications require further investigation.

**Key Words:** plasma; soman; sarin; mass spectrometry; tyrosine residue; transferrin.

We have previously shown that many proteins in plasma react with the organophosphorus agent (OP) FP-biotin (10-fluoroethoxyphosphinyl-N-biotinamido pentyldodecanamide) (Peeples *et al.*, 2005). Our goal is to identify these proteins. The proteins that react most rapidly with FP-biotin and with other OP are enzymes in the serine hydrolase family, for example, butyrylcholinesterase, acetylcholinesterase, acylpeptide hydrolase, fatty acid amide hydrolase, arylformamidase, and neuropathy target esterase-lysophospholipase (Casida and

Quistad, 2004; Richards *et al.*, 2000). The residue that is labeled in these enzymes is the active site serine in the consensus sequence GlyXSerXGly. However, proteins with no consensus active site serine constitute another group of OP-reactive proteins, where OP bind to tyrosine. Papain and bromelain bind diisopropylfluorophosphate (DFP) on tyrosine (Chaiken and Smith, 1969; Murachi *et al.*, 1965). Mass spectrometry has allowed identification of OP-binding to tyrosines in albumin and tubulin (Ding *et al.*, 2008; Grigoryan *et al.*, 2008; Li *et al.*, 2007, 2008). The present report adds transferrin to this list. Analysis of the reactive peptides from these proteins shows that a new motif of OP binding has emerged.

Our strategy uses FP-biotin, initially, to label the OP-reactive proteins in plasma. Through the use of the fluorescent probe Streptavidin-Alexa 680 and the biotin tag, the proteins that are OP-reactive in serum can be visualized. The biotin tag also provides a means for purification of the labeled proteins and peptides by binding to avidin-agarose beads. The FP-biotin-labeled proteins and peptides are identified by mass spectrometry. It is relatively simple to identify a protein by mass spectrometry because only a few peptides from a protein are needed for a positive identification. However, it is often difficult to find a specific labeled peptide. Convincing proof that a protein is OP-labeled comes from identifying the labeled peptide and the amino acid in that peptide that is modified by OP. To provide this proof we label pure protein with OP, digest with trypsin, separate and enrich the OP-labeled peptides by reverse phase high-performance liquid chromatography (HPLC), and determine the peptide sequence and site of attachment by collision-induced dissociation in the mass spectrometer.

Not all OP are expected to bind covalently to a particular protein. For example, the positively charged echothiophate and VX react rapidly with acetylcholinesterase, but only poorly with carboxylesterase (Maxwell and Brecht, 2001). Therefore we treated human and mouse transferrin with six different OP. We found human transferrin peptides labeled with six OP, and mouse transferrin peptides labeled with five OP.

<sup>1</sup> To whom correspondence should be addressed at Eppley Institute, University of Nebraska Medical Center, Omaha, NE 68198-6805. Fax: (402) 559-4651. E-mail: olockrid@unmc.edu.

The common feature in the motif for OP-reactive tyrosines is the presence of a positively charged arginine or lysine within five residues of the tyrosine. This OP-binding motif was tested with two synthetic peptides, both containing tyrosine, but only one containing nearby arginines. Tyrosine formed a covalent bond with OP in both peptides, but the reaction proceeded more readily with ArgTyrThrArg than with SerTyrSerMet. Additional work with small peptides needs to be done to determine the optimum peptide sequence of the OP reactive peptide and to determine its rate of reaction with OP.

## EXPERIMENTAL PROCEDURES

**Materials.** FP-biotin (Mr 592.32) was custom synthesized in the laboratory of Dr Charles Thompson at the University of Montana, Missoula, MT. A 2mM FP-biotin solution in dimethyl sulfoxide was stored at  $-80^{\circ}\text{C}$ . Chlorpyrifos oxon (ChemService, Inc. West Chester, PA; MET-674B) was dissolved in ethanol and stored at  $-80^{\circ}\text{C}$ . Dichlorvos (ChemService Inc.; PS-89) was dissolved in methanol. Soman and sarin from CEB (Vert-le-Petit, France) were dissolved in isopropanol. Immun-Blot polyvinylidene difluoride (PVDF) membrane for protein blotting, 0.2  $\mu\text{m}$  (162-0177) and Affi-gel blue (153-7301), a cross-linked agarose bead with covalently attached Cibacron Blue F3GA dye, were from Bio-Rad Laboratories, Hercules, CA. Streptavidin Alexa Fluor 680 (S-21378) was from Molecular Probes, Eugene, OR. Porcine trypsin (Promega, Madison, WI; V5113 sequencing grade modified trypsin) at a concentration of 0.4  $\mu\text{g}/\mu\text{l}$  in 50mM acetic acid was stored at  $-80^{\circ}\text{C}$ . Immobilized tetrameric avidin-agarose beads (Pierce 20219) and immobilized monomeric avidin-agarose beads (Pierce 20228) were used to purify FP-biotinylated proteins as well as FP-biotinylated peptides. Human butyrylcholinesterase was purified from outdated human plasma as described (Lockridge *et al.*, 2005) and labeled with FP-biotin as described (Peeples *et al.*, 2005). Mouse plasma was from strain 129Sv mice. Human holo-transferrin (T0665), human apo-transferrin (T4382), mouse apo-transferrin (T0523), bovine holo-transferrin (T1408), human alpha 2-macroglobulin (M6159), human alpha 1-antitrypsin (A9024), human complement C3 (C2910), nitrilotriacetic acid (N9877), Coomassie blue R250 (Brilliant Blue R), and diisopropylfluorophosphate (D0879, a liquid with a concentration of 5.73M) were from Sigma, St Louis, MO. ProbeQuant G50 micro column was from Amersham (27-5335-01). Peptide ArgTyrThrArg (Mr 594.7) was custom synthesized and purified to  $> 95\%$  by Genscript Corp., Piscataway, NJ. Peptide SerTyrSerMet (#20621; Mr 486.5) was from AnaSpec, Inc., San Jose, CA. Alpha-cyano-4-hydroxy cinnamic acid, Glu Fibrinopeptide B, and Cal Mix 1 were from Applied Biosystems (MDS Sciex, Foster City, CA).

**Blot of FP-biotin-labeled proteins from a nondenaturing polyacrylamide electrophoresis gel.** Two hundred microliters of human or mouse plasma was treated with 100 $\mu\text{M}$  FP-biotin

for 24 h at  $37^{\circ}\text{C}$ . Ten- to 30- $\mu\text{l}$  aliquots were subjected to gel electrophoresis on nondenaturing polyacrylamide gradient gels, 4–22.5% (wt/vol), cast in a Hoefer gel apparatus. The polyacrylamide gel electrophoresis (PAGE) gels were 0.75 mm thick, 15 cm wide, and 12 cm high. Nondenaturing gels were used because albumin separates from other plasma proteins on a nondenaturing gel, but not on a sodium dodecyl sulfate (SDS) gel. Proteins were electrophoretically transferred to a PVDF membrane using a Bio-Rad Trans-blot apparatus. The blot was hybridized with a fluorescent probe, Streptavidin Alexa Fluor 680, as described (Peeples *et al.*, 2005). Fluorescence intensity was captured in the Odyssey Infrared Imaging System (LiCor).

**Blot of FP-biotin-labeled proteins from an SDS PAGE gel.** Purified bovine holo-transferrin (76–81 kDa), human alpha 2-macroglobulin (tetramer 720 kDa; monomer 179 kDa), human alpha 1-antitrypsin (52 kDa), and human complement C3 (115 and 70 kDa) were dissolved in phosphate buffered saline to a concentration of 500 pmol in 50  $\mu\text{l}$ . Proteins were treated with 100 $\mu\text{M}$  FP-biotin at  $37^{\circ}\text{C}$  for 20 h. Control samples were treated with dimethyl sulfoxide but no FP-biotin. Unreacted FP-biotin was removed by passing the samples through a G50 spin column. Samples were boiled in the presence of dithiothreitol and SDS and loaded on a 4–22.5% (wt/vol) polyacrylamide gradient SDS gel. After electrophoresis, some gels were stained for protein with Coomassie blue R250. For other gels, the protein was transferred to a PVDF membrane where the biotin tag was detected with Streptavidin Alexa Fluor 680, as described (Peeples *et al.*, 2005). The amount of protein loaded on the Coomassie stained gel ranged from 3.5 to 70  $\mu\text{g}$ , and that on the gel used for transfer to PVDF ranged from 1.5 to 30  $\mu\text{g}$ .

**Isolation of FP-biotin-labeled proteins with avidin-agarose beads.** Plasma was depleted of albumin by chromatography on Affi-gel blue because albumin reacts extensively with FP-biotin and can deplete the FP-biotin pool making reaction with other proteins more difficult. The albumin-depleted plasma was treated with 100 $\mu\text{M}$  FP-biotin for 24 h at  $37^{\circ}\text{C}$ , and dialyzed to remove excess FP-biotin. The FP-biotinylated proteins were purified by binding to tetrameric avidin-agarose beads and separated by SDS gel electrophoresis as described (Peeples *et al.*, 2005).

**Purification of FP-biotin-labeled peptides.** In some experiments the FP-biotin-labeled peptides rather than FP-biotin-labeled proteins were purified by binding to monomeric avidin-agarose beads. After washing with 1M NaCl in pH 8.0 buffer, followed by water washes to desalt the column, the peptides were released with 10% (vol/vol) acetic acid.

**Reaction of pure transferrin with OP.** A 1 mg/ml solution of human or mouse transferrin in 0.1M TrisCl pH 8.5, or in phosphate buffered saline, or in 10mM TrisCl pH 8.5, 0.01% (wt/vol) sodium azide was treated with 0.5mM OP at  $37^{\circ}\text{C}$  for 16 h. The accession numbers in the SwissProt database are

P02787 for human and Q921I1 for mouse transferrin. Their molecular weight is about 75,000 after the 19 amino acid signal peptide is subtracted.

**Tryptic peptides for mass spectrometry.** Three protocols were used to prepare peptides for mass spectrometry. (1) Proteins in SDS PAGE gel slices were digested with trypsin. The peptides were extracted from the gel and analyzed by liquid chromatography tandem mass spectrometry (LC/MS/MS) as described (Peeples *et al.*, 2005). This protocol was used only for the preliminary experiments where the data are not shown. (2) Pure proteins in solution were denatured in 8M urea, reduced with 10mM dithiothreitol at pH 8, carbamidomethylated (CAM) with 50mM iodoacetamide, and desalted by dialysis against 10mM ammonium bicarbonate. The CAM proteins were digested with trypsin at a ratio of 50:1 (w/w) at 37°C for 16 h. Peptides were separated offline by reverse phase HPLC on a 100 × 4.60 mm Phenomenex C18 column eluted with a 60 min gradient from 0 to 60% (vol/vol) acetonitrile versus 0.1% (vol/vol) trifluoroacetic acid at a flow rate of 1 ml/min. Fractions were analyzed by matrix-assisted laser desorption ionization-time of flight (MALDI-TOF) mass spectrometry to locate the OP-labeled peptides. Selected samples were dried, dissolved in 50% acetonitrile, 0.1% formic acid, and infused into the QTRAP 4000 mass spectrometer for MS/MS analysis. Peptides were infused into the mass spectrometer when the mass of the parent ion was known. (3) Trypsin digested pure protein was analyzed a second way to allow for the possibility that the mass of the parent ion was unknown. The offline HPLC step was omitted, and peptides were separated on a nanocolumn whose output was electrosprayed into the QTRAP 2000 mass spectrometer. MS/MS spectra were acquired for three peptides every 2.8 s.

**Reaction of model peptides with OP.** Peptides ArgTyr-ThrArg (0.17mM) and SerTyrSerMet (0.17mM) in 10mM ammonium bicarbonate pH 8.3 were treated with 0.1, 0.2, or 1mM DFP, chlorpyrifos oxon (CPO), or dichlorvos for 16 h at 37°C. Aliquots were spotted on a MALDI target plate, overlaid with CHCA ( $\alpha$ -cyano-4-hydroxy cinnamic acid) matrix, and analyzed by MALDI-TOF as well as by MALDI-TOF-TOF mass spectrometry and by LC/MS/MS on the QTRAP 2000.

**Percent labeling.** The percent labeled peptide in a given MALDI-TOF spectrum was calculated by dividing the cluster area of the labeled peptide by the sum of the cluster areas for the unlabeled and labeled peaks in a given spectrum. The assumption in this calculation is that the labeled and unlabeled peptides ionize equally well. In a previous publication (Lockridge *et al.*, 2008) we checked the validity of our MALDI-TOF quantitation method by using a second method to quantitate labeled and unlabeled peptides. The second method was amino acid composition analysis. Both methods showed that 27% of a particular peptide was labeled, thus validating the MALDI-TOF quantitation method.

**MALDI-TOF mass spectrometry.** All peptide samples were screened by MALDI-TOF before they were analyzed in the QTRAP mass spectrometer because MALDI-TOF is a quick way to obtain peptide masses and thereby a suggestion of whether an OP-labeled peptide is present. Salt-free peptides were spotted on a target plate in 0.5- $\mu$ l aliquots, allowed to dry, and overlaid with 10 mg/ml CHCA matrix in 50% acetonitrile, 0.1% trifluoroacetic acid. Mass spectra were acquired with the MALDI-TOF-TOF 4800 mass spectrometer (Applied Biosystems, MDS Sciex, Foster City, CA). Each scan is the sum of 500 laser shots—50 shots were taken at one location on the spot and then the laser automatically moved to a new location to avoid burning out the sample. Laser intensity was adjusted to obtain maximum signal intensity without exceeding the saturation limit. The mass spectrometer was calibrated against Cal Mix 1 (des-Arg Bradykinin, Glu Fibrinopeptide B, angiotensin I, and neurotensin).

**LC/MS/MS on a tandem quadrupole mass spectrometer.** Tryptic digests of OP-labeled human and mouse transferrin were analyzed by this method. A 10- $\mu$ l aliquot of peptides in 5% acetonitrile, 0.1% formic acid, at a concentration of about 2 pmol/ $\mu$ l, was injected into the HPLC nanocolumn (#218MS3.07515 Vydac C18 polymeric rev-phase, 75 micron ID × 150 mm long; P.J. Cobert Assoc, St Louis, MO). Peptides were separated with a 90 min linear gradient from 0 to 60% acetonitrile at a flow rate of 0.3  $\mu$ l/min and electrosprayed through a nanospray emitter (fused silica, 360  $\mu$ m OD × 75  $\mu$ m ID × 15  $\mu$ m taper; New Objective) directly into the mass spectrometer. Mass spectra, high resolution mass spectra, and product ion spectra (MS/MS) were acquired on a QTRAP 2000 triple quadrupole linear ion trap mass spectrometer (Applied Biosystems) using the trap (enhanced sensitivity) mode. An ion-spray voltage of 1900 volts was maintained between the emitter and the mass spectrometer. Information-dependent acquisition was used to acquire data for the three most intense peaks in each cycle, having a charge of +1 to +4, a mass between 200 and 1700  $m/z$ , and an intensity > 10,000 counts per s. Precursor ions were excluded for 30 s after one MS/MS spectrum had been collected. The collision cell was pressurized to 40  $\mu$ Torr with pure nitrogen and collision energies between 20 and 40 eV were determined automatically by the Analyst 1.4.1 software, based on the mass and charge of the precursor ion. The mass spectrometer was calibrated using fragment ions generated from collision-induced dissociation of Glu fibrinopeptide B (Sigma). The MS/MS data were processed using Analyst 1.4.1 software and submitted to Mascot for identification of peptide sequences modified by OP on Tyr, Ser, or Thr (Perkins *et al.*, 1999).

**Infusion in the QTRAP 4000 mass spectrometer.** HPLC purified OP-labeled human and mouse transferrin tryptic peptides were analyzed by this method when the mass of the parent ion was known from MALDI-TOF experiments. Peptides were dissolved in 50% acetonitrile, 0.1% formic acid

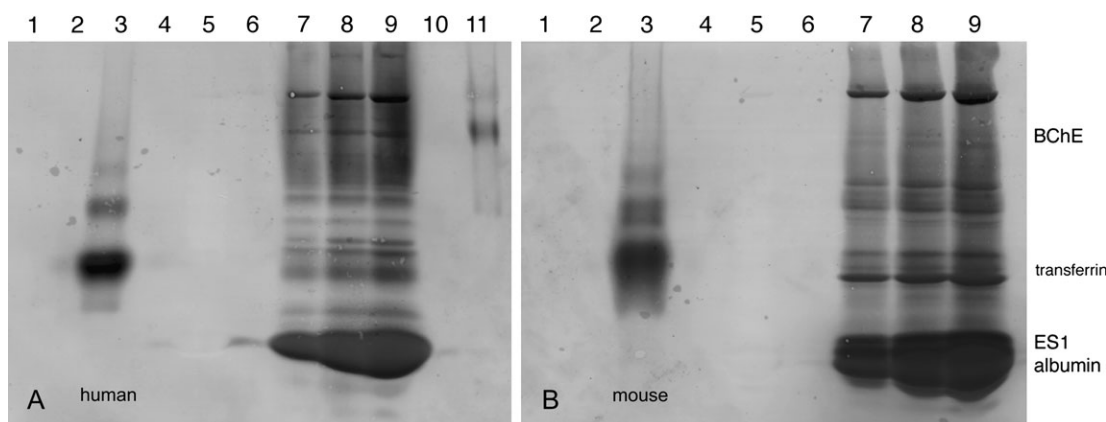


**FIG. 1.** Blots showing FP-biotin-reactive proteins in human (A) and mouse (B) plasma. FP-biotinylated plasma proteins were separated on nondenaturing polyacrylamide gels and transferred to PVDF membranes. Blots were hybridized with the fluorescent probe Streptavidin Alexa Fluor 680. A1, 20  $\mu$ g human transferrin; A2, blank; A3, 20  $\mu$ g FP-biotinylated human transferrin; A4, blank; A5, 5  $\mu$ l of human plasma; A6, blank; A7, 3.3  $\mu$ l of FP-biotinylated human plasma; A8, 6.6  $\mu$ l of FP-biotinylated human plasma; A9, 9.9  $\mu$ l of FP-biotinylated human plasma; A10, blank; A11, 1 pmol FP-biotinylated human butyrylcholinesterase (BChE). B1, 20  $\mu$ g mouse transferrin; B2, blank; B3, 20  $\mu$ g FP-biotinylated mouse transferrin; B4, blank; B5, 5  $\mu$ l of mouse plasma; B6, blank; B7, 5  $\mu$ l of FP-biotinylated mouse plasma; B8, 10  $\mu$ l of FP-biotinylated mouse plasma; B9, 15  $\mu$ l of FP-biotinylated mouse plasma. The heavy band in B contains mouse ES1 carboxylesterase and mouse albumin. ES1 carboxylesterase in mouse plasma does not separate well from albumin on a nondenaturing gel. Human plasma does not contain carboxylesterase.

to a concentration of 2–6 pmol/ $\mu$ l. Peptides were infused into the QTRAP 4000 (Applied Biosystems) mass spectrometer at a flow rate of 0.3  $\mu$ l/min through an 8  $\mu$ m emitter (#FS360-50-8-D, New Objective) via a 25- $\mu$ l Hamilton syringe mounted on a Harvard pump. Five hundred MS/MS spectra were accumulated for each parent ion.

**Binding of ferric ion to transferrin.** The normal function of transferrin is iron transport through the blood. Binding of ferric ion is a measure of the functional viability. Titration of transferrin with ferric ion was performed as described (Welch and Skinner, 1989). A 1 mg/ml solution of apo-human transferrin was prepared in 0.1M TrisCl pH 8.5 containing 5mM Na<sub>2</sub>CO<sub>3</sub>. Half of the transferrin solution was incubated with 100 $\mu$ M FP-biotin at 37°C for 16 h, resulting in the labeling of Tyr 238 and Tyr 574. The other half was the unlabeled control. Protein concentration was determined with the CB-X protein assay kit (Genotech, St Louis, MO; #786-12X). FP-biotin-labeled as well as control apo-transferrin were titrated with ferric nitrilotriacetate (FENTA) to determine the stoichiometry of ferric ion binding. Each 1 ml solution of transferrin was titrated by sequential additions of 5  $\mu$ l of 1mM FENTA. Binding was monitored by following the change in absorbance at 470 nm.

## RESULTS

### Human and Mouse Plasma Proteins that Bind FP-Biotin

The blots in Figures 1A and 1B show at least 12 bands in both human and mouse plasma that bind FP-biotin (Figs. 1A and 1B, lanes 7, 8, 9). The most intense band in human plasma is FP-biotin-labeled albumin. The most intense band in mouse

plasma contains two proteins: FP-biotin-labeled carboxylesterase ES1 and FP-biotin-labeled albumin (Fig. 1B, lanes 7, 8, 9). A major difference between human and mouse plasma is that only mouse plasma contains carboxylesterase (Li *et al.*, 2005). Albumin, ES1 carboxylesterase, and butyrylcholinesterase have previously been identified as proteins in mouse plasma that bind FP-biotin (Peebles *et al.*, 2005).

The search for additional OP-reactive proteins in plasma led to preliminary identification of human transferrin. This preliminary identification resulted from LC/MS/MS mass spectral analysis of an in-gel, tryptic digest of a band from an SDS PAGE gel. Data were acquired on the QTRAP 2000 mass spectrometer. Proteins applied to this gel had been labeled with FP-biotin and purified with avidin-agarose (data not shown). Mass spectra identified transferrin, but not the labeled peptide.

To confirm that transferrin was actually labeled by FP-biotin, pure human and mouse transferrin treated with FP-biotin were visualized on a blot hybridized with Streptavidin Alexa Fluor 680. Lane 3 in Figures 1A and 1B shows an intense band for FP-biotinylated transferrin, thus confirming that human and mouse transferrin bind FP-biotin.

The preliminary LC/MS/MS mass spectral experiments also showed alpha-2-macroglobulin, alpha-1-antitrypsin, and complement C3 as proteins in human plasma that could be labeled with FP-biotin (data not shown). As with transferrin, the FP-biotinylated plasma proteins had been purified on avidin-agarose beads, separated by SDS gel electrophoresis, digested with trypsin, and analyzed by LC/MS/MS. The labeled peptides from these proteins were not found in these preliminary experiments. To confirm that these proteins made a covalent bond with FP-biotin, highly purified preparations of the proteins were treated with FP-biotin and subjected to SDS

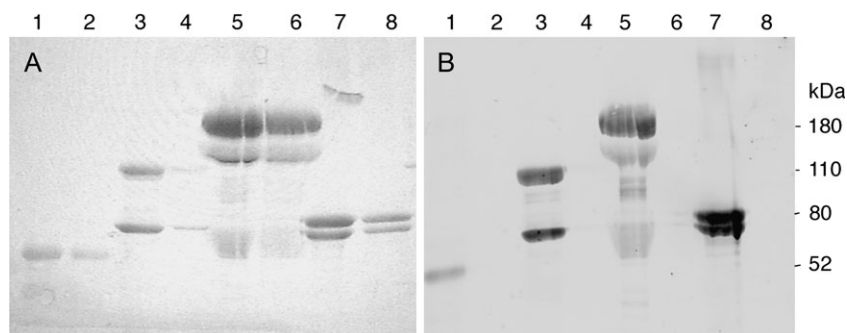


**FIG. 2.** Covalent binding of FP-biotin to human alpha-1-antitrypsin, human complement C3, human alpha-2-macroglobulin, and bovine holo-transferrin. (A) Coomassie stained SDS gel. (B) Blot hybridized with Streptavidin Alexa Fluor 680 to visualize FP-biotinylated proteins transferred to PVDF membrane from the gel. Lane 1, FP-biotinylated alpha-1-antitrypsin; lane 2, unlabeled alpha-1-antitrypsin; lane 3, FP-biotinylated complement C3; lane 4, unlabeled complement C3; lane 5, FP-biotinylated alpha-2-macroglobulin; lane 6, unlabeled alpha-2-macroglobulin; lane 7, FP-biotinylated transferrin; lane 8, unlabeled transferrin.

gel electrophoresis. The labeled proteins were transferred from the gel to PVDF membrane. The membrane was hybridized with Streptavidin Alexa Fluor 680 (Fig. 2B). A second gel, containing higher quantities of protein, was stained with Coomassie blue R250 (Fig. 2A). Figure 2 (lanes 2, 4, 6, 8) shows that control proteins, not treated with FP-biotin, have a Coomassie stained band in panel A, but no fluorescent band in panel B. On the other hand, proteins treated with FP-biotin (lanes 1, 3, 5, 7) have a band in panel A as well as in panel B. The blot confirms that human alpha-1-antitrypsin, human complement C3, human alpha-2-macroglobulin, and bovine holo-transferrin covalently bind FP-biotin.

No further results were obtained for alpha-1-antitrypsin, complement C3, and alpha-2-macroglobulin. The site for covalent attachment of FP-biotin in these proteins is unknown.

#### *Tyr 238 and Tyr 574 of Human Transferrin Bind OP*

Structures of OP are in Figure 3. FP-biotinylated, CAM tryptic peptides of human transferrin were purified on monomeric avidin beads and their masses determined by MALDI-TOF mass spectrometry. Every peak in the MALDI-TOF spectrum was fragmented with the MALDI-TOF-TOF feature of the mass spectrometer. The MS/MS scans were examined for the presence of ions characteristic of FP-biotin at 227, 312, and 329 amu (Schopfer *et al.*, 2005). A peptide that fragmented to yield these ions was labeled with FP-biotin. Additional information about the peptide was obtained in the QTRAP 4000 mass spectrometer.

Two FP-biotin-labeled peptides were identified in human transferrin. The labeled tyrosines are Tyr 238 and Tyr 574, when numbering is for the mature human transferrin protein (MacGillivray *et al.*, 1982) from which the 19 amino acid signal peptide has been deleted (Swiss Prot accession #P02787). Both holo- and apo-human transferrin bound FP-biotin.

The MS/MS spectrum in Figure 4A shows that FP-biotin is covalently attached to tyrosine in peptide LysProValAspGlu-Tyr\**Lys* (KPVDEY\*K). The parent ion mass (726 *m/z*, doubly

charged) is equal to the peptide mass plus the added mass from FP-biotin (572 amu). Fragments at 227.3, 312.5, and 329.5 amu are characteristic for the presence of FP-biotin. Absence of a mass at 591 amu suggests the FP-biotin is bound to tyrosine (Schopfer *et al.*, 2005), because the 591 amu fragment of FP-biotin is released from serine but not from tyrosine. The masses at 708.8 and 691.6 amu are commonly seen in the fragmentation spectrum of FP-biotinylated tyrosine and are consistent with the immonium ion of FP-biotinylated tyrosine and its deamino counterpart (unpublished observations). The y-ion series (y2–y6) is consistent with FP-biotin attached to the C-terminal peptide, TyrLys (YK). Of these two residues, tyrosine is the most likely candidate for carrying the label. Had the lysine been labeled, trypsin would not have recognized that lysine as a cleavage site. The b-ion series (b1–b5) supports the identification of the peptide.

Peptide LysProValAspGluTyr\**Lys* (KPVDEY\*K) of human transferrin also covalently bound DFP, chorpriyfos oxon, dichlorvos, soman, and sarin on Tyr 238 as shown in Figures 4B–F. The isopropyl group of DFP and the pinacolyl group of soman were released by collision-induced dissociation in the QTRAP mass spectrometer (Figs. 4B and 4E). However, the isopropyl group was not released from sarin by matrix-assisted laser desorption ionization (Fig. 4F). The methylphosphotyrosine immonium ion at 214 amu is characteristic for soman and sarin adducts on tyrosine (Figs. 4E and 4F).

The spectrum in Figure 5A shows that FP-biotin is covalently attached to tyrosine in peptide LysProValGluGlu-Tyr\**AlaAsnCysHisLeuAlaArg* (KPVEEY\*ANCHLAR). The parent ion mass (541.4 *m/z*, quadruply charged) is consistent with the mass of the peptide plus the added mass of FP-biotin. The characteristic fragments at 227.3, 312.6, 329.6, 708.7, and 691.6 amu along with the absence of a fragment at 591 amu are indicative of FP-biotin bound to a tyrosine in this peptide. Minor fragments at 1248.6, 1378.0, and 1507.0 amu are consistent with FP-biotinylated peptides y8–y10 that have lost 328 amu during collision-induced dissociation in the mass spectrometer. Three hundred and twenty-eight amu is the

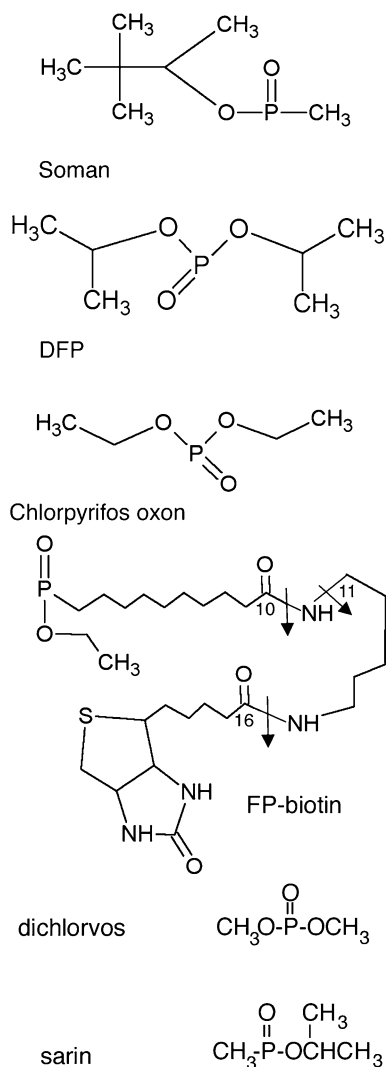


**FIG. 3.** Structures of the phosphoryl moieties that have become attached through phosphorus to tyrosine. Covalent binding to tyrosine results in loss of the fluoride ion from soman, DFP, FP-biotin, and sarin, of the dichlorovinyl alcohol group from dichlorvos, and of the trichloropyridinol group from chlorpyrifos oxon. Tyrosine loses one hydrogen. The added mass is 162.2 for soman, 164.1 for DFP, 136.0 for chlorpyrifos oxon, 572.3 for FP-biotin, 108.0 for dichlorvos, and 120.0 for sarin. The arrows in FP-biotin indicate fragmentation sites. A 227 amu ion is produced by cleavage between carbon 16 and the adjacent nitrogen. A 329 amu ion is produced by cleavage between carbon 10 and the adjacent nitrogen. The 312 amu ion is produced by loss of the amine from the 329 ion.

neutral counterpart of the 329 amu characteristic fragment from FP-biotin. The y-ion series (y1–y7) and the b-ion series (b1–b5) account for all the residues in the peptide except for the tyrosine which appears to carry the FP-biotin label.

Peptide LysProValGluGluTyr\*AlaAsnCysHisLeuAlaArg (KPVEEY\*ANCHLAR) of human transferrin also covalently bound DFP, chlorpyrifos oxon, dichlorvos, soman and sarin on Tyr 574, as shown in Figures 5B–F. The methylphosphotyrosine immonium ion at 214 amu is characteristic of soman and

sarin-labeled tyrosine (Figs. 5E and 5F). Collision-induced fragmentation in the QTRAP mass spectrometer resulted in loss of the pinacolyl group from soman, and the isopropyl group from sarin (Figs. 5E and 5F), indicated by loss of 84 and 42 amu. Analyses of the spectra support the labeling of tyrosine. Details are given in the figure legends.

#### *Mouse Transferrin Labeled on Tyr 238, Tyr 319, Tyr 429, Tyr 491, Tyr 518.*

Five tyrosines in mouse transferrin were labeled by FP-biotin and chlorpyrifos oxon (Table 1). Two tyrosines were labeled by DFP, three by sarin, and two by soman. No residues were labeled by dichlorvos. Both holo- and apo- mouse transferrin bound FP-biotin (data not shown).

#### *No Aging*

Aging of OP-modified acetylcholinesterase and butyrylcholinesterase involves the loss of an alkyl group from the OP. For example, soman-inhibited acetylcholinesterase loses the pinacolyl group during aging so that the added mass for aged soman is 72 rather than 162 amu. The LC/MS/MS data sets for soman and CPO-labeled transferrin peptides were manually searched for parent ions with an added mass of 72 for aged soman, or an added mass of 108 for aged CPO, as well as for parent ions with an added mass of 162 for nonaged soman and 136 for nonaged CPO. No masses for aged OP adducts were found, though the data sets did contain masses for nonaged adducts. In conclusion, no evidence for aging of the OP-tyrosine adducts of transferrin was found.

#### *Motif for OP Binding to Tyrosine*

Comparison of the sequences of the transferrin peptides that bind OP shows no definite consensus sequence around the tyrosine to which the OP binds. What the peptides do have in common is the presence of a positively charged Arginine, Lysine, or Histidine within one to five amino acids from the labeled tyrosine, or within a certain distance in the tertiary structure. Figure 6 shows a distance of 3.37 Å between Tyr 238 and Lys 239, and a distance of 4.06 Å between Tyr 574 and His 535 in the tertiary structure of apo-transferrin. Nearby positively charged residues probably interact with the phenolic hydroxyl group of tyrosine to lower the pKa. Tyrosines with a lower pKa value would be better nucleophiles and thus be better able to attack OP.

#### *Peptide ArgTyrThrArg Covalently Binds OP*

The hypothesis was tested that a positively charged amino acid located near a tyrosine could activate tyrosine, enabling it to covalently bind OP. Incubation of peptide ArgTyrThrArg with 0.1, 0.2, or 1mM CPO, dichlorvos, or DFP in pH 8.3 buffer at 37°C for 16 h resulted in covalent labeling of tyrosine (Fig. 7). Thirty-seven percent of a 170μM solution of ArgTyrThrArg was labeled by 1mM DFP, 24% by 1mM

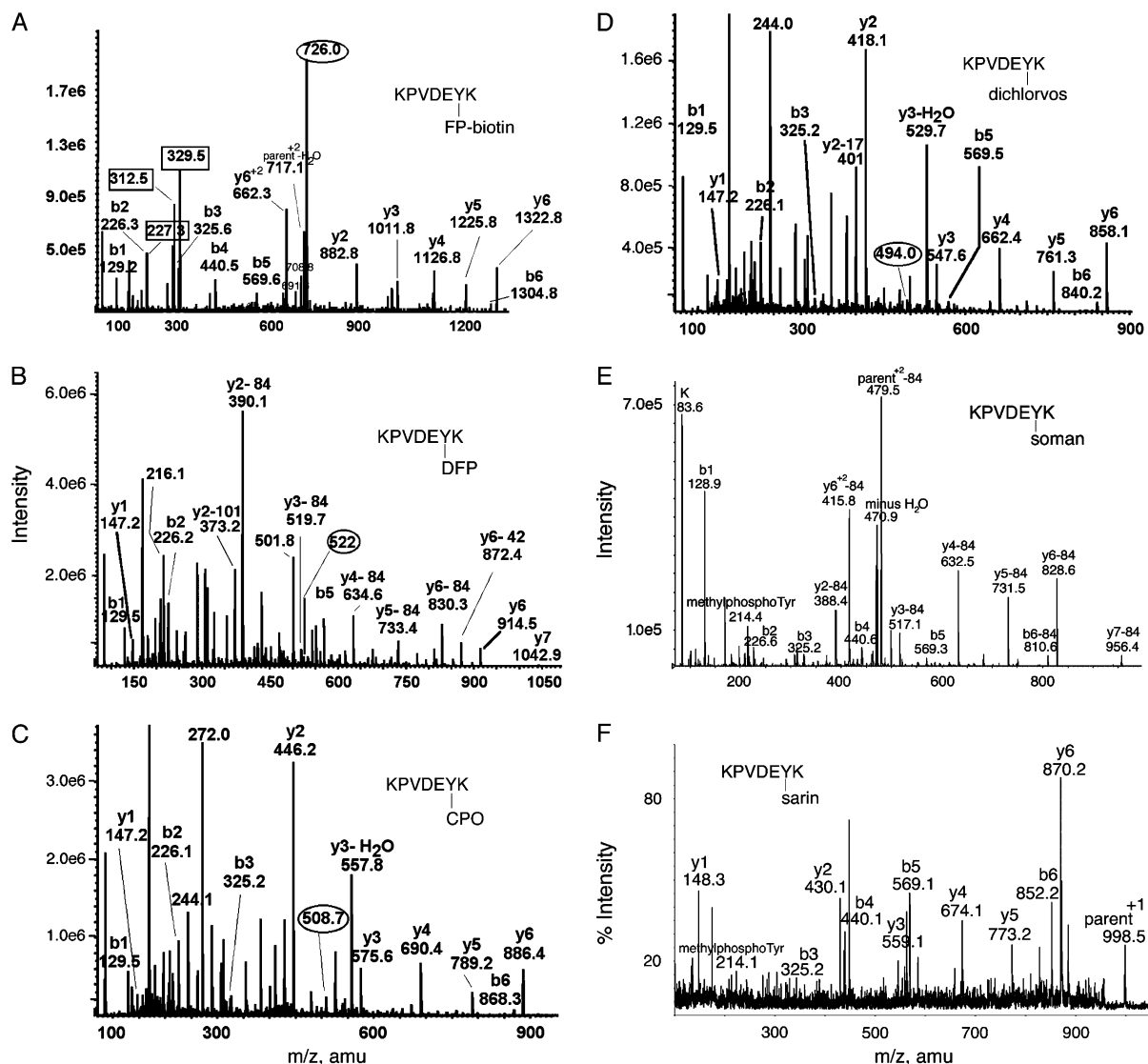


**FIG. 4.** MS/MS spectra of OP labeled Tyr 238 in peptide KPVDEYK of human transferrin. Mass spectra in (A–D) were acquired on the QTRAP 4000 mass spectrometer by infusion, in panel E on the QTRAP 2000 by LC/MS/MS, and in panel F on the MALDI-TOF-TOF mass spectrometer. The b and y ion masses in all panels are consistent with OP covalently bound to Tyr 238. (A) The doubly charged parent ion of the FP-biotin-labeled peptide is at 726.0 *m/z*. Masses enclosed in boxes at 227.3, 312.5, and 329.5 amu are fragments of FP-biotin. The immonium ion of FP-biotinylated tyrosine is at 708.8 amu. Its partner ion at 691.6 amu has lost 17 amu. (B) The doubly charged parent ion of the DFP-labeled peptide is at 522.0 *m/z*. Loss of one or both isopropyl groups during collision-induced dissociation yields y-ions minus 42 or minus 84 amu, confirming the presence of diisopropylphosphate. Loss of both isopropyl groups is the most common observation (Grigoryan *et al.*, 2008; Li *et al.*, 2007). The y-ion series (y1 and y2–84 through y6–84) indicates that tyrosine is labeled. The delta mass (242.9 amu) between y1 (147.2 amu) and y2–84 (390.1 amu) is consistent with the appearance of tyrosine phosphate at fragment y2 (163 amu for tyrosine and 80 amu for phosphate). The mass at 373.2 amu is the y2 ion minus 101 amu, representing loss of two isopropyl groups as well as ammonia. The mass at 501.8 *m/z* is the doubly charged parent ion minus one isopropyl group. The mass at 216.1 amu is consistent with the phosphotyrosine immonium ion. (C) The doubly charged parent ion of the chlorpyrifos oxon-labeled peptide is at 508.7 *m/z*. The y-ion series (y1–y6) shows the presence of all residues. The mass difference (299.0 amu) between y1 (147.2 amu) and y2 (446.2 amu) clearly shows the diethoxyphosphate on tyrosine in fragment y2 (163 amu for tyrosine and 136 amu for diethoxyphosphate). The mass at 244.1 amu is consistent with the monoethoxyphosphotyrosine immonium ion. The mass at 272.0 amu is consistent with the diethoxyphosphotyrosine immonium ion. (D) The doubly charged parent ion of the dichlorvos-labeled peptide is at 494.0 *m/z*. The y-ion series (y1–y6) shows the presence of all residues. The mass difference (270.9 amu) between y1 (147.2 amu) and y2 (418.1 amu) clearly shows the dimethoxyphosphate on tyrosine in fragment y2 (163 amu for tyrosine and 108 amu for dimethoxyphosphate). The mass at 244.0 amu is consistent with dimethoxyphosphotyrosine immonium ion. (E) The parent ion of the soman-labeled peptide has a mass to charge ratio of 520.7, but this mass does not appear in the scan. The prominent peak at 479.5 is the doubly charged parent ion that has lost the pinacolyl group from soman. The y2–y7 ions have all lost 84 amu due to release of pinacolyl from soman. The peak at 214.4 is the methylphosphotyrosine immonium ion. (F) The parent ion of the sarin-labeled peptide is the singly charged ion at 998.5 amu. The masses of the y-ion series, and the 214.1 mass for methylphosphotyrosine immonium, support labeling on tyrosine.

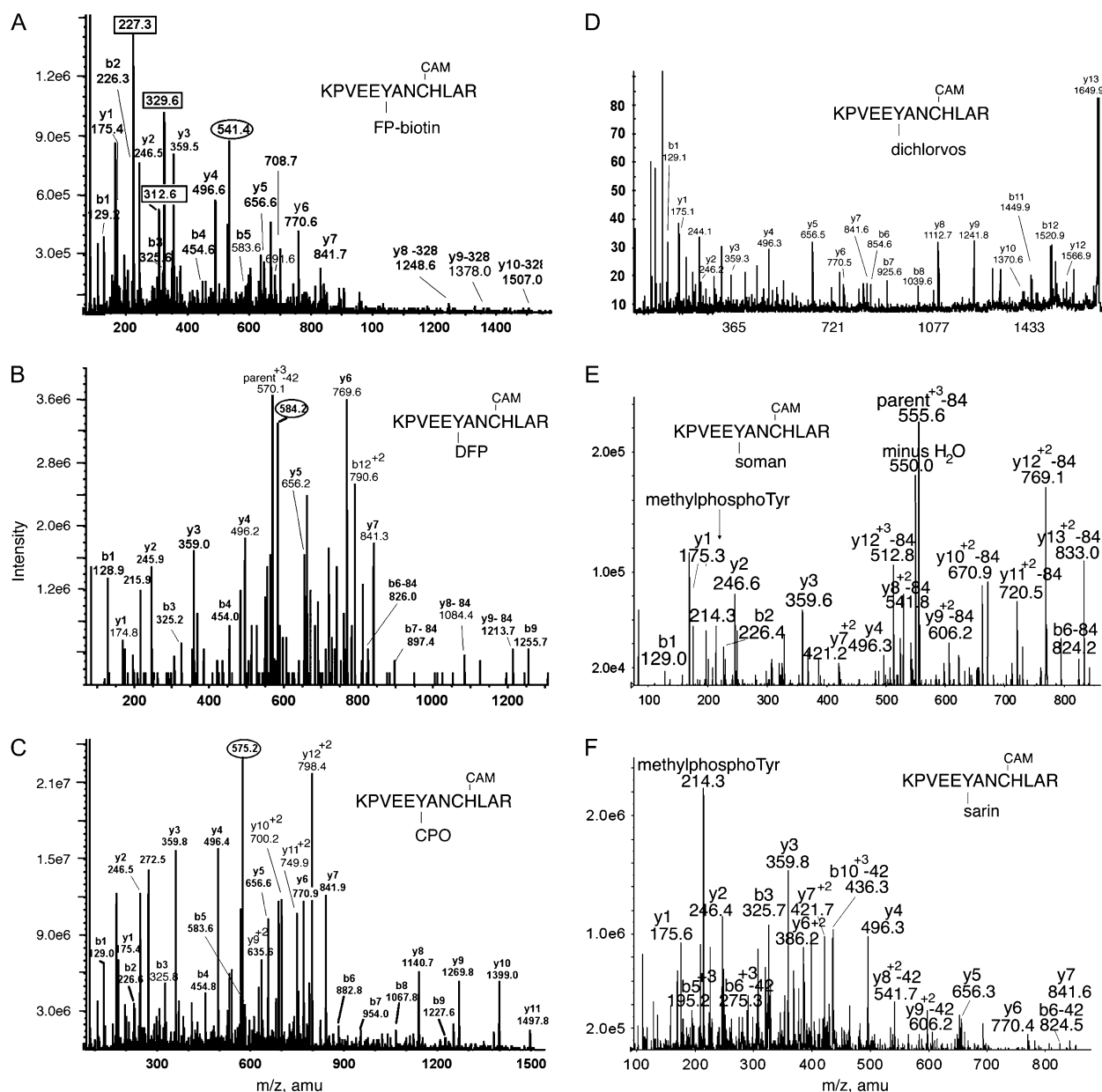


**FIG. 5.** MS/MS spectra of OP labeled Tyr 574 in peptide KPVEEYANCHLAR of human transferrin. Mass spectra in (A), (B), and (C) were acquired on the QTRAP 4000 mass spectrometer by infusion, in (D) on the MALDI-TOF-TOF, in panels E and F by LC/MS/MS on the QTRAP 2000 mass spectrometer. The b and y ion masses in all panels are consistent with OP covalently bound to Tyr 574. Cysteine has been CAM, which adds a mass of 57 amu. (A) The quadruply charged parent ion of the FP-biotin-labeled peptide is at 541.4  $m/z$ . Masses enclosed in boxes at 227.3, 312.6, and 329.6 amu, are fragments of FP-biotin. The immonium ion of FP-biotinylated tyrosine is at 708.7 amu. Its partner ion at 691.6 amu has lost 17 amu. Three y-ions have lost 328 amu from FP-biotin. (B) The triply charged parent ion of the DFP-labeled peptide is at 584.2  $m/z$ . Loss of one or both isopropyl groups yields ions minus 42 or minus 84 amu. The y-ion series (y1–y7) supports the identification of the peptide and indicates that the OP label is not in that portion of the peptide. The delta mass (243.2 amu) between y7 (841.3 amu) and y8-84 (1084.4 amu) fits with the appearance of tyrosine-phosphate in fragment y8 (163 amu for tyrosine and 80 amu for phosphate). The presence of tyrosine-phosphate is expected for tyrosine-diisopropylphosphate that has lost both isopropyl groups. Masses at 1213.7 (y9-84), 826.0 (b6-84) and 897.4 amu (b7-84) support this assignment. The mass at 215.9 amu is consistent with the phosphotyrosine immonium ion. (C) The triply charged parent ion of the chlorpyrifos oxon-labeled peptide is at 575.2  $m/z$ . The y-ion series (y1–y11) shows a delta mass (299.4 amu) between y7 (841.3 amu) and y8 (1140.7 amu) that is consistent with the appearance of tyrosine-diethoxyphosphate at fragment y8 (163 amu for tyrosine and 136 amu for diethoxyphosphate). This is supported by the b-ion series (b1–b9) which shows the appearance of the same tyrosine as tyrosine-diethoxyphosphate at fragment b6. The mass at 272.5 amu is consistent with the diethoxyphosphotyrosine immonium ion. (D) The singly charged parent ion of the dichlorvos-labeled peptide is at 1649.9  $m/z$ . This is a MALDI-TOF-TOF spectrum, where parent ions are typically singly charged. The y-ion series (y1–y10) shows a delta mass (271.1 amu) between y7 (841.6 amu) and y8 (1112.7 amu) which is consistent with the appearance of tyrosine-dimethoxyphosphate at fragment y8 (163 amu for tyrosine and 108 amu for dimethoxyphosphate). The mass at 244.1 amu is consistent with dimethoxyphosphotyrosine immonium ion. (E) The triply charged parent ion of the soman-labeled peptide has a mass of 583.9, but this mass does not appear in the

**TABLE 1**  
**Human and Mouse Transferrin (Swiss Prot accession# P02787**  
**and Q92111) Labeled with OP Agents**

OP	Human-labeled peptide	Mouse-labeled peptide	OP-Tyr
FP-biotin	KPVDEY*K	KPVDQY*EDCYLAR	Y238
FP-biotin		LYLGHNY*VTAIR	Y319
FP-biotin		GY*YAVAVVK	Y429
FP-biotin		FDEFFSQGCAPGY*EK	Y491
FP-biotin		EEYNGY*TGAFR	Y518
FP-biotin	KPVEEY*ANCHLAR		Y574
DFP	KPVDEY*K	KPVDQY*EDCYLAR	Y238
DFP		GY*YAVAVVK	Y429
DFP	KPVEEY*ANCHLAR		Y574
CPO	KPVDEY*K	KPVDQY*EDCYLAR	Y238
CPO		LYLGHNY*VTAIR	Y319
CPO		GY*YAVAVVK	Y429
CPO		FDEFFSQGCAPGY*EK	Y491
CPO		EEYNGY*TGAFR	Y518
CPO	KPVEEY*ANCHLAR		Y574
Dichlorvos	KPVDEY*K		Y238
Dichlorvos	KPVEEY*ANCHLAR		Y574
Sarin	KPVDEY*K	KPVDQY*EDCYLAR	Y238
Sarin		GY*YAVAVVK	Y429
Sarin		GY*YAVAVVK	Y430
Sarin	KPVEEY*ANCHLAR		Y574
Soman	KPVDEY*K	KPVDQY*EDCYLAR	Y238
Soman		GY*YAVAVVK	Y430
Soman	KPVEEY*ANCHLAR		Y574

*Note.* Single letter codes for amino acids are A, ala; C, cys; D, asp; E, glu; F, phe; G, gly; H, his; I, ile; K, lys; L, leu; M, met; N, asn; P, pro; Q, gln; R, arg; S, ser; T, thr; V, val; W, trp; Y, tyr. The labeled tyrosine is designated by an asterisk Y\*. The table shows the amino acid sequences of the tryptic peptides containing OP-labeled tyrosine. The location of the labeled tyrosine in the transferrin protein is given in the last column. Tyrosine 238 of transferrin was labeled in both species. Tyr 319, 429, 430, 491, and 518 was labeled only in mouse transferrin. Tyr 574 was labeled only in human transferrin. Transferrin 1 mg/ml in pH 8.5 buffer was treated in vitro with 0.5mM OP at 37°C for 16 h.

CPO, and 21% by 1mM dichlorvos. MS/MS spectra showed that the OP-labeled residue in peptide ArgTyrThrArg was tyrosine. Peptide SerTyrSerMet was also labeled by 1mM DFP, CPO, and dichlorvos, but no labeling was detected with 0.1 and 0.2mM OP. MS/MS spectra showed that the OP-labeled residue in SerTyrSerMet was tyrosine. Peptide SerTyrSerMet ionized poorly in the MALDI-TOF, giving a weak signal with large standard deviation. It was concluded that tyrosines in general could be labeled by OP, but that the most reactive tyrosines were located near a positively charged arginine or lysine.

The higher reactivity of DFP compared with other OP has been explained by formation of a hydrogen-bonded intermediate between fluoride and the hydroxyl group of tyrosine (Ashbolt and Rydon, 1957).

#### *Function of Transferrin is not Disrupted by OP Binding*

It was unknown whether covalent binding of an OP to transferrin affected the ability of transferrin to bind ferric ions. Tyrosines 95, 188, 426, and 517 are involved in the binding of ferric ions in human transferrin (Sargent *et al.*, 2005).

Human apo-transferrin, labeled with FP-biotin on Tyr 238 and Tyr 574, as well as control apo-transferrin were titrated with ferric nitriloacetate to determine binding stoichiometry. Figure 8 shows that both transferrin preparations bound approximately 2 mol of ferric ion per mole of transferrin, a result in agreement with the known number of ferric ion binding sites in transferrin (Bates and Schlabach, 1973). It was concluded that modification of human transferrin by FP-biotin did not interfere with binding of ferric ion.

## DISCUSSION

#### *Serine Hydrolases are not the only OP-Binding Proteins in Human Plasma*

Our expectation when we started this project was that OP-labeled proteins would all be serine esterases and serine proteases. We expected butyrylcholinesterase to be the dominant OP-binding protein in human plasma (Fidder *et al.*, 2002; Van Der Schans *et al.*, 2004). Our results show that this expectation was not met. OP bind not only to serine esterases and serine proteases, but also to proteins that have an activated tyrosine. Using mass spectrometry, we have conclusively demonstrated OP binding to 18 tyrosines in five proteins: human albumin (Ding *et al.*, 2008; Li *et al.*, 2007), alpha- and beta-tubulin (Grigoryan *et al.*, 2008), human transferrin and mouse transferrin. In addition we have shown that human alpha-1-antitrypsin, human complement C3, human alpha-2-macroglobulin covalently bind FP-biotin, though the site of attachment is unknown. Tyrosine in small synthetic peptides was also the site of attachment of OP.

#### *New OP-Binding Motif*

The OP-binding motif in the serine hydrolase family is GlyXSerXGly where OP is covalently bound to serine. Though OP binding to Tyr 411 of human albumin has been recognized (Li *et al.* 2007, 2008; Williams *et al.*, 2007), OP binding to

spectrum. The mass at 555.5 is the triply charged parent ion that has lost 84 amu from the pinacolyl group of soman. The doubly charged y8–y13 ions have all lost 84 amu from soman; the y8–y13 masses support labeling on tyrosine. The methylphosphotyrosine immonium ion is present at 214.3 amu. (F) The quadruply charged parent ion for sarin-labeled peptide has a mass of 427.7, but this mass does not appear in the spectrum. The most prominent peak is the methylphosphotyrosine immonium ion at 214.3 amu, supporting labeling of tyrosine by sarin. The doubly charged y8 and y9 ions, and the triply charged b5 and b6 ions also support labeling on tyrosine. These ions have lost 42 amu due to loss of the isopropyl group from sarin.

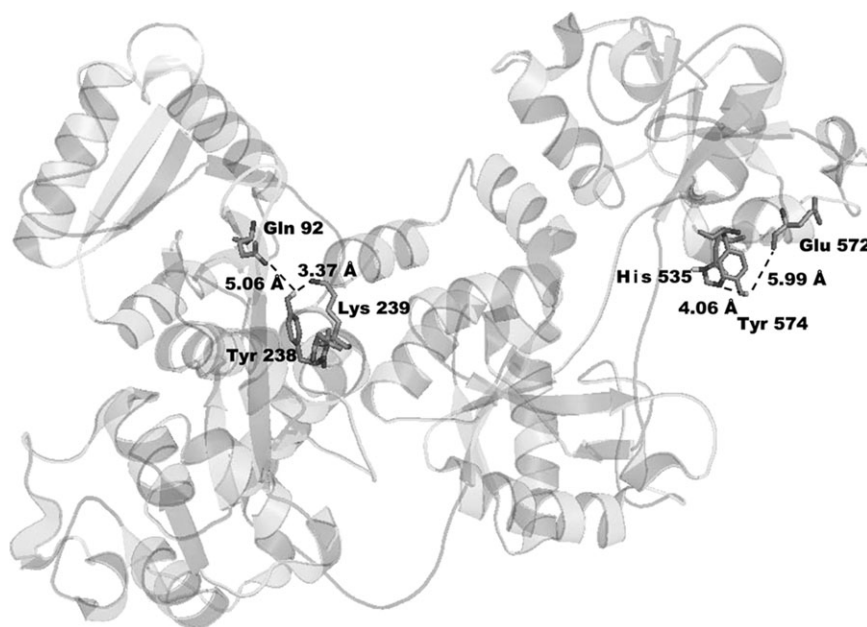


**FIG. 6.** OP-labeled Tyr 238 and Tyr 574 in the crystal structure of human apo-transferrin (PDB code 2hav). The phenolic hydroxyl of Tyr 238 is 3.37 Å from the amine of Lys 239 and 5.06 Å from Gln 92. The phenolic hydroxyl of Tyr 574 is 4.06 Å from the imidazole nitrogen of His 535 and 5.99 Å from oxygen in the carbonyl of Glu 572 (Wally *et al.*, 2006).

tyrosine as a general phenomenon has not been appreciated. Our results show that OP binding to tyrosine is not limited to Tyr 411 of albumin, but is found on many tyrosines in many proteins. Even the small peptide ArgTyrThrArg made a covalent bond with OP. Our analysis of OP-labeled tyrosine peptides reveals no consensus amino acid sequence around the labeled tyrosine. The chief requirement for OP binding to

tyrosine appears to be a nearby positively charged arginine or lysine. The positively charged groups stabilize the phenolate anion of tyrosine, thus lowering the pKa of tyrosine. The unusually low pKa enables the negatively charged phenolic anion to react with OP at physiological pH values.

It is anticipated that many more proteins than those we have already identified can be modified by OP. Proteins with no active site serine have been implicated in OP-induced neurodevelopmental, behavioral, and immunological effects. These proteins include neurotransmitter receptors (Aldridge *et al.*, 2003; Bomser and Casida, 2001; Katz *et al.*, 1997; Lein and Fryer, 2005; Pope, 1999; Quistad *et al.*, 2002; Smulders *et al.*, 2004), proteins in the adenylyl cyclase signaling cascade (Song *et al.*, 1997), cyclic AMP response element binding protein (Schuh *et al.*, 2002), immune function proteins (Kassa *et al.*, 2003), and kinesin in the axonal transport system (Gearhart *et al.*, 2007; Prendergast *et al.*, 2007; Terry *et al.*, 2007). Whether OP bind to tyrosine in these proteins is unknown.

#### Biomarkers of OP Exposure

Our *in vitro* conditions used high concentrations of OP that would not be found during *in vivo* poisoning. It is unknown whether live animals treated with a nonlethal dose of OP would have OP-labeled transferrin. However, it is known that mice treated with a nontoxic dose of FP-biotin (1 and 5 mg/kg ip) (Peeples *et al.*, 2005) and guinea pigs treated with sarin, soman, cyclosarin, and tabun have OP-labeled albumin in their blood (Williams *et al.*, 2007). The guinea pigs received 0.5–5 LD<sub>50</sub> doses of nerve agent, but were alive up to 7 days later

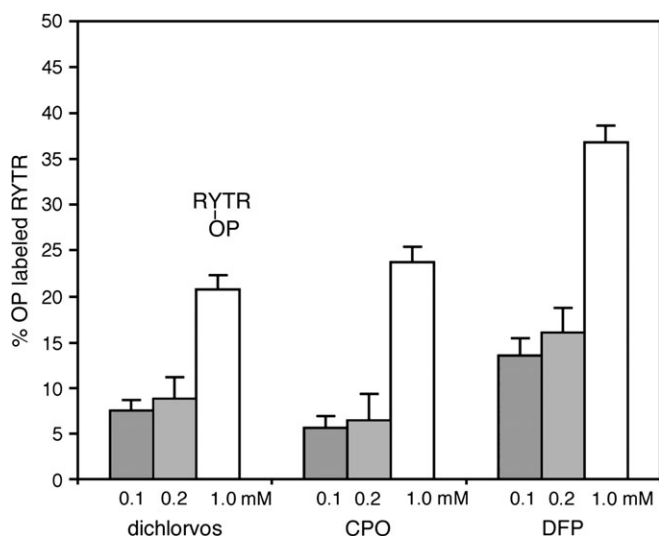


**FIG. 7.** Labeling of peptide ArgTyrThrArg by dichlorvos, chlorpyrifos oxon, and DFP. The reaction of 170 μM peptide with 0.1, 0.2, or 1 mM OP was in ammonium bicarbonate buffer pH 8.3, at 37°C for 16 h. MALDI-TOF cluster areas were used to calculate % labeling. MS/MS spectra identified the labeled residue as tyrosine.

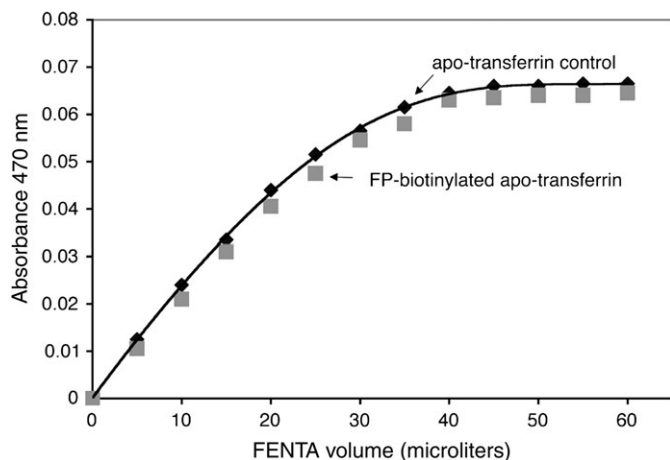


**FIG. 8.** FP-biotinylation of Tyr 238 and Tyr 574 in human transferrin does not interfere with ferric ion binding. One milliliter of 12.1  $\mu$ M apo-transferrin control ( $\blacklozenge$ ) titrated with FENTA had an endpoint of 27.3  $\mu$ M FENTA, which calculates to 2.26 mol of ferric ion bound per mole of transferrin. One milliliter of 14.67  $\mu$ M FP-biotinylated apo-transferrin ( $\blacksquare$ ) had an endpoint of 31.3  $\mu$ M FENTA, which calculates to 2.11 mol of ferric ion bound per mole of transferrin. Assays for each type of transferrin were performed in duplicate.

because they had been protected with pyridostigmine, oximes, atropine, and midazolam. Tyrosine-modified proteins could serve as biomarkers for OP exposure.

#### No Aging

The serine hydrolases, acetylcholinesterase, butyrylcholinesterase, and acylpeptide hydrolase have been shown to serve as biomarkers of OP exposure in mice and rats (Quistad *et al.*, 2005; Richards *et al.*, 2000). OP-labeled serine hydrolases lose part of the OP in a process called aging, making it impossible to distinguish between exposure to sarin and soman. In contrast, OP-labeled tyrosines do not undergo aging, so that labeling by sarin is clearly distinguished from labeling by soman.

#### Significance

Our findings may have application to diagnosis and treatment of OP exposure. Proteins that have no active site serine may serve as biomarkers of exposure. In the future it may be possible to develop antibodies to the new OP-labeled biomarkers to use for screening OP exposure. Synthetic peptides containing arginine, lysine, and tyrosine may find application as scavengers to clear the body of OP. The recognition of a new OP-binding motif to tyrosine suggests new directions to search for mechanisms of long-term effects of OP exposure.

#### FUNDING

U.S. Army Medical Research and Materiel Command (W81XWH-07-2-0034 to OL, W81XWH-06-1-0102 to S.H.H.); National Institutes of Health (U01 NS058056-02 to OL, P30CA36727 to Epplery Cancer Center, ES016102) to

C.M.T.; and the Direction Générale de l'Armement of the French Ministry of Defense (DGA grant 03co010-05/PEA01 08 7) to P.M.

#### ACKNOWLEDGMENTS

Mass spectra were obtained with the support of the Mass Spectrometry and Proteomics core facility at the University of Nebraska Medical Center.

#### REFERENCES

- Aldridge, J. E., Seidler, F. J., Meyer, A., Thillai, I., and Slotkin, T. A. (2003). Serotonergic systems targeted by developmental exposure to chlorpyrifos: Effects during different critical periods. *Environ. Health Perspect.* **111**, 1736–1743.
- Ashbolt, R. F., and Rydon, H. N. (1957). The action of diisopropyl phosphorofluoridate and other anticholinesterases on amino acids. *Biochem. J.* **66**, 237–242.
- Bates, G. W., and Schlabach, M. R. (1973). The reaction of ferric salts with transferrin. *J. Biol. Chem.* **248**, 3228–3232.
- Bomser, J. A., and Casida, J. E. (2001). Diethylphosphorylation of rat cardiac M2 muscarinic receptor by chlorpyrifos oxon in vitro. *Toxicol. Lett.* **119**, 21–26.
- Casida, J. E., and Quistad, G. B. (2004). Organophosphate toxicology: Safety aspects of nonacetylcholinesterase secondary targets. *Chem. Res. Toxicol.* **17**, 983–998.
- Chaiken, I. M., and Smith, E. L. (1969). Reaction of a specific tyrosine residue of papain with diisopropylfluorophosphate. *J. Biol. Chem.* **244**, 4247–4250.
- Ding, S. J., Carr, J., Carlson, J. E., Tong, L., Xue, W., Li, Y., Schopfer, L. M., Li, B., Nachon, F., Asojo, O., *et al.* (2008). Five tyrosines and two serines in human albumin are labeled by the organophosphorus agent FP-biotin. *Chem. Res. Toxicol.* **21**, 1787–1794.
- Fidder, A., Hulst, A. G., Noort, D., de Ruiter, R., van der Schans, M. J., Benschop, H. P., and Langenberg, J. P. (2002). Retrospective detection of exposure to organophosphorus anti-cholinesterases: Mass spectrometric analysis of phosphorylated human butyrylcholinesterase. *Chem. Res. Toxicol.* **15**, 582–590.
- Gearhart, D. A., Sickles, D. W., Buccafusco, J. J., Prendergast, M. A., and Terry, A. V., Jr. (2007). Chlorpyrifos, chlorpyrifos-oxon, and diisopropyl-fluorophosphate inhibit kinesin-dependent microtubule motility. *Toxicol. Appl. Pharmacol.* **218**, 20–29.
- Grigoryan, H., Schopfer, L. M., Thompson, C. M., Terry, A. V., Masson, P., and Lockridge, O. (2008). Mass spectrometry identifies covalent binding of soman, sarin, chlorpyrifos oxon, diisopropyl fluorophosphate, and FP-biotin to tyrosines on tubulin: A potential mechanism of long term toxicity by organophosphorus agents. *Chem. Biol. Interact.* **175**, 180–186.
- Kassa, J., Krocova, Z., Sevelova, L., Sheshko, V., Kasalova, I., and Neubauerova, V. (2003). Low-level sarin-induced alteration of immune system reaction in inbred BALB/c mice. *Toxicology* **187**, 195–203.
- Katz, E. J., Cortes, V. I., Eldefrawi, M. E., and Eldefrawi, A. T. (1997). Chlorpyrifos, parathion, and their oxons bind to and desensitize a nicotinic acetylcholine receptor: Relevance to their toxicities. *Toxicol. Appl. Pharmacol.* **146**, 227–236.
- Lein, P. J., and Fryer, A. D. (2005). Organophosphorus insecticides induce airway hyperreactivity by decreasing neuronal M2 muscarinic receptor function independent of acetylcholinesterase inhibition. *Toxicol. Sci.* **83**, 166–176.

- Li, B., Nachon, F., Froment, M. T., Verdier, L., Debouzy, J. C., Brasme, B., Gillon, E., Schopfer, L. M., Lockridge, O., and Masson, P. (2008). Binding and hydrolysis of soman by human serum albumin. *Chem. Res. Toxicol.* **21**, 421–431.
- Li, B., Schopfer, L. M., Hinrichs, S. H., Masson, P., and Lockridge, O. (2007). Matrix-assisted laser desorption/ionization time-of-flight mass spectrometry assay for organophosphorus toxicants bound to human albumin at Tyr411. *Anal. Biochem.* **361**, 263–272.
- Li, B., Sedlacek, M., Manoharan, I., Boopathy, R., Duysen, E. G., Masson, P., and Lockridge, O. (2005). Butyrylcholinesterase, paraoxonase, and albumin esterase, but not carboxylesterase, are present in human plasma. *Biochem. Pharmacol.* **70**, 1673–1684.
- Lockridge, O., Schopfer, L. M., Winger, G., and Woods, J. H. (2005). Large scale purification of butyrylcholinesterase from human plasma suitable for injection into monkeys; a potential new therapeutic for protection against cocaine and nerve agent toxicity. *J. Med. CBR Def.* **3**, online publication
- Lockridge, O., Xue, W., Gaydess, A., Grigoryan, H., Ding, S. J., Schopfer, L. M., Hinrichs, S. H., and Masson, P. (2008). Pseudo-esterase activity of human albumin: Slow turnover on tyrosine 411 and stable acetylation of 82 residues including 59 lysines. *J. Biol. Chem.* **283**, 22582–22590.
- MacGillivray, R. T., Mendez, E., Sinha, S. K., Sutton, M. R., Lineback-Zins, J., and Brew, K. (1982). The complete amino acid sequence of human serum transferrin. *Proc. Natl. Acad. Sci. U. S. A.* **79**, 2504–2508.
- Maxwell, D. M., and Brecht, K. M. (2001). Carboxylesterase: specificity and spontaneous reactivation of an endogenous scavenger for organophosphorus compounds. *J. Appl. Toxicol.* **21**(Suppl. 1), S103–S107.
- Murachi, T., Inagami, T., and Yasui, M. (1965). Evidence for alkylphosphorylation of tyrosyl residues of stem bromelain by diisopropylphosphorofluoridate. *Biochemistry* **4**, 2815–2825.
- Peebles, E. S., Schopfer, L. M., Duysen, E. G., Spaulding, R., Voelker, T., Thompson, C. M., and Lockridge, O. (2005). Albumin, a new biomarker of organophosphorus toxicant exposure, identified by mass spectrometry. *Toxicol. Sci.* **83**, 303–312.
- Perkins, D. N., Pappin, D. J., Creasy, D. M., and Cottrell, J. S. (1999). Probability-based protein identification by searching sequence databases using mass spectrometry data. *Electrophoresis* **20**, 3551–3567.
- Pope, C. N. (1999). Organophosphorus pesticides: Do they all have the same mechanism of toxicity? *J. Toxicol. Environ. Health B Crit. Rev.* **2**, 161–181.
- Prendergast, M. A., Self, R. L., Smith, K. J., Ghayoumi, L., Mullins, M. M., Butler, T. R., Buccafusco, J. J., Gearhart, D. A., and Terry, A. V., Jr. (2007). Microtubule-associated targets in chlorpyrifos oxon hippocampal neurotoxicity. *Neuroscience* **146**, 330–339.
- Quistad, G. B., Klintonberg, R., and Casida, J. E. (2005). Blood acylpeptide hydrolase activity is a sensitive marker for exposure to some organophosphate toxicants. *Toxicol. Sci.* **86**, 291–299.
- Quistad, G. B., Nomura, D. K., Sparks, S. E., Segall, Y., and Casida, J. E. (2002). Cannabinoid CB1 receptor as a target for chlorpyrifos oxon and other organophosphorus pesticides. *Toxicol. Lett.* **135**, 89–93.
- Richards, P. G., Johnson, M. K., and Ray, D. E. (2000). Identification of acylpeptide hydrolase as a sensitive site for reaction with organophosphorus compounds and a potential target for cognitive enhancing drugs. *Mol. Pharmacol.* **58**, 577–583.
- Sargent, P. J., Farnaud, S., and Evans, R. W. (2005). Structure/function overview of proteins involved in iron storage and transport. *Curr. Med. Chem.* **12**, 2683–2693.
- Schopfer, L. M., Champion, M. M., Tamblyn, N., Thompson, C. M., and Lockridge, O. (2005). Characteristic mass spectral fragments of the organophosphorus agent FP-biotin and FP-biotinylated peptides from trypsin and bovine albumin (Tyr410). *Anal. Biochem.* **345**, 122–132.
- Schuh, R. A., Lein, P. J., Beckles, R. A., and Jett, D. A. (2002). Noncholinesterase mechanisms of chlorpyrifos neurotoxicity: Altered phosphorylation of Ca<sup>2+</sup>/cAMP response element binding protein in cultured neurons. *Toxicol. Appl. Pharmacol.* **182**, 176–185.
- Smulders, C. J., Bueters, T. J., Vailati, S., van Kleef, R. G., and Vijverberg, H. P. (2004). Block of neuronal nicotinic acetylcholine receptors by organophosphate insecticides. *Toxicol. Sci.* **82**, 545–554.
- Song, X., Seidler, F. J., Saleh, J. L., Zhang, J., Padilla, S., and Slotkin, T. A. (1997). Cellular mechanisms for developmental toxicity of chlorpyrifos: Targeting the adenylyl cyclase signaling cascade. *Toxicol. Appl. Pharmacol.* **145**, 158–174.
- Terry, A. V., Jr., Gearhart, D. A., Beck, W. D., Jr., Truan, J. N., Middlemore, M. L., Williamson, L. N., Bartlett, M. G., Prendergast, M. A., Sickles, D. W., and Buccafusco, J. J. (2007). Chronic, intermittent exposure to chlorpyrifos in rats: Protracted effects on axonal transport, neurotrophin receptors, cholinergic markers, and information processing. *J. Pharmacol. Exp. Ther.* **322**, 1117–1128.
- Van Der Schans, M. J., Polhuijs, M., Van Dijk, C., Degenhardt, C. E., Pleijsier, K., Langenberg, J. P., and Benschop, H. P. (2004). Retrospective detection of exposure to nerve agents: Analysis of phosphofluoridates originating from fluoride-induced reactivation of phosphorylated BuChE. *Arch. Toxicol.* **78**, 508–524.
- Wally, J., Halbrooks, P. J., Vornrhein, C., Rould, M. A., Everse, S. J., Mason, A. B., and Buchanan, S. K. (2006). The crystal structure of iron-free human serum transferrin provides insight into inter-lobe communication and receptor binding. *J. Biol. Chem.* **281**, 24934–24944.
- Welch, S., and Skinner, A. (1989). A comparison of the structure and properties of human, rat and rabbit serum transferrin. *Comp. Biochem. Physiol. B* **93**, 417–424.
- Williams, N. H., Harrison, J. M., Read, R. W., and Black, R. M. (2007). Phosphorylated tyrosine in albumin as a biomarker of exposure to organophosphorus nerve agents. *Arch. Toxicol.* **81**, 627–639.

# Matrix-assisted laser desorption/ionization time-of-flight mass spectrometry assay for organophosphorus toxicants bound to human albumin at Tyr411

Bin Li <sup>a</sup>, Lawrence M. Schopfer <sup>a</sup>, Steven H. Hinrichs <sup>b</sup>, Patrick Masson <sup>c</sup>, Oksana Lockridge <sup>a,\*</sup>

<sup>a</sup> *Eppley Institute, University of Nebraska Medical Center, Omaha, NE 68198, USA*

<sup>b</sup> *Department of Pathology and Microbiology, University of Nebraska Medical Center, Omaha, NE 68198, USA*

<sup>c</sup> *Centre de Recherches du Service de Santé des Armées, La Tronche 38702, France*

Received 3 October 2006

Available online 4 December 2006

## Abstract

Our goal was to determine whether chlorpyrifos oxon, dichlorvos, diisopropylfluorophosphate (DFP), and sarin covalently bind to human albumin. Human albumin or plasma was treated with organophosphorus (OP) agent at alkaline pH, digested with pepsin at pH 2.3, and analyzed by matrix-assisted laser desorption/ionization time-of-flight (MALDI-TOF) mass spectrometry. Two singly charged peaks  $m/z$  1718 and 1831, corresponding to the unlabeled peptide fragments containing the active site Tyr411 residue, were detected in all samples. The sequences of the two peptides were VRYTKKVPQVSTPTL and LVRYTKKVPQVSTPTL. The peptide–OP adducts of these peptides were also found. They had masses of 1854 and 1967 for chlorpyrifos oxon, 1825 and 1938 for dichlorvos, 1881 and 1994 for DFP, and 1838 and 1938 for sarin; these masses fit a mechanism whereby OP bound covalently to Tyr411. The binding of DFP to Tyr411 of human albumin was confirmed by electrospray tandem mass spectrometry and analysis of product ions. None of the OP–albumin adducts lost an alkoxy group, leading to the conclusion that aging did not occur. Our results show that OP pesticides and nerve agents bind covalently to human albumin at Tyr411. The presence of Tyr411 on an exposed surface of albumin suggests that an antibody response could be generated against OP–albumin adducts.

© 2006 Elsevier Inc. All rights reserved.

**Keywords:** Biomarker organophosphate exposure; Pepsin; Sarin; Soman; Dichlorvos; Diisopropylfluorophosphate; Chlorpyrifos oxon; Nerve agents; Pesticides

The acute toxicity of organophosphorus (OP)<sup>1</sup> toxicants is known to be due to inhibition of acetylcholinesterase. However, other proteins also bind OP, although their role

in toxicity is less defined [1]. Albumin is a potential new biomarker of OP exposure. Mice treated with a nontoxic dose of a biotinylated nerve agent analog, FP-biotin (10-fluoroethoxyphosphinyl-*N*-biotinamidopentyldecanamide), had 1000 times more FP-biotinylated albumin than FP-biotinylated butyrylcholinesterase in their blood [2].

Albumin has been shown to covalently bind radiolabeled diisopropylfluorophosphate (DFP). Human albumin incorporated 1 mol DFP per mole of albumin when 20 to 70  $\mu$ M albumin was incubated with a sevenfold molar excess of DFP at pH 8.0 for 2 h at 23 °C [3,4]. Bovine albumin also incorporated 1 mol DFP per mole of albumin [5]. The site of covalent binding of DFP to human albumin was identified by amino acid sequencing. The labeled peptide

\* Corresponding author. Fax: +1 402 559 4651.

E-mail address: [olockrid@unmc.edu](mailto:olockrid@unmc.edu) (O. Lockridge).

<sup>1</sup> *Abbreviations used:* OP, organophosphorus; FP-biotin, 10-fluoroethoxyphosphinyl-*N*-biotinamidopentyldecanamide; DFP, diisopropylfluorophosphate; MS, mass spectrometry; MALDI-TOF, matrix-assisted laser desorption/ionization time-of-flight; HPLC, high-performance liquid chromatography; TFA, trifluoroacetic acid; DHBA, 2,5-dihydroxybenzoic acid; CHCA,  $\alpha$ -cyano 4-hydroxycinnamic acid; ACTH, adrenocorticotrophic hormone; MS/MS, tandem mass spectra; LC–MS, liquid chromatography–mass spectrometry; GC–MS, gas chromatography–mass spectrometry.

had the sequence ArgTyrThrLys with DFP bound to Tyr [6]. Later, when the complete amino acid sequence of human albumin was known, the active site tyrosine was identified as Tyr411 (Tyr435 when residue 1 is Met of the signal peptide). Mass spectrometry (MS) identified Tyr410 of bovine albumin (equivalent to Tyr411 of human albumin) as the covalent binding site for FP-biotin [7]. The nerve agents soman and sarin were shown to bind covalently to human albumin on tyrosine [8,9] and to be released by treatment with potassium fluoride [9].

Albumin has also been demonstrated to be an OP hydrolase, hydrolyzing chlorpyrifos oxon, *O*-hexyl *O*-2,5-dichlorophenylphosphoramidate, and paraoxon at measurable rates [10–13]. The apparent  $K_m$  of bovine albumin is 0.41 mM for chlorpyrifos oxon and 1.85 mM for paraoxon [12], and the apparent  $K_m$  of human albumin is 3.6 mM for DFP [3]. Despite this seemingly consistent body of results, some issues have been raised regarding the reaction of OP with albumin. It has been questioned whether the observed OP hydrolase activity was associated with the albumin molecule itself or with minor phosphotriesterase contaminants in the albumin preparation [10]. In addition, the possibility has been raised that DFP binds to one site in albumin but that other OP toxicants bind to a different site [12,14].

Our goal was to determine whether Tyr411 of human albumin was the site for covalent attachment of a variety of OP toxicants. For this purpose we developed a matrix-assisted laser desorption/ionization time-of-flight (MALDI-TOF) MS assay applicable to purified human albumin and to human plasma.

## Materials and methods

### Materials

Purified human serum albumin, essentially fatty acid free, was obtained from Fluka via Sigma (Cat. No. 05418, St. Louis, MO, USA). Pepsin from porcine gastric mucosa was obtained from Sigma (Cat. No. P6887). Modified trypsin, sequencing grade, was purchased from Promega (Cat. No. V5113, Madison, WI, USA). DFP was obtained from Sigma (Cat. No. D0879). Dichlorvos and chlorpyrifos oxon were purchased from Chem Services (Cat Nos. PS-89 and MET-674B, West Chester, PA, USA). Sarin-treated human plasma was a gift from Patrick Masson. Acetonitrile high-performance liquid chromatography (HPLC)-grade 99% ACROS, was purchased from Fisher Scientific (Cat. No. 61001-0040, Pittsburgh, PA, USA). Trifluoroacetic acid (TFA), sequencing grade, was purchased from Beckman Instruments (Cat. No. 290203, Palo Alto, CA, USA). 2,5-Dihydroxybenzoic acid (DHBA) matrix was purchased from Applied Biosystems (Foster City, CA, USA).  $\alpha$ -Cyano 4-hydroxycinnamic acid (CHCA, Cat. No. 70990, Sigma) was recrystallized before use. Calibration standards for MALDI-TOF were obtained from New England Biolabs (Cat. No. P7720S, Beverly, MA, USA) and included angiotensin 1 (1297.51 amu), adrenocorticotrophic hormone

(ACTH) (7–38) (3660.19 amu), and ACTH (18–39) (2466.73 amu). Double distilled water was prepared in-house and was autoclaved.

### Sample preparation for DFP-, dichlorvos-, and chlorpyrifos oxon-treated samples

Fatty acid-free human albumin at a concentration of 10 mg/ml, which is 150  $\mu$ M, was dissolved in 25 mM ammonium bicarbonate (pH 8.6) and treated with an equimolar concentration of OP for 24 h at 37°C. The pH of 1000  $\mu$ l reaction mixture was reduced to 2.3 by the addition of 500  $\mu$ l of 1% TFA. Pepsin was dissolved in 10 mM HCl to make 1 mg/ml and was stored at –80°C. The albumin was digested with pepsin (1:250 ratio) for 2 h at 37°C and was diluted to 1 pmol/ $\mu$ l with 0.1% TFA.

A 200- $\mu$ l aliquot of human plasma was treated with 6.85  $\mu$ l of 20 mM OP (660  $\mu$ M final OP concentration) for 24 h at 37°C. The pH was adjusted to 2.3 to 2.5 by the addition of 200- $\mu$ l of 1% TFA. Proteins were digested with 50  $\mu$ l of 1 mg/ml pepsin for 2 h at 37°C. Before spotting the digest on the target plate, a 10- $\mu$ l aliquot of the digest was diluted with 390  $\mu$ l of 0.1% TFA so that the final plasma dilution was 1000-fold.

### MALDI-TOF

A 1- $\mu$ l aliquot of diluted peptic digest was applied to a stainless-steel target plate, air-dried, and overlaid with 1  $\mu$ l of 2,5-dihydroxybenzoic acid matrix. The CHCA matrix gave similar results. Mass spectra were acquired with the Voyager DE-PRO MALDI-TOF mass spectrometer (Applied Biosystems/MDS Sciex) in linear positive ion mode, 20,000 V accelerating voltage, 94% grid voltage, 0.1% guide wire, 350 ns extraction delay time, and automated laser intensity adjustment from 1000 to 1600. The instrument was calibrated with a peptide calibration mixture from New England Biolabs. Mass accuracy for each standard was within 0.05% of the corresponding average molecular weight. Spectra were acquired in automatic mode by examining signals from random spots on a target. The signals from the first 10 spots that met the acceptance criteria were summed into one final profile mass spectrum. The acceptance criteria were signal intensities between 1000 and 55,000 counts with signal/noise ratios of 10 or greater and minimum resolution of 50. The final spectrum was the average of 1000 shots.

The MS-Digest program from the UCSF Mass Spectrometry Facility was used to calculate the masses of the peptic peptides expected from digests of human serum albumin.

### Quadrupole mass spectrometer

Tandem mass spectra (MS/MS) were acquired on a Q-Trap 2000 triple quadrupole linear ion trap mass spectrometer (Applied Biosystems/MDS Sciex) with a nano electro-

spray ionization source. DFP-labeled albumin digested with trypsin was infused into the mass spectrometer via a fused silica emitter (360  $\mu\text{m}$  o.d., 20  $\mu\text{m}$  i.d., 10  $\mu\text{m}$  taper, New Objective, Woburn, MA, USA) using a Harvard syringe pump to drive a 100- $\mu\text{l}$  Hamilton syringe equipped with an inline 0.25- $\mu\text{m}$  filter at a flow rate of 1  $\mu\text{l}/\text{min}$ . Samples were prepared in 50% acetonitrile and 0.1% formic acid. Positive ion spectra were obtained. Mass spectra were calibrated using fragment ions generated from collision-induced dissociation of Glu fibrinopeptide B (Sigma). Enhanced product ion scans were obtained with collision energy of  $40 \pm 5$  V and nitrogen gas pressure of  $4 \times 10^{-5}$  Torr. The final enhanced product ion scan was the average of 212 scans.

#### *Sample preparation of sarin-treated plasma*

Human plasma (100  $\mu\text{l}$ ) was treated with 600  $\mu\text{M}$  sarin and stored at ambient temperature for 3 days. This concentration of sarin is equimolar with the concentration of albumin in plasma. Then 10  $\mu\text{l}$  was digested with 0.5  $\mu\text{g}$  of pepsin at 37  $^{\circ}\text{C}$  for 2 h at pH 2.3, and the peptides were separated by HPLC on a Waters 625 LC system. A C18 reverse-phase column (Prodigy 5- $\mu\text{m}$  ODS(2), 100  $\times$  4.6 mm, 5  $\mu\text{m}$ , 00 D-3300-E0, Phenomenex, Torrance, CA, USA) was used to trap the peptides from the digest, which were then eluted with a 40-min gradient starting with 85% buffer A (0.1% TFA in water) and 15% buffer B (acetonitrile containing 0.07% TFA) and ending with 65% buffer A and 35% buffer B. Then 1-ml fractions were reduced in volume to 200  $\mu\text{l}$  in a vacuum centrifuge, and 1  $\mu\text{l}$  was analyzed by MALDI-TOF. A control plasma sample was treated identically except that it was incubated with 3.5% isopropanol rather than with sarin.

## Results

#### *Reaction of pure human albumin with OP*

The assay was developed with pure human albumin and later tested with human plasma. Fatty acid-free albumin was used because fatty acids and OP bind to the same albumin domain and therefore fatty acids could block the binding of OP [3,15]. The covalent attachment site for human albumin, Tyr411, is located near the surface of the albumin molecule, where it is accessible to proteases. Digestion with trypsin at pH 8.6 or with pepsin at pH 2.0 to 2.5 released peptides of the expected masses without the need to denature or to reduce and alkylate the disulfide bonds of albumin. Peptides containing Tyr411 had the sequence YTK ( $m/z$  411, singly charged mass) when the protease was trypsin and had the sequences VRYTKKVPQVSTPTL ( $m/z$  1718) and LVRYTKKVPQVSTPTL ( $m/z$  1831) when the protease was pepsin. Pepsin routinely missed one cleavage in our experiments.

The tryptic YTK peptide ( $m/z$  411) and the dichlorvos, chlorpyrifos oxon, and DFP adducts had masses that over-

lapped with matrix peaks, making them difficult to detect by MALDI-MS. Furthermore, the YTK peptide and YTK-OP adducts did not seem to ionize when irradiated by the nitrogen laser in the Voyager DE-PRO, although they did ionize in the electrospray source of the Q-Trap mass spectrometer. In contrast, the larger peptides produced by digestion of albumin with pepsin separated well from matrix and ionized to give good signals in the Voyager DE-PRO. Therefore, samples intended for analysis by MALDI-TOF were digested with pepsin rather than with trypsin.

Table 1 lists the expected peptic peptide masses before and after covalent binding of dichlorvos, chlorpyrifos oxon, DFP, and sarin to Tyr411 of human albumin. The leaving group in Table 1 is that portion of the OP molecule that detaches from the OP on covalent binding of the OP to protein. The mass of the leaving group is absent from the final adduct. The added OP mass comes from the phosphorus atom, the two phosphorus ligands, and the phosphoryl oxygen atom, less one hydrogen.

Fig. 1 shows the MALDI-TOF spectra obtained for pepsin-digested human albumin before and after treatment with OP. The top panel shows masses at  $m/z$  1718 and 1831, which are consistent with the peptides from unlabeled albumin that contain Tyr411. Additional albumin peptides are also present, but they do not contain Tyr411 and therefore are not discussed. The dichlorvos panel shows peaks at  $m/z$  1718 and 1831 as well as two new peaks at  $m/z$  1826 and 1939. The two new peaks have the expected sizes for the dimethoxyphosphate adducts of the  $m/z$  1718 and 1831 peptides. The amount of labeled albumin estimated from the relative peak areas is 65%. The chlorpyrifos oxon panel shows two new peaks at  $m/z$  1854 and 1967 for the diethoxyphosphate adducts. Approximately 30% of the albumin is labeled. The DFP panel shows two new peaks at  $m/z$  1882 and 1995 for the diisopropoxyphosphate adducts. Approximately 70% of the albumin is labeled. Because the MALDI conditions disrupt noncovalent interactions, the OP-peptide adducts must be covalently formed. These results support the conclusion that human albumin is labeled by dichlorvos, chlorpyrifos oxon, and DFP and are consistent with the site for covalent attachment being Tyr411. The masses correspond to the dialkoxy adducts rather than to the monoalkoxy adducts. Masses for monoalkoxy adducts were not found, supporting the conclusion that OP-albumin adducts do not age.

#### *Saturating the albumin binding sites*

Unlabeled  $m/z$  1718 and 1831 peptides always were present when the concentration of OP was the same as the concentration of albumin. However, when the dichlorvos or DFP concentration was 40-fold higher than the albumin concentration, all of the Tyr411 sites were occupied and no unlabeled peptides of  $m/z$  1718 and 1831 were detected. OP labeling reactions with albumin were performed at pH 8.5 because labeling occurs at high pH but is decreased markedly at neutral pH [3,5].

Table 1  
Pepsin digested human albumin

Human albumin peptide	Peptide <i>m/z</i>	Peptide <i>m/z</i> after dichlorvos	Dichlorvos	Leaving group	Added mass
VR <u>Y</u> TKKVPQVSTPTL	1718	1826			108
LVR <u>Y</u> TKKVPQVSTPTL	1831	1939			
		Peptide <i>m/z</i> after chlorpyrifos oxon	Chlorpyrifos oxon		
VR <u>Y</u> TKKVPQVSTPTL	1718	1854			136
LVR <u>Y</u> TKKVPQVSTPTL	1831	1967			
		Peptide <i>m/z</i> after DFP	DFP		
VR <u>Y</u> TKKVPQVSTPTL	1718	1882		F	164
LVR <u>Y</u> TKKVPQVSTPTL	1831	1995			
		Peptide <i>m/z</i> after sarin	Sarin		
VR <u>Y</u> TKKVPQVSTPTL	1718	1838		F	120
LVR <u>Y</u> TKKVPQVSTPTL	1831	1951			

Note. The  $[M+H]^+$  masses of peptic peptides containing Tyr411 are listed before and after covalent binding of OP. Tyr411 is underlined. The accession number for human albumin is GI:28592 where Tyr411 is Tyr435 because numbering begins with the signal peptide.

### Limit of detection

It was essential to dilute the albumin and plasma digests before applying the sample on the target plate. Undiluted samples did not show the desired peptides due to ion suppression and charge competition effects. The limit of detection of OP-labeled peptide was determined from dilutions of peptides in which all of the Tyr411 sites were occupied. The diluent was 0.1% TFA in water. Peaks of interest were detected after 100-, 1000-, 3000-, and 9000-fold dilutions of a sample whose starting concentration was 600  $\mu$ M (40 mg/ml) albumin. The signal/noise ratio for the 1:9000 diluted sample was 3:1. At 18,000-fold dilution, the peak height was only twofold above the noise. Thus, the minimum detectable signal from an OP-labeled peptide occurred at 0.07 pmol/ $\mu$ l.

### Missed cleavage

We hoped to increase the sensitivity of the assay by changing digestion conditions so that pepsin would consistently cleave Leu from the N terminus of the active site peptide. If there were no missed cleavage, the area of the 1721 peak would increase relative to the background noise, thereby increasing the sensitivity of the assay. We increased the pepsin/albumin ratio to 1:25, lowered the pH in

increments to 1.5, and increased the digestion time to 4 h. A pepsin/albumin ratio of 1:25 at pH 1.8 incubated for 2.5 h at 37 °C did eliminate the 1831 peptide but did not increase the signal for 1721.

### Detection of dichlorvos bound to albumin in human plasma

The concentration of albumin in human plasma is approximately 40 to 50 mg/ml (600–770  $\mu$ M). No other protein in plasma is present at such a high concentration. This overwhelming concentration of albumin in plasma suggested that it might be possible to detect OP–albumin adducts without separating albumin from other proteins in plasma. This was tested by incubating an aliquot of human plasma with a concentration of dichlorvos equimolar to the albumin concentration in plasma. The pH was not adjusted, and no buffer was added for the reaction with dichlorvos. Then the plasma was digested with pepsin at pH 2.3 and diluted 600-fold with 0.1% TFA to yield an albumin peptide concentration of approximately 1 pmol/ $\mu$ l. A 1- $\mu$ l aliquot of the diluted digest was applied to the MALDI target. The control sample was human plasma treated in parallel with everything except dichlorvos. Fig. 2 shows that albumin peptides at *m/z* 1718 and 1831 stand out, despite the presence of normal plasma components, and that the OP-labeled form of these peptides at *m/z* 1826 and

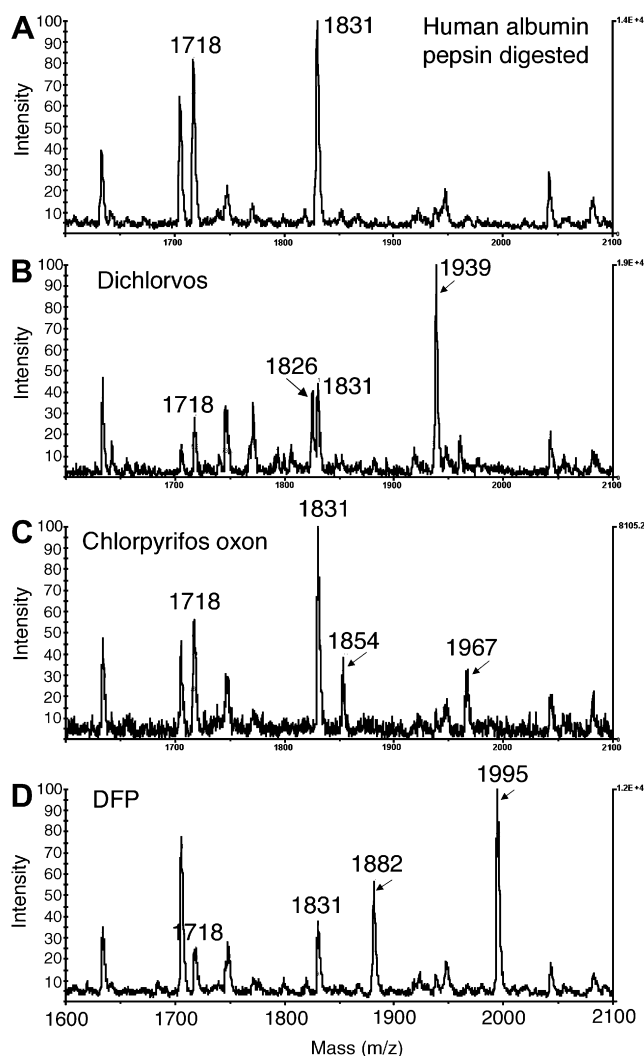


Fig. 1. MALDI-TOF analysis of human albumin-OP adducts. (A) Digestion of human albumin with pepsin at pH 2.3 yields two peptides containing Tyr411 whose average mass/charge ratios are 1718 and 1831 (singly protonated). (B) Incubation of human albumin with dichlorvos in ammonium bicarbonate (pH 8.5), followed by digestion with pepsin (pH 2.3), yields dimethoxyphosphate adducts of  $m/z$  1826 and 1939. (C) Incubation with chlorpyrifos oxon yields diethoxyphosphate adducts of  $m/z$  1854 and 1967. (D) Incubation with DFP yields diisopropoxyphosphate adducts of  $m/z$  1882 and 1995. Samples were diluted to 1 pmol/ $\mu$ l before plating 1  $\mu$ l on the MALDI target with 2,5-dihydroxybenzoic acid matrix.

1939 can be detected by MALDI-TOF. We conclude that human plasma can be assayed for OP bound to albumin. The 1826 and 1939 masses are 108 amu larger than their unlabeled counterparts, identifying the OP as a dimethoxy OP and thus classifying it as a pesticide rather than as a nerve agent. For forensic purposes, it is valuable to know whether the OP is a pesticide or a nerve agent.

#### Detection of sarin bound to albumin in human plasma

MALDI-TOF analysis of peptic digests of human plasma labeled by reaction with 600  $\mu$ M sarin did not show the sarin-labeled peptides after simple dilution. We suspected that the absence of signal was due to ion suppression.

Therefore, the digests were fractionated by reverse-phase chromatography prior to mass spectral analysis, as shown in Fig. 3. Fractions were collected at 1-min intervals. Each HPLC fraction was analyzed by MALDI-TOF. Peptides of interest eluted between 8 and 16 min. The unlabeled active site peptides of albumin, of masses 1718 and 1831, eluted at 8 to 10 min. The sarin-labeled peptides of masses 1838 and 1951 eluted at 14 to 16 min (Fig. 4, fractions 14 and 16). The peptides of interest separated from a large peak of UV absorbing material in the HPLC. Elimination of this material would be expected to reduce ion suppression, thereby accounting for the appearance of the sarin-labeled peptide signals in MALDI-TOF analysis.

Fig. 4 shows the MALDI-TOF spectra for the two sarin-labeled peptides of human albumin with masses of 1838 and 1951. These masses are consistent with the 1718 and 1831 albumin peptides to which 120 amu from sarin has been added. The fact that the sarin-peptide complex survived the MALDI conditions indicates that sarin has made a covalent complex. These results show that sarin covalently binds to human albumin on Tyr411. They also show that binding can be detected in plasma and that the sarin adduct of albumin does not lose an alkoxy group during storage for 3 days at room temperature.

#### Confirmation of DFP binding to Tyr411 of the YTK peptide

DFP-labeled human albumin was digested with trypsin, and the digest was infused into the Q-Trap mass spectrometer. The enhanced mass spectrum showed a peak at  $m/z$  575.4, which is consistent with the singly charged YTK peptide covalently bound to DFP ( $[M+H]^+ = 411$  amu for the YTK peptide plus 164 amu added mass from DFP [Table 1]). This peptide was subjected to collision-induced dissociation with nitrogen as the collision gas. The resulting enhanced product ion spectrum yielded amino acid sequence information consistent with the sequence YTK where DFP is covalently bound to tyrosine (Fig. 5). A mass was found at 147.2 amu, indicative of the C-terminal lysine from a  $y$ -series. This was followed by masses at 248.3, for the Thr-Lys dipeptide, and at 575.4, for the Tyr\*ThrLys tripeptide, including the N terminus, from a  $y$ -series (where Tyr\* represents the diisopropylphospho adduct of tyrosine). No relevant signals were found at higher masses. No evidence for the diisopropylphospho adduct of threonine was found.

Furthermore, convincing evidence for covalent binding of DFP to Tyr411 comes from the presence of six masses, all of which are consistent with various fragments of DFP attached to tyrosine alone or in conjunction with the YTK peptide. The structures of these six ions are shown in Fig. 5. As mentioned earlier, the ion at 575.4 amu is consistent with the singly protonated YTK peptide plus the added mass from covalent attachment of DFP. Neutral loss of 42 amu yields the 533.4-amu ion. Loss of 42 amu is predicted for  $\beta$ -elimination of propylene from the diisopropylphosphate adduct. This  $\beta$ -elimination-type reaction, also referred to as a McLafferty rearrangement [16,17], is a facile

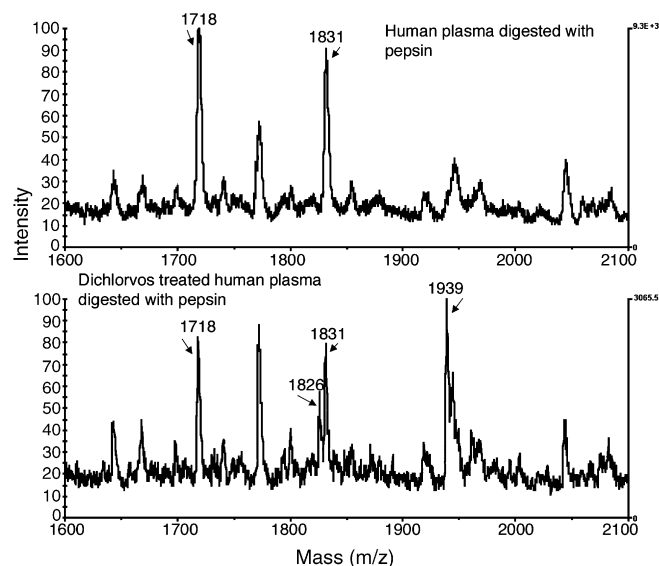


Fig. 2. MALDI-TOF analysis of OP-albumin adducts in human plasma. The top panel is the control sample. Human plasma digested with pepsin shows the Tyr411 containing albumin peptides of  $m/z$  1718 and 1831. The bottom panel shows two new peaks at  $m/z$  1826 and 1939 in dichlorvos-treated human plasma, representing peptides containing dichlorvos covalently bound to Tyr411 of albumin.

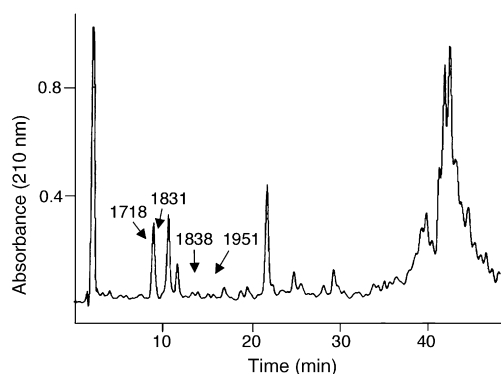


Fig. 3. HPLC trace. A peptic digest of human plasma (10  $\mu$ l) that had been treated with sarin was subjected to reverse-phase chromatography. Unlabeled active site albumin peptides of masses 1718 and 1831 separated from sarin-labeled albumin peptides of masses 1838 and 1951 and from a large peak of UV absorbing material. The marked peaks contain a mixture of peptides; therefore, the relative UV intensities do not represent the relative amounts of labeled and unlabeled albumin.

reaction commonly seen during collision-induced dissociation of phosphopeptides [18]. A second neutral loss of 42 amu yields the 491.3-amu ion; this mass is consistent with a phosphorylated YTK peptide. In theory, all three of these masses are consistent with DFP adducts of either tyrosine or threonine. However, the mass at 244.2 amu is characteristic of an N-terminal phosphotyrosine, *b*-series aziridone ion, and the 226.2-amu ion is consistent with its dehydration product [19]. In addition, the mass at 216.2 amu is characteristic of a phosphotyrosine immonium ion [20]. Furthermore, no indication of phosphorylated or organophosphorylated threonine was found. These results prove that DFP covalently binds to Tyr411 of human albumin.

No evidence for any form of the dephosphorylated YTK peptide was found. This probably reflects the relative difficulty of releasing OP from tyrosine compared with the other

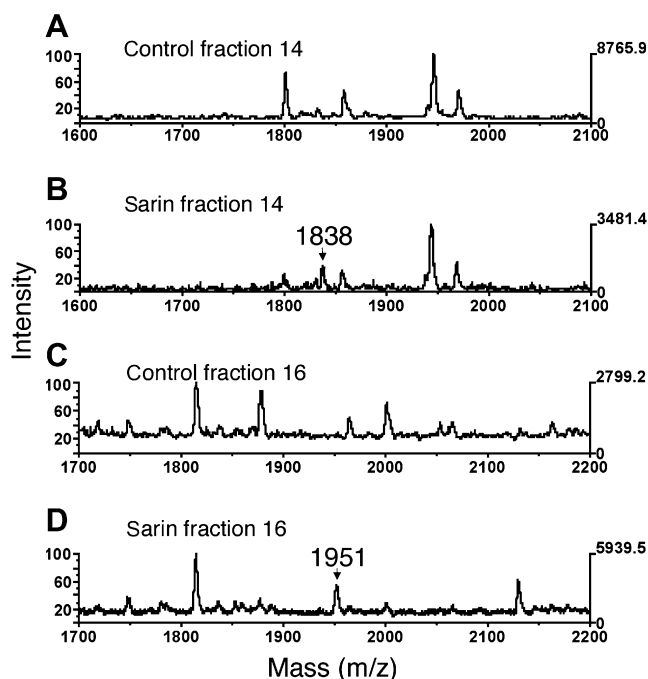


Fig. 4. MALDI-TOF analysis of sarin covalently attached to human albumin. (A and C) Control human plasma digested with pepsin and fractionated by HPLC but not treated with sarin. (B and D) Human plasma treated with sarin before digestion with pepsin and fractionation by HPLC. Fractions were collected at 1-min intervals. Sarin-labeled albumin peptides of 1838 and 1951 amu include 120 amu from sarin.

fragmentation pathways available to the diisopropylphospho-YTK peptide. Facile dephosphorylation of phosphotyrosine via a  $\beta$ -elimination-type mechanism is not available because tyrosine does not afford a suitable environment.  $\beta$ -Elimination would require the shift of a proton from the  $\beta$ -carbon of the leaving group to the phosphate oxygen, with concomitant formation of a double bond between the  $\alpha$ - and

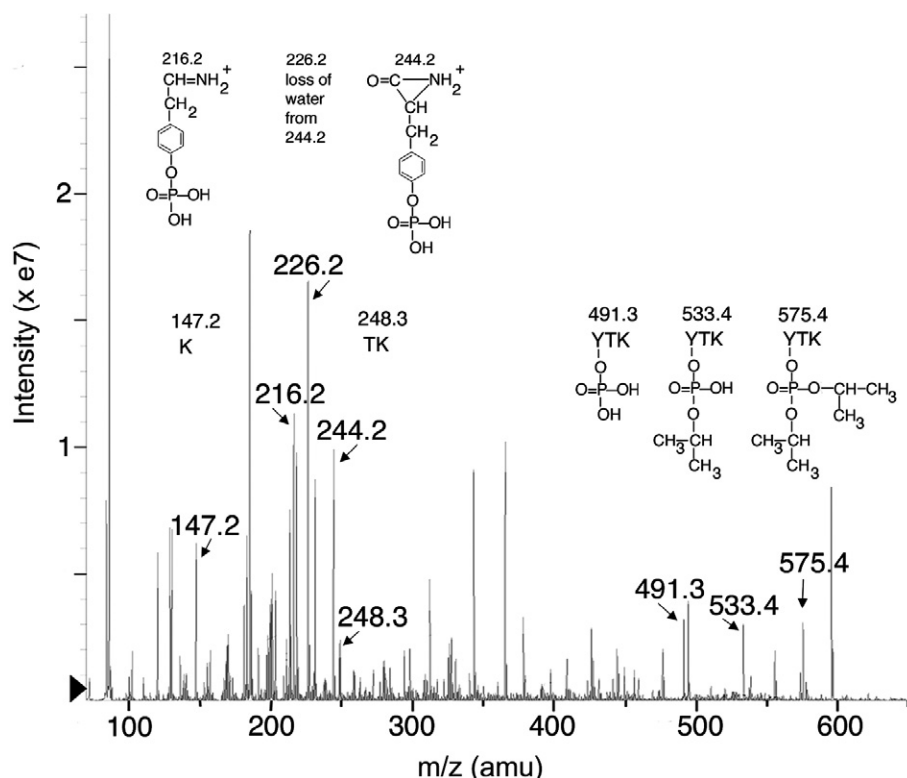


Fig. 5. Product ion spectrum of DFP-labeled human albumin peptide 575.4. DFP-labeled albumin was digested with trypsin and infused into the Q-Trap mass spectrometer. The singly charged parent ion of  $m/z$  575.4 has the sequence YTK and has the diisopropylphosphate group covalently bound to tyrosine. Fragment masses and their corresponding structures are shown. In addition to information on the DFP–YTK peptide, fragments from a second albumin peptide (LVNEVTEFAK, doubly protonated) can be extracted from the fragmentation information.

$\beta$ -carbons of the leaving group. For phosphotyrosine, the  $\beta$ -proton of the leaving tyrosine is aromatic and therefore not readily released; furthermore, formation of the double bond requires introduction of a triple bond into the aromatic ring of tyrosine—another difficult operation. Although phosphate can be released from tyrosine during collision-induced dissociation, it seems to require the presence of hydroxyl moieties on the phosphate. Even then, the yield of dephosphorylation is poor [17,21]. Thus, it would appear that elimination of propylene from the diisopropoxy moieties and fragmentation of the peptide backbone provide energetically more acceptable routes for use of the collision energy than does dephosphorylation of the tyrosine.

The spectrum in Fig. 5 contains a number of major peaks that were not used in the analysis of the DFP–YTK adduct. Most of these are attributable to fragments from a second albumin peptide. The doubly charged form of LVNEVTEFAK appears at  $m/z$  575. The peaks at 218, 365, 494, and 595 amu (plus additional peaks at the higher masses of 694, 823, 937, and 1036 amu) correspond to the complete  $y$ -series for this contaminating peptide. Peaks at 213, 327, 456, and 555 amu can be assigned to a  $b$ -series from this same peptide, whereas peaks at 312, 343, 426, and 444 amu reflect internal fragments. The large peak at 86 amu is the immonium ion of Leu/Ile.

The presence of two isopropyl groups in parent ion 575.4 supports the conclusion that the DFP–albumin adduct does not age.

The unique set of six phosphorylated fragment ions in Fig. 5 for DFP–albumin could be useful for identifying exposure to DFP in an MS method that selectively searches for characteristic fragment ions.

#### Only one covalent binding site for OP

Human albumin labeled with dichlorvos or DFP and digested with pepsin was searched for additional peptides that might bind OP. MALDI-TOF and Q-Trap analysis revealed no other OP adducts. The only identified OP binding site was Tyr411.

## Discussion

#### Mechanism of OP labeling of albumin

Each of the OP toxicants tested in this work labeled Tyr411 of human albumin. The stoichiometry of labeling has been shown to be 1 mol  $^3\text{H}$ [DFP] or  $^{14}\text{C}$ [DFP] incorporated per mole of albumin [3–5,12]. The specific labeling of 1 tyrosine in a molecule that contains 18 tyrosines suggests that Tyr411 is in a special environment. This tyrosine has an unusually low  $\text{pK}_a$  of 7.9 to 8.3 [3,22], in contrast to the  $\text{pK}_a$  of 10 for the average tyrosine.

Tyr411 is the active site residue not only for reaction with OP but also for reaction with esters such as  $p$ -nitrophenyl acetate, carbamates such as carbaryl, and amides

such as *o*-nitroacetanilide [3,23–25]. The esterase and amidase activity of albumin can be inhibited by pretreatment with DFP. Conversely, labeling with DFP can be prevented by pretreatment with *p*-nitrophenyl acetate, which forms a stable acylated albumin adduct [3]. The sensitivity of albumin esterase activity to ionic strength led Means and Wu to conclude that the reactive tyrosine residue is located on the surface of albumin in an apolar environment adjacent to several positively charged groups [3]. This description of the OP binding site of albumin was proven to be correct when the crystal structure was solved [26,27]. Subdomain IIIa of albumin contains a pocket lined by hydrophobic side chains. The hydroxyl of Tyr411 is close to the side chains of Arg410 and Lys414.

Site-directed mutagenesis experiments have shown that albumin esterase activity is abolished when Tyr411 is mutated to Ala and is severely diminished when Arg410 is mutated to Ala [28]. These results support Tyr411 as the active site for albumin esterase activity and support a role for Arg410 in stabilizing the reactive anionic form of Tyr411. The negatively charged Tyr411 is available for nucleophilic attack on ester and amide substrates. Although crystal structures of several ligand albumin complexes have been solved [29], the crystal structure of an OP–albumin adduct is not yet available.

#### *No aging of OP–albumin adducts*

Aging of OP-labeled acetylcholinesterase and butyrylcholinesterase is defined as the loss of an alkoxy group from the OP-labeled active site serine [30,31]. The nerve agents sarin, soman, and VX yield the same aged OP derivative, so that these agents may be difficult to distinguish when bound to acetylcholinesterase or butyrylcholinesterase [32,33].

Three of the OP agents studied in this work—sarin, DFP, and chlorpyrifos oxon—are known to age when bound to acetylcholinesterase and butyrylcholinesterase. However, these OP toxicants did not age when bound to albumin. Aging is a catalytic process that requires the participation of nearby histidine and glutamic acid residues [34]. Residues that promote aging are not present in the active site pocket of albumin. The absence of aging allows the bound OP to be spontaneously released from Tyr411. This makes albumin an OP hydrolase, albeit a very slow one. Albumin hydrolyzes chlorpyrifos oxon, *O*-hexyl *O*-2,5-dichlorophenylphosphoramidate, and paraoxon [10–13]. We recently measured the hydrolysis of soman by human albumin and found a deacylation rate of 0.0052 per hour (unpublished).

The observation that OP–albumin adducts do not age is supported by the findings of others [8,9]. Using liquid chromatography–mass spectrometry (LC–MS), Black and coworkers found *O*-(pinacolyl methylphosphonyl)tyrosine in human plasma as well as in albumin samples that had been treated with soman, and they found *O*-(isopropyl methylphosphonyl)tyrosine in samples treated with sarin [8]. If aging had occurred, the products would have been (methyl-

phosphonyl)tyrosine for both soman and sarin. Adams and coworkers used gas chromatography–mass spectrometry (GC–MS) to measure sarin and soman recovered from human plasma and albumin samples [9]. The plasma and albumin were reacted with sarin or soman, excess agent was removed by solid phase extraction, and the samples were treated with potassium fluoride to release the bound OP. Intact sarin and soman were recovered, demonstrating that aging had not occurred. The absence of aging in OP–albumin adducts suggests that albumin could be a useful biomarker to distinguish between soman and sarin exposure. In the same manner, OP–albumin adducts could distinguish between pesticide and nerve agent exposure.

#### *Advantages and disadvantages of MALDI-TOF–MS*

The MALDI-TOF–mass spectrometer is an easy instrument to use. Samples need to be free of salt, and the concentration of peptide needs to be approximately 1 pmol/μl. As little as 0.5 μl of a 1-pmol/μl solution gives a good signal. Results are acquired in seconds.

The disadvantage of MALDI is that not all peptides ionize when the sample contains a mixture of peptides. For example, the FP-biotin-labeled bovine albumin YTR peptide gave an intense signal at 1012 amu (data not shown). In contrast, FP-biotin-labeled human albumin YTK peptide gave no signal. In both experiments, the sample was a mixture of tryptic peptides. Ion suppression is a common problem in MS, and one way of solving the problem is to separate the peptide of interest from other peptides by HPLC before examining it by MALDI-TOF MS. This strategy allowed us to detect sarin-labeled albumin in human plasma. Alternatively, the peptides can be separated by step elution from a C18 ZipTip, a procedure that was successful for nerve agent adducts of acetylcholinesterase [35].

#### *OP–albumin as a biomarker of OP exposure*

Many proteins in human plasma are labeled by OP. MS assays have been developed for OP–butyrylcholinesterase adducts [36–38]. The current article has provided an assay for OP–albumin adducts. Albumin is far less reactive with OP than butyrylcholinesterase, but the 10,000-fold higher concentration of albumin in plasma compared with butyrylcholinesterase (40,000–50,000 vs. 4–5 mg/ml) means that both albumin and butyrylcholinesterase will be labeled when a person is exposed to OP. New assays that use precursor and fragment ion *m/z* values in selected reaction monitoring experiments are expected to be capable of diagnosing low-dose exposure [38].

#### *Antibody to OP–albumin*

The information presented in this article could have application to the monitoring of individuals exposed to

OP. It may be possible to detect exposure through the use of an antibody detection assay directed toward the OP–albumin adduct at Tyr411. There is precedent for the generation of antibodies to very small haptens bound to protein. For example, antibodies that distinguish among phosphotyrosine, phosphoserine, and phosphothreonine have been successfully produced [39,40]. Antibodies to soman, sarin, and VX bound to carrier proteins through a chemical linker have been produced [41–43]. The proposed OP–albumin epitope could be more useful for detection of OP exposure than existing antibodies because the OP–albumin adduct has no chemical linker and no foreign protein environment.

An OP–albumin adduct at Tyr411 may generate an antibody response in exposed individuals, and the antibody could be detected to determine a history of exposure to OP. This would facilitate monitoring exposure to OP long after the exposure incident and long after the antigen has disappeared.

### Acknowledgments

Mass spectra were obtained with the support of the Protein Structure Core Facility at the University of Nebraska Medical Center. This work was supported by U.S. Army Medical Research and Materiel Command contract W81XWH-06-1-0102, Edgewood Biological Chemical Center contract W911SR-04-C-0019, Eppley Cancer Center Grant P30CA36727, National Institutes of Health Grant 1 U01 NS058056-01, and Grants DGA/DSP/STTC-PEA 010807 and EMA/LR 06 from France.

### References

- [1] J.E. Casida, G.B. Quistad, Organophosphate toxicology: safety aspects of nonacetylcholinesterase secondary targets, *Chem. Res. Toxicol.* 17 (2004) 983–998.
- [2] E.S. Peeples, L.M. Schopfer, E.G. Duysen, R. Spaulding, T. Voelker, C.M. Thompson, O. Lockridge, Albumin, a new biomarker of organophosphorus toxicant exposure, identified by mass spectrometry, *Toxicol. Sci.* 83 (2005) 303–312.
- [3] G.E. Means, H.L. Wu, The reactive tyrosine residue of human serum albumin: characterization of its reaction with diisopropylfluorophosphate, *Arch. Biochem. Biophys.* 194 (1979) 526–530.
- [4] N. Hagag, E.R. Birnbaum, D.W. Darnall, Resonance energy transfer between cysteine-34, tryptophan-214, and tyrosine-411 of human serum albumin, *Biochemistry* 22 (1983) 2420–2427.
- [5] T. Murachi, A general reaction of diisopropylphosphorofluoridate with proteins without direct effect on enzymic activities, *Biochim. Biophys. Acta* 71 (1963) 239–241.
- [6] F. Sanger, Amino-acid sequences in the active centers of certain enzymes, *Proc. Chem. Soc.* 5 (1963) 76–83.
- [7] L.M. Schopfer, M.M. Champion, N. Tamblyn, C.M. Thompson, O. Lockridge, Characteristic mass spectral fragments of the organophosphorus agent FP-biotin and FP-biotinylated peptides from trypsin and bovine albumin (Tyr410), *Anal. Biochem.* 345 (2005) 122–132.
- [8] R.M. Black, J.M. Harrison, R.W. Read, The interaction of sarin and soman with plasma proteins: the identification of a novel phosphorylation site, *Arch. Toxicol.* 73 (1999) 123–126.
- [9] T.K. Adams, B.R. Capacio, J.R. Smith, C.E. Whalley, W.D. Korte, The application of the fluoride reactivation process to the detection of sarin and soman nerve agent exposures in biological samples, *Drug Chem. Toxicol.* 27 (2004) 77–91.
- [10] E.G. Erdos, L.E. Boggs, Hydrolysis of paraoxon in mammalian blood, *Nature* 190 (1961) 716–717.
- [11] J. Ortigoza-Ferado, R.J. Richter, S.K. Hornung, A.G. Motulsky, C.E. Furlong, Paraoxon hydrolysis in human serum mediated by a genetically variable arylesterase and albumin, *Am. J. Hum. Genet.* 36 (1984) 295–305.
- [12] L.G. Sultatos, K.M. Basker, M. Shao, S.D. Murphy, The interaction of the phosphorothioate insecticides chlorpyrifos and parathion and their oxygen analogues with bovine serum albumin, *Mol. Pharmacol.* 26 (1984) 99–104.
- [13] M.A. Sogorb, N. Diaz-Alejo, M.A. Escudero, E. Vilanova, Phosphotriesterase activity identified in purified serum albumins, *Arch. Toxicol.* 72 (1998) 219–226.
- [14] J. Mourik, L.P. de Jong, Binding of the organophosphates parathion and paraoxon to bovine and human serum albumin, *Arch. Toxicol.* 41 (1978) 43–48.
- [15] T. Peters Jr., *All About Albumin: Biochemistry, Genetics, and Medical Applications*, Academic Press, London, 1996.
- [16] F.W. McLafferty, Mass spectrometric analysis: molecular rearrangements, *Anal. Chem.* 31 (1959) 82–87.
- [17] S.A. Fredriksson, L.G. Hammarstrom, L. Henriksson, H.A. Lakso, Trace determination of alkyl methylphosphonic acids in environmental and biological samples using gas chromatography/negative-ion chemical ionization mass spectrometry and tandem mass spectrometry, *J. Mass Spectrom.* 30 (1995) 1133–1143.
- [18] D.T. McLachlin, B.T. Chait, Analysis of phosphorylated proteins and peptides by mass spectrometry, *Curr. Opin. Chem. Biol.* 5 (2001) 591–602.
- [19] M. Mann, R.C. Hendrickson, A. Pandey, Analysis of proteins and proteomes by mass spectrometry, *Annu. Rev. Biochem.* 70 (2001) 437–473.
- [20] H. Steen, B. Kuster, M. Fernandez, A. Pandey, M. Mann, Detection of tyrosine phosphorylated peptides by precursor ion scanning quadrupole TOF mass spectrometry in positive ion mode, *Anal. Chem.* 73 (2001) 1440–1448.
- [21] A. Tholey, J. Reed, W.D. Lehmann, Electrospray tandem mass spectrometric studies of phosphopeptides and phosphopeptide analogues, *J. Mass Spectrom.* 34 (1999) 117–123.
- [22] N. Ahmed, D. Dobler, M. Dean, P.J. Thornalley, Peptide mapping identifies hotspot site of modification in human serum albumin by methylglyoxal involved in ligand binding and esterase activity, *J. Biol. Chem.* 280 (2005) 5724–5732.
- [23] M.A. Sogorb, A. Monroy, E. Vilanova, Chicken serum albumin hydrolyzes dichlorophenyl phosphoramidates by a mechanism based on transient phosphorylation, *Chem. Res. Toxicol.* 11 (1998) 1441–1446.
- [24] M.A. Sogorb, V. Carrera, E. Vilanova, Hydrolysis of carbaryl by human serum albumin, *Arch. Toxicol.* 78 (2004) 629–634.
- [25] I. Manoharan, R. Boopathy, Diisopropylfluorophosphate-sensitive aryl acylamidase activity of fatty acid free human serum albumin, *Arch. Biochem. Biophys.* 452 (2006) 186–188.
- [26] X.M. He, D.C. Carter, Atomic structure and chemistry of human serum albumin, *Nature* 358 (1992) 209–215.
- [27] S. Sugio, A. Kashima, S. Mochizuki, M. Noda, K. Kobayashi, Crystal structure of human serum albumin at 2.5 Å resolution, *Protein Eng.* 12 (1999) 439–446.
- [28] H. Watanabe, S. Tanase, K. Nakajou, T. Maruyama, U. Kragh-Hansen, M. Otagiri, Role of Arg-410 and Tyr-411 in human serum albumin for ligand binding and esterase-like activity, *Biochem. J.* 349 (2000) 813–819.
- [29] J. Ghuman, P.A. Zunszain, I. Petitpas, A.A. Bhattacharya, M. Otagiri, S. Curry, Structural basis of the drug-binding specificity of human serum albumin, *J. Mol. Biol.* 353 (2005) 38–52.
- [30] H.P. Benshop, J.H. Keijer, On the mechanism of ageing of phosphorylated cholinesterases, *Biochim. Biophys. Acta* 128 (1966) 586–588.
- [31] H.O. Michel, B.E. Hackley Jr., L. Berkowitz, G. List, E.B. Hackley, W. Gillilan, M. Pankau, Ageing and dealkylation of soman (pin-

- acetylthymolphosphonofluoridate)-inactivated eel cholinesterase, *Arch. Biochem. Biophys.* 121 (1967) 29–34.
- [32] C.B. Millard, G. Koellner, A. Ordentlich, A. Shafferman, I. Silman, J. Sussman, Reaction products of acetylcholinesterase and VX reveal a mobile histidine in the catalytic triad, *J. Am. Chem. Soc.* 121 (1999) 9883–9884.
- [33] C.B. Millard, G. Kryger, A. Ordentlich, H.M. Greenblatt, M. Harel, M.L. Raves, Y. Segall, D. Barak, A. Shafferman, I. Silman, J.L. Sussman, Crystal structures of aged phosphonylated acetylcholinesterase: nerve agent reaction products at the atomic level, *Biochemistry* 38 (1999) 7032–7039.
- [34] I.M. Kovach, R. Akhmetshin, I.J. Enyedy, C. Viragh, A self-consistent mechanism for dealkylation in soman-inhibited acetylcholinesterase, *Biochem. J.* 324 (1997) 995–996.
- [35] E. Elhanany, A. Ordentlich, O. Dgany, D. Kaplan, Y. Segall, R. Barak, B. Velan, A. Shafferman, Resolving pathways of interaction of covalent inhibitors with the active site of acetylcholinesterases: MALDI-TOF/MS analysis of various nerve agent phosphyl adducts, *Chem. Res. Toxicol.* 14 (2001) 912–918.
- [36] A. Fidler, A.G. Hulst, D. Noort, R. de Ruiter, M.J. van der Schans, H.P. Benschop, J.P. Langenberg, Retrospective detection of exposure to organophosphorus anti-cholinesterases: mass spectrometric analysis of phosphylated human butyrylcholinesterase, *Chem. Res. Toxicol.* 15 (2002) 582–590.
- [37] M.J. Van Der Schans, M. Polhuijs, C. Van Dijk, C.E. Degenhardt, K. Pleijsier, J.P. Langenberg, H.P. Benschop, Retrospective detection of exposure to nerve agents: analysis of phosphofluoridates originating from fluoride-induced reactivation of phosphylated BuChE, *Arch. Toxicol.* 78 (2004) 508–524.
- [38] K. Tsuge, Y. Seto, Detection of human butyrylcholinesterase–nerve gas adducts by liquid chromatography–mass spectrometric analysis after in-gel chymotryptic digestion, *J. Chromatogr. B Anal. Technol. Biomed. Life Sci.* 838 (2006) 21–30.
- [39] J.R. Glenney Jr., L. Zokas, M.P. Kamps, Monoclonal antibodies to phosphotyrosine, *J. Immunol. Methods* 109 (1988) 277–285.
- [40] L. Levine, H.B. Gjika, H. Van Vunakis, Antibodies and radioimmunoassays for phosphoserine, phosphothreonine, and phosphotyrosine: serologic specificities and levels of the phosphoamino acids in cytoplasmic fractions of rat tissues, *J. Immunol. Methods* 124 (1999) 239–249.
- [41] J.M. Grognet, T. Ardouin, M. Istin, A. Vandais, J.P. Noel, G. Rima, J. Satge, C. Pradel, H. Sentenac-Roumanou, C. Lion, Production and characterization of antibodies directed against organophosphorus nerve agent VX, *Arch. Toxicol.* 67 (1993) 66–71.
- [42] Y.X. Zhou, Q.J. Yan, Y.X. Ci, Z.Q. Guo, K.T. Rong, W.B. Chang, Y.F. Zhao, Detection of the organophosphorus nerve agent sarin by a competitive inhibition enzyme immunoassay, *Arch. Toxicol.* 69 (1995) 644–648.
- [43] J.K. Johnson, D.M. Cerasoli, D.E. Lenz, Role of immunogen design in induction of soman-specific monoclonal antibodies, *Immunol. Lett.* 96 (2005) 121–127.

# Carbofuran poisoning detected by mass spectrometry of butyrylcholinesterase adduct in human serum

He Li,<sup>a</sup> Ivan Ricordel,<sup>b</sup> Larry Tong,<sup>a</sup> Lawrence M. Schopfer,<sup>a</sup> Frédéric Baud,<sup>c</sup> Bruno Mégarbane,<sup>c</sup> Eric Maury,<sup>d</sup> Patrick Masson<sup>e</sup> and Oksana Lockridge<sup>a\*</sup>

**ABSTRACT:** Carbofuran is a pesticide whose acute toxicity is due to inhibition of acetylcholinesterase. Butyrylcholinesterase (BChE) in plasma is inhibited by carbofuran and serves as a biomarker of poisoning by carbofuran. The goal was to develop a method to positively identify poisoning by carbofuran. Sera from an attempted murder and an attempted suicide were analyzed for the presence of carbofuran adducts on BChE. The BChE from 1 ml of serum was rapidly purified on a 0.2 ml procainamide-Sepharose column. Speed was essential because the carbofuran-BChE adduct decarbamylates with a half-life of about 2 h. The partially purified BChE was boiled to denature the protein, thus stopping decarbamylation and making the protein vulnerable to digestion with trypsin. The labeled peptide was partially purified by HPLC before analysis by LC/MS/MS in the multiple reaction monitoring mode on the QTRAP 2000 mass spectrometer. Carbofuran was found to be covalently bound to Ser 198 of human BChE in serum samples from two poisoning cases. Multiple reaction monitoring triggered MS/MS spectra positively identified the carbofuran-BChE adduct. In conclusion a mass spectrometry method to identify carbofuran poisoning in humans has been developed. The method uses 1 ml of serum and detects low-level exposure associated with as little as 20% inhibition of plasma butyrylcholinesterase. Copyright © 2008 John Wiley & Sons, Ltd.

**Keywords:** carbofuran; butyrylcholinesterase; multiple reaction monitoring; pesticide; carbamate; human plasma

## Introduction

Carbofuran (Fig. 1) is a carbamate pesticide used to control beetles, nematodes and rootworm in fields of alfalfa, rice, grapes and sugar beet (Gupta, 1994). The acute toxicity of carbofuran for both insects and mammals is due to inhibition of acetylcholinesterase. In people, activity assays of red blood cell acetylcholinesterase and serum butyrylcholinesterase (BChE) can verify that poisoning has occurred but cannot identify the type of poison. Gas-chromatography followed by mass spectrometry has been used to detect carbofuran metabolites in plasma and urine (Barr *et al.*, 2002; Petropoulou *et al.*, 2006a, 2006b). However, intact carbofuran has been difficult to find because it is rapidly degraded in plasma and liver. The presence of carbofuran metabolites in plasma and urine could mean that a person ingested or inhaled the metabolites rather than the parent compound. An alternative strategy to obtain proof of exposure takes advantage of the fact that carbofuran makes a covalent bond

with the active site serine of butyrylcholinesterase (Fig. 2). Metabolites do not make this covalent bond. Therefore, identification of the methylcarbamate-butylcholinesterase adduct in a person's serum provides conclusive proof that the individual has been exposed to a carbamate.

This is the first report to describe a mass spectrometry method for detection of the methylcarbamate-BChE adduct. The method extends previous work on detection of organophosphorus-BChE adducts in human plasma (Fidder *et al.*, 2002).

Carbamates are used to slow the progression of Alzheimer's disease (Weinstock and Groner, 2008). Toxicity from these drugs could be monitored by the mass spectrometry method described in this report.

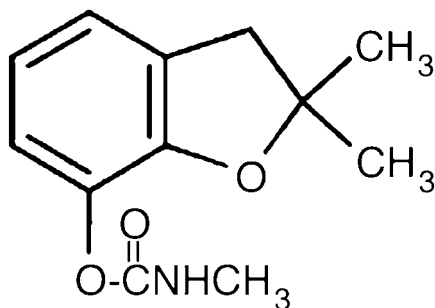


**Figure 1.** Structure of carbofuran.

\* Correspondence to: O. Lockridge, 986805 Nebraska Medical Center, Omaha, NE 68198-6805, USA. E-mail: olockrid@unmc.edu

a Eppley Institute, University of Nebraska Medical Center, Omaha, NE 68198, USA.

b Institut National de Police Scientifique, Laboratoire de toxicologie de la préfecture de police, 2 Place Mazas, 75012 Paris, France.

c Service de Réanimation Médicale et Toxicologique and INSERM U705, Université Paris-Diderot, Hôpital Lariboisière, 2 Rue Ambroise Paré, 75010, Paris, France.

d Réanimation Médicale, Hôpital Saint Antoine, Assistance Publique-Hôpitaux de Paris, 184 rue du Faubourg Saint Antoine, 75571 Paris Cedex 12 France.

e Centre de Recherches d Service de Santé des Armées, Département de Toxicologie-Unité d'Enzymologie, BP87, 38702 La Tronche Cedex, France.

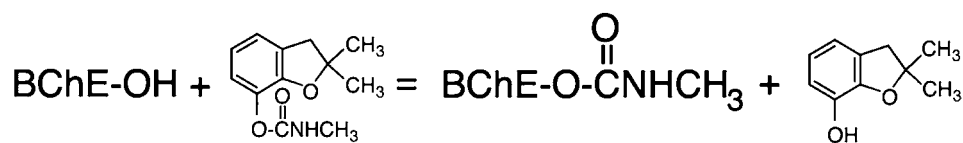


**Figure 2.** Covalent binding of carbofuran to BChE. The active site serine 198 of human BChE makes a covalent bond with the carbamate group of carbofuran, releasing the hydroxybenzofuran ring structure. The mass added to BChE by the carbamate is 57.05 amu.

## Methods

### Materials

Human BChE was purified from 70 l of outdated human plasma by ion exchange chromatography at pH 4.0, followed by procainamide affinity chromatography, and ion exchange chromatography at pH 7.4 (Lockridge *et al.*, 2005). The 574 amino acid sequence of the secreted human BChE protein plus the 28 amino acid signal peptide sequence for a total of 602 amino acids are in file accession no. gi: 116353. Carbofuran (2,3-dihydro-2,2-dimethyl-7-benzofuranol *N*-methyl carbamate) was from Aldrich (no. 426008). Carbofuran was dissolved in dimethylsulfoxide just before use. Sequencing grade modified trypsin (Promega V5113) at a concentration of 20 µg in 50 µl of 50 mM acetic acid was stored at -80 °C.

### Pure Human BChE Labeled with Carbofuran for Mass Spectrometry

An aliquot of 87 µl of 1 mg/ml BChE (1 nmole) in 10 mM ammonium bicarbonate was treated with 5 µl of freshly prepared 0.4 mM carbofuran (2 nmol) for 30 min at room temperature. BChE activity fell from 720 to 122 u/ml, indicating 83% inhibition. A BChE control sample was prepared in the same way except that exposure to carbofuran was omitted. Both the carbofuran-treated and the control BChE samples were boiled for 10 min in a water bath to denature the protein in preparation for digestion with 5 µl of 0.4 µg/µl trypsin. Digestion was at 37 °C for 22 h. The active site peptide was purified using a Phenomenex Prodigy, 5 µm, ODS(2) C<sub>18</sub> column (100 × 4.60 mm) on a Waters HPLC system. Peptides were eluted with a 60 min gradient starting at 0.1% trifluoroacetic acid, and ending at 60% acetonitrile–40% 0.1% trifluoroacetic acid, at a flow rate of 1 ml/min. A 0.5 µl aliquot from each 1 ml fraction was analyzed by MALDI-TOF mass spectrometry to identify samples containing the active site peptide. HPLC fractions were dried in a vacuum centrifuge and redissolved in 100 µl of 50% acetonitrile, 0.1% formic acid in preparation for infusion into the QTRAP 4000 tandem quadrupole mass spectrometer, or in 100 µl of 5% acetonitrile, 0.1% formic acid for LC/MS/MS on the QTRAP 2000 tandem quadrupole mass spectrometer.

### BChE Activity

BChE activity was assayed with 1 mM butyrylthiocholine iodide in 0.1 M potassium phosphate pH 7.0 in the presence of 0.5 mM dithiobisnitrobenzoic acid, at 25 °C by measuring the increase in absorbance at 412 nm. The slope per min was converted to µmoles per min using the extinction coefficient  $E = 13\,600\text{ M}^{-1}\text{ cm}^{-1}$  (Ellman *et al.*, 1961).

### Serum

Serum samples (no anticoagulant) from an attempted murder and an attempted suicide were obtained from Professor Ivan Ricordel, Paris Police. Samples were shipped to Nebraska on dry ice and stored at -80 °C.

The attempted murder victim was a 63-year-old man who had been repeatedly poisoned. He was admitted to the Intensive Care Unit for respiratory failure requiring mechanical ventilation. Clinical examination revealed myosis, hypersialorrhea and some paralysis. Plasma cholinesterase activity measured 6 and 17 h after admission was 2.5 and 4.8 U/ml (normal: 7–9 U/ml). Clinical symptoms improved rapidly, allowing extubation by 12 h. The rapid recovery was consistent with poisoning by a carbamate rather than an organophosphorus agent. Hair analysis revealed the presence of carbofuran and its main metabolite, 3-hydroxycarbofuran (Dulaurent *et al.*, 2008).

The suicidal female patient had ingested 20 mg of carbofuran (Curater 5%) and alcohol. Diagnosis of the nature of the toxicant was based on interview of the patient and the pesticide bottle brought to the hospital. The patient had abdominal pain, but no other cholinergic symptoms of toxicity. Her alcohol level was 1.37 g/l. She was treated with atropine to block muscarinic receptors, and with rivotril for anxiety. The interval between exposure and blood sampling was 7 h. After centrifugation to remove coagulated blood, the serum was frozen at -30 °C until it was shipped on dry ice.

### Purification of BChE from 1 ml Serum

Human serum contains about 0.05 nmol of BChE in 1 ml. This amount was expected to be detectable in the mass spectrometer, based on studies with highly purified BChE. BChE from 1 ml serum was purified by passage over 0.2 ml of procainamide affinity gel packed in a 1.5 ml microfuge spin column. The affinity gel had been custom synthesized by Dr Yacov Ashani (Grunwald *et al.*, 1997) and had a specific activity of 34 µmol procainamide bound per ml Sepharose. The gel was equilibrated with 2 ml of 20 mM potassium phosphate pH 7.0 buffer. One milliliter of serum was loaded on the column by gravity flow at a rate of 1 ml in 10 min. Centrifugation was not used for this step because binding was more complete when loading was slow. The column was washed four times with 1 ml of 0.2 M NaCl in 20 mM potassium phosphate pH 7.0 buffer. The wash time was reduced to less than 0.5 min per ml by briefly centrifuging the spin column. The column was eluted three times with 0.5 ml of 1 M sodium chloride in 20 mM potassium phosphate pH 7.0 buffer to remove the BChE. The total time elapsed from thawing the plasma to elution was 15 min. Speed was critical because the carbamate is easily released from intact BChE. A 10 µl aliquot of each fraction was saved for nondenaturing gel electrophoresis.

### Trypsin Digestion and HPLC Purification of the Carbofuran-BChE Peptide

The 0.5 ml BChE fraction in 1 M NaCl containing the majority of the BChE was immediately boiled for 10 min to denature the protein, and thus prevent decarbamylation of the active site serine. A second reason for boiling the BChE was to unfold the protein to allow trypsin access to cleavage sites that otherwise are blocked by the sugar-coated surface of the BChE molecule. There was no need to reduce and alkylate disulfide bonds. The BChE was digested with 20  $\mu$ l of 0.4  $\mu$ g/ $\mu$ l trypsin for 18 h at 37 °C. The active site peptide was partially purified on a Waters HPLC as described above. The sample that eluted between 34 and 35% acetonitrile was analyzed in the QTRAP 4000 and QTRAP 2000 mass spectrometers.

### Nondenaturing Gel Electrophoresis

A 4–30% polyacrylamide gradient gel was prepared in a Hoefer apparatus (Hoefer became Pharmacia then Amersham and is now GE Healthcare). Electrophoresis was for 5000 V h (250 V, 20 h) at 4 °C. Bromophenol Blue eluted off the gel long before electrophoresis was stopped. The gel was stained for BChE activity with butyrylthiocholine by the method of Karnovsky and Roots, and counterstained with Coomassie blue (Karnovsky and Roots, 1964).

### Infusion into the QTRAP 4000 Mass Spectrometer

HPLC fractions containing the partially purified carbofuran-labeled BChE peptide were infused into the QTRAP 4000 hybrid, quadrupole, linear ion-trap mass spectrometer (Applied Biosystems, Foster City, CA, USA) at a flow rate of 0.3  $\mu$ l/min through an 8  $\mu$ m emitter (no. FS360-50-8-D, New Objective) via a 25  $\mu$ l Hamilton syringe mounted on a Harvard syringe pump. An ion spray potential of 1900 V was maintained between the emitter and the mass spectrometer. Selected masses were fragmented by collision induced dissociation in a collision cell pressurized to 40  $\mu$ Torr with pure nitrogen, using a collision energy of 40 eV. The mass spectrometer was calibrated on selected fragments from the MS/MS spectrum of Glu Fibrinopeptide B. 500 MS/MS scans were summed to produce the final spectrum. The sequence of the peptide was determined by manual inspection of the fragmentation spectra.

### Multiple Reaction Monitoring on the QTRAP 2000 Mass Spectrometer

Ten microliters of HPLC-purified, tryptic peptides were injected onto a nanocolumn (no. 218MS3.07515 Vydac C<sub>18</sub> polymeric rev-phase, 75  $\mu$ m i.d.  $\times$  150 mm long; P.J. Cobert Assoc, St Louis, MO, USA) for a second phase of HPLC separation. Peptides were separated with a 90 min linear gradient from 0 to 60% acetonitrile at a flow rate of 0.3  $\mu$ l/min and electrosprayed through a fused silica emitter (360  $\mu$ m o.d., 75  $\mu$ m i.d., 15  $\mu$ m taper, New Objective) directly into the QTRAP 2000, a hybrid quadrupole linear ion trap mass spectrometer (Applied Biosystems, Foster City, CA, USA). An ion-spray voltage of 1900 V was maintained between the emitter and the mass spectrometer. The collision cell was pressurized to 40  $\mu$ Torr with pure nitrogen and collision energies between 20 and 40 eV were used. The collision energy for a given peptide was determined automatically by the Analyst software, based on the mass and charge of the precursor ion. The mass spectrometer was calibrated on selected fragments

from the MS/MS spectrum of Glu-Fibrinopeptide B. The MS/MS data were collected and processed using Analyst 1.4.1 software (Applied Biosystems).

The QTRAP 2000 was operated in MRM mode. MRM transition ions were selected based on the fragmentation pattern of the carbofuran-labeled BChE active site peptide determined from the infusion experiments. The Q1 mass was set to 747.6  $m/z$  for the quadruply-charged parent ion SVTLFGES\*AGAASVSLHLLSPGSHSLFTR, where the labeled Ser198 is indicated by an asterisk. The Q3 masses were set to 1001.5 amu for the singly-charged y9 ion, and to 1201.6 amu for the singly-charged y11 ion. The BChE peptide AILQSGSFNAPWAVTSLYEAR co-purified with the active site peptide. It was included in the MRM search as a positive control. The Q1 mass for that peptide was set to 761.5  $m/z$  for the triply-charged parent ion. The Q3 masses were set to 839.4 amu for the singly-charged y7 ion, and to 1009.5 amu for the singly-charged y9 ion. The reference peptide served as assurance that the MRM method was working.

### MALDI-TOF-TOF 4800 Mass Spectrometer (Applied Biosystems, Foster City, CA, USA)

Essentially salt-free 0.5  $\mu$ l samples from the offline HPLC fractions were spotted on a MALDI target plate, air dried and overlaid with 0.5  $\mu$ l of 10 mg/ml  $\alpha$ -cyano-4-hydroxycinnamic acid in 50% acetonitrile, 0.1% trifluoroacetic acid. MS spectra were acquired with laser power at 3000 V in positive reflector mode. The mass spectrometer was calibrated against des-Arg-Bradykinin, Angiotensin 1, Glu Fibrinopeptide B and neurotensin (Cal Mix 1, Applied Biosystems). Each spectrum was the average of 500 laser shots.

### Decarbamylation Rate of Carbofuran-labeled BChE

Highly purified human BChE with an activity of 540 u/ml (0.75 mg/ml) was dissolved in phosphate buffered saline pH 7.4. A 560  $\mu$ l aliquot (4.94 nmol) was treated with 1  $\mu$ l of 10 mM carbofuran (10 nmol) for 1 h at 25 °C, at which time 88% of the BChE was inhibited. A 5  $\mu$ l aliquot was diluted into 500  $\mu$ l of phosphate buffered saline to make the solution used for measuring the rate of decarbamylation. Seven replicate dilutions were prepared in seven tubes. At various times after dilution, 20  $\mu$ l was removed for assay of BChE activity.

## Results

### Pure BChE Labeled with Carbofuran

HPLC fractions were analyzed by MALDI-TOF to identify the elution positions of the 2985.5 amu carbofuran-BChE peptide and the 2928.5 amu unlabeled active site peptide. The methylcarbamyl-labeled as well as the unlabeled active site tryptic peptides started to elute at 34% acetonitrile and continued to elute with lower intensity to 42% acetonitrile. The highest concentration was in the 34–35% acetonitrile fraction.

The 34–35% fraction, containing the partially purified, methylcarbamyl-labeled peptide was infused into the QTRAP 4000 mass spectrometer where collision-induced dissociation of the triply-charged parent ion at 996.4  $m/z$  yielded the MS/MS spectrum in Fig. 3. The b- and y-ion masses in Fig. 3 are consistent with the sequence SVTLFGES\*AGAASVSLHLLSPGSHSLFTR where S\* has an added mass of 57 due to covalent binding of carbamate. Masses for the doubly-charged ions from y22<sup>+2</sup> to y27<sup>+2</sup> are

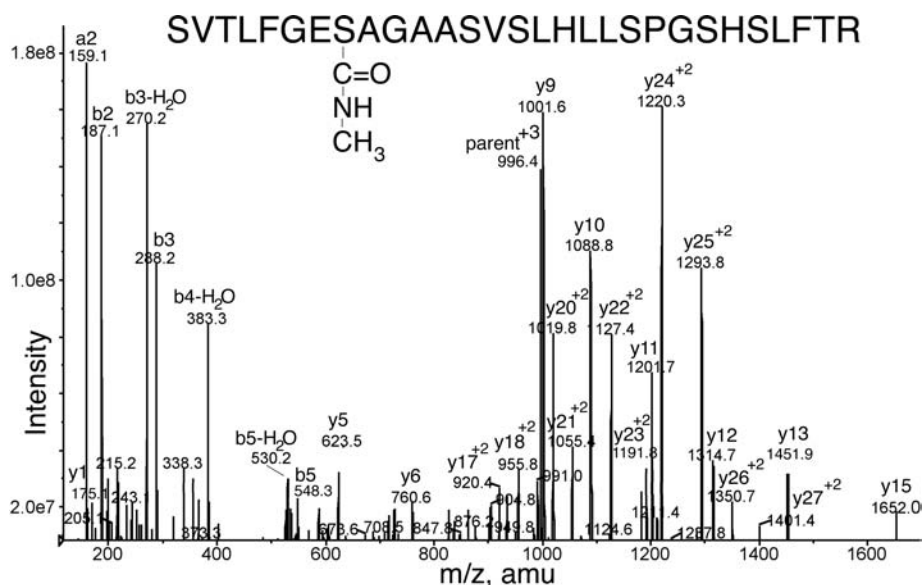


**Figure 3.** MS/MS spectrum of the carbofuran (methylcarbamyl)-labeled tryptic peptide from pure human BChE (accession no. gi:116353). The doubly-charged  $y_{22}^{+2}$  to  $y_{27}^{+2}$  ions carry the carbamate on Ser 198. This increases their mass by 57 amu compared with the unlabeled ions. The spectrum was obtained on the QTRAP 4000 mass spectrometer by infusing purified peptide.

consistent with the presence of carbamate on Ser 198. Carbamate increases each of their masses by 57 amu compared to the unlabeled ions. The  $y_{22}^{+2}$  ion (S\*AGAASVSLHLLSPGSHSLFTR) is 144 amu heavier than the  $y_{21}^{+2}$  ion (AGAASVSLHLLSPGSHSLFTR), a mass that exactly fits Ser (87 amu) plus carbamate (57 amu).

No ions for dehydrated serine were found. Unlike organophosphorus-modified serine (Fidder *et al.*, 2002; Tsuge and Seto, 2006; Sun and Lynn, 2007) and pyridostigmine (dimethylcarbamyl)-modified serine (Fidder *et al.*, 2002), carbofuran (methylcarbamyl)-modified serine did not undergo beta-elimination during fragmentation when the collision energy was 40 V in the QTRAP mass spectrometer. Beta-elimination would have yielded ions that were missing the carbamate as well as water for a total loss of 75 amu.

#### Rate of Decarbamylation of Carbofuran (Methylcarbamyl)-labeled Pure BChE

The half-life for decarbamylation of the carbofuran-BChE adduct was measured by regain of BChE activity as a function of time, during incubation at pH 7.4, 25 °C. Figure 4 shows that the half-life was  $142 \pm 8$  min, which corresponds to a first-order rate constant of  $k = 0.00488 \text{ min}^{-1}$ . A half-life of about 2 h for reactivation of the adduct means that a BChE purification method would have to be rapid if any of the labeled, active site peptide were to be recovered.

#### Residual BChE Activity in the Serum from Victims of Carbofuran Poisoning

The serum from the attempted murder victim had a BChE activity of 0.5 u/ml, while serum from the attempted suicide had an activity of 2.3 u/ml. The average BChE activity in unexposed serum is about 3.0 u/ml, indicating that BChE from the murder victim was 83% inhibited, while BChE from the suicide attempt was 23% inhibited.

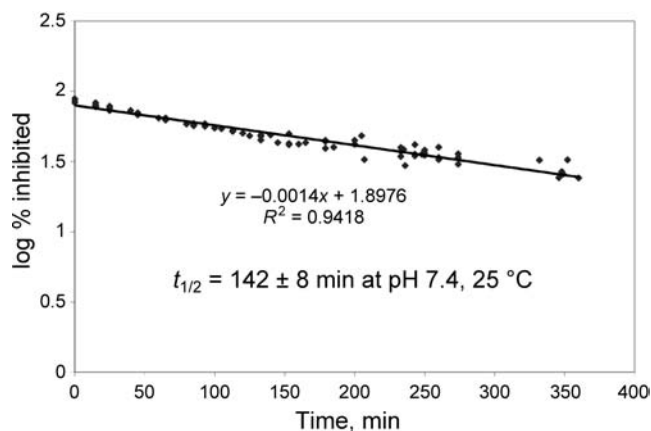


**Figure 4.** Decarbamylation rate of carbofuran (methylcarbamyl)-BChE. BChE activity was 88% inhibited at time zero, but became less inhibited with time as carbofuran was released from the active site Ser 198. The points are the data, while the line is a linear regression. The equation describes the regression line and  $R^2$  indicates the standard error. The experiment was repeated seven times.

#### Purification of BChE from 1 ml Serum

Fifty-seven percent of the starting BChE activity was recovered when the procainamide affinity column was eluted with the first 0.5 ml of 1 M sodium chloride. An additional 20% was recovered with the subsequent 1 ml of 1 M sodium chloride. Only 13% of the activity was lost during washing with 0.2 M NaCl (Table 1). The BChE in the first eluate was purified about 60-fold, for the example shown in Table 1. With other samples this purification method has yielded up to 600-fold purified BChE.

The nondenaturing gel stained for BChE activity in Fig. 5(A) shows that the majority of BChE in human serum is a tetramer

**Table 1.** Fifteen-minute purification of carbofuran-BChE from 1 ml of serum, on a 0.2 ml procainamide-Sepharose column

Sample	Composition	Volume, ml	Units/ml	Total units	A280	Units/mg
Serum	Serum	1	2.32	2.32	55.7	0.075
Flow-thru	Loading	1	0.071	0.071	39.46	0.003
Wash	0.2 M NaCl	1	0.205	0.205	14.22	0.026
Wash	0.2 M NaCl	1	0.059	0.059	1.492	0.071
Wash	0.2 M NaCl	1	0.024	0.024	0.243	0.178
Wash	0.2 M NaCl	1	0.022	0.022	0.196	0.202
Elute	1 M NaCl	0.5	2.61	1.30	1.060	4.41
Elute	1 M NaCl	0.5	0.98	0.49	0.372	4.74
Elute	1 M NaCl	0.5	0.073	0.037	0.120	1.11

Sodium chloride solutions are in 20 mM potassium phosphate, pH 7, 1 mM EDTA, 0.01% sodium azide.

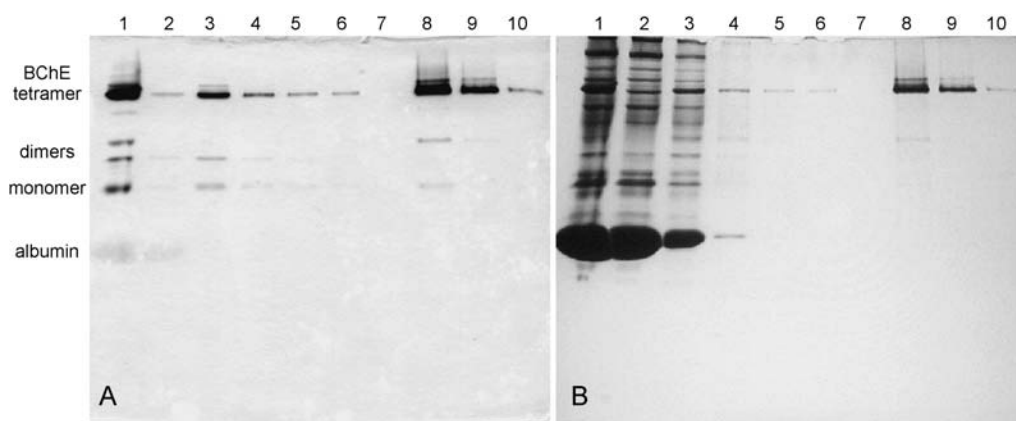


**Figure 5.** Nondenaturing gel stained for BChE activity (A) and counterstained with Coomassie blue (B). Aliquots of 10  $\mu$ l of serum and fractions from the affinity column purification of BChE were loaded into each lane of a 4–30% polyacrylamide, gradient gel. Lane 1, serum; lane 2, flow-thru; lane 3, first wash, with 1 ml of 0.2 M sodium chloride; lane 4, second wash; lane 5, third wash; lane 6, fourth wash; lane 7, blank; lane 8, first eluate, with 0.5 ml of 1 M sodium chloride; lane 9, second eluate; lane 10, third eluate.

(lane 1). Two bands of activity appear in the dimer region. The faster migrating dimer is composed of one BChE subunit linked to one albumin molecule through a disulfide bond (Masson, 1989). The BChE–albumin dimer eluted during the wash with 0.2 M NaCl (lane 3) and was not recovered with the partially-purified BChE shown in lane 8. Bromophenol blue binds to human albumin and is visible as a rapidly migrating band in lane 1 of panel A. The same gel was counterstained with Coomassie blue in Fig. 5(B). The most intense Coomassie-staining band is for albumin. The affinity gel did not bind albumin as can be seen by the albumin bands in lanes 2, 3 and 4. No Coomassie blue stained bands are present in lanes 8–10 of Fig. 5(B). The bands that appear in the figure are the brownish red bands of copper ferrocyanide precipitate formed during the activity staining reaction.

Though the BChE appears to be relatively pure in Fig. 5(B), it still is contaminated with many proteins. These contaminating proteins generate peptides during tryptic digestion that interfere with ionization of the BChE active site peptide in the mass spectrometer. Therefore the tryptic digest of the BChE eluate was further purified offline using a Waters HPLC system. The 2985.5 amu peak for the carbofuran-labeled active site peptide of BChE was barely detectable by MALDI-TOF analysis of the HPLC fractions; however from the control experiments we knew

that this peptide would elute in the 34–35% acetonitrile fraction. Therefore this fraction was collected and analyzed by tandem, quadrupole mass spectrometry.

#### Tandem Quadrupole Ion Trap Mass Spectrometry

The purified carbofuran (methylcarbamylo)–BChE peptide that had been isolated from 1 ml of serum was infused into the QTRAP 4000 mass spectrometer. MS/MS spectra for the quadruply-charged parent ion at 747.1 and the triply-charged parent ion at 995.8 had 20–30 singly-, doubly-, and triply-charged ions that fit the carbofuran (methylcarbamylo)–BChE peptide sequence. Both the attempted murder and suicide samples gave spectra consistent with the carbofuran (methylcarbamylo)–BChE peptide. The signal-to-noise ratio ranged from 2 to 10, and peak intensities were about 100-fold lower than for pure BChE.

#### Multiple Reaction Monitoring

The carbofuran (methylcarbamylo)-labeled peptide from the murder and suicide victims was also characterized by a multiple reaction monitoring (MRM) strategy. The mass spectrometer was instructed to ignore all masses except for the quadruply-charged parent ion at 747.6 *m/z* and two singly-charged daughter ions at

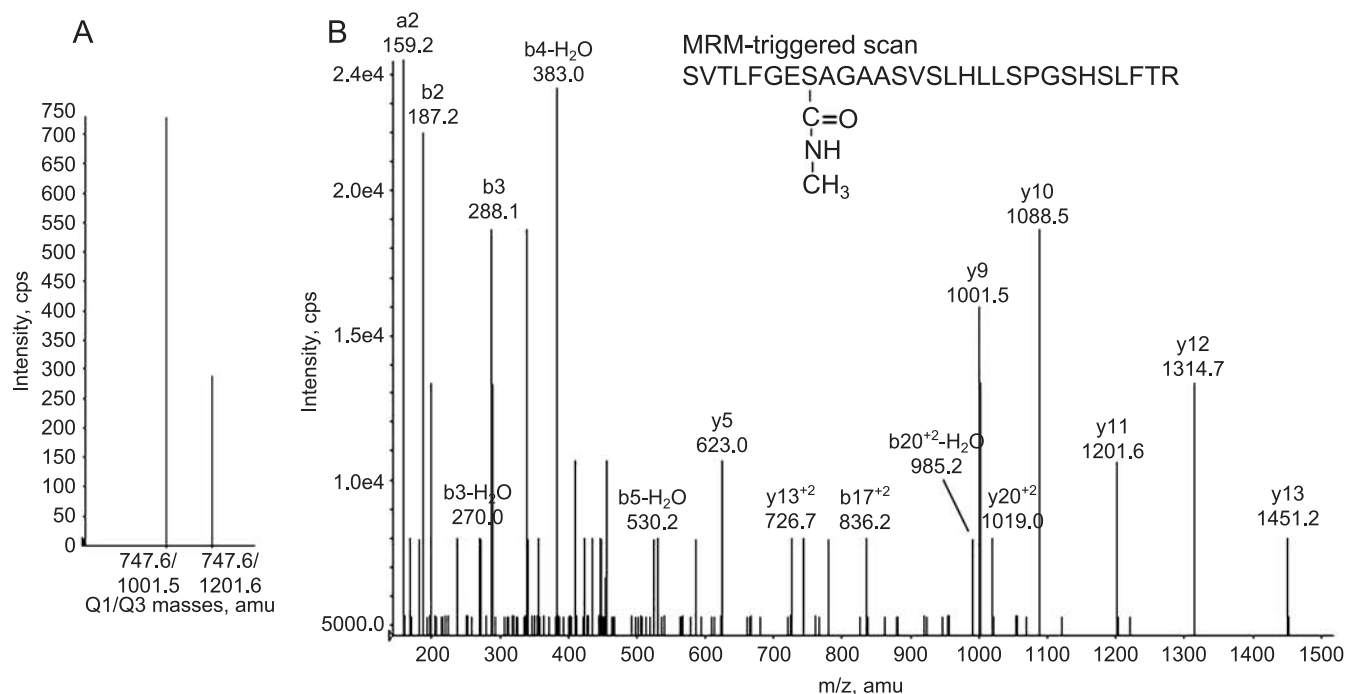


**Figure 6.** MRM-triggered MS/MS scan of carbofuran (methylcarbamyl)-labeled BChE peptide from 1 ml of serum taken from the attempted murder victim. (A) MRM transitions for the quadruply-charged parent ion at 747.6 *m/z* and singly-charged daughter ions at 1001.5 and 1201.5 amu. (B) The MS/MS spectrum of the 747.6 *m/z* parent ion was triggered by the MRM scan. The MS/MS scan confirms that the parent ion is the carbofuran-labeled active site peptide of human BChE.

1001.5 and 1201.6 amu. These masses are referred to as the Q1 and Q3 transitions [Fig. 6(A)]. When the mass spectrometer identified a peptide with these transitions, it automatically acquired an MS/MS spectrum for that parent ion [Fig. 6(B)].

The MRM-triggered MS/MS scan in Fig. 6(B) has an intensity that is 4 orders of magnitude lower than the MS/MS scan in Fig. 3, and it has fewer ions. Nevertheless, the ions in the MRM-triggered scan have the masses expected for fragments from the carbofuran(methylcarbamyl)-labeled peptide SVTLFGES\*AGAASVSLHLLSPGSHSLFTR. Comparison of the MS/MS spectrum in Fig. 6(B) with that in Fig. 3 revealed 16 ions characteristic of the carbofuran (methylcarbamyl)-labeled BChE active site tryptic peptide. The mass of the parent ion is consistent with the active site peptide of BChE modified with an added mass of 57 amu. The doubly-charged b17 and b20 minus H<sub>2</sub>O ions support modification on Ser 198.

Serum samples from both the murder and suicide victims yielded MRM-triggered MS/MS scans that supported the presence of carbofuran-labeled BChE in their sera.

## Discussion

### Carbamate Adducts on BChE are Unstable

The *N*-methyl carbamate adduct of human BChE has been reported to have a half-life of 11 min at pH 7.4, 37 °C (Wetherell and French, 1991) or 3 h at pH 7.4, 25 °C (Reiner, 1971). In our hands the half-life at pH 7.4, 25 °C was about 2.4 h. The short half-life of the carbofuran adduct meant the BChE had to be purified rapidly to prevent loss of the carbofuran label. This was achieved by purifying BChE on affinity gel packed in a spin column. The short half-life also means there is a need to collect

the serum samples in a timely manner from the victims. If several days pass between exposure and serum collection, it is likely that all the carbofuran (methylcarbamyl)-BChE adduct will have been lost.

The *N*-dimethyl carbamate adduct of human BChE (e.g., BChE carbamylated by pyridostigmine or by M7C or by an analog of rivastigmine) is more stable than the *N*-methyl carbamate. The half-life of the *N*-dimethyl carbamylated BChE is 277 min at pH 7.4, 25 °C, a value that calculates to a rate of decarbamylation of 0.0025 min<sup>-1</sup> (Lockridge and La Du, 1978). The rate of decarbamylation is 0.0063 min<sup>-1</sup> at pH 8.0, 37 °C (Weinstock and Groner, 2008).

### Decarbamylation is a Catalytic Process

The partially purified BChE was boiled immediately after it was eluted from the affinity column. This step was used because decarbamylation is a catalytic process requiring the native conformation of BChE (Main, 1979), and therefore decarbamylation can be halted by denaturing the enzyme. This concept was proven to be correct by the fact that the carbofuran (methylcarbamyl)-labeled peptide was recovered despite the passage of many days between the time the BChE was boiled and the peptide was analyzed.

### Mass Spectrometry to Identify the Poison

The method introduced in this work identifies poisons that add methylcarbamate, a mass of 57 amu, to the BChE active site. Carbofuran is not the only poison that adds a mass of 57 amu. Physostigmine, carbaryl, aldicarb, aldoxycarb, formetanate, methiocarb, methomyl, oxamyl, propoxur and physovenine all

give the same added mass of 57 amu. Analysis of degradation products present in urine can be used to discriminate between these toxins (Barr *et al.*, 2002; Petropoulou *et al.*, 2006a). However, other carbamates such as pyridostigmine and pirimicarb add dimethylcarbamate to BChE, an added mass of 71 amu. The method described in this report can be used to discriminate between these classes of carbamate toxins. The presence of an adduct on BChE means the person was exposed to the intact carbamate pesticide.

### Significance

The presence of metabolites of carbofuran in blood and urine provides evidence of exposure, but this evidence can be interpreted to mean that degradation products rather than the active poison were ingested. Indisputable proof of exposure to active poison is the finding of butyrylcholinesterase adducts.

### Acknowledgements

Supported by US Army Medical Research and Materiel Command W81XWH-07-2-0034 (to O.L.), NIH CounterACT grant U01 NS058056 (to O.L.), Eppley Cancer Center grant P30CA36727 and DGA grant 03co010-05/PEA 01 08 7 to (P.M.). Mass spectra were obtained with the support of the Mass Spectrometry and Proteomics Core Facility at the University of Nebraska Medical Center.

### References

- Barr DB, Barr JR, Maggio VL, Whitehead RD, Jr, Sadowski MA, Whyatt RM, Needham LL. 2002. A multi-analyte method for the quantification of contemporary pesticides in human serum and plasma using high-resolution mass spectrometry. *J. Chromatogr. B Analyt. Technol. Biomed. Life Sci.* **778**: 99–111. DOI: 10.1016/S0378-4347(01)00444-3.
- Dulaurent S, Gaulier JM, Baudel JL, Fardet L, Maury E, Lachatre G. 2008. Hair analysis to document non-fatal pesticide intoxication cases. *Forensic Sci. Int.* **176**: 72–75. DOI: 10.1016/j.forsciint.2007.07.018.
- Ellman GL, Courtney KD, Andres V Jr, Feather-Stone RM. 1961. A new and rapid colorimetric determination of acetylcholinesterase activity. *Biochem Pharmacol* **7**: 88–95.
- Fidder A, Hulst AG, Noort D, de Ruiter R, van der Schans MJ, Benschop HP, Langenberg JP. 2002. Retrospective detection of exposure to organophosphorus anti-cholinesterases: mass spectrometric analysis of phosphorylated human butyrylcholinesterase. *Chem. Res. Toxicol.* **15**: 582–590. DOI: 10.1021/tx0101806 S0893-228x(01)00180-1.
- Grunwald J, Marcus D, Papier Y, Raveh L, Pittel Z, Ashani Y. 1997. Large-scale purification and long-term stability of human butyrylcholinesterase: a potential bioscavenger drug. *J. Biochem. Biophys. Meth.* **34**: 123–135. DOI: 10.1016/S0165-022X(97)01208-6.
- Gupta RC. 1994. Carbofuran toxicity. *J. Toxicol. Environ. Hlth* **43**: 383–418.
- Karnovsky MJ, Roots L. 1964. A 'direct-coloring' thiocholine method for cholinesterases. *J. Histochem. Cytochem.* **12**: 219–221.
- Lockridge O, La Du BN. 1978. Comparison of atypical and usual human serum cholinesterase. Purification, number of active sites, substrate affinity, and turnover number. *J. Biol. Chem.* **253**: 361–366.
- Lockridge O, Schopfer LM, Winger G, Woods JH. 2005. Large scale purification of butyrylcholinesterase from human plasma suitable for injection into monkeys; a potential new therapeutic for protection against cocaine and nerve agent toxicity. *J. Med. CBR Def.* **3**. DOI: 10.1901/jaba.2005.3-nihms5095.
- Main AR. 1979. Mode of action of anticholinesterases. *Pharmac. Ther.* **6**: 579–628.
- Masson P. 1989. A naturally occurring molecular form of human plasma cholinesterase is an albumin conjugate. *Biochim. Biophys. Acta* **998**: 258–266.
- Petropoulou SS, Gikas E, Tsarbopoulos A, Siskos PA. 2006a. Gas chromatographic-tandem mass spectrometric method for the quantitation of carbofuran, carbaryl and their main metabolites in applicators' urine. *J. Chromatogr. A* **1108**: 99–110. DOI: 10.1016/j.chroma.2005.12.058.
- Petropoulou SS, Tsarbopoulos A, Siskos PA. 2006b. Determination of carbofuran, carbaryl and their main metabolites in plasma samples of agricultural populations using gas chromatography-tandem mass spectrometry. *Anal. Bioanal. Chem.* **385**: 1444–1456. DOI: 10.1007/s00216-006-0569-0.
- Reiner E. 1971. Spontaneous reactivation of phosphorylated and carbamylated cholinesterases. *Bull. WHO* **44**: 109–112.
- Sun J, Lynn BC. 2007. Development of a MALDI-TOF-MS method to identify and quantify butyrylcholinesterase inhibition resulting from exposure to organophosphate and carbamate pesticides. *J. Am. Soc. Mass Spectrom.* **18**: 698–706. DOI: 10.1016/j.jasms.2006.11.009.
- Tsuge K, Seto Y. 2006. Detection of human butyrylcholinesterase-nerve gas adducts by liquid chromatography-mass spectrometric analysis after in gel chymotryptic digestion. *J. Chromatogr. B Analyt. Technol. Biomed. Life Sci.* **838**: 21–30. DOI: 10.1016/j.jchromb.2006.02.054.
- Weinstock M, Groner E. 2008. Rational design of a drug for Alzheimer's disease with cholinesterase inhibitory and neuroprotective activity. *Chem. Biol. Interact.* DOI: 10.1016/j.cbi.2008.03.014.
- Wetherell JR, French MC. 1991. A comparison of the decarbamylation rates of physostigmine-inhibited plasma and red cell cholinesterases of man with other species. *Biochem. Pharmacol.* **42**: 515–520. DOI: 10.1016/0006-2952(91)90313-T.

# Aging Pathways for Organophosphate-Inhibited Human Butyrylcholinesterase, Including Novel Pathways for Isomalathion, Resolved by Mass Spectrometry

He Li,\* Lawrence M. Schopfer,\* Florian Nachon,† Marie-Thérèse Froment,† Patrick Masson,† and Oksana Lockridge\*<sup>1</sup>

\*Eppley Institute and Department of Biochemistry and Molecular Biology, University of Nebraska Medical Center, Omaha, Nebraska 68198-6805; and

†Centre de Recherches du Service de Santé des Armées, Département de Toxicologie-Unité d'Enzymologie, 24 avenue des Maquis du Grésivaudan-BP87, 38702 La Tronche cedex, France

Received June 27, 2007; accepted July 24, 2007

Some organophosphorus compounds are toxic because they inhibit acetylcholinesterase (AChE) by phosphorylation of the active site serine, forming a stable conjugate: Ser–O–P(O)–(Y)–(XR) (where X can be O, N, or S and Y can be methyl, OR, or SR). The inhibited enzyme can undergo an aging process, during which the X–R moiety is dealkylated by breaking either the P–X or the X–R bond depending on the specific compound, leading to a non-reactivatable enzyme. Aging mechanisms have been studied primarily using AChE. However, some recent studies have indicated that organophosphate-inhibited butyrylcholinesterase (BChE) may age through an alternative pathway. Our work utilized matrix-assisted laser desorption/ionization-time-of-flight mass spectrometry to study the aging mechanism of human BChE inhibited by dichlorvos, echothiophate, diisopropylfluorophosphate (DFP), isomalathion, soman, sarin, cyclohexyl sarin, VX, and VR. Inhibited BChE was aged in the presence of H<sub>2</sub>O<sup>18</sup> to allow incorporation of <sup>18</sup>O, if cleavage was at the P–X bond. Tryptic-peptide organophosphate conjugates were identified through peptide mass mapping. Our results showed no aging of VX- and VR-treated BChE at 25°C, pH 7.0. However, BChE inhibited by dichlorvos, echothiophate, DFP, soman, sarin, and cyclohexyl sarin aged exclusively through O–C bond cleavage, i.e., the classical X–R scission pathway. In contrast, isomalathion aged through both X–R and P–X pathways; the main aged product resulted from P–S bond cleavage and a minor product resulted from O–C and/or S–C bond cleavage.

**Key Words:** butyrylcholinesterase; organophosphate; aging; mass spectrometry.

than acetylcholinesterase (AChE) in mouse and human (Li *et al.*, 2000). BChE reacts with a broad range of toxicants more effectively than AChE. BChE has been suggested to function as a scavenger protein that protects the cholinergic system against anticholinesterase poisons (Lockridge and Masson, 2000).

Organophosphorus (OP) compounds account for a large portion of pesticides and chemical warfare agents. These compounds exert their acute toxicity mainly through inhibition of AChE. OP inhibition of AChE and BChE proceeds in a progressive manner by phosphorylation of the active site Ser, to form a Ser–O–P(O)–(Y)–(XR) adduct (where X can be O, N, or S and Y can be methyl, OR, or SR). The phosphorylated enzyme can be reactivated by treating with strong nucleophilic agents such as oximes. The phosphorylated enzyme can also undergo a spontaneous time-dependent process called “aging” during which the P–X–R component of the OP-serine conjugate is dealkylated, leaving the enzyme irreversibly inhibited (Casida and Quistad, 2004).

Aging has been studied in detail using AChE as the model enzyme. The generally accepted aging mechanism for alkoxy-OP adducts invokes the catalytic participation of residues from the enzyme. Dealkylation of the OP adduct is facilitated primarily by the protonated histidine of the catalytic triad, a glutamic acid residue adjacent to the catalytic serine, and a nearby tryptophan residue (Shafferman *et al.*, 1996; Viragh *et al.*, 1997). It is agreed that these residues combine to promote the cleavage of the O–C bond with formation of a carbocation on the leaving alkyl group and a negatively charged phospho-oxygen (Shafferman *et al.*, 1996; Viragh *et al.*, 1997). The resultant carbocation is then vulnerable to nucleophilic attack by water. A variety of pH, mutational, crystallographic, and kinetic studies support the catalytic involvement of the amino acid residues (Barak *et al.*, 1997; Harris *et al.*, 1966; Jennings *et al.*, 2003; Michel *et al.*, 1967; Millard *et al.*, 1999; Saxena *et al.*, 1993; Shafferman *et al.*, 1996). Studies on BChE inhibited with diisopropylfluorophosphate (DFP) are also consistent with this mechanism (Masson *et al.*, 1997a).

## INTRODUCTION

Butyrylcholinesterase (BChE) is a serine hydrolase that catalyzes the hydrolysis of a variety of choline and noncholine esters (Lockridge and Masson, 2000). BChE is more abundant

<sup>1</sup> To whom correspondence should be addressed at Eppley Institute, University of Nebraska Medical Center, Box 986805, 600 South 42nd Street, Omaha, NE 68198. Fax: (402) 559-4651. E-mail: olockrid@unmc.edu.

On the other hand, recent studies have provided evidence for alternative aging pathways. First, studies on aging of tabun-inhibited human AChE suggested a P–N bond cleavage and elimination of the dimethylamine moiety from the tabun-enzyme conjugate (Barak *et al.*, 2000). This result is also corroborated by the x-ray structure of tabun-aged murine AChE (Ekstrom *et al.*, 2006). Second, isomalathion-inhibited equine BChE was shown to age through breaking the P–S bond and releasing either a thiomethyl or a diethylthiosuccinate moiety (Doorn *et al.*, 2001a). Third, a crystal structure study on echothiophate-inhibited human BChE presented the possibility of aging through both P–O scission and O–C scission (Nachon *et al.*, 2005). Given the diversity of aging pathways invoked for various OP compounds and the indication that different aging pathways may be used by BChE and AChE when inhibited by the same OP, systematic investigation of the BChE aging pathway was needed. The use of BChE as an antidote against OP toxicity also calls for a better understanding of its aging mechanism.

In the current study, we investigated the possibility that OP-inhibited human BChE ages through breakage of the P–X bond (where X may be O or S), as opposed to the classical pathway, i.e., breaking the X–C bond. We evaluated the aging pathway by using matrix-assisted laser desorption/ionization-time-of-flight (MALDI-TOF) mass spectrometry to determine the mass of the aged product. Including  $\text{H}_2\text{O}^{18}$  in the aging medium enabled us to distinguish between the two pathways. Discrimination was possible because the inhibition step employed OP made with common  $^{16}\text{O}$ . If aging occurred via cleavage at P– $^{16}\text{O}$ , then the phosphorus would pick up an  $^{18}\text{OH}$  from the medium to form P– $^{18}\text{O}$ –H. If the cleavage occurred at O–C, then the carbon would pick up the  $^{18}\text{OH}$  and the phosphorus would retain the  $^{16}\text{O}$  as P– $^{16}\text{OH}$ . The net effect would be a 2-Da increase in the mass of the aged adduct if cleavage of the P–O bond occurred. Consequently, the mass of the aged OP-enzyme conjugate revealed which aging pathway had been taken (Fig. 1). The aged enzyme was digested with trypsin, and

the resulting tryptic peptides were analyzed by MALDI-TOF mass spectrometry to determine the mass of the OP-labeled, active-site peptide conjugate. Nine OP compounds were tested, including dichlorvos, echothiophate, DFP, soman, sarin, cyclohexyl sarin (GF), VX, VR (Russian VX), and isomalathion (Fig. 2).

Aging of all the alkoxy adducts followed the classical pathway, with cleavage of the O–C bond. Isomalathion-inhibited BChE, however, gave two aged products. Besides the main aged product resulting from breaking the P–S bond, a minor product resulted from breaking the O–C and/or S–C bond, which had not been reported before.

## MATERIALS AND METHODS

**Chemicals and reagents.** Dichlorvos and isomalathion were from CIL Cluzeau Info Labo (Sainte-Foy-La-Grande, France). Echothiophate iodide was from Wyeth-Ayerst (Rouses Point, NY). DFP was from Acros (Belgium). Soman, sarin, cyclohexyl sarin, VX, and VR were from Centre d'Etudes du Bouchet (Vert-le-Petit, France).  $\text{H}_2\text{O}^{18}$  (95% pure) was from Aldrich (Milwaukee, WI). Sequence-grade modified trypsin was from Promega (Madison, WI).  $\alpha$ -Cyano-4-hydroxycinnamic acid (CHCA) matrix-assisted laser desorption/ionization (MALDI) matrix and external MALDI mass calibration standard mix were purchased from Applied Biosystems (Framingham, MA).

**Purification and deglycosylation of human BChE.** Human BChE (gi:116353; Swiss protein P06276) was purified from plasma as previously described (Lockridge *et al.*, 2005). Recombinant GST-PNGaseF was expressed and purified as previously described (Grueninger-Leitch *et al.*, 1996). Two milligrams of purified human BChE was deglycosylated by treating with 3.2 mg of GST-PNGaseF for 5 min at 37°C in 6.66 ml of 100mM Tris-HCl, pH 7.5. GST-PNGaseF was removed by loading the sample onto GSH-agarose (Sigma, St Louis, MO) packed in a 5-ml column, equilibrated with 100mM Tris-HCl, pH 8.0. The flow through containing human BChE was concentrated to 4.5 mg/ml in a Centricon PM 10 microconcentrator (Millipore, Bedford, MA). BChE was deglycosylated because the deglycosylated protein released the active-site tryptic peptide upon digestion with trypsin. By contrast, when the BChE was not deglycosylated, the active-site peptide was not available to trypsin unless the protein was first denatured and its disulfide bonds reduced and alkylated.

**Organophosphate treatment of BChE.** A 10- $\mu\text{l}$  aliquot of deglycosylated human BChE stock at a concentration of 53 $\mu\text{M}$  enzyme (4.5 mg/ml) was diluted with 90  $\mu\text{l}$  of  $\text{H}_2\text{O}^{16}$  or  $\text{H}_2\text{O}^{18}$  and 1  $\mu\text{l}$  of 1M sodium phosphate pH 7.0. Each 100- $\mu\text{l}$  diluted BChE sample received 1  $\mu\text{l}$  of dichlorvos (6.5M stock), echothiophate (10mM stock), DFP (50mM stock), soman (27.4mM stock), sarin (35.6mM stock), cyclohexyl sarin (27.7mM stock), VX (18.6mM stock), VR (18.6mM stock), or isomalathion (32mM stock). The final concentration of OP is at least 20 times higher than the BChE concentration in the reaction system, ensuring that the inhibition and aging reaction can reach completion under the experimental conditions. The excess OP should not affect the aging reaction pathways. The  $\text{H}_2\text{O}^{18}$  level in the final reaction mixture was at least 85%. Enzyme inhibition and aging proceeded at room temperature for 4 days or more. The BChE used in this study was purified from sterilized human plasma, and we kept the sterilization condition throughout the OP treatment to prevent the microbial contamination. Samples were stored at  $-80^\circ\text{C}$ .

**Tryptic digestion of BChE.** To remove excess OP,  $\text{H}_2\text{O}^{18}$ , and salts, 50  $\mu\text{l}$  of OP-treated BChE was subjected to buffer exchange using Millipore Microcon YM-3 centrifuge filters with 3000 MW cutoff. The protein was diluted with 25mM ammonium bicarbonate pH 8.3, concentrated to 50  $\mu\text{l}$ ,

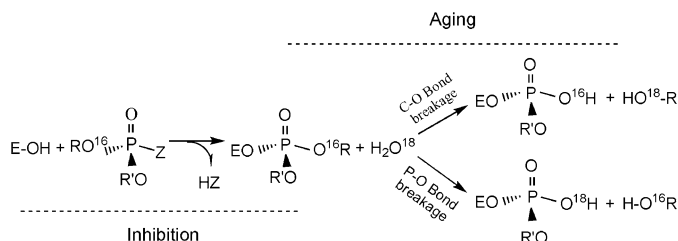


**FIG. 1.** Inhibition and aging of BChE with organophosphate in a  $\text{H}_2\text{O}^{18}$  environment. Two aging pathways give two OP-BChE conjugates with the same chemical structure, but a mass difference of 2 Da, which can be detected by MALDI-TOF mass spectrometry. The generalized OP structure in the scheme represents dichlorvos, echothiophate, and DFP. Aging of isomalathion-, soman-, sarin-, cyclohexyl sarin-, VX-, and VR-inhibited BChE can be studied in the same fashion. E–OH: catalytic serine; R, R': alkyl groups; Z: OP leaving group.

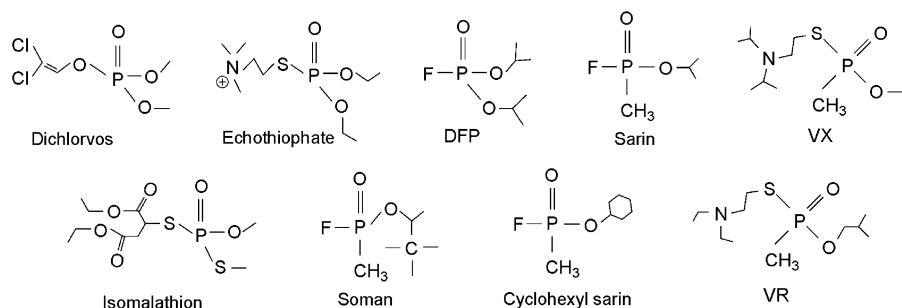


FIG. 2. Chemical structures of dichlorvos, echothiophate, DFP, soman, sarin, cyclohexyl sarin, VX, VR, and isomalathion.

rediluted, and reconcentrated 5 times before digestion. The final  $\text{H}_2\text{O}^{18}$  level was no more than 0.5% of the total volume. The BChE was incubated with modified porcine trypsin at a trypsin:BChE ratio of 1:30, at room temperature, overnight. To wash off salts from the digestion that may interfere with mass spectrometric analysis, trypsinized BChE was adsorbed onto a C18 ZipTip (Millipore) and washed with 0.1% trifluoroacetic acid (TFA). Peptides were eluted from the ZipTip with 15  $\mu\text{l}$  of 30% acetonitrile, 0.1% TFA, followed by 15  $\mu\text{l}$  of 60% acetonitrile, 0.1% TFA. The active-site peptide was eluted with 60% acetonitrile, 0.1% TFA.

**MALDI-TOF mass spectrometry.** All MALDI-TOF mass spectrometry experiments were performed on an Applied Biosystems Voyager DE-PRO workstation equipped with a 337-nm pulsed nitrogen laser. The OP-labeled, trypsinized, BChE active-site peptide that had been adsorbed to a reverse phase C18 ZipTip was eluted into a microcentrifuge tube with 15  $\mu\text{l}$  of 60% acetonitrile, 0.1% TFA. One microliter of eluant was mixed 1:1 (vol/vol) with the matrix solution CHCA (10 mg/ml in 50% acetonitrile, 0.3% TFA) on the MALDI target plate and allowed to dry at room temperature.

Mass spectra were acquired in positive ion, linear, or reflector mode under delayed extraction conditions, using an acceleration voltage of 20 kV. Laser intensity was adjusted so that the strongest ion intensity in a spectrum did not exceed 80% of the maximum, saturated intensity value. Laser positioning on the sample spot was monitored with a video camera. Spectra shown are the average of 500 laser shots collected from multiple locations on the target spot. Calibration for the mass spectra was performed both externally using adrenocorticotrophic hormone peptides (amino acid residues 1–17, 18–39, and 7–38) and internally by reference to BChE tryptic fragments other than the labeled, active-site peptide. The sequence of human BChE (accession number: P06276) was obtained from the SwissProt database (<http://ca.expasy.org/cgi-bin/sprot-search-ful>). The reference masses of the tryptic BChE peptides were obtained using the MS-Digest feature of ProteinProspector version 4.0.6 (<http://prospector.ucsf.edu/>), a comprehensive proteomic data analysis software package. The MS-Fit feature of ProteinProspector was used to identify human BChE from MALDI peptide mass data, where the mass tolerance was set at 100 ppm.

**Half-life of aging.** To determine the aging half-life of echothiophate-inhibited BChE, a time course experiment was conducted. Twenty-five microliters of deglycosylated human BChE (150  $\mu\text{M}$  enzyme in 15mM 2-(N-morpholino)ethanesulfonic acid buffer, pH 6.5) was mixed with 25  $\mu\text{l}$  of 100mM Tris-Cl, pH 8.6 to give a final pH of 8.4. Five microliters of enzyme solution were taken immediately after mixing and diluted into 100  $\mu\text{l}$  of 25mM ammonium bicarbonate, pH 8.3. This enzyme fraction served as the 0-min time point and was stored in the  $-80^\circ\text{C}$  freezer until trypsin digestion. After the 0-min time point had been taken, a 2.2-fold molar excess of echothiophate (1  $\mu\text{l}$  of 7.5mM echothiophate iodide dissolved in water) was added to the enzyme solution. The OP inhibition and aging process proceeded in a  $37^\circ\text{C}$  water bath. A total of nine time points were taken (5 min, 1 h, 2 h, 4 h, 8 h, 12 h, 16 h, 23 h and 28 h). For each time point, a 5- $\mu\text{l}$  aliquot was taken from the reaction solution and diluted to 100  $\mu\text{l}$  with 25mM ammonium bicarbonate. Excess OP was removed from the mixture by gel filtration on a spin column (Performa SR

gel filtration cartridge, Edge BioSystems, Gaithersburg, MD). Samples were stored at  $-80^\circ\text{C}$  until trypsin digestion.

When all time points had been collected, the samples were thawed, subjected to tryptic digestion (as described under Tryptic digestion of BChE), and prepared for MALDI-TOF mass spectrometry (as described under MALDI-TOF mass spectrometry).

The Data Explorer software for the Voyager DE-PRO mass spectrometer provided the area of the peptide peaks for the initial and aged adduct in each spectrum. The aging half-life was calculated from a semilog plot of the normalized peak area for unaged OP peptide against time. The normalized peak area was obtained by taking the ratio of the unaged peak area to the sum of the areas for the aged and unaged peak areas, at each time point. This ratio compensated for the variation in MALDI peak intensities from shot-to-shot and sample-to-sample. It was assumed that the signal response of the aged and unaged peptides would be essentially the same in the same sample (i.e., each individual time point) because there is only a small difference between the structures of the two peptides (i.e., an ethoxy phosphate in the unaged form is converted to a hydroxy in the aged form). SigmaPlot (SigmaPlot for Windows version 10.0, Systat Software, Inc.) was used to generate the equation describing the plot and to run statistic tests on the data. The data set passed the Durbin-Watson test, the normality test, and the constant variance test.

## RESULTS

### Identification of the BChE Tryptic Peptide Containing the Catalytic Serine

MALDI mass spectra of trypsinized BChE were obtained in both reflector mode for high peak resolution and in linear mode for maximum signal intensity. In reflector mode, the isotopic envelope of each peptide can be resolved and the observed peak values represent the mass of each isotope of a peptide. Peak values observed in linear mode are the average mass of the isotopic variants of the peptides. For a molecule that has a monoisotopic mass around 3000 Da, as the OP-BChE peptides in this study, the average mass of the molecule will be about 2 Da heavier than the monoisotopic mass.

Amino acid numbers are for the mature secreted protein, which has no signal peptide and is therefore shorter by 28 amino acids than the sequence in accession number P06276. Tryptic digestion of BChE generates a 29 amino acid, active-site peptide extending from Ser 191 to Arg 219, where Ser 198 (in bold) is the catalytic Ser: <sup>191</sup>SVTLFGESA-GAASVSLHLLSPGSHSLFTR<sup>219</sup>. In the reflector mode

spectrum, 11 peaks can be assigned to the tryptic peptides of BChE (Fig. 3A). The isotopic peaks for each peptide are well resolved. The theoretical monoisotopic  $m/z$  for the singly protonated  $[M+H]^+$  active-site peptide is 2928.5, the observed  $m/z$  is 2928.4. In the linear mode spectrum (Fig. 3B), 13 peaks can be assigned to tryptic peptides of human BChE, including the active-site peptide. The average mass of the active-site peptide is 2930.3  $m/z$ .

The peptide mass data acquired in both linear and reflector mode were submitted to the protein identification program MS-Fit to validate the peptide assignments. The *Homo sapiens* subset of the SwissProt database (2005.01.06 released version) was selected for the search. Human BChE was successfully identified as the first hit using either monoisotopic or average peptide mass.

*Aging of Echothiophate-, DFP-, Dichlorvos-, Soman-, Sarin-, and Cyclohexyl Sarin-Inhibited BChE Occurs via O–C Bond Breakage*

Aging of echothiophate-treated BChE was allowed to occur in  $^{18}\text{O}$  water. The active-site tryptic peptide was analyzed by

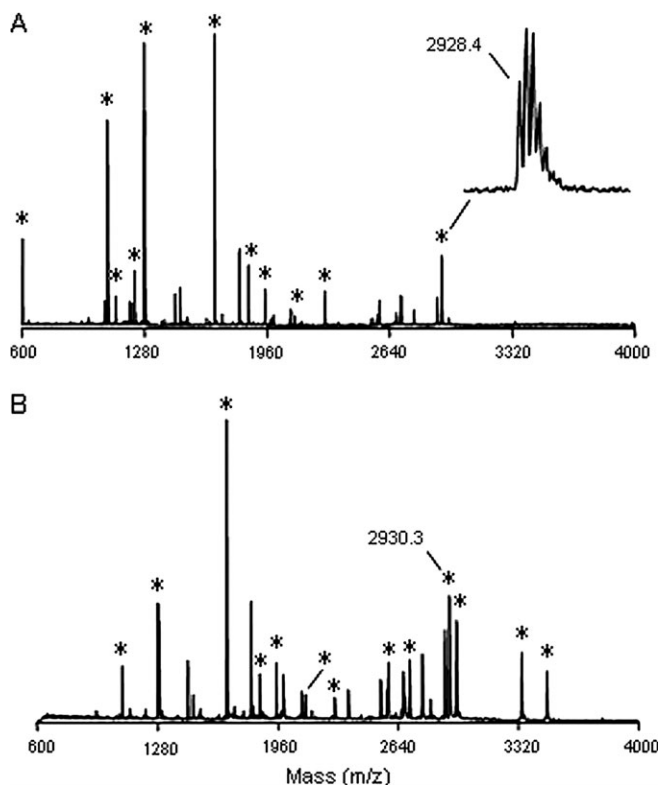


**FIG. 3.** MALDI mass spectrum of BChE tryptic peptides. BChE was subjected to tryptic digestion, and the resulting peptides were analyzed by MALDI-TOF mass spectrometry. Peptide mass spectra were acquired in reflector mode (A) as well as linear mode (B). Peaks labeled with an asterisk match the theoretical masses of BChE tryptic peptides. Peak 2928.4 in A represents the monoisotopic  $m/z$  of the active-site peptide. Peak 2930.3 in B represents the average  $m/z$  of the active-site peptide.

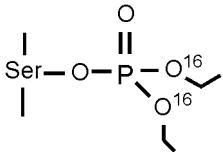
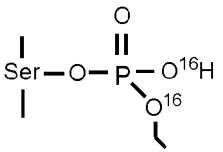
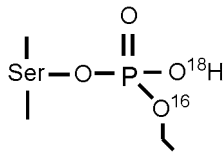
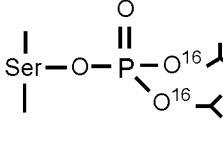
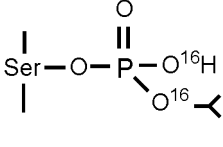
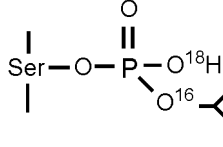
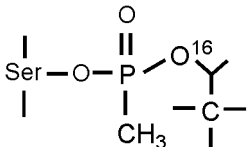
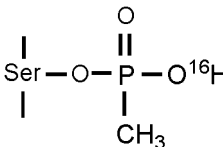
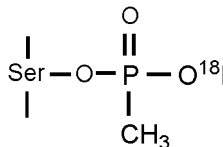
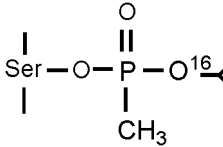
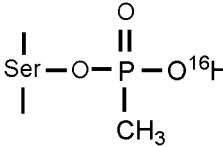
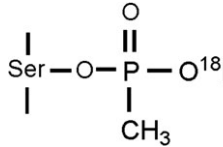
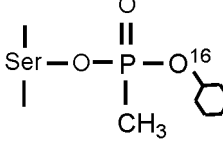
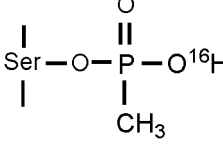
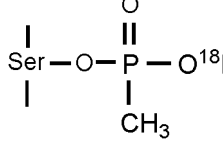
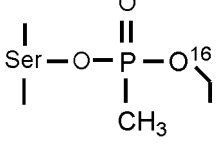
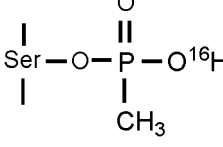
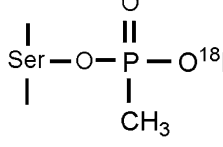
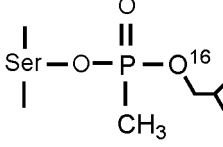
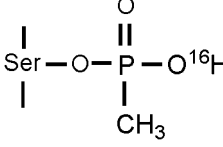
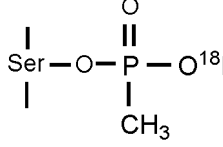
MALDI-TOF. It was calculated that if aging resulted from P–O bond breakage (predicted monoisotopic mass 3038.5 Da), the active-site peptide would be 2 Da heavier than if aging resulted from O–C bond breakage (predicted monoisotopic mass 3036.5 Da) (Table 1). As shown in Figure 4, a peak with  $m/z$  of 3036.3 can be matched to the theoretical monoisotopic  $m/z$  of the echothiophate peptide conjugate, indicating O–C bond scission. Neither peak 2928.5 (monoisotopic  $m/z$  of unlabeled BChE) nor peak 3064.5 (for unaged BChE) were detected, indicating that all the BChE had been inhibited and that the aging was complete. The observed isotopic distribution is exactly that expected for the aged, active-site conjugate (data not shown). The absence of any trace of a peak at 3038.5  $m/z$  indicates that for echothiophate-inhibited human BChE, aging follows the O–C bond breaking pathway exclusively, under the applied experimental conditions.

To rule out the possibility that peak 3036.3 observed in the spectrum from echothiophate-treated BChE (Fig. 4) may be from an unknown peptide which happens to have the same  $m/z$  value as the aged echothiophate BChE peptide conjugate, we monitored the disappearance of unaged echothiophate peptide conjugate (average  $m/z$ : 3066.4, Table 1) and the appearance of aged echothiophate peptide conjugate (average  $m/z$ : 3038.3, Table 1) as a function of time. To avoid confusion, the 3038.3  $m/z$  mass observed in this experiment is the average mass for the aged, active-site peptide; the monoisotopic mass for this peptide is 3036.3  $m/z$ , as described in Figure 3. A total of nine time points were taken after adding echothiophate into the enzyme solution. A MALDI mass spectrum was acquired for each time point, as shown in Figure 5. The predominant peak after 5 min incubation with OP was peak 3066.4, corresponding to the unaged echothiophate BChE peptide conjugate. Peak 3066.4 diminished while peak 3038.3 grew, as the incubation time became longer. After 28 h incubation, peak 3066.4 almost completely disappeared from the spectrum, indicating that aging was essentially complete. This result confirmed that peak 3038.3 was the echothiophate active-site peptide conjugate resulting from O–C bond breakage during aging. The aging half-life of echothiophate-inhibited human BChE was calculated to be  $7.2 \pm 0.7$  h (Fig. 6) under the experimental conditions, which is consistent with previous studies on BChE inhibited by OP with diethoxy moieties on the phosphorus atom (Mason *et al.*, 1993, Masson *et al.*, 1997b).

DFP-treated BChE was analyzed the same way as echothiophate-treated BChE in Figure 4. The peptide mass spectrum of aged, DFP-inhibited BChE revealed a new monoisotopic peak at 3050.4 Da, indicating that aging of this OP-enzyme conjugate is through breaking the O–C bond of one of the isopropoxy groups (Fig. 7, Table 1). The observed isotopic distribution was consistent with that expected for the 3050.4 Da peptide.

Similarly, the O–C bond was cleaved during aging of dichlorvos-inhibited BChE (spectrum not shown).

TABLE 1  
Structures and Theoretical Monoisotopic m/z of Organophosphate-Peptide Conjugates

Before aging	After aging	
	thru O-C bond	thru P-O bond
Echothiophate <sup>a</sup>	<div></div> <div>m/z: 3064.5</div>	<div></div> <div>3036.5</div> <div></div> <div>3038.5</div>
DFP	<div></div> <div>m/z: 3092.5</div>	<div></div> <div>3050.5</div> <div></div> <div>3052.5</div>
Soman	<div></div> <div>m/z: 3090.6</div>	<div></div> <div>3006.5</div> <div></div> <div>3008.5</div>
Sarin	<div></div> <div>m/z: 3048.6</div>	<div></div> <div>3006.5</div> <div></div> <div>3008.5</div>
Cyclohexyl sarin	<div></div> <div>m/z: 3088.6</div>	<div></div> <div>3006.5</div> <div></div> <div>3008.5</div>
VX	<div></div> <div>m/z: 3034.5</div>	<div></div> <div>3006.5</div> <div></div> <div>3008.5</div>
VR	<div></div> <div>m/z: 3062.6</div>	<div></div> <div>3006.5</div> <div></div> <div>3008.5</div>

<sup>a</sup>The theoretical average m/z of unaged echothiophate-peptide conjugate, the aged echothiophate-peptide conjugate from the O-C bond breakage and the P-O bond breakage are 3066.4, 3038.3, and 3040.3, respectively.

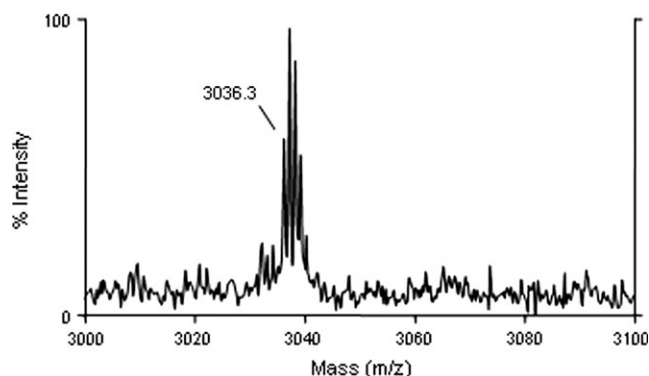


**FIG. 4.** MALDI mass spectrum of tryptic peptides from echothiophate-inhibited BChE. The spectrum was acquired in positive ion reflector mode. Peak 3036.3 represents the monoisotopic mass of the aged, echothiophate-labeled, active-site peptide conjugate resulting from O–C bond breakage.

We also investigated the aging pathways for sarin- (Fig. 8, Table 1), cyclohexyl sarin-, and soman- (Table 1, spectra not shown) inhibited BChE. Aging of these three compounds involved only O–C bond cleavage of the alkoxy groups. Peak 3048.4 in Figure 8 and peak 3088.6 (see Table 1, spectrum not shown) represent the monoisotopic  $m/z$  of unaged sarin and cyclohexyl sarin BChE conjugate peptides, respectively, indicating that the aging of BChE treated with these two compounds was not complete under the experimental conditions applied in this study.

Aging of VX-inhibited human AChE and human BChE has been previously found to be slow. Seventy percent of the human erythrocyte AChE activity can be restored by incubation with 2-pralidoxime (2-PAM) 48 h after VX inhibition (Sidell and Groff, 1974). Aging half-life of VX- and VR-inhibited human erythrocyte AChE has recently been measured to range between 36 and 138 h, respectively (Aurbek *et al.*, 2006). Aging of VX-inhibited BChE is so slow that BChE spontaneously reactivates to 50% of its original activity, without any need of 2-PAM treatment (van der Schans *et al.*, 2004). In our experiment, the expected peak of the aged VX active-site peptide conjugate with monoisotopic  $m/z$  of 3006.5 was absent from the sample spectrum, whereas peak 3034.7 matched the unaged VX active-site peptide conjugate. This result indicated that aging of VX-inhibited BChE did not occur under our experimental conditions (Fig. 9, Table 1). Similarly, the VR-inhibited BChE did not age (spectrum not shown).

#### *Trypsin Proteolysis of Echothiophate-Inhibited BChE in H<sub>2</sub>O<sup>18</sup> Medium*

These experiments are controls to prove that a two mass unit shift can be detected in linear mode. The mass spectra in Figures 3A,4, and 7–9 had been acquired in reflector mode. However, signal intensities for isomalathion- and tabun-inhibited BChE were not high enough to support data

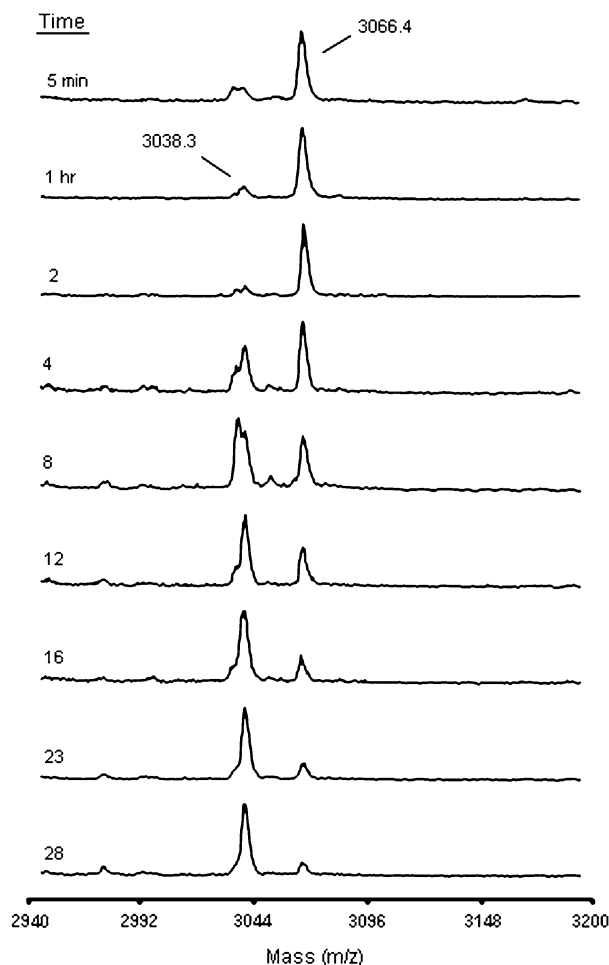


**FIG. 5.** A time course for the aging of echothiophate-inhibited BChE. Mass spectra were acquired in linear mode from samples with various echothiophate incubation times, as indicated. Peaks 3066.4 and 3038.3 represent the average  $m/z$  of echothiophate active-site peptide conjugates before and after aging, respectively.

collection in reflector mode. Mass spectra were therefore acquired using linear mode settings because linear mode data have better signal intensities than those acquired using reflector mode settings. However, the linear mode spectrum is less well resolved than a reflector mode spectrum, and the observed mass represents the average mass of the isotopes of a peptide rather than the monoisotopic mass. For a molecule that has a monoisotopic mass around 3000 Da, as the OP-BChE peptide conjugates in this study, the average mass of the molecule will be 2 Da heavier than the monoisotopic mass (as shown in Figure 3 for BChE active-site peptide and in Table 1 for echothiophate BChE peptide conjugates). To prove that a two mass unit shift, occurring as a consequence of adding the hydroxyl group from H<sub>2</sub>O<sup>18</sup> to a peptide, can be detected from linear mode spectra, we carried out the tryptic digestion of echothiophate-treated BChE without removing the H<sub>2</sub>O<sup>18</sup> from the reaction medium. The hydroxyl group from water is added

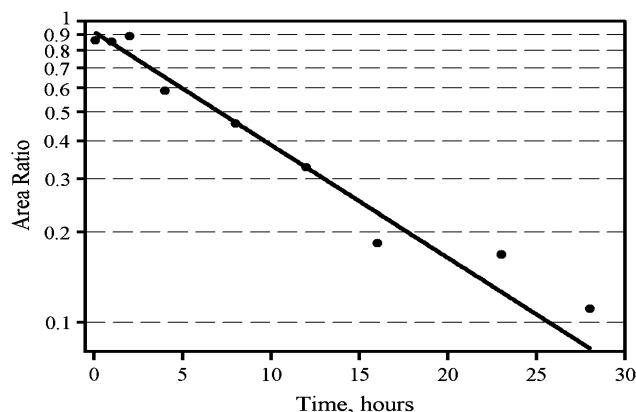


**FIG. 6.** Aging half-life of echothiophate-inhibited BChE. At each time point, the area of peak 3066.4 was divided by the sum of the peak areas of peaks 3066.4 and 3038.3 to generate an area ratio. The area ratio was plotted against its corresponding time point in a semilog fashion using SigmaPlot. The plot can be described by equation:  $y = a \times \exp(-bx)$ , where “ $a$ ” is a proportionality constant =  $0.92 \pm 0.039$  and “ $b$ ” is the apparent rate constant =  $0.086 \pm 0.0090/\text{h}$ . Aging half-life was measured from the plot as  $7.2 \pm 0.7$  h, representing the time when there are equal amounts of aged and unaged OP-peptide conjugates, i.e., the time when the area ratio equals 0.5 on the plot.

to the C-terminus of a tryptic peptide when the amide bond is cleaved. Thus, peptides created in  $\text{H}_2\text{O}^{18}$  will be two mass units heavier than comparable peptides made in  $\text{H}_2\text{O}^{16}$ .

The echothiophate-treated BChE was digested with trypsin in 85%  $\text{H}_2\text{O}^{18}$ . Thus 85% of each tryptic peptide, including the echothiophate active-site peptide conjugate, will carry an  $^{18}\text{O}$  hydroxyl group at the C-terminus. The observed mass of a peptide from this  $\text{H}_2\text{O}^{18}$  digestion medium should be 2 Da heavier than the same peptide digested in  $\text{H}_2\text{O}^{16}$  medium. We observed a peak with an  $m/z$  of 3040.2 from this sample (spectrum not shown), which is two units heavier than the mass of the aged, echothiophate-labeled, active-site peptide conju-

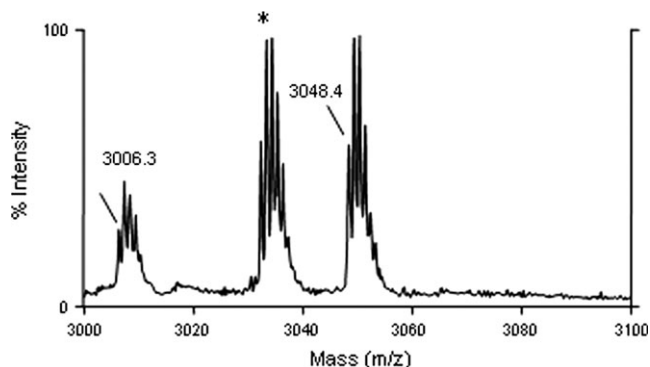


**FIG. 8.** MALDI mass spectrum of tryptic peptides from sarin-inhibited BChE. The spectrum was acquired in positive ion reflector mode. The peak labeled with an asterisk has a monoisotopic  $m/z$  of 3032.4, which matches a BChE tryptic peptide. Peak 3006.3 represents the monoisotopic  $m/z$  of the aged, sarin-labeled, active-site peptide conjugate resulting from O–C bond breakage. Peak 3048.4 represents the monoisotopic  $m/z$  of the unaged, sarin-labeled, active-site peptide conjugate.

gate resulting from tryptic digestion in an  $\text{H}_2\text{O}^{16}$  medium. Seven other peaks in the spectrum from the  $\text{H}_2\text{O}^{18}$  medium were found to be 2 Da heavier than the theoretical masses of the same peptides digested in  $\text{H}_2\text{O}^{16}$  medium. This result demonstrates that MALDI data collected in linear mode are capable of discerning a two mass unit shift resulting from incorporation of an  $^{18}\text{O}$  hydroxyl group into a peptide.

#### *Aging of Isomalathion-Inhibited BChE Occurs via both P–S and O–C/S–C Bond Breakage*

Previous studies showed that stereoisomers of isomalathion take different inhibitory and aging pathways when reacting with BChE, depending on the stereo configuration of the inhibitor. Inhibition of the enzyme with (1R)-isomalathion proceeds with loss of diethylthiosuccinate as the primary leaving group, resulting in an O,S-dimethyl phosphate adduct;

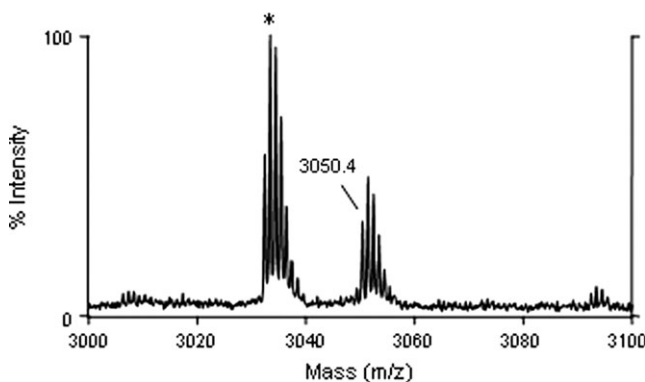


**FIG. 7.** MALDI mass spectrum of tryptic peptides from DFP-inhibited BChE. The spectrum was acquired in positive ion reflector mode. Peak labeled with an asterisk has a monoisotopic  $m/z$  of 3032.4, which matches a BChE tryptic peptide. Peak 3050.4 represents the monoisotopic  $m/z$  of the aged DFP active-site peptide conjugate resulting from O–C bond breakage. Trace amount of unaged DFP-peptide conjugate can also be seen in the spectrum at  $m/z$  of 3092.6.

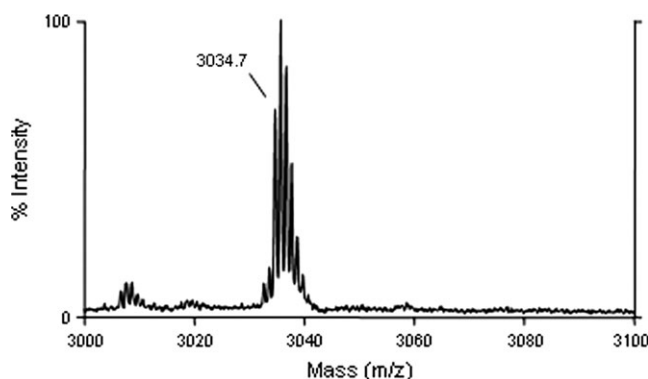


**FIG. 9.** MALDI mass spectrum of tryptic peptides from VX-inhibited BChE. The spectrum was acquired in positive ion reflector mode. Peak 3034.7 represents the monoisotopic  $m/z$  of the unaged, VX-labeled, active-site peptide conjugate.

aging of this adduct occurs through breaking the P–S bond and loss of the thiomethyl moiety. On the other hand, the primary leaving group for (1S)-isomalathion inhibition of the enzyme is the thiomethyl group. Inhibition is followed by a quick aging reaction, which also involves breaking a P–S bond. In this case, the diethylthiosuccinate moiety is released (Doorn *et al.*, 2001a,b). In both cases, aging of isomalathion-inhibited BChE occurs via the P–X bond scission pathway.

The isomalathion used in the present study was a mixture of all stereoisomers. The chemical structures and corresponding theoretical masses after inhibition of BChE are summarized in Table 2. The mass spectrum of tryptic peptides of isomalathion-treated BChE (Fig. 10) does not have peaks matching the unaged isomalathion active-site peptide conjugates, regardless of the primary leaving group (theoretical *m/z* should be 3054.4 when diethylthiosuccinate is the primary leaving group or 3198.5 when thiomethyl is the primary leaving group). This indicates that aging is complete. Peak 3026.6 in the spectrum matches the theoretical *m/z* of an aged isomalathion peptide conjugate formed as a result of a P–S bond scission. Formation of this fragment can occur from either primary adduct (see Table 2). This result is consistent with the reports in the literature (Doorn *et al.*, 2001a,b).

In addition, a comparatively minor peak with *m/z* of 3040.6 is present, which matches the theoretical *m/z* of the aged isomalathion peptide conjugate resulting from O–C or S–C bond scission. An O–C cleavage pathway would generate this mass only from a primary adduct that was formed by elimination of the diethylthiosuccinate moiety, whereas the 3040.6 mass is consistent with an S–C cleavage starting with either primary adduct. This result indicates that isomalathion-inhibited human BChE can age not only via the P–X pathway,

as indicated in previous studies, but also via the X–R pathway. The relative intensities of peaks 3026.6 and 3040.6 suggest that the P–X pathway is the predominant aging pathway under the experimental conditions of this study.

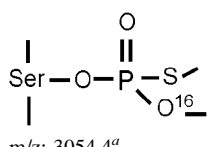
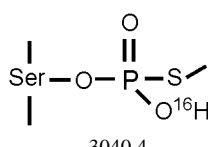
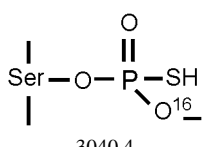
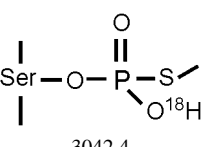
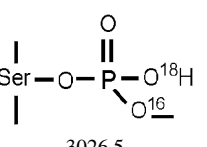
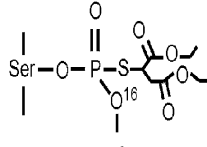
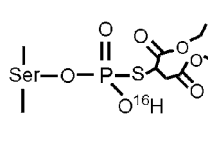
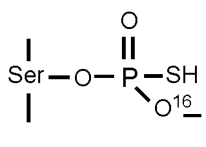
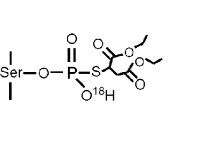
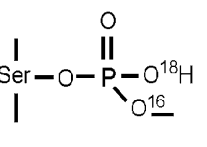
## DISCUSSION

### *Direct Evidence Supporting the X–R Scission Pathway for Aging of Human BChE Inhibited by Alkoxy-OP*

Classical aging theory for alkoxy-OP-inhibited cholinesterases states that aging involves activation of the alkoxy oxygen, O–C bond scission, and formation of a carbonium ion (Shafferman *et al.*, 1996; Viragh *et al.*, 1997). Numerous studies involving a wide range of alkoxy-type OP have demonstrated that aging results in the net loss of an alkyl group (Doorn *et al.*, 2001b; Michel *et al.*, 1967; Millard *et al.*, 1999; Nachon *et al.*, 2005; Viragh *et al.*, 1999). However, cleavage at either the P–O or the O–C bond could account for these observations. Only in the case of soman-inhibited AChE has cleavage of the O–C bond been conclusively demonstrated (Michel *et al.*, 1967; Viragh *et al.*, 1999).

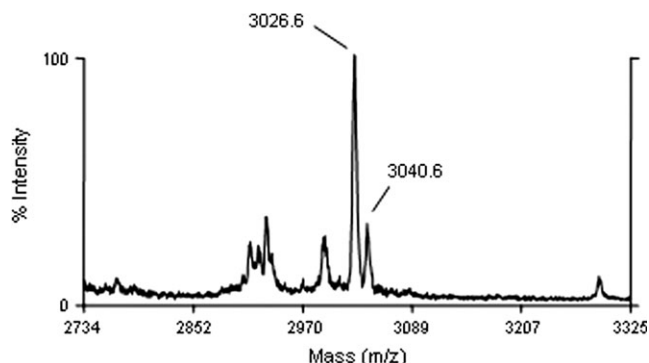
To test whether aging of other alkoxy-OP adducts proceeds via an O–C cleavage, we studied the aging of human BChE inhibited by dichlorvos, echothiophate, DFP, soman, sarin, cyclohexyl sarin, VX, and VR. Our results showed that for all of these OP except VX and VR (in which aging did not occur), aging did indeed occur via cleavage of the O–C bond, i.e., they aged through the X–R scission pathway (see Figs. 4,7,8, and related text). Based on these observations, it seems fair to predict that whenever BChE is inhibited by an OP that leaves an alkoxy group in the inhibited adduct, aging will proceed

TABLE 2  
Structures and Theoretical Average *m/z* of Isomalathion-Peptide Conjugates Aged in <sup>18</sup>O Water

Before aging	After aging			
	thru O–C bond	thru S–C bond	thru P–O bond	thru P–S bond
 <i>m/z</i> : 3054.4 <sup>a</sup>	 3040.4	 3040.4	 3042.4	 3026.5
 <i>m/z</i> : 3212.5 <sup>b</sup>	 3198.5	 3040.4	 3200.5	 3026.5

<sup>a</sup>This OP-peptide conjugate results from the inhibition of BChE by (1R)-isomalathion, where diethylthiosuccinate is the primary leaving group (Doorn *et al.* 2001a).

<sup>b</sup>This OP-peptide conjugate results from the inhibition of BChE by (1S)-isomalathion, where thiomethyl is the primary leaving group (Doorn *et al.* 2001a).



**FIG. 10.** MALDI mass spectrum of tryptic peptides from isomalathion-inhibited BChE. The spectrum was acquired in positive ion linear mode. Peaks 3026.6 and 3040.6 represent the aged isomalathion active-site peptide conjugate resulting from P-S and O-C/S-C bond breakage, respectively.

through the X-R scission pathway. Although AChE demonstrates different kinetic characteristics from BChE upon OP treatment (Giacobini, 2003), it is reasonable to predict that AChE conjugated with an OP retaining an alkoxy group after inhibition will age through the same pathway.

#### *Isomalathion-Inhibited Human BChE Ages via both X-R and P-X Scission Pathways*

The two asymmetric centers of isomalathion, one at the phosphorus and the other at the  $\alpha$ -carbon of the diethylthiosuccinate group, yield four stereoisomers for this compound. Among the four stereoisomers, two belong to the (1R)-stereoisomer group and the other two belong to the (1S)-stereoisomer group, based on the phosphorus asymmetric center (Berkman *et al.*, 1993b). Previous studies have demonstrated that (1R)- and (1S)-isomers have different inhibition and aging mechanisms when reacting with cholinesterases (Berkman *et al.*, 1993a; Doorn *et al.*, 2001a,b; Jianmongkol *et al.*, 1999). For (1R) isomers, the primary leaving group upon conjugation with the catalytic serine is the diethylthiosuccinate, yielding an O,S-dimethyl phosphate adduct; aging of this adduct appears to proceed through a P-X scission reaction where the P-S bond is cleaved and the end product is the *o*-methyl phosphate adduct (refer to Table 2). For (1S)-isomers, the inhibitory reaction is believed to proceed with loss of the thiomethyl. The aging reaction follows quickly with release of the bulky diethylthiosuccinate, through breakage of the P-S bond, another P-X scission reaction. These reaction pathways have been investigated in rat and bovine AChE and horse BChE (Berkman *et al.*, 1993a; Doorn *et al.*, 2001a,b; Jianmongkol *et al.*, 1999).

We have reexamined this reaction with human BChE. The isomalathion used in our study was from a commercial source and was a mixture of stereoisomers. It is thus necessary for us to consider all the possible OP-BChE conjugates that can result from the primary inhibition and aging (see Table 2). The OP was added to human BChE at room temperature, and the

reaction proceeded for at least 4 days. Due to this relatively long incubation time, we did not see peaks for the unaged isomalathion conjugates (3054.4 and 3198.5 *m/z*), and there was no unmodified active-site peptide in the spectrum (2930.3 *m/z*), indicating that the BChE was completely inhibited and had completely aged (see Fig. 10). A peak with *m/z* of 3026.5, for the *o*-methyl phosphate adduct containing  $O^{18}H$ , appeared in the spectrum as expected for a P-X bond scission. This confirmed the results from previous studies.

More interestingly, a minor peak with *m/z* corresponding to the aged OP adduct resulting from either O-C or S-C bond scission (3040.4 *m/z*) appeared in the spectrum. This minor peak was not observed in tryptic peptide spectra of isomalathion-treated equine BChE (Doorn *et al.*, 2001a). We suggest that this new aged product is due to subtle differences in the geometry of the active-site gorge between human and equine BChE (e.g., Phe398 in human BChE is an Ile in equine BChE at the equivalent position, which may affect the conformation stability of the catalytic histidine) that render either O-C or S-C bond cleavage possible for human BChE but not for equine BChE.

It is noteworthy that a consistent difference was found in the reactivation rates of human BChE inhibited with the (1S, 3R) or the (1S, 3S) isomers of isomalathion (Doorn *et al.*, 2001b). The (1S, 3S)-isomer-inhibited enzyme cannot be reactivated at all, whereas a small portion of the (1S, 3R)-isomer-inhibited enzyme was reactivated after adding 2-PAM. This suggests that there is something different about the two 1S adducts. Possibly, one of the (1S)-isomers ages via the P-S bond scission, which proceeds very fast after initial enzyme inhibition, thus leaves no opportunity for reactivation; and the other ages via the relatively slow S-C bond scission, so a partial reactivation was observed.

In conclusion, the aging pathways for BChE inhibited by nine different organophosphates were studied. The organophosphates which were chosen included nerve agents such as soman, sarin, and cyclohexyl sarin. The toxicity of the nerve agents is generally considered to be due to their rapid rate of aging, which results in irreversible inhibition of AChE. BChE is being considered for use as a prophylactic against nerve agent exposure. The nature of the aging pathways for these compounds, as described herein, may help in designing a mutant BChE that has better resistance to aging and thus serves as a more potent anti-organophosphate intoxication drug.

#### FUNDING

U.S. Army Medical Research and Materiel Command Contract (W81XWH-06-1-0102); Edgewood Biological Chemical Center Contract (W911SR-04-C-0019); Epplery Cancer Center grant (P30CA36727); National Institute of Health (1 U01 NS058056-01); and grants DGA/DSP/STTC-PEA 010807 and EMA/LR 06 from France.

## ACKNOWLEDGMENTS

Mass spectra were obtained with the support of the Protein Structure Core Facility at the University of Nebraska Medical Center.

## REFERENCES

- Aurbek, N., Thiermann, H., Szinicz, L., Eyer, P., and Worek, F. (2006). Analysis of inhibition, reactivation and aging kinetics of highly toxic organophosphorus compounds with human and pig acetylcholinesterase. *Toxicology* **224**, 91–99.
- Barak, D., Ordentlich, A., Kaplan, D., Barak, R., Mizrahi, D., Kronman, C., Segall, Y., Velan, B., and Shafferman, A. (2000). Evidence for P-N bond scission in phosphoramidate nerve agent adducts of human acetylcholinesterase. *Biochemistry* **39**, 1156–1161.
- Barak, D., Ordentlich, A., Segall, Y., Velan, B., Benshop, H. P., De Jong, L. P. A., and Shafferman, A. (1997). Carbocation-mediated processes in biocatalysts. Contribution of aromatic moieties. *J. Am. Chem. Soc.* **119**, 3157–3158.
- Berkman, C. E., Ryu, S., Quinn, D. A., and Thompson, C. M. (1993a). Kinetics of the postinhibitory reactions of acetylcholinesterase poisoned by chiral isomalathion: A surprising nonreactivation induced by the RP stereoisomers. *Chem. Res. Toxicol.* **6**, 28–32.
- Berkman, C. E., Thompson, C. M., and Perrin, S. R. (1993b). Synthesis, absolute configuration, and analysis of malathion, malaoxon, and isomalathion enantiomers. *Chem. Res. Toxicol.* **6**, 718–723.
- Casida, J. E., and Quistad, G. B. (2004). Organophosphate toxicology: Safety aspects of nonacetylcholinesterase secondary targets. *Chem. Res. Toxicol.* **17**, 983–998.
- Doorn, J. A., Schall, M., Gage, D. A., Talley, T. T., Thompson, C. M., and Richardson, R. J. (2001a). Identification of butyrylcholinesterase adducts after inhibition with isomalathion using mass spectrometry: Difference in mechanism between (1R)- and (1S)-stereoisomers. *Toxicol. Appl. Pharmacol.* **176**, 73–80.
- Doorn, J. A., Talley, T. T., Thompson, C. M., and Richardson, R. J. (2001b). Probing the active sites of butyrylcholinesterase and cholesterol esterase with isomalathion: Conserved stereoselective inactivation of serine hydrolases structurally related to acetylcholinesterase. *Chem. Res. Toxicol.* **14**, 807–813.
- Ekstrom, F., Akfur, C., Tunemalm, A. K., and Lundberg, S. (2006). Structural changes of phenylalanine 338 and histidine 447 revealed by the crystal structures of tabun-inhibited murine acetylcholinesterase. *Biochemistry* **45**, 74–81.
- Giacobini, E. (2003). Cholinesterases and Cholinesterase Inhibitors. pp. 1–19. Informa Healthcare, London.
- Grueninger-Leitch, F., D'Arcy, A., D'Arcy, B., and Chene, C. (1996). Deglycosylation of proteins for crystallization using recombinant fusion protein glycosidases. *Protein Sci.* **5**, 2617–2622.
- Harris, L. W., Fleisher, J. H., Clark, J., and Cliff, W. J. (1966). Dealkylation and loss of capacity for reactivation of cholinesterase inhibited by sarin. *Science* **154**, 404–407.
- Jennings, L. L., Malecki, M., Komives, E. A., and Taylor, P. (2003). Direct analysis of the kinetic profiles of organophosphate-acetylcholinesterase adducts by MALDI-TOF mass spectrometry. *Biochemistry* **42**, 11083–11091.
- Jianmongkol, S., Marable, B. R., Berkman, C. E., Talley, T. T., Thompson, C. M., and Richardson, R. J. (1999). Kinetic evidence for different mechanisms of acetylcholinesterase inhibition by (1R)- and (1S)-stereoisomers of isomalathion. *Toxicol. Appl. Pharmacol.* **155**, 43–53.
- Li, B., Stribley, J. A., Ticu, A., Xie, W., Schopfer, L. M., Hammond, P., Brimijoin, S., Hinrichs, S. H., and Lockridge, O. (2000). Abundant tissue butyrylcholinesterase and its possible function in the acetylcholinesterase knockout mouse. *J. Neurochem.* **75**, 1320–1331.
- Lockridge, O., and Masson, P. (2000). Pesticides and susceptible populations: People with butyrylcholinesterase genetic variants may be at risk. *Neurotoxicology* **21**, 113–126.
- Lockridge, O., Schopfer, L. M., Winger, G., and Woods, G. H. (2005). Large scale purification of butyrylcholinesterase from human plasma suitable for injection into monkeys; a potential new therapeutic for protection against cocaine and nerve agent toxicity. *J. Med. CBR. Def.* **3**, online.
- Mason, H. J., Waite, E., Stevenson, A., and Wilson, H. K. (1993). Aging and spontaneous reactivation of human plasma cholinesterase activity after inhibition by organophosphorus pesticides. *Hum. Exp. Toxicol.* **12**, 497–503.
- Masson, P., Fortier, P. L., Albaret, C., Froment, M. T., Bartels, C. F., and Lockridge, O. (1997a). Aging of di-isopropyl-phosphorylated human butyrylcholinesterase. *Biochem. J.* **327**(Pt. 2), 601–607.
- Masson, P., Froment, M. T., Bartels, C. F., and Lockridge, O. (1997b). Importance of aspartate-70 in organophosphate inhibition, oxime re-activation and aging of human butyrylcholinesterase. *Biochem. J.* **325**(Pt. 1), 53–61.
- Michel, H. O., Hackley, B. E., Jr, Berkowitz, L., List, G., Hackley, E. B., Gillilan, W., and Pankau, M. (1967). Ageing and dealkylation of Soman (pinacolylmethylphosphonofluoridate)-inactivated eel cholinesterase. *Arch. Biochem. Biophys.* **121**, 29–34.
- Millard, C. B., Kryger, G., Ordentlich, A., Greenblatt, H. M., Harel, M., Raves, M. L., Segall, Y., Barak, D., Shafferman, A., Silman, I., et al. (1999). Crystal structures of aged phosphorylated acetylcholinesterase: Nerve agent reaction products at the atomic level. *Biochemistry* **38**, 7032–7039.
- Nachon, F., Asojo, O. A., Borgstahl, G. E., Masson, P., and Lockridge, O. (2005). Role of water in aging of human butyrylcholinesterase inhibited by echothiophate: The crystal structure suggests two alternative mechanisms of aging. *Biochemistry* **44**, 1154–1162.
- Saxena, A., Doctor, B. P., Maxwell, D. M., Lenz, D. E., Radic, Z., and Taylor, P. (1993). The role of glutamate-199 in the aging of cholinesterase. *Biochem. Biophys. Res. Commun.* **197**, 343–349.
- Shafferman, A., Ordentlich, A., Barak, D., Stein, D., Ariel, N., and Velan, B. (1996). Aging of phosphorylated human acetylcholinesterase: Catalytic processes mediated by aromatic and polar residues of the active centre. *Biochem. J.* **318**(Pt. 3), 833–840.
- Sidell, F. R., and Groff, W. A. (1974). The reactivability of cholinesterase inhibited by VX and sarin in man. *Toxicol. Appl. Pharmacol.* **27**, 241–252.
- van der Schans, M. J., Polhuijs, M., van Dijk, C., Degenhardt, C. E., Pleijsier, K., Langenberg, J. P., and Benschop, H. P. (2004). Retrospective detection of exposure to nerve agents: Analysis of phosphofluoridates originating from fluoride-induced reactivation of phosphorylated BuChE. *Arch. Toxicol.* **78**, 508–524.
- Viragh, C., Akhmetshin, R., Kovach, I. M., and Broomfield, C. (1997). Unique push-pull mechanism of dealkylation in soman-inhibited cholinesterases. *Biochemistry* **36**, 8243–8252.
- Viragh, C., Kovach, I. M., and Pannell, L. (1999). Small molecular products of dealkylation in soman-inhibited electric eel acetylcholinesterase. *Biochemistry* **38**, 9557–9561.

# Lamellipodin proline rich peptides associated with native plasma butyrylcholinesterase tetramers

He LI\*, Lawrence M. SCHOPFER\*, Patrick MASSON† and Oksana LOCKRIDGE\*<sup>1</sup>

\*Eppley Institute and Department of Biochemistry and Molecular Biology, University of Nebraska Medical Center, Omaha, NE 68198-6805, U.S.A., and †Centre de Recherches du Service de Santé des Armées, Département de Toxicologie-Unité d'Enzymologie, 24 avenue des Maquis du Grésivaudan-BP87, 38702 La Tronche cedex, France

BChE (butyrylcholinesterase) protects the cholinergic nervous system from organophosphorus nerve agents by scavenging these toxins. Recombinant human BChE produced from transgenic goat to treat nerve agent intoxication is currently under development. The therapeutic potential of BChE relies on its ability to stay in the circulation for a prolonged period, which in turn depends on maintaining tetrameric quaternary configuration. Native human plasma BChE consists of 98 % tetramers and has a half-life ( $t_{1/2}$ ) of 11–14 days. BChE in the neuromuscular junctions and the central nervous system is anchored to membranes through interactions with ColQ (AChE-associated collagen tail protein) and PRiMA (proline-rich membrane anchor) proteins containing proline-rich domains. BChE prepared in cell culture is primarily monomeric, unless expressed in the presence of proline-rich peptides. We hypothesized that a poly-proline peptide is an intrinsic component of soluble plasma BChE tetramers, just as it is for membrane-bound BChE. We found that a series of proline-rich peptides was released from denatured human and horse plasma BChE. Eight peptides, with masses from 2072 to 2878 Da, were purified by

HPLC and sequenced by electrospray ionization tandem MS and Edman degradation. All peptides derived from the same proline-rich core sequence PSPPLPPPPPPPPPPPPPPPPPLP (mass 2663 Da) but varied in length at their N- and C-termini. The source of these peptides was identified through database searching as RAPH1 [Ras-associated and PH domains (pleckstrin homology domains)-containing protein 1; lamellipodin, gi:82581557]. A proline-rich peptide of 17 amino acids derived from lamellipodin drove the assembly of human BChE secreted from CHO (Chinese-hamster ovary) cells into tetramers. We propose that the proline-rich peptides organize the 4 subunits of BChE into a 340 kDa tetramer, by interacting with the C-terminal BChE tetramerization domain.

**Key words:** acetylcholinesterase (AChE)-associated collagen tail protein (ColQ), butyrylcholinesterase (BChE), lamellipodin, proline-rich attachment domain (PRAD), proline-rich membrane anchor (PRiMA), tetramer assembly.

## INTRODUCTION

BChE (butyrylcholinesterase; EC 3.1.1.8) is a serine hydrolase found in most vertebrate tissues and is especially abundant in serum, liver, intestine and lung [1,2]. BChE is capable of hydrolysing a wide range of choline and non-choline esters [3]. BChE has been suggested to have a role in controlling the activity of the neurotransmitter acetylcholine in brain as well as in the peripheral neuromuscular junction [2,4–6]. BChE protects the cholinergic nervous system from the toxicity of OP (organophosphorus toxin) nerve agents and pesticides by scavenging OP in a one-to-one stoichiometry. Purified human plasma BChE injected intravenously or intramuscularly into rodents and non-human primates has a prophylactic effect against acute and long-term toxicity of sarin, soman and VX {*O*-ethyl *S*-[2-(di-isopropylamino)ethyl]methylphosphonothioate} [7–9]. Recombinant human BChE produced in the milk of transgenic goats is a promising protein drug currently under development to treat nerve agent intoxication [10].

Approx. 98 % of human BChE in serum is a tetramer of four identical subunits whose combined molecular mass is 340 000 Da [3]. The molecule is a soluble globule, protected from proteolysis by a heavy sugar coating from nine N-linked carbohydrate chains. Human plasma BChE is synthesized in the liver and secreted into the blood where it has a half-life ( $t_{1/2}$ ) of 11–14 days

[3,11]. The residence time of cholinesterases in blood shows a positive correlation with glycosylation state and tetrameric quaternary configuration, the latter factor being more crucial [12,13]. Wild-type human BChE expressed from HEK-293 cells (human embryonic kidney cells) and CHO (Chinese-hamster ovary) cell lines forms only approx. 10–30 % tetramers. However, addition of poly(L-proline) to the culture medium or co-expression with the N-terminus of ColQ [AChE (acetylcholinesterase)-associated collagen tail protein] including the PRAD (proline-rich attachment domain) increased the amount of tetrameric BChE to 70 % [14,15]. The PRAD-containing peptide co-purified with BChE tetramers [15], indicating that this proline-rich peptide not only drives the formation of tetramers but also is part of the final tetrameric complex. These observations raised the question of whether native plasma BChE tetramers contain a proline-rich peptide.

In the present study, we investigated the possibility that a poly-proline peptide is an intrinsic component of the native plasma BChE tetramer. Both purified human and horse BChEs were studied. The proteins were denatured by boiling or by lowering the pH with formic acid. Released peptides were purified by HPLC and analysed by MS. A series of peptides was identified by MALDI (matrix-assisted laser-desorption ionization)–TOF-MS (MALDI–time-of-flight MS). The same series of peptides was found in horse and human BChE samples. The peptides were

Abbreviations used: AChE, acetylcholinesterase; a.m.u., atomic mass unit; BChE, butyrylcholinesterase; CHO, Chinese-hamster ovary; ColQ, AChE-associated collagen tail protein; EPI, enhanced product ion; ER, endoplasmic reticulum; ESI-MS/MS, electrospray ionization tandem MS; OP, organophosphorus toxin; PRAD, proline-rich attachment domain; PRiMA, proline-rich membrane anchor; MALDI, matrix-assisted laser-desorption ionization; MALDI–TOF-MS, MALDI–time-of-flight MS; MWCO, molecular-mass cut-off; PH domain, pleckstrin homology domain; RAPH1, Ras-associated and PH domain-containing protein 1; TAP, transporter associated with antigen processing.

<sup>1</sup> To whom correspondence should be addressed (email olockrid@unmc.edu).

sequenced by ESI-MS/MS (electrospray ionization tandem MS) and Edman degradation. These peptides all derived from a common, proline-rich sequence in lamellipodin (gi:82581557), which is a membrane-associated protein that participates in the regulation of lamellipodial protrusion, a component of directed cell motility [16]. When we added a proline-rich peptide of 17 amino acids derived from lamellipodin into the culture medium of CHO cells expressing wild-type human BChE, the peptide caused the formation of BChE tetramers.

## EXPERIMENTAL

### Human and horse BChEs

Human BChE (accession number gi:116353; Swiss-Prot database accession number P06276) was purified from plasma as described previously [17]. The purified human BChE was at least 90 % pure. It was dissolved in 0.19 M NaCl, 20 mM Tris/HCl and 0.02 % sodium azide (pH 7.5) to an activity of 1823 units/ml (2.5 mg/ml). Horse BChE was from Sigma (St. Louis, MO, U.S.A.). The purified horse BChE, freeze-dried out of PBS, was reconstituted by the addition of water to a concentration of 2.36 mg of BChE protein/ml with an activity of 1700 units/ml. Activity was assayed with 1 mM butyrylthiocholine in 0.1 M potassium phosphate buffer (pH 7.0) at 25 °C, in the presence of 0.5 mM DTNB [5,5'-dithiobis-(2-nitrobenzoic acid); Ellman's reagent]. One unit of activity is defined as micromoles of butyrylthiocholine hydrolysed per minute. Pure BChE has an activity of 720 units/mg.

### Non-denaturing gradient gel electrophoresis

Polyacrylamide gradient gels (40–30 %), 1.5 mm thick, were prepared in a Hoefer SE6000 gel apparatus (Hoefer Scientific Instruments, San Francisco, CA, U.S.A.). Electrophoresis was at 250 V constant voltage for 16 h at 4 °C. BChE samples were diluted with PBS (pH 7.2) and mixed with 50 % (v/v) glycerol in 0.1 M Tris/HCl (pH 7.5) to a final glycerol concentration of 10 %. The equivalent of 8 µg of human or horse BChE was loaded on to each lane for gel staining with Coomassie Brilliant Blue R-250 (Fisher Scientific).

### Preparation of peptides for MALDI-TOF-MS

A 2 ml portion of 1823 units/ml human BChE and 2 ml of 1700 units/ml of horse BChE were put into dialysis bags with an MWCO (molecular-mass cut-off) of 3000 Da (Spectrum Laboratories, Rancho Dominguez, CA, U.S.A.) and dialysed against 4 × 4 litres of double-distilled water for 3 days at 4 °C. Approx. 2 ml of BChE solution was recovered from both human and horse samples after dialysis. Each BChE sample was divided into two fractions of equal volume. One fraction was heated in boiling water for 5 min to denature the protein. The horse BChE solution appeared turbid after heating, so it was briefly centrifuged and the precipitate was discarded. All samples were loaded into Centricon YM-10 centrifugal filters (MWCO = 10 kDa; Millipore, Bedford, MA, U.S.A.) to separate peptides from protein. The centrifugation was in a Beckman CPR centrifuge with swinging bucket rotor at 3200 g for 40 min at 10 °C. The solution that passed through the filter membrane contained peptides and was recovered. Peptide solutions were concentrated to approx. 50–100 µl in a SpeedVac prior to MALDI analysis.

### Reverse-phase HPLC

To prepare BChE peptide samples for sequencing and amino acid composition analysis, we used a Waters 625 HPLC system

(Milford, MA, U.S.A.) equipped with a Zorbax 300 SB C-18 reverse-phase column (Agilent Technologies, Santa Clara, CA, U.S.A.). Purified human or horse BChE was boiled to release peptides. An alternative method for releasing peptides was to mix 1 mg of BChE in 0.5 ml with 0.5 ml of formic acid. Samples were filtered through a 0.2 µm syringe filter before injection into the HPLC.

The HPLC was operated at room temperature (22 °C) at a flow rate of 1 ml/min. Buffer A was 0.1 % trifluoroacetic acid in water; buffer B was 0.07 % trifluoroacetic acid in acetonitrile. Peptides were eluted with a gradient of 0–60 % buffer B in 60 min. The absorbance was monitored at 220 nm. The HPLC eluent was collected into 1 min fractions and saved for analysis.

### MALDI-TOF-MS

All MALDI-TOF-MS experiments were performed on an Applied Biosystems Voyager DE-PRO workstation equipped with a 337 nm pulsed nitrogen laser (Applied Biosystems, Framingham, MA, U.S.A.). A 1 ml portion of peptide sample was mixed 1:1 (v/v) with the matrix solution  $\alpha$ -CHCA ( $\alpha$ -cyano-4-hydroxycinnamate; 10 mg/ml in 50 % (v/v) acetonitrile and 0.3 % trifluoroacetic acid) on the MALDI target plate and allowed to dry at room temperature. Mass spectra were acquired in positive-ion, linear mode under delayed extraction conditions, using an acceleration voltage of 20 kV. Laser intensity was adjusted so that the strongest ion intensity in a spectrum did not exceed 80 % of the maximum saturated intensity value. Laser positioning on the sample spot was monitored with a video camera. Spectra shown are the average of 500 laser shots collected from multiple locations on the target spot. Calibration for the mass spectra was performed externally using corticotropin peptides (amino acid residues 1–17, 18–39 and 7–38).

### Q-Trap mass spectrometer

The amino acid sequence of peptides released from human and horse BChEs was determined by collision-activated dissociation in a Q-Trap 2000, a hybrid quadrupole linear ion trap mass spectrometer equipped with a nanospray interface (Applied Biosystems). The spectrometer was calibrated daily on selected fragments from the collision-activated spectrum of [glutamic acid]fibrinopeptide B. HPLC eluent fractions containing target peptides (identified by MALDI-TOF-MS) were reconstituted into 60 % (v/v) acetonitrile and 0.1 % formic acid and then loaded into a silver-coated nano-infusion emitter (Econo12; New Objective, Woburn, MA, U.S.A.) using a gel-loading pipette tip (GELoader, Eppendorf, Westbury, NY, U.S.A.). The emitter can hold up to 12 µl of sample. The loaded emitter was fitted into the Discrete Nanospray™ head of the nanospray source on the Q-Trap mass spectrometer. Peptides were introduced into the mass spectrometer by means of static infusion, at room temperature, using an ion spray voltage of 1300 V (which creates a voltage differential of 1300 V between the emitter and the curtain plate). The emitter position was optimized to obtain maximum signal intensity. Mass spectra were collected in the enhanced mode, i.e. using the ion trap. Enhanced mass spectra were collected to identify the target peptide. EPI (enhanced product ion) was used for fragmenting the target peptide. The collision cell was pressurized to 40 µtorr (1 torr = 0.133 kPa) with pure nitrogen and collision energies of 40–50 V were used. The default trap fill time for each EPI scan was 20 ms. A total of 200 EPI scans were accumulated to generate the final EPI spectrum. The EPI spectra of the target peptide were manually analysed to determine the sequence of the peptide.

### Amino acid composition analysis

Peptide samples were subjected to acid hydrolysis in which peptides were heated at 110°C in 6 M HCl for 20 h. Composition analysis was performed by a Hitachi L-8800 amino acid analyser (Hitachi, Tokyo, Japan), using post-column derivatization, as previously described [18].

### Edman degradation sequencing of peptides

A Procise 494 N-terminal sequencer (Applied Biosystems) was used to sequence peptides by Edman degradation. Standard company settings and running cycles were applied. Samples were immobilized on to a PVDF membrane for the experiment. A detailed description of the method can be found in [19].

### Lamellipodin proline-rich peptide experiment

A 17-amino-acid proline-rich peptide derived from lamellipodin was custom-synthesized by GenScript (Piscataway, NJ, U.S.A.). The sequence of the peptide was: PPPPPPPPPPPPPPLP. The peptide, dissolved in water and filter-sterilized, was added to the culture medium of CHO cells to final concentrations of 5 and 50 µM. The CHO cells used in this experiment express and secrete wild-type human BChE as described previously [15]. A 20 µl portion of culture medium (with or without the proline-rich peptide), along with 20 µl of human plasma as a control, were loaded on to a non-denaturing polyacrylamide gel and electrophoresed at 250 V constant voltage for 16 h at 4°C. The gel was stained for BChE activity by using the method of Karnovsky and Roots [20].

## RESULTS

### Peptides were released from denatured BChE tetramers

The purity of the BChE preparations used in the present study was determined by non-denaturing PAGE. Coomassie Brilliant Blue staining of the gel showed a heavy band migrating at the position of tetrameric BChE (for the gel picture, see Supplementary material at <http://www.BiochemJ.org/bj/411/bj4110425add.htm>). No other bands can be clearly seen on the gel. The absence of an albumin band from both samples rules out the possibility that the peptides released by boiling originated from albumin. This was a concern because albumin sequesters low-molecular-mass peptide fragments in blood [21].

Peptides released by boiling were separated from BChE protein on a centrifugal filter with a 10000 Da cut-off. The pass-through solution was collected and analysed by MALDI-TOF-MS. Control native BChE samples, treated identically except that they were not boiled, were also analysed by MALDI-TOF. As shown in Figure 1(A), the pass-through solution from native human BChE sample (upper panel) gave virtually no peptides, whereas the pass-through solution from boiled human BChE (lower panel) gave a series of peptides, ranging from approx. 2000 Da to 3000 Da. Similar observations were made for the horse BChE samples (Figure 1B).

Table 1 lists the masses of the peptides released from horse and human BChEs observed in the MALDI spectra. The differences between masses show that most of these peptides differ by single amino acids. For example, in the human preparation, the difference between the 2171.5 and 2074.3 masses is 97.2 a.m.u. (atomic mass unit), which is the dehydro-mass of proline [19]. The difference between the 2171.5 and 2285.1 masses is 113.6 (leucine or isoleucine), between 2452.8 and 2566.7 is 113.9 (asparagine), between 2566.7 and 2663.7 is 97.0 (proline) and between 2663.7 and 2878.5 is 214.8 (consistent with serine plus glutamine). These

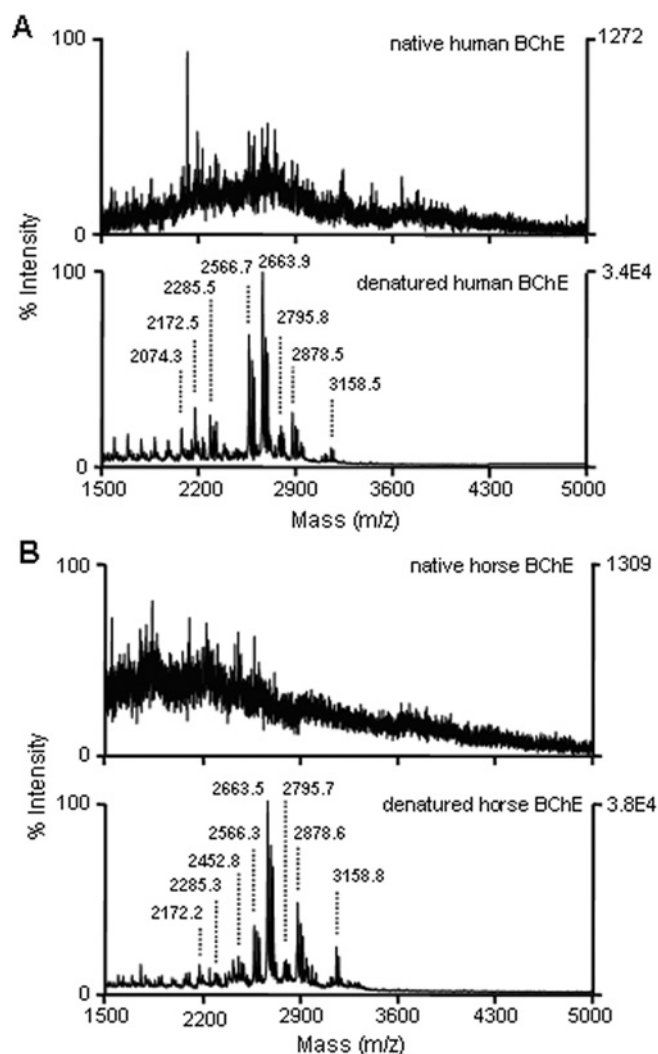


**Figure 1** MALDI mass spectra of peptides released from native or denatured plasma BChE

Purified plasma BChE from either human (A) or horse (B) was divided into two fractions. One fraction was boiled and the other was not boiled. Peptides were separated from the native and denatured proteins and subjected to MALDI analysis. Native human and horse BChE samples (upper panels of A and B) released no peptides. A series of peptides can be identified from both denatured human and horse BChE samples (lower panels of A and B).

**Table 1** Summary of the peptide masses released from denatured human and horse plasma BChE tetramers

Only peaks greater than 2000 Da are recorded in the Table. Each peak is the most intense peak in a group of three related peaks. A detailed explanation for the nature of the peaks in each group is given in the text.

Sample	Observed peptide mass (Da)								
Human	2074.3	2171.5	2285.1	—	2566.7	2663.7	2795.8	2878.5	3158.5
Horse	—	2171.2	2285.3	2452.8	2566.3	2663.5	2795.7	2878.6	3158.8

observations suggest that these masses represent a family of related peptides and not a collection of wholly different sequences. Similar observations can be made for the peptides from the horse BChE preparation.

The denatured samples from both horse and human BChEs contain nearly identical sets of peptides (Table 1), even though

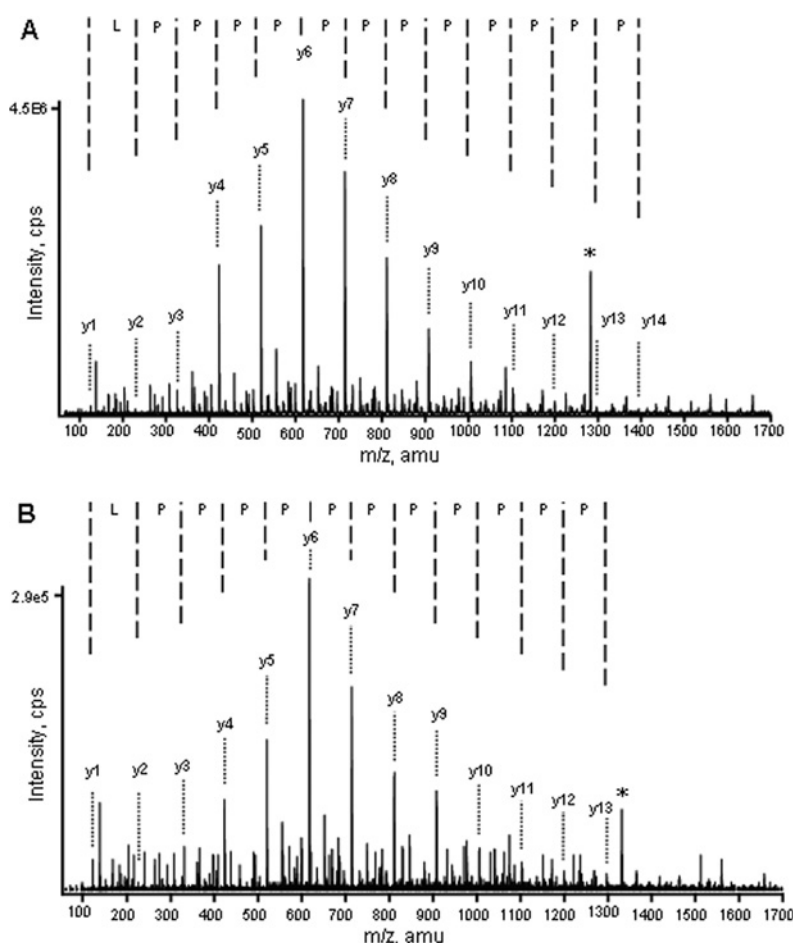


**Figure 2** Sequencing of peptide 2566 (A) and peptide 2663 (B) by using ESI-MS/MS fragment ion spectra

The peak labelled with an asterisk in (A) has an  $m/z$  value of 1283.6, which represents the doubly charged state of peptide 2566. The peak labelled with an asterisk in (B) has an  $m/z$  value of 1332.3, which represents the doubly charged state of peptide 2663. Major  $y$ -series fragment ions used in sequencing the peptides are labelled. Major  $b$ -series product ions can also be readily identified in the two spectra and were used to sequence the peptides from the N-terminus. cps, counts per s.

they are from two different species and two different preparations. These results strongly suggest that the peptides are not due to contamination of the BChE samples during purification. The fact that this series of peptides can only be found after denaturation of BChE further suggests that the peptides are part of the BChE tetrameric structure and are not adventitiously bound to the surface of BChE. Finally, the peptides are not attached through disulfide bonds, as no reducing agent was required for their release.

One final point concerning the complexity of the MALDI spectrum should be mentioned. Each labelled peptide in Figure 2 is the most intense peak in a group of three peaks. The second most intense peak is 22 a.m.u. heavier than the first and the least intense peak is 22 a.m.u. heavier than the second. This is consistent with sodium ion adducts contributing the positive charge, instead of a hydrogen ion.

#### The peptides released from denatured BChE are proline-rich

Peptides released from BChE by boiling were separated from BChE protein and partially resolved from one another by HPLC. HPLC-purified peptides were electrosprayed into the Q-Trap mass spectrometer where fragment ion spectra of selected peptides were generated through collision-activated dissociation. Figures 2(A) and 2(B) show the fragment ion spectra of peptides 2566 and

2663 respectively. The peptide sequences were determined from the fragment ion spectra.

The spectrum of peptide 2566 revealed  $y$ -series ions that contained 12 proline residues in a row with a Pro(Leu/Ile)Pro sequence at the C-terminus. The  $b$ -ion series, although present in the spectrum, was less easily interpreted. This is because several different  $b$ -series sequences of equivalent intensity could be identified. We attribute this multitude of sequences to internal fragmentation. Each of these sequences included an N-terminal residue (either proline or serine), but the true N-terminus could not be unequivocally assigned. A leucine/isoleucine was also frequently observed in the first five N-terminal residues. After the first few N-terminal residues, each  $b$ -ion sequence became a string of proline residues. Up to 12 proline residues in a row were observed. Because of this complexity, the complete sequence of this peptide could not be determined from the Q-Trap data alone. However, the sequence data together with the peptide mass suggested that peptide 2566 contained at least 20 consecutive proline residues, as well as one serine and two leucine/isoleucine residues. The fragmentation pattern of peptide 2663 was nearly identical with that of peptide 2566. It also revealed a Pro(Leu/Ile)Pro C-terminus followed by a string of proline residues (at least 19). The similarity of these

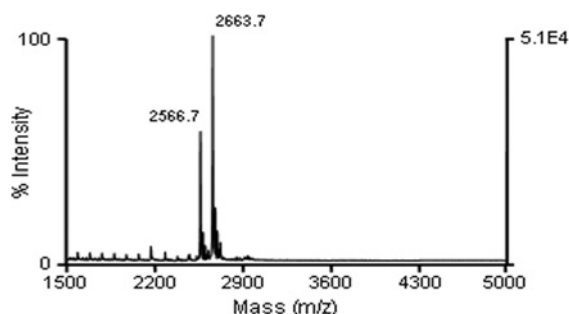


**Figure 3** MALDI mass spectrum of human BChE-associated peptides

This peptide sample was purified on a C-18 reverse-phase HPLC column (see the Experimental section) and sequenced by Edman degradation.

fragmentation patterns supports the proposal that these peptides are representative members of a family.

The HPLC fraction containing peptides 2566 and 2663 was further purified by using reverse-phase HPLC. The resulting sample, which contained only peptides 2566 and 2663 (Figure 3), was subjected to amino acid composition analysis and amino acid sequencing by Edman degradation. The composition analysis data indicated that the unit composition of the sample was 24 proline, two leucine and one serine residues. This is comparable with the composition obtained from the mass spectral sequence analysis.

Edman degradation generated the complete sequence of the two peptides: the sequence of one peptide was SPPLPPPPPPPPPPPPPPPPPLP, and the sequence of the other peptide was PSPPLPPPPPPPPPPPPPPPPPLP. The two sequences match the sequences for the peptides 2566 and 2663 obtained by MS and confirm that they indeed differ only by an N-terminal proline residue.

Similar purification and sequencing experiments were applied to the horse BChE peptide samples (results not shown) and the results showed that horse peptides 2566 and 2663 had exactly the same sequences as their human counterparts.

ESI-MS/MS sequencing was also performed on other peptides in Table 1. All peptides contained a string of proline residues, indicating the poly-proline core sequence. This supports the proposal that they all derived from a common source protein.

### Peptides released from denatured BChE originate from RAPH1 [Ras-associated and PH domain (pleckstrin homology domain)-containing protein 1], also called lamellipodin

Peptide PSPPLPPPPPPPPPPPPPPPPPLP (molecular mass = 2663.2 Da) was used to query the NCBI (National Center for Biotechnology Information) non-redundant human protein database by using BLAST. RAPH1 (gi:82581557) was the only protein that exactly matched the query sequence. This protein is also called lamellipodin, or proline-rich EVH1 [Ena/VASP (vasodilator-stimulated phosphoprotein) homology 1] ligand 2 [16]. The partial sequence information that we obtained from all the other peptides also fit the lamellipodin sequence. Lamellipodin is thus identified as the source of the peptides released from denatured human BChE.

By combining the peptide masses from the MALDI-TOF-MS with the ESI-MS/MS sequencing results and the sequence of human lamellipodin, we were able to obtain complete sequences that were consistent with all of the masses observed in the MALDI spectra from the denatured BChE tetramers, except one. Only the sequence of peptide 3158 was not identified. No portion of the proline-rich core sequence of lamellipodin yielded this mass. A list of the peptides is given in Table 2.

There is no horse protein database available for a BLAST-like query at this time. However, given the observed similarity between the peptide masses and peptide sequences from human and horse BChEs, it is reasonable to predict that peptides released from horse BChE originate from a horse protein closely related to human lamellipodin.

### Proline-rich peptide derived from lamellipodin caused assembly of BChE into tetramers

Previous studies showed that addition of poly(L-proline) peptide into the culture media of CHO cells expressing wild-type human BChE increased the proportion of BChE tetramers and decreased the amount of dimers and monomers [15]. To investigate whether the proline-rich peptides we identified from plasma BChE can drive the formation of BChE tetramers, we expressed wild-type human BChE in CHO cells in the presence of a 17-mer proline-rich peptide with the sequence PPPPPPPPPPPPPPLP. This peptide accounts for amino acids 686–702 in the human lamellipodin sequence (gi:82581557). As shown

**Table 2** Amino acid sequences of BChE-associated peptides

Observed $m/z$ *	Theoretical $m/z$ †	Peptide sequence‡
2074.3	2074.5	<sup>682</sup> PPPPPPPPPPPPPPPPPPPLP <sup>702</sup>
2171.5	2171.6	<sup>681</sup> PPPPPPPPPPPPPPPPPPPLP <sup>702</sup>
2285.1	2284.8	<sup>680</sup> LPPPPPPPPPPPPPPPPPPPLP <sup>702</sup>
2452.8§	2452.9	<sup>676</sup> PSPPLPPPPPPPPPPPPPPPPPP <sup>700</sup>
2566.7	2566.1	<sup>677</sup> SPPLPPPPPPPPPPPPPPPPPPPLP <sup>702</sup>
2663.7	2663.2	<sup>676</sup> PSPPLPPPPPPPPPPPPPPPPPPPLP <sup>702</sup>
2795.8	2795.2	<sup>683</sup> PPPPPPPPPPPPPPPPPPPLPSQSAPSAGSAAP <sup>714</sup>
2878.5	2878.4	<sup>676</sup> PSPPLPPPPPPPPPPPPPPPPPPPLPSQ <sup>704</sup>

\* Masses are from Table 1.

† The theoretical  $m/z$  value of a peptide reflects the singly charged state of the peptide and was calculated using an online tool provided by the University of Cambridge (<http://www.ch.cam.ac.uk/magnus/MolWeight.html>).

‡ To more clearly demonstrate the relationships between the peptides, each peptide sequence is labelled at its N- and C-termini with its position in human lamellipodin (gi:82581557), and all peptides are aligned in accordance with their relative position in lamellipodin. A peptide from lamellipodin that encompasses all the observed data has the sequence:  $\gamma^{671}$ TASQSPPLPPPPPPPPPPPPPPPLPSQSAPSAGSAAPMFVKYS<sup>720</sup>.

§ Peptide 2452 was only observed in the horse BChE sample. It is listed here because it fits well in the sequence assignment from the lamellipodin protein.

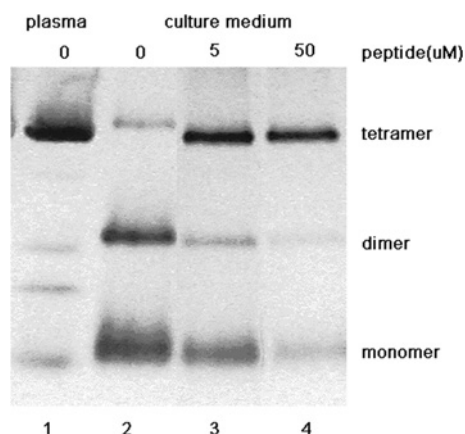


**Figure 4** Lamellipodin proline-rich peptide promotes BChE tetramerization

A non-denaturing gel was stained for BChE activity. Lane 1, human plasma; lane 2, culture medium without proline-rich peptide; lane 3, culture medium with 5  $\mu$ M proline-rich peptide; lane 4, culture medium with 50  $\mu$ M proline-rich peptide.

in Figure 4, addition of the lamellipodin-derived proline-rich peptide to the culture medium increased the proportion of BChE tetramers from approx. 10% to approx. 60% (5  $\mu$ M final peptide concentration in the culture medium) or 80% (50  $\mu$ M final peptide concentration in the culture medium). The proportion of BChE dimers and monomers in the culture medium was correspondingly decreased. These results indicated that the proline-rich peptides we found in plasma BChE can guide the tetramerization of BChE.

## DISCUSSION

### The tetramer-organizing function of proline-rich peptides

Our finding that the serum BChE tetramer is associated with a family of proline-rich peptides derived from lamellipodin establishes the identity of the tetramer-organizing peptide as PSPPLPPPPPPPPPPPPPPPPPLP (and variations thereof). It thereby defines a new, naturally occurring tetramerization peptide. Previously, membrane-bound forms of BChE and AChE have been shown to be associated with the proline-rich regions of ColQ and PRiMA (proline-rich membrane anchor) [22,23]. Our finding reinforces the requirement for a proline-rich peptide in the formation of tetrameric cholinesterase structures. Also, it opens the possibility that other, yet unidentified forms of tetramer-organizing peptide may exist for cholinesterases in other tissues.

### Association of BChE with lamellipodin-derived peptide

Plasma BChE is secreted into the blood from the liver. Secreted proteins are synthesized in the rough ER (endoplasmic reticulum) and transported into the Golgi complex where they are glycosylated, assembled and packed into vesicles that are destined for secretion. Lamellipodin, on the other hand, is a cytosolic protein [16]. The molecular pathway that directs the association of BChE and lamellipodin-derived proline-rich peptide is unclear. However, the events leading to the generation of peptides used by MHC class I molecules for cellular immune response may provide a hint for the answer.

Approximately one-third of newly synthesized proteins are rapidly degraded by proteasomes in the cytosol under physiological conditions [24]. The peptides needed for antigen presentation are generated in the cytosol by cleavage of endogen-

ous proteins and are displayed on the cell surface by MHC class I molecules, which are present on nearly all nucleated cells [25]. TAPs (transporters associated with antigen processing) are located on the ER membrane and are responsible for moving peptides from the cytosol into the ER for binding with MHC class I molecules. TAPs translocate peptides with broad specificity. Although it is most efficient for peptides of 8–12 amino acids, peptides of up to 40 amino acids can also be transported into the ER by TAPs [26]. It is conceivable that the cytosolic protein lamellipodin is degraded in the cytosol by proteasomes and the resulting peptides, including the proline-rich peptides we identified in the present study, are transported into ER by TAPs, where they associate with newly synthesized BChE molecules to form tetramers.

### The heterogeneity of the proline-rich peptide

A total of eight proline-rich peptides were identified from human and horse BChE samples, all inter-related and originating from the same protein (see Table 2). The proteasome in the cytosol is a protein complex and can cleave at nearly every position of a protein [27]. Other proteases in the cytosol, such as IFN (interferon)- $\gamma$ -inducible leucine aminopeptidase and tripeptidyl peptidase II, have been shown to work along with proteasomes in processing peptides to be transported into the ER by TAPs [28,29]. All the above-mentioned proteases may contribute to produce a mixture of lamellipodin-derived proline-rich peptides that are imported into the ER for interaction with BChE.

Alternatively, the peptides we observed might all derive from a single progenitor peptide that was progressively proteolysed, from both the N- and C-termini, while attached to the BChE tetramer during circulation in the blood. Koomen et al. [30] found progressive N- and C-terminal proteolysis of naturally occurring peptides by aminopeptidases and carboxypeptidases in blood to be the general rule. This resulted in families of peptides with variously truncated N- and C-termini [30]. However, if the observed heterogeneity in the proline-rich peptides is due to proteolysis in the circulation, then that proteolysis would have had to have happened while the peptide was bound to BChE. Dvir et al. [22] showed that the 14-residue ColQ PRAD peptide (LLTPPPPLFPFF) was longer than the tetramerization domain of AChE and the length of the tetramerization domain was about the same as the thickness of the AChE tetramer. Furthermore, they showed that if a larger proline-rich peptide was complexed with AChE, the C-terminus could pass easily between the AChE subunits in one direction while the N-terminus could pass out beyond the end of the tetramerization domain in the other direction. BChE is nearly identical in structure with AChE [31]. Therefore the AChE models should apply equally well to BChE. We found various proline-rich peptides attached to BChE that included residues 676–714 from lamellipodin. That suggests that the original peptide may have been up to 39 residues long. As such, it should have been long enough to extend beyond the protection of the BChE molecule in both directions, making it accessible to the peptidases in blood, and thus susceptible to degradation during circulation.

### C<sub>5</sub> genetic variant of human BChE

Approx. 8% of Caucasians have a variant form of serum BChE, named C<sub>5</sub>, which migrates more slowly than the normal serum BChE during electrophoresis on non-denaturing polyacrylamide gels [32,33]. Studies on the C<sub>5</sub> BChE showed that it consists of the normal BChE tetramer non-covalently associated with an unknown protein component with an estimated molecular mass of 60 kDa. The coding gene for this unknown protein is located

on chromosome 2q33–q35 [34]. The human lamellipodin gene is also located on chromosome 2q33 (obtained from NCBI GENE database under the gene name RAPH1). This striking coincidence suggests that the unknown protein component of C<sub>5</sub> BChE could actually be a truncated form of lamellipodin. If this is true, the presence of C<sub>5</sub> BChE in blood may suggest malfunctioning of a certain protease or a protein-processing pathway in the liver. Although C<sub>5</sub> BChE carriers do not show any pathology, further investigation in this direction may have broader clinical significance.

### Tetrameric BChE has a longer half-life in the circulation

Proteins and peptides in blood are constantly subjected to renal clearance and enzymatic degradation. Their circulation half-life ranges from a few minutes to several days [35]. The therapeutic potential of BChE against organophosphate toxicants (nerve agents and pesticides) relies heavily on its ability to stay in the circulation for a prolonged period. Native and recombinant BChE tetramers showed a half-life of 16–56 h in rodents in various studies, whereas recombinant human BChE monomers and dimers only have a half-life of 2–300 min [12,36]. Therefore expression of the tetrameric form of recombinant BChE is an important factor in creating a viable therapeutic agent. Our discovery of the native proline-rich peptide that is responsible for the formation of the human serum BChE tetramer should contribute to the creation of an expressed, tetrameric form of BChE that will be stable in the circulation. This fulfils critical criteria in developing BChE into an antinerve agent therapeutic.

MS, Edman degradation and amino acid composition analysis were performed with the support of the Protein Structure Core Facility at the University of Nebraska Medical Center. This work was supported by U.S. Army Medical Research and Materiel Command contract W81XWH-06-1-0102, Edgewood Biological Chemical Center contract W911SR-04-C-0019, Eppley Cancer Center grant P30CA36727 and NIH (National Institutes of Health) grant 1 U01 NS058056-01.

### REFERENCES

- Jbilo, O., Bartels, C. F., Chatonnet, A., Toutant, J. P. and Lockridge, O. (1994) Tissue distribution of human acetylcholinesterase and butyrylcholinesterase messenger RNA. *Toxicol.* **32**, 1445–1457
- Li, B., Stribley, J. A., Ticu, A., Xie, W., Schopfer, L. M., Hammond, P., Brimijoin, S., Hinrichs, S. H. and Lockridge, O. (2000) Abundant tissue butyrylcholinesterase and its possible function in the acetylcholinesterase knockout mouse. *J. Neurochem.* **75**, 1320–1331
- Lockridge, O. and Masson, P. (2000) Pesticides and susceptible populations: People with butyrylcholinesterase genetic variants may be at risk. *Neurotoxicology* **21**, 113–126
- Mesulam, M. M., Guillozet, A., Shaw, P., Levey, A., Duysen, E. G. and Lockridge, O. (2002) Acetylcholinesterase knockouts establish central cholinergic pathways and can use butyrylcholinesterase to hydrolyze acetylcholine. *Neuroscience* **110**, 627–639
- Mesulam, M., Guillozet, A., Shaw, P. and Quinn, B. (2002) Widely spread butyrylcholinesterase can hydrolyze acetylcholine in the normal and Alzheimer brain. *Neurobiol. Dis.* **9**, 88–93
- Giacobini, E. (2003) Cholinesterases and Cholinesterase Inhibitors, pp. 1–19, Informa Healthcare, London
- Raveh, L., Grunwald, J., Marcus, D., Papier, Y., Cohen, E. and Ashani, Y. (1993) Human butyrylcholinesterase as a general prophylactic antidote for nerve agent toxicity. *In vitro* and *in vivo* quantitative characterization. *Biochem. Pharmacol.* **45**, 2465–2474
- Raveh, L., Grauer, E., Grunwald, J., Cohen, E. and Ashani, Y. (1997) The stoichiometry of protection against soman and VX toxicity in monkeys pretreated with human butyrylcholinesterase. *Toxicol. Appl. Pharmacol.* **145**, 43–53
- Lenz, D. E., Maxwell, D. M., Koplovitz, I., Clark, C. R., Capacio, B. R., Cerasoli, D. M., Federko, J. M., Luo, C., Saxena, A., Doctor, B. P. and Olson, C. (2005) Protection against soman or VX poisoning by human butyrylcholinesterase in guinea pigs and cynomolgus monkeys. *Chem. Biol. Interact.* **157–158**, 205–210
- Huang, Y. J., Huang, Y., Baldassarre, H., Wang, B., Lazaris, A., Leduc, M., Bilodeau, A. S., Bellemare, A., Cote, M., Herskovits, P. et al. (2007) Recombinant human butyrylcholinesterase from milk of transgenic animals to protect against organophosphate poisoning. *Proc. Natl. Acad. Sci. U.S.A.* **104**, 13603–13608
- Ostergaard, D., Viby-Mogensen, J., Hanel, H. K. and Skovgaard, L. T. (1988) Half-life of plasma cholinesterase. *Acta Anaesthesiol. Scand.* **32**, 266–269
- Saxena, A., Ashani, Y., Raveh, L., Stevenson, D., Patel, T. and Doctor, B. P. (1998) Role of oligosaccharides in the pharmacokinetics of tissue-derived and genetically engineered cholinesterases. *Mol. Pharmacol.* **53**, 112–122
- Chittlaru, T., Kronman, C., Velan, B. and Shafferman, A. (2001) Effect of human acetylcholinesterase subunit assembly on its circulatory residence. *Biochem. J.* **354**, 613–625
- Blong, R. M., Bedows, E. and Lockridge, O. (1997) Tetramerization domain of human butyrylcholinesterase is at the C-terminus. *Biochem. J.* **327**, 747–757
- Altamirano, C. V. and Lockridge, O. (1999) Conserved aromatic residues of the C-terminus of human butyrylcholinesterase mediate the association of tetramers. *Biochemistry* **38**, 13414–13422
- Krause, M., Leslie, J. D., Stewart, M., Lafuente, E. M., Valderrama, F., Jagannathan, R., Strasser, G. A., Robinson, D. A., Liu, H., Way, M. et al. (2004) Lamellipodin, an Ena/VASP ligand, is implicated in the regulation of lamellipodial dynamics. *Dev. Cell* **7**, 571–583
- Lockridge, O., Schopfer, L. M., Winger, G. and Woods, G. H. (2005) Large scale purification of butyrylcholinesterase from human plasma suitable for injection into monkeys; a potential new therapeutic for protection against cocaine and nerve agent toxicity. *J. Med. Chem. Biol. Radiol. Def.* **3**, nihms5095
- Smith, A. J. (2002) Post column amino acid analysis. In *Protein Sequencing Protocols* (Smith, B. J., ed.), pp. 133–142, Humana Press, Totowa, NJ
- Jackson, P. J. (1998) Quality control and protein primary structure by automated sequencing and mass spectrometry. In *Bioseparation and Bioprocessing: A Handbook* (Subramanian, G., ed.), pp. 291–323, John Wiley & Sons, Hoboken
- Karnovsky, M. J. and Roots, L. (1964) A 'direct-coloring' thiocholine method for cholinesterases. *J. Histochem. Cytochem.* **12**, 219–221
- Lowenthal, M. S., Mehta, A. I., Frogale, K., Bandle, R. W., Araujo, R. P., Hood, B. L., Veenstra, T. D., Conrads, T. P., Goldsmith, P., Fishman, D. et al. (2005) Analysis of albumin-associated peptides and proteins from ovarian cancer patients. *Clin. Chem.* **51**, 1933–1945
- Dvir, H., Harel, M., Bon, S., Liu, W. Q., Vidal, M., Garbay, C., Sussman, J. L., Massoulie, J. and Silman, I. (2004) The synaptic acetylcholinesterase tetramer assembles around a polyproline II helix. *EMBO J.* **23**, 4394–4405
- Feng, G., Krejci, E., Molgo, J., Cunningham, J. M., Massoulie, J. and Sanes, J. R. (1999) Genetic analysis of collagen Q: roles in acetylcholinesterase and butyrylcholinesterase assembly and in synaptic structure and function. *J. Cell Biol.* **144**, 1349–1360
- Schubert, U., Anton, L. C., Gibbs, J., Norbury, C. C., Yewdell, J. W. and Bennink, J. R. (2000) Rapid degradation of a large fraction of newly synthesized proteins by proteasomes. *Nature* **404**, 770–774
- Lankat-Buttgerit, B. and Tampe, R. (2002) The transporter associated with antigen processing: function and implications in human diseases. *Physiol. Rev.* **82**, 187–204
- Koopmann, J. O., Post, M., Neefjes, J. J., Hammerling, G. J. and Momburg, F. (1996) Translocation of long peptides by transporters associated with antigen processing (TAP). *Eur. J. Immunol.* **26**, 1720–1728
- Ehring, B., Meyer, T. H., Eckerskorn, C., Lottspeich, F. and Tampe, R. (1996) Effects of major-histocompatibility-complex-encoded subunits on the peptidase and proteolytic activities of human 20S proteasomes. Cleavage of proteins and antigenic peptides. *Eur. J. Biochem.* **235**, 404–415
- Bening, J., Rock, K. L. and Goldberg, A. L. (1998) Interferon- $\gamma$  can stimulate post-proteasomal trimming of the N terminus of an antigenic peptide by inducing leucine aminopeptidase. *J. Biol. Chem.* **273**, 18734–18742
- Geier, E., Pfeifer, G., Wilm, M., Lucchiarini-Hartz, M., Baumeister, W., Eichmann, K. and Niedermann, G. (1999) A giant protease with potential to substitute for some functions of the proteasome. *Science* **283**, 978–981
- Koomen, J. M., Li, D., Xiao, L. C., Liu, T. C., Coombes, K. R., Abbruzzese, J. and Kobayashi, R. (2005) Direct tandem mass spectrometry reveals limitations in protein profiling experiments for plasma biomarker discovery. *J. Proteome Res.* **4**, 972–981
- Nicolet, Y., Lockridge, O., Masson, P., Fontecilla-Camps, J. C. and Nachon, F. (2003) Crystal structure of human butyrylcholinesterase and of its complexes with substrate and products. *J. Biol. Chem.* **278**, 41141–41147
- Masson, P., Chatonnet, A. and Lockridge, O. (1990) Evidence for a single butyrylcholinesterase gene in individuals carrying the C<sub>5</sub> plasma cholinesterase variant (CHE2). *FEBS Lett.* **262**, 115–118

- 33 Simpson, N. E. (1972) Polyacrylamide electrophoresis used for the detection of C5+ cholinesterase in Canadian Caucasians, Indians, and Eskimos. *Am. J. Hum. Genet.* **24**, 317–320
- 34 Eiberg, H., Nielsen, L. S., Klausen, J., Dahlen, M., Kristensen, M., Bisgaard, M. L., Møller, N. and Mohr, J. (1989) Linkage between serum cholinesterase 2 (CHE2) and gamma-crystallin gene cluster (CRYG): assignment to chromosome 2. *Clin. Genet.* **35**, 313–321
- 35 Werle, M. and Bernkop-Schnurch, A. (2006) Strategies to improve plasma half life time of peptide and protein drugs. *Amino Acids* **30**, 351–367
- 36 Duysen, E. G., Bartels, C. F. and Lockridge, O. (2002) Wild-type and A328W mutant human butyrylcholinesterase tetramers expressed in Chinese hamster ovary cells have a 16-hour half-life in the circulation and protect mice from cocaine toxicity. *J. Pharmacol. Exp. Ther.* **302**, 751–758

---

Received 14 November 2007; accepted 12 December 2007

Published as BJ Immediate Publication 12 December 2007, doi:10.1042/BJ20071551



## Fast affinity purification coupled with mass spectrometry for identifying organophosphate labeled plasma butyrylcholinesterase

He Li<sup>a,\*</sup>, Larry Tong<sup>a</sup>, Lawrence M. Schopfer<sup>a</sup>, Patrick Masson<sup>b</sup>, Oksana Lockridge<sup>a</sup>

<sup>a</sup> Eppley Institute, University of Nebraska Medical Center, Omaha, NE 68198-6805, United States

<sup>b</sup> Centre de Recherches du Service de Santé des Armées, Département de Toxicologie, Unité d'Enzymologie, BP 87, 38702 La Tronche cédex, France

### ARTICLE INFO

#### Article history:

Available online 2 May 2008

#### Keywords:

Butyrylcholinesterase  
Biomarker  
Organophosphate exposure  
Sarin  
Soman  
Affinity chromatography  
Mass spectrometry

### ABSTRACT

Classical plasma butyrylcholinesterase (BChE) purification involves dialysis and multiple steps of chromatography. We describe a procainamide affinity gel purification scheme that takes 15–30 min to purify BChE from 1 ml plasma. The method uses a microfuge spin column to build a 0.2 ml procainamide affinity column. The eluted BChE contains 3–4 µg of 500-fold purified BChE, free from 99% of contaminating plasma proteins. The BChE was further purified by gel electrophoresis. Tryptic peptides from the BChE containing gel electrophoresis band were prepared by in-gel digestion, separated by reverse phase liquid chromatography and identified by mass spectrometry. The 29 residue active site tryptic peptide labeled with the nerve agents soman or sarin was identified.

© 2008 Elsevier Ireland Ltd. All rights reserved.

### 1. Introduction

Butyrylcholinesterase (BChE) is a scavenger protein that protects the cholinergic system against anticholinesterase poisons [1,2]. Most of the U.S. population has been exposed to organophosphorus (OP) pesticides in their homes, workplaces, outdoors, or through trace contaminants in food [3]. The high reactivity of BChE with OP makes BChE an ideal biomarker of OP exposure. OP inhibits BChE by covalently binding to its active site serine. Proteolysis of OP-inhibited BChE generates an OP-peptide conjugate whose molecular mass distinguishes nerve agents from OP pesticides. Mass spectrometry analysis of the plasma BChE peptide can be used to determine whether a person was exposed to OP and what kind of OP he or she was exposed to [4–6].

The 12 most abundant proteins in plasma make up 96% (by weight) of the total plasma proteins. Their concentrations range from 50 mg/ml (albumin) to 1 mg/ml (apolipoprotein A) [7]. Human BChE concentration in blood is  $4.2 \times 10^{-3}$  mg/ml. Even though mass spectrometry technologies have advanced to high sensitivity, purification steps are still necessary to identify a low abundant protein like BChE in a complex plasma sample [8].

Here we describe a fast and simple affinity purification method for plasma BChE that produces BChE sufficiently pure that it can be identified by mass spectrometry. The purification procedure consumes as little as 1 ml of plasma. A similar procedure has been described by Fidler et al. [5]. However, our purification is substantially simpler and has the potential to be developed into a high throughput method. The procedure was applied to samples of human plasma treated with the nerve agents soman and sarin. Peptides from BChE, isolated from 1 ml of plasma, were identified including the OP-labeled active-site peptide. The identity of the OP-labeled active site serine peptide was confirmed by MS/MS spectrum.

\* Corresponding author. Tel.: +1 5106432394.

E-mail addresses: [heli@berkeley.edu](mailto:heli@berkeley.edu) (H. Li), [pym.masson@free.fr](mailto:pym.masson@free.fr) (P. Masson).

## 2. Experimental methods

### 2.1. OP treatment of human plasma

Human plasma was treated with 200  $\mu$ M soman or sarin, reducing BChE activity to zero. Soman and sarin were provided by CEB (Vert-le-Petit, France). Only trace amounts of intact soman and sarin remained in the plasma after 24 h at room temperature. Samples were stored at  $-80^{\circ}\text{C}$ . Plasma was cleared of solids and fat by centrifugation.

### 2.2. Procainamide-Sepharose micro column purification of plasma BChE

Procainamide-Sepharose gel, custom made by Dr. Yacov Ashani [9], bound 34  $\mu$ mol of procainamide per milliliter gel. 0.2 ml (0.4 ml of 1:1 slurry in 50% ethanol) of procainamide gel was packed into a 1.5 ml microfuge spin column (Princeton Separations, Adelphia, NJ). The column was equilibrated with 2 ml of 20 mM potassium phosphate pH 7.0 buffer. 1 ml of cleared, OP-treated plasma was allowed to flow through the column by gravity flow at a flow rate of 1 ml/10 min. The column was washed 4 times with 1 ml of 0.2 M NaCl in 20 mM potassium phosphate pH 7.0 buffer. Each wash time was reduced to less than 1 min by briefly centrifuging the column. BChE was eluted with 0.5 ml of 1 M sodium chloride in 20 mM potassium phosphate pH 7.0 buffer or alternatively with 0.5 ml of 0.2 M procainamide.

### 2.3. Nondenaturing gradient gel electrophoresis

A four-to-thirty percent, polyacrylamide, nondenaturing, gradient gel, 0.75 mm thick, was prepared in a Hoefer SE6000 gel apparatus (Hoefer Scientific Instruments, San Francisco, CA; presently part of GE Healthcare). Electrophoresis was at 250 V constant voltage for 16 h at  $4^{\circ}\text{C}$ . 10  $\mu$ l samples were mixed with 50% glycerol in 0.1 M Tris/Cl, pH 7.5 to a final glycerol concentration of 10%. The gel was first stained for BChE activity using the Karnovsky & Roots method [10], and then stained with Coomassie blue R-250 (Fisher Scientific).

The BChE intended for mass spectrometry was reduced from 0.5 to 0.06 ml and desalted in an Amicon YM10 centrifugal filter with a molecular weight cutoff of 10 kDa (Millipore, Billerica, MA) before it was loaded on the nondenaturing gel. A nondenaturing gel rather than an SDS gel was used because only the nondenaturing gel separates BChE from albumin.

### 2.4. Protein in-gel digestion and peptide extraction

The protein band corresponding to the position of BChE was cut out and digested with trypsin [11]. Peptides were extracted from the gel and dissolved in 5% acetonitrile, 0.1% formic acid for mass spectrometry analysis.

### 2.5. ESI LC-MS/MS analysis of tryptic peptides

A FAMOS autosampler in conjunction with a SWITCHOS and ULTIMATE capillary liquid chromatography system (LC Packings Dionex, Sunnyvale, CA) was used to deliver peptides to a QTrap hybrid quadrupole, linear ion trap mass spectrometer model 2000 (Applied Biosystems, Foster City, CA). Peptides were eluted from a Vydac C18 nanocolumn (Grace Vydac, Southborough, MA) at a flow rate of 300 nl/min, using an acetonitrile gradient containing 0.1% formic acid. The acetonitrile increased from 5 to 60% in 60 min. Detailed instrument settings and data collection protocols are described by Schopfer et al. [12].

MASCOT (Matrix Science, Boston, MA) was used for database searching to identify proteins [13]. Mascot search parameters: IPI human database, enzyme is trypsin; allow for one missed cleavage; fixed modification consists of carbamidomethylated cysteine; variable modifications consist of oxidized methionine, dehydrated serine, and methylphosphonylated serine; mass values are monoisotopic; peptide mass tolerance  $\pm 2.0$  amu; fragment mass tolerance  $\pm 1.0$  amu. Similar results were obtained if the peptide mass tolerance was  $\pm 1.2$  amu and fragment mass tolerance was  $\pm 0.6$  amu. The Analyst filter was set to allow charge states +1 to +5, the “Discard ions with charge of 5+ or higher” was deactivated; “Determine charge state from Survey scan” was deactivated “Remove peaks with intensity—% of highest” was set to 0.

## 3. Results and discussion

### 3.1. A single-step procainamide affinity purification recovers 70% of the starting BChE

1 ml of control plasma was applied onto a 0.2 ml procainamide-Sepharose column packed into a microfuge spin column. As shown in Table 1, 94% of the BChE was retained on the column and 70% of the starting BChE was recovered by elution with 1 M NaCl. The time elapsed from loading the sample to elution was 15–30 min.

**Table 1**  
Procainamide affinity purification of BChE from 1 ml plasma

Fraction	Composition	Volume (ml)	BChE activity ( $\mu$ /ml)
Loading	Plasma	1	2.95
Flow-through	Plasma eluted during loading	1	0.17
Wash-off	0.2 M NaCl	1	0.17
	0.2 M NaCl	1	0.06
	0.2 M NaCl	1	0.04
	0.2 M NaCl	1	0.03
Elute	1 M NaCl	0.5	4.15

### 3.2. OP labeled BChE tryptic peptide identified from gel extracts by LC–MS/MS

BChE from 1 ml of soman- or sarin-treated human plasma was subjected to the purification procedure described above. Protein eluted from the procainamide column was loaded onto a nondenaturing gel. The gel was first stained for BChE activity, then counter stained with Coomassie blue. Fig. 1A shows the chromatography results for sarin-treated samples. Relatively strong BChE activity staining bands can be seen on the gel (Fig. 1A, lanes 2–4), indicating that plasma BChE activity had partially recovered. Comparison of the Coomassie staining in Fig. 1B, lane 1 (unpurified plasma) and lane 4 (eluate from the

column), shows that the one-step procainamide purification eliminated significant amounts of high abundant proteins including albumin. Although the preparation still contained other proteins (Fig. 1B, lane 6), the sample was pure enough for mass spectrometry identification of BChE.

Soman treated plasma had no BChE activity to pinpoint the location of the labeled BChE on the gel. However, removal of a band from a location adjacent to BChE in the control lane provided a sample from which the tryptic peptides of BChE could be identified by LC–MS/MS. Fragmentation of the peptide typically occurs at the peptide amide bond to produce *y* ions if the carboxyl terminal fragment retains the charge, or *b* ions, if the amino terminal fragment retains the charge. The *m/z* values of *y* and *b*

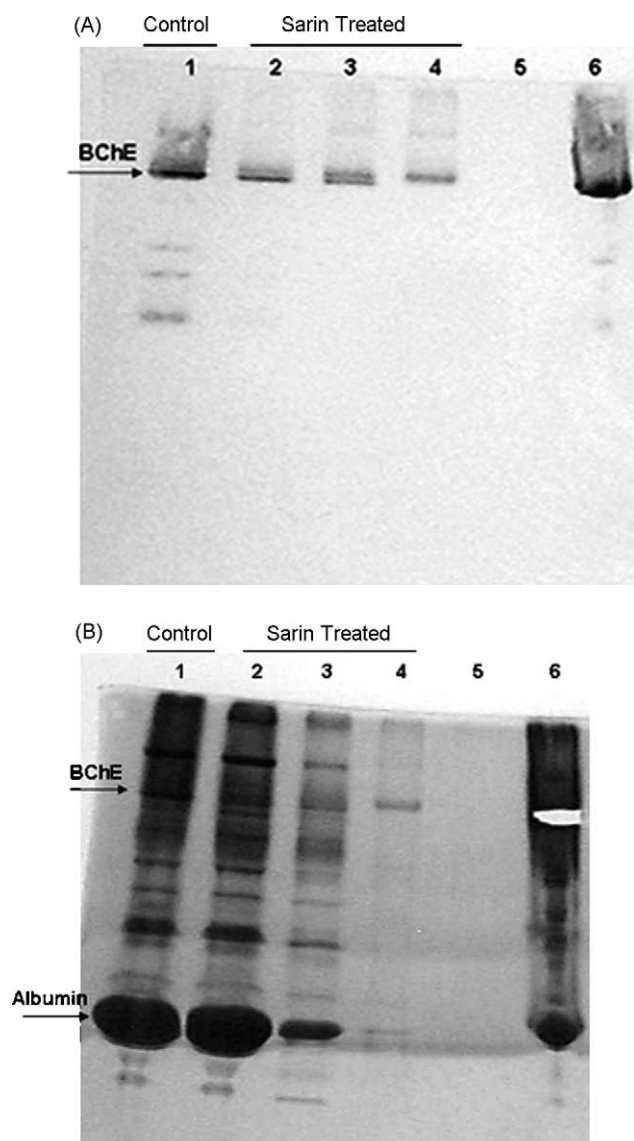


**Fig. 1.** BChE activity (A) followed by Coomassie blue staining (B) on a nondenaturing gel of sarin-treated, plasma proteins from the procainamide affinity column. Lane 1: control human plasma (no sarin treatment, no purification); Lane 2: flow-through fraction from sarin-treated plasma that did not bind to the affinity column; Lane 3: wash-off fraction; Lane 4: eluate from the affinity column; Lane 5: blank; Lane 6: concentrated eluate. The gel slice used for mass spectrometry was cut out of lane 6. Equal volumes (10  $\mu$ l) of sample were loaded in lanes 1–4. Note that significant amounts of protein were in the flow-through fraction. The doublet bands in (A), lane 3 represent BChE tetramers with different glycosylation states.

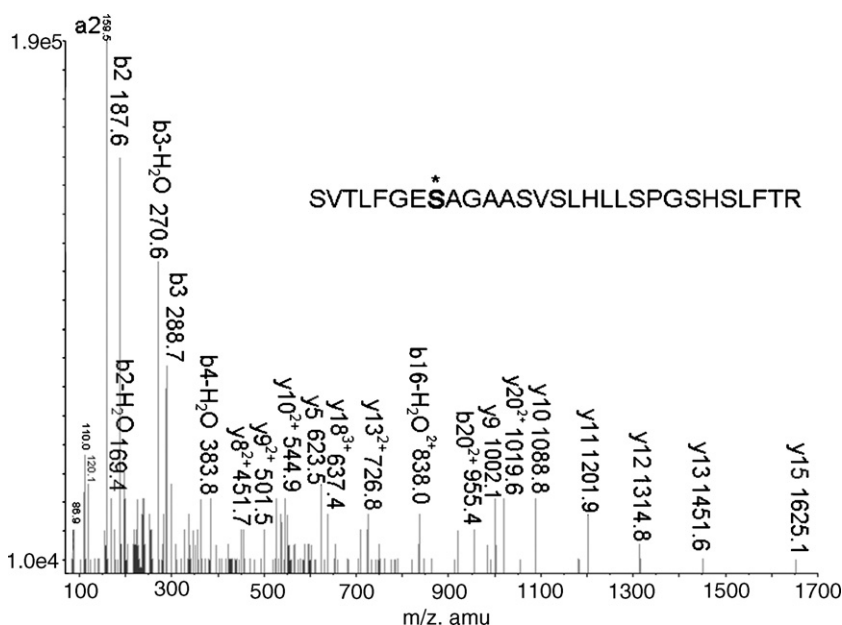


**Fig. 2.** MS/MS spectrum of the aged, soman-labeled BChE active-site peptide. Ions used in the peptide sequence analysis are labeled for their identities and corresponding masses. The sequence of the BChE active-site tryptic peptide is shown. The active-site serine is labeled with \*. The experimental  $m/z$  of the quadruply charged parent ion was 752.7.

series of ions are used by computer programs or manual sequencing to produce the original peptide sequence.

MASCOT identified the aged, soman-labeled, BChE active-site peptide as a quadruply charged parent ion of 752.7  $m/z$ . Manual inspection of the MS/MS spectrum of 752.7 ion confirmed the MASCOT assignment (Fig. 2). As shown in the MS/MS spectrum, a series of  $y$  ions, as well as some  $b$  ions and their derivatives, can be identified. Fragment ion at 838.0  $m/z$  represents the doubly charged form of  $b_{16}$ -H<sub>2</sub>O with the aged soman modification intact (theoretical  $m/z$ : 837.9).

**Table 2**

Peptides identified from a Mascot database search of Soman-labeled Human BChE

	Peptide	Mowse score	ID <sup>a</sup>
1	FWTSFFPK	49	I
2	VIVVSMNYR	49	I
3	YLTLNTESTR	58	I
4	IFFPGVSEFGK	56	I
5	WNNYMMMDWK	12	W
6	DEGTAFLVYGAPFSK	49	I
7	VLEMTGNIDEAEWEWK	36	H
8	FSEWGNNAFFYYFEHR	43	H
9	KFSEWGNNAFFYYFEHR	39	H
10	AILQSGSFNAPWAVTSLYEAR	82	I
11	EALGDVVGDFNFCPALEFTK	40	H
12	ESILFHYTDWVDDQRPENYR	31	W
13	SVTLFGES <sup>b</sup> AGAASVSLHLLSPGS HSLFTR	51	I
14	VGALGFLALPGNPEAPGNMGLF DQQLALQWVQK	20	W

<sup>a</sup> Qualitative description of the Mowse score: I stands for identity, H for homology and W for less than homology.

<sup>b</sup> The active site serine carried a methylphosphonate modification.

Table 2 summarizes the peptides used by MASCOT to identify the aged adduct of soman-labeled BChE. Mascot analysis yielded a Mowse score of 566 for the protein. 14 peptides were identified, covering 39% of the BChE sequence. 7 peptides scored in the identity range, including the aged active-site BChE peptide; 4 in the homology range; and 3 below homology.

Sarin-labeled BChE yielded similar results. The aged products of soman- and sarin-inhibited BChE are expected to have the same mass [14]. The aged, sarin-modified active-site peptide appeared as a quadruply-charged ion at 752.9  $m/z$ . The 752.9 ion was fragmented to generate an MS/MS spectrum from which the peptide sequence could be deduced.

The methods developed in this report can be used to analyze plasma not only for nerve agent exposure, but also for organophosphorus pesticide and carbamate exposure. Future studies will expand to quantitative analysis of OP exposure using Multiple Reaction Monitoring (MRM) on the QTRAP mass spectrometer.

Knowing the mass and structure of the target ion, it is possible to predict the precursor  $m/z$  and a fragment  $m/z$  (MRM transition) for post-translationally modified peptides. MRM experiments can be used to screen for specific transitions, and trigger a dependent product ion scan to confirm the peptide structure. MRM experiments are designed for obtaining the maximum sensitivity for detection of target ions. This type of experiment is widely used to detect and quantify drug and drug metabolites in the pharmaceutical industry. MRM has been successfully applied for both relative and absolute quantitation of protein phosphorylation [15,16]. It will be of significant interest to see its application in determining the relative OP exposure level of an individual within a group or in determining the abso-

lute exposure level in terms of OP concentration based on a pre-generated standard curve.

## Acknowledgements

Supported by NIH CounterACT grant U01 NS058056 (to OL), Eppley Cancer Center grant P30CA36727 and DGA grant 03co010-05/PEA 01 08 7 to (PM). Mass spectra were obtained with the support of the Protein Structure Core Facility at the University of Nebraska Medical Center.

## References

- [1] A. Saxena, W. Sun, C. Luo, T.M. Myers, I. Koplovitz, D.E. Lenz, B.P. Doctor, Bioscavenger for protection from toxicity of organophosphorus compounds, *J. Mol. Neurosci.* 30 (2006) 145–148.
- [2] D.E. Lenz, D. Yeung, J.R. Smith, R.E. Sweeney, L.A. Lumley, D.M. Cerasoli, Stoichiometric and catalytic scavengers as protection against nerve agent toxicity: a mini review, *Toxicology* 233 (2007) 31–39.
- [3] D.B. Barr, R. Bravo, G. Weerasekera, L.M. Calabiano, R.D. Whitehead Jr., A.O. Olsson, S.P. Caudill, S.E. Schober, J.L. Pirkle, E.J. Sampson, R.J. Jackson, L.L. Needham, Concentrations of dialkyl phosphate metabolites of organophosphorus pesticides in the U.S. population, *Environ. Health Perspect.* 112 (2004) 186–200.
- [4] O. Lockridge, L.M. Schopfer, Biomarkers of organophosphate exposure, in: R.C. Gupta (Ed.), *Toxicology of Organophosphate and Carbamate Compounds*, first ed., Academic Press, Inc., USA, 2006, pp. 703–711.
- [5] A. Fidder, A.G. Hulst, D. Noort, R. de Ruiter, M.J. van der Schans, H.P. Benschop, J.P. Langenberg, Retrospective detection of exposure to organophosphorus anti-cholinesterases: mass spectrometric analysis of phosphorylated human butyrylcholinesterase, *Chem. Res. Toxicol.* 15 (2002) 582–590.
- [6] K. Tsuge, Y. Seto, Detection of human butyrylcholinesterase-nerve gas adducts by liquid chromatography–mass spectrometric analysis after in gel chymotryptic digestion, *J. Chromatogr. B. Anal. Technol. Biomed. Life Sci.* 838 (2006) 21–30.
- [7] N.L. Anderson, N.G. Anderson, The human plasma proteome: history, character, and diagnostic prospects, *Mol. Cell. Proteomics* 1 (2002) 845–867.
- [8] Y.Y. Wang, P. Cheng, D.W. Chan, A simple affinity spin tube filter method for removing high-abundant common proteins or enriching low-abundant biomarkers for serum proteomic analysis, *Proteomics* 3 (2003) 243–248.
- [9] J. Grunwald, D. Marcus, Y. Papier, L. Raveh, Z. Pittel, Y. Ashani, Large-scale purification and long-term stability of human butyrylcholinesterase: a potential bioscavenger drug, *J. Biochem. Biophys. Methods* 34 (1997) 123–135.
- [10] M.J. Karnovsky, L.A. Roots, “Direct-Coloring” thiocholine method for cholinesterases, *J. Histochem. Cytochem.* 12 (1964) 219–221.
- [11] K.D. Speicher, O. Kolbas, S. Harper, D.W. Speicher, Systematic analysis of peptide recoveries from in-gel digestions for protein identifications in proteome studies, *J. Biomol. Tech.* 11 (2000) 74–86.
- [12] L.M. Schopfer, M.M. Champion, N. Tamblyn, C.M. Thompson, O. Lockridge, Characteristic mass spectral fragments of the organophosphorus agent FP-biotin and FP-biotinylated peptides from trypsin and bovine albumin (Tyr410), *Anal. Biochem.* 345 (2005) 122–132.
- [13] D.N. Perkins, D.J. Pappin, D.M. Creasy, J.S. Cottrell, Probability-based protein identification by searching sequence databases using mass spectrometry data, *Electrophoresis* 20 (1999) 3551–3567.
- [14] H. Li, L.M. Schopfer, F. Nachon, M.T. Froment, P. Masson, O. Lockridge, Aging pathways for organophosphate-inhibited human butyrylcholinesterase, including novel pathways for isomalathion, resolved by mass spectrometry, *Toxicol. Sci.* 100 (2007) 136–145.
- [15] D.M. Cox, F. Zhong, M. Du, E. Duchoslav, T. Sakuma, J.C. McDermott, Multiple reaction monitoring as a method for identifying protein posttranslational modifications, *J. Biomol. Tech.* 16 (2005) 83–90.
- [16] A. Leigh, C.L. Hunter, Quantitative mass spectrometric multiple reaction monitoring assays for major plasma proteins, *Mol. Cell. Proteomics* 5 (2006) 573–588.



# Reaction of human albumin with aspirin *in vitro*: Mass spectrometric identification of acetylated lysines 199, 402, 519, and 545

Mariya S. Liyasova<sup>a,b</sup>, Lawrence M. Schopfer<sup>b</sup>, Oksana Lockridge<sup>b,\*</sup>

<sup>a</sup> University of Nebraska Medical Center, Department of Environmental, Agricultural & Occupational Health, Omaha, NE 68198-6805, USA

<sup>b</sup> University of Nebraska Medical Center, 986805 Nebraska Medical Center, Eppley Institute, Omaha, NE 68198-6805, USA

## ARTICLE INFO

### Article history:

Received 8 September 2009

Received in revised form 7 October 2009

Accepted 7 October 2009

### Keywords:

Albumin

Aspirin

Mass spectrometry

Acetylated lysine

Pseudo-aspirinase activity

## ABSTRACT

The aspirin esterase activity of human plasma is due to butyrylcholinesterase and albumin. Our goal was to identify the amino acid residues involved in the aspirin esterase activity of albumin. Fatty acid-free human albumin and human plasma were treated with aspirin for 5 min–24 h. Acetylated residues were identified by LC/MS/MS and MALDI-TOF/TOF mass spectrometry of tryptic peptides. Treatment with 0.3 mM aspirin resulted in acetylation of Lys-199, Lys-402, Lys-519, and Lys-545. Treatment with 20 mM aspirin resulted in acetylation of 26 lysines. There was no acetylation of Tyr-411, under any conditions. Acetylated lysine was stable for at least 21 days at pH 7.4, 37 °C. Albumin acetylated by aspirin had reduced esterase activity with  $\beta$ -naphthyl acetate as shown on gels stained for esterase activity. It was concluded that the aspirin esterase activity of albumin is a pseudo-esterase activity in which aspirin stably acetylates lysines and releases salicylate.

© 2009 Elsevier Inc. All rights reserved.

## 1. Introduction

Hawkins et al. reported that aspirin transfers its acetyl to the  $\epsilon$ -amino group of lysine residues of albumin both *in vitro* [1] and *in vivo* [2]. Later the labeled residue was identified as Lys-199 [3]. The crystal structure of human albumin confirmed that aspirin acetylates Lys-199 [4]. To date no other acetylated residues have been identified, though up to 6 additional radiolabeled peptides were found on the radioautograph of the peptide map of aspirin-treated albumin [2].

Albumin is regarded as an aspirin esterase because salicylic acid is produced by incubation of aspirin with albumin [5]. The esterase activity of albumin with p-nitrophenyl acetate is predominantly a pseudo-esterase activity in which up to 59 lysines are stably acetylated. In addition, Tyr-411 of human albumin is rapidly acetylated by p-nitrophenyl acetate ( $t_{1/2}$  = 0.56 min) and slowly deacetylated ( $t_{1/2}$  = 61 h) [6,7]. The three goals of our study were to determine whether the aspirin esterase activity of albumin is also a

pseudo-esterase activity resulting in stable acetylation of many residues; if so, to identify the acetylated residues by mass spectrometry; and to determine whether Tyr-411 is involved in the reaction of albumin with aspirin.

## 2. Materials and methods

### 2.1. Materials

A 1 mg/ml solution of fatty acid-free human albumin (Fluka 05418, via Sigma–Aldrich, St. Louis, MO) was prepared in 100 mM potassium phosphate buffer, pH 7.4. The amino acid sequence for the albumin from this source is given in accession number gi:122920512. This albumin has Glu-396 in peptide QNCELFE\*QLGEYK where other albumin sequences have Lys-396. A 1 mg/ml solution of porcine pepsin (Sigma–Aldrich P6887) in 10 mM HCl, as well as 20  $\mu$ g of sequencing grade modified trypsin (Promega V5113, Madison, WI) in 50  $\mu$ l of 50 mM acetic acid were stored at –80 °C. A saturated solution of  $\alpha$ -cyano-4-hydroxycinnamic acid matrix (CHCA) (Applied Biosystems, Foster City, CA) in 50% acetonitrile, 0.1% trifluoroacetic acid was stored at room temperature. Acetylsalicylic acid (aspirin) (Sigma–Aldrich A5376) was dissolved in ethanol to make 0.1 and 1 M solutions and stored at room temperature.  $\beta$ -Naphthyl acetate, Fast Blue RR, trifluoroacetic acid and iodoacetamide were from Sigma–Aldrich. Affi-Gel Blue was from Bio-Rad, Hercules, CA. Dithiothreitol, sodium azide,

**Abbreviations:** PAGE, polyacrylamide gel electrophoresis; MALDI-TOF/TOF, matrix assisted, laser desorption/ionization tandem mass spectrometer with dual time-of-flight analyzers; Q-TRAP, hybrid triple quadrupole linear ion trap mass spectrometer; MS, mass spectrum; MS/MS, mass spectrum of collision induced dissociation fragments; LC, liquid chromatography; CHCA, alpha-cyano-4-hydroxycinnamic acid.

\* Corresponding author. Tel.: +1 402 559 6032; fax: +1 402 559 4651.

E-mail address: [olockrid@unmc.edu](mailto:olockrid@unmc.edu) (O. Lockridge).

and ammonium bicarbonate were purchased from Fisher Scientific, Fair Lawn, NJ. Acetonitrile was of LC-grade. Water was purified with the Milli-Q system, followed by distillation. Human plasma in heparin anticoagulant was from Innovative Research, Novi, MI.

## 2.2. Incubation of pure human serum albumin with aspirin

In general, 1 ml of a 1 mg/ml solution of fatty acid-free human albumin (15  $\mu$ M) in 100 mM phosphate buffer, pH 7.4 was incubated with 0.05–20 mM aspirin for 24 h at 37 °C. For one experiment, 1 ml of 40 mg/ml solution of human albumin (600  $\mu$ M) in 100 mM phosphate buffer, pH 7.4 was reacted with 0.3 mM aspirin for 24 h at 37 °C. Control albumin solution was treated with 20  $\mu$ l ethanol. Treatment with 10–20 mM concentrations of aspirin caused a pH drop, which was corrected by addition of 1 M NaOH.

## 2.3. Albumin esterase activity staining on nondenaturing PAGE

A 0.75 mm thick, 4–30% polyacrylamide gradient gel was prepared in a Hoefer gel apparatus and run at a constant voltage for 5000 V h (250 V for 20 h) at 4 °C. 5  $\mu$ l of human plasma, estimated to contain 200  $\mu$ g albumin, or 20  $\mu$ l of 10 mg/ml albumin premixed with an equal volume of 50% glycerol, 0.1% bromophenol blue, was loaded per lane. Esterase activity of albumin was visualized by incubating the gel in 100 ml of 50 mM Tris–Cl pH 7.4 solution, containing 50 mg of  $\beta$ -naphthyl acetate dissolved in 1 ml ethanol and 50 mg of Fast Blue RR. Within 10–20 min pink bands formed due to the reaction of released  $\beta$ -naphthol with the diazonium salt of Fast Blue RR [8]. The gel was counterstained with Coomassie Blue.

## 2.4. In vitro modification of human plasma and isolation of albumin

100  $\mu$ l of human plasma was incubated with 0.3 mM aspirin for 1 h 40 min at 37 °C. Non-treated plasma was used as a control. After the incubation albumin was isolated by affinity chromatography on Blue Affi-Gel. Briefly, 200  $\mu$ l of affinity media was packed into a microfuge spin column and equilibrated with binding buffer (50 mM potassium phosphate buffer pH 7.0). Plasma samples were diluted 1:20 and 400  $\mu$ l was applied to the column. Columns were washed with binding buffer until the absorbance of the eluate at 280 nm was zero. Proteins were eluted with 1.5 M KCl in 50 mM potassium phosphate buffer pH 7.0. The absorbance at 280 nm of 1 ml fractions was measured. Albumin concentration was calculated with the formula:  $A_{280} = \epsilon \times l \times c$  where  $\epsilon$  is the extinction coefficient of albumin (35,700 M<sup>-1</sup> cm<sup>-1</sup>) [9],  $c$  is the unknown albumin concentration, and  $l$  is the pathlength of the cuvette (1 cm). Purified albumin was subjected to tryptic digestion as described in Section 2.5.

## 2.5. Trypsin digestion

Human albumin (1 mg/ml) modified by aspirin was denatured by boiling for 10 min in the presence of 10 mM dithiothreitol, carbamidomethylated with 90 mM iodoacetamide (1 h-incubation in the dark at 37 °C), and dialyzed against 2  $\times$  4 l of 10 mM ammonium bicarbonate. Denaturation in urea was avoided because urea adds carbamate (CONH<sub>2</sub>) to lysine. The added mass of +43 amu from carbamate could be confused with the added mass of +42 amu from acetate (COCH<sub>3</sub>). A 100- $\mu$ g aliquot was digested with 2  $\mu$ g of Promega trypsin overnight at 37 °C. The trypsin digest was subjected to MALDI and Q-TRAP mass spectrometric analyses.

## 2.6. Pepsin digestion

Pure human serum albumin (15  $\mu$ M) in 100 mM phosphate pH 7.4 was treated with 0.3, 3, and 20 mM concentrations of aspirin and incubated at 37 °C for 5, 10, 15, 20, 30, 40, 50, 60 min, 3 and 24 h. The reaction between aspirin and albumin was stopped by addition of 50  $\mu$ l of 1% trifluoroacetic acid to 50  $\mu$ l of the reaction mixture. The samples were digested with 2  $\mu$ l of 1 mg/ml pepsin at 37 °C for 1.5 h. Samples were diluted 1:10 in water and analyzed in a MALDI-TOF/TOF 4800 mass spectrometer.

## 2.7. HPLC purification of the acetylated peptide LK\*CASLQK and stability assay

1 ml of 1 mg/ml human albumin in 100 mM potassium phosphate pH 7.4 was treated with 0.3 mM aspirin for 24 h, reduced, carbamidomethylated, dialyzed, and digested with trypsin as described above. The LK\*CASLQK peptide was purified on a Waters 625 LC system using a Phenomenex Prodigy 5 micron C18 100 mm  $\times$  4.60 mm column. Peptides were eluted with a 60-min gradient from 0.1% trifluoroacetic acid in water to 60% acetonitrile, 0.09% trifluoroacetic acid at a flow rate of 1 ml/min. 1 ml fractions were collected. To identify the fraction containing the peptide of interest 1  $\mu$ l of each fraction was analyzed in the MALDI-TOF/TOF mass spectrometer. The acetylated, carbamidomethylated peptide LK\*CASLQK eluted between 16 and 17 min. This fraction was dried in the SpeedVac, dissolved in 30  $\mu$ l of 50 mM potassium phosphate buffer, pH 7.4, containing 0.1% (w/v) sodium azide, and incubated at 37 °C. Aliquots were withdrawn over a period of 3 weeks for measurement of acetylated and deacetylated peptides. A 1- $\mu$ l aliquot was diluted 10-fold in water and analyzed in the MALDI-TOF/TOF 4800 mass spectrometer. The percentage of acetylation was calculated by dividing the cluster area of the acetylated peptide by the sum of the cluster areas for the acetylated and deacetylated peaks [7].

## 2.8. Analysis in a MALDI-TOF/TOF 4800 (Applied Biosystems, Foster City, CA) mass spectrometer

Essentially salt-free 1- $\mu$ l samples were spotted on a MALDI target plate, dried in air, and overlaid with 1  $\mu$ l of saturated CHCA in 50% acetonitrile, 0.1% trifluoroacetic acid. MS spectra were acquired with laser power at 3500 V in positive reflector mode. For MS/MS spectra laser intensity was 4000 V. Each spectrum was the average of 500 laser shots. The mass spectrometer was calibrated against bradykinin (904.47  $m/z$ ), angiotensin 1 (1296.68  $m/z$ ), Glu-fibrinopeptide B (1570.68  $m/z$ ), adrenocorticotrophic hormone (ACTH) 1–17 clip (2093.09  $m/z$ ), ACTH 18–39 clip (2465.20  $m/z$ ), and ACTH 7–38 clip (3657.96  $m/z$ ) (Cal Mix 5 from Applied Biosystems). Spectra were analyzed with Data Explorer Software.

## 2.9. LC/MS/MS with the Q-TRAP 2000 mass spectrometer

Tryptic digests were dried in a vacuum centrifuge and dissolved in 5% acetonitrile, 0.1% formic acid to make 6 pmol/ $\mu$ l. A 10- $\mu$ l aliquot was injected into the HPLC nanocolumn (218MS3.07515 Vydac C18 polymeric rev-phase, 75  $\mu$ m i.d.  $\times$  150 mm long; P.J. Cobert Assoc., St. Louis, MO). Peptides were separated with a 90-min linear gradient from 0 to 60% acetonitrile at a flow rate of 0.3  $\mu$ l/min and electrosprayed through a fused silica emitter (360  $\mu$ m o.d., 75  $\mu$ m i.d., 15  $\mu$ m taper, New Objective) directly into the Q-TRAP 2000 (Applied Biosystems, Foster City, CA), a hybrid quadrupole linear ion trap mass spectrometer. An ion-spray voltage of 1900 V was maintained between the emitter and the mass spectrometer. Information dependent acquisition was used to collect MS, enhanced MS, and MS/MS spectra for the three most

intense peaks in each cycle, having a charge of +1 to +4, a mass between 200 and 1700  $m/z$ , and an intensity >10,000 cps. All spectra were collected in the enhanced mode, using the trap function. Precursor ions were excluded for 30 s after one MS/MS spectrum had been collected. The collision cell was pressurized to 40  $\mu$ Torr with pure nitrogen and collision energies between 20 and 40 eV were determined automatically by the software based on the mass and charge of the precursor ion. The mass spectrometer was calibrated on selected fragments from the MS/MS spectrum of Glu-fibrinopeptide B. The MS/MS data were processed using Analyst 1.4.1 software and submitted to Mascot for identification of peptide sequences [10].

### 3. Results

#### 3.1. Residues acetylated by 0.3 mM aspirin

Two different mass spectrometry methods (MALDI-TOF/TOF and Q-TRAP MS/MS) were applied to identify tryptic peptides of albumin acetylated by aspirin. A 24-h reaction of 15  $\mu$ M human albumin with 0.3 mM aspirin at 37 °C resulted in the acetylation of four albumin residues, namely Lys-199, Lys-402, Lys-519, and Lys-545. No additional acetylation sites were found when the physiological concentration of albumin (600  $\mu$ M) was used. The masses of labeled tryptic peptides were increased by +42  $m/z$  due to acetylation. MS/MS spectra of candidate peptides were analyzed to confirm the identity of the modified peptide as well as to identify the site of modification.

Fig. 1 shows the MALDI MS/MS spectrum of parent ion 989.5  $m/z$ , which corresponds to acetylated peptide LK\*<sup>+</sup>CASLQK. Lys-199 was identified as the adduction site by the presence of unacetylated  $y_3$ ,  $y_4$ ,  $y_5$ , and  $y_6$  ions at  $m/z$  388.2, 475.2, 546.2, and 706.3, respectively and by the presence of the acetylated b-ion series  $b_2^*$ ,  $b_3^*$ ,  $b_4^*$ , and  $b_5^*$  at  $m/z$  284.2, 444.2, 515.2, and 602.2, respectively. The presence of  $\epsilon$ -N-acetyllysine immonium ion at  $m/z$  126.1 provides additional evidence for the assignment of acetyllysine-containing peptide [11].

Lys-402 was confirmed to be acetylated by Q-TRAP MS/MS analysis of parent ion  $[M+3H]^{3+}$  at  $m/z$  881.54 (Fig. 2). The acetylated peptide was unambiguously identified as QNCELFEQLGEYK\*<sup>+</sup>FQNALLVR, characterized by the partial b-series ( $b_3$ – $b_8$ ) and the partial y-series ( $y_1$ – $y_8$ ). Lys-402 was identified as the position of acetylation by the presence of the adducted ions  $y_9^*$ ,  $y_{10}^*$ , and

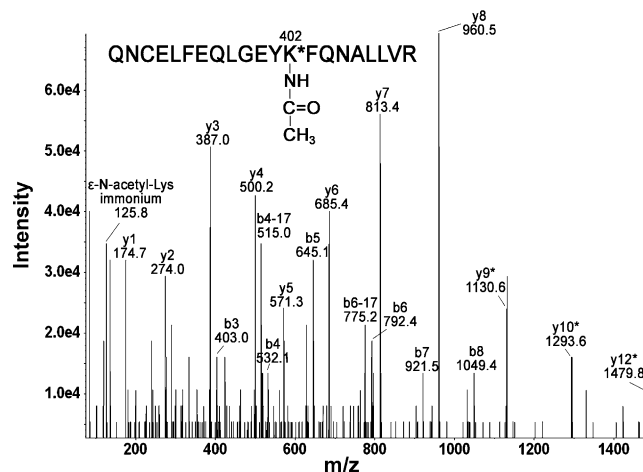


Fig. 2. Identification of Lys-402 as an acetylation site. Q-TRAP MS/MS fragmentation of parent ion  $[M+3H]^{3+}$  at  $m/z$  881.54 yielded y- and b-ion series consistent with acetylated peptide QNC(carbamidomethylated)ELFEQLGEYK\*<sup>+</sup>FQNALLVR. The asterisk \* indicates +42  $m/z$  shift in ion mass as compared to native peptide ions.

$y_{12}^*$ . The presence of  $\epsilon$ -N-acetyllysine immonium ion at  $m/z$  125.8 served as additional confirmation of acetylation on lysine [11].

Q-TRAP MS/MS fragmentation of parent ion  $[M+3H]^{3+}$  at  $m/z$  863.46 is shown in Fig. 3A. The spectrum confirms the identity of this acetylated peptide as EFNAETFTFHADICTLSEK\*<sup>+</sup>ER and confirms that the adducted residue is Lys-519. Supporting ions are  $y_1$ ,  $y_3^*$ ,  $y_4^*$ ,  $y_5^*$ ,  $y_6^*$ ,  $y_7^*$ ,  $y_8^*$ ,  $y_9^*$ ,  $y_{10}^*$ ,  $y_{11}^*$ ,  $y_{12}^*$ ,  $y_{12}^{*+2}$ ,  $y_{19}^{*+2}$ ,  $b_3$ ,  $b_{16}^{*+2}$ , where the asterisk indicates acetylated ions, as well as b-ions that have lost water ( $b-18$ ). The internal fragment at  $m/z$  230.9 has the sequence ET.

The Q-TRAP MS/MS spectrum of parent ion  $[M+2H]^{2+}$  at  $m/z$  942.16, in Fig. 3B, corresponds to the acetylated peptide EQLK\*<sup>+</sup>AVMDDFAAFVEK. The presence of  $\epsilon$ -N-acetyllysine immonium ion at  $m/z$  125.8 confirms the presence of acetylated lysine [11]. The MS/MS fragmentation, yielding a partial b-series ( $b_2$ ,  $b_3$ ,  $b_4^*$ – $b_6^*$ ), a partial y-series ( $y_3$ ,  $y_5$ – $y_{12}$ ,  $y_{13}^*$ ) and internal fragment LK\*<sup>+</sup> at 284.0  $m/z$ , confirms that Lys-545, but not Lys-557 is acetylated. The ions marked with an asterisk are acetylated.

#### 3.2. Residues acetylated by 20 mM aspirin

Incubation of 15  $\mu$ M human albumin with 20 mM aspirin at pH 7.4, 37 °C for 24 h resulted in the acetylation of 26 lysines, listed in Table 1. To identify labeled peptides, *in silico* trypsin digestion of albumin was performed (ProteinProspector v 5.3.0 <http://prospector.ucsf.edu>), taking into account carbamidomethylation of cysteine and possible oxidation of methionine, as well as possible missed cleavages. Theoretical masses of acetylated tryptic peptides were calculated and used to select candidates for acetylated ions from the MALDI MS spectrum. To confirm peptide sequences and identify adducted residues, peptides were analyzed by MALDI MS/MS.

Q-TRAP MS/MS analysis served as an additional tool for the identification of acetylated peptides. All MS/MS spectra were submitted to Mascot for comparison with the NCBI human protein database. Peptides corresponding to 60% coverage of the albumin sequence, in accession # gi:122920512, were obtained. MS/MS spectra of candidates for acetylated peptides were manually evaluated and only strong, well-assigned spectra, comparable to those shown in Figs. 1–3, were considered as evidence for peptide acetylation.

All peptides listed in Table 1 have a missed cleavage at the acetylated lysine. This is because trypsin is unable to recognize

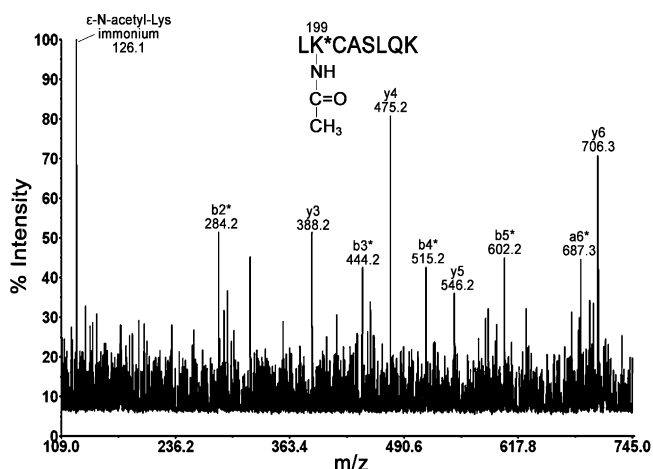
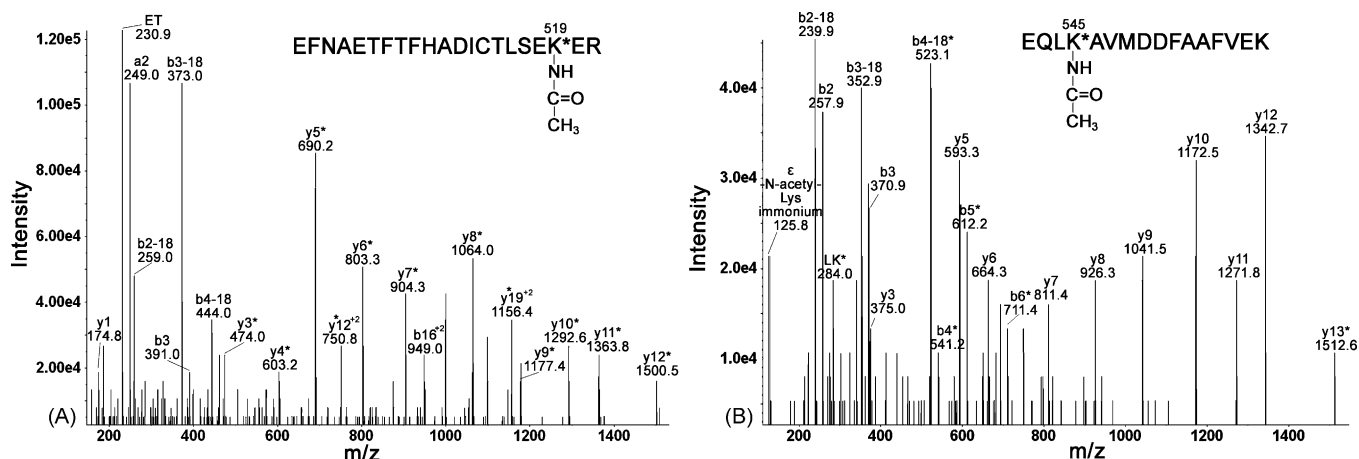


Fig. 1. Identification of acetylated residue Lys-199. MALDI MS/MS spectrum of parent ion 989.5  $m/z$  shows major y- and b-ions of peptide LK\*<sup>+</sup>(carbamidomethylated)ASLQK. The asterisk \* denotes +42  $m/z$  shifted ions as compared to native peptide. Carbamidomethylation of cysteine adds +57  $m/z$ .



**Fig. 3.** Identification of Lys-519 and Lys-545 as adduction sites. Q-TRAP MS/MS spectra of parent ion  $[M+3H]^{3+}$  at  $m/z$  863.46 (panel A) and parent ion  $[M+2H]^{2+}$  at  $m/z$  942.16 (panel B) show major  $y$ - and  $b$ -ions, as well as internal fragments. Acetylated fragment ions are labeled with an asterisk.

**Table 1**

Tryptic peptides found to be acetylated after 24-h reaction of 15  $\mu$ M human albumin with 20 mM aspirin at 37 °C.

Sequence position	Peptide sequence	Acetylated lysine	Mass of unlabeled peptide, $m/z$	Mass of labeled peptide (mass shift 42), $m/z$	Method of identification
11–20	FK*DLGEENFK	12	1226.6	1268.6	MALDI MSMS, Q-TRAP
65–81	SLHTLFGDK*LCTVATLR	73	1932.0	1974.0	MALDI MSMS, Q-TRAP
82–98	ETYGEMADCCAK*QEPER	93	2073.8	2115.8	MALDI MSMS
99–114	NECFLQHK*DDNPNLPR	106	1996.9	2038.9	Q-TRAP
115–137	LVRPEVDVMCTAFHDNEETFLK*K	136	2778.3	2820.3	MALDI MSMS
137–144	K*YLYEIAR	137	1055.6	1097.6	MALDI MSMS, Q-TRAP
146–160	HPYFYAPPELLFAFK*R	159	1899.0	1941.0	MALDI MSMS
161–174	YK*AAFTCCQAADK	162	1662.7	1704.7	MALDI MSMS, Q-TRAP
163–181	AAFTCCQAADK*AACLLPK	174	2125.0	2167.0	Q-TRAP
198–205	LK*CASLQK	199	947.5	989.5	MALDI MSMS
200–209	CASLQK*FGER	205	1195.6	1237.6	MALDI MSMS, Q-TRAP
210–218	AFK*AWAVAR	212	1019.6	1061.6	MALDI MSMS, Q-TRAP
223–233	FPK*AEFAEVSK	225	1252.6	1294.6	Q-TRAP
258–274	ADLAK*YICENQDSISK	262	1941.9	1983.9	MALDI MSMS, Q-TRAP
277–286	ECCEK*PLEK	281	1305.6	1347.6	Q-TRAP
318–336	NYAEAK*DVFLGMFLYEYAR	323	2300.1	2342.1	MALDI MSMS
349–359	LAK*TYETLLEK	351	1296.7	1338.7	Q-TRAP
373–389	VNDEFK*PLVEEPQNLIK	378	2045.1	2087.1	Q-TRAP
390–410	QNCLEFEQLGEYK*FQNALLVR	402	2599.3	2641.3	MALDI MSMS, Q-TRAP
414–428	K*VPQVSTPTLVEVSR	414	1639.9	1681.9	Q-TRAP
473–484	VTK*CCTESLVNR	475	1466.7	1508.7	MALDI MSMS, Q-TRAP
501–521	EFNAETFTFHADICTLSEK*ER	519	2545.2	2587.2	MALDI MSMS, Q-TRAP
525–534	K*QTALVELVK	525	1128.7	1170.7	Q-TRAP
539–545	ATK*EQLK	541	817.5	859.5	MALDI MSMS
542–557	EQLK*AVMDDFAAFVEK	545	1840.9	1882.9	MALDI MSMS, Q-TRAP
546–560	AVMDDFAAFVEK*CCK	557	1790.8	1832.8	MALDI MSMS, Q-TRAP

The asterisk \* indicates the adducted lysine. The albumin sequence is in accession # gi: 122920512 in the NCBI protein database. Monoisotopic masses of singly charged ions are given. Cysteines are carbamidomethylated, adding a mass of +57 amu. Acetylated lysines have an added mass of +42 amu.

adducted lysine as a cleavage site, in agreement with the previous literature reports [12].

### 3.3. Mass spectrometric analysis of commercial albumin

Interestingly, acetylation of non-treated pure human albumin was observed. The acetylated residues in commercial albumin were Lys-199, and Lys-525. Less than 0.1% of commercial albumin was acetylated. In contrast, significant amounts of albumin were acetylated after treatment with aspirin.

### 3.4. Reaction of aspirin with human plasma

To study the reaction between aspirin and albumin under physiological conditions, 100  $\mu$ l of human plasma was incubated directly with 0.3 mM aspirin for 1 h 40 min at 37 °C. Albumin was isolated and digested with trypsin as described in Section 2.

Analysis of the tryptic digest on the MALDI-TOF/TOF mass spectrometer revealed acetylation of Lys-199 and Lys-519.

To model repeated doses of aspirin, 100  $\mu$ l of human plasma was treated with 0.3 mM aspirin 3 times. The time between treatments was 1 h 40 min. Two treatments with 0.3 mM aspirin resulted in acetylation of four residues, Lys-199, Lys-402, Lys-519, and Lys-545. Three serial treatments led to the acetylation of 5 residues, the fifth being Lys-136.

Thus, under physiological conditions the most reactive albumin residues were Lys-199 and Lys-519, appearing after the first treatment with 0.3 mM aspirin. Additional “doses” of aspirin led to accumulation of acetylation.

### 3.5. The role of Tyr-411 in the reaction between aspirin and albumin

To study the involvement of Tyr-411 in the reaction, 15  $\mu$ M fatty acid-free human albumin was treated with different

concentrations of aspirin, digested with pepsin and analyzed on the MALDI mass spectrometer. Pepsin was chosen because experience has shown that peptic peptides containing Tyr-411 are readily observed in both the MALDI and Q-TRAP mass spectrometers. Acetylation of Tyr-411 increases the mass of peptic peptides VRYTKKVPQVSTPTL and LVRYTKKVPQVSTPTL (missed cleavage) at 1717 and 1830  $m/z$  by +42 to 1759 and 1872  $m/z$  [7]. Samples that were incubated with aspirin for 5 min–3 h gave strong signals for the unlabeled peptides but did not result in the appearance of peptides at  $m/z$  1759 and 1872 (data not shown). However, after 24-h reaction with 20 mM aspirin, low intensity masses at  $m/z$  1759 and 1872 were observed. Q-TRAP MS/MS analysis showed that the +42  $m/z$  mass shift was due to acetylation of Lys-414, but not Tyr-411 (data not shown).

### 3.6. The stability of acetylated Lys-199

To estimate the stability of acetylation, peptide LK\**CASLQK* with acetyl on Lys-199 was purified by HPLC and incubated at 37 °C in pH 7.4 buffer. At various time intervals a 1  $\mu$ l aliquot was removed for MALDI-TOF MS analysis to measure the percentage of acetylation. The acetylated peptide at  $m/z$  989.5 would lose 42 amu and shift to a mass of 947.5  $m/z$  if it were deacetylated. Fig. 4 shows that the acetylated peptide was stable for at least 21 days. The absence of non-acetylated peptide after 21 days of incubation leads to the conclusion that acetylation on Lys-199 is stable at pH 7.4, 37 °C.

### 3.7. Acetylation sites: order of reactivity

To measure the reactivity of acetylation sites, 15  $\mu$ M albumin was treated with different concentrations of aspirin for 24 h at 37 °C, digested with trypsin and analyzed in the MALDI mass spectrometer.

Two sites, namely Lys-402 and Lys-519, were acetylated by the lowest aspirin concentration (0.05 mM), when no other sites were labeled. Moreover, peptides containing these acetylated residues rose in abundance with increasing aspirin concentration. Lys-199 was found to be acetylated with 0.1 mM aspirin; however the peak intensity of the peptide containing this lysine was low and did not change with the increase in aspirin concentration.

When albumin was incubated with 0.5 mM aspirin, evidence of acetylation of Lys-73, Lys-136, Lys-137, Lys-159, Lys-212, and Lys-545 appeared in the MS spectrum. Incubation with 20 mM aspirin resulted in acetylation of 26 lysine residues (Table 1).

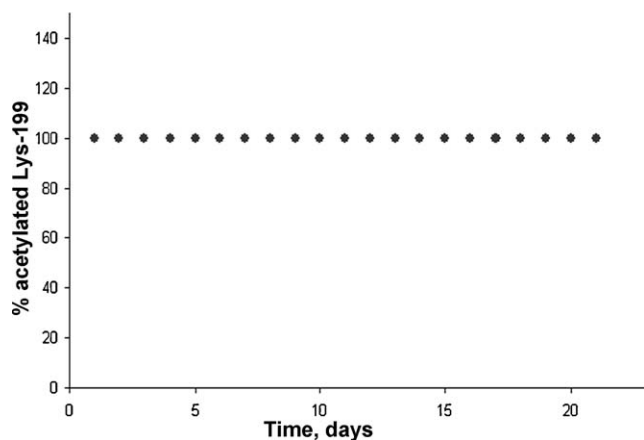


Fig. 4. The stability of acetylated Lys-199. Deacetylation was monitored at pH 7.4, 37 °C for 21 days. Percentage acetylation was calculated from cluster area in the MALDI MS spectrum for peptide LK\**CASLQK*.

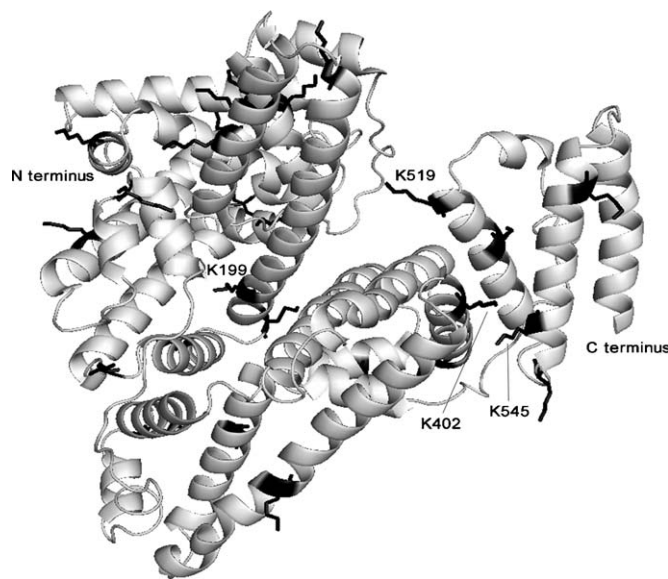


Fig. 5. Molecular modeling to locate lysines acetylated by aspirin. Ribbon model shows the crystal structure of human albumin (Protein Data Bank code 1bmo). The 26 lysines acetylated by 20 mM aspirin are shown in sticks. Lys-199, Lys-402, Lys-519 and Lys-545 are acetylated by 0.3 mM aspirin. The structure was drawn with PyMOL software (DeLano, W.L. The PyMOL Molecular Graphics System (2002) <http://www.pymol.org>).

### 3.8. Surface location of acetylated residues in human serum albumin

The crystal structure of human albumin is shown in Fig. 5. The 26 acetylated lysines are shown as sticks. Lys-199, Lys-402, Lys-519, and Lys-545 are acetylated by 0.3 mM aspirin. To establish the availability of acetylation sites the solvent accessible surface was analyzed. The solvent accessible surface area is defined as the surface traced out by the center of a water sphere, having a radius of 1.4 Å, rolled over the protein atoms [13]. By visual inspection of the molecule, it was concluded that sites Lys-199, Lys-402, Lys-519, as well as Lys-545 are accessible to the solvent.

### 3.9. Albumin esterase activity

Staining of a nondenaturing gradient PAGE gel with  $\beta$ -naphthyl acetate and Fast Blue RR revealed esterase activity of human albumin. The gel in Fig. 6A shows esterase bands of albumin. Fatty acid-free human albumin preincubated for 24 h with different concentrations of aspirin (from 0 to 50 mM) and stained for esterase activity shows decreasing esterase staining with increasing aspirin concentration (lanes 2–8). This result is interpreted to mean that lysines acetylated by aspirin are unavailable for reaction with  $\beta$ -naphthyl acetate. It is concluded that the esterase activity of albumin is due to acetylation of lysines and not to an enzymatic-like hydrolysis. As such albumin exhibits a pseudo-esterase activity. Aspirin by transferring its acetyl group to albumin decreases the number of available esteratic sites.

To show that equivalent protein concentrations were loaded per lane, the gel was counterstained with Coomassie Blue (Fig. 6B). Pure albumin reveals monomeric forms, as well as albumin dimers and multimers. Albumin treated with 50 mM aspirin (lane 8) migrates slightly further compared to native albumin (lane 9). This fact can be explained by partial elimination of positive charge from the  $\epsilon$ -N-amino groups of lysines due to acetylation. Therefore, acetylated protein has a greater net negative charge and migrates more readily to the anode compared to non-treated albumin.

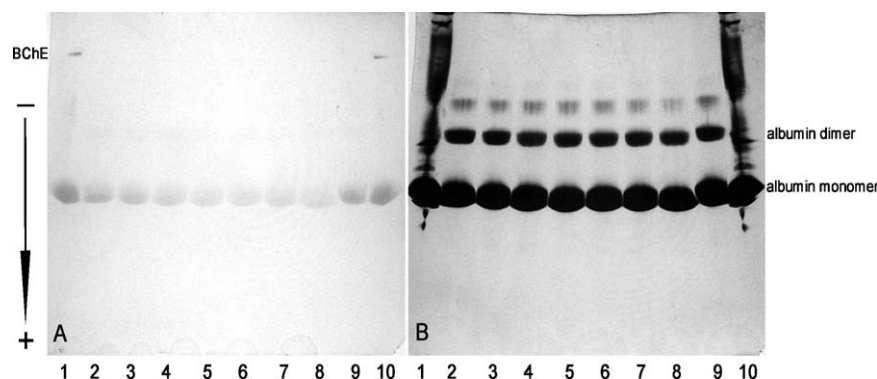


**Fig. 6.** Nondenaturing gradient gel stained for esterase activity (A) and counterstained with Coomassie Blue (B). Lanes 1 and 10, control human plasma (5  $\mu$ l), 0 mM aspirin. Lanes 2–9 contain 200  $\mu$ g of human albumin treated for 24 h with aspirin. Lane 2, 0 mM aspirin; lane 3, 1 mM aspirin; lane 4, 10 mM aspirin; lane 5, 20 mM aspirin; lane 6, 30 mM aspirin; lane 7, 40 mM aspirin; lane 8, 50 mM aspirin; lane 9, 0 mM aspirin. Albumin esterase activity in panel A diminishes with increasing aspirin concentrations. Acetylated albumin in lane 8 migrates more rapidly than untreated albumin in lane 9. The arrow shows the direction of migration of proteins on the gel.

## 4. Discussion

### 4.1. Covalent modification of lysines by aspirin

Aspirin transfers its acetyl group to human albumin *in vitro*. This interaction involves multiple acceptor sites, identified as lysine residues by two different mass spectrometry methods (MALDI TOF/TOF and Q-TRAP). We conclude that the observed adducts are due to covalent binding of the acetyl group to  $\epsilon$ -N-amino groups of lysines. Non-covalent adducts do not survive the MALDI process due to the low pH of the matrix as well as the heat generated by high laser energy [14]. Furthermore, non-covalent adducts would not be expected to survive the low pH and high organic solvent conditions that exist in the HPLC step that precedes electrospraying into the Q-TRAP mass spectrometer. Thus, only covalent modifications of albumin are consistent with our experimental conditions.

### 4.2. Four lysines acetylated by low concentration of aspirin

Aspirin is administered to people in a wide range of doses. Low doses (75–325 mg once a day) are taken to prevent recurrent heart attack and stroke, while high doses (up to 130 mg/kg/day in divided doses) are used to reduce swelling in rheumatoid arthritis patients [15]. The high dose regime amounts to 9100 mg of aspirin per day for a 70 kg (155 lb) individual. Plasma aspirin concentration was found to reach approximately 0.12 mM 20 min after ingestion of 650 mg aspirin [16]. The half-life of aspirin *in vivo* is approximately 20 min with plasma levels essentially undetectable 1–2 h after ingestion [16,17]. In our study, the 0.3 mM aspirin concentration was comparable to therapeutic blood levels.

The reaction of pure albumin with 0.3 mM aspirin, for 24 h, yielded four modified lysines: Lys-199, Lys-402, Lys-519, and Lys-545. Acetylation of Lys-199 by aspirin has been reported previously [3,4], but the identity of the other acetylated lysines is new in this report. The finding that additional lysines are acetylated is consistent with studies that show the involvement of several sites in the reaction of albumin with low (0.1–0.5 mM) concentrations of aspirin [2,18].

Treatment of human plasma with 0.3 mM aspirin, for 1 h 40 min, resulted in the acetylation of two lysines: Lys-199 and Lys-519. The fact that only two of these lysines were found to be acetylated in plasma may be explained by the shorter incubation period as well as faster hydrolysis of aspirin in plasma compared to phosphate buffer. Aspirin hydrolysis in plasma is catalyzed by butyrylcholinesterase. The half-life of aspirin in 0.1 M phosphate buffer, pH 7.4 at 37 °C is 15.4 h [19] vs. 1.6 h in plasma at 37 °C [20] and vs. 0.8 h in whole blood [20].

To mimic repeated doses of aspirin, plasma was treated with 0.3 mM aspirin 3 times with 1 h and 40 min between treatments. Two treatments led to the acetylation of Lys-199, Lys-402, Lys-519, and Lys-545. The third treatment added Lys-136 to residues found with first two “doses”. The time difference between treatments corresponds to 5 half-lives of aspirin *in vivo* [17]; consequently about 96% of the aspirin should have been hydrolyzed in 1 h 40 min. However in isolated plasma aspirin was found to survive longer [20,21]. Thus, 1 h and 40 min is not enough for aspirin to break down completely, meaning that the observed increase in the number of acetylation sites may be due to build up of aspirin concentration. The possibility that repeated doses of aspirin would lead to enhancement of acetylation *in vivo* cannot be ruled out.

### 4.3. 26 Lysines acetylated by high concentration of aspirin

The reaction of pure albumin with 20 mM aspirin resulted in the acetylation of 26 lysine residues. Six peptides were identified only with MALDI MS/MS, eight only with Q-TRAP MS/MS, and twelve peptides were identified with both methods. This difference between mass spectrometers is not surprising. It is generally accepted that different ionization techniques utilized by MALDI and Q-TRAP mass spectrometers allow identification of more peptides than either method used alone [22,23].

However, this high acetylation burden is not likely to occur *in vivo*, since a 20 mM aspirin concentration is well beyond the therapeutic blood level. In addition, concentrations of salicylic acid, the metabolite of aspirin, greater than 5.4 mM cause severe toxicity [24].

Lys-199 was proposed to be the preferential site of acetylation in early studies [2]. Our data support this finding: Lys-199 was among the first few sites to be labeled by 0.1 mM aspirin. Moreover, this site together with Lys-519 were the first to react under physiological conditions. Lys-199 reactivity can be explained by the unusually low pKa of its  $\epsilon$ -N-amino group (pKa  $\approx$  8) [9]. This, in turn, may be due to the close proximity of positively charged residues, Lys-195, Arg-281, Arg-222, which would disfavor protonation of Lys-199 [25].

Additional sites with high reactivity towards aspirin were Lys-402 and Lys-545. All of these residues are located on the surface of albumin where they are available to solvent.

### 4.4. Acetylated lysine is stable

To assess the persistence of acetylation, the stability of acetylated LK\**CASLQK* peptide was measured. It was found that Lys-199 remains 100% acetylated at pH 7.4, 37 °C for up to 21 days.

Assuming an albumin half-life of 20 days in the blood [9], it can be anticipated that once it becomes acetylated, albumin remains acetylated for the remainder of its life-time in the circulation. This idea is supported by the striking finding of a small amount of acetylated albumin in commercial albumin, which indicates that albumin does not lose the acetyl group even under conditions of commercial preparation.

#### 4.5. Tyrosine 411 is not acetylated by aspirin

One of the aims of this study was to establish the role of Tyr-411 in the reaction between aspirin and albumin, since this site was shown to be important in the hydrolysis of other acetyl-containing agents [7,26]. It seemed reasonable to propose that aspirin reacts with albumin by the same mechanism as other phenyl acetates [27]. In which case, labeling of Tyr-411 was expected. In the present study, the reaction with aspirin was stopped after different time points; albumin was digested with pepsin and analyzed by MALDI mass spectrometry to find shifted peptides due to acetylation on Tyr-411. Though the expected mass shift was found, after extended reaction, the labeled residue was Lys-414 not Tyr-411.

Why then does aspirin behave differently from other phenyl esters? Sakurai et al. [28] proposed a mechanism by which p-nitrophenyl esters react with Tyr-411. In their model, the side chain of Arg-410 forms a hydrogen bond with the carbonyl oxygen of the ester, thus facilitating nucleophilic attack by the phenolic oxygen of Tyr-411 on the carbonyl carbon of the ester [28]. However, in the case of aspirin the reaction may be complicated by the presence of carboxylic group. Therefore, it is possible that the carboxylic oxygens rather than the carbonyl oxygen of the acetyl group interact with Arg-410, making the acetylation of Tyr-411 impossible due to a wrong orientation of the aspirin molecule.

In conclusion, the aspirin esterase activity of albumin is a half-reaction in which only lysines are stably acetylated. Aspirin molecules are hydrolyzed in a reaction that consumes albumin binding sites, making them unavailable for reaction with other esters. Tyr-411 does not contribute to these reactions.

#### 4.6. Acetylated albumin has altered binding affinity

Albumin function *in vivo* might be altered by acetylation from aspirin. Interestingly, interaction between aspirin and albumin was first noted because of the increased capacity of aspirin-treated albumin to bind acetrizoate [1]. It was then proposed, that this was a result of structural changes in human albumin induced by acetylation [2]. These early studies generated the idea that albumin affinity for anions that were structurally related to acetrizoate may also be altered by acetylation [1]. Later, acetylation of albumin by aspirin was found to increase the affinity of albumin for phenylbutazone, but decrease its affinity for flufenamic acid [29].

In addition, acetylation of albumin by aspirin was demonstrated to inhibit bilirubin binding [30]. Bilirubin binds to site I located in the IIA subdomain of the albumin molecule [9]. This site also binds aspirin and salicylic acid and includes the reactive residue Lys-199 [4]. Thus, acetylation occurring at binding site I changes the albumin affinity for bilirubin [30].

Finally, binding of aspirin to human albumin was shown to reduce prostaglandins binding to albumin [31]. This was proposed to accelerate clearance of prostaglandins, thus serving as an additional mechanism of the aspirin anti-inflammatory effect [31].

#### 4.7. Summary

Reaction between human albumin and aspirin leads to stable acetylation of multiple lysine residues (see Table 1). Thus the

aspirin esterase activity of albumin is more properly classified as a pseudo-esterase activity. Tyr-411 was found not to play a role in this reaction. Considering the widespread use of aspirin by children and adults, investigation into the consequences of the acetylation of albumin on the various functions of albumin *in vivo* is of interest.

#### Acknowledgements

Mass spectra were obtained with the support of the Mass Spectrometry and Proteomics core facility at the University of Nebraska Medical Center. This work was supported by a grant from the US Army Medical Research and Materiel Command W81XWH-07-2-0034 and an NCI Cancer Center Support Grant CA36727. M.L. was awarded a Fulbright Russia student grant.

#### References

- [1] Hawkins D, Pinckard RN, Farr RS. Acetylation of human serum albumin by acetylsalicylic acid. *Science* 1968;160:780–1.
- [2] Hawkins D, Pinckard RN, Crawford IP, Farr RS. Structural changes in human serum albumin induced by ingestion of acetylsalicylic acid. *J Clin Invest* 1969;48:536–42.
- [3] Walker JE. Lysine residue 199 of human serum albumin is modified by acetylsalicylic acid. *FEBS Lett* 1976;66:173–5.
- [4] Yang F, Bian C, Zhu L, Zhao G, Huang Z, Huang M. Effect of human serum albumin on drug metabolism: structural evidence of esterase activity of human serum albumin. *J Struct Biol* 2007;157:348–55.
- [5] Morikawa M, Inoue M, Tsuboi M, Sugiura M. Studies on aspirin esterase of human serum. *Jpn J Pharmacol* 1979;29:581–6.
- [6] Means GE, Bender ML. Acetylation of human serum albumin by p-nitrophenyl acetate. *Biochemistry* 1975;14:4989–94.
- [7] Lockridge O, Xue W, Gaydess A, Grigoryan H, Ding SJ, Schopfer LM, et al. Pseudo-esterase activity of human albumin: slow turnover on tyrosine 411 and stable acetylation of 82 residues including 59 lysines. *J Biol Chem* 2008;283:22582–90.
- [8] Li B, Sedlacek M, Manoharan I, Boopathy R, Duysen EG, Masson P, et al. Butyrylcholinesterase, paraoxonase, and albumin esterase, but not carboxylesterase, are present in human plasma. *Biochem Pharmacol* 2005;70:1673–84.
- [9] Peters Jr T. All about albumin. *Biochemistry, genetics, and medical applications*. London: Academic Press Ltd; 1996.
- [10] Perkins DN, Pappin DJ, Creasy DM, Cottrell JS. Probability-based protein identification by searching sequence databases using mass spectrometry data. *Electrophoresis* 1999;20:3551–67.
- [11] Trelle MB, Jensen ON. Utility of immonium ions for assignment of epsilon-N-acetyllysine-containing peptides by tandem mass spectrometry. *Anal Chem* 2008;80:3422–30.
- [12] Violand BN, Schlittler MR, Lawson CQ, Kane JF, Siegel NR, Smith CE, et al. Isolation of *Escherichia coli* synthesized recombinant eukaryotic proteins that contain epsilon-N-acetyllysine. *Protein Sci* 1994;3:1089–97.
- [13] [http://www.pymolwiki.org/index.php/Displaying\\_Biochemical\\_Properties#-Display\\_solvent\\_accessible\\_surface](http://www.pymolwiki.org/index.php/Displaying_Biochemical_Properties#-Display_solvent_accessible_surface).
- [14] Bolbach G. Matrix-assisted laser desorption/ionization analysis of non-covalent complexes: fundamentals and applications. *Curr Pharm Des* 2005;11:2535–57.
- [15] Bayer Aspirin. <http://www.wonderdrug.com/index.html>.
- [16] Rowland M, Riegelman S, Harris PA, Sholkoff SD. Absorption kinetics of aspirin in man following oral administration of an aqueous solution. *J Pharm Sci* 1972;61:379–85.
- [17] Levy G. Clinical pharmacokinetics of aspirin. *Pediatrics* 1978;62:867–72.
- [18] Burch JW, Blazer-Yost B. Acetylation of albumin by low doses of aspirin. *Thromb Res* 1981;23:447–52.
- [19] Bakar SK, Niazi S. Stability of aspirin in different media. *J Pharm Sci* 1983;72:1024–6.
- [20] Harthorn L, Hedstrom M. Hydrolysis of salicylsalicylic acid in human blood and plasma: a comparison with acetylsalicylic acid. *Acta Pharmacol Toxicol (Copenh)* 1971;29:155–63.
- [21] Rylance HJ, Wallace RC. Erythrocyte and plasma aspirin esterase. *Br J Clin Pharmacol* 1981;12:436–8.
- [22] Yang Y, Zhang S, Howe K, Wilson DB, Moser F, Irwin D, et al. A comparison of nLC-ESI-MS/MS and nLC-MALDI-MS/MS for GeLC-based protein identification and iTRAQ-based shotgun quantitative proteomics. *J Biomol Tech* 2007;18:226–37.
- [23] Bodnar WM, Blackburn RK, Krise JM, Moseley MA. Exploiting the complementary nature of LC/MALDI-MS/MS and LC/ESI-MS/MS for increased proteome coverage. *J Am Soc Mass Spectrom* 2003;14:971–9.
- [24] Dargan PI, Wallace CI, Jones AL. An evidence based flowchart to guide the management of acute salicylate (aspirin) overdose. *Emerg Med J* 2002;19:206–9.
- [25] Diaz N, Suarez D, Sordo TL, Merz Jr KM. Molecular dynamics study of the IIA binding site in human serum albumin: influence of the protonation state of Lys195 and Lys199. *J Med Chem* 2001;44:250–60.

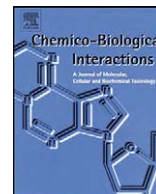
- [26] Watanabe H, Tanase S, Nakajou K, Maruyama T, Kragh-Hansen U, Otagiri M. Role of arg-410 and tyr-411 in human serum albumin for ligand binding and esterase-like activity. *Biochem J* 2000;349(Pt 3):813–9.
- [27] Kuroono Y, Maki T, Yotsuyanagi T, Ikeda K. Esterase-like activity of human serum albumin: structure-activity relationships for the reactions with phenyl acetates and p-nitrophenyl esters. *Chem Pharm Bull (Tokyo)* 1979;27:2781–6.
- [28] Sakurai Y, Ma SF, Watanabe H, Yamaotsu N, Hirono S, Kuroono Y, et al. Esterase-like activity of serum albumin: characterization of its structural chemistry using p-nitrophenyl esters as substrates. *Pharm Res* 2004;21:285–92.
- [29] Chignell CF, Starkweather DK. Optical studies of drug-protein complexes. V. The interaction of phenylbutazone, flufenamic acid, and dicoumarol with acetylsalicylic acid-treated human serum albumin. *Mol Pharmacol* 1971;7:229–37.
- [30] Trynda L, Przywarska-Boniecka H, Kosciukiewicz T. Influence of aspirin and iron(III) tetrasulfonated phthalocyanine on bilirubin binding by human serum albumin. *J Inorg Biochem* 1990;38:153–67.
- [31] Attallah AA, Lee JB. Indomethacin, salicylates and prostaglandin binding. *Prostaglandins* 1980;19:311.



Contents lists available at ScienceDirect

# Chemico-Biological Interactions

journal homepage: [www.elsevier.com/locate/chembioint](http://www.elsevier.com/locate/chembioint)



## Mini review

# Review of tyrosine and lysine as new motifs for organophosphate binding to proteins that have no active site serine

Oksana Lockridge\*, Lawrence M. Schopfer

*Eppley Institute, 985950 University of Nebraska Medical Center, Omaha, NE 68198-5950, United States*

## ARTICLE INFO

**Article history:**  
Available online 6 March 2010

**Keywords:**  
Pesticides  
Nerve agents  
Organophosphorus agents  
Tyrosine  
Lysine

## ABSTRACT

The accepted target for organophosphorus agent (OP) binding to enzymes is the active site serine in the consensus sequence Gly X Ser X Gly. New motifs have been identified by using mass spectrometry to fragment OP-labeled peptides. It has been found that OP can make covalent bonds with tyrosine and lysine in proteins that have no active site serine. The OP-tyrosine bond is stable, and does not undergo the decay seen with OP-serine. Information on OP binding to tyrosine has been applied to diagnosis of OP exposure, through the use of mass spectrometry to detect OP-labeled albumin in human and animal plasma. It is expected that the new OP binding motif will aid in the search for a mechanism of low dose OP toxicity. It is hypothesized that proteins involved in axonal transport, especially proteins whose function depends on reversible phosphorylation, are prime candidates for a role in OP-induced neurodegeneration. Treatment of neurodegenerative disorders could be developed by identifying methods to reverse OP binding to tyrosine.

© 2010 Elsevier Ireland Ltd. All rights reserved.

## Contents

1. Introduction.....	345
1.1. Historical perspective on OP binding to the active site serine in the serine hydrolase superfamily.....	345
2. OP binding to histidine.....	345
3. OP binding to proteins without inhibiting activity.....	345
4. OP binding to tyrosine.....	345
4.1. Low dose toxicity.....	345
4.2. Albumin.....	345
4.3. Tubulin.....	346
4.4. OP binding to tyrosine as a general phenomenon.....	346
4.5. OP binding to free tyrosine and to tyrosine in short peptides.....	347
5. OP binding to lysine.....	347
6. Potential applications and significance of the new OP binding motif.....	347
6.1. Biomarker of OP exposure.....	347
6.2. Antibodies for detection of OP exposure.....	347
6.3. Peptide scavengers for decontamination.....	347
6.4. Understanding low dose toxicity.....	347
6.5. Treatment of low dose toxicity.....	347
7. Conclusion.....	347
Conflict of interest statement.....	347
Acknowledgements.....	347
References.....	347

\* Corresponding author. Tel.: +1 402 559 6032; fax: +1 402 559 4651.  
E-mail addresses: [olockrid@unmc.edu](mailto:olockrid@unmc.edu) (O. Lockridge), [lschopf@unmc.edu](mailto:lschopf@unmc.edu) (L.M. Schopfer).

## 1. Introduction

### 1.1. Historical perspective on OP binding to the active site serine in the serine hydrolase superfamily

In 1953, scientists knew that organophosphorus agents irreversibly inhibit chymotrypsin, trypsin, acetylcholinesterase, and butyrylcholinesterase (pseudocholinesterase). It was argued that the OP binding site had to be histidine. However, Norwood Schaffer isolated L-serine phosphoric acid from diisopropylfluorophosphate-inhibited chymotrypsin, thus providing the first evidence that the label was on serine [1]. This result was unacceptable to biochemists because they argued that serine could not ionize at physiological pH and therefore could not be directly involved in a reaction with OP. It was suggested that histidine was the original reactive group and that the OP was transferred from histidine to serine [2]. Labeling experiments with eel acetylcholinesterase [3], trypsin [4], horse serum butyrylcholinesterase [5], and horse liver aliesterase [6] confirmed that the OP-labeled residue in these proteins was serine. OP-labeled histidine was never found in these proteins. Determination of the crystal structure of chymotrypsin by Blow et al., led to the understanding that ionization of the active site serine was promoted by interaction with histidine and aspartic acid [7]. Thus, the concept of the catalytic triad for serine proteases and esterases was born. A catalytic triad of serine, glutamic acid, and histidine has been found in the crystal structures of acetylcholinesterase [8] and butyrylcholinesterase [9]. Today it is generally accepted that serine, in the consensus sequence GXSG, is the active site nucleophile and that this serine makes a covalent bond with organophosphorus agents directly. Covalent binding to the active site serine results in irreversible inhibition of enzymes in the serine hydrolase superfamily. It is generally accepted that the acute toxicity of OP is due to inhibition of acetylcholinesterase in nerve synapses.

## 2. OP binding to histidine

A 60 kDa glycosylated carboxylesterase isolated from rabbit liver was treated with [ $H^3$ ]-diisopropylfluorophosphate and digested with proteases [10,11]. Peptides were purified by HPLC and sequenced. Radiolabeled diisopropylphosphate was found on the active site serine as well as on the histidine of the catalytic triad. The covalent bond to histidine was stable in 88% formic acid, used during peptide purification. Covalent binding of OP to histidine had long been hypothesized but has never before or since been demonstrated to occur in a protein.

## 3. OP binding to proteins without inhibiting activity

A single tyrosine residue was covalently labeled by treatment of papain, egg-white lysozyme, and Taka-amylase A with diisopropylfluorophosphate [12–14]. The OP-modified enzymes retained full activity with casein, glycol chitin, and amylose [12]. Up to four tyrosines were labeled in stem bromelain by treatment with a 400-fold molar excess of diisopropylfluorophosphate in pH 8.2 buffer [15]. Activity toward casein was unaffected. At pH 11 one tyrosine and three additional residues, that were not tyrosine, were modified by treatment of egg-white lysozyme with a 300-fold molar excess of diisopropylfluorophosphate [14]. At pH 9.5 only one residue was labeled, and that residue was tyrosine. The organophosphorylated lysozyme retained full activity on glycol chitin and p-nitrophenyl acetate, but showed 25% decrease in lytic activity on *Micrococcus lysodeikticus* cells.

## 4. OP binding to tyrosine

### 4.1. Low dose toxicity

Low doses of OP that do not inhibit acetylcholinesterase nevertheless cause cognitive deficits in some people. Epidemiologists have linked chronic low dose OP exposure to Parkinson's disease, neurologic dysfunction, Gulf War Illness [16], and depression [16–19].

Bronchoconstriction is caused by low doses of organophosphorus pesticides that inhibit M2 muscarinic receptor function without inhibiting acetylcholinesterase activity [20]. M2 muscarinic receptors covalently bind chlorpyrifos oxon [21] at an unknown site. The M2 muscarinic receptor has no active site serine. Therefore it is a clear example of a protein outside the serine hydrolase superfamily for which reaction with low doses of OP disrupts function.

Chlorpyrifos oxon, at concentrations far below those required to inhibit acetylcholinesterase, reduces neurite outgrowth in primary cultures of sympathetic neurons derived from the embryonic rat superior cervical ganglia. This is an example of disruption of neuron morphogenesis by doses of OP too low to bind to the classical active site serine [22].

Proteins important for axonal transport have been implicated in neurodegenerative diseases [23] and are prime candidates for proteins responsible for OP low dose neurotoxicity. Neurons rely heavily on phosphorylation-dependent intracellular signaling mechanisms [23], suggesting that irreversible OP binding to a site that is normally reversibly phosphorylated will result in neuron dysfunction. If multiple proteins are involved, it follows that different OP will react differently with the different targets, and that the identity of the OP target will depend on the identity of the OP.

### 4.2. Albumin

Our search for additional OP targets was begun by treating live mice with a biotin-labeled OP called FP-biotin [24]. Doses of FP-biotin that did not inhibit acetylcholinesterase were found to label albumin. Mass spectral analysis of pure human albumin, pure mouse albumin, and human plasma identified tyrosine 411 as the amino acid that is labeled by soman, sarin, chlorpyrifos oxon, dichlorvos, diisopropylfluorophosphate, and FP-biotin [25,26]. Additional tyrosines as well as serines are labeled when the experimental conditions are maximized, but tyrosine 411 is always the most reactive residue in human albumin [27,28].

Human plasma treated ex vivo with OP was found to have OP-labeled albumin [25]. Human plasma from individuals who attempted suicide by drinking dichlorvos had dichlorvos-labeled albumin in their blood; the OP label was on tyrosine 411 (Li et al., unpublished). Live guinea pigs treated with nerve agents had OP-labeled tyrosine in plasma digests, the tyrosine presumably originating from albumin [29,30].

OP-albumin adducts on tyrosine have several advantages over OP-cholinesterase as biomarkers of OP exposure. The OP-tyrosine adduct on albumin is more stable than the OP-serine adduct on butyrylcholinesterase as shown by the finding that OP-tyrosine is detectable in guinea pigs 24 days after treatment with nerve agents, at a time when OP-butyrylcholinesterase is undetectable [29]. In vitro studies have shown that the half-life of the tyrosine 411 adduct with soman is 20 days at pH 7.4 and 22 °C [26]. The chlorpyrifos oxon adduct on tyrosine 411 of human albumin loses only 25% of the OP after 8 months incubation at pH 7.4 and 22 °C [28]. The stability of the OP-tyrosine adduct makes OP-albumin a suitable biomarker of exposure to OP nerve agents and OP pesticides.

Another characteristic of OP-tyrosine adducts is that they do not age [25,26,30–32]. For example, the pinacolyl group of soman is retained in the soman-tyrosine adduct [26]. This contrasts with

soman-serine adducts on cholinesterases which lose the pinacolyl group about 2 min after covalent binding to the active site serine. Thus, the character of the OP-albumin adduct is more closely akin to that of the original OP than is the OP-cholinesterase adduct. This makes identification of the original OP more reliable.

Oxime therapy displaces the OP from serine, but not from tyrosine [29]. Therefore, identification of the OP to which a patient was exposed can be made after the patient has been treated with oxime.

#### 4.3. Tubulin

OP-labeling of albumin is not an explanation for low dose toxicity. However, covalent binding of OP to tyrosine in albumin suggests that proteins other than the serine hydrolases could be involved in low dose OP toxicity. Tubulin is a candidate protein for this role. Tubulin polymerizes to microtubules. Microtubules play an integral part in axonal transport, and behavioral studies correlate chronic low dose chlorpyrifos exposure with cognitive dysfunction and with disruptions in axonal transport [33,34]. Microtubules are essential for the architecture of neuronal cells, as well as for transport of cell organelles from the cell body to the axon. Drugs such as taxol that target microtubule structure result in cell death.

Studies with pure bovine tubulin have shown that tubulin is readily labeled by chlorpyrifos oxon, soman, sarin, dichlorvos, and FP-biotin [35,36]. The labeled residues are tyrosine and lysine. Tubulin function is disrupted by OP binding as visualized by atomic force microscopy nanoimages of microtubule structure, which show that in the presence of 0.005 mM chlorpyrifos oxon, tubulin polymerizes to abnormally short microtubules [37]. Mice treated with chlorpyrifos at a dose that does not inhibit acetylcholinesterase have diethoxyphosphorylated tubulin in the brain [38].

A broader view of low dose toxicity suggests that OP may be modifying many proteins associated with tubulin in addition to tubulin itself, and that OP modification of these axonal transport proteins results in the loss of synaptic function, alterations in axonal connectivity, and finally in cell death [23,39,40].

#### 4.4. OP binding to tyrosine as a general phenomenon

The question arose whether OP binding to albumin and tubulin was a special case or whether other proteins could also make

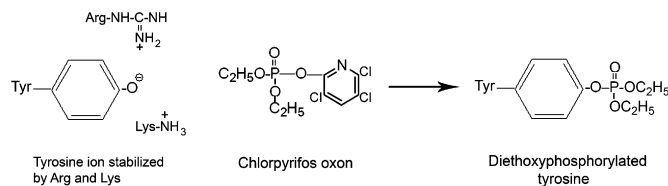


**Fig. 1.** Reaction of tyrosinate anion with chlorpyrifos oxon to yield diethoxyphosphorylated tyrosine. The anion of tyrosine is stabilized by interaction with positively charged arginine and lysine side chains. The tyrosine anion reacts with chlorpyrifos oxon to make a covalent bond with diethoxyphosphate while displacing 3,5,6-trichloro-2-pyridinol.

a covalent bond with OP. Purified proteins were treated with diisopropylfluorophosphate, chlorpyrifos oxon, FP-biotin, soman, or sarin and the labeled peptide and labeled amino acid were identified by mass spectrometry. Table 1 summarizes the proteins and the OP-modified tyrosines in proteins that have been identified to date. Only the most reactive tyrosine, Tyr 411, is listed in Table 1 for human albumin. Additional OP-labeled tyrosines in human albumin can be found in Ding et al. [28]. A more complete list of proteins labeled by OP on tyrosine and the sequences of OP-labeled peptides is found in Schopfer et al. [41]. It is concluded that OP binding to tyrosine is a general phenomenon. Many proteins can be labeled on tyrosine by OP.

Not all tyrosines in a protein are labeled by OP. The most reactive tyrosines are accessible to solvent and are presumably in an environment that stabilizes the ionized form of the phenolic group of tyrosine. Table 1 summarizes the amino acid sequences around the OP-labeled tyrosines. There is no consensus sequence for the reactive tyrosines, but a positively charged group (Arg, Lys and His) is usually present within five residues of the reactive tyrosine. The nearby positively charged residue could stabilize the tyrosinate form of the tyrosine making it a better nucleophile in reactions with OP (Fig. 1).

The proteins in Table 1 react slowly with OP compared to the rate of reaction of OP with the cholinesterases. The fact that a particular tyrosine in albumin is more reactive than other tyrosines suggests that the reactivity of tyrosine is enhanced by its environment. This further suggests that proteins with even higher reactivity than albumin may exist. If these proteins are in low abundance but have an essential physiological function, then OP binding to such proteins could contribute to low dose toxicity.

**Table 1**  
Proteins labeled by OP on tyrosine.

Protein	Accession number	OP-labeled tyrosine	Reference
Human albumin	gi 28592	NALLVRY <sub>411</sub> TKKVPQ	[25,27]
Bovine albumin	gi 30794280	NALIVRY <sub>410</sub> TRKVPQ	[45]
Guinea pig albumin	gi 33518896	NALAVRY <sub>411</sub> TQKAPQ	[29]
Mouse albumin	gi 3647327	NAILVRY <sub>411</sub> TQKAPQ	Present report
Mouse albumin	gi 3647327	YEKLGEY <sub>401</sub> GFQNAI	Present report
Bovine tubulin alpha	gi 73586894	EVRTGTY <sub>83</sub> RQLFHP	[36]
Bovine tubulin beta	gi 75773583	EATGGKY <sub>59</sub> VPRAVL	[36]
Bovine tubulin beta	gi 75773583	SRGSQQY <sub>281</sub> RALTVP	[36]
Bovine tubulin beta	gi 75773583	SKIREEY <sub>159</sub> PDRIMN	[36]
Mouse tubulin beta	gi 21746161	LERINVY <sub>50</sub> Y <sub>51</sub> NEATGN	[41]
Human transferrin	gi 136191	RKPVDEY <sub>257</sub> KDCHLA	[46]
Human transferrin	gi 136191	RKPVVEY <sub>593</sub> ANCHLA	[46]
Human kinesin 3C motor domain	gi 160286524	YLVRSAY <sub>157</sub> LEIYQE	[47]
Mouse transferrin	gi 21363012	RKPVDQY <sub>257</sub> EDCY <sub>261</sub> LARIPS	[46]
Mouse transferrin	gi 21363012	RMDYRLY <sub>333</sub> LGHNY <sub>338</sub> VTAINR	[46]
Mouse transferrin	gi 21363012	GIFPKGY <sub>448</sub> Y <sub>449</sub> AVAVVK	[46]
Mouse transferrin	gi 21363012	QGCAPGY <sub>510</sub> EKNSTL	[46]
Mouse transferrin	gi 21363012	PNNKEEY <sub>534</sub> NGY <sub>537</sub> TGAFCR	[46]
Mouse ATP synthase	gi 20455479	QKILQDY <sub>431</sub> KSLQDI	[47]
Papain	gi 129614	NEGALLY <sub>256</sub> SIANQP	[13]

Numbering for residues in albumin is for mature albumin minus the signal peptide. Numbering for other proteins uses Met in the signal peptide as residue 1. Accession numbers are from the NCBI nonredundant protein database.

#### 4.5. OP binding to free tyrosine and to tyrosine in short peptides

Free tyrosine in pH 7 buffer is labeled by DFP, but is not labeled by paraoxon (E600) [42]. Short peptides containing four to five amino acids including tyrosine are readily labeled by OP when the peptide is treated with a 10-fold molar excess of OP in 10 mM Tris–Cl pH 8.0 or in 10 mM ammonium bicarbonate pH 8.3. For example, a 1 mg/ml solution of peptide RYGRK (1.47 mM) treated with 14.7 mM soman for 2 days at 37 °C labels up to 80% of the tyrosine in that peptide.

#### 5. OP binding to lysine

Mass spectrometry analysis of purified proteins treated with chlorpyrifos oxon or diisopropylfluorophosphate identified OP-labeled lysine. OP-labeled lysines were found in human albumin, human keratins 1 and 10, bovine tubulin alpha and beta, bovine actin, and mouse transferrin [43]. These same proteins also had OP-labeled tyrosine.

Lysine acetylation contributes to RNA splicing, regulation of the cell cycle, chromatin remodeling, DNA replication, transcription, actin cytoskeleton remodeling, nuclear transport, and the function of chaperone proteins [44]. Binding of OP to lysine could interfere with acetylation of lysine and therefore with the function of proteins involved in biological processes.

#### 6. Potential applications and significance of the new OP binding motif

##### 6.1. Biomarker of OP exposure

The recognition of tyrosine 411 in albumin as a binding site for OP has led to the development of mass spectrometry assays for detection of OP-labeled albumin in animals and humans exposed to OP. Advantages of using albumin as a biomarker of exposure are (1) OP-labeled albumin is stable; (2) OP-labeled albumin does not age and (3) albumin is present in saliva, suggesting that an assay using saliva could be developed.

##### 6.2. Antibodies for detection of OP exposure

Antibodies for detection of OP-tyrosine and OP-lysine adducts could be developed. Antibodies against OP-tyrosine adducts are more likely to be useful than antibodies against OP-serine adducts because OP-tyrosine adducts are stable, whereas OP-serine adducts undergo spontaneous decay to dehydroalanine as well as to dealkylated “aged” adducts. Decay of the OP-serine adducts complicates their use as antigens for the production of OP-specific antibodies. Decay of OP-serine adducts formed in vivo reduces their potential to be identified.

##### 6.3. Peptide scavengers for decontamination

Short peptides could be developed for use as decontaminants of nerve agent spills. These short peptides would include tyrosine and positively charged amino acids to activate the tyrosine for reaction with OP.

##### 6.4. Understanding low dose toxicity

The molecular mechanism by which low dose OP exposure results in cognitive dysfunction is not yet understood. Advances in this area are slowed, because it is not yet known which proteins in the brain are involved. Progress in understanding the relationship between low dose OP exposure and disease will be accelerated

once the relevant OP-modified proteins have been identified. The new OP binding motifs to tyrosine and lysine suggest that almost any protein should be considered when searching for proteins that could be involved in low dose, OP-induced cognitive dysfunction.

#### 6.5. Treatment of low dose toxicity

Oximes do not remove the OP from binding to tyrosine. A search for methods to reverse OP binding to tyrosine could lead to a treatment for cognitive dysfunction from low dose exposure to OP.

#### 7. Conclusion

Mass spectrometry has provided conclusive proof that proteins with no active site serine covalently bind organophosphorus agents on tyrosine and lysine. This result suggests new directions to search for mechanisms of low dose OP toxicity.

#### Conflict of interest statement

The authors have no competing interests.

#### Acknowledgements

This work was supported by the U.S. Army Medical Research and Materiel Command W81XWH-07-2-0034 and the National Institutes of Health U01 NS058056 and P30CA36727.

#### References

- [1] N.K. Schaffer, S.C. May Jr., W.H. Summerson, Serine phosphoric acid from diisopropylphosphoryl chymotrypsin, *J. Biol. Chem.* 202 (1953) 67–76.
- [2] F. Bergmann, Fine structure of the active surface of cholinesterases and the mechanism of enzymatic ester hydrolysis, *Disc. Faraday Soc.* 20 (1955) 126–134.
- [3] N.K. Schaffer, S.C. May Jr., W.H. Summerson, Serine phosphoric acid from diisopropylphosphoryl derivative of eel cholinesterase, *J. Biol. Chem.* 206 (1954) 201–207.
- [4] G.H. Dixon, D.L. Kauffman, H. Neurath, Amino acid sequence in the region of diisopropyl phosphoryl binding in DIP-trypsin, *J. Am. Chem. Soc.* 80 (1958) 1260–1261.
- [5] H.S. Jansz, D. Brons, M.G. Warringa, Chemical nature of the DFP-binding site of pseudocholinesterase, *Biochim. Biophys. Acta* 34 (1959) 573–575.
- [6] H.S. Jansz, C.H. Posthumus, J.A. Cohen, On the active site of horse-liver aliesterase. II. Amino acid sequence in the DFP-binding site of the enzyme, *Biochim. Biophys. Acta* 33 (1959) 396–403.
- [7] D.M. Blow, J.J. Birktoft, B.S. Hartley, Role of a buried acid group in the mechanism of action of chymotrypsin, *Nature* 221 (1969) 337–340.
- [8] J.L. Sussman, M. Harel, F. Frolow, C. Oefner, A. Goldman, L. Toker, I. Silman, Atomic structure of acetylcholinesterase from *Torpedo californica*: a prototypic acetylcholine-binding protein, *Science* 253 (1991) 872–879.
- [9] Y. Nicolet, O. Lockridge, P. Masson, J.C. Fontecilla-Camps, F. Nachon, Crystal structure of human butyrylcholinesterase and of its complexes with substrate and products, *J. Biol. Chem.* 278 (2003) 41141–41147.
- [10] G. Korza, J. Ozols, Complete covalent structure of 60-kDa esterase isolated from 2,3,7,8-tetrachlorodibenzo-p-dioxin-induced rabbit liver microsomes, *J. Biol. Chem.* 263 (1988) 3486–3495.
- [11] J. Ozols, Isolation and characterization of a 60-kilodalton glycoprotein esterase from liver microsomal membranes, *J. Biol. Chem.* 262 (1987) 15316–15321.
- [12] T. Murachi, A general reaction of diisopropylphosphorofluoridate with proteins without direct effect on enzymic activities, *Biochim. Biophys. Acta* 71 (1963) 239–241.
- [13] I.M. Chaiken, E.L. Smith, Reaction of a specific tyrosine residue of papain with diisopropylfluorophosphate, *J. Biol. Chem.* 244 (1969) 4247–4250.
- [14] T. Murachi, T. Miyake, N. Yamasaki, Alkylphosphorylation of hen egg-white lysozyme by diisopropylphosphorofluoridate, *J. Biochem.* 68 (1970) 239–244.
- [15] T. Murachi, T. Inagami, M. Yasui, Evidence for alkylphosphorylation of tyrosyl residues of stem bromelain by diisopropylphosphorofluoridate, *Biochemistry* 4 (1965) 2815–2825.
- [16] R. Toomey, R. Alpern, J.J. Vasterling, D.G. Baker, D.J. Reda, M.J. Lyons, W.G. Henderson, H.K. Kang, S.A. Eisen, F.M. Murphy, Neuropsychological functioning of U.S. Gulf War veterans 10 years after the war, *J. Int. Neuropsychol. Soc.* 15 (2009) 717–729.
- [17] F. Kamel, L.S. Engel, B.C. Gladen, J.A. Hoppin, M.C. Alavanja, D.P. Sandler, Neurologic symptoms in licensed pesticide applicators in the Agricultural Health Study, *Hum. Exp. Toxicol.* 26 (2007) 243–250.

- [18] C.L. Beseler, L. Stallones, J.A. Hoppin, M.C. Alavanja, A. Blair, T. Keefe, F. Kamel, Depression and pesticide exposures among private pesticide applicators enrolled in the Agricultural Health Study, *Environ. Health Perspect.* 116 (2008) 1713–1719.
- [19] D.B. Hancock, E.R. Martin, G.M. Mayhew, J.M. Stajich, R. Jewett, M.A. Stacy, B.L. Scott, J.M. Vance, W.K. Scott, Pesticide exposure and risk of Parkinson's disease: a family-based case-control study, *BMC Neurol.* 8 (2008) 6.
- [20] P.J. Lein, A.D. Fryer, Organophosphorus insecticides induce airway hyperreactivity by decreasing neuronal M2 muscarinic receptor function independent of acetylcholinesterase inhibition, *Toxicol. Sci.* 83 (2005) 166–176.
- [21] J.A. Bomser, J.E. Casida, Diethylphosphorylation of rat cardiac M2 muscarinic receptor by chlorpyrifos oxon in vitro, *Toxicol. Lett.* 119 (2001) 21–26.
- [22] A.S. Howard, R. Bucelli, D.A. Jett, D. Bruun, D. Yang, P.J. Lein, Chlorpyrifos exerts opposing effects on axonal and dendritic growth in primary neuronal cultures, *Toxicol. Appl. Pharmacol.* 207 (2005) 112–124.
- [23] G.A. Morfini, M. Burns, L.I. Binder, N.M. Kanaan, N. LaPointe, D.A. Bosco, R.H. Brown Jr., H. Brown, A. Tiwari, L. Hayward, J. Edgar, K.A. Nave, J. Garberrn, Y. Atagi, Y. Song, G. Pigino, S.T. Brady, Axonal transport defects in neurodegenerative diseases, *J. Neurosci.* 29 (2009) 12776–12786.
- [24] E.S. Peeples, L.M. Schopfer, E.G. Duysen, R. Spaulding, T. Voelker, C.M. Thompson, O. Lockridge, Albumin, a new biomarker of organophosphorus toxicant exposure, identified by mass spectrometry, *Toxicol. Sci.* 83 (2005) 303–312.
- [25] B. Li, L.M. Schopfer, S.H. Hinrichs, P. Masson, O. Lockridge, Matrix-assisted laser desorption/ionization time-of-flight mass spectrometry assay for organophosphorus toxicants bound to human albumin at Tyr411, *Anal. Biochem.* 361 (2007) 263–272, PMID: 1828685.
- [26] B. Li, F. Nachon, M.T. Froment, L. Verdier, J.C. Debouzy, B. Brasme, E. Gillon, L.M. Schopfer, O. Lockridge, P. Masson, Binding and hydrolysis of soman by human serum albumin, *Chem. Res. Toxicol.* 21 (2008) 421–431.
- [27] G.E. Means, H.L. Wu, The reactive tyrosine residue of human serum albumin: characterization of its reaction with diisopropylfluorophosphate, *Arch. Biochem. Biophys.* 194 (1979) 526–530.
- [28] S.J. Ding, J. Carr, J.E. Carlson, L. Tong, W. Xue, Y. Li, L.M. Schopfer, B. Li, F. Nachon, O. Asajo, C.M. Thompson, S.H. Hinrichs, P. Masson, O. Lockridge, Five tyrosines and two serines in human albumin are labeled by the organophosphorus agent FP-biotin, *Chem. Res. Toxicol.* 21 (2008) 1787–1794, PMID: 2646670.
- [29] R.W. Read, J.R. Riches, J.A. Stevens, S.J. Stubbs, R.M. Black, Biomarkers of organophosphorus nerve agent exposure: comparison of phosphorylated butyrylcholinesterase and phosphorylated albumin after oxime therapy, *Arch. Toxicol.* 84 (2010) 25–36.
- [30] N.H. Williams, J.M. Harrison, R.W. Read, R.M. Black, Phosphorylated tyrosine in albumin as a biomarker of exposure to organophosphorus nerve agents, *Arch. Toxicol.* 81 (2007) 627–639.
- [31] R.M. Black, J.M. Harrison, R.W. Read, The interaction of sarin and soman with plasma proteins: the identification of a novel phosphorylation site, *Arch. Toxicol.* 73 (1999) 123–126.
- [32] T.K. Adams, B.R. Capacio, J.R. Smith, C.E. Whalley, W.D. Korte, The application of the fluoride reactivation process to the detection of sarin and soman nerve agent exposures in biological samples, *Drug Chem. Toxicol.* 27 (2004) 77–91.
- [33] A.V. Terry Jr., D.A. Gearhart, W.D. Beck Jr., J.N. Truan, M.L. Middlemore, L.N. Williamson, M.G. Bartlett, M.A. Prendergast, D.W. Sickles, J.J. Buccafusco, Chronic, intermittent exposure to chlorpyrifos in rats: protracted effects on axonal transport, neurotrophin receptors, cholinergic markers, and information processing, *J. Pharmacol. Exp. Ther.* 322 (2007) 1117–1128.
- [34] A.V. Terry Jr., J.D. Stone, J.J. Buccafusco, D.W. Sickles, A. Sood, M.A. Prendergast, Repeated exposures to subthreshold doses of chlorpyrifos in rats: hippocampal damage, impaired axonal transport, and deficits in spatial learning, *J. Pharmacol. Exp. Ther.* 305 (2003) 375–384.
- [35] H. Grigoryan, L.M. Schopfer, E.S. Peeples, E.G. Duysen, M. Grigoryan, C.M. Thompson, O. Lockridge, Mass spectrometry identifies multiple organophosphorylated sites on tubulin, *Toxicol. Appl. Pharmacol.* 240 (2009) 149–158, NIHMS: 135197.
- [36] H. Grigoryan, L.M. Schopfer, C.M. Thompson, A.V. Terry, P. Masson, O. Lockridge, Mass spectrometry identifies covalent binding of soman, sarin, chlorpyrifos oxon, diisopropyl fluorophosphate, and FP-biotin to tyrosines on tubulin: a potential mechanism of long term toxicity by organophosphorus agents, *Chem. Biol. Interact.* 175 (2008) 180–186, PMID: 2577157.
- [37] H. Grigoryan, O. Lockridge, Nanoimages show disruption of tubulin polymerization by chlorpyrifos oxon: Implications for neurotoxicity, *Toxicol. Appl. Pharmacol.* 240 (2009) 143–148, NIHMS: 134468.
- [38] W. Jiang, E.G. Duysen, H. Hansen, L. Shlyakhtenko, L.M. Schopfer, O. Lockridge, Mice treated with chlorpyrifos or chlorpyrifos oxon have organophosphorylated tubulin in the brain and disrupted microtubule structures, suggesting a role for tubulin in neurotoxicity associated with exposure to organophosphorus agents, *Toxicol. Sci.* (2010).
- [39] D.A. Gearhart, D.W. Sickles, J.J. Buccafusco, M.A. Prendergast, A.V. Terry Jr., Chlorpyrifos, chlorpyrifos-oxon, and diisopropylfluorophosphate inhibit kinesin-dependent microtubule motility, *Toxicol. Appl. Pharmacol.* 218 (2007) 20–29.
- [40] M.A. Prendergast, R.L. Self, K.J. Smith, L. Ghayoumi, M.M. Mullins, T.R. Butler, J.J. Buccafusco, D.A. Gearhart, A.V. Terry Jr., Microtubule-associated targets in chlorpyrifos oxon hippocampal neurotoxicity, *Neuroscience* 146 (2007) 330–339.
- [41] L.M. Schopfer, H. Grigoryan, B. Li, F. Nachon, P. Masson, O. Lockridge, Mass spectral characterization of organophosphate-labeled, tyrosine-containing peptides: characteristic mass fragments and a new binding motif for organophosphates, *J. Chromatogr. B: Anal. Technol. Biomed. Life Sci.* (in press).
- [42] R.F. Ashbolt, H.N. Rydon, The action of diisopropyl phosphorofluoridate and other anticholinesterases on amino acids, *Biochem. J.* 66 (1957) 237–242.
- [43] H. Grigoryan, B. Li, W. Xue, M. Grigoryan, L.M. Schopfer, O. Lockridge, Mass spectral characterization of organophosphate-labeled lysine in peptides, *Anal. Biochem.* 394 (2009) 92–100.
- [44] C. Choudhary, C. Kumar, F. Gnad, M.L. Nielsen, M. Rehman, T.C. Walther, J.V. Olsen, M. Mann, Lysine acetylation targets protein complexes and co-regulates major cellular functions, *Science* 325 (2009) 834–840.
- [45] L.M. Schopfer, M.M. Champion, N. Tamblin, C.M. Thompson, O. Lockridge, Characteristic mass spectral fragments of the organophosphorus agent FP-biotin and FP-biotinylated peptides from trypsin and bovine albumin (Tyr410), *Anal. Biochem.* 345 (2005) 122–132.
- [46] B. Li, L.M. Schopfer, H. Grigoryan, C.M. Thompson, S.H. Hinrichs, P. Masson, O. Lockridge, Tyrosines of human and mouse transferrin covalently labeled by organophosphorus agents: a new motif for binding to proteins that have no active site serine, *Toxicol. Sci.* 107 (2009) 144–155, PMID: 2638647.
- [47] H. Grigoryan, B. Li, E.K. Anderson, W. Xue, F. Nachon, O. Lockridge, L.M. Schopfer, Covalent binding of the organophosphorus agent FP-biotin to tyrosine in eight proteins that have no active site serine, *Chem. Biol. Interact.* 180 (2009) 492–498, PMID: 2700782.

# Pseudo-esterase Activity of Human Albumin

## SLOW TURNOVER ON TYROSINE 411 AND STABLE ACETYLATION OF 82 RESIDUES INCLUDING 59 LYSINES<sup>\*[5]</sup>

Received for publication, April 2, 2008, and in revised form, June 2, 2008. Published, JBC Papers in Press, June 24, 2008, DOI 10.1074/jbc.M802555200

Oksana Lockridge<sup>‡</sup>, Weihua Xue<sup>‡</sup>, Andrea Gaydoss<sup>§</sup>, Hasmik Grigoryan<sup>‡</sup>, Shi-Jian Ding<sup>¶</sup>, Lawrence M. Schopfer<sup>‡</sup>, Steven H. Hinrichs<sup>¶</sup>, and Patrick Masson<sup>||1</sup>

From the <sup>‡</sup>Eppley Institute, <sup>§</sup>Environmental Health and Toxicology, and the <sup>¶</sup>Department of Pathology and Microbiology, University of Nebraska Medical Center, Omaha, Nebraska 68198 and the <sup>||</sup>Unité d'Enzymologie, Centre de Recherches d Service de Santé des Armées, BP87, 38702 La Tronche Cedex, France

Human albumin is thought to hydrolyze esters because multiple equivalents of product are formed for each equivalent of albumin. Esterase activity with *p*-nitrophenyl acetate has been attributed to turnover at tyrosine 411. However, *p*-nitrophenyl acetate creates multiple, stable, acetylated adducts, a property contrary to turnover. Our goal was to identify residues that become acetylated by *p*-nitrophenyl acetate and determine the relationship between stable adduct formation and turnover. Fatty acid-free human albumin was treated with 0.5 mM *p*-nitrophenyl acetate for 5 min to 2 weeks, or with 10 mM *p*-nitrophenyl acetate for 48 h to 2 weeks. Aliquots were digested with pepsin, trypsin, or GluC and analyzed by mass spectrometry to identify labeled residues. Only Tyr-411 was acetylated within the first 5 min of reaction with 0.5 mM *p*-nitrophenyl acetate. After 0.5–6 h there was partial acetylation of 16–17 residues including Asp-1, Lys-4, Lys-12, Tyr-411, Lys-413, and Lys-414. Treatment with 10 mM *p*-nitrophenyl acetate resulted in acetylation of 59 lysines, 10 serines, 8 threonines, 4 tyrosines, and Asp-1. When Tyr-411 was blocked with diisopropylfluorophosphate or chlorpyrifos oxon, albumin had normal esterase activity with  $\beta$ -naphthyl acetate as visualized on a nondenaturing gel. However, after 82 residues had been acetylated, esterase activity was almost completely inhibited. The half-life for deacetylation of Tyr-411 at pH 8.0, 22 °C was  $61 \pm 4$  h. Acetylated lysines formed adducts that were even more stable. In conclusion, the pseudo-esterase activity of albumin is the result of irreversible acetylation of 82 residues and is not the result of turnover.

Human albumin has been reported to have esterase activity with *p*-nitrophenyl acetate (1, 2),  $\alpha$ -naphthyl acetate, phenyl acetate, 1-naphthyl *N*-methylcarbamate (3),  $\beta$ -naphthyl acetate

(4), aspirin (5), ketoprofen glucuronide (6), carprofen acylglucuronide (7), cyclophosphamide (8), nicotinate esters (9), long- and short-chain fatty acid esters (10), octanoyl ghrelin (11), organophosphorus pesticides (12), carbaryl (13), *o*-nitrotrifluoroacetanilide (14), *o*-nitroacetanilide (15), and nerve agents (16).

One site in albumin is rapidly acetylated by *p*-nitrophenyl acetate, showing a burst of product, but up to 5.2 molar equivalents are incorporated when albumin is treated with a 9-fold excess of *p*-nitrophenyl [<sup>14</sup>C]acetate (1). The 5 equivalents of label are not removable by extensive dialysis. The esteratic site has been identified as Tyr-411 based on site-directed mutagenesis studies (17). Mass spectrometry (MS)<sup>2</sup> has identified Tyr-411 as the residue labeled by organophosphorus esters including diisopropylfluorophosphate (DFP), soman, sarin, dichlorvos, FP-biotin, and chlorpyrifos oxon (16, 18) confirming the report by Sanger that a tyrosine in albumin is labeled by DFP (19), and reports that a tyrosine in albumin is labeled by the nerve agents soman, sarin, cyclosarin, and tabun (20). When albumin is labeled with 1 mol of DFP, albumin loses the fast phase of its esterase activity (the burst), supporting the conclusion that DFP and *p*-nitrophenyl acetate bind to the same site, namely to Tyr-411 (21).

Our goal was to identify the additional sites labeled by *p*-nitrophenyl acetate. We wanted an explanation for the apparently inconsistent observation that albumin hydrolyzes *p*-nitrophenyl acetate at measurable rates, yet the [<sup>14</sup>C]-acetylated albumin formed by *p*-nitrophenyl acetate is a stable adduct.

### EXPERIMENTAL PROCEDURES

**Materials**—A 1 mg/ml solution of fatty acid-free human albumin (Fluka 05418, via Sigma) was dissolved in 10 mM Tris-Cl, pH 8.0. A 1 mg/ml solution of porcine pepsin (Sigma P6887) in 10 mM HCl was stored at –80 °C. Sequencing grade modified trypsin (Promega V5113) at a concentration of 20  $\mu$ g in 50  $\mu$ l of 50 mM acetic acid was stored at –80 °C. Endoproteinase GluC (*Staphylococcus aureus* protease V8) was from Worthington Biochemical Corp (Lakewood, NJ, LS003608). 1 mg of GluC powder was dissolved in 210  $\mu$ l of water, aliquoted into micro-

<sup>\*</sup> This work was supported, in whole or in part, by the National Institutes of Health NIH CounterACT U01 NS058056-02 (to O. L.) and NIH Eppley Cancer Center Grant P30CA36727. This work was also supported by U.S. Army Medical Research and Materiel Command W81XWH-07-2-0034 (to O. L.), W81XWH-06-1-0102 (to S. H. H.), and DGA Grant 03co010-05/PEA01 08 7 (to P. M.). The costs of publication of this article were defrayed in part by the payment of page charges. This article must therefore be hereby marked "advertisement" in accordance with 18 U.S.C. Section 1734 solely to indicate this fact.

<sup>[5]</sup> The on-line version of this article (available at <http://www.jbc.org>) contains supplemental Figs. S1–S3 and Table S1.

<sup>1</sup> To whom correspondence should be addressed: Eppley Institute, University of Nebraska Medical Center, Omaha, NE 68198-6805. Tel.: 402-559-6032; Fax: 402-559-4651; E-mail: olockrid@unmc.edu.

<sup>2</sup> The abbreviations used are: MS, mass spectrometry; DFP, diisopropylfluorophosphate; amu, atomic mass unit; CHCA,  $\alpha$ -cyano-4-hydroxycinnamic acid; LC/MS/MS, liquid chromatography tandem mass spectrometry; MALDI-TOF, matrix-assisted laser desorption/ionization time of flight mass spectrometry; i.d., inner diameter.

centrifuge tubes each containing 10  $\mu\text{L}$  (50  $\mu\text{g}$ ), dried in a vacuum centrifuge, and stored at  $-80^\circ\text{C}$ . A 10 mg/ml solution of  $\alpha$ -cyano-4-hydroxycinnamic acid matrix (CHCA) (Applied Biosystems) in 50% acetonitrile, 0.1% trifluoroacetic acid was stored at room temperature. A 0.1 M solution of *p*-nitrophenyl acetate (Sigma N8130) in acetonitrile was stored at  $-20^\circ\text{C}$ . DFP, a liquid with a concentration of 5.73 M, was from Sigma (D0879). Chlorpyrifos oxon (ChemService Inc. West Chester, PA; MET-674B) was dissolved in methanol to make a 1 M solution and stored at  $-80^\circ\text{C}$ .  $\beta$ -naphthyl acetate, Fast Blue RR, and fluorodinitrobenzene (>99% pure) were from Sigma. Albumin samples were concentrated in a Microcon centrifugal device with a YM10 membrane whose molecular weight cutoff was 10,000 (Millipore 42406).

**Pure Albumin Labeled with *p*-Nitrophenyl Acetate, Digested with Pepsin While Albumin Disulfides Were Intact**—1 ml of a 1 mg/ml solution of fatty acid-free human albumin (15  $\mu\text{M}$ ) in 10 mM Tris-Cl, pH 8.0 was treated with a 33-fold molar excess of *p*-nitrophenyl acetate (5  $\mu\text{L}$  of 0.1 M in acetonitrile) at  $22^\circ\text{C}$ . 1 ml of control albumin solution was treated with 5  $\mu\text{L}$  of acetonitrile. A 50- $\mu\text{L}$  aliquot was removed into 50  $\mu\text{L}$  of 1% trifluoroacetic acid containing 2  $\mu\text{L}$  of 1 mg/ml pepsin after 5, 10, 15, 20, 30, 40, 50, 60 min, 6 h, 24 h, 9 days, and 14 days. The drop in pH to 1.4 stopped the reaction with *p*-nitrophenyl acetate. Digestion with pepsin was at  $37^\circ\text{C}$  for 1 to 2 h. A 0.5- $\mu\text{L}$  aliquot of the digest was spotted on a MALDI target plate, dried, and overlaid with 0.5  $\mu\text{L}$  of CHCA matrix, for analysis in a MALDI-TOF/TOF 4800 mass spectrometer.

**Absorbance at 400 nm to Measure *p*-Nitrophenolate Produced by Albumin Hydrolysis of *p*-Nitrophenyl Acetate**—1 ml of 1 mg/ml human albumin in 10 mM Tris-Cl, pH 8.0 was incubated with 5  $\mu\text{L}$  of 0.1 M *p*-nitrophenyl acetate at  $22^\circ\text{C}$ . At various times after mixing, a 50- $\mu\text{L}$  aliquot was withdrawn and diluted to 2 ml for measurement of absorbance at 400 nm. The reaction was followed until all of the *p*-nitrophenyl acetate was consumed. A control sample, without albumin, was followed in a similar manner to measure spontaneous hydrolysis of *p*-nitrophenyl acetate, in 10 mM Tris-Cl, pH 8.0. The amount of *p*-nitrophenolate ion formed in the albumin reaction was corrected for spontaneous hydrolysis.

The extinction coefficient for the *p*-nitrophenolate ion at pH 8.0 is  $16,900\text{ M}^{-1}\text{ cm}^{-1}$  at 400 nm (1). Therefore, the completely hydrolyzed 500  $\mu\text{M}$  *p*-nitrophenyl acetate should have an absorbance at 400 nm of 8.45.

**Albumin Incubated with Potassium Acetate**—To determine whether acetylation of lysines was accomplished by reaction with *p*-nitrophenyl acetate or by reaction with free acetate, we measured acetylated lysines after incubation of albumin with potassium acetate. 1 ml of 1 mg/ml albumin in 10 mM Tris-Cl, pH 8.0 was incubated with 500  $\mu\text{M}$  potassium acetate for 15 h at  $22^\circ\text{C}$ . A 50- $\mu\text{L}$  aliquot of the reaction mixture was removed into 50  $\mu\text{L}$  of 1% trifluoroacetic acid containing 2  $\mu\text{L}$  of 1 mg/ml pepsin and incubated for 2 h at  $37^\circ\text{C}$ . The digest was analyzed with a MALDI-TOF-TOF 4800 mass spectrometer, with CHCA matrix.

**HPLC Purification of the 1872-amu Acetylated Peptide LVRYTKKVPQVSTPTL**—This peptide was purified to make it possible to get an MS/MS spectrum of acetylated YTK. The

acetylated YTK peptide ionized in the mass spectrometer only when the number of ions in the mixture was minimal. 10 mg of human albumin in 1 ml of 10 mM Tris-Cl, pH 8.0 was treated with a 33-fold molar excess of *p*-nitrophenyl acetate for 5 min. The reaction was stopped by the addition of 1 ml of 1% trifluoroacetic acid and 0.1 ml of 1 mg/ml pepsin. After 1 h at  $37^\circ\text{C}$ , the pepsin-digested albumin was purified on a Waters 625 LC system on a Phenomenex Prodigy 5 micron C18  $100 \times 4.6$  mm column. Peptides were eluted with a 60-min gradient from 0.1% trifluoroacetic acid in water to 60% acetonitrile, 0.09% trifluoroacetic acid at a flow rate of 1 ml/min. An aliquot from each 1-min fraction was spotted on a MALDI target plate to identify the fractions that contained the 1872 mass. It was found that the 1872 mass eluted with 26% acetonitrile in fractions 26 and 27. These fractions were combined, dried, and injected into the same Phenomenex column, but this time the elution solvents were 10 mM potassium phosphate pH 7.0 and acetonitrile. In a 60-min gradient from 0 to 60% acetonitrile, the 1872 mass eluted in fractions 37–44. About 5000 pmol of the purified 1872-amu peptide in 225  $\mu\text{L}$  of 50 mM ammonium bicarbonate were digested with 2  $\mu\text{g}$  of Promega trypsin for 4 h at  $37^\circ\text{C}$ , dried, dissolved in 50  $\mu\text{L}$  of 5% acetonitrile, 0.1% formic acid, and infused into the QTRAP 4000 mass spectrometer.

**Percent Acetylation Calculated from Cluster Areas in a MALDI-TOF-TOF 4800 (Applied Biosystems, Foster City) Mass Spectrometer**—Essentially salt-free 0.5- $\mu\text{L}$  samples were spotted on a MALDI target plate, air-dried, and overlaid with 0.5  $\mu\text{L}$  of 10 mg/ml CHCA in 50% acetonitrile, 0.1% trifluoroacetic acid. MS spectra were acquired with laser power at 3000 volts in positive reflector mode. Each spectrum was the average of 500 laser shots. The percentage of acetylation was calculated by dividing the cluster area of the unlabeled peptide by the sum of the cluster areas for the unlabeled and labeled peaks. The mass spectrometer was calibrated against des-Arg-bradykinin (904.468 Da), angiotensin 1 (1296.685 Da), Glu-fibrinopeptide B (1570.677 Da), and neurotensin (1672.918 Da) (Cal Mix 1 from Applied Biosystems).

**LC/MS/MS with the QTRAP 2000 and LCQ Deca XP Mass Spectrometers**—Human albumin treated with *p*-nitrophenyl acetate was denatured by boiling 10 min in the presence of 10 mM dithiothreitol, carbamidomethylated with 90 mM iodoacetamide, and dialyzed against  $2 \times 4$  liters of 10 mM ammonium bicarbonate. A 500- $\mu\text{g}$  aliquot was digested with 10  $\mu\text{g}$  of Promega trypsin overnight at  $37^\circ\text{C}$ , or with 50  $\mu\text{g}$  of GluC. The digest was dried in a vacuum centrifuge and dissolved in 5% acetonitrile, 0.1% formic acid to make 6.7 pmol/ $\mu\text{L}$ . A 10- $\mu\text{L}$  aliquot was injected into the HPLC nanocolumn (218MS3.07515 Vydac C18 polymeric rev-phase, 75  $\mu\text{m}$  i.d.  $\times$  150 mm long; P.J. Cobert Assoc, St. Louis, MO). Peptides were separated with a 90-min linear gradient from 0 to 60% acetonitrile at a flow rate of 0.3  $\mu\text{L}/\text{min}$  and electrosprayed through a fused silica emitter (360  $\mu\text{m}$  o.d., 75  $\mu\text{m}$  i.d., 15  $\mu\text{m}$  taper, New Objective) directly into the QTRAP 2000 (Applied Biosystems, Foster City, CA), a hybrid quadrupole linear ion trap mass spectrometer. An ion-spray voltage of 1900 V was maintained between the emitter and the mass spectrometer. Information-dependent acquisition was used to collect MS, enhanced MS, and MS/MS spectra for the three most intense peaks in each

cycle, having a charge of +1 to +4, a mass between 200 and 1700  $m/z$ , and an intensity >10,000 cps. All spectra were collected in the enhanced mode, using the trap function. Precursor ions were excluded for 30 s after one MS/MS spectrum had been collected. The collision cell was pressurized to 40  $\mu$ Torr with pure nitrogen and collision energies between 20 and 40 eV were determined automatically by the software based on the mass and charge of the precursor ion. The mass spectrometer was calibrated on selected fragments from the MS/MS spectrum of Glu-fibrinopeptide B. The MS/MS data were processed using Analyst 1.4.1 software and submitted to Mascot for identification of peptide sequences (22).

A pepsin digest of the same carbamidomethylated preparation was analyzed on the LCQ Deca XP mass spectrometer (Thermo-Finnigan, San Jose, CA) coupled to the Ultimate 3000 HPLC system (Dionex, Sunnyvale, CA). The 75- $\mu$ m i.d. C18 column was from LCPackings. HPLC solvents were: A) 0.1 M acetic acid and B) 80% acetonitrile, 0.1 M acetic acid. Peptides were eluted with a gradient from 0 to 55% B in 90 min. Data were collected with Xcalibur 2.0 and analyzed with OMMSA search engine (23).

**Infusion in QTRAP 4000 Mass Spectrometer**—Peptides dissolved in 50% acetonitrile, 0.1% formic acid were infused into the QTRAP 4000 (Applied Biosystems, Foster City, CA) mass spectrometer at a flow rate of 0.3  $\mu$ l/min through an 8- $\mu$ m emitter (FS360-50-8-D, New Objective) via a 25- $\mu$ l Hamilton syringe mounted on a Harvard syringe pump. 500 MS/MS spectra were accumulated for each parent ion.

**Deacetylation of Tyr-411**—The production and disappearance of acetylated Tyr-411 was followed by MALDI-TOF mass spectrometry. A 15  $\mu$ M solution of human albumin in 10 mM Tris-Cl, pH 8.0 was treated with an equimolar concentration of *p*-nitrophenyl acetate at 22 °C. After various times, a 10- $\mu$ l aliquot was mixed with 10  $\mu$ l of 1% trifluoroacetic acid and 1  $\mu$ l of 1 mg/ml pepsin. After 1–2 h at 37 °C a 0.5  $\mu$ l aliquot of the digest was spotted on a MALDI target plate. Cluster areas for the unlabeled peptides at 1717 and 1830 amu and the labeled peptides at 1759 and 1872 amu were used to calculate % labeling on Tyr-411.

**Percentage of Acetylated Lysines Calculated from Amino Acid Composition Analysis**—Quantitation of the acetylated lysine was obtained by the use of fluorodinitrobenzene (Allfrey *et al.*, Ref. 30). Fluorodinitrobenzene reacts with un-acetylated lysine to form  $\epsilon$ -N-dinitrobenzylated lysine. Acid hydrolysis, in preparation for amino acid composition analysis hydrolyzes the  $\epsilon$ -N-acetyl lysines to yield free lysine, but the dinitrobenzylated lysines are relatively stable to acid hydrolysis. The amount of free lysine appearing in the amino acid composition analysis, corrected for hydrolysis of dinitrobenzylated lysine, represents the amount of lysine that was originally acetylated.

Fluorodinitrobenzylation employs the method originally described by Sanger (24). Acetylated and control albumin were dialyzed into NaHCO<sub>3</sub> (20 mg/ml). Two hundred micrograms of dialyzed albumin were adjusted to 1 ml with NaHCO<sub>3</sub> and mixed with 2 ml of absolute ethanol. The mixture was shaken at room temperature for 1 h, at which time 30  $\mu$ l of fluorodinitrobenzene was added and that mixture shaken for an additional 2 h. The insoluble yellow product was washed twice with water,

twice with absolute ethanol, twice with diethyl ether, air-dried, and submitted for amino acid composition analysis.

**Nondenaturing Gel Electrophoresis**—Albumin esterase activity was demonstrated on a nondenaturing 4–30% polyacrylamide gradient gel, stained for esterase activity with  $\beta$ -naphthyl acetate and Fast Blue RR (25). Gels were shaken in 100 ml of 0.05 M Tris-Cl, pH 7.4 containing 50 mg of  $\beta$ -naphthylacetate in 1 ml ethanol, and 50 mg of solid Fast Blue RR. Though most of the Fast Blue RR does not dissolve, pink bands of esterase activity appear within 15–30 min. The gel was counterstained with Coomassie Blue to show protein concentration.

The positive control samples, not acetylated on any residues, were 5  $\mu$ l of human serum and 200  $\mu$ g of fatty acid-free human albumin. The negative control was albumin that had been denatured in 8 M urea, reduced with 10 mM dithiothreitol, carbamidomethylated with iodoacetamide, dialyzed to remove salts, and concentrated to 10  $\mu$ g/ $\mu$ l. Albumin acetylated on 100% of Tyr-411 only, was prepared by incubating 10 mg/ml albumin with 5 mM *p*-nitrophenyl acetate (33-fold excess) in 10 mM Tris-Cl, pH 8.0 for 5 min, followed immediately by gel electrophoresis. Albumin acetylated on 100% Tyr-411 and 20% of the lysines was prepared by incubating 1 mg/ml albumin with 0.5 mM *p*-nitrophenyl acetate for 6 h at 22 °C. Albumin with free Tyr-411 and 20% acetylated lysines was prepared by incubating 1 mg/ml albumin with 0.5 mM *p*-nitrophenyl acetate, 0.01% sodium azide for 2 weeks at 22 °C, during which time Tyr-411 was completely deacetylated as shown by mass spectrometry. Albumin with 100% acetylated Tyr-411 and 60–100% acetylated lysines was prepared by incubating 1 mg/ml albumin with 10 mM *p*-nitrophenyl acetate for 48 h. Percent acetylation of Tyr-411 and lysines was determined by mass spectrometry as described above, and by amino acid composition analysis after reaction with fluorodinitrobenzene.

Albumin labeled with DFP on 80% of Tyr-411 was prepared by treating 2 mg/ml albumin with a 20-fold excess of DFP in 10 mM Tris-Cl, pH 8.0 for 2 h at 22 °C. Albumin labeled with chlorpyrifos oxon on 95% of Tyr-411 was prepared by treating 1 mg/ml albumin in 10 mM Tris-Cl, pH 8.0 with a 7.5-fold excess of chlorpyrifos oxon for 48 h at 22 °C. The percent free and modified Tyr-411 was determined by mass spectrometry. No lysines were labeled by DFP or chlorpyrifos oxon.

## RESULTS

**Tyrosine 411 Is Rapidly Acetylated by *p*-Nitrophenyl Acetate**—A 5-min reaction of albumin (15  $\mu$ M) with *p*-nitrophenyl acetate (500  $\mu$ M) results in complete acetylation of Tyr-411. This is indicated by the mass shift of +42 amu for peptic peptides VRYTKKVPQVSTPTL and LVRYTKKVPQVSTPTL (missed cleavage), which have masses of 1717 and 1830 amu in the control albumin digest (Fig. 1A), but masses of 1759 and 1872 amu after treatment with *p*-nitrophenyl acetate (Fig. 1B). No unlabeled masses at 1717 and 1830 amu remain after treatment with *p*-nitrophenyl acetate, indicating 100% labeling. No other peptides were found to have a mass shift at this time point.

The labeled residue was identified as tyrosine 411 by fragmentation of the doubly charged parent ion 936.5  $m/z$  (corresponding to the singly charged 1872 amu ion) in the QTRAP mass spectrometer. Fig. 2A shows fragmentation of parent ion

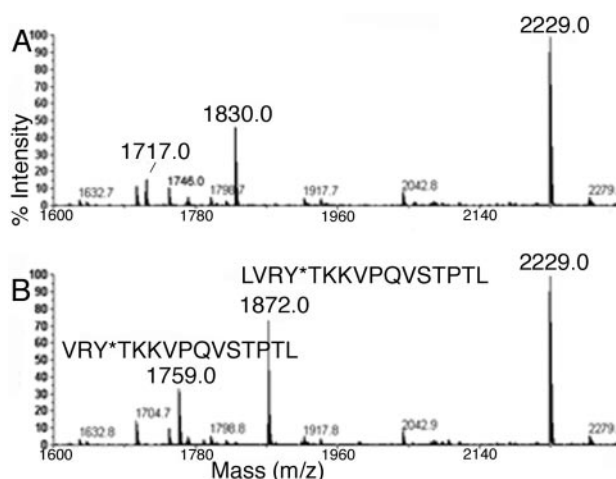


FIGURE 1. MALDI-TOF mass spectra of peptic peptides of human albumin before (A) and after (B) 5 min reaction with 0.5 mM *p*-nitrophenyl acetate. The mass of peptides at 1717 and 1830 amu increased by +42 amu due to acetylation of Tyr-411.

936.5 *m/z*. All major peaks are assigned to fragments of LVRYTKKVPQVSTPTL. The presence of the b<sub>4</sub> ion (representing residues LVRY\* plus acetyl) at 574.3 amu indicates acetylation of that fragment. The most likely candidate for acetylation is tyrosine. The b<sub>4</sub>–17 ion at 557.3 amu, and the b-ion fragments b<sub>5</sub> ion at 675.3 amu through b<sub>13</sub>–18 at 1524.8 amu are all 42 amu larger than predicted from the amino acid sequence, further supporting acetylation of tyrosine in LVRYTKKVPQVSTPTL.

To obtain additional support for acetylation on tyrosine, peptide LVRYTKKVPQVSTPTL from Fig. 2A was purified by HPLC, digested with trypsin, and analyzed by mass spectrometry. Fig. 2B shows fragmentation of the 453.2 amu singly charged parent ion. The labeled peaks in the spectrum support the sequence YTK where the acetyl group is on the phenolic oxygen of Tyr-411. The mass at 178.1 is the *O*-acetyl-tyrosine immonium ion. The 178.1 mass was found in other peptides that had an acetylated tyrosine. A peak at 178.1 can be used as a marker for *O*-acetylated tyrosine.

There is no possibility that the acetyl group is on the amino group of tyrosine, because the reaction with *p*-nitrophenyl acetate was performed while the amino group of Tyr-411 was in a peptide bond and therefore unavailable for modification. Taken together, the data indicate that Tyr-411 is the first albumin residue to be acetylated by *p*-nitrophenyl acetate.

**Lysine 413 and Lysine 414 Are Slowly Acetylated by *p*-Nitrophenyl Acetate**—After 6 h of reaction of 15  $\mu$ M albumin with 500  $\mu$ M *p*-nitrophenyl acetate, a second and third site on peptides VRYTKKVPQVSTPTL and LVRYTKKVPQVSTPTL were acetylated, as indicated by peaks with mass shifts of +42, +84, and +126 amu. The 1717 amu peak (supplemental Fig. S1A) shifted to 1759 amu, 1801 amu, and 1843 amu (supplemental Fig. S1B), while the 1830 amu peak shifted to 1872, 1914, and 1956 amu (supplemental Fig. S1B). At 6 h, about 50% of peptides VRYTKKVPQVSTPTL and LVRYTKKVPQVSTPTL were labeled with one acetate, about 50% with 2 acetates, and 1–2% with 3 acetates (percentage estimates are based on the cluster areas of the peaks). The percentage of acetylated pep-

tides did not increase after 6 h, because 90% of the *p*-nitrophenyl acetate had been hydrolyzed by that time. The possibility that acetate (rather than *p*-nitrophenyl acetate) might be acetylating lysines was ruled out by the finding that no mass shifts occurred when 1 mg/ml albumin was treated with 0.5 mM potassium acetate.

Peptides VRYTKKVPQVSTPTL and LVRYTKKVPQVSTPTL with a mass shift of +84 amu were acetylated on Tyr-411 and Lys-413, or on Tyr-411 and Lys-414. Supplemental Fig. S2 shows the MS/MS spectrum for doubly charged parent ion 957.5 of peptide LVRYTKKVPQVSTPTL at the 6-h time point. The b<sub>4</sub> ion at 574.1 amu (representing residues LVRY\* plus 1 acetyl) and the b<sub>5</sub> ion at 675.7 amu (representing residues LVRY\*T plus 1 acetyl) support acetylation of Tyr-411. The b<sub>6</sub> ion at 844.3 amu (representing residues LVRY\*TK\* plus 2 acetyls) supports acetylation of Lys-413 in addition to Tyr-411. The existence of the b<sub>6</sub> ion mass at 803.3 amu (representing residues LVRY\*TK plus 1 acetyl) suggests that Lys-413 can appear without being acetylated. The appearance of an un-acetylated form of Lys-413 together with acetylated b<sub>7</sub> to b<sub>11</sub> ions is consistent with the second acetyl group on Lys-414. Other +84 ions were found (data not shown) where the second acetyl group was exclusively on Lys-413 or on Lys-414. Based on the relative intensities of the peaks at 803.3 and 844.3 amu, acetylated Lys-414 was more abundant than acetylated Lys-413. From the above analysis, it follows that triply acetylated peptides, with a mass shift of +126 amu, were acetylated on Tyr-411, Lys-413, and Lys-414.

**The N Terminus of Albumin, Lysine 4, Lysine 12, and Serine 5 Are Slowly Acetylated by *p*-Nitrophenyl Acetate**—Another prominent peptide in pepsin-digested albumin was DAHKSEVAHRFKDLGEENF at 2229 amu (supplemental Fig. S1A). After 6 h of reaction of 15  $\mu$ M albumin with 500  $\mu$ M *p*-nitrophenyl acetate, 20% of this peak had acquired a mass of +42 amu (supplemental Fig. S1B), 2% had acquired a mass of +84 amu, and about 0.5% had increased in mass by +126 amu. Incubation with 10 mM *p*-nitrophenyl acetate for 48 h resulted in complete disappearance of the 2229 and 2271 amu peaks and appearance of +84, +126, and +168 amu ions at 2313, 2355, and 2397 amu (data not shown). MS/MS spectra showed that the +42 amu parent ion was acetylated on Asp-1, the N terminus of albumin, the +84 amu parent ion was acetylated on Asp-1 and Lys-12, and the +126 amu ion was acetylated on Asp-1, Lys-12, and Lys-4 (data not shown).

The +168 amu ion was acetylated on Asp-1, Lys-4, Ser-5, and Lys-12 (supplemental Fig. S3). Most of the major peaks in the spectrum could be assigned to the DAHKSEVAHRFKDLGEENF peptide. The 366.1 amu mass was consistent with the b<sub>3</sub> ion (representing D\*AH plus 1 acetyl). Though histidine is a potential candidate for acetylation, *N*-acetylhistidine is unstable (26). Therefore, acetylation is on the N terminus. The mass at 536.2 amu is consistent with the b<sub>4</sub> ion (representing D\*AHK\* plus 2 acetyls). The 665.2 amu mass is consistent with the b<sub>5</sub> ion (representing D\*AHK\*S\* plus three acetyls). Additional b-ions at 794.4 amu (b<sub>6</sub>), 893.0 amu (b<sub>7</sub>), and 964.3 amu (b<sub>8</sub>) support the presence of 3 acetyls. The mass at 1296.5 amu is consistent with the y<sub>10</sub> ion (representing RFK\*DLGEENF plus 1 acetyl) where acetylation is on the lysine.

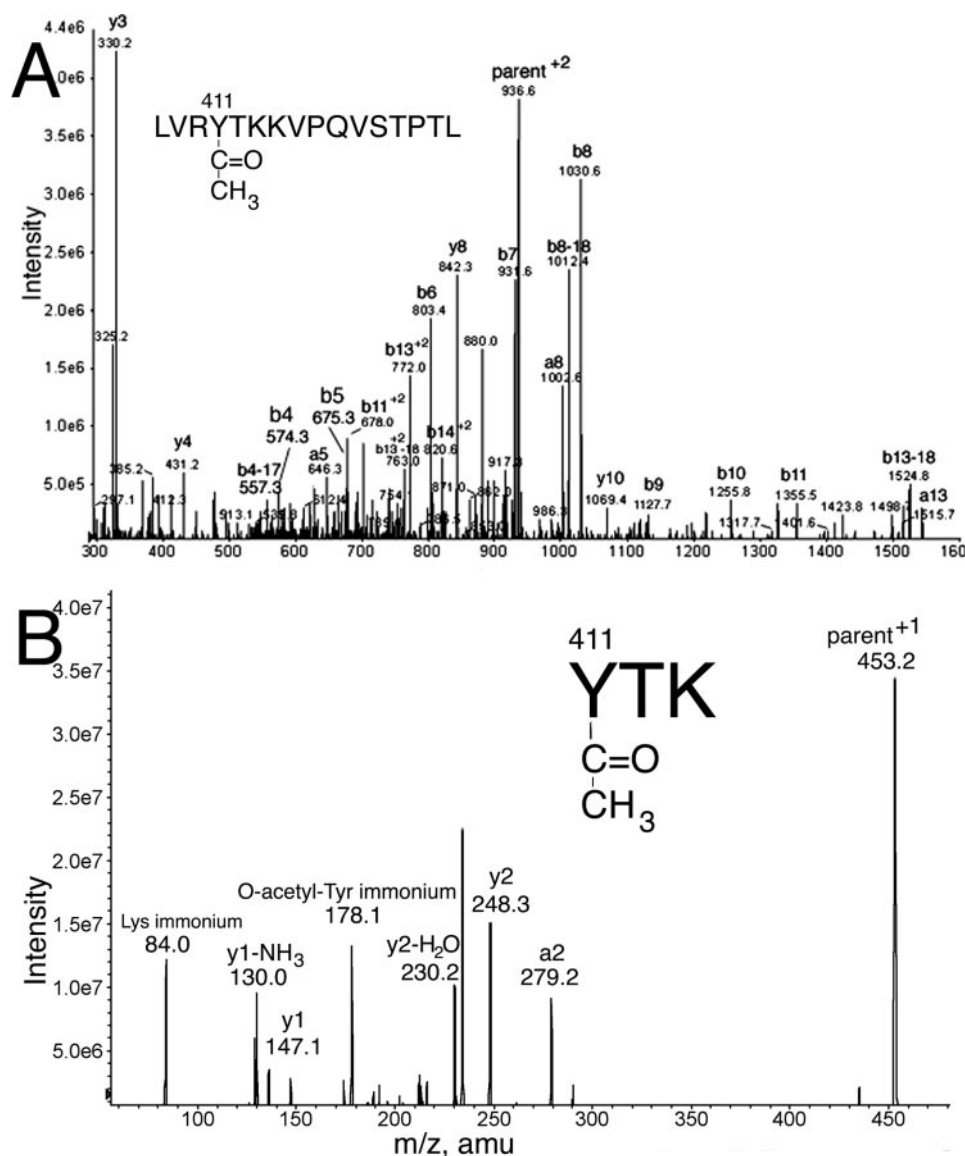


FIGURE 2. MS/MS spectra to identify the residue acetylated after 5 min reaction of 1 mg/ml albumin with 0.5 mM *p*-nitrophenyl acetate. A, fragmentation of the doubly charged form of peptide 1872 identifies acetylated Tyr 411 in LVRYTKKVPQVSTPTL. B, fragmentation of the singly charged peptide of mass 453.2 identifies acetylated Tyr-411 in YTK. The peak at 178.1 is the *O*-acetyl-tyrosine immonium ion.

Analysis of cluster areas in the MALDI-TOF spectra showed that the N-terminal Asp-1 and Lys-12 were 100% acetylated, consistent with the disappearance of peaks at 2229 and 2271 amu. About 65% of Lys-4 and 6% of Ser-5 residues were acetylated, indicating that serine is not nearly as reactive with *p*-nitrophenyl acetate as lysine.

**Residues Acetylated by 0.5 mM *p*-Nitrophenyl Acetate—**Within the first 5 min of reaction of 15  $\mu$ M albumin with 0.5 mM *p*-nitrophenyl acetate, Tyr-411 was acetylated 99–100%. No other residue was significantly acetylated within 5 min. Six hours after addition of *p*-nitrophenyl acetate, residues Asp-1, Lys-12, Lys-413, and Lys-414 were acetylated about 20–25% while Tyr-411 was still acetylated 100%. An additional 19 peptides had a mass shift of +42 amu as observed by MALDI-TOF, however peak intensities were low, and the peptide sequences could not be determined. After 50 h, all of the *p*-nitrophenol had been exhausted, and half of the Tyr-411 was free. By 2

weeks, none of the Tyr-411 was labeled. The albumin still carried a lot of label, but the label was on lysines and on the N-terminal Asp-1.

**Residues Acetylated by 10 mM *p*-Nitrophenyl Acetate—**Supplemental Table S1 lists the residues in human albumin acetylated by treatment of 15  $\mu$ M albumin with 10 mM *p*-nitrophenyl acetate at pH 8.0, 22 °C for 48 h. The Mascot search engine matched 215 peptides to albumin in accession gi:3212456, yielding 76% coverage in the tryptic digest, and matched 331 peptides for 85% coverage in the GluC digest. Three peptides from a pepsin digest are included in supplemental Table S1. MS/MS spectra were manually evaluated before a labeled peptide was included in supplemental Table S1. MS/MS spectra positively identified acetylation of 59 lysines, 10 serines, 8 threonines, 4 tyrosines, and the N-terminal aspartate. Albumin has 59 lysines; every lysine was at least partially acetylated. The 10 acetylated serines were Ser-5, Ser-65, Ser-192, Ser-202, Ser-287, Ser-312, Ser-419, Ser-427, Ser-435, and Ser-454. The 8 acetylated threonines were Thr-68, Thr-76, Thr-79, Thr-83, Thr-467, Thr-474, Thr-527, and Thr-540. The four acetylated tyrosines were Tyr-84, Tyr-161, Tyr-401, and Tyr-411. The N-terminal aspartate Asp-1 was acetylated. Tyrosine 138, the ligand binding site in subdomain IB, which is modified by metabolites of poly-

cyclic hydrocarbons (27) and by nitric oxide (28), was not modified by *p*-nitrophenyl acetate.

Both chemical and *in vivo*  $\epsilon$ -*N*-acetylation of lysines has precedent (26, 29–32). Chemical *O*-acetylation of tyrosines also has precedent (33). Reports on acetylation of serines and threonines are more rare, though indirect evidence has been reported for bovine growth hormone-treated with acetic anhydride (34).

The peptides in supplemental Table S1 do not have an acetylated Lys at the C terminus, with the exception of Lys-162. The vast majority of acetylated lysines appear as missed cleavages within the peptide. This confirms reports in the literature (29) that trypsin generally does not recognize acetylated lysine as a cleavage site.

Carbamylation by ammonium cyanate, a degradation product of urea, would add a mass of +43, a value close to the mass of +42 from acetylation. To avoid carbamylation artifacts, we did not use urea in our protocol.

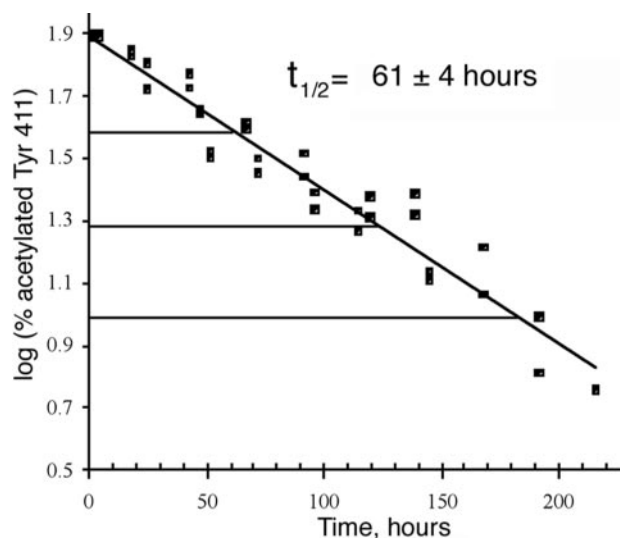


FIGURE 3. **Deacetylation rate of Tyr-411.** At time 0, Tyr-411 was acetylated 80%. After 61 h at pH 8.0, 22 °C, Tyr-411 was acetylated 40%. Deacetylation was monitored for 3.5 half-lives until only 5% of Tyr-411 was still acetylated. The three horizontal lines mark 3 half-lives. % acetylation was calculated from cluster areas in the MALDI-TOF mass spectrometer for peptides VRYT-KKVPQVSTPTL and LVRYTKKVPQVSTPTL.

**Lysines Are Stably Acetylated**—An estimate of the stability of acetylated lysines was obtained by measuring % acetylation of Lys-225 in peptide SQRFPK\*AEF with time. After 6 h of reaction of 15  $\mu$ M albumin with 0.5 mM *p*-nitrophenyl acetate, 9% of Lys-225 was acetylated. No change in % acetylation of this peptide was observed for up to 9 days. The lack of an increase in % acetylation with time is explained by the fact that 90% of the *p*-nitrophenyl acetate had been consumed after 6 h. The absence of a loss in % acetylation supports the conclusion that acetylated lysine is stable at pH 8.0. A peptide with 9% acetylated lysines was chosen for this example to make the point that a particular residue may be only partially acetylated.

A second example of stable acetylation was obtained by MALDI-TOF analysis of peptide D\*AHK\*S\*EVAHRFK\*DLG-EENF. After 48 h reaction of 15  $\mu$ M albumin with 10 mM *p*-nitrophenyl acetate, followed by dialysis to remove excess reagent, 100% of the N terminus (Asp-1), 100% of Lys-12, 78% of Lys-4, and 5% of Ser-5 were acetylated. After 18 days, the % acetylations were unchanged. We conclude that acetylated lysines, as well as the acetylated N terminus and acetylated serine, are stable at pH 8.0 and 22 °C.

**Deacetylation of Tyr-411**—Treatment of 15  $\mu$ M albumin with 15  $\mu$ M *p*-nitrophenyl acetate in 10 mM Tris-Cl, pH 8.0 resulted in exclusive acetylation of Tyr-411. No other residues were significantly acetylated. Tyr-411 was maximally acetylated after 1 h. Fig. 3 shows the maximum acetylation level of 80% and loss of the acetyl group with time. The half-life for deacetylation of Tyr-411 at pH 8.0, 22 °C was  $61 \pm 4$  h. This very slow deacetylation rate ( $k = 0.0002 \text{ min}^{-1}$ ) confirms a previous report that deacetylation is the rate-limiting step for reaction of human albumin with *p*-nitrophenyl acetate (14). On the other hand, turnover with *o*-nitrotrifluoroacetanilide is explained by the instability of the trifluoroacetyl adduct due to the electronic effect of the fluorine atoms (14).

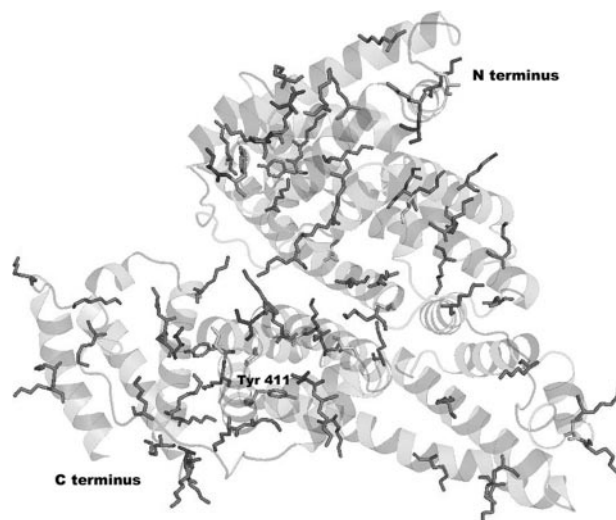


FIGURE 4. **Surface location of acetylated residues in human albumin.** The crystal structure of human albumin (Protein Data Bank code 1bm0) shows side-chains for acetylated lysines, tyrosines, serines, and threonines. Asp-1 and Lys-4 are missing from the structure (41).

**Location of Ester-reactive Residues**—The location of the reactive residues in the crystal structure of human albumin is shown in Fig. 4. All acetylated lysines, serines, and threonines are exposed to the surface. Tyr-411 is in a pocket 4.5 Å from Arg-410. Acetylated Tyr-84, -161, and -401 may also have been activated by interaction with nearby arginines.

**Time to Complete Hydrolysis of 0.5 mM *p*-Nitrophenyl Acetate**—Six hours after addition of *p*-nitrophenyl acetate to 15  $\mu$ M albumin in 10 mM Tris-Cl, pH 8.0, 22 °C, 90% of the 0.5 mM *p*-nitrophenyl acetate had been consumed, and the rate of *p*-nitrophenol production by albumin had slowed so it was indistinguishable from the rate by buffer alone. By 24 h, the end point absorbance of 8.42, at 400 nm, was reached, and no further change in absorbance was obtained. The theoretical end point calculated from the extinction coefficient of  $16,900 \text{ M}^{-1} \text{ cm}^{-1}$  for *p*-nitrophenolate ion at pH 8.0 was 8.45 (1), a value in close agreement with the observed end point.

**Percent Acetylated Lysines**—About 50% of the hydrolysis of 0.5 mM *p*-nitrophenyl acetate was due to reaction with 15  $\mu$ M albumin, and about 50% to reaction with pH 8.0 buffer. Assuming that the 250  $\mu$ M *p*-nitrophenyl acetate that reacted with 15  $\mu$ M albumin resulted in stable acetylation of albumin, one can calculate about 16–17 molar equivalents of acetate bound per mol of albumin. If 16 of 59 lysines are acetylated, then on average 27% of each lysine was acetylated. This value is close to the 20–25% acetylation calculated for Lys-414 by MALDI-TOF analysis.

A third method was used to calculate % acetylated lysines. This method is based on the principle that lysines labeled with fluorodinitrobenzene are relatively stable to acid hydrolysis, whereas acetylated lysines are deacetylated to free lysines. Standard acid hydrolysis followed by amino acid composition analysis allows an estimate of the number of acetylated lysines (30). It was found that 27% of the lysines were acetylated in albumin treated with 0.5 mM *p*-nitrophenyl acetate, while 67% of the lysines were acetylated in albumin treated with 10 mM *p*-nitrophenyl acetate.

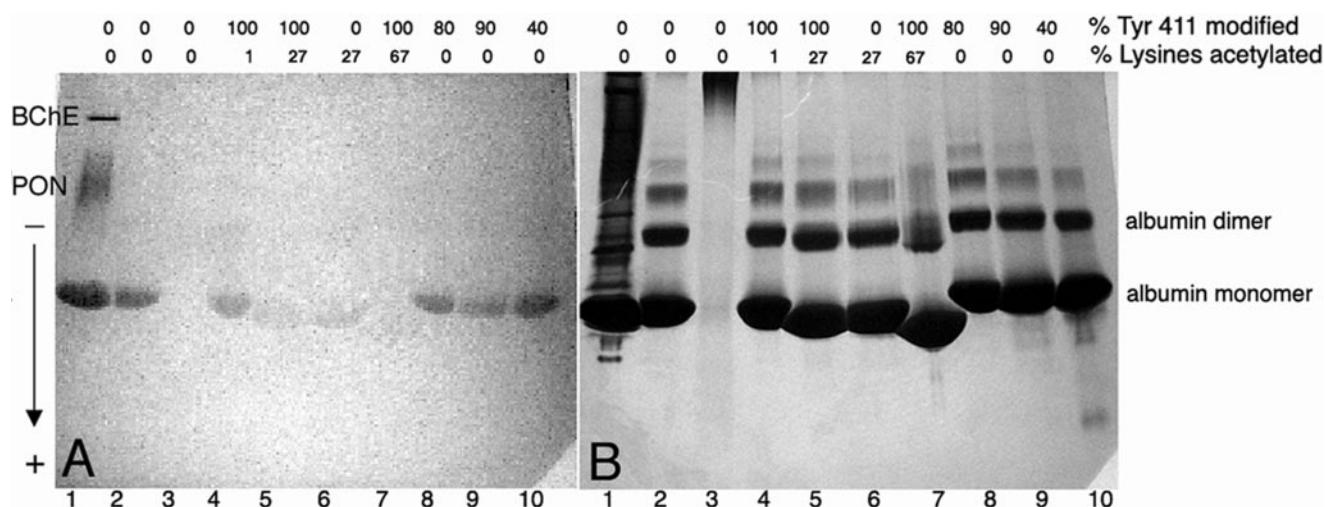


FIGURE 5. **Nondenaturing gel stained for esterase activity (A) and counterstained with Coomassie Blue (B).** Lane 1, 5  $\mu$ l of human serum where the esterase bands are butyrylcholinesterase (BChE), paraoxonase (PON), and albumin. Lane 2, 200  $\mu$ g of 99% pure fatty acid-free human albumin. Lane 3, 200  $\mu$ g of denatured, carbamidomethylated albumin. Lane 4, 200  $\mu$ g of albumin treated 5 min with 0.5 mM *p*-nitrophenyl acetate to acetylate 100% of Tyr-411. Lane 5, 200  $\mu$ g of albumin treated with 0.5 mM *p*-nitrophenyl acetate for 6 h. Lane 6, 200  $\mu$ g of albumin treated with 0.5 mM *p*-nitrophenyl acetate for 2 weeks. Lane 7, 200  $\mu$ g of albumin treated with 10 mM *p*-nitrophenyl acetate for 48 h. Lane 8, 200  $\mu$ g of albumin treated with DFP to label 80% of Tyr-411. Lane 9, 200  $\mu$ g of albumin treated with chlorpyrifos oxon to label 90% of Tyr-411. Lane 10, 200  $\mu$ g of albumin treated with chlorpyrifos oxon to label 40% of Tyr-411. The percent labeling of Tyr-411 was estimated from cluster areas of peaks in the MADLI-TOF mass spectrometer. The percent labeling of lysines was estimated from amino acid composition analysis. The arrow indicates the direction of migration of proteins on the gel.

**Esterase Activity of Albumin**—The esterase activity of human albumin can be visualized on a nondenaturing gel stained for esterase activity with  $\beta$ -naphthyl acetate and Fast Blue RR. The  $\beta$ -naphthol reacts with the diazonium salt of Fast Blue RR to produce a pink, insoluble azodye, which precipitates at the site where naphthol is released.

The gel in Fig. 5A shows naphthol production by the albumin present in 5  $\mu$ l of human plasma (lane 1), as well as by 200  $\mu$ g of pure human albumin (lane 2). Additional esterase bands in lane 1 are from butyrylcholinesterase and paraoxonase. The question of interest was how much of the apparent esterase activity of albumin was due to Tyr-411 and how much to irreversible acetylation of lysines? To answer this question, albumin preparations with various percent acetylation of Tyr-411 and lysines were loaded on the gel. The esterase activity in lane 4 where 100% of Tyr-411 was acetylated, was similar to that in lane 2 where none of the Tyr-411 was acetylated. The esterase activity in lane 5 where 100% of the Tyr-411 was acetylated, and 27% of the lysines were acetylated, was substantially decreased. The albumin in lane 6 was acetylated only on lysines, because Tyr-411 had completely deacetylated during 2 weeks incubation; the esterase activity in lane 6 was similar to that in lane 5, showing that lysines contributed more to albumin esterase activity than Tyr-411. The albumin in lane 7 was maximally acetylated by 10 mM *p*-nitrophenyl acetate, corresponding to the 82 residues acetylated in supplemental Table S1. The esterase activity in lane 7 was nearly abolished. Blocking Tyr-411 by covalent modification with DFP (lane 8) or chlorpyrifos oxon (lanes 9 and 10) had little effect on the apparent esterase activity.

The gel was counterstained with Coomassie Blue in Fig. 5B to show that protein loading per lane was equivalent. Slower migrating bands are consistent with higher molecular weight forms of albumin. Pure albumin is predominantly monomeric, but also forms dimers, and higher multimers. Fig. 5B clearly shows that the highly acetylated albumin (67%) in lane 7

migrated substantially further than native albumin in lane 2. Albumin that was 27% acetylated migrated slightly further than native. This behavior is consistent with elimination of positive charge from the protein by acetylation of the  $\epsilon$ -N-amino groups of the lysines, thus giving the acetylated protein a greater net negative charge so that it would be attracted more readily to the positively charged electrode at the bottom of the gel.

The esterase activity of albumin is characterized by an initial burst of product formation that is equal to one equivalent of albumin, followed by slower formation of multiple equivalents of product (1). The fast phase has been attributed to initial acetylation of Tyr-411 (21), which is consistent with the rapid labeling of Tyr-411 described in Fig. 1. From the activity shown in Fig. 5, it can be concluded that the apparent slow phase esterase activity of albumin is due to release of *p*-nitrophenol upon acetylation of 59 lysines, and to some extent the surface accessible serines, threonines, and other tyrosines. This myriad of acetylations creates the appearance of enzymatic turnover, but it is not a true turnover process. Lysine, serine, and threonine are acetylated but do not release the acetate. Acetylated Tyr-411 does release the bound acetate (that is, it turns over), but the release rate is too slow to account for a significant part of the apparent esterase activity of albumin in a 30-min assay. Albumin must therefore be regarded as a pseudo-esterase, not an enzymatic esterase.

## DISCUSSION

**Albumin Esterase Activity**—In our previous reports we had identified Tyr-411 as the residue in albumin that is labeled by soman, sarin, DFP, chlorpyrifos oxon, FP-biotin, and dichlorvos (16, 18). Others have also identified tyrosine as the site of covalent binding of soman, sarin, cyclosarin, and tabun to albumin (20). Organophosphorus agents inhibit the esterase activity of butyrylcholinesterase and other serine esterases by covalent binding to the active site serine (35). By analogy, we had

expected that OP binding to albumin would inhibit the esterase activity of albumin because it is commonly assumed that Tyr-411 is the active site residue on albumin that is responsible for esterase activity. The burst activity of albumin with *p*-nitrophenyl acetate is indeed inhibited by labeling Tyr-411 with an organophosphorus agent (21). However our results show that the slow steady state esterase activity of albumin is not inhibited by binding OP to Tyr-411, but instead is inhibited by acetylation of lysines. These results lead to a revised model of the esterase activity of albumin.

In this revised model of the esterase activity of albumin up to 82 residues participate. The most reactive residue is Tyr-411. Deacetylation of Tyr-411 occurs with a half-life of  $61 \pm 4$  h, which means the *p*-nitrophenolate product formed in a 30-min reaction cannot come from turnover on Tyr-411. The majority of the "esterase" activity of albumin is due to a half-reaction with lysines, serines, threonines, and tyrosines. These acetylated residues do not turnover but form stable adducts. At high *p*-nitrophenyl acetate concentration a total of 59 lysines, 10 serines, 8 threonines, 4 tyrosines, and the N-terminal aspartate are acetylated.

The lysines of albumin are acetylated by *p*-nitrophenyl acetate, but are not labeled by organophosphorus esters. We have found no evidence for labeling of lysines by organophosphorus agents.

**Confirmation of Means and Bender**—When Means and Bender (1) found stable incorporation of [ $^{14}$ C]acetate into albumin they concluded that accelerated formation of *p*-nitrophenolate ion in the presence of serum albumin was not due to increased hydrolysis, but to rapid acetylation of serum albumin by *p*-nitrophenyl acetate. Means and Bender did not identify the residues involved and therefore their conclusion has been overlooked during the past 30 years while investigators focused on Tyr-411 as the esteratic site (36). With the availability of mass spectrometry we have identified the specific residues in albumin that become acetylated by *p*-nitrophenyl acetate and therefore provide proof for the concept introduced by Means and Bender to explain albumin esterase activity. Our results support their conclusion that the overall reaction rate, as reflected by appearance of *p*-nitrophenolate ion, corresponds to the sum of a large number of simultaneous reactions at different sites on the protein plus spontaneous hydrolysis.

Additional support for the conclusion that lysines and tyrosine participate in the esterase activity of albumin comes from studies of chemically modified albumin (7). Modification of tyrosine and lysine suppressed hydrolysis of carprofen glucuronide, leading to the conclusion that Tyr and Lys have roles in hydrolysis.

**Significance**—It is expected that other esters will also acetylate albumin. Acetyl salicylic acid (aspirin) has been shown to acetylate up to 3 residues on human albumin, though only one acetylation site has been identified to date, namely Lys-199 (37–39). Though acetylation rates must be very slow, the high concentration of albumin in plasma (0.6 mM) makes these reactions pharmacologically relevant.

Albumin is unusual in the family of plasma proteins because it has no carbohydrates. This makes the amino acids of albumin more accessible to acetylation than those of a protein like

butyrylcholinesterase whose surface is sugar-coated. Nevertheless, it is possible that other proteins including butyrylcholinesterase are acetylated by carboxylic acid esters on multiple sites. Several lysines on ubiquitin are acetylated by aspirin (26). In some cases chemical acetylation has an important physiological consequence. For example, the anti-inflammatory action of aspirin is explained by acetylation of the N-terminal serine of prostaglandin synthetase (40).

**Acknowledgments**—Mass spectra and amino acid composition analysis were obtained with the support of the Mass Spectrometry and Proteomics core facility and the Protein Structure core facility at the University of Nebraska Medical Center.

## REFERENCES

- Means, G. E., and Bender, M. L. (1975) *Biochemistry* **14**, 4989–4994
- Tildon, J. T., and Ogilvie, J. W. (1972) *J. Biol. Chem.* **247**, 1265–1271
- Casida, J. E., and Augustinsson, K. B. (1959) *Biochim. Biophys. Acta* **36**, 411–426
- Morikawa, M., Inoue, M., Tsuboi, M., and Sugiura, M. (1979) *Jpn. J. Pharmacol.* **29**, 581–586
- Rainsford, K. D., Ford, N. L., Brooks, P. M., and Watson, H. M. (1980) *Eur. J. Clin. Invest.* **10**, 413–420
- Dubois-Presle, N., Lapique, F., Maurice, M. H., Fournel-Gigleux, S., Magdalou, J., Abiteboul, M., Siest, G., and Netter, P. (1995) *Mol. Pharmacol.* **47**, 647–653
- Georges, H., Presle, N., Buronfosse, T., Fournel-Gigleux, S., Netter, P., Magdalou, J., and Lapique, F. (2000) *Chirality* **12**, 53–62
- Kwon, C. H., Maddison, K., LoCastro, L., and Borch, R. F. (1987) *Cancer Res.* **47**, 1505–1508
- Salvi, A., Carrupt, P. A., Mayer, J. M., and Testa, B. (1997) *Drug Metab. Dispos.* **25**, 395–398
- Tove, S. B. (1962) *Biochim. Biophys. Acta* **57**, 230–235
- De Vriese, C., Hacquebard, M., Gregoire, F., Carpentier, Y., and Delporte, C. (2007) *Endocrinology* **148**, 2355–2362
- Sogorb, M. A., Diaz-Alejo, N., Escudero, M. A., and Vilanova, E. (1998) *Arch. Toxicol.* **72**, 219–226
- Sogorb, M. A., Carrera, V., and Vilanova, E. (2004) *Arch. Toxicol.* **78**, 629–634
- Masson, P., Froment, M. T., Darvesh, S., Schopfer, L. M., and Lockridge, O. (2007) *J. Enzyme Inhib. Med. Chem.* **22**, 463–469
- Manoharan, I., and Boopathy, R. (2006) *Arch. Biochem. Biophys.* **452**, 186–188
- Li, B., Nachon, F., Froment, M. T., Verdier, L., Debouzy, J. C., Brasme, B., Gillon, E., Schopfer, L. M., Lockridge, O., and Masson, P. (2008) *Chem. Res. Toxicol.* **21**, 421–431
- Watanabe, H., Tanase, S., Nakajou, K., Maruyama, T., Kragh-Hansen, U., and Otagiri, M. (2000) *Biochem. J.* **349**, 813–819
- Li, B., Schopfer, L. M., Hinrichs, S. H., Masson, P., and Lockridge, O. (2007) *Anal. Biochem.* **361**, 263–272
- Sanger, F. (1963) *Proc. Chem. Soc.* **5**, 76–83
- Williams, N. H., Harrison, J. M., Read, R. W., and Black, R. M. (2007) *Arch. Toxicol.* **81**, 627–639
- Means, G. E., and Wu, H. L. (1979) *Arch. Biochem. Biophys.* **194**, 526–530
- Perkins, D. N., Pappin, D. J., Creasy, D. M., and Cottrell, J. S. (1999) *Electrophoresis* **20**, 3551–3567
- Geer, L. Y., Markey, S. P., Kowalak, J. A., Wagner, L., Xu, M., Maynard, D. M., Yang, X., Shi, W., and Bryant, S. H. (2004) *J. Proteome Res.* **3**, 958–964
- Sanger, F. (1945) *Biochem. J.* **39**, 507–515
- Li, B., Sedlacek, M., Manoharan, I., Boopathy, R., Duysen, E. G., Masson, P., and Lockridge, O. (2005) *Biochem. Pharmacol.* **70**, 1673–1684
- Macdonald, J. M., LeBlanc, D. A., Haas, A. L., and London, R. E. (1999) *Biochem. Pharmacol.* **57**, 1233–1244
- Brunmark, P., Harriman, S., Skipper, P. L., Wishnok, J. S., Amin, S., and

## Pseudo-esterase Activity of Albumin

- Tannenbaum, S. R. (1997) *Chem. Res. Toxicol.* **10**, 880–886
28. Jiao, K., Mandapati, S., Skipper, P. L., Tannenbaum, S. R., and Wishnok, J. S. (2001) *Anal. Biochem.* **293**, 43–52
29. Violand, B. N., Schlittler, M. R., Lawson, C. Q., Kane, J. F., Siegel, N. R., Smith, C. E., Kolodziej, E. W., and Duffin, K. L. (1994) *Protein Sci.* **3**, 1089–1097
30. Allfrey, V. G., Di Paola, E. A., and Sterner, R. (1984) *Methods Enzymol.* **107**, 224–240
31. Lapko, V. N., Smith, D. L., and Smith, J. B. (2001) *Protein Sci.* **10**, 1130–1136
32. Gershey, E. L., Vidali, G., and Allfrey, V. G. (1968) *J. Biol. Chem.* **243**, 5018–5022
33. Riordan, J. F., and Vallee, B. L. (1972) *Methods Enzymol.* **25**, 500–506
34. Oikawa, A., Dellacha, J. M., and Sonenberg, M. (1967) *Biochem. J.* **104**, 947–952
35. Nachon, F., Asojo, O. A., Borgstahl, G. E., Masson, P., and Lockridge, O. (2005) *Biochemistry* **44**, 1154–1162
36. Sakurai, Y., Ma, S. F., Watanabe, H., Yamaotsu, N., Hirono, S., Kuroono, Y., Kragh-Hansen, U., and Otagiri, M. (2004) *Pharm. Res.* **21**, 285–292
37. Hawkins, D., Pinckard, R. N., and Farr, R. S. (1968) *Science* **160**, 780–781
38. Walker, J. E. (1976) *FEBS Lett.* **66**, 173–175
39. Yang, F., Bian, C., Zhu, L., Zhao, G., Huang, Z., and Huang, M. (2007) *J. Struct. Biol.* **157**, 348–355
40. Roth, G. J., and Siok, C. J. (1978) *J. Biol. Chem.* **253**, 3782–3784
41. Sugio, S., Kashima, A., Mochizuki, S., Noda, M., and Kobayashi, K. (1999) *Protein Eng.* **12**, 439–446



Contents lists available at ScienceDirect

## Archives of Biochemistry and Biophysics

journal homepage: [www.elsevier.com/locate/yabbi](http://www.elsevier.com/locate/yabbi)

## Review

## Butyrylcholinesterase for protection from organophosphorus poisons: Catalytic complexities and hysteretic behavior

Patrick Masson<sup>a,b</sup>, Oksana Lockridge<sup>a,\*</sup><sup>a</sup> Eppley Institute, University of Nebraska Medical Center, Omaha, NE 68198-5950, USA<sup>b</sup> Centre de Recherches du Service de Santé des Armées, Department of Toxicology, Enzymology Unit, BP 87, 38702 La Tronche Cedex, France

## ARTICLE INFO

## Article history:

Received 9 October 2009  
and in revised form 24 November 2009  
Available online 11 December 2009

## Keywords:

Bioscavenger  
Mass spectrometry  
Phosphylation  
Dehydroalanine  
Aryl acylamidase  
Hysteresis

## ABSTRACT

Butyrylcholinesterase is a promiscuous enzyme that displays complex kinetic behavior. It is toxicologically important because it detoxifies organophosphorus poisons (OP) by making a covalent bond with the OP. The OP and the butyrylcholinesterase are both inactivated in the process. Inactivation of butyrylcholinesterase has no adverse effects. However, inactivation of acetylcholinesterase in nerve synapses can be lethal. OP-inhibited butyrylcholinesterase and acetylcholinesterase can be reactivated with oximes provided the OP has not aged. Strategies for preventing the toxicity of OP include (a) treatment with an OP scavenger, (b) reaction of non-aged enzyme with oximes, (c) reactivation of aged enzyme, (d) slowing down aging with peripheral site ligands, and (e) design of mutants that rapidly hydrolyze OP. Option (a) has progressed through phase I clinical trials with human butyrylcholinesterase. Option (b) is in routine clinical use. The others are at the basic research level. Butyrylcholinesterase displays complex kinetic behavior including activation by positively charged esters, ability to hydrolyze amides, and a lag time (hysteresis) preceding hydrolysis of benzoylcholine and *N*-methylindoxyl acetate. Mass spectrometry has identified new OP binding motifs on tyrosine and lysine in proteins that have no active site serine. It is proposed, but not yet proven, that low dose exposure involves OP modification of proteins that have no active site serine.

© 2009 Elsevier Inc. All rights reserved.

## Introduction

Humans have two cholinesterases: acetylcholinesterase (AChE, accession # gi:177975)<sup>1</sup> and butyrylcholinesterase (BChE, accession # gi:116353). Acetylcholinesterase in nerve synapses terminates nerve impulse transmission by hydrolyzing the neurotransmitter acetylcholine. Butyrylcholinesterase acts as a backup for acetylcholinesterase, and as a scavenger for poisons that might inhibit acetylcholinesterase activity. Butyrylcholinesterase was of little interest to research scientists until the US Department of Defense allocated millions of dollars for the mass production of pure human butyrylcholinesterase to use for protection against the toxicity of nerve agents. Animal studies had demonstrated that pretreatment with butyrylcholinesterase gave complete protection from up to 5 LD<sub>50</sub> of nerve agents [1]. Chemical warfare agents were used by Iraq against Kurdish civilians in the war between Iraq and Iran (1980–1988), and

by Aum Shinrikyo cult members in the 1995 sarin attack in the Tokyo subway, and in Matsumoto city the previous year.

Nerve agents are a threat because they are extremely toxic at low doses. Their acute toxicity is due to inhibition of acetylcholinesterase. Nerve agents are organophosphorus esters, similar in structure (Fig. 1) and mechanism of toxicity to organophosphorus pesticides.

This review focuses on human butyrylcholinesterase and unanswered questions about butyrylcholinesterase. New mass spectrometry evidence suggests that proteins other than the cholinesterases may be involved in disorders that arise from low dose exposure.

## Function of butyrylcholinesterase

The human body has ten times more butyrylcholinesterase than acetylcholinesterase [2]: about 680 nmol of butyrylcholinesterase and 62 nmol of acetylcholinesterase. Butyrylcholinesterase protein or mRNA has been found in almost every tissue including plasma, liver, brain, muscle, saliva, kidney, heart, lining of blood vessels, skin, colon, small intestine, spleen, and lung (see AceView in the NCBI database). According to AceView, the *BCHE* gene is expressed at very high levels, 4.0 times the average gene. The sequence of the *BCHE* gene is defined by 439 GenBank accessions from 433

\* Corresponding author. Fax: +1 402 559 4651.

E-mail addresses: [pmasson@unmc.edu](mailto:pmasson@unmc.edu) (P. Masson), [olockrid@unmc.edu](mailto:olockrid@unmc.edu) (O. Lockridge).

<sup>1</sup> Abbreviations used: AChE, acetylcholinesterase; BChE, butyrylcholinesterase; DFP, diisopropyl fluorophosphate; G117H, mutation of glycine 117 to histidine; OP, organophosphorus compound; 2-PAM, pralidoxime; VX, nerve agent, O-ethyl S-[2-(diisopropylamino)ethyl] methylphosphonothioate.

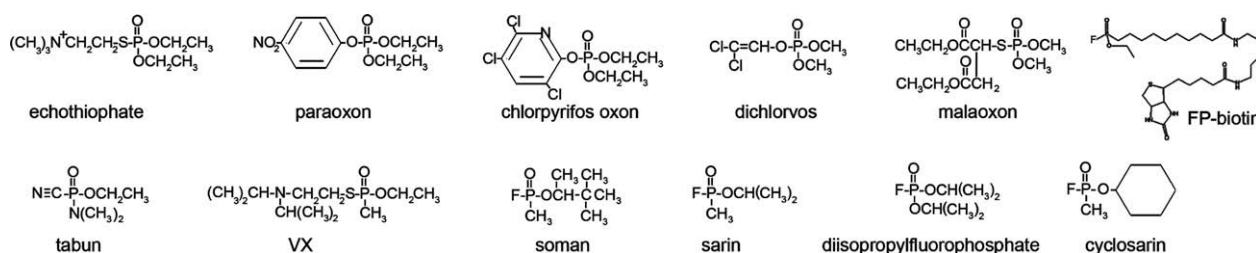


**Fig. 1.** Structures of organophosphorus agents. Paraoxon, chlorpyrifos oxon, dichlorvos, and malaoxon are the active metabolites of pesticides. Echothiophate has been used in eyedrops to treat glaucoma. Tabun, VX, soman, sarin, and cyclosarin are nerve agents developed for use as chemical warfare agents. FP-biotin and diisopropylfluorophosphate are research reagents.

cDNA clones. Certain neurons in the thalamus of the human brain express butyrylcholinesterase exclusively, whereas others express both butyrylcholinesterase and acetylcholinesterase as shown by specific activity staining [3].

#### Acetylcholine hydrolysis

The high amount of butyrylcholinesterase present in nearly every tissue suggests that butyrylcholinesterase has a function. The neurotransmitter acetylcholine is an excellent substrate for butyrylcholinesterase; butyrylcholinesterase hydrolyzes acetylthiocholine at a rate just 2-fold lower than it hydrolyzes butyrylthiocholine [4]. Butyrylcholinesterase does not appear to have a significant role in acetylcholine hydrolysis under normal conditions as shown in muscle preparations where complete inhibition of butyrylcholinesterase activity has no effect on muscle contraction. However, butyrylcholinesterase does have a role in neurotransmission in mice that have no acetylcholinesterase. The AChE<sup>-/-</sup> mice have normal levels of butyrylcholinesterase activity. Treatment of AChE<sup>-/-</sup> mice with OP results in inhibition of butyrylcholinesterase activity and lethality at concentrations well below those that cause lethality in wild-type mice [5,6]. This suggests that butyrylcholinesterase performs the function of the missing acetylcholinesterase in these mice by hydrolyzing acetylcholine.

Additional evidence of a role for butyrylcholinesterase in terminating neurotransmission comes from studies of the Gly117His transgenic mouse. This mouse expresses low levels of the butyrylcholinesterase mutant G117H in all tissues [7]. The G117H mutant is resistant to inhibition by OP and is capable of hydrolyzing acetylcholine in the presence of OP. Live G117H mice treated with DFP survive even though their acetylcholinesterase is inhibited. Under the same conditions wild-type mice die. The survival of the G117H mice is attributed to the ability of G117H to hydrolyze acetylcholine in the presence of DFP. Though the G117H mutant hydrolyzes OP, the rate of OP hydrolysis is slow, so that OP hydrolysis does not explain survival. If OP hydrolysis were significant, then the level of acetylcholinesterase and butyrylcholinesterase inhibition should be lower in the G117H mouse than in the wild-type mice treated with DFP. This was not the case. The levels of inhibition were similar. It was concluded that G117H hydrolysis of acetylcholine, rather than hydrolysis of OP, explained survival of these mice.

Acetylcholine levels in the hippocampus of live AChE<sup>-/-</sup> mice were measured by microdialysis followed by HPLC and electrochemical detection [8]. Infusion of a selective butyrylcholinesterase inhibitor (bambuterol, tolserine, or bis-norcymserine) through the microdialysis probe caused a 5-fold increase in acetylcholine levels in AChE<sup>-/-</sup> mice, but not in AChE<sup>+/+</sup> mice. It was concluded that in the absence of acetylcholinesterase, the levels of extracellular acetylcholine in the brain are controlled by the activity of butyrylcholinesterase.

Neurons in the human thalamus were stained specifically for acetylcholinesterase or butyrylcholinesterase activity. In some nuclei, for example the anteroventral nucleus, virtually all neurons stained positive for butyrylcholinesterase activity and none stained positive for acetylcholinesterase activity. In contrast, some nuclei for example the anterodorsal nucleus, had only acetylcholinesterase positive neurons. It was concluded that the distinct distribution of butyrylcholinesterase in neurons is consistent with an important role for butyrylcholinesterase in neurotransmission in the human nervous system [3].

The action of acetylcholine on bronchial airway smooth muscle is prolonged following inhibition of butyrylcholinesterase, indicating that butyrylcholinesterase has a role in acetylcholine hydrolysis in this tissue [9,10].

#### Butyrylcholine hydrolysis

Butyrylcholine is the optimum substrate for human butyrylcholinesterase. Butyrylcholine has been found in bovine corneal epithelium [11] and in bovine brain [12] where its function is unknown. Local application of butyrylcholine to intrinsic cardiac neurons increases neuronal activity [13], suggesting that butyrylcholine can act as a neurotransmitter.

#### Protection from neurotoxins

It is generally agreed that butyrylcholinesterase functions to protect from man-made and naturally occurring poisons. The man-made poisons include OP nerve agents, OP pesticides, carbamate pesticides, and the Alzheimer drugs donepezil and rivastigmine [14,15]. Naturally occurring poisons include physostigmine (also called eserine) in the calabar bean, cocaine from the *Erythroxylum coca* plant, solanidine in green potatoes, huperzine A from the club moss *Huperzia serrata*, and anatoxin-a(S) an OP in blue-green algae [16]. Butyrylcholinesterase inactivates these poisons by reversible or irreversible binding or by hydrolysis. These poisons inhibit the activity of butyrylcholinesterase, but inhibition of butyrylcholinesterase has no known adverse effects. Many of these poisons are acetylcholinesterase inhibitors. By scavenging the poisons, butyrylcholinesterase protects acetylcholinesterase from inhibition.

#### Gaps in knowledge of butyrylcholinesterase deficiency

It is suspected but not proven that people with butyrylcholinesterase deficiency are more susceptible to the toxicity of organophosphorus pesticides, as well as to anti-Alzheimer drugs, and recreational doses of cocaine. Butyrylcholinesterase deficiency is due to genetic variation as well as to malnutrition and liver disease [17]. The activity of butyrylcholinesterase genetic variants ranges from about 70% of normal in the K variant, to 0% of normal in the silent variant. People with zero butyrylcholinesterase activity

have normal health, are fertile, and live to old age [2]. However, they are paralyzed for 2 h after treatment with a dose of succinylcholine that paralyzes most people for only 3 min.

The presence of neurons in the brain that express butyrylcholinesterase exclusively suggests that butyrylcholinesterase in those neurons may be acting on a neurotransmitter substrate that is hydrolyzed specifically by butyrylcholinesterase. A logical substrate would be butyrylcholine, but this has not been demonstrated. Mice completely deficient in butyrylcholinesterase have normal health and behavior [18], suggesting that other enzymes compensate for the missing butyrylcholinesterase activity.

### Purification of butyrylcholinesterase and specific activity

Butyrylcholinesterase is purified from up to 100 l of outdated human plasma by ion exchange chromatography at pH 4.0, followed by affinity chromatography on procainamide–Sephrose, and ion exchange at pH 7.4 [19]. Other protocols are also in the literature [20,21]. All use chromatography on procainamide–Sephrose as one of the steps. Recombinant human acetylcholinesterase is also purified by binding to procainamide–Sephrose [22].

The specific activity of pure human butyrylcholinesterase is  $720 \mu\text{mol min}^{-1} \text{mg}^{-1}$  assayed at pH 7.0 in 0.1 M potassium phosphate,  $25^\circ\text{C}$  with 1 mM butyrylthiocholine. Protein concentration is measured by absorbance at 280 nm where a 1 mg/ml solution of butyrylcholinesterase has an absorbance of 1.8.

Butyrylcholinesterase has a non-linear response in plots of 1/activity versus 1/butyrylthiocholine concentration. The phase from 0.01 to 0.1 mM butyrylthiocholine yields a  $k_{\text{cat}}$  of  $24,000 \text{ min}^{-1}$ . The substrate activation phase from 0.4 to 40 mM yields a  $k_{\text{cat}}$  value that is 3.2 times higher,  $76,800 \text{ min}^{-1}$  [23] measured at pH 7.0 and  $25^\circ\text{C}$ . At pH 8.0 the values are  $k_{\text{cat}} = 45,500 \text{ min}^{-1}$  with butyrylthiocholine, and  $k_{\text{cat}} = 30,600 \text{ min}^{-1}$  with acetylthiocholine for the substrate range 0.02–0.1 mM [20].

The specific activity of pure human acetylcholinesterase is  $6000 \mu\text{mol min}^{-1} \text{mg}^{-1}$  assayed at pH 8.0,  $25^\circ\text{C}$  with 1 mM acetylthiocholine, which corresponds to a  $k_{\text{cat}}$  value of  $400,000 \text{ min}^{-1}$  [24].

### Gaps in knowledge of purification method

Procainamide was selected as a ligand for affinity column purification because the inhibition constant for procainamide ( $K_i = 9 \times 10^{-6} \text{ M}$ ) [25,26] is tight enough to give good binding, but not so tight as to make it impossible to release the bound butyrylcholinesterase. The procainamide affinity column does not purify butyrylcholinesterase in a single step. Two additional chromatography steps are required before the butyrylcholinesterase is pure.

Protocols with multiple chromatography steps are not ideal for sample preparation for mass spectrometry where the goal is to identify the OP-labeled peptide in a small clinical sample. What is needed is a one-step purification method. A one-step purification on procainamide–Sephrose is inadequate for identification of the OP-labeled active site tryptic peptide of butyrylcholinesterase, because this affinity gel does not yield highly purified butyrylcholinesterase. Ion suppression by contaminating peptides prevents the OP-labeled peptide from ionizing in the mass spectrometer. A more useful affinity column would bind butyrylcholinesterase with such high affinity that almost all contaminating proteins could be washed off. It would not be necessary to elute the butyrylcholinesterase from the affinity column because the bound butyrylcholinesterase could be digested with trypsin using protocols similar to those used to digest proteins embedded in acrylamide gel slices. Beads that do not dissolve in 50% acetonitrile would be optimal,

because it would allow extraction of peptides with 50% acetonitrile.

### Structure of the butyrylcholinesterase tetramer

The butyrylcholinesterase tetramer consists of 4 identical subunits, each containing 574 amino acids. The C-terminal 40 amino acids comprise the tetramerization domain. Assembly of butyrylcholinesterase subunits into a tetramer requires a polyproline-rich peptide derived from lamellipodin [27]. A crystal of the native butyrylcholinesterase tetramer has not yet been obtained. Crystallization is difficult because of the flexible tetramerization domain which protrudes from the tetramer like a stem from a flower. A model of the butyrylcholinesterase tetramer including its tetramerization domain interleaved with a polyproline-rich peptide has been constructed and is shown in Fig. 2. The model is supported by biochemical data that indicate the tetramerization domain can be cleaved off with proteases without affecting the catalytic properties of the enzyme. Knowledge of the tetramer organization is important: (a) it will confirm the presence of a polyproline peptide within the tetramerization domain; (b) it will reveal the relationship of the tetramerization domain to the subunit assembly; (c) it will provide information about the structure of membrane-anchored butyrylcholinesterase; (d) it will reveal the relative orientation of subunits in the tetramer and might tell whether cooperativity exists between subunits, (e) it will help in design of butyrylcholinesterase-based bioscavengers with longer residence times in the circulation.

### Catalytic issues

Site-directed mutagenesis studies, the crystal structure of butyrylcholinesterase and molecular dynamic studies support the formal minimum mechanistic model (Scheme 1) proposed from steady-state kinetic analysis of cholinesterases [28]. This minimum model implies a conformational link between residues located at the rim of the gorge, the peripheral anionic site, and the active center located at the bottom of the gorge. Conformational linkage occurs through motion of the omega loop that connects Asp70, the main component of the peripheral anionic site, and Trp82, the main component of the “choline”-binding site in the catalytic center.

The non-Michaelian behavior of butyrylcholinesterase with excess positively charged substrates ( $b < 1$  or  $b > 1$ ) results from the binding of a second substrate molecule ( $S_p$ ) on the peripheral anionic site. Neutral substrates in excess do not bind to the peripheral anionic site, thus butyrylcholinesterase follows the Michaelis–Menten model ( $b = 1$ ) with neutral substrates. For most esters, the acylation and deacylation steps are partially rate limiting, so that the turnover number,  $k_{\text{cat}}$ , is determined by the magnitude of both rate constants ( $k_{\text{cat}} = k_2 k_3 / (k_2 + k_3)$ ). The charge of the substrate is important for binding. The  $K_m$  values for positively charged esters are of the order of microM, while for neutral and negatively charged esters,  $K_m$  values are 3 orders of magnitude higher. After substrate is bound, electric charge is not the determining factor of catalytic efficiency. A negatively charged substrate like aspirin ( $k_{\text{cat}} = 6200 \text{ min}^{-1}$ ) is hydrolyzed at a rate only 2 times lower than the positively charged acetylcholine ( $13,000 \text{ min}^{-1}$ ) and 8 times lower than its related neutral ester phenylacetate ( $32,000 \text{ min}^{-1}$ ). Because the active site pocket of butyrylcholinesterase is larger than that of acetylcholinesterase ( $\approx 500 \text{ \AA}^3$  against  $300 \text{ \AA}^3$ ) [29], butyrylcholinesterase is less specific and can accommodate bulkier substrates. The catalytic efficiency of butyrylcholinesterase to hydrolyze esters is in fact mostly dependent on the size and enantiomeric configuration of the acyl or alcohol moieties.

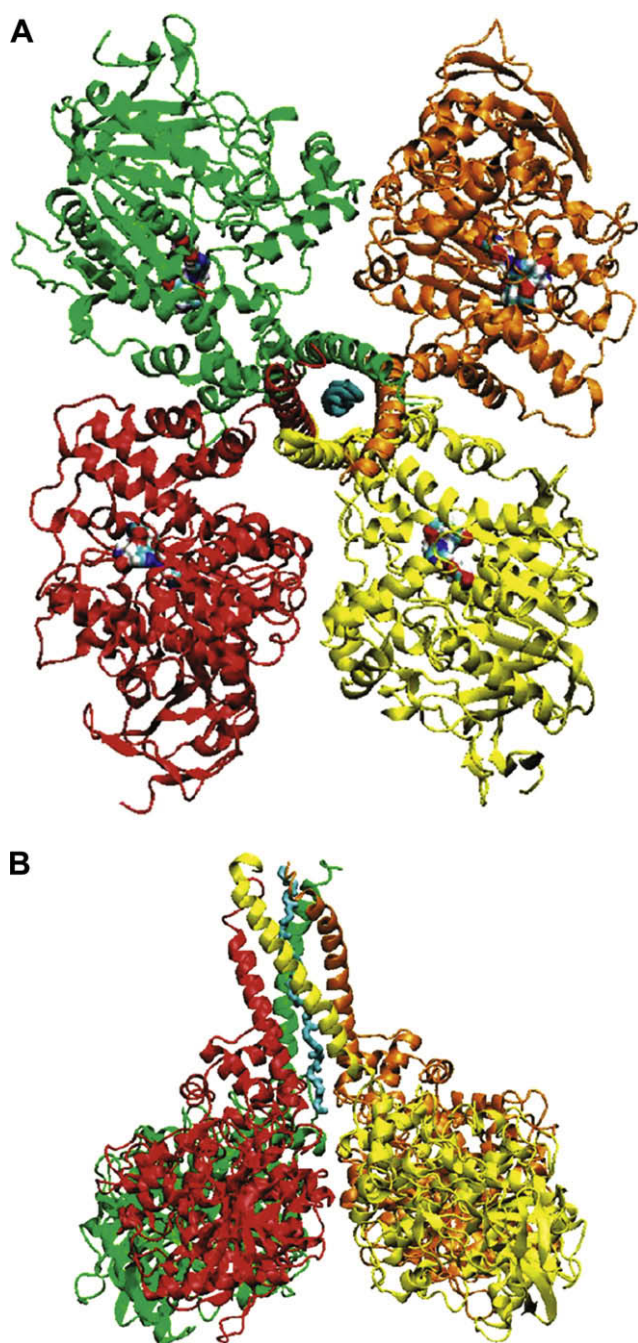
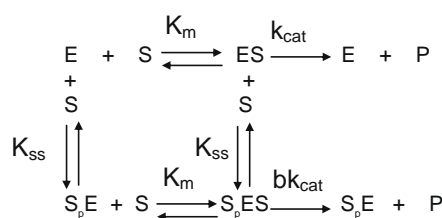


**Fig. 2.** Model of the human butyrylcholinesterase tetramer. Four subunits assemble through the tetramerization domain at the C-terminus. The tetramerization domain has four parallel alpha helices wrapped around a single antiparallel polyproline helix. The polyproline peptide derives from lamellipodin. The tetramer is a dimer of dimers. Dimers have an interchain disulfide bond at Cys571. (A) Viewed from the top, with the tetramerization domain and the polyproline peptide in the center. Two of the active sites are exposed to solvent, while two face the central cavity of the butyrylcholinesterase tetramer. (B) Viewed from the side. Reproduced from [185].

For instance,  $k_{\text{cat}}$  for (+)-cocaine is  $7500 \text{ min}^{-1}$  while it is  $3.9 \text{ min}^{-1}$  for (–)-cocaine [30]. The substrate slides down the gorge to form a first enzyme–substrate complex,  $\text{ES}_1$ , that is non-productive. Then  $\text{ES}_1$  rotates to a position favorable for nucleophilic attack by Ser198. This second complex,  $\text{ES}_2$ , is the productive Michaelis complex [23,31].

The promiscuity of butyrylcholinesterase and its hysteretic behavior with certain substrates raise interesting questions related to putative catalytic functions.



**Scheme 1.**

#### Aryl acylamidase activity

Like acetylcholinesterase, butyrylcholinesterase displays a genuine aryl acylamidase activity with *o*-nitroacetanilide, by hydrolyzing an amide bond [32]. See Fig. 3. This activity reflects the conformational plasticity of the active site to adjust to different types of substrates [33]. Clear evidence has been provided that the aryl acylamidase activity of butyrylcholinesterase is fully explained by its single active site serine (Ser198) [34,35]. Echothiophate completely inhibits both aryl acylamidase and esterase activities. Titration with echothiophate shows that echothiophate inhibits both aryl acylamidase and esterase activities with the same bimolecular rate constant. Plasma from a silent butyrylcholinesterase genetic variant with a frame shift at amino acid 117 (FS117) has neither aryl acylamidase nor esterase activity. Mutation of the active site serine to cysteine or aspartate yields butyrylcholinesterase with neither aryl acylamidase nor esterase activity. It is concluded that Ser198 is the active site for both aryl acylamidase and esterase activity.

Study of highly purified monomers and tetramers of butyrylcholinesterase showed that the aryl acylamidase activity of butyrylcholinesterase does not depend on quaternary structure [34]. Yet, it was reported that enzyme molecular forms isolated by sucrose gradient ultracentrifugation differ in aryl acylamidase activity, the monomer being more active than the tetramer [36,37]. The discrepancy could be explained by contamination of butyrylcholinesterase monomer fractions by tissue-specific carboxylesterase-amidase isozymes in gut and kidney [38,39] or albumin since carboxylesterase-amidases and albumin have aryl acylamidase activity [40].

The question of the possible physiological significance of the aryl acylamidase activity of cholinesterases has repeatedly been addressed [32,41,42]. With the exception of melatonin, no endogenous aryl acylamide compound has been isolated so far, and it should be noted that melatonin is not hydrolyzed by cholinesterases (Masson and Froment, unpublished result). Thus, the hypothetical function of butyrylcholinesterase and acetylcholinesterase in the metabolism of putative endogenous aryl acylamide substrates remains to be demonstrated.

Moreover, we should point out that the aryl acylamidase activity of butyrylcholinesterase is very low, with acylation as the rate-limiting step ( $k_2 \ll k_3$ ), and that the  $K_m$  with neutral aryl acylamide substrates is high. Therefore, under Michaelis–Menten conditions (enzyme concentration much less than substrate concentration), hydrolysis of aryl acylamide substrates at non-lethal concentrations is pseudo-first order. The neutral aryl acylamides, propanilil

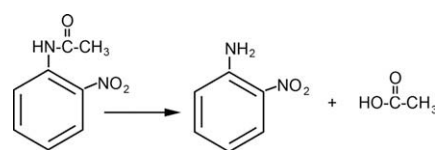


**Fig. 3.** Hydrolysis of *o*-nitroacetanilide by acetylcholinesterase and butyrylcholinesterase.

(fungicide), acetaminophen and phenacetin (drugs), and the negatively charged aryl acylamide, *N*-acetylthranilic acid (drug precursor), are not hydrolyzed by butyrylcholinesterase under these conditions. These results suggest that it is unlikely that plasma butyrylcholinesterase plays a role in the metabolism of exogenous aryl acylamide drugs and xenobiotics [34,35].

### Hysteretic behavior

The establishment of a steady state for butyrylcholinesterase-catalyzed hydrolysis of certain substrates is preceded by a long induction phase. This phenomenon was first described with *N*-methylindoxyl acetate as the substrate where a lag of several minutes is needed to reach steady state [43]. Actually, “chaotic” lags preceding steady state have been observed for decades by investigators using benzoylcholine as the substrate, but the nature of this phenomenon had not been investigated. Investigators using benzoylcholine just recorded hydrolysis kinetics after establishment of “equilibrium”. Kinetic analysis of benzoylcholine hydrolysis showed that the pre-steady state phase can be described by damped oscillations that superimpose on a mono-exponential lag [44]. The dependence of induction time on substrate concentration was interpreted according to hysteretic models developed by Frieden [45]. Accordingly, the enzyme exists in two interconvertible states, E and E' in slow equilibrium (Scheme 2). Substrate can bind on E and/or on E'. Depending on the affinity of E and E' for S, ( $K_S$  and  $K'_S$  are dissociation constants of enzyme–substrate complexes), and whether ES and E'S make products (P) or not, induction time will be a lag or a burst. With *N*-methylindoxyl acetate, only E' binds S and makes products, while with benzoylcholine, E and E' bind S, but only E'S makes products. With both substrates induction times are lags. With an anilide, 3-(acetamido) *N,N,N*-trimethylanilinium both enzyme states bind substrate and make products, but  $K'_S < K_S$  and E'S is catalytically less active than ES. In that case, a burst is observed [34,46]. Damped oscillations with benzoylcholine and long-alkyl chain homologues of benzoylcholine [44,47] were the result of an additional time-dependent constraint: the slow formation of a suitable substrate molecule due to multiple slow equilibria between different forms of the substrate (conformers, oligomers and micelles) [46].

The molecular mechanism for the hysteretic behavior of butyrylcholinesterase and acetylcholinesterase [46,48,49] is still unknown. Site-directed mutagenesis, pH-dependence studies, and occurrence of hysteresis with both cholinesterases suggest that hysteresis originates in the function of the catalytic triad. Effects of temperature, hydrostatic pressure, organic solvents and lyotropic salts indicate that hysteresis is related to enzyme hydration change. Water in the active site gorge of enzyme form E' appears to be more structured than in the gorge of the unprimed form E. A preliminary kinetic crystallography study indicates that water structure change in the gorge may induce a flip in the position of the catalytic histidine (Colletier, unpublished work).

The physiological relevance of the hysteretic behavior of the cholinesterases is questionable because acetylcholinesterase-cata-

lyzed hydrolysis of acetylcholine does not require hysteresis. However, affinity and reaction with inhibitors may differ between E and E'. Thus, it can be hypothesized that hysteresis could act as a “retarder” mechanism in natural defenses against toxicity of anticholinesterase agents. In fact, ligand binding and inhibition studies provided evidence for slow isomerization between two cholinesterase forms differing in affinity for ligands of the peripheral site [50,51]. Also, biphasic inhibition kinetics of butyrylcholinesterase by the carbamylating agent *N*-methyl-*N*-(2-nitrophenyl)carbamoyl chloride was explained by a mechanism in which both E and E' forms have the same affinity for the inhibitor but are inactivated at different rates ( $k'_{carb} = 10 k_{carb}$ ) [52]. Therefore, if reaction with certain irreversible inhibitors is faster for E' than for E as in slow-binding inhibition of type c [53], then it may be hypothesized that hysteresis could play a protective role in damping the cholinergic response to these agents.

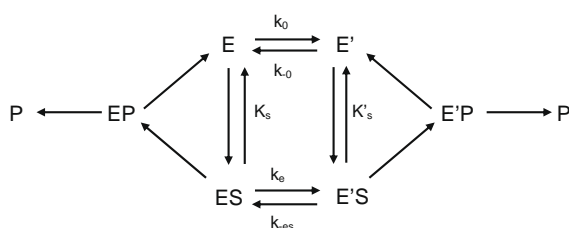
### Inhibition by OP and aging of the inhibited enzyme

#### Phosphorylation of cholinesterases

Organophosphorus compounds are progressive irreversible inhibitors of acetylcholinesterase and butyrylcholinesterase. After stereoselective formation of the enzyme–OP complex, the OP makes a covalent bond with the catalytic serine and simultaneously releases the leaving group (Fig. 4). The stereochemistry of the groups attached to phosphorus is inverted. The catalytic histidine remains protonated, so that water-mediated dephosphorylation is very slow or zero. After aging (dealkylation of the organophosphate), the positively charged catalytic histidine stabilizes the negatively charged aged OP adduct. Bimolecular rate constants for phosphorylation of cholinesterases are  $10^7$ – $10^{10} \text{ M}^{-1} \text{ min}^{-1}$ . Fast phosphorylation of acetylcholinesterase fully explains the acute lethal toxicity of OP [54]. However, the sub-lethal toxicity of OP with no inhibition of acetylcholinesterase, but with chronic effects can be explained by inhibition of other enzymes [15] or phosphorylation of other protein targets.

#### Reactivation of phosphorylated cholinesterases

The term “phosphylated” denotes both phosphorylation and phosphonylation. Phosphylated cholinesterases can be reactivated by nucleophilic compounds such as fluorides, hydroxamates and



Scheme 2.

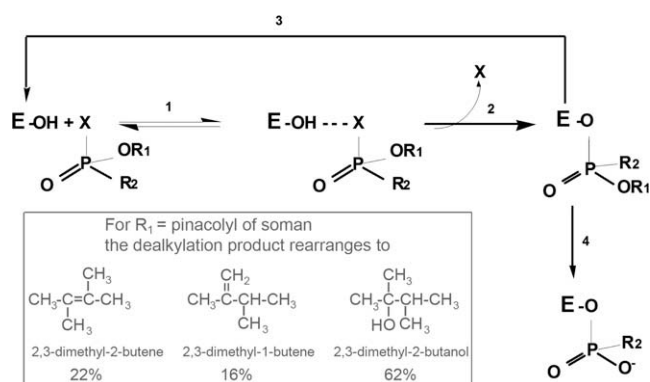


Fig. 4. Reaction of butyrylcholinesterase and acetylcholinesterase with OP. (1) formation of reversible complex; (2) phosphorylation of the active site serine, with departure of the leaving group X and inversion of the stereochemistry of the OP; (3) reactivation of phosphorylated enzyme by oximes or by 2 M potassium fluoride; (4) aging to produce a negatively charged OP stabilized by interaction with the positively charged histidine of the catalytic triad. Inset. When the OP is soman, R<sub>1</sub> is pinacolyl alcohol. Dealkylation does not yield pinacolyl alcohol, but instead yields 3 rearranged products [75].

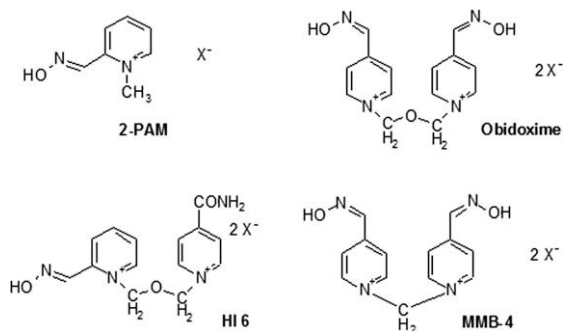


Fig. 5. Oxime structures.

oximates. The pyridinium oximes 2-PAM and obidoxime (toxogonin) are currently used as antidotes to OP poisoning. The more potent oximes HI-6 and MMB-4 are under advanced development. The structures of oximes are in Fig. 5. The efficacy of oximes to reactivate phosphorylated cholinesterases depends on the type of enzyme, and the chemical structure of the organophosphorus agent bound to the catalytic serine. Phosphorylated human butyrylcholinesterase is reactivated less efficiently than phosphorylated human acetylcholinesterase. Cholinesterases inhibited by tabun are resistant to most oximes at concentrations compatible with medical use [55]. Hydroxamates and fluoride ions release OP *in vitro* at conditions (2 M potassium fluoride pH 4) incompatible for therapeutic use *in vivo*, but well suited for biomonitoring of exposure [56].

#### Aging of OP-inhibited cholinesterases

Reactivation of phosphorylated enzymes is complicated by post-inhibitory reactions. Phosphorylated cholinesterases as well as the serine proteases trypsin and chymotrypsin [57] may become progressively resistant to reactivators. On the other hand, phosphorylated serine enzymes like carboxylesterases [58] and phospholipase A2[59] can be reactivated. Carboxylesterase spontaneously reactivates.

Progressive loss of reactivability of phosphorylated enzymes is called “aging”. Aging is the functional consequence of unimolecular dealkylation of the OP adduct. Aging is catalyzed by residues in the active site, His 438 and Glu 197 [36]. The rate of aging depends on

both the enzyme structure and the OP structure. The rate of aging is modulated by temperature, pH, and ligand binding. Aging can be halted by denaturing the protein. The half time of aging ranges from a few minutes to several days (Table 1). Treatment of OP poisoning may be dramatically impaired when there is rapid aging. In particular, in the case of poisoning by soman, aging of phosphorylated acetylcholinesterase is so fast that treatment with a potent oxime like HI-6 is ineffective. In the case of poisoning by sarin, which has a slow aging rate, treatment by pralidoxime (2-PAM) effectively reactivates acetylcholinesterase as was observed in Tokyo casualties after release of sarin in the subway [60].

#### Beta-elimination to form dehydroalanine

When the pH of a solution of phosphorylated butyrylcholinesterase is raised to 11 the organophosphorus agent and the active site serine are both lost during beta-elimination (Fig. 6). As a result the active site serine is converted to dehydroalanine. Both aged and non-aged phosphorylated butyrylcholinesterase undergo beta-elimination. The dehydroalanine peptide is detectable by mass spectrometry. For human butyrylcholinesterase, the masses of the tryptic peptides are 2910.5 *m/z* for the dehydroalanine form of the active site peptide, 2928.5 for the unlabeled active site peptide, 3006.5 for aged sarin, soman, and cyclosarin peptide, and 3090.5 for the soman-labeled peptide before aging. Dehydroalanine also forms at pH 7.4 though the rate of formation is much slower than at pH 11.

Another way to generate dehydroalanine is to bombard the phosphorylated peptide with high energy during acquisition of MS/MS fragmentation data [68]. The dehydroalanine form of the peptide is among the most intense peaks in the MS/MS spectrum indicating that beta-elimination occurs more easily than fragmentation of the backbone bonds in the peptide. OP-inhibited butyrylcholinesterase undergoes beta-elimination regardless of the structure of the OP.

The curious mass spectrometry observation is that a dehydroalanine peptide is also observed in MS spectra. A peak at 2910.5 *m/z* is observed in MS spectra acquired on the MALDI-TOF mass spectrometer (Fig. 7). 2910.5 is the mass of the dehydroalanine form of the human butyrylcholinesterase tryptic peptide. MS spectra acquired on the QTRAP tandem quadrupole ion trap mass spectrometer also have the 2910.5 peptide. Fragmentation

Table 1  
Half-time of aging for human acetylcholinesterase and human butyrylcholinesterase inhibited by organophosphorus compounds.

$\begin{array}{c} \text{O} \\ \parallel \\ \text{E}-\text{O}-\text{P}-\text{R}_1 \\   \\ \text{R}_2 \end{array}$						
OP	R <sub>1</sub>	R <sub>2</sub>	<i>t</i> (°C)	pH	<i>t</i> <sub>1/2</sub>	Reference
<b>Human AChE</b>						
Soman*	(CH <sub>3</sub> ) <sub>3</sub> C(CH <sub>3</sub> )CHO	CH <sub>3</sub>	27	8.0	6.3 min	[61]
Sarin	(CH <sub>3</sub> ) <sub>2</sub> CHO	CH <sub>3</sub>	37	8.0	3.9 h	[62]
Cyclosarin	Cyclohexyl-O	CH <sub>3</sub>	37	7.4	8.7 h	[63]
Tabun	(CH <sub>3</sub> ) <sub>2</sub> N	CH <sub>3</sub> CH <sub>2</sub> O	37	7.4	13.6 h	[64]
DFP	(CH <sub>3</sub> ) <sub>2</sub> CHO	(CH <sub>3</sub> ) <sub>2</sub> CHO	37	7.8	4.4 h	[65]
Paraoxon-ethyl	CH <sub>3</sub> CH <sub>2</sub> O	CH <sub>3</sub> CH <sub>2</sub> O	37		41 h	[63]
Paraoxon-methyl	CH <sub>3</sub> O	CH <sub>3</sub> O	37	7.4	3.7 h	[66]
<b>Human BChE</b>						
Soman*	(CH <sub>3</sub> ) <sub>3</sub> C(CH <sub>3</sub> )CHO	CH <sub>3</sub>	25	8.0	9 min	[67]
Sarin	(CH <sub>3</sub> ) <sub>2</sub> CHO	CH <sub>3</sub>	37	7.4	5.8–6.4 h	[64]
Cyclosarin	Cyclohexyl-O	CH <sub>3</sub>	37	7.4	2.2 h	[63]
Tabun	(CH <sub>3</sub> ) <sub>2</sub> N	CH <sub>3</sub> CH <sub>2</sub> O	37	7.4	6.1–6.4 h	[64]
DFP	(CH <sub>3</sub> ) <sub>2</sub> CHO	(CH <sub>3</sub> ) <sub>2</sub> CHO	37	7.8	28 min	[65]
Paraoxon-ethyl	CH <sub>3</sub> CH <sub>2</sub> O	CH <sub>3</sub> CH <sub>2</sub> O	20	8	11.6 h	[63]
Paraoxon-methyl	CH <sub>3</sub> O	CH <sub>3</sub> O	37	7.4	3.9 h	[66]

\* Racemic soman.

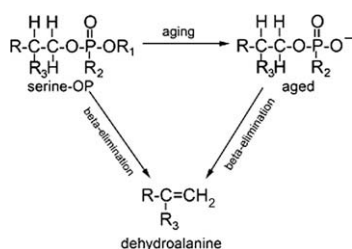


**Fig. 6.** Beta-elimination. OP-labeled serine loses the OP and a molecule of water in the beta-elimination reaction. The active site serine is converted to dehydroalanine.

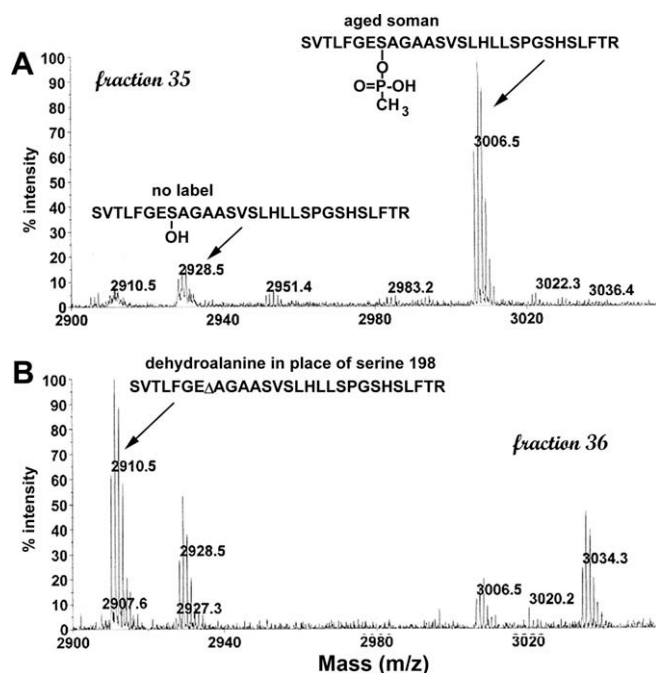


**Fig. 7.** MS spectrum of tryptic digest of soman-labeled human butyrylcholinesterase. Peptides were separated by HPLC and 1 ml fractions collected. A 0.5- $\mu$ l aliquot of each fraction was analyzed in the MALDI-TOF mass spectrometer. Panel A shows that fraction 35 contains the aged soman-labeled peptide at 3006.5  $m/z$  and a small amount of unlabeled peptide at 2928.5  $m/z$ . Panel B shows that fraction 36 contains the dehydroalanine form of the peptide at 2910.5  $m/z$ , unlabeled peptide at 2928.5  $m/z$ , and a small amount of aged-soman-labeled peptide at 3006.5  $m/z$ . The active site serine of human butyrylcholinesterase is Ser198 (accession # gi:116353).

shows that the sequence of the 2910.5 peptide is SVTLFGE $\Delta$ AGAASVSLHLLSPGSHSLFTR where the symbol  $\Delta$  represents dehydroalanine. The energy for acquisition of MS spectra is low so that the energy of ionization is not likely to be the cause of beta-elimination. The beta-elimination could have occurred during sample preparation or it could reflect spontaneous formation of dehydroalanine under mild conditions. It is not known whether dehydroalanine forms spontaneously under physiological conditions from OP-inhibited butyrylcholinesterase and OP-inhibited acetylcholinesterase. Dehydroalanine forms of the cholinesterases cannot be reactivated by treatment with oximes.

#### Gaps in knowledge of rate of beta-elimination to make dehydroalanine

It is not certain that phosphorylated cholinesterases undergo beta-elimination under physiological conditions. The possibility that artifacts are introduced during preparation of samples for analysis in the mass spectrometer needs to be ruled out. It is not known whether a substantial amount of dehydroalanine forms *in vivo*. The rate of formation of dehydroalanine under physiologi-

cal conditions has not yet been determined. It is assumed that phosphorylated acetylcholinesterase undergoes the same beta-elimination as phosphorylated butyrylcholinesterase, but this has not been demonstrated. Since the dehydroalanine form of cholinesterases cannot be reactivated, it is important to know how much of an aged acetylcholinesterase preparation is in the dehydroalanine form when attempting to evaluate oxime drugs for their reactivation efficacy.

#### Mechanism of dealkylation of phosphorylated cholinesterase

Dealkylation of phosphorylated cholinesterase is an  $S_N1$  reaction. The reaction has been thoroughly investigated for aging of soman-inhibited cholinesterase where it involves a carbocation-like transition state and then scission of the P–O–C chain to form a carbocation on the pinacolyl chain. For organophosphates like echothiophate and DFP, and organophosphonates like sarin and soman, phosphorylation and aging of human butyrylcholinesterase were carried out in  $^{18}O$ -water and compared to aging in  $^{16}O$ -water. Analysis of tryptic peptides by MALDI-TOF mass spectrometry provided evidence that dealkylation occurs by breaking of the O–C bond and not the P–O bond [69]. For the phosphoramidate, tabun, mass spectrometry and X-ray structure analyses provided evidence that aging of cholinesterase occurs through O-dealkylation, not N-dealkylation [70]. For the phosphorodithioate, isomalathion, aging is more complex, involving O–C, P–S and S–C cleavages, depending on the enantiomer that reacted with the enzyme [69].

Chemical modification of histidine by diethylpyrocarbonate implicated the active site histidine in aging [71]. Studies of pH dependence and site-directed mutagenesis provided evidence for participation of the catalytic histidine and the glutamate vicinal to the catalytic serine in the mechanism of dealkylation [72]. Other residues in the active center of cholinesterase have been found to play a role in the aging process. In particular, tryptophan (W82 in human butyrylcholinesterase), the main component of the choline-binding pocket, has been found to stabilize the developing carbocationic chain that will be released [61].

Identification of products released by dealkylation of the pinacolyl chain of soman bound to acetylcholinesterase [73–75] as well as pH profiles and solvent isotope effects support a “push–pull” mechanism for aging in which tryptophan (W82 in human butyrylcholinesterase) and glutamate (E197 in human butyrylcholinesterase) exert electrostatic and steric “push”, and histidine (H438 in human butyrylcholinesterase) and the oxyanion hole act as “pullers” [76,77]. This mechanism involves migration of methyl from C $\beta$  to C $\alpha$  in the pinacolyl chain in the dealkylation transition state. Another proposed mechanism supported by mutagenesis and structural data involves protonation of the pinacoloxyl oxygen by the protonated catalytic histidine, and then scission of the O–C bond [61]. More recently, the high-resolution crystal structure of non-aged and aged soman-acetylcholinesterase conjugates led to a critical reexamination of both models, highlighting the role of a conserved water molecule in dealkylation [78].

Dealkylation is accompanied by formation of a salt bridge between the negatively charged P–O $^-$  and the protonated catalytic histidine [79,80]. Crystal structures of aged butyrylcholinesterase (Fig. 8) and other serine hydrolases confirm the existence of this strong salt bridge in the active center of aged conjugates [57,70,78,81].

#### Consequence of aging on cholinesterase structure

Fluorescence decay of pyrenebutyl-containing organophosphates bound to acetylcholinesterase was found to have a lower quantum yield for non-aged conjugates than for aged ones [82]. This suggested that the pyrenebutyl group in aged conjugates is

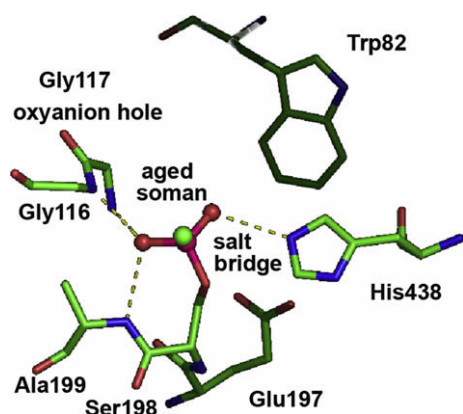


**Fig. 8.** Salt bridge between the negatively charged aged soman bound to Ser198 and the positively charged catalytic His438 of human butyrylcholinesterase. The crystal structure is in pdb code 1p0q [81].

more deeply buried than in non-aged conjugates. Later, kinetic and equilibrium studies showed alteration in binding of peripheral anionic site ligands in aged acetylcholinesterase compared to non-aged acetylcholinesterase [83]. This was interpreted to be the result of a change in the topographic relationships between the active center and the peripheral anionic site.

Cross-linking of butyrylcholinesterase with dimethylimidates of different chain length showed that upon aging there was no change in the quaternary structure of butyrylcholinesterase or in the overall conformation of subunits [26]. However, enzyme denaturation studies showed that the conformational stability of aged cholinesterase is dramatically increased compared to non-inhibited and non-aged enzymes [84–87]. See Fig. 9.

Neutron scattering studies as a function of temperature up to 90 °C showed that the increase in stability of aged butyrylcholinesterase correlated to decrease in molecular flexibility [88]. Formation of a salt bridge and partial dehydration of the active site gorge upon dealkylation may explain the stability and molecular dynamic changes of aged butyrylcholinesterase.

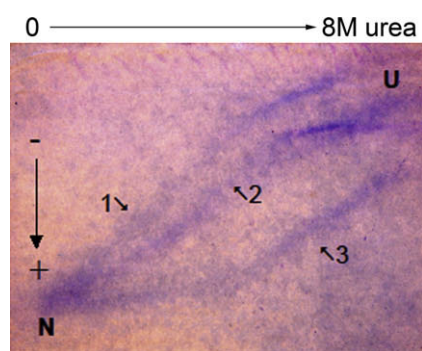


**Fig. 9.** Soman-inhibited butyrylcholinesterase tetramer is resistant to unfolding. A mixture of native unlabeled butyrylcholinesterase, non-aged soman-butylcholinesterase, and aged soman-butylcholinesterase, 0.5 mg butyrylcholinesterase protein total, was layered on a polyacrylamide gel containing a 0–8 M transverse gradient of urea. After electrophoresis the gel was stained with Coomassie blue. Three well-separated curves of butyrylcholinesterase protein are seen. (1) Not labeled butyrylcholinesterase tetramer swells into an unfolded structure as the urea concentration increases from 0 to 8 M. The unfolded butyrylcholinesterase migrates more slowly through the gel. The urea concentration at the mid-point for unfolding is 3.5 M. (2) Non-aged soman-phosphylated butyrylcholinesterase begins to unfold at a higher urea concentration. (3) Aged soman-butylcholinesterase retains its folded structure up to 4 M urea and has a mid-point for unfolding at 6 M urea. N indicates the migration of normal folded tetrameric butyrylcholinesterase in the absence of urea. U indicates migration of unfolded butyrylcholinesterase in 8 M urea. The direction of migration is from minus (–) to plus (+).

## Resistance to oxime reactivation of aged cholinesterases

Shortly after the discovery of aging, Hobbiger suggested that a new bond was formed between aged adduct and the active center, thus preventing reactivation [89]. It was proposed that the presence of the negatively charged oxygen in the adducted phosphorus atom formed an electrostatic shield opposing nucleophilic attack by negatively charged oximates [90]. In fact, studies of reactions between different acylmethylphosphonates and neutral or negatively charged nucleophiles showed that the presence of a negative charge slows down the rate of nucleophilic displacement at phosphorus due to the electrostatic effect, but does not prevent reaction between compounds [91–93]. Conformational rigidity of the aged enzymes cannot explain by itself the loss of reactivation. Moreover, the crystal structure of soman-aged acetylcholinesterase, compared to native or non-aged acetylcholinesterase, revealed only a slight displacement of the catalytic histidine upon formation of a salt bridge at the bottom of the gorge [78]. An explanation for the resistance to reactivation was provided by the crystal structure of the complex of soman-aged acetylcholinesterase and 2-PAM. The oximate function of 2-PAM points away from the phosphorus atom, in an orientation that does not permit nucleophilic attack on the phosphorus atom. This provides a new explanation for the failure of 2-PAM to reactivate aged soman-acetylcholinesterase.

In the case of aged phosphoramidate-inhibited cholinesterase, resistance to reactivators results from the conjunction of steric factors imposed by the salt bridge, and electron delocalization along the P–N–R chain due to the nitrogen doublet [70,94].

## Perspectives

### Modulation of aging velocity

Because reactivation of aged cholinesterase is not yet possible, medical counter-measures could be improved by using drugs capable of slowing the aging process. The D70G mutation on the peripheral anionic site of human butyrylcholinesterase was found to slow the aging process, and molecular dynamic simulations indicated that the peripheral anionic site and the catalytic binding site are coupled via conformational change of the omega loop that connects both sites [95]. Therefore, occupation of the peripheral anionic site may affect the rate of aging by altering interactions between the adduct and the active center residues. In fact, the effects of several peripheral anionic site ligands of acetylcholinesterase, i.e., bispyridinium compounds like SAD-128, HH54 [96–98], and gallamine [99], acting as allosteric effectors have been investigated. Other ligands have been found to slow down the aging of phosphorylated cholinesterases, e.g., ketamine [100] and tacrine [101]. None of these compounds was found to be of practical interest for slowing down aging *in vivo* in association with other medical counter-measures. However, new generations of peripheral anionic site and bifunctional ligands are emerging. Screening of libraries of tethered ligands and cyclic peptides [102], and bifunctional ligands produced by click chemistry [103] may be a strategy for discovery of such compounds. Alternatively, a computer-aided approach based on flexible docking in the crystal structure of cholinesterase appears to be a very promising strategy [104].

### Is reactivation of aged cholinesterase possible?

Reactivation of aged cholinesterase is a challenge. Solving this major issue would greatly improve medical counter-measures, in particular against acute poisoning by soman. Direct reactivation of aged conjugates using oximes has not been possible so far. Yet

hundreds of oximes have been synthesized. However, most oximes have been designed without knowledge of the three-dimensional structure and molecular dynamics of phosphorylated enzymes. Very few structures of complexes between oximes and phosphorylated cholinesterase have been reported so far. The three-dimensional structure of complexes such as that of the non-aged tabun-acetylcholinesterase conjugate with the oxime HIö-7 explains why reactivation of cholinesterase inhibited by tabun is so difficult [105]. Recent work of Sanson et al. [78] provides a rationale to understand why non-aged soman-acetylcholinesterase is not reactivatable by 2-PAM, and why 2-PAM cannot reactivate the aged enzyme. Therefore, lessons from crystallography and molecular dynamics are expected to provide information for improving the orientation of the oxime function for effective attack on phosphorus. *In silico* design of new oximes, as well as other chemical strategies mentioned above, including click chemistry and combinatorial chemistry, should lead to a new generation of reactivators. Another strategy would be to realkylate the aged adduct by using an electrophilic molecule, and then to displace the phosphotriester by a nucleophilic compound.

#### *Aging-resistant cholinesterase mutants as potential pseudo-catalytic bioscavengers*

Bioscavengers are proteins that neutralize nerve agents before they damage the nervous system. Bioscavenger-based cholinesterase is an alternative to prophylaxis against organophosphate poisoning [1], and administration of bioscavengers may improve efficacy of treatment of acute nerve agent poisoning. However, cholinesterases act as stoichiometric scavengers, so that efficacy of cholinesterase in OP poisoned humans needs administration of 200–300 mg of costly enzymes. Efforts to convert cholinesterases into efficient catalytic bioscavengers have not been successful so far [106]. Thus, selected mutants of cholinesterase non-susceptible to aging, i.e., reactivatable, could be used in association with oximes as pseudo-catalytic bioscavengers. Several attempts have been made [107–109], and this approach looks promising.

#### *Butyrylcholinesterase as a bioscavenger for protection against OP*

OP poisoning is a major public-health concern. According to the World Health Organization, OP self-poisoning is responsible for 200,000 deaths a year in the world [110]. Though 188 countries are now part of the Chemical Weapons Convention, OP nerve agents still represent military and terrorist threats. The pharmacological approach for prophylaxis and treatment of OP poisoning has reached its limit [55,111–115]. Thus, alternative approaches have been considered. In particular, acute toxicity of OP can be countered by lowering OP concentration in the blood compartment. This prevents the transfer of OP molecules to physiological targets. The bioscavenger approach is based on the concept of inactivation of OP molecules in the blood stream before they reach their central and peripheral neuronal and neuromuscular targets. The importance of endogenous esterases in inactivation of poisonous esters has been recognized. Multiple cellular and plasma enzymes constitute barriers that play a role in natural defenses against toxicants. The presence of OP detoxifying enzymes in skin contributes to reduction of the amount of OP that penetrates into the body [116]. Tissue carboxylesterases react with OP, and participate in protection [58,117]. Certain secondary targets of OP also play a detoxifying role [118–120]. Finally, blood esterases significantly contribute to detoxication of OP molecules. Unlike plasma of most mammals, there are no carboxylesterases in human plasma [121]. However, human plasma contains two enzymes capable of degrading poisonous esters: paraoxonase (PON1; EC 3.1.8.1) that displays arylesterase, lactonase and phosphotriesterase activities,

and butyrylcholinesterase that hydrolyzes numerous poisonous esters and reacts stoichiometrically with OP. The concentration of paraoxonase in human serum is 500 nM, and its catalytic efficiency with OP is about  $10^5 \text{ M}^{-1} \text{ min}^{-1}$ . Albumin reacts with OP, but its reactivity is very slow compared to that of butyrylcholinesterase [122]. Though the concentration of butyrylcholinesterase in human serum is about 50 nM, its apparent second-order rate constant with OP is high  $\approx 10^7\text{--}10^9 \text{ M}^{-1} \text{ min}^{-1}$ . Thus, butyrylcholinesterase is the most significant stoichiometric OP scavenger in human plasma.

In the past decade, fast inactivation of OP in blood by pretreatment of animals with pure human butyrylcholinesterase has proven to be safe and efficient for protection against nerve agents [1]. In 2006, plasma-derived human butyrylcholinesterase was registered as an Investigational New Drug by the FDA [123,124]. In 2009 a phase I clinical trial on healthy volunteers (NCT 00333528) was completed by Baxter Healthcare Corporation and butyrylcholinesterase became the first stoichiometric bioscavenger for prophylaxis of organophosphorus poisoning. It is estimated that protection from a dose of nerve agent lethal to 50% of the population requires 200–300 mg of butyrylcholinesterase per adult. Multiple 200–300 mg of butyrylcholinesterase are needed for human protection against higher doses of nerve agents [125]. Natural tetrameric butyrylcholinesterase purified from human plasma [21] and recombinant human butyrylcholinesterase (Protexia™) from the milk of transgenic goat [126,127] are costly GMP-produced enzymes. Thus, it is important to develop new therapeutics that catalyze the destruction of OP. New mutants of human butyrylcholinesterase, paraoxonase, or phospholipase A2 [59] capable of degrading OP with a high turnover, would greatly reduce the cost of treatment and improve the bioscavenger approach against OP.

#### *Conversion of butyrylcholinesterase into an OP-hydrolyzing enzyme*

OP are hemi-substrates of butyrylcholinesterase and acetylcholinesterase. When butyrylcholinesterase reacts with carboxylesters, the acyl group is rapidly displaced from the planar acyl-enzyme intermediate by a water molecule. In contrast, the reaction with phosphyl-esters yields a stable tetrahedral adduct that restricts accessibility of water to the phosphorus atom and impairs proton transfer from the protonated catalytic histidine (H438) to the substrate [77]. Thus, spontaneous hydrolysis of phosphorylated enzyme is very slow or even impossible. Jarv postulated that introduction of a second nucleophile in the active center could activate a water molecule. This water molecule could then attack the phosphorus atom on the back face, causing the P-serine bond to break [128]. Resolution of the three-dimensional structure of Torpedo californica acetylcholinesterase [129] opened the way to rational re-design of cholinesterases to make enzymes capable of hydrolyzing OP. Human butyrylcholinesterase was selected because its active center is larger ( $500 \text{ \AA}^3$ ) than that of acetylcholinesterase ( $300 \text{ \AA}^3$ ) and it is less stereospecific. A molecular model of human butyrylcholinesterase based on the crystal structure of Torpedo acetylcholinesterase was made for the design of butyrylcholinesterase mutants. The second nucleophile was created in the oxyanion hole where a glycine residue was replaced by a histidine. The first mutant, G117H, was capable of hydrolyzing paraoxon, DFP, sarin, echothiophate and VX at a slow rate [130,131]. Interestingly, the mutation G117H is in a position homologous to that of the carboxylesterase mutant, G137D, from a blowfly (*Lucilia cuprina*) resistant to OP. Though the OP hydrolase activity of the G137D carboxylesterase is very low, it is balanced by the abundance of the enzyme in insect organs [132]. The X-ray structure of the carboxylesterase has recently been solved to 2.5 Å resolution [133]. The G117H mutant of butyrylcholinesterase, did not self-reactivate with soman because dealkylation of adduct (aging) was faster than

dephosphorylation. Therefore, a second mutation was made on the glutamate residue important for the aging reaction: Glu197Gln. As expected, the double mutant G117H/E197Q was capable of hydrolyzing soman because the rate of aging was considerably reduced [134]. However, the catalytic activity of this double mutant was too slow to be of pharmacological interest.

More than 60 double and triple mutants of human butyrylcholinesterase with mutated Gly117 [135] and mutants of human acetylcholinesterase and *Bungarus fasciatus* acetylcholinesterase were made, using the same rationale [136]. Unfortunately, none of the mutated cholinesterases was more active than the first mutant, G117H. For a review see [106].

#### Strategies for designing new OP scavengers

Enzymes that hydrolyze or oxidize OP are of potential interest for detection, decontamination, protection and treatment of OP poisoning [137–139]. Among them, phosphotriesterases from bacteria (OP hydrolase), squid (DFPase) and human plasma (paraoxonase) are the most promising, but they are enantioselective, and pose immunological and pharmacotechnological problems. Because of the large variety of OP molecules and enantiomeric preference of cholinesterases and OP hydrolases, it will be impossible to make a universal mutant for protection against all OP. Rather, multiple mutated OP-degrading enzymes, differing in specificity, should be combined to make effective catalytic bioscavengers for prophylaxis and treatment of acute OP poisoning. Mixtures of effective enzymes against a large spectrum of OP could also be incorporated into active topical skin protectants, decontamination solutions and other protection equipment.

The considerable body of data obtained with human butyrylcholinesterase as the first bioscavenger, encourages further research for designing butyrylcholinesterase mutants capable of degrading nerve agents and pesticides [106]. However, new strategies for designing these enzymes have to be implemented. Computational design of mutants also called “intelligent” site-directed mutagenesis is the most promising strategy. Directed evolution of butyrylcholinesterase could be an alternative to computer-based methods. A recent study on the blowfly carboxylesterase mutant G137D showed that directed evolution of this enzyme led to 400-fold increase in OP hydrolase activity in 3 generations [133]. The drawback of directed evolution is that it requires expression in bacteria or yeast. However, expression of functional cholinesterases is difficult in yeast and has failed in bacteria so far. Such approaches in combination with chemical modifications and medium manipulations have been successfully used to improve properties of selected enzymes [140].

#### Basic requirements for operational butyrylcholinesterase-based catalytic bioscavengers

The concentration of toxic OP molecules in blood, [OP], even in the most severe cases of poisoning, is always very low (<11 nM), well below the  $K_m$  of OP-hydrolyzing enzymes [141]. Enzyme-catalyzed hydrolysis of OP in blood is a pseudo-first-order process described by the equation  $v = k_{cat}/K_m [E] [OP]$ . The product of the bimolecular rate constant ( $k_{cat}/K_m$ ) and enzyme active site concentration ([E]) is the pseudo-first-order rate constant. Thus, the higher the catalytic efficiency ( $k_{cat}/K_m$ ), the lower the dose of enzyme required to clean the blood of toxic molecules in a short time. Given that the molecular weight of butyrylcholinesterase per active site is 85,000, and taking the total volume of plasma as 3 l per person, it can be calculated that an enzyme dose of 4.7 mg will reduce [OP] by 100-fold in 4.6 min if  $k_{cat}/K_m = 10^8 \text{ M}^{-1} \text{ min}^{-1}$ . A dose of 47 mg enzyme will be needed if  $k_{cat}/K_m$  is 10 times lower. Therefore, the catalytic efficiency of operational mutants of butyrylcholinesterase

needs to be increased by 3–4 orders of magnitude compared to the catalytic efficiency of G117H towards OP [130,136]. The success of strategies to increase the cocaine hydrolase activity of butyrylcholinesterase suggests that a butyrylcholinesterase mutant with improved OP hydrolase activity may be achieved.

#### Lessons from mutagenesis of butyrylcholinesterase as an efficient cocaine esterase

Plasma butyrylcholinesterase is the major detoxifying enzyme of cocaine in humans [142]. However, wild-type butyrylcholinesterase slowly hydrolyzes (–)-cocaine with a  $k_{cat}/K_m$  of about  $2.8 \text{ M min}^{-1}$ , so that under normal conditions, a large part of an administered dose of cocaine reaches its biological targets and triggers toxic effects. Efficient mutants of human butyrylcholinesterase have been made that hydrolyze cocaine at a high rate. A first mutation, A328Y, enhanced  $k_{cat}/K_m$  4-fold [143]. See Table 2. Then, molecular dynamics simulation and computer-based ligand docking led to the A328W/Y332A double mutant that displays a higher  $k_{cat}/K_m = 8.6 \text{ M min}^{-1}$  [144]. Using the three-dimensional X-ray structure of human butyrylcholinesterase [81], molecular dynamic simulations of the deacylation transition state led to the design of highly active mutants against (–)-cocaine. A butyrylcholinesterase with 4 mutations A199S/S287G/A328W/Y332G had a catalytic efficiency 1500–5000-fold greater than wild-type butyrylcholinesterase [145,146]. Introduction of 5 mutations, A199S/F227A/S287G/A328W/Y332G, led to an enzyme 6500-fold more active than wild-type butyrylcholinesterase [147]. Thus, this strategy led to a progressive increase in  $k_{cat}/K_m$  for (–)-cocaine of more than 3 orders of magnitude in 5 steps. The most active mutant is of therapeutic interest [148]. Computational (transition state simulations, free energy barrier perturbation simulations) and mutagenesis approaches are expected to lead to even more efficient mutants [149]. Application of this computational design approach on dephosphorylation transition states should lead to new mutants of butyrylcholinesterase displaying high OP hydrolase activity.

#### Lessons from self-reactivating butyrylcholinesterase inhibited by OP

Though human butyrylcholinesterase is irreversibly inhibited by OP, mouse butyrylcholinesterase spontaneously self-reactivates after inhibition by paraoxon, DFP or echothiophate [121]. The DFP-inhibited mouse butyrylcholinesterase reactivated to a lesser extent than the echothiophate-inhibited enzyme, suggesting that the fast aging of DFP-inhibited enzyme competed with self-reactivation. Other investigators have reported the peculiar behavior of phosphorylated butyrylcholinesterase from some species (see [121]). An activity rebound of pig plasma butyrylcholinesterase after challenge of animals by VX was attributed to release of butyrylcholinesterase to the blood stream from organs [151]. However, study of highly purified pig butyrylcholinesterase inhibited by VX

**Table 2**  
Cocaine esterase activity of mutants of human butyrylcholinesterase.

Enzyme	$k_{cat}/K_m$ ( $\text{M}^{-1} \text{ min}^{-1}$ )	Fold-increase	Reference
Wild-type BChE	$2.8 \times 10^5$	1	[143]
A328Y	$11.3 \times 10^5$	4	[143]
A328W/Y332A	$8.6 \times 10^6$	30	[144]
F227A/S287G/A328W/Y332A	$3.1 \times 10^7$	100	[150]
A199S/S287G/A328W/Y332G	$4.15 \times 10^8$	1500	[145]
A199S/S287G/A328W/Y332G	$1.35 \times 10^9$	5000	[148]
A199S/F227A/S287G/A328W/Y332G	$1.84 \times 10^9$	6500	[147]

showed full spontaneous reactivation of the enzyme in less than 1 h (Dorandeu et al., unpublished work). Comparison of butyrylcholinesterase sequences of mouse and pig with other species, as well as molecular modeling of structures of pig and mouse butyrylcholinesterase (Nachon, unpublished works) did not reveal any feature in the active center that could explain spontaneous reactivation of phosphorylated enzymes. The amino acid differences responsible for spontaneous reactivation have not yet been identified, but it is clear that they are not within the active site gorge.

These observations, coming after the success of transition state simulations for the re-design of butyrylcholinesterase as a cocaine esterase, indicate that the key is in the molecular dynamics of these enzymes. It may be hypothesized that the “breathing” of self-reactivable butyrylcholinesterase causes transient adjustment of the active site geometry with unmasking of nucleophilic groups and polarization of a water molecule that acts to release the OP from serine. The functional architecture of the active center and the dynamics of butyrylcholinesterase in action result from a delicate balance between numerous interacting groups, suggesting that multiple mutations will be needed to convert human butyrylcholinesterase to an efficient OP hydrolase.

#### *Lessons from the G117H mutant family*

The crystal structure of the Gly117 His mutant of human butyrylcholinesterase [152,153] indicated that His117 is mobile enough to adopt a favorable conformation to activate a vicinal water molecule. However, the main conformation adopted by His117 in the phosphorylated enzyme is not favorable for dephosphorylation, so that an activated water molecule is produced infrequently. This explains the low turnover with OP substrates. In addition, evidence was provided that mutations at position Gly117 cause dislocation and loss of functionality of the oxyanion hole toward carboxyl-esters and carboxyl-thioesters [154]. Molecular modeling and empirical calculations on acetylation of the G117H mutant by acetylthiocholine are in agreement with these structural and kinetic data [155]. Therefore, the nucleophile needed for general base catalysis of future mutants of butyrylcholinesterase will have to be introduced in a location that does not impair enzyme functionality. Re-design of the active center pocket of butyrylcholinesterase with creation of a stable dyad as in Tyr124His/Tyr72Asp-based new mutants of human acetylcholinesterase [106] may be a starting point. However, “intelligent re-design” of multiple mutations in butyrylcholinesterase for high OP hydrolase activity will need implementation of an integrated computational-mutagenesis strategy as proposed above.

#### **New OP binding motif to tyrosine and lysine in proteins that have no active site serine**

There is general agreement that the acute toxicity of OP is due to inhibition of acetylcholinesterase. What is not understood is why low doses cause chronic illness in some people. Symptoms of low dose toxicity include headache, memory loss, inability to learn, difficulty sleeping, fatigue, and muscle weakness. Low dose is defined as a dose that causes no obvious signs of cholinergic toxicity and no significant acetylcholinesterase inhibition. A hypothesis to explain low dose effects is that non-cholinesterase targets are modified by OP, and that modification damages nerve function.

A search for additional OP targets was begun by treating mice with a biotinylated OP [156] at a dose that did not inhibit acetylcholinesterase. The biotinylated OP made a covalent bond with albumin in plasma, muscle, and liver. The labeled peptide and the labeled amino acid were identified by mass spectrometry. In human albumin (accession # gi:122920512) the OP-labeled resi-

due is Tyr411 [157,158]. When a homogenate of rat thymus was treated with radiolabeled DFP, the labeled protein was identified as albumin [159].

The question we asked next, was whether albumin was a special case or whether tyrosine in other proteins could also be modified by OP. Almost every pure protein when treated with a 20-fold molar excess of chlorpyrifos oxon, dichlorvos, DFP, soman, sarin, or FP-biotin had one or more OP-labeled tyrosines. In each case we isolated the labeled peptide and identified the labeled residue by mass spectrometry. Tyrosine was a common motif for OP binding in bovine tubulin alpha (Tyr 83), bovine tubulin beta (Tyr 59, Tyr 159, Tyr 281), mouse transferrin (Tyr 238, Tyr 319, Tyr 429, Tyr 491, Tyr 518), human transferrin (Tyr 238, Tyr 574), human alpha-2-glycoprotein 1 zinc-binding protein (Tyr 138, Tyr 174, Tyr 181), human kinesin 3C motor domain (Tyr 145), human keratin 1 (Tyr 230), bovine actin Tyr55, Tyr 200), murine ATP synthase beta (Tyr 431), murine adenine nucleotide translocase 1 (Tyr 81), bovine chymotrypsinogen (Tyr 201), and porcine pepsin (Tyr 310) [160–162]. In addition we found OP covalently bound to lysine in keratin, albumin, bovine tubulin alpha, tubulin beta, bovine actin, and mouse transferrin [163]. A review of the 102 OP-labeled tyrosine peptides identified to date by mass spectrometry is in [164]. This review notes that certain ion masses always appear in the MS/MS spectrum of an OP-tyrosine labeled peptide and that these immonium ions can be used to help identify OP-labeled tyrosine.

#### *Gaps in knowledge of proteins modified by low dose OP exposure*

The studies with pure proteins suggest that the search for OP-labeled proteins should be broadened to include almost every protein in the body. The search is no longer restricted to enzymes with an active site serine. OP-labeled tubulin has been found in the brains of mice. Whether or not tubulin function is disrupted after low dose OP treatment is not yet known. Tubulin is an abundant protein in brain, but it is possible that a protein in low abundance could be responsible for symptoms of low dose OP toxicity. Likely candidates are enzymes that regulate axonal transport in nerve cells, because disruption of axonal transport is a common feature of neurodegenerative diseases [165].

#### **Methods for detection of low dose exposure to organophosphorus agents**

##### *Why measure low dose exposure?*

One reason for measuring low dose exposure is to understand why some people become chronically ill from a dose that has no ill effects on the majority. People with chemical sensitivity, chronic fatigue, toxic airline illness ([www.toxicairlines.com](http://www.toxicairlines.com)), and Gulf War Illness suspect their illness is due to exposure to organophosphorus agents [166–168], but this belief is based on correlation rather than direct laboratory evidence. A method that detects low dose exposure could provide this missing evidence. This could lead to an understanding of the mechanism of illness from low doses of organophosphorus agents.

Forensic scientists could use a low dose exposure assay to identify persons who unlawfully synthesize and distribute nerve agents. Even though these people would have no symptoms of toxicity, nerve agent adducts in their blood would provide absolute evidence that they had been in contact with nerve agents. Workers involved in destruction and transportation of nerve agents could be tested for low dose exposure to provide assurance that their protective equipment is functioning properly. In the event of an incident where nerve agent is released, many people who report to emergency facilities would be the worried-well who need

assurance that they have not been exposed. A highly sensitive method that can provide this assurance would calm the public. Pesticide applicators, including farmers and aerial sprayers, could be tested for low dose exposure to pesticides. This could protect them from Parkinson's disease and depression, as these diseases have been linked to pesticide exposure [169,170].

#### Methods for measuring OP exposure

1. Laboratory tests for poisoning by nerve agents and pesticides measure the enzyme activity of acetylcholinesterase in red blood cells and the butyrylcholinesterase in plasma. Low levels indicate poisoning. The advantage of this method is that it is simple, inexpensive, and well established. However, activity assays are not useful for low dose exposures because normal levels of activity have a broad range, making it difficult to distinguish low endogenous levels from low dose exposure. Another disadvantage of this method is that it does not identify the inhibitor. Many chemicals inhibit cholinesterases including the carbamate pesticide carbaryl and the Alzheimer drug tacrine.
2. Intact nerve agent, nerve agent metabolites, pesticides, and pesticide metabolites in air, water, soil, fabric and urine can be extracted and identified by gas chromatography/mass spectrometry and liquid chromatography tandem mass spectrometry [171–173]. These methods identify the agent based on its mass and fragmentation pattern. The results leave no doubt as to the identity of the agent. Analysis of metabolites by gas chromatography has the drawback that several agents can yield identical metabolites, and most metabolites must be derivatized, thus adding an extra step to sample preparation. Identification of metabolites in urine does not allow one to know whether exposure was to the active agent or to breakdown products.
3. Organophosphorus agents bound to the active site serine of butyrylcholinesterase or acetylcholinesterase can be regenerated by treatment of blood with potassium fluoride. The freed agent is extracted and identified by gas chromatography/mass spectrometry [174,175]. The identification is highly reliable. The drawback of this method is that nerve agent or pesticide that has lost an alkyl group in the process called “aging”, cannot be regenerated. This means soman and other aged OP will give a negative result, indicating no exposure. Most pesticides yield identical dimethyl or diethylphosphate adducts of butyrylcholinesterase and acetylcholinesterase, so that identification of the pesticide is incomplete.
4. Electrospray mass spectrometry identifies adducts on the active site serine 198 of human butyrylcholinesterase. The butyrylcholinesterase is first purified from 0.5 to 1 ml plasma and then digested with trypsin or pepsin [68,176]. HPLC followed by mass spectrometry yields the mass of the poison. The advantage of this method is that it gives a positive result for “aged” adducts. The limitation is that most pesticides yield identical adducts on butyrylcholinesterase, so that one can confirm exposure but not identify the poison. For example, chlorpyrifos oxon and paraoxon both yield diethylphosphate adducts with an added mass of +136, while dichlorvos and malaoxon both yield dimethyl phosphate adducts with an added mass of +108.
5. Electrospray mass spectrometry can also be used to detect organophosphorus adducts on tyrosine 411 of human albumin [177]. The advantage of analyzing adducts on albumin is that organophosphorus labeled tyrosine does not age [178,179]. Therefore soman exposure can be distinguished from sarin exposure. The disadvantage of analyzing tyrosine adducts is that the percent labeling on albumin is low. Plasma from a patient poisoned with dichlorvos has been found to contain

dichlorvos-labeled albumin by this method (unpublished). Guinea pigs poisoned with soman and tabun have OP-labeled albumin [178]. However, humans poisoned with OP other than dichlorvos have not yet been demonstrated to have OP-labeled albumin.

6. Mass spectrometers equipped with a source that requires no sample preparation are being evaluated but are not yet in routine use. The DESI source electrosprays boric acid solution onto a Teflon surface on which OP hydrolysate has been deposited [180]. The ions are analyzed in an LTQ mass spectrometer.
7. A drawback of mass spectrometry methods is that mass spectrometers are very expensive and require highly trained personnel to run them. Portable mass spectrometers are used by the military but they give a high rate of false positives [181].
8. An ELISA kit that uses a polyclonal antibody to detect chlorpyrifos in river and lake water is available from Strategic Diagnostics Inc, Newark, DE (catalog # 7250000). The limit of detection is in the nanomolar range. ELISA kits for detection of diazinon and carbofuran are also available. Analysis of environmental samples by commercial ELISA kits is less costly and labor intensive than analysis by gas or liquid chromatography. ELISA kit results tend to overestimate pesticide levels [182].

#### Gaps in knowledge on how to detect low dose exposure

Antibodies that recognize OP-modified proteins in human fluids (plasma, saliva, and urine) are not yet available. Several laboratories are developing antibody-based detection devices using Quantum dots [183], an array biosensor [184], and a fluorogenic sensor (Ateris Technologies, Missoula, MT) but no antibody has as yet been made with adequate binding affinity and specificity to serve in these devices. It is anticipated that a hand held device, and possibly even a dip-stick type of assay, will become available in the future after suitable antibodies have been created.

#### Conclusion

Human butyrylcholinesterase is highly effective for preventing the toxicity of nerve agents and OP pesticides. Its limitation is that one molecule of butyrylcholinesterase can inactivate only one molecule of OP. A more cost effective therapeutic would rapidly destroy many OP molecules. Such a therapeutic has not yet been made, though several laboratories are designing mutant proteins with OP hydrolase activity. The low dose toxicity of OP is not due to inhibition of cholinesterases, but may involve modification of proteins that have no active site serine.

#### Acknowledgments

Supported by NIH Grant U01 NS058056-03, NIH Cancer Center Support Grant CA036727, US Army Medical Research & Materiel Command W81XWH-07-2-0034, French Procurement Agency DGA/PEA 08co501 and Agence Nationale pour la Recherche ANR-06-BLAN-0163.

#### References

- [1] A. Saxena, W. Sun, C. Luo, T.M. Myers, I. Koplovitz, D.E. Lenz, B.P. Doctor, J. Mol. Neurosci. 30 (2006) 145–148.
- [2] I. Manoharan, R. Boopathy, S. Darvesh, O. Lockridge, Clin. Chim. Acta 378 (2007) 128–135.
- [3] S. Darvesh, D.A. Hopkins, J. Comp. Neurol. 463 (2003) 25–43.
- [4] J.R. Wetherell, M.C. French, Biochem. Pharmacol. 35 (1986) 939–945.
- [5] E.G. Duysen, B. Li, W. Xie, L.M. Schopfer, R.S. Anderson, C.A. Broomfield, O. Lockridge, J. Pharmacol. Exp. Ther. 299 (2001) 528–535.
- [6] F. Chatonnet, E. Boudinot, A. Chatonnet, L. Taysse, S. Daulon, J. Champagnat, A.S. Foutz, Eur. J. Neurosci. 18 (2003) 1419–1427.

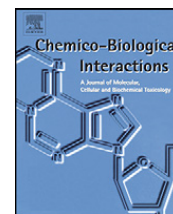
- [7] Y. Wang, A.T. Boeck, E.G. Duysen, M. Van Keuren, T.L. Saunders, O. Lockridge, *Toxicol. Appl. Pharmacol.* 196 (2004) 356–366.
- [8] J. Hartmann, C. Kiewert, E.G. Duysen, O. Lockridge, N.H. Greig, J. Klein, J. Neurochem. 100 (2007) 1421–1429.
- [9] M. Adler, M.G. Filbert, *FEBS Lett.* 267 (1990) 107–110.
- [10] X. Norel, M. Angrisani, C. Labat, I. Gorenne, E. Dulmet, F. Rossi, C. Brink, *Br. J. Pharmacol.* 108 (1993) 914–919.
- [11] J.L. Reusset, A. Ringvold, *J. Chromatogr. Sci.* 43 (2005) 401–405.
- [12] D. Henschler, Hoppe Seyler's Z. Physiol. Chem. 305 (1956) 97–104.
- [13] S. Darvesh, S.E. MacDonald, A.M. Losier, E. Martin, D.A. Hopkins, J.A. Armour, *J. Auton. Nerv. Syst.* 71 (1998) 75–84.
- [14] E.G. Duysen, B. Li, S. Darvesh, O. Lockridge, *Toxicology* 233 (2007) 60–69.
- [15] J.E. Casida, G.B. Quistad, *Chem. Res. Toxicol.* 17 (2004) 983–998.
- [16] N.A. Mahmood, W.W. Carmichael, *Toxicol.* 25 (1987) 1221–1227.
- [17] M. Whittaker, *Anaesthesia* 35 (1980) 174–197.
- [18] B. Li, E.G. Duysen, M. Carlson, O. Lockridge, *J. Pharmacol. Exp. Ther.* 324 (2008) 1146–1154.
- [19] O. Lockridge, L.M. Schopfer, G. Winger, J.H. Woods, *J. Med. CBR Def.* 3 (2005).
- [20] J. Grunwald, D. Marcus, Y. Papier, L. Raveh, Z. Pittel, Y. Ashani, *J. Biochem. Biophys. Methods* 34 (1997) 123–135.
- [21] A. Saxena, C. Luo, B.P. Doctor, *Protein. Expr. Purif.* 61 (2008) 191–196.
- [22] C. Kronman, B. Velan, Y. Gozes, M. Leitner, Y. Flashner, A. Lazar, D. Marcus, T. Sery, Y. Papier, H. Grosfeld, et al., *Gene* 121 (1992) 295–304.
- [23] P. Masson, P. Legrand, C.F. Bartels, M.T. Froment, L.M. Schopfer, O. Lockridge, *Biochemistry* 36 (1997) 2266–2277.
- [24] D. Barak, A. Ordentlich, A. Bromberg, C. Kronman, D. Marcus, A. Lazar, N. Ariel, B. Velan, A. Shafferman, *Biochemistry* 34 (1995) 15444–15452.
- [25] R.S. Rush, A.R. Main, B.F. Kilpatrick, G.D. Faulkner, *J. Pharmacol. Exp. Ther.* 216 (1981) 586–591.
- [26] P. Masson, B. Marnot, J.Y. Lombard, P. Morelis, *Biochimie* 66 (1984) 235–249.
- [27] H. Li, L.M. Schopfer, P. Masson, O. Lockridge, *Biochem. J.* 411 (2008) 425–432.
- [28] Z. Radic, N.A. Pickering, D.C. Vellom, S. Camp, P. Taylor, *Biochemistry* 32 (1993) 12074–12084.
- [29] A. Saxena, A.M. Redman, X. Jiang, O. Lockridge, B.P. Doctor, *Chem. Biol. Interact.* 119–120 (1999) 61–69.
- [30] J.R. Cashman, C.E. Berkman, G. Underiner, C.A. Kolly, A.D. Hunter, *Chem. Res. Toxicol.* 11 (1998) 895–901.
- [31] C.G. Zhan, F. Zheng, D.W. Landry, *J. Am. Chem. Soc.* 125 (2003) 2462–2474.
- [32] A.S. Balasubramanian, C.D. Bhanumathy, *FASEB J.* 7 (1993) 1354–1358.
- [33] D. Quinn, *Chem. Rev.* 87 (1987) 955–979.
- [34] P. Masson, M.T. Froment, E. Gillon, F. Nachon, S. Darvesh, L.M. Schopfer, *Biochim. Biophys. Acta* 1774 (2007) 1139–1147.
- [35] P. Masson, M.T. Froment, E. Gillon, F. Nachon, O. Lockridge, L.M. Schopfer, *FEBS J.* 275 (2008) 2617–2631.
- [36] M.F. Montenegro, T.M. Maria, M.P. de la Cadena, F.J. Campoy, E. Munoz-Delgado, C.J. Vidal, *Biol. Chem.* 389 (2008) 425–432.
- [37] M.F. Montenegro, M.T. Moral-Naranjo, E. Munoz-Delgado, F.J. Campoy, C.J. Vidal, *FEBS J.* 276 (2009) 2074–2083.
- [38] T. Imai, *Drug Metab. Pharmacokinet.* 21 (2006) 173–185.
- [39] S.P. Sanghani, P.C. Sanghani, M.A. Schiel, W.F. Bosron, *Protein Pept. Lett.* 16 (2009) 1207–1214.
- [40] P. Masson, M.T. Froment, S. Darvesh, L.M. Schopfer, O. Lockridge, *J. Enzyme Inhib. Med. Chem.* 22 (2007) 463–469.
- [41] S. Darvesh, D.A. Hopkins, C. Geula, *Nat. Rev. Neurosci.* 4 (2003) 131–138.
- [42] R.V. Rajesh, L. Chitra, P.G. Layer, R. Boopathy, *Biochimie* 91 (2009) 1087–1094.
- [43] P. Masson, M.T. Froment, S. Fort, F. Ribes, N. Bec, C. Balny, L.M. Schopfer, *Biochim. Biophys. Acta* 1597 (2002) 229–243.
- [44] P. Masson, B.N. Goldstein, J.C. Debouzy, M.T. Froment, O. Lockridge, L.M. Schopfer, *Eur. J. Biochem.* 271 (2004) 220–234.
- [45] C. Frieden, *J. Biol. Chem.* 245 (1970) 5788–5799.
- [46] P. Masson, L.M. Schopfer, M.T. Froment, J.C. Debouzy, F. Nachon, E. Gillon, O. Lockridge, A. Hrabovska, B.N. Goldstein, *Chem. Biol. Interact.* 157–158 (2005) 143–152.
- [47] A. Hrabovska, J.C. Debouzy, M.T. Froment, F. Devinsky, I. Paulikova, P. Masson, *FEBS J.* 273 (2006) 1185–1197.
- [48] M.H. Sadar, K.J. Laidler, *Can. J. Biochem.* 53 (1975) 380–387.
- [49] A. Badiou, M.T. Froment, D. Fournier, P. Masson, L.P. Belzunces, *Chem. Biol. Interact.* 175 (2008) 410–412.
- [50] S. Pattison, S. Bernhard, *Proc. Natl. Acad. Sci. USA* 75 (1978) 3613–3617.
- [51] M.B. Bolger, P. Taylor, *Biochemistry* 18 (1979) 3622–3629.
- [52] S. Loudwig, Y. Nicolet, P. Masson, J.C. Fontecilla-Camps, S. Bon, F. Nachon, M. Goeldner, *Chembiochem* 4 (2003) 762–767.
- [53] J.F. Morrison, S.R. Stone, *Comments Mol. Cell. Biophys.* 2 (1985) 347–368.
- [54] D.M. Maxwell, K.M. Brecht, I. Kopolovitz, R.E. Sweeney, *Arch. Toxicol.* 80 (2006) 756–760.
- [55] M. Jokanovic, M. Prostran, *Curr. Med. Chem.* 16 (2009) 2177–2188.
- [56] M. Polhuijs, J.P. Langenberg, H.P. Benschop, *Toxicol. Appl. Pharmacol.* 146 (1997) 156–161.
- [57] M. Harel, C.T. Su, F. Frolov, Y. Ashani, I. Silman, J.L. Sussman, *J. Mol. Biol.* 221 (1991) 909–918.
- [58] C.D. Fleming, C.C. Edwards, S.D. Kirby, D.M. Maxwell, P.M. Potter, D.M. Cerasoli, M.R. Redinbo, *Biochemistry* 46 (2007) 5063–5071.
- [59] T.M. Epstein, U. Samanta, S.D. Kirby, D.M. Cerasoli, B.J. Bahnson, *Biochemistry* 48 (2009) 3425–3435.
- [60] N. Yanagisawa, H. Morita, T. Nakajima, *J. Neurol. Sci.* 249 (2006) 76–85.
- [61] A. Shafferman, A. Ordentlich, D. Barak, D. Stein, N. Ariel, B. Velan, *Biochem. J.* 318 (Pt. 3) (1996) 833–840.
- [62] D.R. Davies, A.L. Green, *Biochem. J.* 63 (1956) 529–535.
- [63] F. Nachon, O.A. Asajo, G.E. Borgstahl, P. Masson, O. Lockridge, *Biochemistry* 44 (2005) 1154–1162.
- [64] E. Heilbronn, *Biochem. Pharmacol.* 12 (1963) 25–36.
- [65] F. Hobbiger, *Br. J. Pharmacol. Chemother.* 11 (1956) 295–303.
- [66] F. Worek, C. Diepold, P. Eyer, *Arch. Toxicol.* 73 (1999) 7–14.
- [67] P. Masson, P.L. Fortier, C. Albaret, M.T. Froment, C.F. Bartels, O. Lockridge, *Biochem. J.* 327 (Pt. 2) (1997) 601–607.
- [68] A. Fidler, A.G. Hulst, D. Noort, R. de Ruiter, M.J. van der Schans, H.P. Benschop, J.P. Langenberg, *Chem. Res. Toxicol.* 15 (2002) 582–590.
- [69] H. Li, L.M. Schopfer, F. Nachon, M.T. Froment, P. Masson, O. Lockridge, *Toxicol. Sci.* 100 (2007) 136–145.
- [70] E. Carletti, H. Li, B. Li, F. Ekstrom, Y. Nicolet, M. Loidice, E. Gillon, M.T. Froment, O. Lockridge, L.M. Schopfer, P. Masson, F. Nachon, *J. Am. Chem. Soc.* 130 (2008) 16011–16020.
- [71] G. Beauregard, J. Lum, B.D. Roufogalis, *Biochem. Pharmacol.* 30 (1981) 2915–2920.
- [72] A. Saxena, B.P. Doctor, D.M. Maxwell, D.E. Lenz, Z. Radic, P. Taylor, *Biochem. Biophys. Res. Commun.* 197 (1993) 343–349.
- [73] T.E. Smith, E. Usdin, *Biochemistry* 5 (1966) 2914–2918.
- [74] H.O. Michel, B.E. Hackley Jr., L. Berkowitz, G. List, E.B. Hackley, W. Gillilan, M. Pankau, *Arch. Biochem. Biophys.* 121 (1967) 29–34.
- [75] C. Viragh, I.M. Kovach, L. Pannell, *Biochemistry* 38 (1999) 9557–9561.
- [76] C. Viragh, R. Akhmetshin, I.M. Kovach, C. Broomfield, *Biochemistry* 36 (1997) 8243–8252.
- [77] I.M. Kovach, *J. Phys. Org. Chem.* 17 (2004) 602–614.
- [78] B. Sanson, F. Nachon, J.P. Colletier, M.T. Froment, L. Toker, H.M. Greenblatt, J.L. Sussman, Y. Ashani, P. Masson, I. Silman, M. Weik, *J. Med. Chem.* 52 (2009) 7593–7603.
- [79] Y. Segall, D. Waysbort, D. Barak, N. Ariel, B.P. Doctor, J. Grunwald, Y. Ashani, *Biochemistry* 32 (1993) 13441–13450.
- [80] J. Grunwald, Y. Segall, E. Shirin, D. Waysbort, N. Steinberg, I. Silman, Y. Ashani, *Biochem. Pharmacol.* 38 (1989) 3157–3168.
- [81] Y. Nicolet, O. Lockridge, P. Masson, J.C. Fontecilla-Camps, F. Nachon, *J. Biol. Chem.* 278 (2003) 41141–41147.
- [82] G. Amitai, Y. Ashani, A. Gafni, I. Silman, *Biochemistry* 21 (1982) 2060–2069.
- [83] H.A. Berman, M.M. Decker, *J. Biol. Chem.* 261 (1986) 10646–10652.
- [84] P. Masson, J.L. Goasdoue, *Biochim. Biophys. Acta* 869 (1986) 304–313.
- [85] P. Masson, P. Gouet, C. Clerly, *J. Mol. Biol.* 238 (1994) 466–478.
- [86] P. Masson, C. Clerly, P. Guerra, A. Redslob, C. Albaret, P.L. Fortier, *Biochem. J.* 343 (Pt. 2) (1999) 361–369.
- [87] Y. Ashani, M.K. Gentry, B.P. Doctor, *Biochemistry* 29 (1990) 2456–2463.
- [88] F. Gabel, P. Masson, M.T. Froment, B.P. Doctor, A. Saxena, I. Silman, G. Zaccari, M. Weik, *Biophys. J.* 96 (2009) 1489–1494.
- [89] F. Hobbiger, in: G.B. Koelle (Ed.), *Cholinesterases and Anticholinesterase Agents*, Springer-Verlag, Berlin, 1963, pp. 941–943.
- [90] L.W. Harris, J.H. Fleisher, J. Clark, W.J. Cliff, *Science* 154 (1966) 404–407.
- [91] A.J. Kirby, *J. Chem. Soc. B* (1970) 1165–1172.
- [92] E.J. Behrman, M.J. Biallas, H.J. Brass, J.O. Edwards, M. Isaks, *J. Org. Chem.* 35 (1970) 3063–3069.
- [93] E.J. Behrman, M.J. Biallas, H.J. Brass, J.O. Edwards, M. Isaks, *J. Org. Chem.* 35 (1970) 3069–3075.
- [94] E. Carletti, N. Aurbek, E. Gillon, M. Loidice, Y. Nicolet, J.C. Fontecilla-Camps, P. Masson, H. Thiermann, F. Nachon, F. Worek, *Biochem. J.* 421 (2009) 97–106.
- [95] P. Masson, M.T. Froment, C.F. Bartels, O. Lockridge, *Biochem. J.* 325 (Pt. 1) (1997) 53–61.
- [96] K. Schoene, *Biochim. Biophys. Acta* 525 (1978) 468–471.
- [97] K. Schoene, J. Steinhanses, A. Wertmann, *Biochim. Biophys. Acta* 616 (1980) 384–388.
- [98] A. Stalc, M. Sentjurc, *Biochem. Pharmacol.* 40 (1990) 2511–2517.
- [99] R.M. Dawson, M.H. Dowling, M. Poretski, *Neurochem. Int.* 19 (1991) 125–133.
- [100] G. Puu, *Biochem. Pharmacol.* 37 (1988) 969–970.
- [101] R.M. Dawson, *Neurosci. Lett.* 100 (1989) 227–230.
- [102] J.L. Johnson, B. Cusack, T.F. Hughes, E.H. McCullough, A. Fauq, P. Romanovskis, A.F. Spatola, T.L. Rosenberry, *J. Biol. Chem.* 278 (2003) 38948–38955.
- [103] P. Taylor, Z. Kovarik, E. Reiner, Z. Radic, *Toxicology* 233 (2007) 70–78.
- [104] M.Y. Mizutani, A. Itai, *J. Med. Chem.* 47 (2004) 4818–4828.
- [105] F.J. Ekstrom, C. Astot, Y.P. Pang, *Clin. Pharmacol. Ther.* 82 (2007) 282–293.
- [106] P. Masson, F. Nachon, C.A. Broomfield, D.E. Lenz, L. Verdier, L.M. Schopfer, O. Lockridge, *Chem. Biol. Interact.* 175 (2008) 273–280.
- [107] A. Saxena, D.M. Maxwell, D.M. Quinn, Z. Radic, P. Taylor, B.P. Doctor, *Biochem. Pharmacol.* 54 (1997) 269–274.
- [108] Z. Kovarik, Z. Radic, H.A. Berman, P. Taylor, *Toxicology* 233 (2007) 79–84.
- [109] O. Mazar, O. Cohen, C. Kronman, L. Raveh, D. Stein, A. Ordentlich, A. Shafferman, *Mol. Pharmacol.* 74 (2008) 755–763.
- [110] M. Eddleston, N.A. Buckley, P. Eyer, A.H. Dawson, *Lancet* 371 (2008) 597–607.
- [111] P. Aas, *Prehosp. Disaster Med.* 18 (2003) 208–216.
- [112] E.X. Albuquerque, E.F. Pereira, Y. Aracava, W.P. Fawcett, M. Oliveira, W.R. Randall, T.A. Hamilton, R.K. Kan, J.A. Romano Jr., M. Adler, *Proc. Natl. Acad. Sci. USA* 103 (2006) 13220–13225.
- [113] J. Wetherell, M. Price, H. Mumford, S. Armstrong, L. Scott, *Toxicology* 233 (2007) 120–127.
- [114] P. Eyer, L. Szinicz, H. Thiermann, F. Worek, T. Zilker, *Toxicology* 233 (2007) 108–119.

- [115] H. Thiermann, L. Szinicz, P. Eyer, N. Felgenhauer, T. Zilker, F. Worek, *Toxicology* 233 (2007) 145–154.
- [116] K.U. Schallreuter, N.C. Gibbons, S.M. Elwary, S.M. Parkin, J.M. Wood, *Biochem. Biophys. Res. Commun.* 355 (2007) 1069–1074.
- [117] M.R. Redinbo, P.M. Potter, *Drug Discov. Today* 10 (2005) 313–325.
- [118] Q. Wang, M. Sun, H. Zhang, C. Huang, *J. Biochem. Mol. Toxicol.* 12 (1998) 213–217.
- [119] D.K. Nomura, K. Fujioka, R.S. Issa, A.M. Ward, B.F. Cravatt, J.E. Casida, *Toxicol. Appl. Pharmacol.* 228 (2008) 42–48.
- [120] D.K. Nomura, D. Leung, K.P. Chiang, G.B. Quistad, B.F. Cravatt, J.E. Casida, *Proc. Natl. Acad. Sci. USA* 102 (2005) 6195–6200.
- [121] B. Li, M. Sedlacek, I. Manoharan, R. Boopathy, E.G. Duysen, P. Masson, O. Lockridge, *Biochem. Pharmacol.* 70 (2005) 1673–1684.
- [122] B. Li, F. Nachon, M.T. Froment, L. Verdier, J.C. Debouzy, B. Brasme, E. Gillon, L.M. Schopfer, O. Lockridge, P. Masson, *Chem. Res. Toxicol.* 21 (2008) 421–431.
- [123] A. Saxena, C. Luo, N. Chilukuri, D.M. Maxwell, B.P. Doctor, in: J.A. Romano, B.J. Lukey, H. Salem (Eds.), *Chemical Warfare Agents Chemistry, Pharmacology, Toxicology and Therapeutics*, CRC Press, Boca Raton, FL, 2007, pp. 145–173.
- [124] D.E. Lenz, C.A. Broomfield, D.T. Yeung, P. Masson, D.M. Maxwell, D.M. Cerasoli, in: J.A. Romano, B.J. Lukey, H. Salem (Eds.), *Chemical Warfare Agents Chemistry, Pharmacology, Toxicology and Therapeutics*, CRC Press, Boca Raton, FL, 2007, pp. 175–202.
- [125] Y. Ashani, S. Pistinner, *Toxicol. Sci.* 77 (2004) 358–367.
- [126] Y.J. Huang, Y. Huang, H. Baldassarre, B. Wang, A. Lazaris, M. Leduc, A.S. Bilodeau, A. Bellemare, M. Cote, P. Herskovits, M. Touati, C. Turcotte, L. Valeanu, N. Lemee, H. Wilgus, I. Begin, B. Bhatia, K. Rao, N. Neveu, E. Brochu, J. Pierson, D.K. Hockley, D.M. Cerasoli, D.E. Lenz, C.N. Karatzas, S. Langermann, *Proc. Natl. Acad. Sci. USA* 104 (2007) 13603–13608.
- [127] Y.J. Huang, P.M. Lundy, A. Lazaris, Y. Huang, H. Baldassarre, B. Wang, C. Turcotte, M. Cote, A. Bellemare, A.S. Bilodeau, S. Brouillard, M. Touati, P. Herskovits, I. Begin, N. Neveu, E. Brochu, J. Pierson, D.K. Hockley, D.M. Cerasoli, D.E. Lenz, H. Wilgus, C.N. Karatzas, S. Langermann, *BMC Biotechnol.* 8 (2008) 50.
- [128] J. Jarv, in: E. Reiner, W.N. Aldridge, F.C.G. Hoskin (Eds.), *Enzymes Hydrolysing Organophosphorus Compounds*, Ellis Horwood Ltd., Chichester, UK, 1989, pp. 221–225.
- [129] J.L. Sussman, M. Harel, F. Frolow, C. Oefner, A. Goldman, L. Toker, I. Silman, *Science* 253 (1991) 872–879.
- [130] O. Lockridge, R.M. Blong, P. Masson, M.T. Froment, C.B. Millard, C.A. Broomfield, *Biochemistry* 36 (1997) 786–795.
- [131] C.B. Millard, O. Lockridge, C.A. Broomfield, *Biochemistry* 34 (1995) 15925–15933.
- [132] R.D. Newcomb, P.M. Campbell, D.L. Ollis, E. Cheah, R.J. Russell, J.G. Oakeshott, *Proc. Natl. Acad. Sci. USA* 94 (1997) 7464–7468.
- [133] C.J. Jackson, J. Liu, R. Russell, M. Weik, D.S. Tawfik, J.G. Oakeshott, 10th International Meeting on Cholinesterases, Sibenik, Croatia, 2009, p. 61.
- [134] C.B. Millard, O. Lockridge, C.A. Broomfield, *Biochemistry* 37 (1998) 237–247.
- [135] L.M. Schopfer, A. Ticu-Boeck, C.A. Broomfield, O. Lockridge, *J. Med. Chem. Def.* 2 (2004) 1–21 (online journal).
- [136] T. Poyot, F. Nachon, M.T. Froment, M. Loiodice, S. Wieseler, L.M. Schopfer, O. Lockridge, P. Masson, *Biochim. Biophys. Acta* 1764 (2006) 1470–1478.
- [137] L.G. Costa, C. Furlong, in: R.C. Gupta (Ed.), *Handbook of Toxicology of Chemical Warfare Agents*, Elsevier-Academic Press, Amsterdam, 2009, pp. 1023–1031.
- [138] R.J. Kern, M.E. Wales, E. Tiffany-Castiglioni, J.R. Wild, in: R.C. Gupta (Ed.), *Handbook of Toxicology of Chemical Warfare Agents*, Elsevier-Academic Press, Amsterdam, 2009, pp. 1041–1051.
- [139] P. Masson, D. Rochu, in: R.C. Gupta (Ed.), *Handbook of Toxicology of Chemical Warfare Agents*, Elsevier-Academic Press, Amsterdam, 2009, pp. 1053–1065.
- [140] S. Bershtein, D.S. Tawfik, *Curr. Opin. Chem. Biol.* 12 (2008) 151–158.
- [141] R.E. Sweeney, D.M. Maxwell, *Math. Biosci.* 181 (2003) 133–143.
- [142] T. Inaba, D.J. Stewart, W. Kalow, *Clin. Pharmacol. Ther.* 23 (1978) 547–552.
- [143] W. Xie, C.V. Altamirano, C.F. Bartels, R.J. Speirs, J.R. Cashman, O. Lockridge, *Mol. Pharmacol.* 55 (1999) 83–91.
- [144] H. Sun, Y.P. Pang, O. Lockridge, S. Brimijoin, *Mol. Pharmacol.* 62 (2002) 220–224.
- [145] Y. Pan, D. Gao, W. Yang, H. Cho, G. Yang, H.H. Tai, C.G. Zhan, *Proc. Natl. Acad. Sci. USA* 102 (2005) 16656–16661.
- [146] F. Zheng, C.G. Zhan, *Org. Biomol. Chem.* 6 (2008) 836–843.
- [147] F. Zheng, W. Yang, M.C. Ko, J. Liu, H. Cho, D. Gao, M. Tong, H.H. Tai, J.H. Woods, C.G. Zhan, *J. Am. Chem. Soc.* 130 (2008) 12148–12155.
- [148] S. Brimijoin, Y. Gao, J.J. Anker, L.A. Gliddon, D. Lafleur, R. Shah, Q. Zhao, M. Singh, M.E. Carroll, *Neuropsychopharmacology* 33 (2008) 2715–2725.
- [149] W. Yang, Y. Pan, F. Zheng, H. Cho, H.H. Tai, C.G. Zhan, *Biophys. J.* 96 (2009) 1931–1938.
- [150] J.D. Pancook, G. Pecht, M. Ader, O. Lockridge, J.D. Watkins, *FASEB J.* 17 (2003) A565.
- [151] F. Dorandeu, A. Foquin, R. Briot, C. Delacour, J. Denis, A. Alonso, M.T. Froment, F. Renault, G. Lallement, P. Masson, *Toxicology* 248 (2008) 151–157.
- [152] P. Masson, E. Carletti, F. Nachon, *Protein Pept. Lett.* (2009).
- [153] F. Nachon, Y. Nicolet, A. Ticu-Boeck, P. Masson, O. Lockridge, in: IXth International Meeting on Cholinesterases, Poster P-IV-2, Suzhou, China, 2007.
- [154] P. Masson, M.T. Froment, E. Gillon, F. Nachon, O. Lockridge, L.M. Schopfer, *Biochim. Biophys. Acta* 1774 (2007) 16–34.
- [155] M. Amitay, A. Shurki, *Proteins* 77 (2009) 370–377.
- [156] E.S. Peeples, L.M. Schopfer, E.G. Duysen, R. Spaulding, T. Voelker, C.M. Thompson, O. Lockridge, *Toxicol. Sci.* 83 (2005) 303–312.
- [157] N.H. Williams, J.M. Harrison, R.W. Read, R.M. Black, *Arch. Toxicol.* 81 (2007) 627–639.
- [158] B. Li, L.M. Schopfer, S.H. Hinrichs, P. Masson, O. Lockridge, *Anal. Biochem.* 361 (2007) 263–272.
- [159] W.G. Carter, M. Tarhoni, A.J. Rathbone, D.E. Ray, *Hum. Exp. Toxicol.* 26 (2007) 347–353.
- [160] H. Grigoryan, L.M. Schopfer, C.M. Thompson, A.V. Terry, P. Masson, O. Lockridge, *Chem. Biol. Interact.* 175 (2008) 180–186 (PMCID2577157).
- [161] B. Li, L.M. Schopfer, H. Grigoryan, C.M. Thompson, S.H. Hinrichs, P. Masson, O. Lockridge, *Toxicol. Sci.* 107 (2009) 144–155 (PMCID2638647).
- [162] H. Grigoryan, B. Li, E.K. Anderson, W. Xue, F. Nachon, O. Lockridge, L.M. Schopfer, *Chem. Biol. Interact.* 180 (2009) 492–498 (PMCID2700782).
- [163] H. Grigoryan, B. Li, W. Xue, M. Grigoryan, L.M. Schopfer, O. Lockridge, *Anal. Biochem.* 394 (2009) 92–100.
- [164] L.M. Schopfer, H. Grigoryan, B. Li, P. Masson, O. Lockridge, *J. Chromatogr. B* (2009), in press.
- [165] G.A. Morfini, M. Burns, L.I. Binder, N.M. Kanaan, N. LaPointe, D.A. Bosco, R.H. Brown Jr., H. Brown, A. Tiwari, L. Hayward, J. Edgar, K.A. Nave, J. Garberrn, Y. Atagi, Y. Song, G. Pigino, S.T. Brady, J. Neurosci. 29 (2009) 12776–12786.
- [166] C.S. Miller, H.C. Mitzel, *Arch. Environ. Health* 50 (1995) 119–129.
- [167] N. Tahmaz, A. Soutar, J.W. Cherrie, *Ann. Occup. Hyg.* 47 (2003) 261–267.
- [168] B.A. Golomb, *Proc. Natl. Acad. Sci. USA* 105 (2008) 4295–4300.
- [169] D.B. Hancock, E.R. Martin, G.M. Mayhew, J.M. Stajich, R. Jewett, M.A. Stacy, B.L. Scott, J.M. Vance, W.K. Scott, *BMC Neurol.* 8 (2008) 6.
- [170] C. Beseler, L. Stallones, J.A. Hoppin, M.C. Alavanja, A. Blair, T. Keefe, F. Kamel, *J. Occup. Environ. Med.* 48 (2006) 1005–1013.
- [171] D.B. Barr, R. Allen, A.O. Olsson, R. Bravo, L.M. Caltabiano, A. Montesano, J. Nguyen, S. Udunka, D. Walden, R.D. Walker, G. Weerasekera, R.D. Whitehead Jr., S.E. Schober, L.L. Needham, *Environ. Res.* 99 (2005) 314–326.
- [172] M.L. Shih, J.R. Smith, J.D. McMonagle, T.W. Dolzine, V.C. Gresham, *Biol. Mass Spectrom.* 20 (1991) 717–723.
- [173] P.A. D'Agostino, J.R. Hancock, C.L. Chenier, C.R. Lepage, *J. Chromatogr. A* 1110 (2006) 86–94.
- [174] M.J. Van Der Schans, M. Polhuijs, C. Van Dijk, C.E. Degenhardt, K. Pleijsier, J.P. Langenberg, H.P. Benschop, *Arch. Toxicol.* 78 (2004) 508–524.
- [175] E.M. Jakubowski, J.M. McGuire, R.A. Evans, J.L. Edwards, S.W. Hulet, B.J. Benton, J.S. Forster, D.C. Burnett, W.T. Muse, K. Matson, C.L. Crouse, R.J. Mioduszewski, S.A. Thomson, *J. Anal. Toxicol.* 28 (2004) 357–363.
- [176] H. Li, I. Ricordel, L. Tong, L.M. Schopfer, F. Baud, B. Megarbane, E. Maury, P. Masson, O. Lockridge, *J. Appl. Toxicol.* 29 (2009) 149–155.
- [177] B. Li, L.M. Schopfer, S.H. Hinrichs, P. Masson, O. Lockridge, *Anal. Biochem.* 361 (2007) 263–272 (PMCID:1828685).
- [178] N.H. Williams, J.M. Harrison, R.W. Read, R.M. Black, *Arch. Toxicol.* 81 (2007) 627–639.
- [179] B. Li, F. Nachon, M.T. Froment, L. Verdier, J.C. Debouzy, B. Brasme, E. Gillon, L.M. Schopfer, O. Lockridge, P. Masson, *Chem. Res. Toxicol.* 21 (2008) 421–431.
- [180] Y. Song, R.G. Cooks, *J. Mass Spectrom.* 42 (2007) 1086–1092.
- [181] Y. Seto, in: R.C. Gupta (Ed.), *Handbook of Toxicology of Chemical Warfare Agents*, Academic Press, 2009, pp. 813–825 (Chapter 53).
- [182] J.J. Sullivan, Y.G. Chen, K.S. Goh, *J. Agric. Food Chem.* 55 (2007) 6407–6416.
- [183] H. Wang, J. Wang, C. Timchalk, Y. Lin, *Anal. Chem.* 80 (2008) 8477–8484.
- [184] F.S. Ligler, K.E. Sapsford, J.P. Golden, L.C. Shriver-Lake, C.R. Taitt, M.A. Dyer, S. Barone, C.J. Myatt, *Anal. Sci.* 23 (2007) 5–10.
- [185] Y. Pan, J.L. Muzyka, C.G. Zhan, *J. Phys. Chem. B* 113 (2009) 6543–6552.



Contents lists available at ScienceDirect

## Chemico-Biological Interactions

journal homepage: [www.elsevier.com/locate/chembioint](http://www.elsevier.com/locate/chembioint)

# A collaborative endeavor to design cholinesterase-based catalytic scavengers against toxic organophosphorus esters<sup>☆</sup>

Patrick Masson<sup>a,\*</sup>, Florian Nachon<sup>a</sup>, Clarence A. Broomfield<sup>b</sup>, David E. Lenz<sup>b</sup>,  
Laurent Verdier<sup>c</sup>, Lawrence M. Schopfer<sup>d</sup>, Oksana Lockridge<sup>d</sup>

<sup>a</sup> Toxicology Department, Enzymology Unit, Centre de Recherches du Service de Santé des Armées, BP 87, 38702 La Tronche Cedex, France

<sup>b</sup> US Army Medical Research Institute of Chemical Defense, 3100 Ricketts Point Road, Aberdeen PG, MD 21010-5400, USA

<sup>c</sup> Centre d'Etudes du Bouchet, BP 3, 91740 Vert-le-Petit, France

<sup>d</sup> Eppley Institute, University of Nebraska Medical Center, 986805 Nebraska Medical Center, Omaha, NE 68198-6805, USA

## ARTICLE INFO

## Article history:

Available online 16 April 2008

## Keywords:

Butyrylcholinesterase  
Acetylcholinesterase  
Catalytic bioscavenger  
Organophosphorus compound

## ABSTRACT

Wild-type human butyrylcholinesterase (BuChE) has proven to be an efficient bioscavenger for protection against nerve agent toxicity. Human acetylcholinesterase (AChE) has a similar potential. A limitation to their usefulness is that both cholinesterases (ChEs) react stoichiometrically with organophosphorus (OP) esters. Because OPs can be regarded as pseudo-substrates for which the dephosphorylation rate constant is almost zero, several strategies have been attempted to promote the dephosphorylation reaction. Oxime-mediated reactivation of phosphorylated ChEs generates a turnover, but it is too slow to make pseudo-catalytic scavengers of pharmacological interest. Alternatively, it was hypothesized that ChEs could be converted into OP hydrolases by using rational site-directed mutagenesis based upon the crystal structure of ChEs. The idea was to introduce a nucleophile into the oxyanion hole, at an appropriate position to promote hydrolysis of the phospho-serine bond via a base catalysis mechanism. Such mutants, if they showed the desired catalytic and pharmacokinetic properties, could be used as catalytic scavengers.

The first mutant of human BuChE that was capable of hydrolyzing OPs was G117H. It had a slow rate. Crystallographic study of the G117H mutant showed that hydrolysis likely occurs by activation of a water molecule rather than direct nucleophilic attack by H117. Numerous BuChE mutants were made later, but none of them was better than the G117H mutant at hydrolyzing OPs, with the exception of soman. Soman aged too rapidly to be hydrolyzed by G117H. Hydrolysis was however accomplished with the double mutant G117H/E197Q, which did not age after phosphorylation with soman.

Multiple mutations in the active center of human and *Bungarus* AChE led to enzymes displaying low catalytic activity towards OPs and unwanted kinetic complexities. A new generation of human AChE mutants has been designed with the assistance of molecular modelling and computational methods. According to the putative water-activation mechanism of G117H BChE, a new histidine/aspartate dyad was introduced into the active center of human AChE at the optimum location for hydrolysis of the OP adduct. Additional mutations were made for optimizing activity of the new dyad. It is anticipated that these new mutants will have OP hydrolase activity.

© 2008 Elsevier Ireland Ltd. All rights reserved.

**Abbreviations:** AChE, acetylcholinesterase; BuChE, butyrylcholinesterase; CaE, carboxylesterase; ChE, cholinesterase; DFP, diisopropylfluorophosphate; DFPase, diisopropylfluorophosphate hydrolase; OP, organophosphorus compound; OPAH, organophosphorus acid anhydride hydrolase; PON1, paraoxonase.

<sup>☆</sup> The opinions or assertions contained herein are the private views of the authors, and are not to be construed as reflecting the view of the French Ministry of Defense or the US Department of Defense.

\* Corresponding author. Tel.: +33 4 76636959; fax: +33 4 76636962.

E-mail address: [pmasson@unmc.edu](mailto:pmasson@unmc.edu) (P. Masson).

0009-2797/\$ – see front matter © 2008 Elsevier Ireland Ltd. All rights reserved.

doi:10.1016/j.cbi.2008.04.005

## 1. Introduction

Organophosphorus (OP) compounds are among the most toxic compounds synthesized. They have been used as pesticides and drugs for several decades. Certain of them are dangerous nerve agents [1,2]. For example, based on animal data the calculated lethal dose of VX, the most toxic nerve agent, is 0.3 mg (inhalation route) and 5 mg (percutaneous absorption) in humans. After rapid absorption mostly through skin and/or lungs, OPs distribute from the blood compartment into biological targets, tissue depot sites and sites of elimination. OPs are irreversible inhibitors of acetylcholinesterase (EC. 3.1.1.7; AChE) and butyrylcholinesterase (EC. 3.1.1.8; BuChE). Inhibition of AChE is responsible for acute toxicity [3,4]. However, OPs interact with numerous biological systems, and reactions with secondary targets are responsible for non-cholinergic and/or delayed toxicity [5].

After some 60 years of research, medical countermeasures against OP poisoning are reaching their optimum [6–8]. Yet they are still imperfect. They prevent lethality, but not incapacitation and irreversible brain damage. It is unlikely that more potent and universal drugs and antidotes devoid of side effects will be discovered in the near future. Therefore, bioscavengers represent an alternative approach to pharmacological pre- and post-exposure treatments. Scavengers can be antibodies, chemicals, e.g. functionalized cyclodextrins, and enzymes that sequester and inactivate highly toxic compounds before they reach their biological targets.

The bioscavenger concept for challenging OPs originated with the observation by Main [9] that “A esterase” (an old name for PON 1), injected i.v. into rats, “significantly reduced the i.v. toxicity of paraoxon”. Because of concern that soman intoxication was resistant to conventional treatment, a search for catalytic soman scavengers was begun that extended over the course of several years. “DFPases” (a general designation for any enzyme that would catalyse the hydrolysis of organophosphorus cholinesterase inhibitors) from a variety of sources were discovered [10–12] and some of them tested [13–16], but practical considerations dictated that human enzymes would be most suitable for use as scavengers in humans. Subsequent studies including active immunization and passive immunization with monoclonal antibodies, revealed that antibodies, by their nature, bind their substrates without changing them and thus might bind an OP and take it out of circulation temporarily but eventually will release it to exercise its toxicity [17,18]. At that point it was realized that catalytic activity was not needed; a stoichiometric scavenger could protect an animal if present in a high enough concentration. The problem was to obtain a relatively large amount of an enzyme that would react with an OP rapidly and irreversibly and would be innocuous in the circulation at artificially high concentrations. This challenge was met initially by Alan Wolfe, who isolated enough AChE from foetal bovine serum to attempt a test in mice, using VX for the challenge. Indeed, administration of foetal bovine serum AChE to mice provided protection against nerve agent poisoning. It was concluded that highly toxic OPs could be sequestered *in*

*vivo*, thus providing a new approach to treatment of OP intoxication [19]. Numerous enzymes have been found to react with OPs [5]. OPs are either irreversible inhibitors or substrates of these enzymes. Skin and plasma BuChE, erythrocyte AChE and liver carboxylesterases are endogenous stoichiometric bioscavengers. Plasma PON1 hydrolyzes OPs, liver glutathione S-transferase and cytochrome P450 (CYP2P) oxidize OP side-chains. Though albumin, the most abundant plasma protein (0.6 mM), reacts with OPs, its reactivity is too slow to contribute significantly to detoxification of these compounds in acute poisoning [20]. Recent reviews on the bioscavenger approach for protection against organophosphorus exposure are available [21–24].

## 2. Stoichiometric scavengers versus catalytic scavengers

An effective bioscavenger detoxifies OP molecules in the blood compartment before they reach their biological targets. Four overall constants control the concentration of OP in blood (Fig. 1): the overall infusion or feeding constant of OP molecules across the skin (or other routes, e.g. lungs, stomach) toward the circulation system ( $k_{on}$ ), the diffusion constant from blood toward biological targets ( $k_{off}$ ), the inactivation constant of reactive enzymes present in the blood ( $k_{OP}$ ), and the clearance constant ( $k_c$ ) of these enzymes. Efficient detoxification by bioscavengers requires that  $k_{OP}$  be as high as possible. In addition,  $k_{OP}$  has to be much higher than  $k_{off}$ , and  $k_c$  must be very slow.

There are two types of scavenger to consider. There are stoichiometric scavengers, which react on a one-to-one basis with the OP, thereby inactivating one OP per scavenger. And, there are catalytic scavengers that hydrolyze the OP, thereby inactivating multiple OP per scavenger.

Butyrylcholinesterase (EC. 3.1.1.8; BuChE) is the most important stoichiometric scavenger in human plasma. The concentration of BuChE in blood (about 50 nM) is 20 times higher than the concentration of erythrocyte AChE

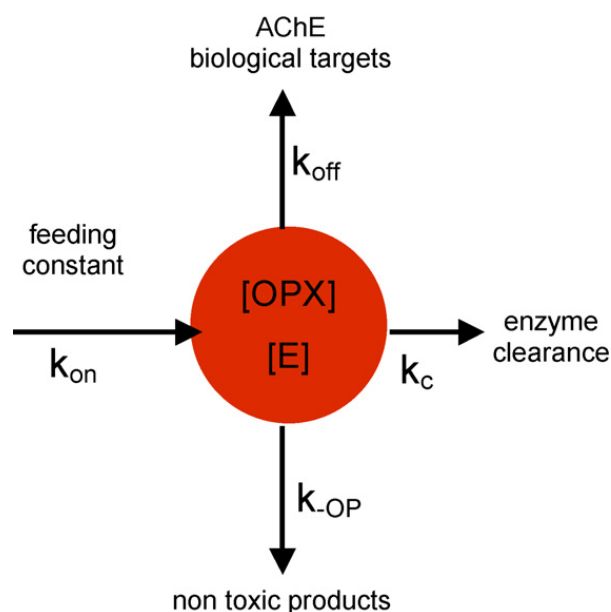
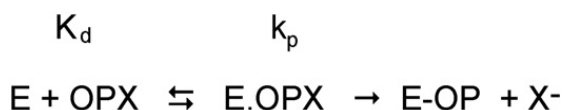


Fig. 1. Kinetic control of OP concentration ([OPX]) in human blood.



Scheme 1.

(2.5 nM), another potential stoichiometric scavenger. Reactions of BuChE with OPs of various types are very rapid (maximum apparent second-order rate constants of about  $10^7 \text{ M}^{-1} \text{ min}^{-1}$ ). In practice, BuChE is capable of protecting against concentrations of OP up to 50 nM, in blood (about 350 nM). To a first approximation, it is only when this level is exceeded that acute intoxication occurs.

Rapid reactivity is a critical feature of BuChE's effectiveness, because even in the most severe intoxications the maximum concentration of OP in blood [OPX] is very low, less than 11 nM [25], which is well below the  $K_d$  of BuChE or AChE for OP molecules (OPX). Thus, the reaction of OPX with ChEs is pseudo-first order. The low maximum level of OP is a consequence of the competition between the feeding rate and the diffusion, inactivation and clearance rates.

Reaction of a stoichiometric bioscavenger (E) with OP is depicted by Scheme 1.

The stoichiometric neutralization of OPs in blood can be conveniently described by a pseudo-first order process in [OPX] (Eqs. (1) and (2)).

$$v = -\frac{d[OPX]}{dt} = k_{-OP}[OPX] \quad (1)$$

in which

$$k_{-OP} = k_{II} \cdot [E] \quad (2)$$

with

$$k_{II} = \frac{k_p}{K_d} \quad (3)$$

Hydrolysis of OP by a catalytic bioscavenger can be described by the minimum Michaelis–Menten mechanism (Scheme 2).

$$\text{with } K_m = \frac{K_d k_r}{k_p + k_r} \quad (4)$$

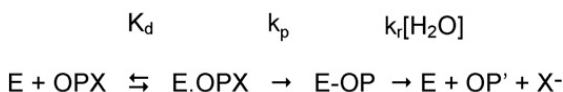
$$\text{and } k_{cat} = \frac{k_p k_r}{k_p + k_r} \quad (5)$$

If  $[OPX] \ll K_m$ , the pseudo first-order rate constant of hydrolysis is

$$k_{-OP} = \frac{k_{cat} \cdot [E]}{K_m} \quad (6)$$

with

$$k_{II} = \frac{k_{cat}}{K_m} \quad (7)$$



Scheme 2.

In order to be optimally effective, a scavenger should be capable of reducing the concentration of OPX to a non-toxic level in less than one median circulation time ( $t \approx 1 \text{ min}$ ). To protect against a severe intoxication, for example, 4000 nmol of OPX, huge amounts of a stoichiometric bioscavenger (such as BuChE, i.e. 340 mg) would have to be injected (Eq. (8)) [23]. In contrast, by virtue of the turnover, much lower doses of a catalytic scavenger would have to be injected for the same detoxifying effect [26,27]. The higher the enzyme catalytic efficiency,  $k_{cat}/K_m$ , the less catalytic scavenger needs to be administered. The necessary concentration of scavenger (either stoichiometric or catalytic) can be calculated from Eq. (8).

$$[E] = \frac{X}{K_{II} \cdot t} \quad (8)$$

X, the factor by which [OPX] is reduced, is equal to  $\ln[OPX]_0/[OPX]_t$ .

The general requirements for a bioscavenger are: (1) high reaction rate ( $k_{-OP}$ ) with OPs; (2) long biological life (very low  $k_c$ ); (2) immuno-tolerance; (3) no side effects; (4) storage and thermal stability; (5) availability from natural source or expression system at reasonable cost; (6) a convenient delivery system. The reaction rate and enantioselectivity can be considerably improved by site-directed mutagenesis or directed evolution [28,29]. Biological life and immuno-tolerance can be improved by encapsulation in nano-containers, e.g. liposomes [30,31], or by chemical modifications of the protein surface, e.g. PEGylation [32–34]. Animal studies are mandatory to evaluate safety and iatrogenic risk, in particular behavioral effects, of administered bioscavengers. Care must be taken if a bioscavenger candidate displays promiscuous activities and has no known physiological function, e.g. PON1 [27,35]. Storage and thermal stability can be solved by lyophilization and/or addition of stabilizers to the enzyme preparations. Improving thermal stability by mutagenesis or by selecting enzyme candidates in an extremophile biotope, e.g. thermophilic bacteria [36], could be an alternative solution, but it needs to be a compromise between thermodynamic stability, catalytic efficiency, and immuno-genicity. At the moment, bioscavengers are administered intravenously or intramuscularly. Future delivery systems for transdermal needleless injection, skin permeation, and inhalation have to be considered for emergency treatment of large populations.

### 3. Human butyrylcholinesterase-based bioscavengers: from stoichiometric to catalytic scavengers

Human BuChE has proven to be a safe and efficient stoichiometric bioscavenger. Based on animal data, it is calculated that injection of a 200 mg dose of recombinant or natural plasma BuChE will protect humans against 2–5 LD<sub>50</sub> of soman or VX with no side effects [23,37–40]. Human plasma derived BuChE was granted Investigational New Drug status by the FDA in 2006 for protection against nerve agents. Because AChE reacts specifically with toxic stereoisomers of soman, whereas BuChE is less enantioselective, administration of 200 mg of AChE is expected to

detoxify larger doses of racemic soman [41]. In addition, 200 mg of AChE is equivalent to 2800 nmol of enzyme, whereas 200 mg of BuChE is equivalent to 2200 nmol. Therefore, 1.27 time more OP molecules can potentially be neutralized by AChE than by BuChE administered at the same dose. However, scaled production of human AChE has not yet begun. Human BuChE has been produced from outdated plasma under GMP by Baxter Healthcare Corporation (<http://www.baxter.com>). Efforts have also been made to engineer human carboxylesterases for the same purpose [42,43]. Stoichiometric bioscavengers, the first generation bioscavengers, are intended for pre-exposure treatment of soldiers, first responders and medical personnel [23].

Second generation scavengers will be catalytic scavengers. Several enzymes are promising candidates, such as *Pseudomonas diminuta* organophosphorus acid anhydride hydrolase (OPAH) [29,44] and human paraoxonase [22,27] that is also an OPAH. Although the bacterial enzyme is not suitable for injection in humans, after chemical capping or encapsulation in stable nano-containers, it could be administered without immunological response. Because evolved mutants of bacterial PTE have been found to be the most efficient enzyme for nerve agent detoxification [29], research efforts have to continue on this enzyme. However, more research has to be done to overcome the immunological issue. Human cholinesterases may represent another alternative. Indeed, because OPs are hemi-substrates of ChEs, it was hypothesized that ChE could be changed into an OP hydrolase. The idea of making mutants of cholinesterases capable of hydrolysing OPs was based on Jarv's hypothesis [45]. Jarv observed that the stereochemistry required for nucleophilic displacement of a carbonyl-ester from ChEs is different from that for displacement of a phosphyl-ester. Acyl-enzyme intermediates have a short life because the acyl group is rapidly displaced with a water molecule. On the contrary, in phosphorylated ChEs, the stereochemistry of the phosphorylated serine prevents accessibility of water. Jarv proposed that this difference in stereochemistry was the reason that the phosphorylated enzyme intermediate is stable. For efficient reaction with a phosphorylated ChE, the nucleophile needs to approach from the vicinity of the oxy-anion hole. This nucleophile could either activate a water molecule or be the primary nucleophile for direct attack on the phosphorus atom.

Broomfield and Millard used computer-aided molecular modelling based on the crystal structure of *Torpedo californica* AChE to design the first mutant of BuChE with OP hydrolase activity. Histidine residues were introduced into the oxyanion hole of human BuChE at positions 115, 117, 119 and 121 [46] (Fig. 2). The imidazole group was intended to promote hydrolysis of the phospho-serine bond in phosphorylated BuChE conjugates either by direct nucleophilic attack on the phosphorus atom or by activating a water molecule. The G117H mutant was successful. It had a decreased phosphorylation rate ( $k_p$ ) for DFP and nerve agents, and a spontaneous reactivation rate ( $k_r$ ), i.e. there was hydrolysis of the phospho-serine bond. Conjugates of BuChE with nerve agents, DFP, paraoxon, and echothiophate slowly self-reactivated [46,48]. However, due to rapid "aging", soman-phosphonylated enzyme did not reacti-

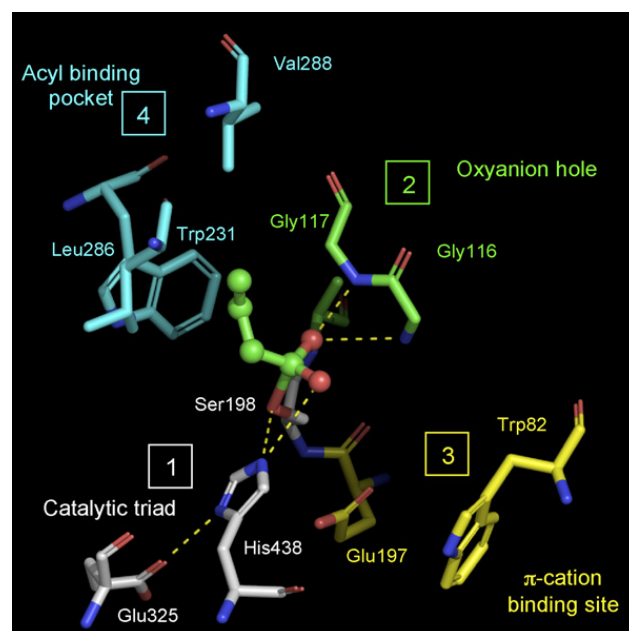


**Fig. 2.** Active center pocket of human butyrylcholinesterase, in complex with butyrate, taken from crystal structure at 2.0 Å resolution [47]. Area 1, Active serine (S198), vicinal E197, and catalytic histidine (H438); area 2, oxyanion hole (G116, G117, A199); area 3,  $\pi$ -cation binding site (W82); area 4, acyl-binding pocket (L286, V288, W231).

vate. The aging reaction involves stabilization of a positive charge on the developing carbocationic alkoxy chain by the carboxylate of E197 (Fig. 2). The mutation E197Q was introduced to make the double mutant G117H/E197Q. This mutation abolished the aging reaction, and allowed time for hydrolysis to occur [49]. Unfortunately, this second mutation decreased both the rate of phosphorylation and dephosphorylation of other OPs.

Numerous multiple mutations were subsequently created in different loci: the oxyanion hole (introduction of other nucleophiles D, Y, S, C in position 117), the  $\pi$ -cation binding site and the acyl-binding pocket (Fig. 2) [50]. None of these mutants was more active than G117H. In fact, we recently provided evidence that mutation in the oxyanion hole causes distortion of this area with deleterious effects on transition state stabilization [51].

The X-ray structure of the G117H mutant phosphorylated by echothiophate, i.e. the diethylphosphorylated enzyme conjugate was recently solved at 2.1 Å (Fig. 3) [52]. Results indicate that H117 is mobile enough to both activate a vicinal water molecule and stabilize the trigonal bipyramidal dephosphorylation transition state.

#### 4. Mutagenesis of acetylcholinesterases

Transposition of the G117H mutation into *Bungarus fasciatus* and human AChE yielded inactive enzyme. In those enzymes, the mutated residue was G122. In an effort to activate the G122H mutant, two additional mutations were introduced to enlarge the active site pocket. This triple mutant, G122H/Y124Q/S125T, might be referred to as "butyrylized" AChE. These mutations dramatically altered the catalytic properties of AChE with ester substrates, conferred resistance to inhibition by OPs, and created OP

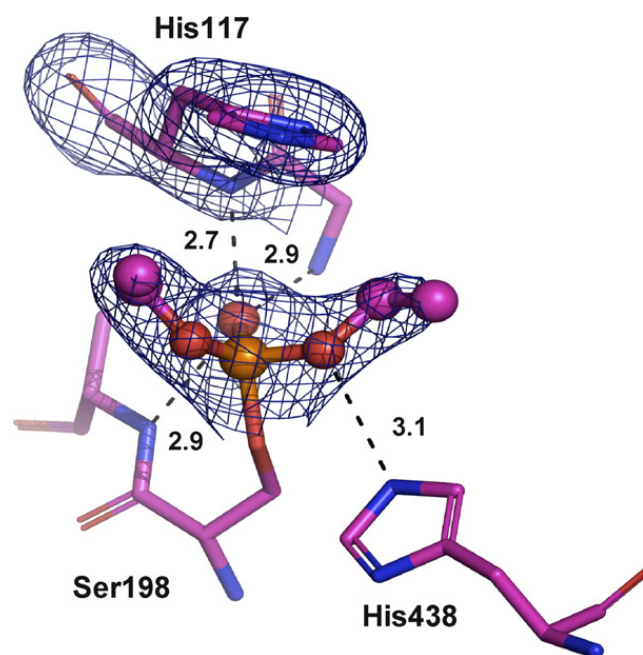
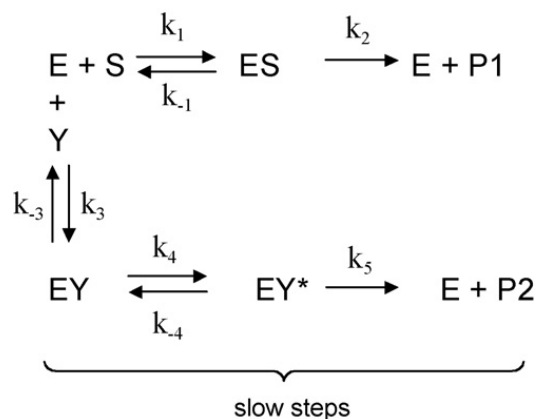


**Fig. 3.** X-ray structure of the active center of diethylphosphorylated G117H mutant of human butyrylcholinesterase (DEP-G117H) at 2.1 Å resolution [52].

hydrolase activity, though the OP hydrolase activity was extremely low. However, these mutants are the first AChE mutants capable of hydrolysing OPs [53]. The reactivity with OPs was accompanied by kinetic complexities: first, there was slow binding of certain OPs (e.g. DFP), which meant that the phosphorylation reaction started after a long induction time. The dependence of the induction time on OP concentration is hyperbolic. This meant that slow-binding inhibition is of type B, that is, there is rapid formation of complex EY between enzyme and OP followed by slow isomerization of EY to EY\*, then slow hydrolysis of EY\* (Scheme 3). Second, with other OPs (e.g. paraoxon) there was a transient increase of the enzyme-catalyzed hydrolysis of acetylthiocholine in the presence of low OP concentrations. A similar phenomenon was recently reported for interaction of chlorpyrifos-oxon with recom-



**Scheme 3.**

binant human AChE [54]. This was interpreted in terms of binding of OP on a secondary site.

Cholinesterases engineered for hydrolysing OPs so far display a catalytic efficiency much less than that of phosphotriesterases (Table 1). To be of medical interest, cholinesterase mutants should display  $k_{cat}/K_m$  values several orders of magnitude higher than the values for the mammalian enzymes in Table 1. In addition, mutated enzyme should not display unwanted kinetic complexities such as a long induction period or hysteresis, preceding establishment of steady-state OP hydrolysis.

To take up this challenge we have modified our mutagenesis strategy. A histidine was introduced into the active center of human AChE in a position that does not affect the oxyanion hole. An aspartate was added to activate the histidine, making the His/Asp dyad (Y124H/Y72D) (Fig. 4). Molecular dynamics showed that H-bonding and orientation of the dyad are optimal for hydrolysis of phosphyl-adducts and that the structure is stable. In particular, the D72 carboxylate, the H124 imidazolium and the phosphorus atom in diisopropylated enzyme (DFP conjugate) remain aligned throughout the simulation. This mutant was expressed in 293K cells. Unlike previous ChE mutants that displayed altered catalytic properties with carboxyl-esters compared to wild-type enzymes,

**Table 1**

Catalytic efficiency ( $k_{cat}/K_m$   $10^6$   $M^{-1}$   $min^{-1}$ ) of different natural and engineered OP hydrolases towards different OPs

Enzyme	Paraoxon	DFP	Soman	Sarin	Echothiophate	VX
Human Q192 PON1	0.68 [55]	0.04 [56]	2.8 [57]	0.91 [57]		+ *
Human R192 PON1	2.4 [55]		2.1 [57]	0.07 [57]		+ *
Mammalian G3C9_rPON1	0.72 [58]					
Human G117H BuChE	0.0057 [53]	0.0052 [53]	-	0.00016 [48]	0.0101 [53]	0.0015 [48]
Blowfly G117D CaE	0.2 [59]					
<i>B. fasciatus</i> HQT AChE	0.000064 [53]	0.00076 [53]			0.000024 [53]	
<i>Loligo vulg.</i> DFPase		78 [60]	2.4 [60]	2.4 [60]		0 [60]
<i>P. diminuta</i> OPAH	2000 [61]	580 [62]	0.6 [63]	4.8 [63]		0.04 [64]
<i>Alteromonas</i> OPAA		46 [65]				

Mammalian enzymes are in the grey box (see Refs. [48,53,55–65]). \* C.A. Broomfield, unpublished result.

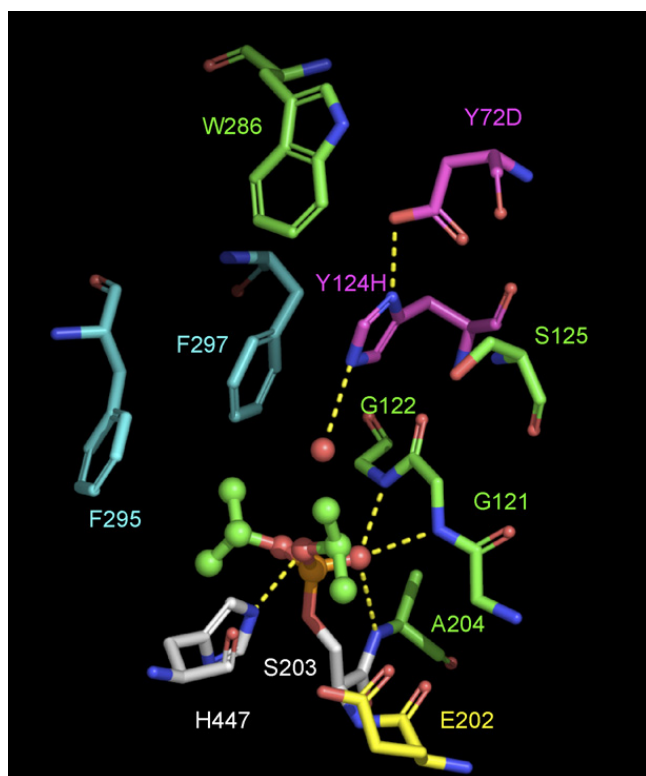


**Fig. 4.** New human AChE mutant: simulation of DFP covalently docked into the active center of Y124H/Y72D mutant of human AChE. S203 is the active site serine.

this mutant is very active with acetylthiocholine as the substrate. This mutant is the first one of a new generation of ChE mutants designed for hydrolyzing OPs. Additional mutations were introduced for optimising the efficiency of the dyad. Two generic mutants were made: Y124H/Y72D/E285Q and Y124H/Y72D/E285M. The catalytic OP hydrolase activity of these new generic mutants will be improved by computational design.

## 5. Prospects

Rational design of ChE mutants with high OP hydrolase activity requires a better knowledge of the detailed reaction mechanism of mutant-catalyzed OP hydrolysis. The key to rational redesign is to further understand the protein environmental effects on the reaction pathway, particularly on the transition states. Knowledge of the configuration of the trigonal bipyramidal transition state of phosphorus conjugates is needed to enable lowering the activation free energy barrier of the rate-limiting step, and increasing the fraction of reactive trajectories that successfully cross the transition state barrier and become productive. However, reaction coordinate calculations by quantum mechanics with an active site model can only account for breaking the P–Oγ–serine bond during the nucleophilic attack. Thus, complex protein environmental effects on the reaction pathway and the energy barriers have to be examined. Hybrid quantum mechanical/molecular mechanical (QM/MM) calculations are the method of choice for including the protein environment. Because it is not yet possible to treat entire proteins by QM methods, the system has to be

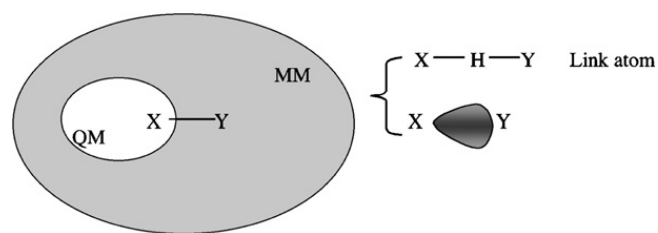


**Fig. 5.** In QM/MM method the protein is divided into a QM part and a MM part. The QM subsystem must include all atoms that are directly involved in the bond breaking and forming process. This partition may require cutting a covalent bond (between a QM atom X and a MM atom Y) in the boundary and thus special techniques should be applied to fulfil the valence of the QM atom (X).

partitioned as follows: the smallest ‘important’ part of the protein is treated at a high quantum chemical level (QM), whereas the much larger remainder is dealt with using classical force-field methods (MM) as displayed in Fig. 5 [66].

However, the QM/MM process is time consuming even if using large computational resources and screening a large panel of ChE mutants would be prohibitive. A new methodology called “transition state modelling with empirical force-field” (TS-MD) has demonstrated its power in design of a human BuChE mutant that hydrolyses (–)-cocaine at a rate more than 400-times higher than wild-type BuChE [67]. MD simulations using a classical force field (molecular mechanics) can only simulate a stable structure corresponding to a local energy minimum. To associate the transition state structure to a local minimum on the energy potential surface, one needs to create a non-standard residue and to maintain the bond lengths of the forming and breaking covalent bonds. In the case of phosphylate–AChE, the non-standard residue consists of the OP adduct and the hydroxyl ion of water, leading to the trigonal bipyramidal transition state (Fig. 6). Geometry of the transition state structure is obtained by previous QM/MM calculations or by *ab initio* calculations on a model reaction system. These types of MD simulations on transition states would provide quantitative information about the dynamic change in the environment surrounding the reaction center and on the multiple interactions between the reaction center and the protein environment. The speed of this method compared to QM/MM or QM is expected to allow screening of a large number of mutants.

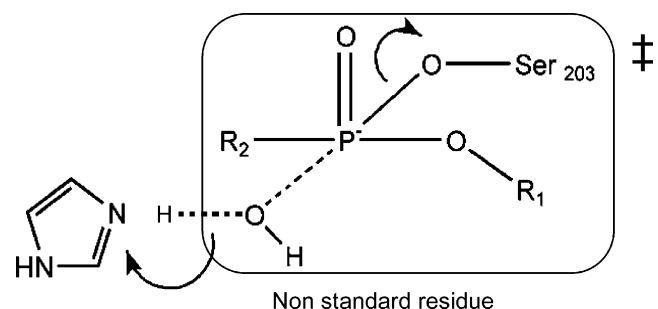


**Fig. 6.** Non-standard residue in transition state for phosphylated human AChE. Non-standard residue contains the phosphorus adduct, the catalytic serine (S203) and hydroxyl ion from a water molecule, that simulates the transition state (TS1) of forming covalent bond during hydrolysis.

## 6. Conclusion

Human BChE was awarded Investigational New Drug status by the FDA in 2006, and it is now undergoing Phase I safety trials in humans. If taken to full FDA licensure, BuChE would be the first marketed bioscavenger for protection against organophosphorus agent exposure. Because catalytic scavengers show advantages over first generation stoichiometric scavengers, efforts have been made for more than 15 years to convert ChEs into OP hydrolase enzymes. Though mutated ChEs displaying turnover with OPs have been made, no operational mutants are available so far.

In the future, much significant progress is expected, using the site-directed mutagenesis approach with the help of computational methods like QM/MM or TS-MD simulations for predicting mutations that will optimize the geometry and the stability of the dephosphorylation transition state in ChEs. Alternatively, if expression of functional ChEs in microorganisms, like *E. coli*, becomes possible, then directed evolution of ChEs should be a promising method to generate new ChE-based catalytic scavengers.

## Acknowledgements

This work was supported by US Army Medical Research and Materiel Command DAMD17-01-2-0036 to OL and DGA (03-CO 010-05)/PEA 01.08.07) to PM.

## References

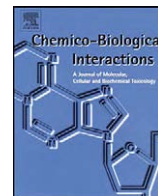
- [1] B. Balantyne, T.C. Marrs (Eds.), *Clinical and Experimental Toxicology of Organophosphates and Carbamates*, Butterworth, Oxford & London, 1992.
- [2] A.A. Weinbroum, Pathophysiological and clinical aspects of combat anticholinesterase poisoning, *Br. Med. Bull.* 72 (2005) 119–133.
- [3] L.C. Costa, Current issues in organophosphate toxicology, *Clin. Chim. Acta* 366 (2006) 1–13.
- [4] D.M. Maxwell, K.M. Brecht, I.M. Koplovitz, R.E. Sweeney, Acetylcholinesterase inhibition: does it explain the toxicity of organophosphorus compounds? *Arch. Toxicol.* 80 (2006) 756–760.
- [5] J.E. Casida, G.B. Quistad, Organophosphate toxicity: safety aspects of non acetylcholinesterase secondary targets, *Chem. Res. Toxicol.* 17 (2004) 983–998.
- [6] P. Aas, Future considerations for the medical management of nerve-agent intoxication, *Prehosp. Disast. Med.* 18 (2003) 208–216.
- [7] J. Wetherell, M. Price, H. Mumford, S. Armstrong, L. Scott, Development of next generation medical countermeasures to nerve agent poisoning, *Toxicology* 233 (2007) 120–127.
- [8] M. Eddleston, N.A. Buckley, P. Eyer, A.H. Dawson, Management of acute organophosphorus pesticide poisoning, *Lancet* 371 (2008) 597–607.
- [9] A.R. Main, The role of A-esterase in the acute toxicity of paraoxon, TEPP, and parathion, *Can. J. Biochem. Physiol.* 34 (1956) 197–216.
- [10] F.C. Hoskin, A.H. Roush, Hydrolysis of nerve gas by squid-type diisopropylphosphorofluoridate hydrolyzing enzyme on agarose resin, *Science* 215 (1982) 1255–1257.
- [11] W.G. Landis, R.E. Savage, F.C. Hoskin, An organofluorophosphate-hydrolyzing activity in *Tetrahymena thermophila*, *J. Protozool.* 32 (1985) 517–519.
- [12] C.M. Serdar, D.T. Gibson, Enzymatic hydrolysis of organophosphates: cloning and expression of a parathion hydrolase gene from *Pseudomonas diminuta*, *Bio/Technology* 3 (1985) 567–571.
- [13] D.E. Lenz, C.A. Broomfield, J.S. Little, R. Ray, The kinetics of hydrolysis of soman stereoisomers by diisopropylfluorophosphatase, in: Frank, Holmstedt, Testa (Eds.), *Chirality and Biological Activity*, Alan R. Liss, New York, 1990, pp. 169–176.
- [14] J.S. Little, C.A. Broomfield, M.K. Fox-Talbot, L.J. Boucher, B. MacIver, D.E. Lenz, Partial Characterization of an Enzyme that Hydrolyzes Sarin, Soman, Tabun and DFP, *Biochem. Pharmacol.* 38 (1989) 23–29.
- [15] C.A. Broomfield, J.S. Little, D.E. Lenz, R. Ray, Organophosphorus acid anhydride hydrolase that lack chiral specificity, in: E. Reiner, W.N. Aldridge, F.C.G. Hoskin (Eds.), *Enzymes Hydrolyzing Organophosphorus Compounds*, Horwood, Chichester, 1989, pp. 79–89.
- [16] C.A. Broomfield, A purified recombinant organophosphorus acid anhydride protects mice against soman, *Chem. Biol. Interact.* 87 (1993) 279–284.
- [17] D.E. Lenz, A.A. Brimfield, K.W. Hunter, H.P. Benschop, L.P.A. de Jong, C. van Dijk, T.R. Clow, Studies using a monoclonal antibody against soman, *Fundam. Appl. Toxicol.* 4 (1984) S156–S164.
- [18] A.A. Brimfield, D.E. Lenz, H.P. Benschop, L.A.P. de Jong, C. van Dijk, K.W. Hunter, Structural and stereochemical specificity of mouse monoclonal antibodies to the organophosphorus compound soman, *Mol. Pharmacol.* 28 (1985) 32–39.
- [19] A.D. Wolfe, A.R.S. Rush, B.P. Doctor, I. Koplovitz, D. Jones, Acetylcholinesterase prophylaxis against organophosphate toxicity, *Fundam. Appl. Toxicol.* 9 (1987) 266–270.
- [20] B. Li, F. Nachon, M.-T. Froment, L. Verdier, J.-C. Debouzy, B. Brasme, E. Gillon, L.M. Schopfer, O. Lockridge, P. Masson, Binding and hydrolysis of soman by human serum albumin, *Chem. Res. Toxicol.* 21 (2008) 421–431.
- [21] P. Masson, F. Nachon, D. Rochu, Ingénierie d'enzymes pour la protection, la décontamination et le traitement des agressions par les composés organophosphorés, *Bull. Acad. Méd.* 191 (2007) 93–112.
- [22] D.E. Lenz, D. Yeung, R.E. Sweeney, L.A. Lumley, D.M. Cerasoli, Stoichiometric and catalytic scavengers as protection against nerve agent toxicity: a mini review, *Toxicology* 233 (2007) 31–39.
- [23] D.E. Lenz, C.A. Broomfield, D.T. Yeung, P. Masson, D.M. Maxwell, D.M. Cerasoli, Nerve agent bioscavengers: progress in development of a new mode of protection against organophosphorus exposure, in: J.A. Romano, B.J. Luckey, H. Salem (Eds.), *Chemical Warfare Agents Chemistry, Pharmacology, Toxicology and Therapeutics*, CRC Press, Boca Raton, FL, 2007, pp. 175–202.
- [24] A. Saxena, C. Luo, N. Chilukuri, D.M. Maxwell, B.P. Doctor, Novel approaches to medical protection against chemical warfare nerve agents, in: J.A. Romano, B.J. Luckey, H. Salem (Eds.), *Chemical Warfare Agents Chemistry, Pharmacology, Toxicology and Therapeutics*, CRC Press, Boca Raton, FL, 2007, pp. 145–173.
- [25] R.E. Sweeney, D.M. Maxwell, A theoretical expression for the protection associated with stoichiometric and catalytic scavengers in a single compartment model of organophosphate poisoning, *Math. Biosci.* 181 (2003) 133–143.
- [26] D. Josse, O. Lockridge, W. Xie, C.F. Bartels, L.M. Schopfer, P. Masson, The active site of human paraoxonase (PON1), *J. Appl. Toxicol.* 38 (Suppl. 1) (1999) 7–11.
- [27] D. Rochu, E. Chabriere, P. Masson, Human paraoxonase: a promising approach for pre-treatment and therapy of organophosphate poisoning, *Toxicology* 233 (2007) 47–59.
- [28] C.M. Hill, W.-S. Li, J.B. Thoden, H.M. Holden, F.M. Raushel, Enhanced degradation of chemical warfare agents through molecular engineering of the phosphotriesterase active site, *J. Am. Chem. Soc.* 125 (2003) 8990–8991.
- [29] E. Ghanem, F.M. Raushel, Detoxification of organophosphate nerve agents by bacterial phosphotriesterase, *Toxicol. Appl. Pharmacol.* 207 (Suppl. 2) (2005) 459–470.
- [30] S. Fisher, A. Aya, R. Margalit, Liposome-formulated enzymes for organophosphate scavenging: butyrylcholinesterase and demeton-S, *Arch. Biochem. Biophys.* 434 (2005) 108–115.
- [31] I. Petrikovics, T.-C. Cheng, D. Papahadjopoulos, K. Hong, R. Yin, J.J. DeFrank, J. Jaing, Z.H. Song, W.D. McGuinn, D. Sylvester, L. Pei, J. Madec, C. Tamulinas, J.C. Jaszberenyi, T. Barcza, J.L. Way, Long circulating liposomes encapsulating organophosphorus acid anhydrolase in diisopropylfluorophosphate antagonism, *Toxicol. Sci.* 57 (2000) 16–21.
- [32] N. Chilukuri, K. Parikh, W. Sun, R. Naik, P. Tipparaju, B.P. Doctor, A. Saxena, Polyethylene glycosylation prolongs the circulatory stability of recombinant human butyrylcholinesterase, *Chem. Biol. Interact.* 157–158 (2005) 115–121.
- [33] O. Cohen, C. Kronman, L. Raveh, O. Mazor, A. Ordentlich, A. Shafferman, Comparison of polyethylene glycol-conjugated recombinant human acetylcholinesterase and serum butyrylcholinesterase as bioscavengers of organophosphate compounds, *Mol. Pharmacol.* 70 (2006) 1121–1131.
- [34] C. Kronman, O. Cohen, L. Raveh, O. Mazor, A. Ordentlich, A. Shafferman, Polyethylene-glycol conjugated recombinant human acetylcholinesterase serves as an efficacious bioscavenger against soman intoxication, *Toxicology* 233 (2007) 40–46.

- [35] R.W. James, A long and winding road: defining the biological role and clinical importance of paraoxonases, *Clin. Chem. Lab. Med.* 44 (2006) 1052–1059.
- [36] L. Merone, L. Mandrich, M. Rossi, G. Manco, A thermostable phosphotriesterase from the archaeon *Sulfolobus solfataricus*: cloning, overexpression and properties, *Extremophiles* 9 (2005) 297–305.
- [37] Y. Ashani, Prospective of human butyrylcholinesterase as a detoxifying antidote and potential regulator of controlled-release drugs, *Drug. Dev. Res.* 50 (2000) 298–308.
- [38] Y. Ashani, S. Pistinner, Estimation of the upper limit of human butyrylcholinesterase dose required for protection against organophosphates toxicity: a mathematically based toxicokinetic model, *Toxicol. Sci.* 77 (2004) 358–367.
- [39] A. Saxena, W. Sun, C. Luo, T.M. Myers, I. Koplovitz, D.E. Lenz, B.P. Doctor, Bioscavengers for protection from toxicity of organophosphorus compounds, *J. Mol. Neurosci.* 30 (2006) 145–147.
- [40] Y.-J. Huang, Y. Huang, H. Baldassarre, B. Wang, A. Lazaris, M. Leduc, A.S. Bilodeau, A. Bellemare, M. Côté, P. Herskovits, M. Touati, C. Turcotte, L. Vaeleau, N. Lemée, H. Wilgus, I. Bégin, B. Bhatia, K. Rao, N. Neveu, E. Brochu, J. Pierson, D.K. Hockley, D.M. Cerasoli, D.E. Lenz, C.N. Karatzas, S. Langermann, Recombinant human butyrylcholinesterase from milk of transgenic animals to protect against organophosphate poisoning, *Proc. Natl. Acad. Sci. U.S.A.* 104 (2007) 13603–13608.
- [41] O. Cohen, C. Kronman, L. Raveh, O. Mazor, A. Ordentlich, A. Shaf-ferman, Comparison of polyethylene glycol-conjugated recombinant human acetylcholinesterase and serum cholinesterase as bioscavengers of organophosphate compounds, *Mol. Pharmacol.* 70 (2006) 1121–1131.
- [42] P.M. Potter, R.M. Wadkins, Carboxylesterases—detoxifying enzymes and targets for drug therapy, *Curr. Med. Chem.* 13 (2006) 1045–1054.
- [43] C.D. Fleming, C.C. Edwards, S.D. Kirby, D.M. Maxwell, P.M. Potter, D.M. Cerasoli, M.R. Redinbo, Crystal structure of human carboxylesterase 1 in covalent complexes with the chemical agents soman and tabun, *Biochemistry* 46 (2007) 5063–5071.
- [44] M.A. Sogorb, E. Vilanova, V. Carrera, Future applications of phosphotriesterases in the prophylaxis and treatment of organophosphorus insecticide and nerve agent poisonings, *Toxicol. Lett.* 151 (2004) 219–233.
- [45] J. Järvi, Insight into the putative mechanism of esterase acting simultaneously on carboxyl and phosphoryl compounds, in: E. Reiner, W.N. Aldridge, F.C.G. Hoskin (Eds.), *Enzymes Hydrolyzing Organophosphorus Compounds*, Ellis Horwood Ltd Pub., Chichester, UK, 1989, pp. 221–225.
- [46] C.B. Millard, O. Lockridge, C.A. Broomfield, Design and expression of organophosphorus acid anhydride hydrolase activity in human butyrylcholinesterase, *Biochemistry* 34 (1995) 15925–15933.
- [47] Y. Nicolet, O. Lockridge, P. Masson, J.C. Fontecilla-Camps, F. Nachon, Crystal structure of human butyrylcholinesterase and of its complexes with substrate and products, *J. Biol. Chem.* 278 (2003) 41141–41147.
- [48] O. Lockridge, R.M. Blong, P. Masson, M.-T. Froment, C.B. Millard, C.A. Broomfield, A single amino acid substitution, Gly117His, confers phosphotriesterase (organophosphorus acid anhydride hydrolase) activity on human butyrylcholinesterase, *Biochemistry* 36 (1997) 786–795.
- [49] C.B. Millard, O. Lockridge, C.A. Broomfield, Organophosphorus acid anhydride hydrolase activity in human butyrylcholinesterase: synergy results in a somanase, *Biochemistry* 37 (1998) 237–247.
- [50] L.M. Schopfer, A. Ticu-Boeck, C.A. Broomfield, O. Lockridge, Mutants of human butyrylcholinesterase with organophosphate hydrolase activity; evidence that His 117 is a general base catalyst for hydrolysis of echothiophate, *J. Med. Chem. Def.* 2 (2004) 1–21.
- [51] P. Masson, M.-T. Froment, E. Gillon, F. Nachon, O. Lockridge, L.M. Schopfer, Hydrolysis of oxo- and thio-esters by human butyrylcholinesterase, *Biochim. Biophys. Acta* 1774 (2007) 16–34.
- [52] F. Nachon, Y. Nicolet, A. Ticu-Boeck, P. Masson, O. Lockridge, Crystal structure of the G117H mutant of human butyrylcholinesterase, a designed organophosphate hydrolase, in: IXth International Meeting on Cholinesterases, Suzhou (China), 6–10 May 2007, Poster P-IV-2, 2007.
- [53] T. Poyot, F. Nachon, M.-T. Froment, M. Loiodice, S. Wieseler, L.M. Schopfer, O. Lockridge, P. Masson, Mutant of *Bungarus fasciatus* acetylcholinesterase with low affinity and low hydrolase activity toward organophosphorus esters, *Biochim. Biophys. Acta* 1764 (2006) 1470–1478.
- [54] R. Kaushik, C.A. Rosenfeld, L.G. Sultatos, Concentration-dependent interactions of the organophosphates chlorpyrifos oxon and methyl paraoxon with human recombinant acetylcholinesterase, *Toxicol. Appl. Pharmacol.* 221 (2007) 243–250.
- [55] A. Smolen, H.W. Eckerson, K.N. Gan, N. Hailat, B.N. La Du, Characteristics of the genetically determined polymorphic forms of human serum paraoxonase/arylesterase, *Drug. Metab. Dispos.* 19 (1991) 107–112.
- [56] P. Masson, D. Josse, O. Lockridge, N. Viguie, C. Taupin, C. Buhler, Enzymes hydrolyzing organophosphates as potential catalytic scavengers against organophosphate poisoning, *J. Physiol.* 92 (1998) 357–362.
- [57] H.G. Davis, R.J. Richter, M. Keifer, C.A. Broomfield, J. Sowalla, C.E. Furlong, The effect of the human serum paraoxonase polymorphism is reversed with diazoxon, soman and sarin, *Nat. Genet.* 14 (1996) 334–336.
- [58] M. Harel, A. Aharoni, L. Gaidukov, B. Brumshtein, O. Khersonsky, R. Meged, H. Dvir, R.B.G. Ravelli, A. McCarty, L. Tokar, I. Silman, J. Sussman, Structure and evolution of the serum paraoxonase family of detoxifying and anti-atherosclerotic enzymes, *Nat. Struct. Mol. Biol.* 11 (2004) 412–419.
- [59] R.D. Newcomb, P.M. Campbell, D.L. Ollis, E. Cheah, R.J. Russell, J.G. Oakeshott, A single amino acid substitution converts a carboxylesterase to an organophosphorus hydrolase and confers insecticide resistance on a blowfly, *Proc. Natl. Acad. Sci. U.S.A.* 94 (1997) 7464–7468.
- [60] J. Hartlieb, H. Ruterjans, Insights into the reaction mechanism of the diisopropyl fluorophosphatase from *Loligo vulgaris* by means of kinetic studies, chemical modification and site-directed mutagenesis, *Biochim. Biophys. Acta* 1546 (2001) 312–324.
- [61] J.N. Kuo, M.Y. Chae, F.M. Raushel, Perturbation of the active site of phosphotriesterase, *Biochemistry* 36 (1997) 1982–1988.
- [62] K. Lai, N.J. Stolowich, J.R. Wild, Characterization of P–S bond hydrolysis in organophosphorothioate pesticides by organophosphorus hydrolase, *Arch. Biochem. Biophys.* 318 (1995) 59–64.
- [63] D.P. Dumas, H.D. Durst, W.G. Landis, F.W. Raushel, Inactivation of organophosphorus nerve agents by the phosphotriesterase from *Pseudomonas diminuta*, *Arch. Biochem. Biophys.* 277 (1990) 155–159.
- [64] V.K. Rastogi, J.J. DeFrank, T.-C. Cheng, J.R. Wild, Enzymatic hydrolysis of Russian-VX by organophosphorus hydrolase, *Biochem. Biophys. Res. Comm.* 241 (1997) 294–296.
- [65] T.-C. Cheng, J.J. DeFrank, V.K. Rastogi, Alteromonas prolidase for organophosphorus G-agent decontamination, *Chem. Biol. Interact.* 119–120 (1999) 455–462.
- [66] S. Marti, R. Maite, J. Andrés, V. Moliner, E. Silla, I. Tuñón, J. Bertrán, Theoretical insights in enzyme catalysis, *Chem. Soc. Rev.* 33 (2004) 98–107.
- [67] Y. Pan, D. Gao, W. Yang, H. Cho, G. Yang, H.-H. Tai, C.-G. Zhan, Computational redesign of human butyrylcholinesterase for anticocaine medication, *Proc. Nat. Ac. Sci. U.S.A.* 15 (2005) 16656–16661.



Contents lists available at ScienceDirect

## Chemico-Biological Interactions

journal homepage: [www.elsevier.com/locate/chembioint](http://www.elsevier.com/locate/chembioint)Structural approach to the aging of phosphylated cholinesterases<sup>☆</sup>Patrick Masson<sup>a,b,c,\*</sup>, Florian Nachon<sup>a</sup>, Oksana Lockridge<sup>c</sup><sup>a</sup> Centre de Recherches du Service de Santé des Armées, Dept. Toxicology, 38702 La Tronche Cedex, France<sup>b</sup> Institute of Structure Biology, Molecular Biophysics Laboratory, 38027 Grenoble Cedex1, France<sup>c</sup> University of Nebraska Medical Center, Eppler Institute, Omaha, United States

## ARTICLE INFO

## Article history:

Available online 23 March 2010

## Keywords:

Cholinesterase

Organophosphorus compounds

Aging

## ABSTRACT

Phosphylated cholinesterases (ChE) can undergo a side reaction that progressively decreases their reactivatability. This process, termed “aging”, results from dealkylation of the adduct and depends on the structure of the organophosphoryl moiety. Aged ChEs are resistant to reactivation by oximes.

Owing to the toxicological importance of OPs, the molecular mechanism of aging has been the subject of research for decades. It was not clear whether aging involves the same bond breakage regardless the type of OP or is a scission of P–O–C bonds (P–O or O–C) in phosphates/phosphonates, P–N–C bonds in phosphoramidates, and P–S–C bonds in phosphonothionates. It was assumed that the resulting negatively charged atom on phosphorus of the aged adduct prevented nucleophilic attack by oximates, but studies on negatively charged model molecules do not support this hypothesis. Decrease in conformational flexibility of aged enzymes may contribute to their non-reativatability by preventing proper adjustment of reactivators in the active site gorge.

MALDI-TOF mass spectrometry of phosphylated human butyrylcholinesterase (hBChE) in water and in <sup>18</sup>O-water provided evidence that aging results from O–C breakage, i.e. O-dealkylation. In contrast, the isomalathion–BChE conjugate ages mostly through P–S bond cleavage, but a minor product results from O–C and/or S–C breakage. The crystal structures of hBChE and hAChE inhibited by tabun showed that aging of tabun–ChE conjugates results from O-dealkylation. However, depending on the nature of O-alkyl and N-alkyl chains, aging of BChE inhibited by other phosphoramidates results either from O–C breakage or deamination, i.e. P–N breakage. It was found that dealkylation of branched alkoxy involves a transient carbocation. Dealkylation of OP–ChE conjugates is accompanied by enzyme conformational changes. Urea, organic solvent, heat and pressure denaturation of human BChE showed that the conformational stability of aged OP–BChE conjugates is dramatically increased compared to native enzyme. Determination of the three-dimensional structure of BChE and AChE conjugated to different OPs showed that aged adducts form a salt bridge with the protonated catalytic histidine. Structure alteration of aged enzymes is accompanied by exit of water molecules from the enzyme's active site gorge. In addition, neutron scattering studies provided evidence that the structural dynamics of aged BChE is dramatically altered compared to native enzyme. Knowledge of the molecular basis of aging will help to design reactivators of aged ChEs, molecules capable of slowing the aging process, and pseudocatalytic ChE-based bioscavengers.

© 2010 Elsevier Ireland Ltd. All rights reserved.

**Abbreviations:** AChE, acetylcholinesterase; BChE, butyrylcholinesterase; ChE, cholinesterase; DFP, diisopropylfluorophosphate; MALDI-TOF, matrix-assisted laser desorption/ionization-time-of-flight; OP, organophosphorus compound; PAS, peripheral anionic site; 2-PAM, pralidoxime.

<sup>☆</sup> Amino acid numbering refers to residues in human butyrylcholinesterase and human acetylcholinesterase. For example, the catalytic serine is S198/S203 in these enzymes.

\* Corresponding author at: IRBA-CRSSA, BP 87, 38702 La Tronche Cedex, France. Tel.: +33 476636959; fax: +33 476636962.

E-mail address: [pmasson@unmc.edu](mailto:pmasson@unmc.edu) (P. Masson).

## 1. Introduction

Cholinesterases (ChEs) and serine hydrolases are progressively inhibited by organophosphorus compounds (OPs) through phosphorylation of the active site serine (S198/S203)<sup>\*</sup>. Inhibition of AChE is responsible for the acute toxicity of OPs. OPs have been widely used as pesticides for decades [1]. Some OPs are potent chemical warfare agents now considered as potential terrorist agents (Fig. 1) [2]. OP poisoning is a major public health concern. Indeed, self-poisoning by pesticides is responsible for some 200,000 deaths a year in the world [3].

Acetylcholinesterase (EC 3.1.1.7; AChE) and butyrylcholinesterase (EC 3.1.1.8; BChE) have a very similar three-

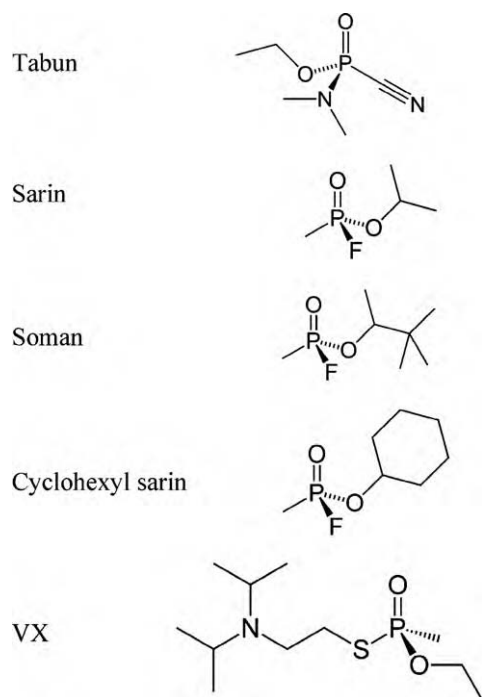


Fig. 1. Chemical structure of nerve agents.

dimensional structure [4]. The major structural differences are: AChE possesses a large peripheral anionic site (PAS) at the entrance of the active site gorge compared to BChE [4]; there are more aromatic residues lining the active site gorge of AChE than in BChE, so that the volume of the gorge is 300 Å<sup>3</sup> in AChE against 500 Å<sup>3</sup> in BChE [5]. These differences have important consequences on reactivity, specificity and stereoselectivity of both enzymes.

After stereoselective formation of the ChE–OP complex, phosphorylation of the catalytic serine is accompanied by release of the OP leaving group [6]. Water-mediated dephosphorylation is very slow or zero, so that inhibition of ChEs by OPs can be regarded as “irreversible”. Bimolecular rate constants for phosphorylation of ChEs range from 10<sup>7</sup> to 10<sup>10</sup> M<sup>−1</sup> min<sup>−1</sup>. Fast phosphorylation of AChE leads to major dysfunction of the cholinergic system that fully

explains the acute lethal toxicity of OPs [7]. However, sub-lethal toxicity of OPs with no inhibition of ChEs, delayed, and chronic effects of OPs may result from inhibition of other serine enzymes [8] and/or phosphorylation of numerous protein targets on tyrosine or lysine residues [9].

Phosphorylated ChEs can be reactivated by nucleophilic compounds such as fluoride ions, hydroxamates and oximes, if they have not undergone aging. Pyridinium oximes: 2-PAM and obidoxime (toxogonin) are currently used as antidotes of OP poisoning. More potent oximes, HI-6 and MMB-4, are under advanced development (Fig. 2). However, the therapeutic efficacy of oximes in emergency treatment of OP poisoning is still the subject of debate [10,11]. As a consequence of structural differences between AChE and BChE, phosphorylated BChE is reactivated with less efficiency than phosphorylated AChE. However, it should be remembered that oxime reactivators have initially been developed for AChE reactivation, not reactivation of phosphorylated BChE. Moreover, reactivation depends also on the structure of reactivator and the structure of OP that caused inhibition. ChEs inhibited by the nerve agent tabun are resistant to oximes at concentrations compatible with medical use [12,13]. However, design of new oximes capable of reactivating AChE and BuChE inhibited by tabun and others OPs at low concentrations is a very active field of research. Improving reactivation of phosphorylated BChE will lead to development of efficient BChE-based pseudocatalytic bioscavengers [14,15].

## 2. Loss in reactivatability of phosphorylated cholinesterases: aging

Due to post-inhibitory reactions, reactivation of phosphorylated ChEs may be progressively spoiled. This loss in reactivatability is called «aging». Unlike ChEs, carboxylesterases and phospholipases do not age [16,17]. Certain phosphorylated serine proteases, e.g. trypsin and chymotrypsin are susceptible to aging. Aging is generally the functional consequence of dealkylation of the OP adduct [18]. However, other types of chemical deteriorations of phosphorylated serine may occur, such as β elimination of the adduct, leading to formation of dehydroalanine [19]. Though slow formation of dehydroalanine has been observed on MS/MS spectra of aged ChE adducts after inhibition by nerve agent analogues [20], it has not yet been established whether dehydroalanine forms spontaneously under mild alkaline conditions or is an artifact of MS analysis.

The dealkylation reaction of adducts depends on the structure of the phosphorylated enzyme active site pocket. The rate constant of aging (*k<sub>a</sub>*) is modulated by temperature, pH, other environmental factors, and binding of ligands on the enzyme's peripheral anionic site (PAS). In general, phosphorylated BChE ages faster than phosphorylated AChE, but the rate of aging depends on the OP structure. Branched alkyl side chains dealkylate much faster than short alkyl chains. Thus, the half-time of aging (*t*<sub>1/2</sub> = ln 2/*k<sub>a</sub>*) ranges from a few minutes to several days. For instance, human acetylcholinesterase ages with *t*<sub>1/2</sub> = 6.3 min after inhibition by soman (dealkylation of pinacolyl chain) [21], *t*<sub>1/2</sub> = 8.7 h after inhibition by cyclohexyl-sarin (loss of cyclohexyl chain) [22], and *t*<sub>1/2</sub> = 1.5 days after inhibition by VX (loss of ethyl chain) [23]. Thus, antidotal treatment of OP poisoning may be dramatically impaired when there is fast aging.

## 3. Mechanism of dealkylation

Dealkylation of phosphorylated ChEs is a unimolecular S<sub>N</sub>1 reaction involving a carbocationic intermediate. The aging reaction has been thoroughly investigated for soman-inhibited ChEs and serine proteases [24]. The active site residues involved in the molecular mechanism of dealkylation have been identified. First, chemical modification of histidine by diethylpyrocarbonate implicated his-

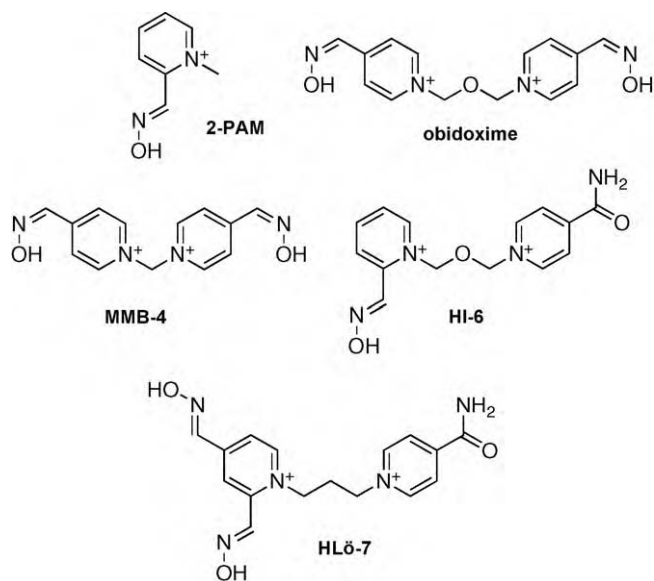


Fig. 2. Chemical structures of some oxime reactivators.

tidine in aging [25]. pH dependence and site-directed mutagenesis studies provided evidence for participation of catalytic histidine (H438/H447) and glutamate (E197/E202; E199 in *Torpedo californica* AChE) vicinal to the catalytic serine in the mechanism of dealkylation [26]. The main component of the choline-binding pocket, tryptophan residue (W82/W86), has been found – together with E197/E202 – to stabilize the developing carbocation that will be cleaved [21,27]. Another residue, F329/F338, in the acyl-binding pocket has been found to play a role in the aging process by stabilizing the imidazolium ring of H447 [21]. Mutation of this phenylalanine residue to alanine considerably slows the rate of aging of phosphorylated AChE [21] but has a moderate effect on aging of phosphorylated BChE [28]. The slower aging rate of human AChE compared to that of human BChE is related to a difference in mobility of the catalytic histidine. H438 of BChE, stabilized by F398, is always in a conformation favorable to aging [29,30]. By contrast, the catalytic histidine is rather mobile in AChE as shown by crystallographic [31,32] and NMR analyses [33], so that it is not always in a conformation favorable to aging.

Lastly, D70/D74, the main component of the PAS has been found to modulate the rate of aging. This residue is part of the  $\Omega$  loop (C65–C92) that allosterically links the peripheral anionic site (PAS) to the choline-binding site. The mutation D70G in human BChE [34] or D74N in human AChE [21] likely induces a change in the position of W82/W86, and disorganizes the water molecule network, which in turn alters stabilization of the carbocationic intermediate. In addition, in AChE, the H-bond between D74 and Y341, at the rim of the active site gorge, stabilizes helix 334–341. Destabilization of this helix affects the position of F338, and, therefore, the position of H447. Double-mutant (Y332A/D70G) cycle kinetic analysis of BChE under high hydrostatic pressure showed that water molecules move more freely in the active gorge of BChE mutated in the PAS than in the gorge of wild-type enzyme [35]. Participation of water molecule(s) in the dealkylation catalysis has been inferred from study of the dependence of the aging rate on hydrostatic pressure versus osmotic pressure [36] and from X-ray structure analysis [29,37].

Products released from dealkylation of the pinacolyl chain of soman bound to AChE [38–40] as well pH profiles and solvent isotope effects support a “push–pull” mechanism for aging in which tryptophan (W82/W86) and glutamate (E197/E202) exert electrostatic and steric “push”, and histidine (H438/H447) and the oxyanion hole act as “pullers” [41,24] (Fig. 3). The critical step of this mechanism involves migration of methyl from C $\beta$  to C $\alpha$  in the pinacolyl chain in the dealkylation transition state. Another proposed mechanism supported by mutagenesis involves protonation of the pinacoloxo oxygen by protonated catalytic histidine, and then scission of the O–C bond [21,42]. Recent high-resolution crystal structures of non-aged and aged soman-*Torpedo californica* AChE conjugates led to a critical reexamination of both models, and highlighted the role of a water molecule (H-bonded to Y121; Y124 in human AChE) in dealkylation [37]. However, these structural data are in favor of the push–pull mechanism. It is expected that crystallokinetic studies of soman-phosphorylated AChE will provide direct evidence for the push–pull mechanism.

Aging of human BChE by organophosphates like echothiophate and diisopropylfluorophosphate (DFP), and organophosphonates like sarin and soman, involves scission of the P–O–C chain. To determine whether there is breakage of the P–O bond or O–C bond, inhibition and aging were carried out in  $^{18}\text{O}$ -water and the products compared to inhibition and aging in water. Analysis of aged BChE tryptic peptides by MALDI-TOF mass spectrometry provided evidence that the chemical reaction corresponded to O–C breakage assisted by a water molecule and not P–O breakage [43]. For phosphoramidates like tabun, mass spectrometry and X-ray structure analyses provided evidence that aging of ChEs proceeds

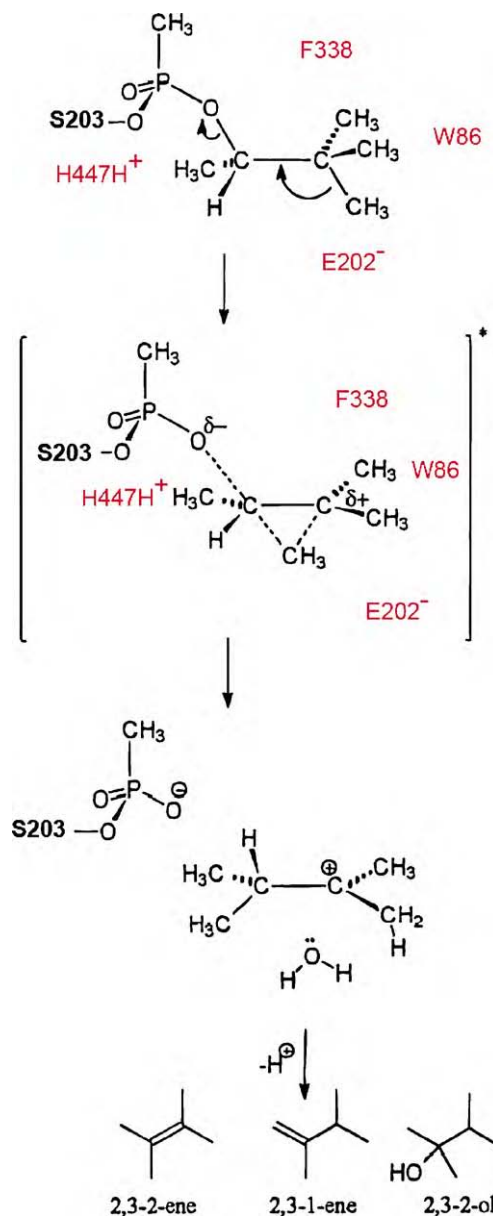


**Fig. 3.** Push–pull mechanism for aging of acetylcholinesterase inhibited by  $\text{P}_3\text{C}_3$ -soman stereoisomer proposed by the group of Kovach [40,41]. Numbering of residues is for human AChE. Electrostatic and steric “push” involves W86 and E202; concomitant “pull” effect is provided by protonated H447 and the oxyanion hole. Small molecular products of pinacolyl dealkylation are 2,3-dimethyl-2-butene (14%), 2,3-dimethyl-1-butene (24.5%) and 2,3-dimethyl-2-butanol (60%).

through O-dealkylation, not deamination [30] (Fig. 4). For phosphorodithioates like isomalathion aging is more complex, involving O–C, P–S and S–C cleavages, depending on the enantiomer that reacted with the enzyme [43]. It is noteworthy that aging of human AChE is generally slower than aging of human BChE.

#### 4. Molecular hypotheses for the resistance of aged ChEs to oxime reactivators

To explain the non-reativatability of aged ChEs, it was initially suggested that a new bond was formed between aged adduct and an active center residue, thus preventing reactivation [44]. Later it was proposed that the negatively charged oxygen on the phosphorus atom formed an electrostatic shield opposing nucleophilic attack of oximates on the phosphorus atom [45]. However, studies

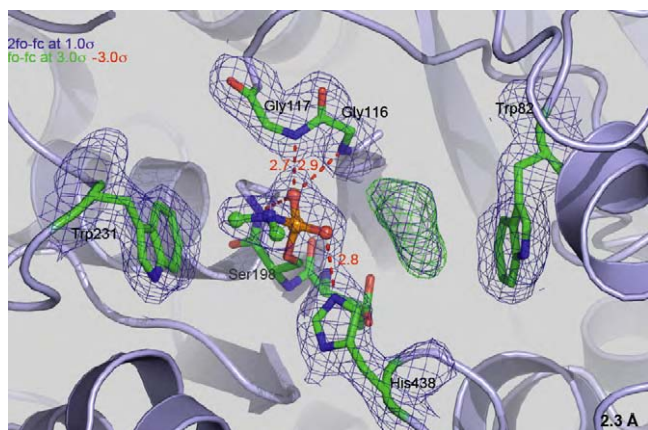


**Fig. 4.** X-ray structure of the active site of tabun-aged human butyrylcholinesterase at 2.3 Å (PDB code 2COP) [30]. Electron density  $2|F_o| - |F_c|$  is represented by a blue mesh, contoured at  $1\sigma$ , and  $|F_o| - |F_c|$  omit map is represented by green mesh contoured at  $3\sigma$ . Important active site residues are represented as sticks with carbon atoms in green, nitrogen atoms in blue, phosphorus atom in orange, and oxygen atoms in red. H bonds are represented by red dashes. The dimethylamine moiety of the tabun adduct is located in the acyl-binding pocket. The imidazolium  $N^+$  of protonated H438 forms a strong salt bridge (2.8 Å) with the negatively charged oxygen atom of the tabun-aged adduct. The positive density close to W82 is an unknown ligand. (For interpretation of the references to color in this figure legend, the reader is referred to the web version of the article.)

of reactions between various acylmethylphosphonates and neutral or negatively charged nucleophiles showed that the presence of a negative charge slows down the rate of nucleophilic displacement at phosphorus due to the electrostatic effect, but does not prevent reaction between compounds [46–48]. NMR studies provided evidence for formation of a salt bridge between  $P-O^-$  and protonated catalytic histidine [49]. Moreover, the role of histidine as a base for dephosphorylation catalysis is impaired because of its protonation. Crystal structures of aged ChEs and other serine hydrolases confirmed the existence of a strong salt bridge in the active center of aged conjugates (Fig. 4) that raises the energy barrier for the reactivation reaction [4,18,30,37].

## 5. Consequence of dealkylation on structure and conformational stability of cholinesterases

Structural investigations have been aimed at understanding whether bonding interaction was the sole cause of resistance to reactivators of aged ChEs or whether enzyme conformational changes occurred upon dealkylation. Measurement of fluorescence decay of pyrenebutyl-containing organophosphates bound to AChE showed that decay was shorter for non-aged conjugates than for aged conjugates [50]. This suggested that the pyrenebutyl group in aged conjugates is more deeply buried than in non-aged conjugates. Later, kinetic and equilibrium spectroscopic studies showed that the binding of ligands was altered in aged AChE compared to non-aged AChE [51]. Differences in the binding properties of non-aged and aged AChE were interpreted to be a consequence of a change in topographic relationships between the active center and the PAS. Affinity electrophoresis of human BChE on procainamide immobilized in a polyacrylamide gel revealed a significant decrease in binding affinity of soman-aged BChE compared to non-inhibited enzyme and enzyme inhibited by methyl sulfonyl fluoride [52]. At the same time, cross-linking of non-inhibited and soman-aged BChE with dimethylimidates of different chain length between reactive functions showed no change in quaternary structure of BChE or in overall conformation of subunits between both enzyme forms [52]. This suggested that only minor conformation changes occur upon dealkylation. However, enzyme denaturation

studies with urea, heat, hydrostatic pressure and organic solvent showed that the conformational stability of aged ChEs is dramatically increased compared to non-inhibited and non-aged ChEs [41,53–55]. Analysis of pressure-induced molten globule transition of BChE also indicated a shift in denaturation onset of aged BChE [36]. Molecular dynamics of non-inhibited and soman-aged BChE studied by incoherent elastic neutron scattering as a function of temperature in the range 50–90 °C showed a significant change in molecular flexibility on the Ångström–nanosecond scale between both enzyme forms. The increase in stability of aged BChE correlates with a decrease in molecular flexibility [56]. Formation of a salt bridge and partial dehydration of the active site gorge upon dealkylation explain stability and molecular dynamics changes of aged BChE. Thus, decrease in conformational flexibility of aged enzymes may contribute to their non-reactivability by preventing proper adjustment of reactivators in the active site gorge.

Comparison of the crystal structures of soman-aged AChE to native and non-aged AChE, showed only a slight displacement of the catalytic histidine upon formation of a salt bridge at the bottom of the gorge [37]. In fact, determination of the crystal structure of the ternary complex between soman-aged AChE and 2-PAM provided a clue. This structure revealed that the oximate function points away from the phosphorus atom, and therefore cannot attack it. Moreover, in the case of aged phosphoramidate-inhibited ChEs, resistance to reactivators may result from the conjunction of steric factors, electron delocalization along the P–N–R chain due to the N lone pair, and stabilization by the salt bridge [30,57].

## 6. Perspectives

### 6.1. Modulation of aging velocity

Medical counter measures against OP poisoning in cases of fast aging, e.g. acute intoxication by soman, could be improved by using drugs capable of slowing the aging process. Molecular dynamic simulations indicated that the PAS and the catalytic binding site are coupled via conformational change of the  $\Omega$  loop, and that mutation of D70/D74 slows the rate of aging [21,34]. Therefore, it is conceivable that occupation of the PAS may affect the rate of aging by altering interactions between aged adduct and active center residues. Allosteric effectors of the PAS have been investigated. Bispyridinium compounds [58–60] and gallamine [61] showed a moderate reducing effect on the aging rate. Other ligands have been found to slow down the aging rate, e.g. ketamine [62] and tacrine [63]. None of these compounds was found to be of practical interest for slowing down aging in vivo in association with other medical counter measures. However, new generations of PAS ligands and bifunctional ligands (i.e. ligands that interact with both PAS and active center residues) are emerging. Screening of libraries of tethered ligands [64], cyclic peptides [65], and bifunctional ligands produced by click chemistry [66] has already been fruitful for discovery of new cholinesterase ligands. Alternatively, a computer-aided approach based on flexible docking in the crystal structure of ChEs appears to be a very promising strategy [67].

### 6.2. Is reactivation of aged ChEs possible?

Reactivation of aged ChEs is a challenge. Solving this major issue would greatly improve medical counter measures, in particular against acute poisoning by soman. Direct reactivation of aged conjugates using oximes has not been possible so far. Yet thousands of oximes have been synthesized. However, most oximes have been designed without knowledge of the three-dimensional structure and molecular dynamics of phosphorylated enzymes. Few structures of complexes between oximes and non-aged and aged

phosphylated ChEs have been reported so far [37,68,69]. The three-dimensional structure of complexes such as that of the non-aged tabun–AChE conjugate with the oxime HI-6 (Fig. 2) explains why reactivation of ChEs inhibited by tabun is so difficult [68]. Indeed, the X-ray structure shows that the oximate function is not oriented toward the P atom. In addition, partial electronic delocalization reinforces interactions of adduct with the acyl-binding pocket and the oxyanion hole [30]. Recent works of Sanson et al. [37] provide a rationale to understand why 2-PAM cannot reactivate the aged enzyme: X-ray structure of complex between 2-PAM and soman-aged TcAChE conjugate shows that the pyridinium ring of 2-PAM is stacked against W84 and the oximate function points away from the adduct. Therefore, lessons from crystallography and molecular dynamics are expected to provide information for improving the orientation of the oxime function for effective attack on phosphorus. *In silico* design of new oximes, as well as other chemical strategies mentioned above (click chemistry, combinational chemistry) should lead to new generations of reactivators. Another strategy would be to realkylate aged adduct by using an electrophilic molecule, and then to displace the phosphotriester with a nucleophilic compound. Such an approach is difficult because of possible non-specific reactions between the designed electrophilic compound and multiple biological targets. However, several electrophilic molecules have already been synthesized, and the proof of concept established (M. Goeldner et al., unpublished results).

### 6.3. Aging-resistant cholinesterase mutants as potential pseudocatalytic bioscavengers

Bioscavenger-based ChEs are an alternative to prophylaxis against organophosphate poisoning [70], and administration of bioscavengers may improve efficacy of treatment of acute nerve agent poisoning. However, ChEs act as stoichiometric scavengers, so that efficacy of ChEs in OP poisoned humans needs administration of large doses of costly enzymes. The future of the bioscavenger approach is certainly in the use of catalytic scavengers capable of degrading OPs with high efficiency. Efforts to convert ChEs into efficient catalytic OP-hydrolases have not been successful so far [71]. However, mutants of ChEs that do not age after phosphylation could be used in association with oximes as pseudocatalytic bioscavengers. Several attempts have been made with AChE mutants [72–75], and this approach looks promising.

### Conflict of interest statement

There are no conflicts of interest.

### Acknowledgments

This work was supported by the Délégation Générale pour l'Armement under contract DGA/PEA 03CO10-05/01 08 7 to PM, DGA/PEA 08CO501, and Agence Nationale de la Recherche, grant number ANR-06-BLAN-0163 and ANR-09-BLAN-0192 to F.N.

### References

- [1] R.C. Gupta (Ed.), *Toxicology of Organophosphate and Carbamate Compounds*, Academic Press-Elsevier, Amsterdam, 2006, xvi + 763 pp.
- [2] R.C. Gupta (Ed.), *Handbook of Toxicology of Chemical Warfare Agents*, Academic Press-Elsevier, Amsterdam, 2009, xviii + 1147 pp.
- [3] M. Eddleston, N.A. Buckley, P. Eyer, A.H. Dawson, Management of acute organophosphorus pesticide poisoning, *Lancet* 371 (2008) 597–607.
- [4] Y. Nicolet, O. Lockridge, P. Masson, J.C. Fontecilla-Camp, F. Nachon, Crystal structure of human butyrylcholinesterase and of its complexes with substrate and products, *J. Biol. Chem.* 278 (2003) 41141–41147.
- [5] A. Saxena, A.M. Redman, X. Jiang, O. Lockridge, B.P. Doctor, Differences in active site gorge dimensions of cholinesterases revealed by binding of inhibitors to human butyrylcholinesterase, *Biochemistry* 36 (1997) 14642–14651.
- [6] J. Jarv, Stereochemical aspects of cholinesterase catalysis, *Bioorg. Chem.* 12 (1984) 259–278.
- [7] D.M. Maxwell, K.M. Brecht, I.M. Koplovitz, R.E. Sweeney, Acetylcholinesterase inhibition: does it explain the toxicity of organophosphates? *Arch. Toxicol.* 80 (2006) 756–760.
- [8] J.E. Casida, G.B. Quistad, Organophosphate toxicology: safety aspects of nonacetylcholinesterase secondary targets, *Chem. Res. Toxicol.* 17 (2004) 983–998.
- [9] L.M. Schopfer, H. Grigoryan, B. Li, F. Nachon, P. Masson, O. Lockridge, Mass spectral characterization of organophosphate-labeled tyrosine-containing peptides: characteristic mass fragments and a new binding motif for organophosphates, *J. Chromatogr. B*, in press.
- [10] F. Worek, N. Aurbek, N.M. Herkert, H. John, M. Eddleston, P. Eyer, H. Thiermann, Evaluation of medical countermeasures against organophosphorus compounds: the value of experimental data and computer simulations, *Chem.-Biol. Interact.* 187 (2010) 259–264.
- [11] P. Eyer, F. Worek, H. Thiermann, M. Eddleston, Paradox findings may challenge orthodox reasoning in acute organophosphate poisoning, *Chem.-Biol. Interact.* 187 (2010) 270–278.
- [12] B. Antonijevic, M.P. Stojiljkovic, Unequal efficacy of pyridinium oximes in acute organophosphate poisoning, *Clin. Med. Res.* 5 (2007) 71–82.
- [13] M. Jokanovic, M. Prostran, Pyridinium oximes as cholinesterase reactivators. Structure–activity relationship and efficacy in the treatment of poisoning with organophosphorus compounds, *Curr. Med. Chem.* 16 (2009) 2177–2188.
- [14] Z. Kovarik, M. Katalinic, G. Sinko, J. Binder, O. Hlas, Y.-S. Jung, L. Musilova, D. Jun, K. Kuca, Pseudo-catalytic scavenging: searching for a suitable reactivator of phosphorylated butyrylcholinesterase, *Chem.-Biol. Interact.* 187 (2010) 167–171.
- [15] P. Masson, O. Lockridge, Butyrylcholinesterase for protection from organophosphorus poisons: catalytic complexities and hysteretic behavior, *Arch. Biochem. Biophys.* 494 (2010) 107–120.
- [16] C.D. Fleming, C.C. Edwards, S.D. Kirby, D.M. Maxwell, P.M. Potter, D.M. Cerasoli, M.R. Redinbo, Crystal structure of human carboxylesterase 1 in covalent complexes with the chemical warfare agents soman and tabun, *Biochemistry* 46 (2007) 5063–5071.
- [17] T.M. Epstein, U. Samanta, S.D. Kirby, D.M. Cerasoli, B.J. Bahnsen, Crystal structures of brain group-VIII phospholipase A2 in non aged complexes with the organophosphorus nerve agents soman and sarin, *Biochemistry* 48 (2009) 3425–3435.
- [18] M. Harel, C.T. Su, F. Frolow, Y. Ashani, I. Silman, J.L. Sussman, Refined crystal structures of “aged” and “non-aged” organophosphoryl conjugates of gamma-chymotrypsin, *J. Mol. Biol.* 221 (1991) 909–918.
- [19] D.H. Strumeyer, W.N. White, D.E. Koshland Jr., Role of serine in chymotrypsin action. Conversion of the active serine to dehydroalanine, *Proc. Natl. Acad. U.S.A.* 50 (1963) 931–935.
- [20] C. Gilley, M. McDonald, F. Nachon, L.M. Schopfer, J. Zhang, J.R. Cashman, O. Lockridge, Nerve agent analogues that produce authentic soman, sarin, tabun, and cyclohexyl methylphosphonate-modified human butyrylcholinesterase, *Biochemistry* 22 (2009) 1680–1688.
- [21] A. Shafferman, A. Ordentlich, D. Barak, D. Stein, N. Ariel, B. Velan, Aging of phosphorylated human acetylcholinesterase: catalytic processes mediated by aromatic and polar residues of the active centre, *Biochem. J.* 318 (1996) 833–840.
- [22] F. Worek, P. Eyer, L. Szinicz, Inhibition, reactivation and aging kinetics of cyclohexylmethylphosphonofluoridate-inhibited human acetylcholinesterases, *Arch. Toxicol.* 72 (1998) 580–587.
- [23] N. Aurbek, H. Thiermann, L. Szinicz, P. Eyer, F. Worek, Analysis of inhibition, reactivation and aging kinetics of highly toxic organophosphorus compounds with human and pig acetylcholinesterase, *Toxicology* 224 (2006) 91–99.
- [24] I.M. Kovach, Stereochemistry and secondary reactions in the irreversible inhibition of serine hydrolases by organophosphorus compounds, *J. Phys. Org. Chem.* 17 (2004) 602–614.
- [25] G. Beauregard, J. Lum, B.D. Roufogalis, Effect of histidine modification on the aging of organophosphate-inhibited acetylcholinesterase, *Biochem. Pharmacol.* 30 (1981) 2915–2920.
- [26] A. Saxena, B.P. Doctor, D.M. Maxwell, D.E. Lenz, Z. Radic, P. Taylor, The role of glutamate-199 in the aging of cholinesterase, *Biochem. Biophys. Res. Commun.* 197 (1993) 343–349.
- [27] D. Barak, A. Ordentlich, Y. Segal, B. Velan, H.P. Benshop, L.P.A. De Jong, A. Shafferman, Carbocation-mediated processes in biocatalysts. Contribution of aromatic moieties, *J. Am. Chem. Soc.* 119 (1997) 3157–3158.
- [28] P. Masson, P.-L. Fortier, C. Albaret, M.-T. Froment, C. Bartels, O. Lockridge, Aging of diisopropyl-phosphorylated human butyrylcholinesterase, *Biochem. J.* 327 (1997) 601–607.
- [29] F. Nachon, O.A. Asojo, G.E.O. Borgstahl, P. Masson, O. Lockridge, Role of water in aging of human butyrylcholinesterase inhibited by echothiophate: the crystal structure suggests two alternative mechanisms of aging, *Biochemistry* 44 (2005) 1154–1162.
- [30] E. Carletti, H. Li, B. Li, F. Ekstrom, Y. Nicolet, M. Loiodice, E. Gillon, M.T. Froment, O. Lockridge, L.M. Schopfer, P. Masson, F. Nachon, Aging of cholinesterases phosphorylated by tabun proceeds through O-dealkylation, *J. Am. Chem. Soc.* 130 (2008) 16011–16020.
- [31] C.B. Millard, G. Koellner, A. Ordentlich, A. Shafferman, I. Silman, J.L. Sussman, Reaction products of acetylcholinesterase and VX reveal a mobile histidine in the catalytic triad, *J. Am. Chem. Soc.* 121 (1999) 9883–9884.

- [32] F. Ekstrom, C. Akfur, A.-K. Tunemalm, S. Lundberg, Structural changes in phenylalanine 338 and histidine 447 revealed by the crystal structures of tabun-inhibited murine acetylcholinesterase, *Biochemistry* 45 (2006) 74–81.
- [33] M.A. Massiah, C. Viragh, P.M. Reddy, I.M. Kovach, J. Johnson, T.L. Rosenberry, A. Mildvan, Short, strong hydrogen bond at the active site of human acetylcholinesterase: proton NMR studies, *Biochemistry* 40 (2001) 5682–5690.
- [34] P. Masson, M.T. Froment, C.F. Bartels, O. Lockridge, Importance of aspartate-70 in organophosphate inhibition, oxime reactivation and aging of human butyrylcholinesterase, *Biochem. J.* 325 (1997) 53–61.
- [35] P. Masson, Double-mutant thermodynamic cycles under high hydrostatic pressure, in: R. Winter (Ed.), *Advances in High Pressure Bioscience and Biotechnology II*, Springer, Berlin, 2003, pp. 61–68.
- [36] P. Masson, C. Cléry, P. Guerra, A. Redslob, C. Albaret, P.L. Fortier, Hydration change during the aging of phosphorylated human butyrylcholinesterase: importance of residues aspartate-70 and glutamate-197 in the water network as probed by hydrostatic and osmotic pressures, *Biochem. J.* 343 (1999) 361–369.
- [37] B. Sanson, F. Nachon, J.P. Colletier, M.T. Froment, L. Toker, H.M. Greenblatt, J.L. Sussman, Y. Ashani, P. Masson, I. Silman, M. Weik, Crystallographic snapshots of nonaged and aged conjugates of soman with acetylcholinesterase, and of a ternary complex of the aged conjugate with pralidoxime, *J. Med. Chem.* 52 (2009) 7593–7603.
- [38] T.E. Smith, E. Usdin, Formation of nonreactivable isopropylmethylphosphonofluoridate-inhibited acetylcholinesterase, *Biochemistry* 5 (1966) 2914–2918.
- [39] H.O. Michell, B.E. Hackley, L. Berkowitz, G. List, E.B. Hackley, W. Gillilan, M. Pankau, Formation of nonreactivable isopropylmethylphosphonofluoridate-inhibited acetylcholinesterase, *Arch. Biochem. Biophys.* 212 (1967) 29–34.
- [40] C. Viragh, I.M. Kovach, L. Pannell, Small molecular products of dealkylation in soman-inhibited electric eel acetylcholinesterase, *Biochemistry* 38 (1999) 9557–9561.
- [41] C. Viragh, R. Akhmetshin, I.M. Kovach, C. Broomfield, Unique push–pull mechanism of dealkylation in soman-inhibited cholinesterases, *Biochemistry* 36 (1997) 8243–8252.
- [42] A. Shafferman, A. Ordentlich, D. Barak, D. Stein, N. Ariel, B. Velan, Aging of somany-acetylcholinesterase adducts: facts and models, *Biochem. J.* 324 (1997) 996–998.
- [43] H. Li, L.M. Schopfer, F. Nachon, M.T. Froment, P. Masson, O. Lockridge, Aging pathways for organophosphate-inhibited human butyrylcholinesterase, including novel pathways for isomalathion, resolved by mass spectrometry, *Toxicol. Sci.* 100 (2007) 136–145.
- [44] F. Hobbiger, in: G.B. Koelle (Ed.), *Cholinesterases and Anticholinesterase Agents*, Springer, Berlin, 1963, p. 941.
- [45] L.W. Harris, J.H. Fleicher, J. Clark, W.J. Cliff, Dealkylation and loss of capacity for reactivation of cholinesterase inhibited by sarin, *Science* 154 (1966) 404–407.
- [46] A.J. Kirby, M. Younas, The reactivity of phosphate esters. Reactions of diesters with nucleophiles, *J. Chem. Soc. B* (1970) 1165–1172.
- [47] E.J. Behrman, M.J. Biallas, H.J. Brass, J.O. Edwards, M. Isaks, Reactions of phosphonic acid esters with nucleophiles. I. Hydrolysis, *J. Org. Chem.* 35 (1970) 3063–3069.
- [48] E.J. Behrman, M.J. Biallas, H.J. Brass, J.O. Edwards, M. Isaks, Reactions of phosphonic acid esters with nucleophiles. II. Survey of nucleophiles reacting with p-nitrophenyl methylphosphonate anion, *J. Org. Chem.* 35 (1970) 3069–3075.
- [49] Y. Segall, D. Waysbrort, D. Barak, N. Ariel, B.P. Doctor, J. Grunwald, Y. Ashani, Direct observation and elucidation of the structures of aged and nonaged phosphorylated cholinesterases by <sup>31</sup>P NMR spectroscopy, *Biochemistry* 32 (1993) 13350–13441.
- [50] G. Amitai, Y. Ashani, A. Gafni, I. Silman, Novel pyrene-containing organophosphates as fluorescent probes for studying aging-induced conformational changes in organophosphate-inhibited acetylcholinesterase, *Biochemistry* 21 (1982) 2060–2069.
- [51] H.A. Berman, M.M. Decker, Kinetic, equilibrium, and spectroscopic studies on dealkylation (“aging”) of alkyl organophosphonyl acetylcholinesterase. Electrostatic control of enzyme topography, *J. Biol. Chem.* 261 (1986) 10646–10652.
- [52] P. Masson, B. Marnot, J.Y. Lombard, P. Morelis, Electrophoretic study of aged butyrylcholinesterase after inhibition by soman, *Biochimie* 66 (1984) 235–249.
- [53] P. Masson, J.L. Goasdoue, Evidence that the conformational stability of “aged” organophosphate-inhibited cholinesterase is altered, *Biochim. Biophys. Acta* 869 (1986) 304–313.
- [54] P. Masson, P. Gouet, C. Clery, Pressure and propylene carbonate denaturation of native and “aged” phosphorylated cholinesterase, *J. Mol. Biol.* 328 (1994) 466–478.
- [55] Y. Ashani, M.K. Gentry, B.P. Doctor, Differences in conformational stability between native and phosphorylated acetylcholinesterase as evidenced by monoclonal antibody, *Biochemistry* 29 (1990) 2456–2463.
- [56] F. Gabel, P. Masson, M.T. Froment, B.P. Doctor, A. Saxena, I. Silman, G. Zaccari, M. Weik, Direct correlation between molecular dynamics and enzymatic stability: a comparative neutron scattering study of native human butyrylcholinesterase and its “aged” soman conjugate, *Biophys. J.* 96 (2009) 1489–1494.
- [57] E. Carletti, N. Aurbek, E. Gillon, M. Loiodice, Y. Nicolet, J.C. Fontecilla-Camps, P. Masson, H. Thiermann, F. Nachon, F. Worek, Structure-activity analysis of aging and reactivation of human butyrylcholinesterase inhibited by analogues of tabun, *Biochem. J.* 421 (2009) 97–106.
- [58] K. Schoene, Aging of soman-inhibited acetylcholinesterase: inhibitors and accelerators, *Biochim. Biophys. Acta* 525 (1978) 468–471.
- [59] K. Schoene, J. Steinhanses, A. Watermann, Aging of soman-inhibited acetylcholinesterase. pH-rate profiles an temperature dependence in absence and in presence of effectors, *Biochim. Biophys. Acta* 616 (1980) 384–388.
- [60] A. Stalc, M. Sentjurs, A contribution to the mechanism of action of SAD-128, *Biochem. Pharmacol.* 40 (1990) 2511–2517.
- [61] R.M. Dawson, M.H. Dowling, M. Poretski, Assessment of the competition between tacrine and gallamine for binding sites on acetylcholinesterase, *Neurochem. Int.* 19 (1991) 125–133.
- [62] G. Puu, Ketamine protects acetylcholinesterase against in vitro inhibition by sarin, *Biochem. Pharmacol.* 37 (1988) 969–970.
- [63] R.M. Dawson, Tacrine slows the rate of ageing of sarin-inhibited acetylcholinesterase, *Neurosci. Lett.* 100 (1989) 625–634.
- [64] J.L. Johnson, B. Cusack, T.F. Hughes, E.H. McCullough, A. Fauq, P. Romanovskis, A.F. Spatola, T.L. Rosenberry, Inhibitors tethered near the acetylcholinesterase active site serve as molecular rulers of the peripheral and acylation sites, *J. Biol. Chem.* 278 (2003) 38948–38955.
- [65] X. Zheng, N. Baker, G.R. Marshall, T.L. Rosenberry, D. Sept, Cyclic peptides as prophylactic agents for acetylcholinesterase, in: 10th International Meeting on Cholinesterases, Sibenik, Croatia, September 20–25, 2009, p. 41.
- [66] P. Taylor, Z. Kovarik, E. Reiner, Z. Radic, Acetylcholinesterase: converting a vulnerable target to a template for antidotes and detection of inhibitor exposure, *Toxicology* 233 (2007) 70–78.
- [67] M.Y. Mizutani, A. Itai, Efficient method for high-throughput virtual screening based on flexible docking: discovery of novel acetylcholinesterase inhibitors, *J. Med. Chem.* 47 (2004) 4818–4828.
- [68] F.J. Ekström, C. Astot, Y.P. Pang, Novel nerve-agent antidote design based on crystallographic and mass spectrometric analyses of tabun-conjugated acetylcholinesterase in complex with antidotes, *Clin. Pharmacol. Ther.* 82 (2007) 282–293.
- [69] A. Hörnberg, E. Artursson, R. Warne, Y.-P. Pang, F. Ekström, Crystal structure of oxime-bound fenamiphos-acetylcholinesterase: reactivation involving flipping of the His447 ring to form a reactive Glu334-His447-oxime triad, *Biochem. Pharmacol.* 79 (2010) 507–515.
- [70] A. Saxena, W. Sun, C. Luo, T.M. Myers, I. Koplovitz, D.E. Lenz, B.P. Doctor, Bioscavenger for protection from toxicity of organophosphorus compounds, *J. Mol. Neurosci.* 30 (2006) 145–148.
- [71] P. Masson, F. Nachon, C.A. Broomfield, D.E. Lenz, L. Verdier, L.M. Schopfer, O. Lockridge, A collaborative endeavor to design cholinesterase-based catalytic scavengers against toxic organophosphorus esters, *Chem. Biol. Interact.* 175 (2008) 273–280.
- [72] A. Saxena, D.M. Maxwell, D.M. Quinn, Z. Radic, P. Taylor, B.P. Doctor, Mutant acetylcholinesterases as potential detoxification agents for organophosphate poisoning, *Biochem. Pharmacol.* 54 (1997) 269–274.
- [73] Z. Kovarik, Z. Radic, H.A. Berman, P. Taylor, Mutation of acetylcholinesterase to enhance oxime-assisted catalytic turnover of methylphosphonates, *Toxicology* 233 (2007) 79–84.
- [74] O. Mazar, O. Cohen, C. Kronman, L. Raveh, D. Stein, A. Ordentlich, A. Shafferman, Aging-resistant organophosphate bioscavenger based on polyethylene glycol-conjugated F338A human acetylcholinesterase, *Mol. Pharmacol.* 74 (2008) 755–763.
- [75] C. Chronman, O. Cohen, O. Mazar, A. Ordentlich, L. Raveh, B. Velan, A. Shafferman, Next generation of OP-bioscavengers: a circulatory long-lived 4-PEG hypolysine mutant of F338A-huAChE with optimal pharmacokinetics and pseudo-catalytic characteristics, *Chem. - Biol. Interact.* 187 (2010) 253–258.



# Mass spectral characterization of organophosphate-labeled, tyrosine-containing peptides: Characteristic mass fragments and a new binding motif for organophosphates<sup>☆,☆☆</sup>

Lawrence M. Schopfer<sup>a,\*</sup>, Hasmik Grigoryan<sup>a</sup>, Bin Li<sup>a</sup>, Florian Nachon<sup>b</sup>, Patrick Masson<sup>b</sup>, Oksana Lockridge<sup>a</sup>

<sup>a</sup> Eppley Institute, University of Nebraska Medical Center, Omaha, NE 68198-6805, USA

<sup>b</sup> Centre de Recherches du Service de Santé des Armées, Toxicology Department BP87, 38702 La Tronche Cedex, France

## ARTICLE INFO

### Article history:

Received 30 May 2009

Accepted 17 July 2009

Available online 24 July 2009

### Keywords:

Tyrosine

Organophosphorus

Covalent bond

Mass spectrometry

Characteristic ions

## ABSTRACT

We have identified organophosphorus agent (OP)-tyrosine adducts on 12 different proteins labeled with six different OP. Labeling was achieved by treating pure proteins with up to 40-fold molar excess of OP at pH 8–8.6. OP-treated proteins were digested with trypsin, and peptides were separated by HPLC. Fragmentation patterns for 100 OP-peptides labeled on tyrosine were determined in the mass spectrometer. The goals of the present work were (1) to determine the common features of the OP-reactive tyrosines, and (2) to describe non-sequence MSMS fragments characteristic of OP-tyrosine peptides. Characteristic ions at 272 and 244 amu for tyrosine-OP immonium ions were nearly always present in the MSMS spectrum of peptides labeled on tyrosine by chlorpyrifos-oxon. Characteristic fragments also appeared from the parent ions that had been labeled with diisopropylfluorophosphate (216 amu), sarin (214 amu), soman (214 amu) or FP-biotin (227, 312, 329, 691 and 708 amu). In contrast to OP-reactive serines, which lie in the consensus sequence GXSG, the OP-reactive tyrosines have no consensus sequence. Their common feature is the presence of nearby positively charged residues that activate the phenolic hydroxyl group. The significance of these findings is the recognition of a new binding motif for OP to proteins that have no active site serine. Modified peptides are difficult to find when the OP bears no radiolabel and no tag. The characteristic MSMS fragment ions are valuable because they are identifiers for OP-tyrosine, independent of the peptide.

© 2009 Elsevier B.V. All rights reserved.

## 1. Introduction

Organophosphates (OP) have long been known to react with enzymes of the serine esterase family [1,2]. The high-reactivity of

acetylcholinesterase [AChE, EC 3.1.1.7] with a variety of OP is the basis for the acute toxicity of these compounds [3]. Covalent reaction of the OP with the catalytic serine of AChE inactivates the enzyme causing a myriad of cholinergic symptoms, including death [4]. Other enzymes can be covalently labeled by OP [5]. Reaction of OP with some of these may explain non-cholinergic effects of OP.

Recent studies have demonstrated that OP can also react in vitro with tyrosine on a variety of proteins [6–11]. To date, we have found OP-tyrosine adducts on 12 different proteins (transferrin, serum albumin, kinesin 3C, alpha 2-glycoprotein 1 zinc, pro-apolipoprotein A-I, keratin, tubulin, actin, ATP synthase, adenine nucleotide translocase I, chymotrypsinogen and pepsin), from four different species (human, cow, mouse and pig) labeled with six different OP (the chemical warfare agents soman and sarin, the pesticides chlorpyrifos-oxon and dichlorvos, and research compounds FP-biotin and diisopropylfluorophosphate).

Reaction of OP with tyrosine on serum albumin has been detected in vivo. Mice that were treated with 5 mg/kg of FP-biotin showed no signs of OP-toxicity, and still showed 1000-times more OP-labeled serum albumin than OP-labeled butyrylcholinesterase [BChE, EC 3.1.1.8] [12]. BChE is a classical, high-reactivity OP target. In another experiment, guinea pigs treated with either 0.5

**Abbreviations:** AChE, acetylcholinesterase; amu, atomic mass unit; BChE, butyrylcholinesterase; CAM, carbamidomethylated; CID, collision induced dissociation; CPO, chlorpyrifos-oxon, O,O-diethyl-(3,5,6-trichloro-2-pyridyl) phosphate; DCV, dichlorvos, O,O-dimethyl-(2,2-dichloroethenyl) phosphate; DFP, diisopropylfluorophosphate, O,O-diisopropyl fluorophosphate; FP-biotin, 10-(fluoroethoxyphosphinyl)-N-(biotinamidopentyl) decanamide; FPB, FP-biotin; LD<sub>50</sub>, lethal dose for 50% of the population; MSMS, tandem mass spectrometry fragmentation; m/z, mass divided by charge; OP, organophosphate; sarin, O-isopropylmethylphosphonofluoridate; SDS PAGE, sodium dodecyl sulfate polyacrylamide gel electrophoresis; soman, O-pinacolylmethylphosphonofluoridate.

<sup>☆</sup> This paper is part of the special issue: 'Bioanalysis of Organophosphorus Toxicants and Corresponding Antidotes', Harald John and Horst Thiermann (Guest Editors).

<sup>☆☆</sup> Presented at the 12th Medical Chemical Defence Conference, 22–23 April 2009, Munich, Germany.

\* Corresponding author. Tel.: +1 402 559 6014; fax: +1 402 559 4651.

E-mail addresses: [lschopf@unmc.edu](mailto:lschopf@unmc.edu) (L.M. Schopfer), [binli@unmc.edu](mailto:binli@unmc.edu) (H. Grigoryan), [hgrigoryan@berkeley.edu](mailto:hgrigoryan@berkeley.edu) (B. Li), [fnachon@crssa.net](mailto:fnachon@crssa.net) (F. Nachon), [pmasson@unmc.edu](mailto:pmasson@unmc.edu) (P. Masson), [olockrid@unmc.edu](mailto:olockrid@unmc.edu) (O. Lockridge).

LD<sub>50</sub> amounts of sarin or 2–5 LD<sub>50</sub> amounts of soman (together with medical countermeasures against intoxication) survived and were found to have substantial amounts of the OP bound to serum albumin [13].

The fact that a variety of proteins have been found to react with OP at tyrosine, coupled with the fact that this reaction can occur under relatively mild conditions *in vivo*, makes tyrosine an attractive candidate for a new, physiologically relevant target of OP intoxication.

To further explore the role of tyrosine as a physiological target for OP reaction, markers for the reaction products are of value.

Mass spectrometry is an excellent tool for identifying markers of protein modification. Three mass spectral features can be used for the identification: (1) the appearance of a mass in the MS spectrum that is consistent with a known peptide mass plus the mass of the modification, (2) the presence of a gap in the b-ion or y-ion sequence from an MSMS spectrum that is consistent with the mass of a modified amino acid, (3) the presence of fragments in the MSMS spectrum that are characteristic of the modification.

We have employed tandem quadrupole electrospray ionization mass spectrometry in conjunction with collision induced dissociation (CID) to study tyrosine-OP containing peptides. All three types of markers have been found. In all cases, the mass of the parent ion in the MS spectrum was consistent with the presence of the OP label. Manual analysis of the MSMS spectra from the labeled peptides often revealed gaps between b- and/or y-ions that were consistent with the mass of modified tyrosine. These gaps confirmed the presence of the OP and yielded the location of the labeled residue in the peptide sequence. Though each marker provides valuable information for the identification of modified peptides, the characteristic fragments are of particular value because they are specific identifiers for the type of modification, independent of the peptide.

The use of characteristic MSMS fragments for the detection of post-translational modifications was introduced by Huddleston for phosphorylation, glycosylation and sulfonylation [14]. Subsequently, characteristic fragments for a wide variety of modifications have been identified. Characteristic fragments are frequently immonium ions, immonium ion-derived fragments, or side chain fragments [15]. Such fragments can be used for precursor ion scanning or for post-acquisition analysis using extracted ion chromatography. Additional fragments resulting from neutral loss reactions involving the modified amino acid are also common [15].

We have found sets of characteristic fragments for tyrosine adducts with soman, sarin, chlorpyrifos-oxon, dichlorvos, FP-biotin, and diisopropylfluorophosphate. Characteristic fragments include ions that are parts of the labeled tyrosine (immonium ions and immonium ion-derived fragments); ions that appear as the result of neutral loss (neutral bits of the OP that are removed from the parent ion or sequence ions); and ions that there are unique fragments of the OP itself (found for FP-biotin).

This presentation has three goals. The first goal is to describe the characteristic ions for the various OP labels, along with the frequency at which each appears and the relative intensity of the signals. The second goal is to explore the environment of the labeled peptides in an attempt to establish factors that could promote the reaction of tyrosine with OP. We have found that tyrosines which are susceptible to reaction with OP frequently lie within 6 Å of a positively-charged group (lysine, arginine, or histidine). This suggests that charge–charge, through-space ion-pairing may be lowering the pK<sub>a</sub> for these tyrosines, making them better nucleophiles that are more capable of reacting with OP. The third goal is to establish tyrosine as a site for reaction of OP with proteins. This is consistent with the wide distribution of proteins that contain tyrosines which react with OP.

## 2. Methods and materials

The majority of the OP-labeled peptides reported in this article were taken from previously published reports, but a few were never before described. Preparation of the unreported peptides is described below.

### 2.1. Sample preparation for mass spectrometry

Bovine actin was purchased from Sigma (St. Louis, MO, cat# 3653). It was dissolved in 130 µl of 10 mM ammonium bicarbonate, pH 8.3, to give a final concentration of 48 µM. Then it was incubated with 48, 240 or 2400 µM chlorpyrifos-oxon (CPO) at 37 °C for 24 h. The samples were boiled for 10 min to denature the protein then reduced with 10 mM dithiothreitol (Fisher Biotech, Fair Lawn, NJ, cat# BP172-25, electrophoresis grade), alkylated with 50 mM iodoacetamide (Sigma cat# I6125), and dialyzed against 4 l of 10 mM ammonium bicarbonate, pH 8.3, for 18 h with one change of buffer. The dialyzed proteins were digested with trypsin (porcine, sequencing grade modified trypsin cat# V5113, reductively methylated, TPCK treated from Promega, Madison, WI) at 37 °C overnight. This preparation was used directly for MALDI mass spectrometry. A portion of the sample was dried in a vacuum centrifuge and redissolved in 5% acetonitrile/95% water/0.1% formic acid to yield approximately 3–5 pmol of peptide/µl (assuming no losses during processing) for analysis via electrospray-ionization, tandem triple-quadrupole mass spectrometry. Labeled peptides were identified using the MALDI TOF mass spectrometer. Theoretical peak lists were generated for the masses of the tryptic peptides from actin plus the added mass of CPO. These masses were compared to the observed masses. Observed masses that matched the theoretical masses were taken as candidates for CPO labeled peptides. Peptides identified in this manner were confirmed by manual analysis of the MSMS spectrum.

Human epidermal keratin was purchased from Sigma (St Louis, MO) (cat# K0253) as a denatured mixture of keratins in 8 M urea plus 0.1 M beta-mercaptoethanol. It was renatured by dialysis against 25 mM Tris/Cl, pH 7.5 overnight [16]. Then it was treated with 2 mM CPO and analyzed in the same manner as described for bovine actin.

Human pro-apolipoprotein A-I was identified from a human serum sample. A 200 µl aliquot of serum was separated into high abundance and low abundance proteins using the Beckman Coulter Proteome IgY spin column depletion kit (Beckman Coulter, Fullerton, CA, cat# 24331). The high abundance fraction (240 µl containing 7.9 µg protein/µl) was incubated with 1.25 mM diisopropylfluorophosphate (DFP from Sigma cat# D0879) at 37 °C overnight. The sample was denatured in 8 M urea, reduced with 5 mM dithiothreitol, alkylated with 40 mM iodoacetamide, dialyzed against 4 l of 10 mM ammonium bicarbonate overnight (with two changes of buffer) and digested with trypsin (porcine, sequencing grade) at 37 °C for 48 h. The product, containing 4.4 µg protein/µl, was fractionated by strong cation exchange chromatography using a Polysulfoethyl A column (200 mm long × 2.1 mm diameter from PolyLC, Columbia, MD) on a Waters HPLC system (Waters, Milford, MA) with a 40 min gradient starting at 100% solvent A and ending at 50% solvent A and 50% solvent B, where solvent A was 10 mM ammonium formate, pH 3.0, plus 25% acetonitrile and solvent B was 500 mM ammonium formate, pH 6.8, plus 25% acetonitrile. Fractions were dried in a vacuum centrifuge and resuspended in 5% acetonitrile/95% water/0.1% formic acid for analysis by electrospray-ionization triple-quadrupole mass spectrometry.

The preparation of the human serum samples from which the unassigned peptides were obtained, was very similar to that used for pro-apolipoprotein A-I. The first major difference was that the serum was reacted with 200 µM FP-biotin for 48 h at 37 °C. Then

after denaturation, reduction, alkylation, dialysis and tryptic digestion, the FP-biotinylated peptides were extracted using monomeric avidin-agarose beads (Pierce, Rockford, IL cat# 20228). The beads were washed with 0.5 M sodium chloride in 0.1 M Tris/Cl buffer, pH 8.6, followed by 20 mM Tris/Cl, pH 7.5. The FP-biotinylated peptides were eluted with 10% acetic acid. The eluate was dried in a vacuum centrifuge and resuspended in 5% acetonitrile/95% water/0.1% formic acid in preparation for analysis by electrospray-ionization triple-quadrupole mass spectrometry. Labeled peptides were identified by extracted ion chromatography utilizing the characteristic masses of 227, 312 and 329 amu derived from FP-biotin.

## 2.2. MALDI mass spectrometry

Generally, 1  $\mu$ l of tryptic digest (20–50 pmol/ $\mu$ l, assuming no losses during processing) was air dried onto a 384 well Opti-TOF sample plate (Applied Biosystems, Foster City, CA, #1016491) and then overlaid with 1  $\mu$ l of alpha-cyano-4-hydroxy cinnamic acid solution (CHCA, 10 mg/ml from Fluka cat# 70990). CHCA was recrystallized before use then dissolved to 10 mg/ml in 50% acetonitrile/50%water/0.1% trifluoroacetic acid. Mass spectra and collision induced MSMS spectra were collected in positive ion reflector mode with a MALDI TOF 4800 mass spectrometer (Applied Biosystems). The final spectrum was the average of 500 laser shots. The mass spectrometer was calibrated before each use with CalMix 5 (Applied Biosystems).

## 2.3. Quadrupole mass spectrometry

Ten microliters of tryptic digest (30–50 pmol) were injected onto an HPLC nanocolumn (218MS3.07515 Vydac C18 polymeric reverse phase, 75  $\mu$ m I.D. – 150 mm long; P.J. Cobert Assoc, St. Louis, MO). Peptides were separated with a 90 min linear gradient from 5% to 60% acetonitrile at a flow rate of 0.3  $\mu$ l/min and electrosprayed through a fused silica emitter (360  $\mu$ m O.D., 75  $\mu$ m I.D., 15  $\mu$ m taper, New Objective, Woburn, MA) directly into the QTRAP 2000, a hybrid quadrupole linear ion trap mass spectrometer (Applied Biosystems). An ion-spray voltage of 1900 V was maintained between the emitter and the mass spectrometer. Information dependent acquisition was used to collect MS, high resolution MS, and MSMS spectra. All spectra were collected in the enhanced mode, using the trap function. The three most intense MS peaks in each cycle having masses between 200 and 1700  $m/z$ , charge of +1 to +4, and intensities greater than 10,000 counts per second were selected for high resolution MS and MSMS analysis. Precursor ions were excluded for 30 s after one MSMS spectrum had been collected. MSMS fragmentation was obtained by collision induced dissociation (CID). The collision cell was pressurized to 40  $\mu$ Torr with pure nitrogen. Collision energies between 20 and 40 eV were determined automatically by the software, based on the mass and charge of the precursor ion. The mass spectrometer was calibrated on selected fragments from the MSMS spectrum of human Glu-fibrinopeptide B (Sigma cat# F3261).

## 2.4. Strategies for finding OP-labeled peptides

The discovery that tyrosines could be labeled by OP arose from a general search for proteins capable of reacting with OP. The strategy for the initial part of that search was taken from Cravatt and co-workers [17,18], and employed the OP probe that they introduced (FP-biotin). One advantage of using FP-biotin as a probe is that the biotin tag allowed purification of the labeled protein. In general, the strategy consisted of the following: A crude protein preparation was labeled with 10  $\mu$ M FP-biotin in pH 8.0 buffer. The labeled proteins were extracted from the crude mixture using avidin-agarose. The extracted proteins were separated by SDS PAGE. The presence

of the FP-biotinylated proteins was confirmed by staining a blot of the PAGE gel with streptavidin-Alexa 680 (a fluorescent dye). Proteins present in sufficient quantity for mass spectral analysis were identified by staining a second gel with Coomassie Blue. Stained bands were cut from the gel and subjected to in-gel tryptic digestion. Finally, the tryptic digests were subjected to mass spectral analysis to identify the proteins that were present in the stained bands. This process is described in more detail by [12,19,20].

The primary difficulty with the search strategy described above is that the labeled peptides were not observed, so that proof for covalent binding of OP to proteins was indirect. Indirect evidence was acceptable for serine hydrolases, but not for proteins that had no active site serine. To find and characterize the labeled peptides, purified preparations of proteins that were identified in the initial screening were studied. This second-stage strategy consisted of the following: purified proteins were labeled with FP-biotin. Labeled protein was proteolyzed. Labeled peptides were extracted with monomeric avidin-agarose. Finally, the peptides were subjected to mass spectral analysis. Description of this process can be found in [9,10]. In another strategy a crude preparation of human plasma was labeled with FP-biotin, digested with trypsin and the labeled peptides extracted with monomeric avidin-agarose [10,21]. With this process, labeled peptides could be successfully retrieved and characterized.

The third stage of the strategy tested the reactivity of pure proteins with OP that had no biotin tag. The OP-treated preparation was digested, and the peptides were analyzed mass spectrally. The masses of the known OP-reactive peptides plus the added mass from the new OP could be calculated and the MS spectrum searched for their presence. Characteristic ion masses provided means of searching through the MSMS data to locate peptides expected to become labeled, and to locate new peptides that might have become labeled. For most OP, the characteristic ion masses are too small and not sufficiently unique to serve as satisfactory search criteria for MSMS spectra from complex mixtures, unless a mass spectrometer of high mass accuracy is used, but they are fully adequate for searching MSMS spectra from pure protein digests. This means the protein of interest has to be purified from a complex mixture such as brain in order to find the OP-labeled peptide. Support for the conclusion that a peptide is labeled with OP on tyrosine comes from the presence in an MSMS spectrum of the characteristic OP-tyrosine immonium ions identified in this report.

## 3. Results and discussion

### 3.1. Distribution of OP labels

We found OP-labeled tyrosines on 60 different tryptic peptides. These peptides included two from human transferrin; six from human serum albumin; one from human kinesin KIF3C motor domain; four from unidentified proteins in human plasma; three from human alpha 2-glycoprotein 1, zinc; one from human proapolipoprotein A-I; four from human keratin 1; one from human keratin 2; one from human keratin 9; two from human keratin 10; one from bovine serum albumin; nine from bovine tubulin alpha; seven from bovine tubulin beta; six from bovine actin alpha, skeletal muscle; one from bovine chymotrypsinogen; five from mouse transferrin; one from mouse ATP synthase; one from mouse adenine nucleotide translocase I; one from mouse tubulin beta; one from pig pepsin and two synthetic peptides (See Table 1). There were 11 peptides that contained more than one tyrosine. Of these, six could be labeled on more than one tyrosine, and two of those (EEY\*NGY\*TGAFR and LY\*LGHNY\*VTAIR from mouse transferrin) could be labeled on two tyrosines simultaneously, though double labeling was not always observed.

**Table 1**

OP-labeled tyrosine-containing peptides observed in tryptic digests.

No.	Species	Protein	Peptide <sup>a</sup>	gi number <sup>c</sup>	OP <sup>d</sup>	Reference
1	Human	Transferrin	KPVDEY*K	136191	FPB, DFP, DCV, CPO, soman	[10]
2	Human	Transferrin	KPVEEY*ANCHLAR	136191	FPB, DFP, CPO, sarin, soman	[10]
3	Human	Serum Albumin	Y*TK	28592	FPB, CPO, DFP	[7,13,21]
4	Human	Serum Albumin	HPY*FY*APELLFFAK	28592	FPB, CPO	[21]
5	Human	Serum Albumin	Y*LYEIR	28592	FPB, CPO	[21]
6	Human	Serum Albumin	QNCLEFQELGEY*K	28592	FPB, CPO	[21]
7	Human	Serum Albumin	MPCAEDY*LSVVLNQCLHEK	28592	FPB, CPO	[21]
8	Human	Serum Albumin	Y*KAAFTCCQAADK	28592	CPO	[21]
9	Human	Kinesin 3C motor domain 5	ASY*Y*LEIQEEIR	41352705	FPB	[20]
10	Human	Serum Unknown	AY*PR	–	FPB	This work
11	Human	Serum Unknown	Y*PR	–	FPB	This work
12	Human	Serum Unknown	Y*L/IK	–	FPB	This work
13	Human	Serum Unknown	Y*K	–	FPB	This work
14	Human	α2-Glycoprotein 1, zinc	WEAEPVY*VQR	51094610	FPB	[20]
15	Human	α2-Glycoprotein 1, zinc	AY*LEECPATLR	51094610	FPB	[20]
16	Human	α2-Glycoprotein 1, zinc	YY*YDGKDYIEFNK <sup>b</sup>	51094610	FPB	[20]
17	Human	Pro-apolipoprotein A-I	DY*VSQFEGSALGK	178775	DFP	This work
18	Human	Keratin 1 renatured	LLRDY*QELMNTK	119395750	CPO	This work
19	Human	Keratin 1 renatured	SGGGFSSGSAGIINY*QR	119395750	CPO	This work
20	Human	Keratin 1 renatured	THLEPY*FESFINNLR	119395750	FPB, CPO	[20]
21	Human	Keratin 1 renatured	Y*EELQITAR	119395750	CPO	This work
22	Human	Keratin 2 renatured	Y*LDTGLTAER	181402	CPO	This work
23	Human	Keratin 9 renatured	QFSSSY*LSR	435476	CPO	This work
24	Human	Keratin 10 renatured	LKY*ENEVALR	47744568	CPO	This work
25	Human	Keratin 10 renatured	LASY*LDK	47744568	CPO	This work
26	Bovine	Serum albumin	Y*TR	30794280	FPB, CPO, DFP	[6]
27	Bovine	Tubulin alpha	TGT*Y*R	73586894	FPB, DFP, CPO	[9]
28	Bovine	Tubulin alpha	AFVHWY*VGEGMEEGEFSEAR	73586894	CPO	[23]
29	Bovine	Tubulin alpha	EDAANNY*AR	73586894	CPO	[23]
30	Bovine	Tubulin alpha	IHFPLATY*APVISAER	73586894	CPO	[23]
31	Bovine	Tubulin alpha	FDGALNVDLTFQTNLPY*PR	73586894	CPO	[23]
32	Bovine	Tubulin alpha	GHY*TIGK	73586894	CPO	[23]
33	Bovine	Tubulin alpha	VGINY*QPPTVVPGGDLAK	73586894	CPO	[23]
34	Bovine	Tubulin alpha	FDLMY*AK	73586894	CPO	[23]
35	Bovine	Tubulin alpha	LSVDY*GK	73586894	CPO	[23]
36	Bovine	Tubulin beta	Y*VPR	75773583	FPB, DFP, CPO, soman	[9]
37	Bovine	Tubulin beta	GSQQY*R	75773583	FPB, DFP, CPO, sarin, soman	[9]
38	Bovine	Tubulin beta	EEY*PDR	75773583	FPB, DFP, CPO	[9]
39	Bovine	Tubulin beta	Y*LTVAAVFR	75773583	CPO	[23]
40	Bovine	Tubulin beta	GHY*TEGAELVDSVLDVVR	75773583	CPO	[23]
41	Bovine	Tubulin beta	INVY*Y*NEATGGK	75773583	CPO	[23]
42	Bovine	Tubulin beta	NSSY*FVEWIPNNVK	75773583	CPO	[23]
43	Bovine	Actin alpha skeletal muscle	GY*SFVTTAER	62287933	FPB	[20]
44	Bovine	Actin alpha skeletal muscle	DSY*VGDEAQS	62287933	CPO	This work
45	Bovine	Actin alpha skeletal muscle	SY*ELPDGQVITIGNER	62287933	FPB	[20]
46	Bovine	Actin alpha skeletal muscle	IWHHTFY*NELR	62287933	CPO	This work
47	Bovine	Actin alpha skeletal muscle	QEY*DEAGPSIVHR	62287933	CPO	This work
48	Bovine	Actin alpha skeletal muscle	DLDY*LMK	62287933	CPO	This work
49	Bovine	Chymotrypsinogen	Y*TNANTPDR	194674931	FPB	[20]
50	Mouse	Transferrin	KPVDQY*EDCY*LAR	21363012	FPB, DFP, CPO, sarin, soman	[10]
51	Mouse	Transferrin	LY*LGHNY*VTAIR	21363012	FPB, CPO	[10]
52	Mouse	Transferrin	EEY*NGY*TAAR	21363012	FPB, CPO	[10]
53	Mouse	Transferrin	FDEFFSQGCAPGY*EK	21363012	FPB, CPO	[10]
54	Mouse	Transferrin	GY*Y*AVAVVK	21363012	FPB, CPO, DFP, sarin, soman	[10]
55	Mouse	ATP Synthase	ILQDY*K	20455479	FPB	[20]
56	Mouse	Adenine Nucleotide Translocase 1	Y*FPTQALNFAFK	902008	FPB	[20]
57	Mouse	Tubulin beta	INVY*Y*NEAAGNK	21746161	CPO	This work
58	Porcine	Pepsin	QYY*TVFDR	1302650	FPB	[20]
59	Synthetic	peptide	RY*TR		CPO	[10]
60	Synthetic	peptide	SY*SM		DCV	[10]

<sup>a</sup> Y\* indicates the labeled tyrosine. For peptides showing two Y\*, either one or the other tyrosine was labeled.<sup>b</sup> The position of the label is unclear for this peptide. Either the first or second Y from the N-terminus could have been labeled.<sup>c</sup> The gi number is the NCBI accession number for the protein in PubMed.<sup>d</sup> FPB = FP-biotin; CPO = chlorpyrifos-oxon; DFP = diisopropyl fluorophosphate; DCV = dichlorvos.

Each labeled peptide exhibited the mass expected of the OP-adduct (to within 0.1 amu). The sequence of each peptide was confirmed by manual analysis of the CID MSMS spectrum. The location of the labeled amino acid could generally be established directly from the observed sequence. Finally, characteristic, non-sequence masses were identified that supported the proposed labeling.

Proteins for which we could find no FP-biotin-labeled peptides included porcine gelatin, bovine RNase, chicken lysozyme, bovine DNase I, human IgG and bovine insulin. Our inability to find OP-labeled peptides in these pure proteins treated with a 20-fold molar excess of FP-biotin does not rule out the possibility that these proteins can be labeled by OP. For example, hen egg white lysozyme incorporates 1 mol of DFP per mole of lysozyme (on tyrosine) at pH

**Table 2**  
Structures of organophosphorus agents bound to tyrosine.

Structure of the added mass	Added mass (amu)	Organophosphorus agent
	572	FP-biotin
	164	Diisopropylfluorophosphate (DFP)
	136	Chlorpyrifos-oxon (CPO)
	108	Dichlorvos (DCV)
	120	Sarin
	162	Soman

The arrows in the FP-biotin structure indicate fragmentation sites. A 227 amu ion is produced by cleavage between carbon 16 and the adjacent nitrogen. A 329 amu ion is produced by cleavage between carbon 10 and the adjacent nitrogen. The 312 amu ion is produced by loss of amine from the 329 amu ion. Added mass refers to the mass of the OP that remains covalently attached to the target amino acid after the reaction is complete. All OP were attached to the phenolic oxygen of tyrosine through the phosphorus atom.

9.5 when the DFP concentration is in 300-fold molar excess [22]. The OP-labeled lysozyme does not lose its esterase activity with *p*-nitrophenyl acetate.

### 3.2. OP characteristic fragments

We employed six different organophosphorus agents in these studies: soman and sarin (chemical warfare agents), chlorpyrifos-oxon and dichlorvos (commercial pesticides), and FP-biotin and diisopropylfluorophosphate (research reagents). Table 2 gives the OP structures and their added masses, after the OP have made a covalent bond with tyrosine.

The reaction between OP and tyrosine is illustrated in Fig. 1. Soman makes a covalent bond with the phenolic oxygen of tyrosine and simultaneously releases fluoride. The reaction product has an added mass of 162 amu. The OP-tyrosine adduct is stable and does not undergo the dealkylation reaction called “aging” that is typical of soman adducts on acetylcholinesterase.

Many of the 60 peptides described in Table 1 were labeled with more than one OP. Consequently, a total of 100 variously-labeled peptides could be assembled: 6 labeled with soman, 4 with sarin, 45 with chlorpyrifos-oxon, 2 with dichlorvos, 32 with FP-biotin,

and 11 with diisopropylfluorophosphate. Each peptide was labeled on tyrosine. Each type of labeled tyrosine generated characteristic non-sequence ions upon low-energy, collision induced dissociation (CID) in the mass spectrometer (QTRAP 2000, Applied Biosystems). Collision energies were set at 20–60 eV and nitrogen was used as the collision gas, at  $4 \times 10^{-5}$  Torr.

The non-sequence fragments can be divided into three categories: (1) those that arise by neutral loss of a side-chain from an OP-tyrosine adduct of the parent ion or a fragment ion, (2) those that are OP-tyrosine immonium ions or derivatives of OP-tyrosine immonium ions, and (3) those that arise by fragmentation that is specific to FP-biotin (329.4, 312.4 and 227.2 amu, see Table 3 or reference [6]).

### 3.3. Neutral loss of a side-chain from CPO, DFP, soman and sarin adducts

In the context of these experiments, neutral loss from CPO, DFP, soman and sarin refers to the loss of an alkyl side-chain from an OP-tyrosine adduct. It does not refer to loss of the entire OP from the tyrosine. None of the 100 OP-tyrosine peptide MSMS spectra we examined showed loss of the entire OP from tyrosine. In contrast,

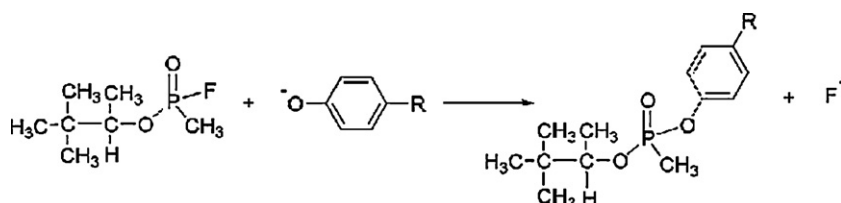


**Fig. 1.** Modification of tyrosine by soman to make a stable covalent bond.

**Table 3**  
OP-tyrosine characteristic product ions<sup>a</sup>.

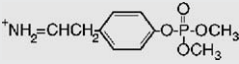
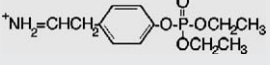
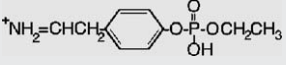
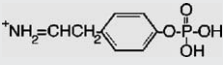
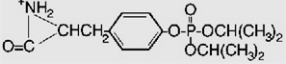
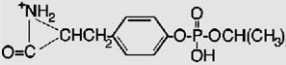
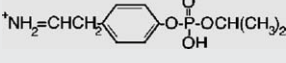
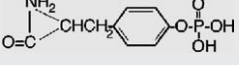
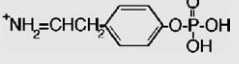
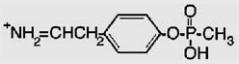
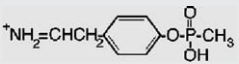
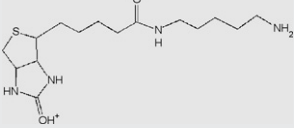
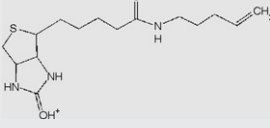
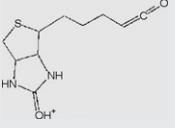
Mass (amu) <sup>b</sup>	Name	Structure	% <sup>c</sup>	Relative intensity <sup>d</sup>
Dichlorvos 2 tryptic peptide analyzed				
244.0	Dimethoxyphospho Tyr immonium		100	100
Chlorpyrifos-oxon 45 tryptic peptides analyzed				
272.3	Diethoxyphospho Tyr immonium		92	6–100
253.5	Diethoxyphospho Tyr immonium-NH3		5	4
254.2	Diethoxyphospho Tyr immonium-H2O		2	4
244.3	Monoethoxyphospho Tyr immonium		75	30–100
226.1	Monoethoxyphospho Tyr immonium-H2O		16	2–38
216.1	Phospho Tyr immonium		30	3–77
198.1	Phospho Tyr immonium-H2O		2	16
Diisopropylfluorophosphate 11 tryptic peptides analyzed				
328.8	Diisopropoxyphospho Tyr		9	23
311.8	Diisopropoxyphospho Tyr-NH3		9	9
286.2	Monoisopropoxyphospho Tyr		9	6
258.1	Monoisopropoxyphospho Tyr immonium		9	4
244.2	Phospho Tyr		9	60
226.0	Phospho Tyr-H2O		18	8–100
216.1	Phospho Tyr immonium		91	4–100
199.2	Phospho Tyr immonium-NH3		9	24
198.1	Phospho Tyr immonium-H2O		27	6–22
Sarin 4 tryptic peptides analyzed				
214.1	Methylphospho Tyr immonium		100	100
Soman 6 tryptic peptides analyzed				
214.2	Methylphospho Tyr immonium		83	10–95
FP-Biotin 32 tryptic peptides analyzed				
329.4	FPB fragment		100	6–100
312.4	FPB fragment		100	7–100
227.2	FPB fragment		89	4–100

Table 3 (Continued)

Mass (amu) <sup>b</sup>	Name	Structure	% <sup>c</sup>	Relative intensity <sup>d</sup>
708.5	Tyr-FPB immonium		86	5–100
691.4	Tyr-FPB immonium-NH <sub>3</sub>		86	5–80
482.5	Tyr-(FPB-226) immonium		31	10–15
465.5	Tyr-(FPB-226) immonium-NH <sub>3</sub>		20	5–20
397.0	Tyr-(FPB-311) immonium		3	14
380.4	Tyr-(FPB-328) immonium		40	15–25
379.3	Tyr-(FPB-329) immonium		17	10–20
362.8	Tyr-(FPB-328) immonium-NH <sub>3</sub>		3	27
355.0	Tyr-FPB immonium (+2 charge)		43	2–100
346.5	Tyr-FPB immonium-NH <sub>3</sub> (+2 charge)		20	10–35

<sup>a</sup> All masses are for the protonated, dehydro form of the amino acid.

<sup>b</sup> Masses are given as the average of all measurements made from the quadrupole tandem mass spectrometer.

<sup>c</sup> % refers to the fraction of the tryptic peptides that exhibited this mass.

<sup>d</sup> Relative intensity is given as a range, which refers to the intensity of the mass relative to the most intense peak in the MSMS spectrum. This value is given as a percentage. Entries without a range represent masses which appeared only once, except for the 214.1 amu entry for sarin which appeared for all 3 peptides as the most intense peak of the spectrum.

phosphorylated-tyrosine can lose the entire phosphate, though in low yield [24].

The neutral loss of alkyl side-chains from OP in the gas phase can be attributed to McLafferty rearrangement [25]. This rearrangement (Fig. 2) requires the availability of a proton on a carbon atom beta to the phosphorus oxygen. Loss of the alkyl group occurs with concomitant transfer of the beta-proton to the phosphoryl-oxygen, via a six-membered transition state, and formation of a carbon–carbon double bond between the alpha and beta carbons in the alkyl group. Under low-energy CID conditions, this is a facile reaction.

McLafferty rearrangement is sometimes referred to as beta-elimination, by analogy with the hydroxide-catalyzed elimination of phosphate from phosphoserine and phosphothreonine in solution chemistry. McLafferty rearrangement/beta elimination is responsible for the well-documented release of phosphate from phosphoserine and phosphothreonine during CID [24]. This mechanism also provides the primary justification for why release of phosphate (or organophosphate) from phosphotyrosine is chemically unfavorable, i.e. the beta proton in phosphotyrosine is on an aromatic ring and therefore not readily released.

Most of the alkoxy side-chains on the OP given in Table 2 are susceptible to McLafferty rearrangement. Methoxy derivatives, such as are found in dichlorvos, do not have a beta-carbon and therefore are not susceptible to McLafferty rearrangement. Alkyl ligands that attach directly to the phosphorus, without the intervention of an

oxygen molecule, are also not susceptible to McLafferty rearrangement, i.e. phosphonyl esters. Ligands of this latter type are found on soman and sarin (methyl) and FP-biotin (biotinylated arm).

McLafferty rearrangements generate neutral losses of 28 amu for ethoxy side-chains (CPO and FP-biotin), 42 amu for isopropoxy side-chains (DFP and sarin), and 84 amu for the pinacolyl side-chain of soman.

Neutral loss of OP side-chains was observed in two contexts. In the first context, loss was directly from the parent ion. This could be detected if the peptide was small enough for the diminished parent ion mass to fall within the mass range of the QTrap 2000 mass spectrometer (upper limit 1500 *m/z*). An example of this sort of neutral loss is shown in Fig. 3 where a doubly-charged form of the parent ion minus the pinacolyl side-chain of the soman label can be found at 524.2 amu. A second example is found in Fig. 6 where the singly-charged, DFP-labeled, YTR parent ion (603.4 amu) loses one isopropyl group (42 amu) to yield the 561.4 ion, and then a second isopropyl group (a total of 84 amu) to yield the 519.2 ion.

In the second context, neutral loss was from OP-labeled tyrosine immonium ions. Loss from immonium ions was a common occurrence and is readily observable in several of the following figures.

The order of neutral loss susceptibility observed for peptides labeled with the various OP, correlated with the complexity of the alkyl chain. Thus, after CID fragmentation of soman-labeled peptides, ions carrying intact soman labels were never observed.

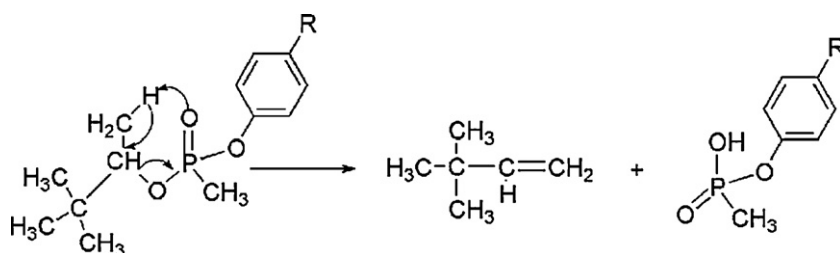


**Fig. 2.** McLafferty rearrangement of a tyrosyl-soman adduct resulting in neutral loss of the pinacolyl side chain. The pinacolyl side-chain is lost during MSMS under CID conditions. Soman-tyrosine adducts do not lose the pinacolyl group outside of the mass spectrometer.

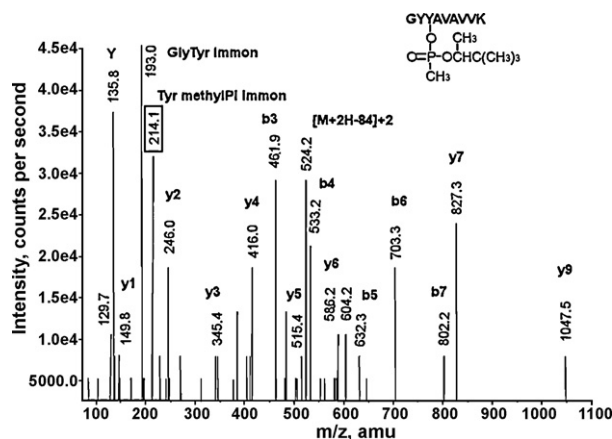


**Fig. 3.** A CID fragmentation spectrum of the soman-labeled mouse transferrin, tryptic peptide GYY\*AVAVVK. The 214.1 value enclosed in the box is the mass of the methylphosphotyrosine immonium ion, the characteristic fragment for soman-labeled tyrosine. The doubly-charged parent ion at 566.5  $m/z$  includes 162 amu from soman. Loss of the pinacolyl group results in the doubly-charged methylphosphonate parent ion at 524.2  $m/z$ . The mass at 135.8 is the immonium ion of tyrosine. The mass at 193.0 amu is the a2 ion, also described as the GlyTyr immonium ion.

Only masses associated with ions missing the pinacolyl group were found (see Fig. 3). On the other hand, the MSMS spectra of DFP-labeled peptides showed ions carrying the intact DFP label as well as ions that had lost one or both of the isopropyl groups (see Fig. 6). This distribution reflects the decreased susceptibility of the isopropoxy group to undergo neutral loss. Finally, the MSMS spectra of CPO-labeled peptides rarely showed parent ion masses consistent with the loss of an ethyl group. Loss of the ethyl group was only seen from the labeled tyrosine immonium ion which created a tyrosine-monoethylphosphate immonium ion at 244.0 amu (see Fig. 5). Neutral loss of methyl was not detected from dichlorvos-labeled peptides (see Fig. 7). Side-chain neutral losses have also been reported for the isolated OP, e.g. sarin, soman, cyclosarin, and analogs of DFP and CPO [26,27].

A similar loss of the alkyl side-chain occurs when OP are bound to cholinesterases in solution. This process is referred to as aging. The gas phase side-chain loss is mechanistically distinct from the aging process and should not be confused with aging.

The observations on neutral loss can be summarized by saying that loss of a side-chain from alkoxy ligands to the phosphorus was the rule for soman-labeled tyrosine; was common for DFP- or sarin-labeled tyrosine; was constrained to tyrosine immonium ions for CPO-labeled tyrosine; and was not observed for the dichlorvos-labeled tyrosine.

### 3.4. OP-tyrosine immonium ions

With the exception of FP-biotinylated samples, the non-sequence masses that appeared most frequently were consistent with forms of OP-tyrosine immonium ions. This is in agreement with a recent review by Lehmann and co-workers, in which they reported that CID-generated characteristic ions (reporter ions) for peptides containing covalently modified amino acids are generally immonium ions or immonium ion-derived fragments [15]. The OP-tyrosine immonium ions and their derivatives appear in the list of characteristic ions in Table 3.

Two dichlorvos-labeled tryptic peptides were analyzed. A mass at 244 amu, consistent with the dimethoxyphospho-tyrosine immonium ion, was the most prominent peak in both MSMS spectra (see Fig. 7 for an example). This mass did not contribute to the peptide sequence information. Though the 244 amu mass is identical to the mass for phospho-tyrosine, the anticipated difficulty in releas-

ing methyl groups from methoxy-OP makes an immonium ion of dimethoxyphospho-tyrosine the more reasonable assignment.

The diethoxyphospho-tyrosine immonium ion, at 272 amu, was the most commonly observed non-sequence ion for chlorpyrifos-oxon labeled peptides. It appeared in 92% of the MSMS spectra (42 out of 45 peptides). In addition to being common, the mass was generally intense. It was the most intense ion in seven spectra. The monoethoxyphospho-tyrosine immonium ion, at 244 amu, was nearly as abundant as the diethoxyphospho-tyrosine immonium ion, appearing in 75% of the spectra (34 out of 45 peptides). It was also intense, being the most intense ion in two spectra. For an example, refer to Fig. 5. Though the 244 amu mass that we have taken to be the monoethoxyphospho-tyrosine immonium ion is the same as that for phospho-tyrosine, the prevalence of immonium ions in Table 3 makes the immonium ion assignment for this mass the more reasonable. Elimination of both ethyl groups to yield the phospho-tyrosine immonium ion, at a mass of 193 amu, was less common, occurring in 30% of the spectra (14 out of 45). The FP-biotin tyrosine adduct also includes an ethoxy substituent on the phosphorus, but no evidence for an FP-biotin tyrosine immonium ion with loss of the ethyl was detected (680 amu).

By far, the most common non-sequence ion seen in the spectra of the DFP-labeled peptides was the 216 amu mass attributable to the phospho-tyrosine immonium ion, i.e. loss of both isopropyl groups (see Table 3 and Fig. 6). It appeared in 91% of the MSMS spectra (10 out of 11 peptides). Though its intensity varied widely, it was always at least 20% that of the most intense peak in the spectrum. On one occasion it was the most intense peak in the spectrum. Loss of a single isopropyl to generate the monoisopropoxyphospho-tyrosine immonium ion at 258 amu appeared in only 9% of the spectra (1 out of 11 peptides). The preponderance of species in which both isopropyl groups had been lost reflects the ease of eliminating the isopropyl under CID conditions. The next most common characteristic ion was the phospho-tyrosine immonium ion minus water at 198 amu, occurring in 27% of the spectra (3 out of 11). This species is a secondary fragmentation of the phospho-tyrosine immonium ion and supports the dominance of the isopropyl free form.

Tyrosine immonium ions from the four sarin-labeled peptides that were examined all had lost their isopropyl moieties (Fig. 8). The resultant methylphospho-tyrosine immonium ion at 214 amu was the only non-sequence ion seen in the MSMS spectra, and it was always the most intense ion in the spectrum (see Table 3).

Formation of the methylphospho-tyrosine immonium ion from soman-labeled tyrosine-containing peptides was also commonplace, appearing in 83% of the MSMS spectra. However, when it did occur, the relative intensity of the peak was generally less than 20% that of the most intense peak in the spectrum (see Table 3 and Fig. 3). By extrapolation of the trend developed from the smaller alkoxy ligands, one might have expected that this immonium ion would have been present for all soman-labeled peptides and that it would have dominated the spectra. A possible rationalization for the unexpected loss in prominence of the methylphospho-tyrosine immonium ion may lie in the extremely facile nature of the neutral loss of pinacolyl from the parent ion. In the same manner that facile loss of phosphate from the parent ions of phospho-peptides suppresses other fragmentation [28,29], facile loss of the pinacolyl group from the soman-labeled parent ions may suppress formation of the methylphospho-tyrosine immonium ion.

The FP-biotinylated tyrosine immonium ion, at 708.5 amu, appeared in 90% of the fragmentation spectra for FP-biotin-labeled tyrosine-containing peptides. It was generally accompanied by a 691.4 amu mass that was consistent with the loss of amine from the tyrosine-FP-biotin immonium ion (see Fig. 4). Even the doubly-charged forms of these ions, at 355.0 and 346.5 amu were common, appearing in 40% and 17% of the spectra, respectively (see Table 3).

Observations on the OP-tyrosine immonium ions can be summarized by saying that they are major non-sequence ions in the MS/MS spectra, and that they are characteristic of OP-labeling of tyrosine.

### 3.5. Fragmentation specific to FP-biotin

In addition to OP-tyrosine immonium ions, fragmentation of FP-biotin labeled tyrosine yielded a unique set of ions. Elimination of the ethyl group from the ethoxy side-chain of the phosphorus was not seen. Rather, fragmentation of the amide linkages in the biotinyl side-chain of the FP-biotin generally dominated the MSMS spectrum. See Table 3 for a list of these fragments and Table 2 for a graphical presentation of the location of the break points.

An FP-biotinylated peptide is invariably multiply-charged. This appears to be due to protonation of the biotin. Thus, even two and three residue peptides are doubly-charged. Scission of FP-biotin's alkyl chain releases the biotin end of the label, along with one charge. This generates positively-charged fragments, as well as creating a loss from the parent ion. A hallmark of FP-biotinylation on tyrosine is the presence of positively-charged fragments at 227, 312 and 329 amu [6], see Fig. 4. Fragments at 329 and 312 amu appeared in 100% of the spectra, while fragments at 227 amu appeared in 89% (31 out of 35 peptides). All three fragments generally yielded very intense signals (see Table 3). The 329 amu mass was the most intense peak on six occasions, the 312 amu peak on two occasions, and the 227 amu peak on three.

A corresponding neutral loss of 226, 311 and 328 amu from the parent ion was detected in 34%, 11% and 31% of the MSMS spectra, respectively. The 328 amu neutral loss peak always appeared as a doublet with the second peak representing loss of 329 amu. The parent ion minus 329 could be discriminated from the +1 isotopic form of the parent ion minus 328 on the basis of the relative intensities of the  $[M+H-328]$  and  $[M+H-329]$  peaks. The intensities of these two masses were always nearly equal.

Neutral loss directly from the parent ion was not observed as frequently as the corresponding positively-charged fragment ion. The parent ion minus 328 (and 329) appeared in 31% of the spectra (11 out of 35); the parent ion minus 311 appeared in 11% of the spectra (4 out of 35); and the parent ion minus 226 appeared in 34% of the spectra (12 out of 35). This can be attributed in part to the large size

of the FP-biotin adduct, which has a 572 amu added mass. Since the upper mass limit for the QTrap 2000 is about 1500 amu, neutral loss fragments from FP-biotinylated peptides larger than seven residues were difficult to detect. Neutral loss fragments were occasionally accompanied by fragments consistent with loss of water (18 amu) or amine (17 amu) or carbon monoxide (28 amu).

Doubly-charged fragments corresponding to the parent ion minus 328, 329 or 226 amu were also detected, as well as fragments corresponding to loss of amine from these species. In addition, tyrosine-FPB immonium ions that had lost 329 amu to give a mass of 379 amu (17%) or 328 amu to give a mass of 380 amu (40%), 226 amu to give a mass of 482 amu (31%) were commonly seen (Table 3).

Ions at 227, 312 and 329 amu generally appear when either FP-biotinylated tyrosine or serine adducts are fragmented [6]. These three ions provide a fingerprint for FP-biotinylated peptides. Since they can be relied upon to appear as a triad and they have moderately large molecular weights, confusing this set of masses with sequence masses from the peptide is minimal. Discrimination between FP-biotinylated tyrosine and FP-biotinylated serine can also be accomplished on the basis of characteristic masses. The FP-biotinylated tyrosine immonium ions at 708 and 691 amu provide a diagnostic sub-set of masses that identify FP-biotinylated tyrosine, while a fragment at 591 amu is characteristic of FP-biotinylated serine [6]. This array of characteristic masses makes FP-biotin very useful in the discovery of unknown proteins that are susceptible to labeling by OP.

### 3.6. Illustration of CID fragmentation for OP-labeled peptides

Figs. 3–8 show representative MSMS fragmentation spectra for peptides containing OP-labeled tyrosine. There is a spectrum for each of the six OP that were used in these studies. Fragmentation spectra from other OP-labeled, tyrosine-containing peptides can be found in the literature [6–9,21].

Fig. 3 illustrates the CID fragmentation of a soman-labeled peptide. This peptide is GYY\*AVAVVK from mouse transferrin, which is labeled on the second tyrosine from the N-terminus. The parent ion was doubly-charged with an  $m/z$  of 566.5 that includes an added mass of 162 amu from soman (O-pinacolyl methylphosphonate). Fragment y9 is consistent with the singly-charged parent ion less the mass of the pinacolyl side-chain (84 amu). This neutral loss leaves a methylphosphonate moiety attached to the peptide fragment (78 amu). The doubly-charged methylphosphonate parent ion was found at 524.2 amu. No fragment mass that included the O-pinacolyl methylphosphonate was detected, reflecting the extreme ease with which the pinacolyl group is eliminated under CID conditions. Fragments y1–y9 represent the entire y-ion series, wanting only y8. Fragments y7 and y9 include the mass for the methylphosphonate as expected. The mass difference of 241.1 amu between y6 and y7 is consistent with tyrosine plus methylphosphonate (163.1 + 78 amu). A b-ion series from b3 to b7 is also present. The b3 mass, at 461.9 amu, and all subsequent b-ion masses include the mass of methylphosphonate. A tyrosine–glycine immonium ion at 193.0 amu does not include the methylphosphonate mass, indicating that the first tyrosine from the N-terminal is not labeled. This observation together with the fact that the b3-ion includes the methylphosphonate places the soman label on the second tyrosine from the N-terminal. The characteristic tyrosine methylphosphonate immonium ion appears at 214.1 amu, confirming the presence of soman on the original peptide.

Fig. 4 illustrates the CID fragmentation of an FP-biotin labeled peptide. This peptide is AY\*LEECPATLR from human alpha 2 glycoprotein 1, zinc, which is labeled on the second residue from the N-terminus. The parent ion is doubly-charged with an  $m/z$  of 1012.7 that includes the 572 amu added mass from FP-biotin (10-(ethoxyphosphinyl)-N-(biotinamidopentyl) decanamide minus a

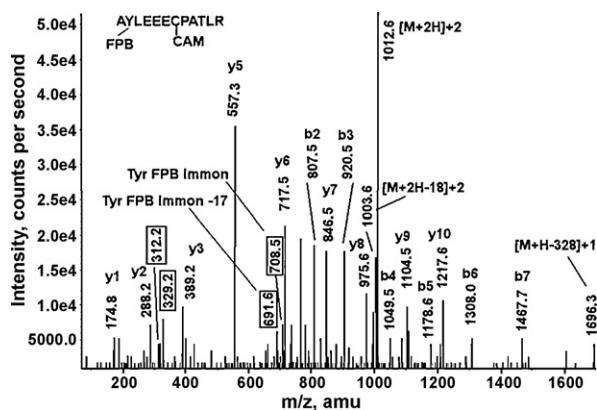


**Fig. 4.** A CID fragmentation spectrum of the FP-biotin labeled human alpha 2 glycoprotein 1, zinc tryptic peptide AY\*LEECPATLR. The 312.2 and 329.2 values enclosed in boxes are fragments of FP-biotin. The 708.5 and 691.6 values enclosed in boxes are the masses of the FP-biotinylated tyrosine immonium ion and of the FP-biotinylated tyrosine immonium ion minus  $\text{NH}_3$  respectively, the characteristic fragments for FP-biotin labeled tyrosine. CAM indicates that the cysteine is carbamidomethylated. The doubly-charged parent ion at 1012.7  $m/z$  includes 572 amu from FP-biotin and 57 amu from iodoacetamide. Loss of water from the parent ion results in a mass at 1003.6  $m/z$ . Neutral loss of a 328 amu portion of FP-biotin results in the 1696.3 amu fragment.

proton) and a carbamidomethyl modification on cysteine (57 amu, due to alkylation by iodoacetamide). Another doubly-charged ion at 1003.6 amu is consistent with the parent ion minus water. A fragment at 1696.3 amu represents the neutral loss of a 328 amu portion of FP-biotin from the parent ion. A y-ion series from y1 to y10 is observed. The masses of all of these fragments fit the unlabeled sequence. A b-ion series from b2 to b7 is also observed. The b2 mass (807.5 amu) is consistent with the presence of alanine, tyrosine and the FP-biotin label ( $164 + 71 + 572 = 807$  amu). Successive b-ion masses all include the mass of the FP-biotin label. Carbamidomethyl Cys (CAM; cysteine plus 57 amu, the result of alkylation of reduced cysteine with iodoacetamide) appears in both the y6 and y7 ions. Characteristic fragments of FP-biotin appear at 312.2 and 329.2 amu, while immonium ions for tyrosine FP-biotin and tyrosine FP-biotin minus amine appear at 708.5 and 691.6 amu, respectively. These are four of the most commonly observed characteristic ions from FP-biotin labeled, tyrosine-containing peptides.

Fig. 5 illustrates the CID fragmentation of a chlorpyrifos-oxon labeled peptide. This peptide is Y\*LDGLTAER from human keratin 2, which is labeled on the N-terminal residue. The parent ion is doubly-charged with an  $m/z$  of 587.3 that includes the 136 amu added mass from CPO (*O,O*-diethylphosphate). The 587.3  $m/z$  ion is not seen in MSMS spectrum. However it was present in the MS spectrum (data not shown). Its absence from the MSMS spectrum indicates that an excessive amount of collision energy was requested by the information directed acquisition algorithm that controlled data acquisition. A y-ion series starts from 175.0 amu for y1 and ends at 874.1 amu for y8. Addition of 299 amu to y8, (*O,O*-diethylphosphate-labeled Tyr,  $163 + 136 = 299$  amu), yields a mass of 1173.1 amu, which is equal to the theoretical mass for the singly-charged parent ion mass ( $1173.6 = 587.3 \times 2 - 1$ ). This indicates the presence of the label on the N-terminus. A mass at 413.0 amu is consistent with the *O,O*-diethylphosphate-labeled tyrosine plus leucine, i.e. the b2-ion ( $164 + 136 + 113 = 413$  amu), which confirms labeling of the N-terminal tyrosine. A strong signal at 385.1 amu corresponds to the labeled a2-ion. Characteristic fragments at 271.9, 244.0 and 215.8 amu are consistent with the *O,O*-diethylphosphate-labeled tyrosine immonium ion, the *O*-ethyl phosphate-labeled tyrosine immonium ion, and the tyrosine phosphate immonium ion, respectively. These are the most commonly observed characteristic ions derived from *O,O*-diethylphosphate-labeled, tyrosine-containing peptides and their

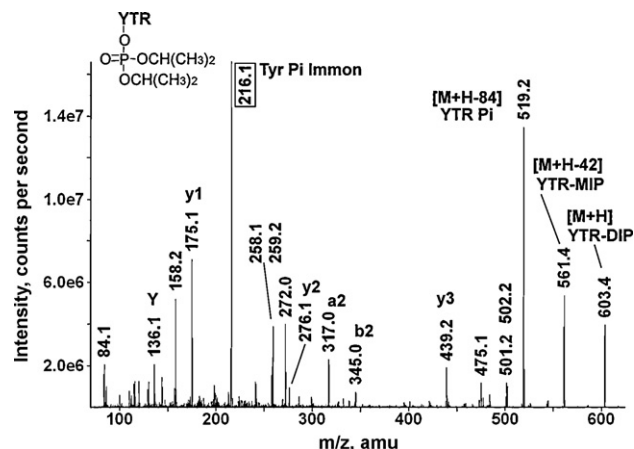


Fig. 6. A CID mass spectrum of the DFP-labeled bovine serum albumin tryptic peptide Y\*TR. The 216.1 amu value enclosed in the box is the mass of the phosphotyrosine immonium ion. The singly-charged parent ion at 603.4  $m/z$  includes 164 amu from DFP. Loss of one isopropylene yields the mass at 561.4 amu. Loss of both isopropylens yields the mass at 519.2 amu. The tyrosine immonium ion, designated Y, has a mass of 136.1 amu.

presence fully establishes the existence of a labeled tyrosine in this peptide.

Fig. 6 illustrates the CID fragmentation of a diisopropylfluorophosphate-labeled peptide. This peptide is Y\*TR from bovine serum albumin, which is labeled on the N-terminal residue. The parent ion is singly-charged with an  $m/z$  of 603.4 that includes the 164 amu added mass from DFP (*O,O*-diisopropylphosphate). Loss of isopropylene (42 amu) yields the 561.4 amu peak, and subsequent loss of a second isopropylene yields the more intense peak at 519.2 amu, which is consistent with YTR-phosphate. These neutral losses are characteristic of a diisopropylphosphate-labeled tyrosine-containing peptide. The relatively large intensities of these masses illustrate the ease with which the isopropylene is eliminated from diisopropylphosphate under CID conditions. The mass difference between 519.2 and 276.1 amu (y2) is consistent with loss of Tyr-phosphate, indicating that tyrosine was the labeled residue. Loss of 80 amu from 519.2 yields the y3 peak at 439.2 amu, which further supports labeling of the tyrosine. A complete y-ion series without phosphate is present. B2 and a2 ions that retain phosphate are seen at 345.0 and 317.0 amu, respectively. A characteristic ion at 216.1 amu, consistent with Tyr-phosphate is one of the most commonly observed characteristic ions derived from *O,O*-diisopropylphosphate-labeled, tyrosine-containing peptides. Its presence is another strong indication of the presence of an *O,O*-diisopropylphosphate labeled tyrosine in the peptide.

Fig. 7 illustrates the CID fragmentation of a dichlorvos-labeled peptide. This peptide is SY\*SM, a synthetic peptide, which is labeled on the tyrosine. The parent ion is singly-charged with a mass of 595.0 amu that includes the 108 amu added mass from dichlorvos (*O,O*-dimethylphosphate). Complete y-ion and b-ion series are present. The mass difference between y2 (237.4 amu) and y3 (507.8 amu) is 271 amu, which is consistent with the presence of *O,O*-dimethylphosphate labeled tyrosine ( $163 + 108 = 271$  amu), indicating that tyrosine is the labeled residue. The mass for the b2-ion (359.4 amu) is consistent with the presence of serine (N-terminal of a b-series) plus tyrosine-*O,O*-dimethylphosphate ( $88 + 163 + 108 = 359$  amu), confirming that the label is on tyrosine. The majority of the remaining masses could be attributed to loss of water, amine or carbon monoxide from the fragments already described. A characteristic ion at 244.3 amu is consistent with the tyrosine-*O,O*-dimethylphosphate immonium ion. There is no

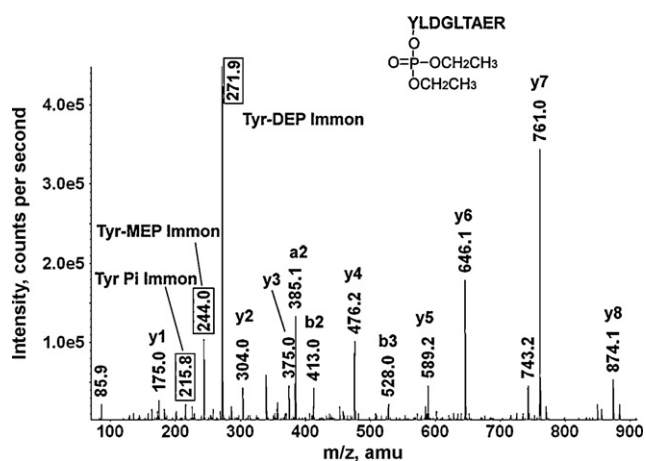
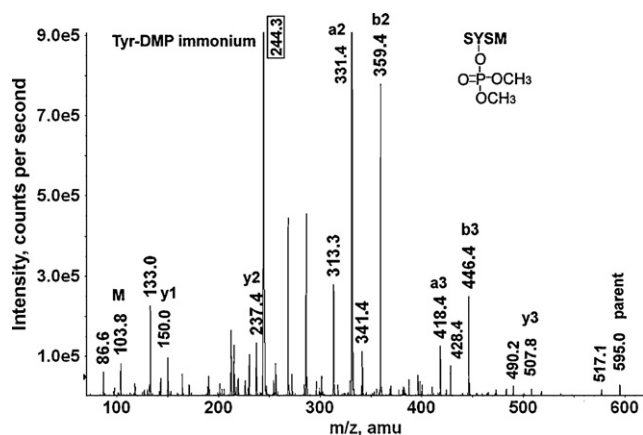


Fig. 5. A CID mass spectrum of the CPO-labeled human keratin 2 tryptic peptide Y\*LDGLTAER. The values enclosed in boxes are the masses of the characteristic fragments for CPO-labeled tyrosine: diethoxyphospho-tyrosine immonium ion at 271.9, monoethoxyphospho-tyrosine immonium ion at 244.0, and phosphotyrosine immonium ion at 215.8 amu. The doubly-charged parent ion at 587.3  $m/z$  includes 136 amu from chlorpyrifos-oxon.



**Fig. 7.** A CID mass spectrum of the dichlorvos-labeled synthetic tryptic peptide SY\*SM. The 244.3 value enclosed in the box is the mass of the dimethoxyphosphotyrosine immonium ion, the characteristic fragment for dichlorvos-labeled tyrosine. The singly-charged parent ion with a mass of 595.0 amu includes 108 amu from dichlorvos. The mass at 103.8 amu is the immonium ion of methionine.

evidence for release of methyl from the side-chain of the *O,O*-dimethylphosphate.

Fig. 8 illustrates the CID fragmentation of a sarin-labeled peptide. This peptide is KPVDQY\*EDCYLAR from mouse transferrin, which is labeled on the sixth residue from the N-terminus. The parent ion is triply-charged with an *m/z* of 592.0 that includes the 120 amu added mass from sarin (*O*-isopropyl methylphosphonate) and a carbamidomethyl modification on cysteine (57 amu). The 592.0 amu mass appeared in the MS spectrum (data not shown) but not in the MSMS spectrum. Its absence from the MSMS spectrum indicates that an excessive amount of collision energy was used during MSMS data acquisition. A partial *y*-ion sequence from *y*1 to *y*6 includes one unlabeled tyrosine (*y*4); the mass difference between *y*3 and *y*4 is 163 (522.1–359.6). The *b*3 ion and its dehydration product are visible at 325.6 and 307.7 amu, respectively. There is no evidence for labeling of the lysine at *b*1. Having thus

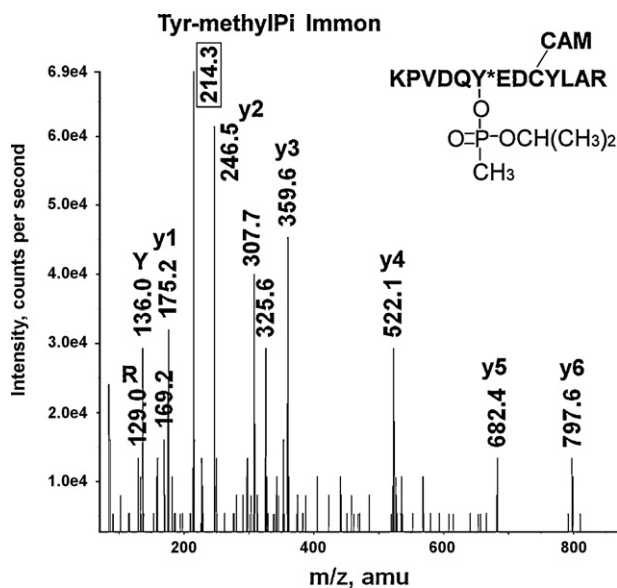


**Fig. 8.** A CID mass spectrum of the sarin-labeled mouse transferrin tryptic peptide KPVDQY\*EDCYLAR. The 214.3 value enclosed in the box is the mass of the methylphosphotyrosine immonium ion, the characteristic fragment for sarin-labeled tyrosine. CAM indicates that the cysteine is carbamidomethylated. The triply-charged parent ion with 592.0 *m/z* includes 120 amu from sarin and 57 amu from iodoacetamide. Immonium ions for tyrosine at 136.0 and for arginine at 129.0 are indicated as Y and R.

eliminated the lysine at *b*1 and the tyrosine at *y*4, the remaining tyrosine in the sequence (*y*8) has been assigned as the labeled residue; no other likely candidates exist in this peptide. The mass at 214.3 amu is consistent with the tyrosine-methylphosphonate immonium ion, which is a characteristic fragment for sarin labeled tyrosine. Absence of the isopropyl group from this characteristic fragment reaffirms the relative lability of the *O*-isopropyl moiety to fragmentation under CID conditions in the mass spectrometer.

### 3.7. Use of characteristic ions to detect OP-tyrosine adducts in unknown samples

Characteristic ions are valuable tools for finding labeled peptides in an unknown sample, especially for those labels that yield more than one characteristic ion. The most productive strategy, in our hands, has been extracted ion chromatographic analysis of MSMS data performed after acquisition of the data. There are two major advantages to this approach. First, post-acquisition analysis allows data to be taken using the trapping function of the QTrap mass spectrometer. This generally improves signal detection by 10-fold over acquisition methods that are restricted to the quadrupole mode. Second, the extracted ion algorithm in the QTrap software (Analyst) will generate separate extracted ion chromatograms for multiple ions, simultaneously. When overlaid, these chromatograms accent those MSMS spectra which include multiple characteristic ion masses, making data analysis more efficient. Once a candidate peptide has been identified, it is necessary to validate the identification by assigning the masses in the MSMS spectrum in order to determine the peptide sequence, to establish that the ions that appear to be characteristic are not part of the sequence, to locate a gap in the sequence that corresponds to a labeled amino acid, and to establish that the parent ion mass is equal to the mass of the peptide plus the mass of the label. Use of precursor ion scanning to look for peptides that generate characteristic fragments is a theoretically viable alternative to extracted ion chromatography. However, precursor ion scanning is a quadrupole function and is restricted to monitoring a single characteristic fragment per run. As such, it is less sensitive and less efficient.

### 3.8. OP-reactivity of tyrosine

Reaction of OP with tyrosine does not appear to be as specific as reaction of OP with the active site serine of the serine esterases. No consensus sequence around the labeled tyrosine was observed. Often, we were able to find multiple reactive tyrosines on a single protein. Sometimes we found more than one reactive tyrosine on a single peptide (see Table 1). Reactive tyrosines were typically on the surface of the protein, however not all surface tyrosines were reactive.

Of those tyrosines on a given protein that were reactive, one was generally much more reactive than the others. For example, five tyrosines from human serum albumin were found to react when plasma was treated with 200  $\mu$ M FP-biotin at 37 °C for 48 h. However, only two labeled peptides, Y\*TK and HPY\*FYAPELFFAK, were detected when 100  $\mu$ M FP-biotin was incubated with 15  $\mu$ M albumin at 22 °C and pH 8 for 2 h. Fifty-two percent of the YTK peptide was labeled while only 10% of the HPY\*FYAPELFFAK peptide was labeled. Thus Y\*TK was the most reactive peptide on human serum albumin [21]. Support for this assignment comes from the observation that the Y\*TR peptide from bovine serum albumin was the only labeled peptide detected after reaction of equimolar amounts of protein and FP-biotin (137  $\mu$ M each, reacted at 37 °C and pH 8.6 for 24 h) [6].

Bovine alpha tubulin provides another example of selective reaction. Out of nine peptides that were labeled by 0.5 mM CPO (pH 8.3 for 24 h at 37 °C) only one, TGT\*YR, was labeled by 0.01 mM CPO

under the same conditions [23]. Bovine actin provides a third example. Out of five peptides found on incubation with 240  $\mu$ M CPO, only one, GY\*SFVTTAER, gave good signals with 48  $\mu$ M CPO.

Such selective reaction strongly suggests that the reactive tyrosine is somehow activated. How might such activation be manifested?

### 3.9. Activation of tyrosine in general

Reaction of tyrosine with OP would be expected to involve nucleophilic attack by the phenolate anion of tyrosine on the phosphorus of the OP [30]. The  $pK_a$  of the tyrosine phenolate is 10.1 [31]. Thus, at pH 8 only 1% of the typical tyrosine would be ionized. Activation could be manifested if the  $pK_a$  value of selected tyrosines were lowered, thereby increasing the fraction of phenolate at pH 8.

Perturbation of  $pK_a$  values can be accomplished by stabilizing or destabilizing the ionized component. A classical example is the increase in  $pK_a$  for ionization of the second acidic group of a dicarboxylic acid [32,33]. The presence of the negative charge on the first carboxylic acid causes an unfavorable electrostatic interaction for the ionization of the second, thereby increasing its  $pK_a$ . Westheimer and Kirkwood calculated that a 0.8 unit difference between  $pK_a$  values for carboxyls of succinic acid corresponded to a distance between carboxylates of 5–6 Å [33].

By analogy with the carboxylate situation, the presence of a positive charge at a moderate distance from a developing anion could stabilize the anion and lower its  $pK_a$ . Or, hydrogen-bond donors could stabilize a developing negative charge, thereby lowering the  $pK_a$ .

This concept has been extended to enzymes. Shafer and coworkers demonstrated that when the active site cysteine of papain (Cys25) is deprotonated, the  $pK_a$  of His159 increases by 4.2 units [34,35] with a comparable decrease in the  $pK_a$  of Cys 25 [36]. They attributed this change to through-space, charge–charge interactions between Cys25 and His159 [36]. They argued that charge–charge interactions do not cause the decrease in nucleophilic reactivity that is seen when  $pK_a$  values are perturbed by charge–dipole interactions [36]. The consequence of this change in  $pK_a$  was an increase in the fraction of nucleophilic cysteine present in the active site. The 4.2 pH unit change in  $pK_a$  corresponded to a distance of 3.4 Å between the cysteine thiol and N3 of the histidine [37].

This sort of  $pK_a$  change is not limited to cysteines. Tyrosines with abnormally low  $pK_a$  values are involved directly or indirectly in the catalytic activity of a number of enzymes including glutathione S-transferase [38], asparaginase [39], beta-lactamases [40], and albumin [41]. A lysine at the active center of acetoacetate decarboxylase was implicated in a 3.7 unit decrease in the  $pK_a$  of a phenolic reporter group [42].

### 3.10. Activation of OP reactive tyrosines

In an effort to determine whether charge–charge interactions might be involved in the activation of the tyrosines that react with OP in our studies, we examined the x-ray structures for proteins on which OP-reactive tyrosines were found (Table 4). Protein structure files from the Protein Data Bank maintained by the Research Collaboratory for Structural Bioinformatics were examined using PyMOL (version 0.99rc6, DeLano, W.L. The PyMOL Molecular Graphics System, 2002, <http://www.pymol.org>). Forty-one tyrosines were evaluated. Two factors were considered: accessibility of the phenolic hydroxyl to solvent and the proximity of the tyrosine hydroxyl to positively charged residues. Solvent accessibility was evaluated visually using the surface feature of PyMOL. The surface that was displayed was defined by the Van der Waals surfaces of water atoms when in contact with the protein. If the phenolic hydroxyl was

visible on the surface, it was considered to be solvent accessible. Positively charged groups were considered to be sufficiently close to the tyrosine hydroxyl to affect ion-pairing if they were within 6 Å. Choice of 6 Å was based on the calculations by Westheimer and Kirkwood which showed effects on the  $pK_a$  of nearly 1 pK unit at this distance [33].

Twenty-three of the 41 tyrosines (56%) were both solvent exposed and within 6 Å of a positively charged residue (Table 4). Ten of the instances in which the distance was greater than 6 Å came from bovine tubulin (alpha and beta). If tubulin is excluded from the analysis (16 tyrosines total), then 18 of the remaining 25 tyrosines (72%) were within ion-pairing distance of a positively charged residue. Exclusion of tubulin might be justified in light of the fact that the crystal structure was of the isolated alpha/beta dimer, whereas in solution tubulin is normally in some polymeric form (e.g., protofilaments or microtubules). charge–charge interactions between residues on adjacent dimers might occur under those circumstances.

Of the seven non-tubulin tyrosines that were not within 6 Å of a positively charged residue, only two (that from pepsin and that from adenine nucleotide translocase) showed more than 10 Å of separation (Table 4). There is reason to believe that these seven residues might still enter into charge–charge interactions if the proteins were not constrained by the crystal packing. That reasoning is based on the fact that, for proteins that had more than one identical subunit in the crystal, the distances between tyrosines and their charged partners varied by up to 1 Å. Examples of this can be found in the measurements given in Table 4 for the human serum albumin dimer, the three beta subunits in bovine ATP synthase, the three subunits of human apolipoprotein A-I, and the dimer of human kinesin 3C. This argument is consistent with the time-honored understanding that proteins in solution undergo substantial conformational change.

Though the evidence in favor of charge–charge interaction lowering the  $pK_a$  of the reactive tyrosines in order to activate them is compelling, it would be naïve to suggest that other factors may not play a role. For example, several instances where a non-reactive tyrosine was found to be 3–6 Å from a positively-charged residue are given in Table 4 (see human serum albumin and human  $\alpha$ 2-glycoprotein, zinc). That these residues are not reactive can be ascribed to steric constraints. An analogous situation exists for 3-nitrotyrosine, which has a  $pK_a$  of 6.5. Based on its  $pK_a$ , 3-nitrotyrosine was expected to react with OP. However, nitration of human serum albumin and the synthetic peptide RYGRK with peroxyntirite resulted in a preparation that showed no reactivity toward OP (PM, unpublished observations). Absence of reactivity might again be due to steric interference, this time from the vicinal nitro group.

In summary, the above correlations strongly suggest that most, if not all, OP-reactive tyrosines are activated by the nearby presence of a positively-charged residue that is capable of forming a charge–charge ion-pair with the phenolate oxygen of the tyrosine, thereby lowering the tyrosine  $pK_a$ , and enhancing its nucleophilic character for reaction with the OP.

### 3.11. Comparison of OP-tyrosine adducts with OP-serine adducts

It is well accepted that activated serine residues, such as those found in the active sites of serine esterases and proteases, react with organophosphorus agents. Recently, it has become apparent that selected tyrosine residues will also react with organophosphorus agents. Not surprisingly, the physical properties of these two classes of organophosphorus adducts are distinct.

For example, serine adducts readily undergo beta elimination (McLafferty rearrangement in the mass spectrometer) to release the organophosphorus moiety, leaving behind a dehydroalanine

**Table 4**

Ion-pairing analysis of protein crystal structures: evaluation of interactions between OP-labeled tyrosines and arginine, lysine and/or histidine residues.

Peptide <sup>a</sup>	Labeled residue <sup>b</sup>	Exposed/buried <sup>c</sup>	Ion-pair residue <sup>b</sup>	Distance <sup>d</sup> (Å)
Human serum albumin [PDB file 1BM0, 2.50 Å resolution]				
There are two monomers in the unit cell for this human serum albumin structure. Measurements are given for both the alpha and beta monomers.				
Y*TK (A subunit)	Y411	Exposed	K414 R410	5.26 4.53
Y*TK (B subunit)	Y411	Exposed	K414 R410	5.47 6.56
HPY*FYAPELLFFAK (A subunit)	Y148	Exposed	K106 R197	5.27 3.58
HPY*FYAPELLFFAK (B subunit)	Y148	Exposed	K106 R197	5.65 4.10
HPYFY*APPELLFFAK (A subunit)	Y150	Exposed	H242-Nε2 R257	3.81 3.75
HPYFY*APPELLFFAK (B subunit)	Y150	Exposed	H242-Nε2 R257	3.44 4.07
MPCAEDDY*LSVVLNQLCVLHEK (A subunit)	Y452	Exposed	K436 K432	4.47 5.69
MPCAEDDY*LSVVLNQLCVLHEK (B subunit)	Y452	Exposed	K436 K432	4.80 6.15
QNCELFEQLGEY*K (A subunit)	Y401	Exposed	K525	4.84
QNCELFEQLGEY*K (B subunit)	Y401	Exposed	K525	3.67
Y*KAAFTCCQAADK (A subunit)	Y161	Exposed	R117	8.46
Y*LYEIAR (A subunit)	Y138	Exposed	R160 R117	7.89 10.06
Note that Y140 was exposed to solvent and was 2.69 Å from a potential ion-pairing partner in R144, but this residue has not been found to be labeled by OP.				
Human Transferrin [PDB file 2HAV, 2.70 Å resolution]				
This is the structure for apo-transferrin. Both apo- and holo- transferrin react with OP at the same sites, and there is no effect of OP labeling on the affinity of apo-transferrin for iron.				
KPVDEY*K	Y238	Exposed	K239 H207-Nε2	4.29 4.46
KPVEEY*ANCHLAR	Y574	Exposed	H535-Nε2	4.36
Human α2-glycoprotein, zinc [PDB file 1T7V, 1.95 Å resolution]				
AY*LEECPATLR	Y161	Exposed	R73	5.03
YY*YDGKDYIEFNK	Y118	Exposed	K116 R100	4.25 5.01
WEAEPV*VQR	Y154	Exposed	R157	5.58
Note that a number of other tyrosines were within ion-pairing distance of positively charged residues, were exposed to solvent, but were not labeled by OP: Y119 was 3.23 Å from H95-Nδ1; Y211 was 4.97 Å from R183; and Y258 was 5.01 Å from R221.				
Bovine Tubulin alpha [PDB file 1JFF-with taxol, 3.5 angstrom resolution]				
IHFPLATY*APVISAER	Y272	Exposed	R320	4.73
EDAANNY*AR	Y103	Exposed	H107-Nε2 H192-Nδ1	4.20 5.13
GHY*TIGK	Y108	Exposed	H107-Nε2	4.67
FDLMY*AK	Y399	Exposed	R402	2.83
TGTY*R	Y83	Exposed	R229	7.47
AFVHWY*VGEGMEEGFSEAR	Y408	Buried	H406-Nε2	11.09
FDGALNVDLTFQTNLVPY*PR	Y262	Exposed	H266-Nδ1 R264	8.52 13.27
VGINY*QPPTVVPGGDLAK	Y357	Exposed	R373 K370	12.75 13.04
LSVDY*GK	Y161	Exposed	R123	7.19
Bovine Tubulin beta [PDB file 1JFF (with taxol), 3.5 angstrom resolution]				
GHY*TEGAELVDSVLDVVR	Y108	Exposed	H107-Nδ1	4.72
NSSY*FVEWIPNNK	Y342	Exposed	R308	4.91
EEY*PDR	Y161	Exposed	R123	6.47
Y*VPR	Y61	Exposed	H28-Nδ1 H37-Nδ1 K60 R64	10.57 10.73 12.92 12.18

Table 4 (Continued)

Peptide <sup>a</sup>	Labeled residue <sup>b</sup>	Exposed/buried <sup>c</sup>	Ion-pair residue <sup>b</sup>	Distance <sup>d</sup> (Å)
GSQQY*R	Y283	Exposed	K218 K372	11.34 15.62
Y*LTVAEFR	Y312	Exposed	R308 R311	11.37 11.47
INVYY*NEATGGK	Y53	Buried	H28-Nε2	6.25
Human Kinesin 3C motor domain [PDB file 3B6U, 1.80 angstrom resolution]				
There are two monomers in the unit cell for this human kinesin structure. Measurements are given for both the alpha and beta monomers.				
ASY*LEIYQEEIR (A subunit)	Y144	Exposed	R201	4.83
ASY*LEIYQEEIR (B subunit)	Y144	Exposed	R201	5.07
Bovine Actin alpha from skeletal muscle in complex with DNAase I [PDB file 2A42, 1.85 Å resolution]				
DSY*VGDEAQS	Y53	Exposed	K50 K61	4.81 5.29
IWHHTFY*NELR	Y91	Exposed	H87-Nε2	5.06
DLTDY*LMK	Y188	Exposed	R256	4.32
GY*SFVTTAER	Y198	Exposed	R196	8.09
QEY*DEAGPSIVHR	Y362	Exposed	K359 K118	6.66 9.00
SY*ELPDGQVITIGNER	Y240	Exposed	K215	6.49
Porcine Pepsin [PDB file 4PEP, 1.80 Å resolution]				
QYY*TVFDDR	Y310	Buried	N-Terminal	10.93
Bovine chymotrypsinogen [PDB file 1EX3, 3.0 Å resolution]				
Y*TNANTPDR	Y146	Exposed	R145	5.29
Bovine ATP synthase beta [PDB file 2CK3, 1.95 Å resolution]				
No crystal structure for mouse ATP synthase could be found. However, the sequence of the beta subunit of bovine ATP synthase is 98.2% identical to that of the mouse beta subunit. Therefore it is reasonable to use the bovine coordinates to represent the mouse protein.				
ATP synthase beta is a component of mitochondrial membrane ATP synthase. The complete structure of the ATP synthase consists of two components, F(1) and F(0). F(0) is composed of 3 subunits (A, B, and C). F(1) is composed of 5 subunits (α, β, γ, δ, and ε in a stoichiometry of 3:3:1:1:1). The three β-subunits are designated D, E and F in the crystal structure.				
ILQDY*K (D subunit)	Y381	Exposed (barely)	R412d R408d	6.52 2.96
ILQDY*K (E subunit)	Y381	Exposed	R412e R408e	5.67 2.99
ILQDY*K (F subunit)	Y381	Exposed	R412f R408f	6.56 3.44
Mouse Adenine Nucleotide Translocase I [PDB file 2C3E, 2.80 Å resolution]				
No crystal structure for mouse Adenine Nucleotide Translocase I could be found. However, the sequence of bovine adenine nucleotide translocase I is 94.6% identical to that of the mouse. Therefore it is reasonable to use the bovine coordinates to represent the mouse protein.				
Y*FPTQALNFAFK	Y80	Exposed	K22 R78	10.38 11.17
Human apolipoprotein A-I [PDB file 2A01, 2.40 Å resolution]				
There are three monomers in the unit cell for this human apolipoprotein A-I structure.				
DY*VSQFEGSALGK (A subunit)	Y29	Exposed	K59	4.63
DY*VSQFEGSALGK (B subunit)	Y29	Exposed (barely)	K59	4.82
DY*VSQFEGSALGK (C subunit)	Y29	Buried	K59	4.75

<sup>a</sup> The asterisk (\*) indicates the labeled tyrosine.

<sup>b</sup> Numbering is for the mature sequence.

<sup>c</sup> Exposed is defined as the phenolic oxygen of the tyrosine being visible when the surface option for the atom display is chosen in PyMOL. Buried is defined as the phenolic oxygen of the tyrosine not being visible.

<sup>d</sup> Distance is defined as the space between the phenolic oxygen of the tyrosine and its ion-pair. For arginine-tyrosine ion-pairs, the shortest distance between the phenolate oxygen and the guanidinium group is taken. For histidine-tyrosine ion-pairs, the distance between the phenolate oxygen and the nearest ring nitrogen is taken.

in place of the original serine. We have found no evidence that OP-tyrosine adducts release the organophosphoryl moiety. As a consequence of the facile elimination of OP from serine adducts under CID conditions in the mass spectrometer, there are no characteristic fragments in the mass spectra of most OP-labeled serine containing peptides. The presence of the OP on the peptide is indicated by the mass of the parent ion and the presence of dehydroalanine in the fragmentation sequence. The relative stability of OP-tyrosine adducts during CID yields an abundance of characteristic fragments

that are diagnostic for the nature of the label. These fragments in combination with the parent ion mass and the characteristic steps in the masses that define the peptide sequence provide strong evidence for the presence and nature of OP-labeled tyrosines in selected peptides.

The organophosphonate FP-biotin is unique among the OP agents in that CID fragmentation in the mass spectrometer yields characteristic masses for both labeled serine and labeled tyrosine. FP-biotinylated tyrosine yields fragments at 227, 312 and

329 amu that correspond to portions of the FP-biotin label, as well as fragments at 708 and 691 amu that correspond to the FP-biotinylated tyrosine immonium ion and its deaminated derivative. FP-biotinylated serine yields the 227, 312 and 329 amu fragments, and in addition a fragment at 591 amu that corresponds to the beta eliminated form of FP-biotin.

Another useful difference in the properties of these two OP-labeled residues concerns the process of aging. Aging is a secondary reaction of OP-labeled serine that is catalyzed by active site residues in certain serine hydrolases such as cholinesterases and serine proteases. Aging results in the hydrolysis of one of the alkoxy ligands to the phosphorus, yielding the corresponding alcohol and a hydroxyl ligand on the phosphorus [43]. OP-labeled tyrosines do not undergo this secondary reaction. This difference becomes noteworthy when trying to diagnose the type of OP agent that has reacted with a sample. For example, sarin-labeled butyrylcholinesterase and soman-labeled butyrylcholinesterase both age to give the same product, methylphosphonate labeled serine [44]. Thus the parent ion masses for the aged active site peptide from samples that were exposed to either of these agents will be the same. In principle, detection of the unaged product is possible because aging of sarin on human BChE is reasonably slow ( $t_{1/2} = 6.4$  h). However, in order to take advantage of this difference, samples from exposed individuals must be taken within 24 h of exposure and aging arrested. On the other hand, since sarin-labeled albumin and soman-labeled albumin do not age, the parent ion masses for the labeled peptides are diagnostic for the agent that was involved in the initial exposure long after the time of exposure.

#### 4. Conclusion

The fragmentation patterns for OP-labeled tyrosine adducts described above should aid in the discovery of proteins and peptides labeled by OP. The presence of characteristic ion masses in the MSMS data provide assurance that a peptide is covalently modified on tyrosine by a particular OP.

These results illustrate the binding of OP to tyrosine on a variety of proteins. Tyrosine is a new target for OP binding, supplementing the traditional active site serine in serine esterases and proteases. As such, tyrosine constitutes a new binding motif for OP reactivity.

#### Acknowledgement

This work was supported by U.S. Army Medical Research and Materiel Command [W81XWH-07-2-0034 to OL]; National Institutes of Health [U01 NS058056 to OL, P30CA36727 to Eppley Cancer Center]; Direction Générale de l'Armement of the French Ministry of Defense [DGA grant 03co010-05/PEA01 08 7 to PM; DGA/PEA 08co501 to FN]; and Agence Nationale pour la Recherche [ANR-06-BLAN-0163 to FN]. Mass spectra were obtained with the support of the Mass Spectrometry and Proteomics core facility at the University of Nebraska Medical Center.

#### References

- [1] N.K. Schaffer, S.C. May Jr., W.H. Summerson, *J. Biol. Chem.* 206 (1954) 201.
- [2] A.R. Main, *Pharmacol. Ther.* 6 (1979) 579.
- [3] D.M. Maxwell, K.M. Brecht, I. Koplovitz, R.E. Sweeney, *Arch. Toxicol.* 80 (2006) 756.
- [4] M.A. Brown, K.A. Brix, *J. Appl. Toxicol.* 18 (1998) 393.
- [5] J.E. Casida, G.B. Quistad, *Chem. Res. Toxicol.* 17 (2004) 983.
- [6] L.M. Schopfer, M.M. Champion, N. Tamblin, C.M. Thompson, O. Lockridge, *Anal. Biochem.* 345 (2005) 122.
- [7] B. Li, L.M. Schopfer, S.H. Hinrichs, P. Masson, O. Lockridge, *Anal. Biochem.* 361 (2007) 263.
- [8] B. Li, F. Nachon, M.T. Froment, L. Verdier, J.C. Debouzy, B. Brasme, E. Gillon, L.M. Schopfer, O. Lockridge, P. Masson, *Chem. Res. Toxicol.* 21 (2008) 421.
- [9] H. Grigoryan, L.M. Schopfer, C.M. Thompson, A.V. Terry, P. Masson, O. Lockridge, *Chem. Biol. Interact.* 175 (2008) 180.
- [10] B. Li, L.M. Schopfer, H. Grigoryan, C.M. Thompson, S.H. Hinrichs, P. Masson, O. Lockridge, *Toxicol. Sci.* 107 (2009) 144.
- [11] R.M. Black, J.M. Harrison, R.W. Read, *Arch. Toxicol.* 73 (1999) 123.
- [12] E.S. Peeples, L.M. Schopfer, E.G. Duysen, R. Spaulding, T. Voelker, C.M. Thompson, O. Lockridge, *Toxicol. Sci.* 83 (2005) 303.
- [13] N.H. Williams, J.M. Harrison, R.W. Read, R.M. Black, *Arch. Toxicol.* 81 (2007) 627.
- [14] M.J. Huddleston, R.S. Annan, M.F. Bean, S.A. Carr, *J. Am. Soc. Mass Spectrom.* 4 (1993) 710.
- [15] C.W. Hung, A. Schlosser, J. Wei, W.D. Lehmann, *Anal. Bioanal. Chem.* 389 (2007) 1003.
- [16] R. Eichner, M. Kahn, *J. Cell Biol.* 110 (1990) 1149.
- [17] Y. Liu, M.P. Patricelli, B.F. Cravatt, *Proc. Natl. Acad. Sci. USA* 96 (1999) 14694.
- [18] D. Kidd, Y. Liu, B.F. Cravatt, *Biochemistry* 40 (2001) 4005.
- [19] H. Li, L. Schopfer, R. Spaulding, C.M. Thompson, O. Lockridge, *Chem. Biol. Interact.* 157–158 (2005) 383.
- [20] H. Grigoryan, B. Li, E.K. Anderson, W. Xue, F. Nachon, O. Lockridge, L.M. Schopfer, *Chem. Biol. Interact.* 180 (2009) 492.
- [21] S.J. Ding, J. Carr, J.E. Carlson, L. Tong, W. Xue, Y. Li, L.M. Schopfer, B. Li, F. Nachon, O. Asojo, C.M. Thompson, S.H. Hinrichs, P. Masson, O. Lockridge, *Chem. Res. Toxicol.* 21 (2008) 1787.
- [22] T. Murachi, T. Miyake, N. Yamasaki, *J. Biochem.* 68 (1970) 239.
- [23] H. Grigoryan, L.M. Schopfer, E.S. Peeples, E.G. Duysen, M. Grigoryan, C.M. Thompson, O. Lockridge, *Toxicol. Appl. Pharmacol.* in press (2009).
- [24] A. Tholey, J. Reed, W.D. Lehmann, *J. Mass Spectrom.* 34 (1999) 117.
- [25] F.W. McLafferty, *Anal. Chem.* 31 (1959) 82.
- [26] A.J. Bell, D. Despeyroux, J. Murrell, P. Watts, *Int. J. Mass Spectrom. Ion Process.* 165/166 (1997) 533.
- [27] P.A. D'Agostino, J.R. Hancock, C.L. Chenier, C.R. Lepage, *J. Chromatogr. A* 1110 (2006) 86.
- [28] H. Steen, J.A. Jebanathirajah, J. Rush, N. Morrice, M.W. Kirschner, *Mol. Cell Proteomics* 5 (2006) 172.
- [29] A. Beck, K. Moeschel, M. Deeg, H.U. Haring, W. Voelter, E.D. Schleicher, R. Lehmann, *J. Am. Soc. Mass Spectrom.* 14 (2003) 401.
- [30] S.J. Benkovic, K.J. Schray, in: P.D. Boyer (Ed.), *The Enzymes*, vol. 8, 1973, p. 201.
- [31] P. Ballinger, F.A. Long, *J. Am. Chem. Soc.* 82 (1960) 795.
- [32] J. Kirkwood, F.H. Westheimer, *J. Chem. Phys.* 6 (1938) 506.
- [33] F.H. Westheimer, J. Kirkwood, *J. Chem. Phys.* 6 (1938).
- [34] F.A. Johnson, S.D. Lewis, J.A. Shafer, *Biochemistry* 20 (1981) 52.
- [35] S.D. Lewis, F.A. Johnson, J.A. Shafer, *Biochemistry* 15 (1976) 5009.
- [36] D.D. Roberts, S.D. Lewis, D.P. Ballou, S.T. Olson, J.A. Shafer, *Biochemistry* 25 (1986) 5595.
- [37] J. Drenth, J.N. Jansonius, R. Koekoek, L.A. Sluyterman, B.G. Wolthers, *Philos. Trans. R. Soc. Lond. B. Biol. Sci.* 257 (1970) 231.
- [38] W.M. Atkins, R.W. Wang, A.W. Bird, D.J. Newton, A.Y. Lu, *J. Biol. Chem.* 268 (1993) 19188.
- [39] C. Derst, A. Wehner, V. Specht, K.H. Rohm, *Eur. J. Biochem.* 224 (1994) 533.
- [40] J. Lamotte-Brasseur, A. Dubus, R.C. Wade, *Proteins* 40 (2000) 23.
- [41] G.E. Means, H.L. Wu, *Arch. Biochem. Biophys.* 194 (1979) 526.
- [42] F.C. Kokesh, F.H. Westheimer, *J. Am. Chem. Soc.* 93 (1971) 7270.
- [43] C. Viragh, I.M. Kovach, L. Pannell, *Biochemistry* 38 (1999) 9557.
- [44] H. Li, L.M. Schopfer, F. Nachon, M.T. Froment, P. Masson, O. Lockridge, *Toxicol. Sci.* 100 (2007) 136.

# Methamidophos, dichlorvos, O-methoate and diazinon pesticides used in Turkey make a covalent bond with butyrylcholinesterase detected by mass spectrometry

Ozden Tacal<sup>a</sup> and Oksana Lockridge<sup>b\*</sup>

**ABSTRACT:** Organophosphorus pesticides used most commonly in Turkey include methamidophos, dichlorvos, O-methoate and diazinon. These toxic chemicals or their metabolites make a covalent bond with the active site serine of butyrylcholinesterase. Our goal was to identify the adducts that result from the reaction of human butyrylcholinesterase with these pesticides. Highly purified human butyrylcholinesterase was treated with a 20-fold molar excess of pesticide. The protein was denatured by boiling and digested with trypsin. MS and MSMS spectra of HPLC-purified peptides were acquired on a MALDI-TOF-TOF 4800 mass spectrometer. It was found that methamidophos added a mass of +93, consistent with addition of methoxy aminophosphate. A minor amount of adduct with an added mass of +109 was also found. Dichlorvos and O-methoate both made dimethoxyphosphate (+108) and monomethoxyphosphate adducts (+94). Diazinon gave a novel adduct with an added mass of +152 consistent with diethoxythiophosphate. Inhibition of enzyme activity in the presence of diazinon developed slowly (15 h), concomitant with isomerization of diazinon via a thiono-thiolo rearrangement. The isomer of diazinon yielded diethoxyphosphate and monoethoxyphosphate adducts with added masses of +136 and +108. MSMS spectra confirmed that each of the pesticides studied made a covalent bond with serine 198 of butyrylcholinesterase. These results can be used to identify the class of pesticides to which a patient was exposed. Copyright © 2010 John Wiley & Sons, Ltd.

**Keywords:** human butyrylcholinesterase; organophosphorus pesticides; mass spectrometry; methamidophos; diazinon; O-methoate; dichlorvos; thiono-thiolo

## INTRODUCTION

Turkey is a major producer and exporter of agricultural products. Pesticides are used in farms, greenhouses and grape vineyards. Pesticide consumption is lower than in European countries probably because of economic constraints. However, ignorance of protective cautions and use of prohibited pesticides cause health problems in Turkey. The Ministry of Agriculture provides financial support for certain pesticides, but since July 1999 the use of very poisonous types of pesticides has been limited. According to the 2008 annual report of the National Poison Center (Refik Saydam Hygiene Center), 8.34% of the 77988 people who were diagnosed as poisoned were poisoned by pesticides. Organophosphorus pesticide (OP) poisonings constituted 20.98% of all pesticide poisonings in Turkey (Ergonen *et al.*, 2005; Turgut *et al.*, 2009).

The OP pesticides most frequently used in Turkey are methamidophos (Tamaron), dichlorvos, O-methoate and diazinon (Ergonen *et al.*, 2005; Fig. 1). These toxic chemicals or their metabolites make a covalent bond with the active site serine of butyrylcholinesterase (BChE, EC 3.1.1.8), resulting in inhibition of BChE activity (Main, 1976; Whittaker, 1986). The inhibited butyrylcholinesterase in plasma serves as a biomarker of OP exposure (Altintop *et al.*, 2005; Yardan *et al.*, 2007; Yurumez *et al.*, 2007; Kavalci *et al.*, 2009).

In Turkey, exposure to OP pesticides is inferred by measuring BChE activity in plasma (Altintop *et al.*, 2005; Yardan *et al.*, 2007; Yurumez *et al.*, 2007; Kavalci *et al.*, 2009). A limitation of this method is that it does not identify the poison. A variety of agents inhibit BChE including the Alzheimer drugs tacrine and rivastigmine (Darvesh *et al.*, 2003), OP nerve agents (Fidder *et al.*, 2002; Nicolet *et al.*, 2003), carbamate pesticides (Li *et al.*, 2009), plant poisons such as physostigmine (eserine) from the Calabar bean (Easson and Stedman, 1936), a naturally occurring OP in the blue-green algae *Anabaena flos-aquea* (Mahmood and Carmichael, 1987; Matsunaga *et al.*, 1989) and OP pesticides. A method that can directly measure the OP-adducted form of the enzyme would distinguish between classes of poisons. Information of this type could be useful for identifying the poison, and for proving exposure.

\*Correspondence to: O. Lockridge, Epplly Institute, 985950 Nebraska Medical Center, Omaha, NE 68198-5950, USA.  
E-mail: olockrid@unmc.edu

<sup>a</sup>Department of Biochemistry, School of Pharmacy, University of Hacettepe 06100 Ankara, Turkey

<sup>b</sup>Epplly Institute, University of Nebraska Medical Center, Omaha, NE 68198, USA

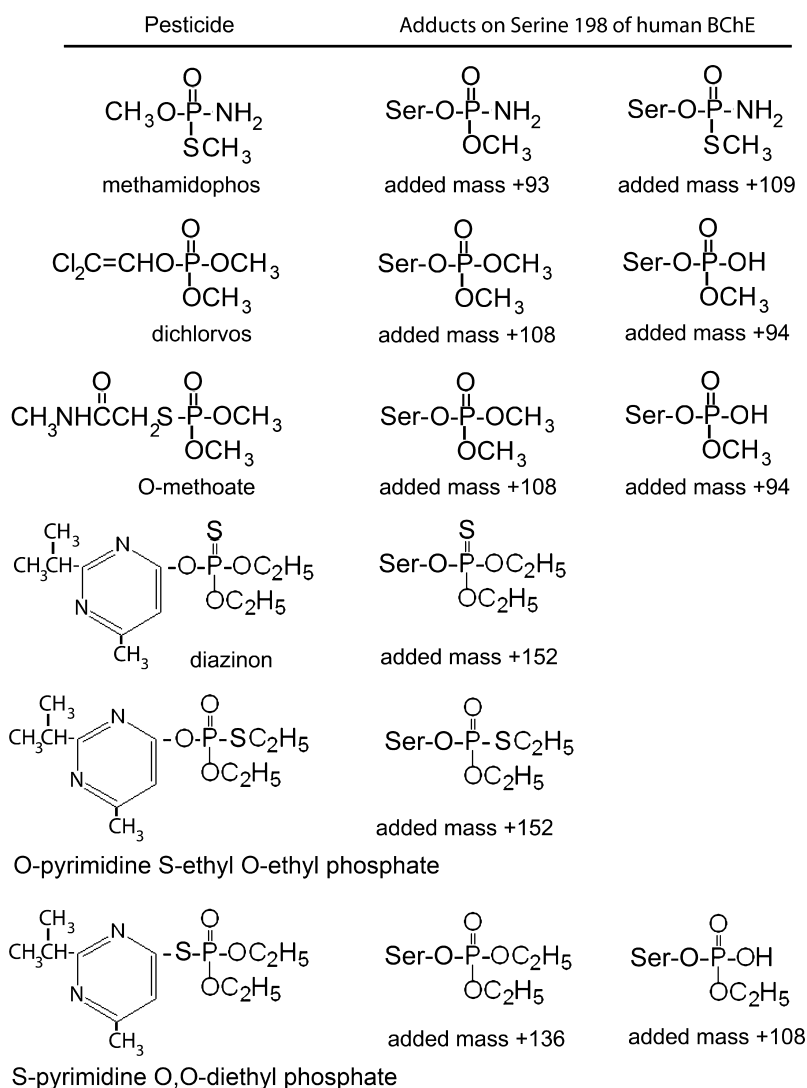


**Figure 1.** Structures of pesticides and the adducts formed by covalent binding to Serine 198 of human BChE. Isomerization of diazinon via a thiono-thiolo rearrangement occurred in solution. The unlabeled active site peptide of BChE (accession number gi:116353) produced by digestion with trypsin has a monoisotopic mass of 2928.5 amu.

## MATERIALS AND METHODS

### Materials

Seventy liters of outdated human plasma were obtained from the University of Nebraska Hospital blood bank. Human BChE was purified from the outdated plasma by ion exchange chromatography at pH 4, followed by procainamide affinity chromatography and ion exchange chromatography at pH 7.4 (Lockridge *et al.*, 2005). Purified BChE (54% pure) had an activity of 2620 U ml<sup>-1</sup> assayed with 1 mM butyrylthiocholine at pH 7.0 and 25 °C, and a BChE protein concentration of 3.64 mg ml<sup>-1</sup>. Butyrylthiocholine iodide and 5,5'-dithiobis(2-nitrobenzoic acid) were from Sigma-Aldrich (St Louis, MO, USA). Methamidophos 98.4% pure (PS-676), dichlorvos 98.0% pure (PS-89) and O-methoate 97.3% pure (PS-2017) were from ChemService (West Chester, PA, USA). Diazinon 96.7% pure (S-87-1185) was from Ciba Crop Protection (Greensboro, NC, USA). OP stock solutions (50 mM) were prepared in methanol or acetonitrile. Sequencing-grade modified porcine

trypsin (V5113) was from Promega (Madison, WI, USA).  $\alpha$ -Cyano-4-hydroxycinnamic acid (CHCA) was from Applied Biosystems (Foster City, CA, USA).

### Inhibition of BChE by OP

Highly purified human BChE (0.2 mg in 0.055 ml of 10 mM NH<sub>4</sub>HCO<sub>3</sub> pH 8.3; 42  $\mu$ M) was reacted with 1  $\mu$ l of 50 mM OP at 22 °C to give a 20-fold molar excess of OP over BChE active sites. The reaction was stopped by heating the sample in a boiling water bath.

The BChE concentration in human plasma is 0.050  $\mu$ M. Humans are unlikely to survive a pesticide dose 20-fold higher than the plasma BChE concentration. Our studies treated purified human BChE with a 20-fold molar excess of pesticide to achieve maximum labeling of BChE. The purpose of our study is to determine the mass of the adducts on human butyrylcholinesterase after butyrylcholinesterase has been modified by organophos-

phorus pesticides. The adduct mass must be known before one can set up a multiple reaction monitoring experiment in the mass spectrometer to search for adducts in human plasma. Our study provides the background information that is needed for analyzing real life blood samples from exposed humans.

### Assay of BChE Activity

BChE activity was assayed at 25 °C by the Ellman method (Ellman *et al.*, 1961). The assay mixture (2 ml) contained 100 mM potassium phosphate buffer (pH 7.0), 1 mM butyrylthiocholine and 0.5 mM 5,5'-dithiobis(2-nitrobenzoic acid). The reactions were initiated by adding enzyme. The rate of butyrylthiocholine hydrolysis was monitored by the increase in absorbance at 412 nm on a Gilford spectrophotometer. BChE activity was calculated in the initial 60 s period using the extinction coefficient ( $E_{412} = 13.6 \text{ mM}^{-1} \text{ cm}^{-1}$ ).

### Trypsin Digestion and HPLC

OP-treated BChE was boiled for 10 min in a water bath to denature and unfold the protein, thereby allowing trypsin access to cleavage sites. BChE (200 µg in 55 µl of 10 mM ammonium bicarbonate pH 8.3) was digested overnight at 37 °C with 20 µl of 0.4 µg µl<sup>-1</sup> trypsin (8 µg in 50 mM acetic acid). A 1 µl aliquot of 1 M ammonium bicarbonate was added to adjust the pH to 8.3.

Trypsinized BChE was injected into a Phenomenex C<sub>18</sub> column (100 × 4.6 mm) on a Waters 625 LC system to purify the labeled active site peptide. Peptides were eluted with a 60 min gradient starting with 100% buffer A (0.1% trifluoroacetic acid in water) and ending with 60% buffer B (acetonitrile containing 0.09% trifluoroacetic acid) at a flow rate of 1 ml min<sup>-1</sup>. One milliliter fractions were collected.

### Matrix-assisted Laser Desorption/Ionization Time of Flight (MALDI-TOF-TOF) Mass Spectrometry

HPLC fractions were analyzed in the MS and MSMS modes of the MALDI-TOF-TOF 4800 mass spectrometer (Applied Biosystems, Foster City, CA, USA). Salt-free HPLC fractions (0.5 µl) were spotted on a MALDI plate (Opti-TOF 384 well Insert from Applied Biosystems), air-dried and overlaid with 0.5 µl of  $\alpha$ -cyano-4-hydroxycinnamic acid (10 mg ml<sup>-1</sup> in 50% acetonitrile, 0.1% trifluoroacetic acid). MS spectra were acquired using positive reflector mode with laser intensity at 4000 V. Each MS spectrum was the sum of 500 laser shots. Parent ion masses corresponding to labeled BChE active site peptides were fragmented in the MSMS mode to determine the peptide sequence and to identify the modified amino acid. Each MSMS spectrum was the sum of 2500 laser shots. The y ions and b ions in the MSMS spectra were assigned with the aid of the Proteomics Toolkit, a free online fragment ion calculator (<http://db.systemsbiology.net>).

## RESULTS

### Inhibition of BChE by Methamidophos, Dichlorvos, O-methoate and Diazinon

After 1 h reaction of BChE with a 20-fold molar excess of OP, enzyme inhibition levels were 97–100% for methamidophos,

dichlorvos and O-methoate. As expected, diazinon did not significantly inhibit BChE in 1 h; phosphorothioates become good inhibitors only after oxidative desulfuration by cytochrome P450 (Sultatos, 1994). After 7 h the diazinon-treated BChE was inhibited 20%. The incubations with methamidophos, dichlorvos and O-methoate were stopped after 7 h. The incubation with diazinon was continued for a total of 15 h, at which time the BChE activity was inhibited 52%.

### Analysis of Methamidophos–BChE Adducts by Mass Spectrometry

Digestion of human BChE with trypsin generates a 29 amino acid active site peptide extending from Ser 191 to Arg 219 (Lockridge *et al.*, 1987). The amino acid sequence of this peptide is <sup>191</sup>SerValThrLeuPheGlyGlu**SER**AlaGlyAlaAlaSerValSerLeuHisLeuLeuSerProGlySerHisSerLeuPheThrArg<sup>219</sup> (gi:116353 is the accession number in the NCBI nonredundant database). The active site serine is shown in bold uppercase letters. The monoisotopic mass of the unlabeled peptide is 2928.5 amu.

When human BChE was reacted with methamidophos, two new masses appeared in the MS spectrum (Fig. 2A). The mass at 3021.5 amu is consistent with addition of methoxy aminophosphate (+93 amu) and release of thiomethyl upon covalent bond formation with BChE (Fig. 1). The small peak at 3037.5 amu is consistent with addition of thiomethyl aminophosphate (+109 amu) and release of the methoxy group. Thus, methamidophos yields two types of adducts. The peak height of the adduct at 3037.5 amu was approximately 5% of that of the adduct at 3021.5 amu. This means thiomethyl is a better leaving group than methoxy, a result supported by the literature (Thompson and Fukuto, 1982). No aging was observed after 7 h at pH 8.3, 22 °C. If aging had occurred, the added mass from methamidophos would have been +79, regardless of which type of adduct was formed initially. No peptides with an added mass of +79 were observed.

Figure 2(B) shows the MSMS spectrum for the singly charged parent ion of mass 3021.5. The labeled masses correspond to fragments of the BChE active site peptide. The most prominent peak, at 2910.5 amu, is the dehydroalanine containing parent ion, designated  $\Delta y_{29}$ . This mass is consistent with loss of the organophosphorus agent together with a molecule of water from the 3021.5 parent ion to yield dehydroalanine in place of the OP-modified active site serine. Facile loss of phosphate from serine to yield dehydroalanine is a commonly observed fragmentation. The y<sub>22</sub> ion at 2288.6 amu and the y<sub>24</sub> ion at 2474.2 amu are consistent with fragments that retain the organophosphorus agent on serine 198. Their presence provides proof that the modified amino acid is Serine 198. Evidence from Fig. 2(B) establishes that the 3021.5 amu ion is the active site peptide of BChE wherein the active site serine is labeled with methoxy aminophosphate.

### O-methoate and Dichlorvos Adducts

O-methoate and dichlorvos both made a dimethoxyphosphate adduct with the BChE active site peptide, to give a singly charged tryptic peptide with a mass of 3036.5 amu. In addition, the aged monomethoxyphosphate adduct with a mass of 3022.5 amu was observed with both reagents. Figure 3 shows the MS spectrum of the BChE peptide labeled with O-methoate, for the sample in

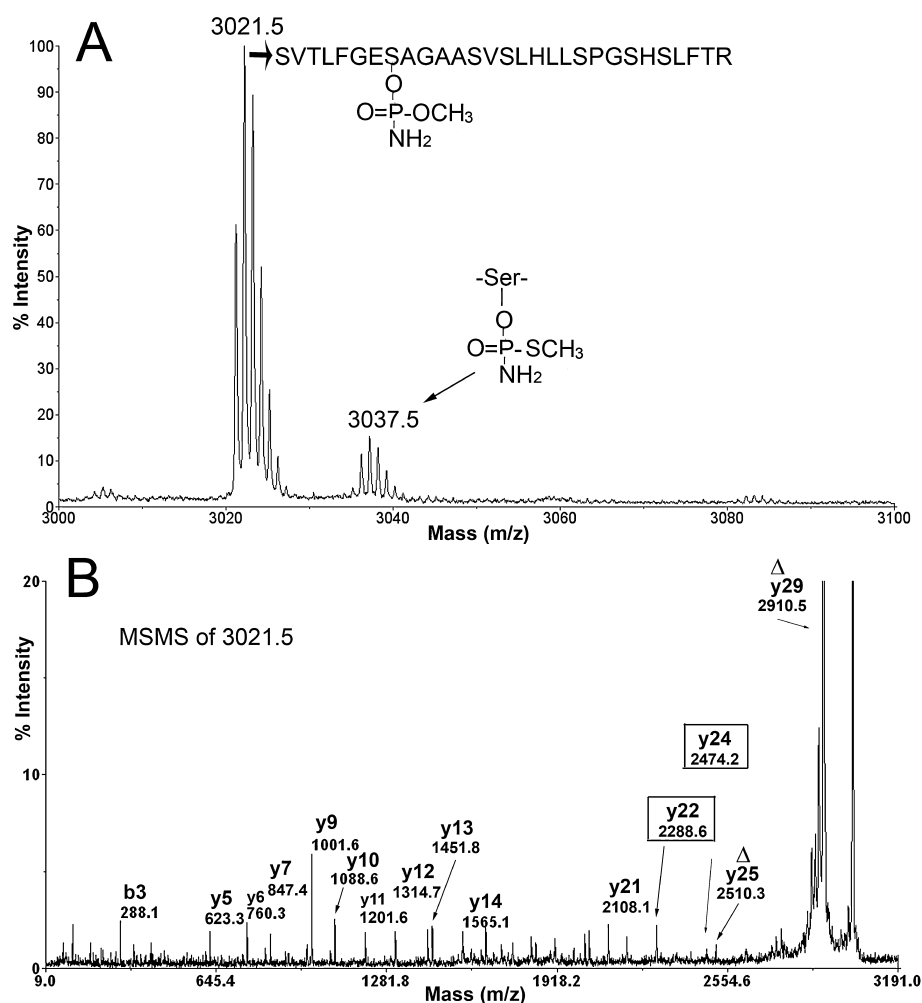


**Figure 2.** Methamidophos adducts of BChE. (A) MS spectrum showing masses of the two adducts produced by covalent binding of methamidophos to BChE. The thiomethyl group is displaced to make the 3021.5 amu adduct. A less favored reaction results in release of the methoxy group to make the 3037.5 amu adduct. (B) MSMS spectrum of the 3021.5 amu parent ion. The  $\Delta y_{29}$  ion at 2910.5 amu has lost the OP and a molecule of water during the fragmentation process. The intensity of  $\Delta y_{29}$  is about 20-fold greater than that of other fragment ions. Loss of OP and water converts the OP-labeled active site serine to dehydroalanine, symbolized by  $\Delta$ . A second dehydroalanine ion is at  $\Delta y_{25}$ . The y22 and y24 ions enclosed in boxes carry the OP on Serine 198.

HPLC fraction 36. The MS spectrum for dichlorvos labeled BChE was indistinguishable from the MS spectrum of *O*-methoate labeled BChE. The relative heights of the peaks in Fig. 3 are not representative of the relative ratio of the aged and unaged peptides because the aged peptide also eluted in fraction 35. MSMS spectra of the 3036.5 and 3022.5 amu parent ions fully supported the assignment of the labeled amino acid as Serine 198 of BChE (data not shown).

Aging is defined as the loss of an alkyl group from the OP-modified enzyme. Aging is catalyzed by Glu 197 and His 438 (Nachon *et al.*, 2005); aging is halted by denaturing the BChE enzyme (Li *et al.*, 2009).

#### Diazinon makes a Covalent Bond without Prior Desulfuration; the 3080.5 Adduct

The reaction of diazinon with BChE yielded three BChE adducts (Fig. 4A). The adduct with a monoisotopic mass of 3080.5 amu (Fig. 4B) appeared in HPLC fraction 35. The 3080.5 mass is consistent with covalent binding of diethoxythiophosphate to the

active site serine. The structure of the adduct indicated in Fig. 4B is the product of the reaction with diazinon and requires no rearrangement of atoms in diazinon. The 3080.5 mass is also consistent with binding of thioethyl ethoxyphosphate. This alternative adduct would be produced from a rearranged diazinon in which the sulfur atom exchanged with an oxygen atom to yield *O*-pyrimidine *S*-ethyl *O*-ethylphosphate (Fig. 1).

Proof that the ion at 3080.5 amu is an OP-modified BChE active site peptide is provided in the MSMS spectrum in Fig. 4C. The singly charged parent ion of mass 3080.5 yielded a prominent peak at 2910.5 amu, designated  $\Delta y_{29}$  in the figure. An intense fragment ion at 2910 amu is commonly seen when the OP-labeled, BChE active-site peptide is subjected to fragmentation in the MALDI-TOF-TOF 4800. It represents loss of the organophosphorus agent and a molecule of water, with conversion of the OP-labeled serine to dehydroalanine. The intensity of the  $\Delta y_{29}$  ion is 25-fold greater than the intensity of other ions. To visualize the other ions it was necessary to cut off most of the signal from the  $\Delta y_{29}$  ion in Fig. 4C. The other annotated peaks are consistent with the fragmentation pattern of the BChE active site

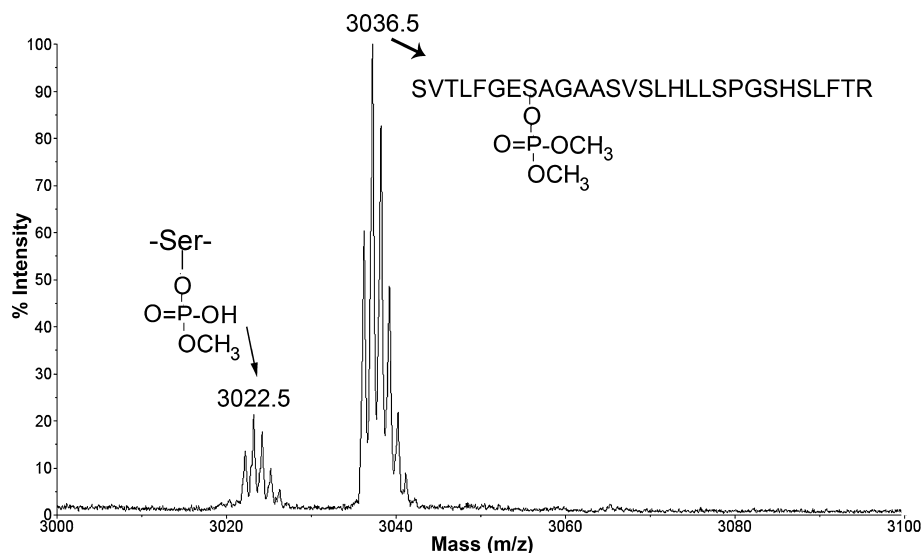


**Figure 3.** O-methoate adduct of BChE, MS spectrum. O-methoate and dichlorvos make the same adducts with BChE. The peptide with mass 3036.5 is the dimethoxyphosphate adduct. The peptide with mass 3022.5 is the monomethoxyphosphate adduct, which has lost a methoxy group as a consequence of aging.

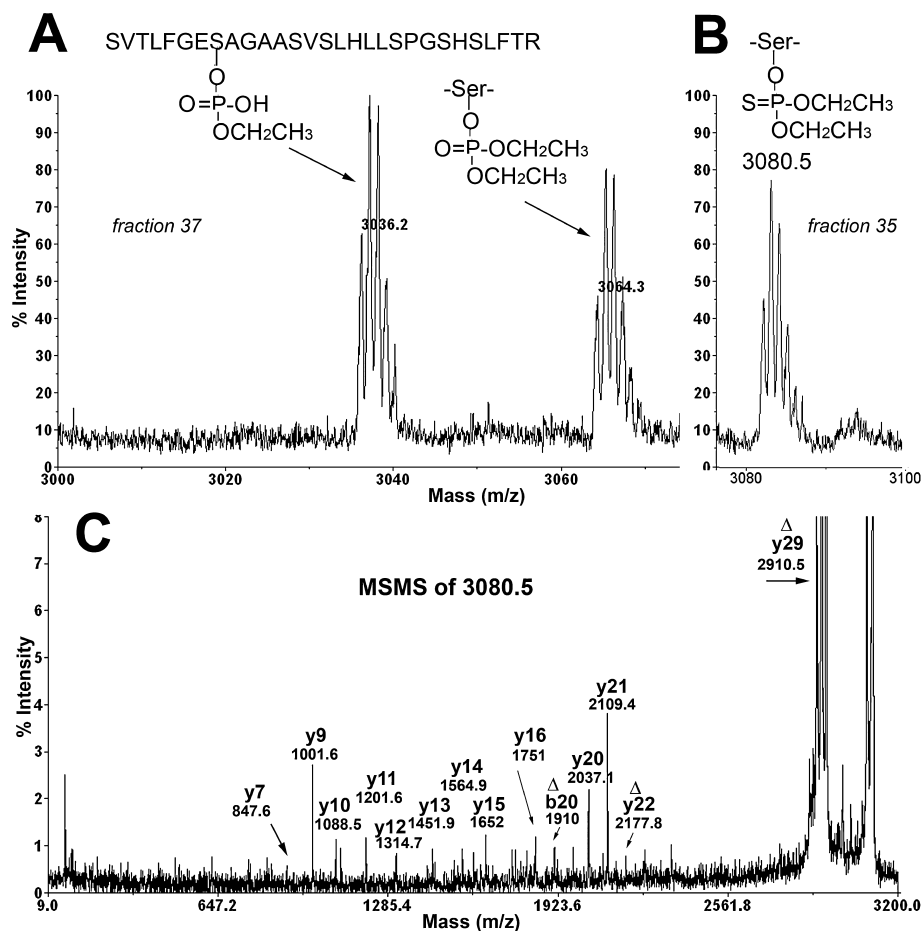


**Figure 4.** Diazinon makes an unusual adduct with BChE. (A) MS spectrum shows adducts with masses of 3036.2 and 3064.3 in fraction 37 from the HPLC. These adducts are from the reaction of an isomer of diazinon with BChE. (B) MS spectrum shows an adduct with a mass of 3080.5 in fraction 35. The peak at 3080.5 is modified on Serine 198 by diethoxythiophosphate. Alternatively, the 3080.5 mass could come from reaction with a rearranged diazinon to yield thioethyl ethoxyphosphate. (C) The MSMS spectrum of the singly charged parent ion  $m/z$  3080.5 demonstrates that the 3080.5 amu peptide is the active site BChE peptide modified on Serine 198 by OP.

peptide. In addition to the 2910.5 fragment, the  $\Delta b_{20}$  ion at 1910 and the  $\Delta y_{22}$  ion at 2177.8 amu are consistent with loss of the organophosphorus agent and a molecule of water, and the appearance of dehydroalanine.

Phosphorothioates, including diazinon, parathion and malathion, are poor inhibitors of acetylcholinesterase and butyrylcholinesterase. Our mass spectrometry results suggest that the inhibition rates observed in kinetic experiments can be attributed in part to the covalent bond formed between the phosphorothioate and BChE. However, a second factor must also be considered and that is the isomerization of phosphorothioates, converting them to oxons. Oxons react rapidly with the cholinesterases, so the rate-limiting step in the inhibition reaction would be the rate of isomerization.

### Isomerization of Diazinon to Explain the 3064.5 and 3036.5 Adducts

The slow inhibition of BChE by diazinon was accompanied by formation of diethoxyphosphate and monoethoxyphosphate adducts with masses of 3064.5 and 3036.5 amu (Fig. 4A). The sulfur originally present in diazinon was lost. The source of the diethoxyphosphate adduct at 3064.5 amu can be rationalized by invoking a thiono–thiolo rearrangement in which the double bonded sulfur on the phosphorus atom is exchanged with the oxygen on the pyrimidinol ring (Thompson *et al.*, 1989; Barr *et al.*, 2005). The rearranged isomer structure, *S*-pyrimidine *O,O*-diethylphosphate, is shown in Fig. 1. The thiono–thiolo rearrangement is an established, facile isomerization that can be induced by heat, light or chemicals (Thompson *et al.*, 1989; Barr *et al.*, 2005). Subsequent reaction of the thiopyrimidine isomer with BChE would eliminate the thiopyrimidine moiety leaving the diethoxyphosphate. Aging with loss of one ethoxy group explains the monoethoxyphosphate adduct at 3036.5 amu.

The 3064.5 and 3036.5 adducts from the reaction of diazinon with BChE are the same as those produced by reaction with diazoxon. The possibility that diazoxon was present as a contaminant was ruled out by the observation that inhibition of BChE occurred slowly over a 15 h incubation period. If the diazoxon had been present as a contaminant in the diazinon solution, inhibition would have been nearly instantaneous on mixing diazinon with BChE. Absence of a diazoxon contamination in the diazinon preparation eliminates diazoxon as a source of adducts with masses of 3064.5 and 3036.5 amu.

MSMS spectra of the 3064.5 and 3036.5 parent ions (data not shown) confirmed that these were BChE peptides and that the OP was covalently bound to the active site serine.

## DISCUSSION

The majority of pesticide poisoning cases in Turkey are suicide attempts (Yurumez *et al.*, 2007). The most frequent clinical signs are miosis, respiratory distress, tachycardia, loss of consciousness and hypertension. Out of 220 cases treated in hospital emergency rooms in Afyonkarahisar and Kayseri, Turkey, 20 patients died. Sometimes the diagnosis of poisoning is difficult. Cases have been misdiagnosed initially as brainstem stroke (Aygun, 2004), opioid overdose (Baydin *et al.*, 2008) and foreign body aspiration (Caksen *et al.*, 2005). Laboratory assays showing that plasma butyrylcholinesterase activity was below normal were helpful for achieving the correct diagnosis of OP poisoning. Treatment strategies depend on a correct diagnosis.

The acute toxicity of organophosphorus pesticides is due to inhibition of acetylcholinesterase in nerve synapses. Inhibition of butyrylcholinesterase has no clinical sequelae. Butyrylcholinesterase is a good marker for OP exposure because BChE reacts rapidly with OP to form covalent adducts that have no enzyme activity, and BChE is 3000-fold more abundant in human plasma than acetylcholinesterase (Brimijoin and Hammond, 1988). It is standard practice to look for inhibition of plasma BChE activity to aid in diagnosis of OP pesticide intoxication.

Although BChE activity assays are helpful for diagnosis, they do not identify the poison. Mass spectrometry can distinguish between classes of poison. Our mass spectrometry study of pure human BChE modified by four OP pesticides will serve as an aid for future work that aims to analyze plasma samples from poisoned individuals.

The pesticides in the present report have not previously been tested by mass spectrometry of adducts with human BChE. The reaction of methamidophos with human and *Torpedo californica* acetylcholinesterase has been studied by mass spectrometry, and has been found to yield adducts on the active site serine similar to the major adduct we found for BChE (Elhanany *et al.*, 2001). A study with radiolabeled methamidophos showed that thiomethyl was the leaving group in the reaction of methamidophos with electric eel acetylcholinesterase (Thompson and Fukuto, 1982), a result consistent with our result for human BChE. Aging of the acetylcholinesterase adducts was not reported, consistent with our result for BChE where aging was not observed for samples treated with methamidophos for 7 h.

Diazinon is widely used as a pesticide in sheep dip formulations, spray pesticides for household use, and cat flea collars (de Blaquiere *et al.*, 2000; Garfitt *et al.*, 2002). Diazinon is a poor inhibitor of acetylcholinesterase and BChE until it is activated to the oxon. Activation to the oxon is mediated by liver microsomal cytochrome P450 (Mutch and Williams, 2006). A second route to the oxon is a thiono–thiolo rearrangement. In the present work the thiono–thiolo rearrangement occurred slowly in aqueous solution to produce an oxon that inhibited the activity of BChE. A full description of the rearrangement products of diazinon is provided by Barr *et al.* (2005).

### Limitations

A mass spectrometry method for detection of OP exposure is not expected to be useful to the clinician, who will treat patients based on their symptoms. Knowing the identity of the poison is, however, likely to be useful to forensic toxicologists. The method distinguishes classes of poisons, but does not distinguish between poisons that add an identical mass. For example, dichlorvos and *O*-methoate both add a mass of 108 for dimethoxyphosphate or a mass of 94 for monomethoxyphosphate. Another limitation of the method is the requirement for highly purified BChE. Purifying 4  $\mu$ g of BChE from 1 ml of plasma that contains 50 000  $\mu$ g of other proteins is a difficult task at this time. A one-step method is needed that selectively extracts BChE from human serum or plasma.

### Application

The information provided in the present work provides the masses of possible adducts and how they fragment in the mass spectrometer. This information is needed to set up sensitive mul-

multiple reaction monitoring mass spectrometry methods to analyze exposure in real-life samples. As of this date, the major application will be for forensic cases, where it is important to distinguish between classes of pesticides, and between nerve agents and pesticides.

### Sensitivity

It has been estimated that mass spectrometry could potentially detect OP-BChE adducts in human plasma where the BChE was inhibited as little as 1% (Tsuge and Seto, 2006). The multiple reaction monitoring method would require purification of BChE from 5 ml of plasma.

## CONCLUSIONS

Mass spectrometry has identified unexpected modifications on the active site serine of human butyrylcholinesterase after highly purified butyrylcholinesterase was treated with selected pesticides. Two types of adducts were produced by reaction of butyrylcholinesterase with methamidophos, and three types of adducts by reaction with diazinon. Knowing what to expect prepares one for analysis of plasma samples from poisoned patients.

### Acknowledgment

This work was supported by NIH grant U01 NS058056, NIH Cancer Center Support grant CA036727, and US Army Medical Research and Materiel Command W81XWH-07-2-0034. Mass spectra were obtained with the support of the Mass Spectrometry and Proteomics core facility at the University of Nebraska Medical Center.

## REFERENCES

- Altintop L, Aygun D, Sahin H, Doganay Z, Guven H, Bek Y, Akpolat T. 2005. In acute organophosphate poisoning, the efficacy of hemoperfusion on clinical status and mortality. *J. Intens. Care Med.* **20**: 346–350.
- Aygun D. 2004. Diagnosis in an acute organophosphate poisoning: report of three interesting cases and review of the literature. *Eur. J. Emerg. Med.* **11**: 55–58.
- Barr JD, Bell AJ, Bird M, Mundy JL, Murrell J, Timperley CM, Watts P, Ferrante F. 2005. Fragmentations and reactions of the organophosphate insecticide diazinon and its oxygen analog diazoxon studied by electrospray ionization ion trap mass spectrometry. *J. Am. Soc. Mass Spectrom.* **16**: 515–523.
- Baydin A, Aygun D, Aydin M, Akdemir HU, Ulger F. 2008. Acute organophosphate poisoning mimicking opioid intoxication. *Eur. J. Emerg. Med.* **15**: 245–246.
- Brimijoin S, Hammond P. 1988. Butyrylcholinesterase in human brain and acetylcholinesterase in human plasma: trace enzymes measured by two-site immunoassay. *J. Neurochem.* **51**: 1227–1231.
- Caksen H, Demirtas M, Tuncer O, Odabas D, Ceylan N, Kati I, Koseoglu B. 2005. A boy with organophosphate poisoning mimicking a foreign body aspiration. *J. Emerg. Med.* **29**: 217–219.
- Darvesh S, Walsh R, Kumar R, Caines A, Roberts S, Magee D, Rockwood K, Martin E. 2003. Inhibition of human cholinesterases by drugs used to treat Alzheimer disease. *Alzheimer Dis. Assoc. Disord.* **17**: 117–126.
- de Blaquiére GE, Waters L, Blain PG, Williams FM. 2000. Electrophysiological and biochemical effects of single and multiple doses of the organophosphate diazinon in the mouse. *Toxicol. Appl. Pharmacol.* **166**: 81–91.
- Easson LH, Stedman E. 1936. The absolute activity of choline-esterase. *Proc. R. Soc. Lond. B.* **121**: 142–164.
- Elhanany E, Ordentlich A, Dgany O, Kaplan D, Segall Y, Barak R, Velan B, Shafferman A. 2001. Resolving pathways of interaction of covalent inhibitors with the active site of acetylcholinesterases: MALDI-TOF/MS analysis of various nerve agent phosphyl adducts. *Chem. Res. Toxicol.* **14**: 912–918.
- Ellman GL, Courtney KD, Andres V Jr, Feather-Stone RM. 1961. A new and rapid colorimetric determination of acetylcholinesterase activity. *Biochem. Pharmacol.* **7**: 88–95.
- Ergonen AT, Salacin S, Ozdemir MH. 2005. Pesticide use among greenhouse workers in Turkey. *J. Clin. Forensic Med.* **12**: 205–208.
- Fidder A, Hulst AG, Noort D, de Ruiter R, van der Schans MJ, Benschop HP, Langenberg JP. 2002. Retrospective detection of exposure to organophosphorus anti-cholinesterases: mass spectrometric analysis of phosphorylated human butyrylcholinesterase. *Chem. Res. Toxicol.* **15**: 582–590.
- Garfitt SJ, Jones K, Mason HJ, Cocker J. 2002. Exposure to the organophosphate diazinon: data from a human volunteer study with oral and dermal doses. *Toxicol. Lett.* **134**: 105–113.
- Kavalci C, Durukan P, Ozer M, Cevik Y, Kavalci G. 2009. Organophosphate poisoning due to a wheat bagel. *Intern. Med.* **48**: 85–88.
- Li H, Ricordel I, Tong L, Schopfer LM, Baud F, Megarbane B, Maury E, Masson P, Lockridge O. 2009. Carbofuran poisoning detected by mass spectrometry of butyrylcholinesterase adduct in human serum. *J. Appl. Toxicol.* **29**: 149–155.
- Lockridge O, Bartels CF, Vaughan TA, Wong CK, Norton SE, Johnson LL. 1987. Complete amino acid sequence of human serum cholinesterase. *J. Biol. Chem.* **262**: 549–557.
- Lockridge O, Schopfer LM, Winger G, Woods JH. 2005. Large scale purification of butyrylcholinesterase from human plasma suitable for injection into monkeys; a potential new therapeutic for protection against cocaine and nerve agent toxicity. *J. Med. Chem. Biol. Radiol. Def.* **3**: nihms5095.10.1901/jaba.2005.3-nihms5095.
- Mahmood NA, Carmichael WW. 1987. Anatoxin-a(s), an anticholinesterase from the cyanobacterium *Anabaena flos-aquae* NRC-525-17. *Toxicon.* **25**: 1221–1227.
- Main AR. 1976. Structure and inhibitors of cholinesterase. In *Biology of Cholinergic Function*, Goldberg AM, Hanin I (eds). Raven Press: New York; 269–353.
- Matsunaga S, Moore RE, Niemczura WP, Carmichael WW. 1989. Anatoxin-a(s), a potent anticholinesterase from *Anabaena flos-aquae*. *J. Am. Chem. Soc.* **111**: 8021–8023.
- Mutch E, Williams FM. 2006. Diazinon, chlorpyrifos and parathion are metabolised by multiple cytochromes P450 in human liver. *Toxicology* **224**: 22–32.
- Nachon F, Asojo OA, Borgstahl GE, Masson P, Lockridge O. 2005. Role of water in aging of human butyrylcholinesterase inhibited by echthiophate: the crystal structure suggests two alternative mechanisms of aging. *Biochemistry* **44**: 1154–1162.
- Nicolet Y, Lockridge O, Masson P, Fontecilla-Camps JC, Nachon F. 2003. Crystal structure of human butyrylcholinesterase and of its complexes with substrate and products. *J. Biol. Chem.* **278**: 41141–41147.
- Sultatos LG. 1994. Mammalian toxicology of organophosphorus pesticides. *J. Toxicol. Environ. Health* **43**: 271–289.
- Thompson CM, Fukuto TR. 1982. Mechanism of cholinesterase inhibition by methamidophos. *J. Agric. Food Chem.* **30**: 282–285.
- Thompson CM, Frick JA, Natke BC, Hansen LK. 1989. Preparation, analysis, and anticholinesterase properties of O,O-dimethyl phosphorothioate isomerides. *Chem. Res. Toxicol.* **2**: 386–391.
- Tsuge K, Seto Y. 2006. Detection of human butyrylcholinesterase-nerve gas adducts by liquid chromatography-mass spectrometric analysis after in gel chymotryptic digestion. *J. Chromatogr. B Analyt. Technol. Biomed. Life Sci.* **838**: 21–30.
- Turgut C, Ornek H, Cutright TJ. 2009. Pesticide residues in dried table grapes from the Aegean region of Turkey. *Environ. Monit. Assess.; doi: 10.1007/s10661-009-1037-z*
- Whittaker M. 1986. *Cholinesterase*. Karger: Basel.
- Yardan T, Baydin A, Aygun D, Karatas AD, Deniz T, Doganay Z. 2007. Late-onset intermediate syndrome due to organophosphate poisoning. *Clin. Toxicol. (Phil.)* **45**: 733–734.
- Yurumez Y, Durukan P, Yavuz Y, Ikizceli I, Avsarogullari L, Ozkan S, Akdur O, Ozdemir C. 2007. Acute organophosphate poisoning in university hospital emergency room patients. *Intern. Med.* **46**: 965–969; doi: 10.2169/internalmedicine.46.6304